CONSTANT SHEAR ALONG A BOUNDARY OF A FLUME

THESIS FOR A DOCTORATE OF PHILOSOPHY PRESENTED BY

A. E. KRAMER

CIVIL ENGINEERING DEPARTMENT
UNIVERSITY OF ASTON IN BIRMINGMAM.

JUNE 1972

ACKNOWLEDGEMENTS

I gratefully acknowledge the assistance afforded me by the Civil Engineering Department of the University of Aston in Birmingham for the use of laboratory space and equipment and in particular for the encouragement given to me by Professor M. Holmes during this programme of research.

I wish also to thank Mr David Hall of the Civil Engineering Department for the help he gave me in the laboratory.

I wish also to record my grateful appreciation to Dr. K. Arumugam for his helpful comments during this investigation.

I would like to thank the Science Research Council for their financial support.

CONTENTS

LIST OF PLATES

LIST OF SYMBOLS

δ = Boundary layer thickness

δ_* = Displacement thickness

δ_2 = Momentum thickness of boundary layer

ρ = Density

μ = Dynamic Viscosity

ν = Kinematic viscosity

ε = Vorticity

γ = Constant

θ = Momentum thickness

τ_o = Bed shearing stress

$\chi = \frac{U}{2.5\ V_*}$ = White's derivative for constant drag

R_e = Reynolds number

$C_{f'}$ = Local friction coefficient

$H = \frac{\delta x}{\theta}$ = Shape factor

k = Mean diameter of grain

f = Function of

R_x = Correlation coefficient with respect to x axis

R_y = Correlation coefficient with respect to y axis

u = Velocity in x direction

v = Velocity in y direction

u' = Turbulent component of velocity in x direction

v' = Turbulent component of velocity in y direction

$\bar{u}$ = Average value of velocity in x direction

$\bar{v}$ = Average value of velocity in y direction

U = Velocity outside boundary layer

U_* = Shear stress velocity

y = Wall distance

ABSTRACT

The accurate measurement of bed shear stress has been extremely difficult due to its changing values until White propounded a theory which would give constant shear along the bed of a flume. In this investigation a flume has been designed according to White's theory and by two separate methods proven to give constant shearing force along the bed.

The first method applied the Hydrogen Bubble Technique to obtain accurate values of velocity thus allowing the velocity profile to be plotted and the momentum at the various test sections to be calculated. The use of a 16 mm Beaulieu movie camera allowed the exact velocity profiles created by the hydrogen bubbles to be recorded whilst an analysing projector gave the means of calculating the exact velocities at the various test sections.

Simultaneously Preston's technique of measuring skin friction using Pitot tubes was applied. Two banks of open ended water manometer were used for recording the static and velocity head pressure drop along the flume. This type of manometer eliminated air locks in the tubes and was found to be sufficiently accurate.

Readings of pressure and velocity were taken for various types and diameters of bed material both natural sands and glass spheres and the results tabulated.

Graphs of particle Reynolds Number against bed shear stress were plotted and gave a linear relationship which dropped off at high values of Reynolds Number.

It was found that bed movement occurred instantaneously along the bed of the flume once critical velocity had been reached. On completion of this test a roof curve inappropriate to the bed material was used and then the test repeated. The bed shearing stress was now no longer constant and yet bed movement started instantaneously along the bed of the flume, showing that there are more parameters than critical shear stress to bed movement.

It is concluded from the two separate methods applied that the bed shear stress is constant along the bed of the flume.

CHAPTER I

Introduction

It has been appreciated for a long time that the shear stress at the bed of an open channel is an important parameter which determines the discharge through it. In natural open channels where the bed is composed of mobile material the bed shear was determined both by their form and their movement. This belief led Shields, Lane and others to propose shear stress as the major criterion for bed movement. To confirm this experimentally would involve the measurement of instantaneous shear stress at the mobile bed, as it is well-known that the shear stress in any natural or laboratory channel varies at any point along the bed. C. M. White[38] while trying to establish criteria for the movement of sand particles in the bed of channels found the drag force, caused by bed shear, to be the major factor. He then, in wanting to study the bed shear, designed what he called a Constant Shear or Drag Nozzle.

The purpose of this nozzle was to develop a constant shear stress along the bed of the channel. He used Prandtl's "Mixing Length Theory" and depending on the size of particles on the bed theoretically developed a shape for a two dimensional nozzle. This he used to confirm his hypothesis of sand grain movement.

He, however, did not confirm completely that the nozzle met all the requirements that it was designed for.

It is the aim of this study

(a) to check and develop the two dimensional nozzle for different bed materials both artificial and natural;

(b) to confirm that the design criteria are fulfilled along the nozzle;

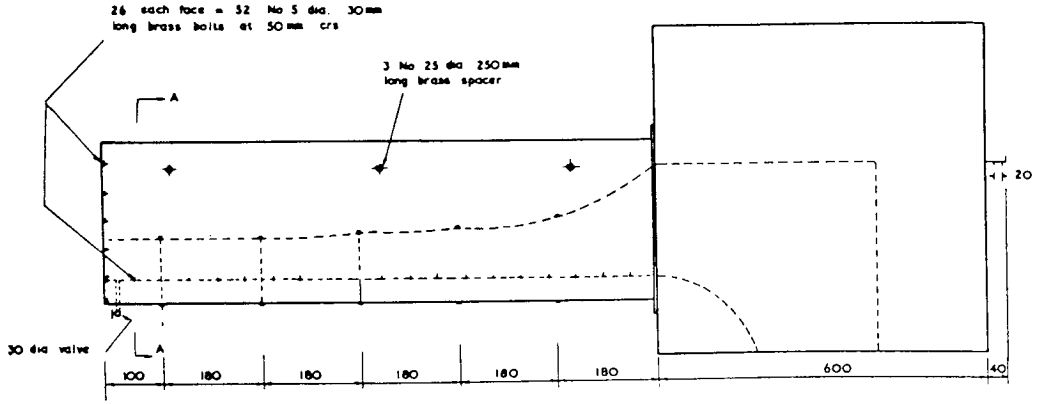

SIDE ELEVATION

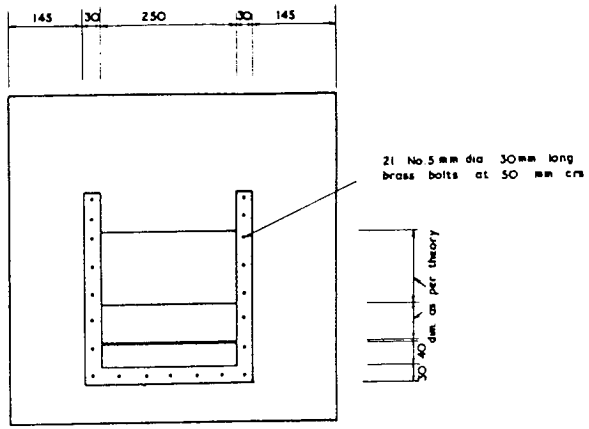

SECTION A-A

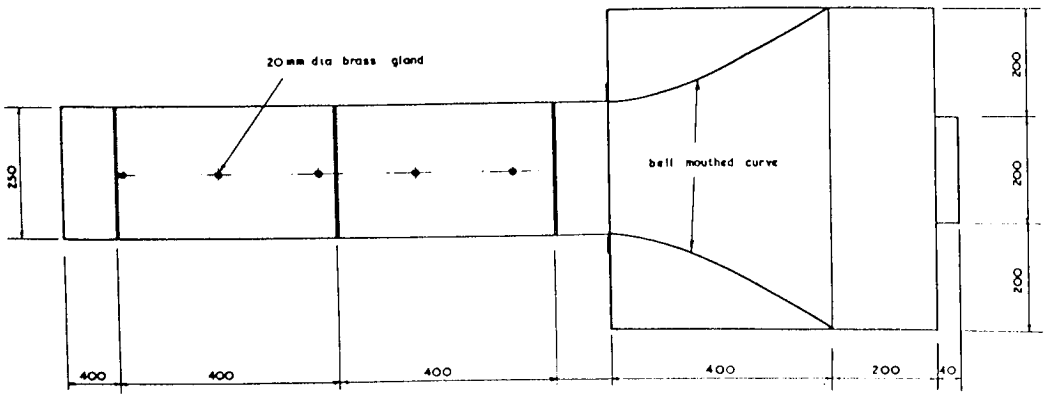

PLAN

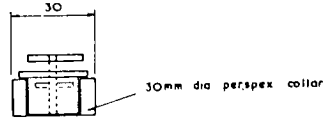

SECTION

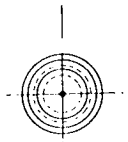

PLAN

Detail of 20mm dia brass gland with 30mm dia perspex collar

Scale full size

NOTE. All dimensions in millimeters

UNIVERSITY OF ASTON IN BIRMINGHAM
CIVIL ENGINEERING DEPARTMENT

CONSTANT SHEAR FLUME

SCALE 1:5

Drawn by

(c) to confirm that a constant shear stress is developed along the nozzle for any flow, but different for different rates of flow;

(d) if the threshold shear stress criterion is reached, whether there was uniform movement of particles along the channel.

Based on White's assumptions depending on the material chosen it was found that a different profile results in each case. The author constructed five different profiles as given in Chapter IV for uniform artificial material 1, 1½, 2 and 3 mm diameter and natural material of ½, 1, 1½ and 3 mm mean diameter.

These nozzles were tested for different rates of flow. In trying to confirm the hypothesis for the design it was necessary to measure the velocity distribution at various stations along the length of the nozzle. Attempts were made by the author to measure this at five equidistant locations as shown in Fig. 1 using a photographic technique. This meant photographing Telcon particles injected into the main stream and obtaining the streak left by this particle for a fixed pulse time. It was hoped that by measuring this length of streak it would be possibl to obtain the velocity. This method was abandoned as it was difficult to identify these particles on the print of the photograph obtained.

The author then decided to try applying the hydrogen bubble technique for the measurement of velocities. Stainless steel tubes are used as anodes as shown in Plate 1 at five different locations and the bubbles were then photographed using a cine camera. The "stills" obtained from these movie films Plates 2-3 give clearly the velocity profiles at these sections. From these photographs, as given in Chapter VI, the momentum and discharges have been computed and used to verify the hypothesis given in Chapter IV for the design of the nozzle.

This nozzle was designed to give constant shear, and according to hypothesis given in Chapter III, the longitudinal pressure gradient has to be a constant. C. M. White made attempts to measure this. The author tried to measure this using micro-manometers with carbon tetrachloride as the measuring fluid. This attempt did not succeed due to the inability to bleed the manometers successfully. Hence it was decided by the author to use inclined tube water manometers to measure the static pressure differences at these sections as given in Plate 9.

It was found by the author that this proved successful and tended to confirm the original hypothesis as a basis for design.

In the original nozzle as designed by White, no serious attempts were made to measure the instantaneous values of the shear stress along the bed of the channel. It was therefore proposed to use some of the techniques used for the measurement of shear stress in air over smooth boundaries to water.

The method used was similar to that used by Preston[25] as shown in Plate 4. The results obtained from these experiments as given in columns 3-6 of Tables 1-9, Chapter V, confirmed the constancy of shear stress according to the theory given in Appendix B.

In order to confirm whether this was true the author used a different sized material for a nozzle designed for another size and the results obtained using the above technique gave non constant values of bed shear.

The results obtained from all the above experiments were analysed for momentum, boundary layer growth, constancy of bed shear, according to the theory given in Chapter III. The conclusions obtained from these are given in Chapter V.

CHAPTER II

2.1. Development of Boundary and Associated Wall Shear Stress

2.1.1. Laminar Boundary Layer

An ideal non-viscous fluid ideally experiences no force on the boundary whilst in the case of a real fluid body experiences drag which early theories could not analyse. This could be due to forces of friction on the boundary, and the form of the boundary, whose surface could be regular, irregular and smooth or rough. The changes in momentum are confined to a thin layer close to the boundary called the boundary layer. If fluid in two dimensional flow flows over a boundary this layer, which from the first instant should be zero, tends to grow parabolically. The growth of this layer is a function of the change of momentum, the thickness of the layer growing as the momentum increases, the momentum change being itself a function of the shear stress in the boundary layer. Two dimensional laminar and turbulent motion were first analysed by Prandtl (1904)[26] when he formulated two dimensional equations governing the performance of the boundary layer.

In laminar flow it is possible in certain cases, as indicated by Schlichting[30], to calculate the wall shear stress. Blasius[1] obtained the solution to the equation of the boundary layer in the form of a series expansion, whilst Polhausen[24] at a later date demonstrated that if a stream function is introduced the resulting partial differential equation can be reduced to an ordinary differential equation by a similarity transform. Simplified forms of the boundary layer equation were also obtained by Falkner and Skan[10], whilst experimental work by Kempf[17] also in 1922 showed tolerable agreement with experimental results.

2.1.2. Turbulent Boundary Layer

Beyond certain velocities there is a breakdown of laminar flow, and the theoretical valuations would not be true. From conceptional dimensional reasoning it can be shown that δ the boundary layer thickness is a function of the square root of the Reynolds Number $(R_e^{\frac{1}{2}})$ (27).

2.1.3. Apparent Turbulent Friction

In this type of turbulent motion the shear stress associated with it is again due to transfer of momentum in the longitudinal and transverse directions. The transfer of energy is difficult to treat theoretically, but Osborne Reynolds (27) introduced the fundamentally important concept of apparent or virtual turbulent friction as early as 1880. Reynolds also derived equations for shear stress at the bed and walls of a flume and these first derivations of his are still the fundamentals of more advanced series. A complete calculation of the boundary layer for a given body with the aid of differential equations is in many cases extremely cumbersome and von Karman (18) devised a momentum integral method to simplify the solution. In this method the mean is taken over the whole thickness of the boundary layer. The point of separation itself is determined, and indeed defined, by the condition that the velocity gradient at the wall should vanish, i.e.

$$\left(\frac{du}{dy}\right) = 0$$

at separation.

2.1.4. Correlation Coefficient Concept

Schubauer and Klebanoff[31] in their investigation into the separation of the boundary layer came to the conclusion that energy is transferred from larger to smaller flow regimes by the means of large eddies and these large eddies account for the average shearing stress. They found that shearing stress per unit energy is much like the correlation coefficient and would be two-thirds of $u\,v/u'v'$ if u', v' and w' were all equal. The correlation coefficient R_y they defined as the transverse coefficient equal to $u_1u_2/u_1'u_2'$ where subscripts 1 and 2 refer to positions y_1 and y_2 whilst R_x was the longitudinal coefficient referring to the positions of x.

They found a great difference between laminar flow shear stress and turbulent flow shear stress. In laminar flow the shearing stress is directly proportional to the local velocity gradient. In turbulent flow the shearing stress may rise abruptly for scarcely any change in the local velocity gradient and again fall with increasing velocity gradient. This illustrates the difficulty of adopting the concepts of viscous flow in turbulent flow. The difference may arise because turbulent phenomena, unlike molecular phenomena, are on a scale of space and velocity of the same order as that of the mean flow.

2.1.5. Drag Coefficient Equation

Schultz-Grunow[33] found that the application of logarithmic laws of velocity distribution for turbulent pipe flow to the free friction layer did not afford a satisfactory resistance law to agree with plate drag measurements. He therefore deemed it desirable to explore the velocity distribution in the free friction layer and check the drag measurements. He checked the momentum, displacement and friction layer thickness obtained from the velocity measurements and found that only a

minor correction was disclosed by recalculating the plate length from the friction layer thickness obtained in the foremost test section by the old power law, which at small Reynolds numbers corresponds to reality quite well.

The momentum thickness δ he found could be tied to the drag coefficient through an equation so that the drag coefficients can be determined from the measured momentum thickness. He found this determination not to be accurate enough and by a mathematical analysis of velocity profiles went on to propose new formulae for the drag constant dependent on the value of the Reynolds Number. The form of these equations corresponded closely to the form of approximate formulae proposed by Prandtl.

2.1.6. Artificially Thickened Boundary Layer

Klebanoff and Diehl (1951)[20] carried out an investigation to determine the feasibility of artificially thickening a turbulent boundary layer. They discussed features of the fully developed turbulent boundary layer with zero pressure gradient. The then lack of satisfactory theory for turbulent shear flow directed their attention to the quantitative measurement of the characteristics of turbulence in shear flow as a means of obtaining information on which to base a theory. Much of the theoretical work that has been done on the turbulent boundary layer is based on the application of the logarithmic laws of velocity distribution derived for flow in pipes and channels. These involve the adoption of the mixing-length concept, a form for the shearing-stress distribution, and the omission of the influence of viscosity on the turbulence.

They compare their experimental results with wall-proximity law and the velocity-defect law for the velocity distribution. The value of V_* in their measurements was determined from the measured velocity profile by means of the von Karman momentum equation. In contrast with the measurements for pipes and channels, they found that there is a systematic increase in the deviation from the logarithmic law as Reynolds number decreases.

2.1.7. Local Friction Coefficient C_f

Because of the unsatisfactory state of knowledge concerning the surface shearing stress of boundary layers with pressure gradients Ludwieg and Tillmann[23] re-examined the problem. They found that the wall shearing stresses in a laminar boundary layer could be computed on a strictly theoretical basis since the relationship between velocity profile and shearing stress is known. This procedure, however, cannot be applied to the turbulent boundary layers since the relationship for the shearing stresses due to turbulent exchange is still unknown. Some investigations have been made also on boundary layers with pressure gradients, both accelerating and decelerating, but the data on wall friction are either absent or partly unsatisfactory. The wall shearing-stress was determined from the measured velocity profile by means of von Karman's momentum equation[18]. One substantial drawback of the experimental set up was the narrowness of the flow compared to the boundary layer thickness. This is likely to produce secondary flows which cancel the two-dimensionality of von Karman's momentum equation.

From the results obtained by previous investigators of pipe and plate flow, Ludwieg and Tillmann decided that C_f, the local friction coefficient depends only on the velocity profile and the material constants of the flowing medium. That is, that if the velocity profile

is known, $C_{f'}$ can be computed.

The results of previous investigations for plate and pipe flows were used to derive fundamental formulae regarding friction drag.

(a) The velocity profile of the boundary layer can be represented in the form

$$\frac{u}{U} = \phi\left(\frac{y}{\delta_2}, R_e\right) \qquad (1)$$

(u = velocity in boundary layer.

U = velocity outside boundary layer.

y = wall distance);

$$\delta_2 = \int_0^\infty \frac{u}{U}\left(1 - \frac{u}{U}\right) dy = \text{momentum thickness of boundary layer}$$

$$R_e = U\,\frac{\delta_2}{\nu} = \text{Reynolds number of boundary layer formed with momentum thickness } \delta_2;$$

ν = kinematic viscosity.

Quantity g in equation (1) is a fixed function which, however, is different for plate, pipe or channel flow. The dependence of $\frac{u}{U}$ on R_e is very small, that is, the velocity profiles differ very little for different Reynolds Numbers.

(b) The local friction coefficient $C_{f'}$ can always be represented in the form

$$C_{f'} = F(R_e)$$

($C_{f'} = \tau_o / \frac{\rho}{2} U^2$; τ_o = wall shearing stress; ρ = density).

Quantity F is again a fixed function for plate, pipe and channel flow; F can be computed for plate flow by the momentum

equation when g is known, because the total friction drag appears as loss of momentum in the boundary layer.

(c) For the part of the velocity profile near the wall the relation

$$\frac{u}{u_*} = f\left(\frac{u_* y}{\nu}\right) \tag{3}$$

was obtained $\left(u_* = \sqrt{\frac{\tau_o}{\rho}} = \text{shearing stress velocity.}\right)$

This relation holds true with the same function f for the part of plate, pipe or channel flow next to the wall. Provided that $\frac{u_* y}{\nu}$ values are not too small (fully turbulent zone $\frac{u_* y}{\nu} > 50$), equation (3) can be replaced very accurately by the approximate formula

$$\frac{u}{u_*} = a \log\left(\frac{u_* y}{\nu}\right) + b \tag{3a}$$

where a and b are universal constants. The logarithmic law can be approximated by a power law

$$\frac{u}{u_*} = C\left(\frac{u_* y}{\nu}\right)^{1/n} \tag{3b}$$

where C and n are constants which are still somewhat dependent on the $\frac{u_* y}{\nu}$ zone for which the approximation is especially good.

With the validity of the law governing equations (3) and (3a) proven by experimental means it is possible to say that u_* and hence, τ_o and C_f, depend only on the velocity profile and the material constants of the flowing medium.

They found that for boundary layers with pressure gradients their value of C_f, did not agree with results obtained by previous experimenters. Therefore they modified their theoretical derivation regarding layers with a pressure drop and arrived at good agreement with experimental data.

Their work on boundary layers with pressure gradients also disproved earlier claims, by previous workers, that the rise of friction coefficient to a multiple of that for plate flows in a boundary with a laminar layer.

2.1.8. Adverse Pressure Gradients

Sandborn and Slogan (1955)[29] investigating the momentum distribution in a turbulent boundary layer found that good agreement existed between skin friction values obtained by instrument measurement and the evaluations of the Ludwieg-Tillman empirical equations. They found, however, that previous investigators like Schubauer and Klebanoff[31] were getting inconsistencies in the shear distribution. They found that other experimenters had also been confronted with inconsistent wall shear stress evaluations.

They found that several methods were available for the evaluation of the wall shear stress; hence after an evaluation of the methods and taking into account the necessary limitations on each they concluded that the empirical equation of Ludwieg and Tillman[23]

$$C_{f'} = 0.246 \times 10^{-0.678H} R_\theta^{-0.268}$$

gives very good agreement with measurements. Attempts to predict shear distribution through the turbulent boundary layer had been largely empirical by nature so they looked at the means available for assessing a simple and yet accurate method for determining the shear distribution.

Analysing their measurements in turbulent boundary layers with adverse pressure gradients they came to the following conclusions. At all pressure gradients good agreement was obtained for the value of skin friction determined from the Ludwieg/Tillmann[23] relation and those measured with their heat-transfer-skin friction instrument.

Use of the measured distributions of turbulent shear stress $-\rho\,\overline{uv}$ and viscous shear stress $\mu \frac{\partial V}{\partial y}$ to predict the wall shearing stress agrees roughly with the values obtained from heat-transfer measurements or predicted by the Ludwieg-Tillmann equation.

Measurements indicated that there is a sub-layer within which the total shear stress obeys the relationship $\frac{\partial \tau}{\partial y} = \frac{p_w}{x}$ where τ is the total shear stress and p_w is the static pressure at the wall.

The universal relation $\frac{u}{U_*}$ against $y \frac{U_*}{\nu}$ (where U is the local mean velocity, U_* is the shear stress velocity, and ν the kinematic vosoosity) that has been observed by many workers was found to hold near the wall and the total shear distributions predicted by use of this universal relation were found to agree qualitatively with the distributions obtained from the measurements.

2.1.9. Adverse Pressure Gradients

Clauser (1953)[3] also made a thorough investigation into Boundary Layers with Adverse Pressure Gradients and compared his results for turbulent and laminar flow. In spite of the great technical importance of turbulent separation he found that the knowledge of the action of pressure gradients was poor. Firstly, no theory worthy of the name

exists for any turbulent shear flow. Secondly, several empirical methods exist for predicting the effect of pressure gradients on turbulent boundary layers, but experience indicates that none of them are reliable. They do little but correlate the data on which they were originally based.

Clauser found that in turbulent layers the situation was not simple as the profiles are not similar. At lower Reynolds numbers the profiles are roughly one-seventh power profiles whilst as the Reynolds number increases they become nearer one-eighth or one-ninth power profiles. It had been known for some time that if one abandoned U as a non dimensionalizing velocity and measured velocities relative to the free stream, using in its place $U_* = \sqrt{\frac{\tau_o}{\rho}}$ the shear velocity, then all constant pressure turbulent profiles are similar.

Most methods of treating turbulent boundary layers in adverse pressure gradients assume that the pressure gradients have no effect on the skin friction. Ludwieg and Tillmann[23] and Schubauer and Klebanoff[31] showed that adverse gradients reduced C_f but neither group was able to make a quantitative statement about the relationship of C_f and $\frac{dp}{dx}$. Early in the course of his investigation Clauser decided that pressure gradients have an unexpectedly large effect on skin friction. Even though his first pressure distribution had relatively gentle gradients the skin friction coefficients were nearly half of those for constant pressure profiles at the same Reynolds number.

Clauser by combining the results of his work with those of others in the field was able to present a relatively complete picture of turbulent skin friction. It is of interest to give a comparison of the results of the paper by Clauser with those of previous authors.

Since an understanding of turbulent processes under the combined influence of shear and pressure gradients did not exist, analyses have necessitated the momentum integral equation

$$\frac{d\theta}{dx} = \frac{C_f}{2} + \frac{(H + 2)}{2} \frac{\theta}{q} \frac{dp}{dx}$$

as a starting point. Since the momentum equation is not complete in itself, it is necessary to make assumptions about how the terms in the equation are to be obtained.

In summary, Clauser states that the experimental results he obtained show little or no agreement with the predictions of other workers. Since his experimental results were relatively simple and well defined he concludes that the field is still wide open for the advent of a reliable method of predicting the behaviour of turbulent layers under the influence of pressure gradients.

2.2. Direct Measurement of Shear Stress at the Wall

2.2.1. Measurement of Drag Forces induced by Shear

Schultz Grunow[33] in developing his new resistance law for smooth plates decided for the sake of greater accuracy to make the measurements in the wind tunnel whilst preserving the conditions of a free surface, i.e. no pressure decrease and a free friction layer. For his experimental measurements he used a new type of blower operated tunnel with the lower horizontally placed wall carrying the surface to be explored. The tunnel height was so chosen that the opposite friction layers were always kept separate, and thus produced free friction layers.

The upper wall of the tunnel was hinged and adjustable so that any prescribed pressure distribution, and for this purpose, also a

pressure equal to the outside pressure could be obtained to within 1/20th millimeter alcohol accuracy. The tunnel height thereby increased in flow direction according to the proportional growth of the displacement thickness at the walls. This made the conditions in the tunnel the same as on free surfaces.

The friction was weighed directly on a rectangular test plate mounted movably in a sector of the principal plate. The test plate rests on an arm in flexure pivots rotatable about a vertical axis. The weight is taken up by a float. Aside from the moment of the friction force an opposite moment is applied in the hinge by a wire stressed in torsion. The wire can be twisted by a hand wheel until it balances the moment of friction force and the scale arm is in the neutral setting, which can be read optically. The torque for the related twist was calibrated so that the frictional force and hence the local resistance could be ascertained.

This arrangement, also used for the same purpose by G. Kempf[17], is only practical where the pressure in the tunnel is the same as in the outside space. In any other case the slots in the sector necessary for free movement of the test plate manifest flows which produce uneven suction and pressure on the plate edges and falsify the measurements.

2.2.2. Use of Small Floating Elements for the Measurement of Shear Stress

The principle of measuring wall shear stress by cutting from the wall a small elemental piece, mounting it in such a way that it can move freely in the direction of the wall stream lines, and measuring the force on it is quite straightforward. Furthermore, since no assumptions need to be made about the nature of the flow near the

wall, the method appears satisfactory for measurements in a three dimensional situation. It was used by early investigators such as Kempf (1929)[17] for their studies of flat plate boundary layers in water. Schultz-Grunow (1940)[33] and Smith and Walker (1959)[35] have made successful measurements of the incompressible two-dimensional flat plate boundary layer in air, whilst Dhawan (1953)[5], Ludwieg[22], Hokkinen (1955)[15], Coles (1953)[4] and others have developed instruments for flat plates at high Mach numbers. However, secondary effects, associated mainly with the pressure gradient and the existence of an air gap around the element have so far restricted the use of the floating element technique to zero pressure gradients.

Brown and Joubert (1968)[2], however, developed the floating element principle so as to obtain accurate measurements of friction in turbulent boundary layers. They show that the shear force on the element is simply the product of the shear stress τ_o and the element area S but that to this shear force there should be added two secondary forces

(i) a pressure force imposed on the edge of the element by penetration of the free-stream pressure into the air gap. If a pressure gradient exists, a net pressure or buoyancy force on the element in a direction opposing the pressure gradient results;

(ii) the pressure gradient besides causing a direct pressure force on the element, will also cause a pressure difference between the boundary layer above any point in the air gap and the instrument case.

The element they designed and built for a three dimensional situation gave reasonable repeatable results and did not depend on the absence of pressure gradients for efficient operation.

Smith and Walker[35] also used a floating element device to measure local surface-shear stress. They decided since little was known about the effect of change of size of gap around the floating element to construct a device whose element could be repositioned and centered. Both Schultz-Grunow and Kempf used such a device while Dhawan and others used a simple deflection-type instrument. In their unit the floating element was repositioned by a small, powerful electro-magnet. The position of the element was indicated by a differential transformer capable of indicating movement of the floating element to an accuracy of a few hundred thousandth of a millimetre. When the position indicator showed that the floating element had started to move from its no-load neutral position, the strength of the electro-magnet was varied until the element returned to its no-load neutral position. Since the electromagnetic force was equal and opposite to the drag force exerted on the element, the average surface-shear stress on the floating element could be deduced from the measured electromagnetic force and a predetermined calibration.

This shear stress measuring device was capable of indicating the drag force on the element with a sensitivity of about 0.1×10^{-3} Newtons for a range of force from 0 to about 1.5×10^{-3} Newtons. The accuracy of determining the load under test conditions was believed to be within ± 2 per cent of applied load throughout the load range encountered.

Tests were made to study the effects of small variations in "flushness" of the floating element with the surrounding fixed surface. Measurements of surface shear at identical test conditions were made for a range of positions of the floating element, both depressed below and protruding above the fixed surface of the plate. It was found that the floating element could be depressed as much as 0.002 millimetres without any change in surface shear. However, when the element protruded above the surface of the wall, there was a noticeable

deviation in the measured shear force. Consequently, the surface element was always maintained flush or slightly below the surface of the channel wall.

2.3. Indirect Measurement of Shear

Successful attempts by direct measurement of the force on a small element of surface have been made for flat plates as described in previous paragraphs. Unfortunately the method needs great care and is not suitable as a general method of determining skin friction on aircraft in flight or on ships at sea, and even in the laboratory its difficulties are formidable.

J. H. Preston[25] in 1954 made full use of the experimental work done by Ludwieg and Tillmann[23] when they established that, near the surface $\frac{u}{U_*} = f\left(\frac{y/U_*}{\nu}\right)$. He focussed his attention on this equation assuming it to be true in a limited region near the wall. This, it seemed must imply a kind of local or restricted dynamical similarity in this region, for which τ_o, ρ, ν and some representative length are the only variables. Thus by tracking a pitot tube along the surface made it possible for Preston to convert the readings of such a tube relative to the local static pressure into local skin friction. This line of thought, in conjunction with the idea of a kind of restricted dynamical similarity is developed in detail in Appendix B.

Preston chose geometrically similar circular pitot tubes having as nearly as possible a ratio of internal to external diameter of 0.600. This ratio was chosen as previous work had been done, using this ratio, to measure the displacement of the effective centre. Secondly, the larger sizes of hypodermic tubing in stock have approximately this ratio. Also preliminary experiments showed that it was important to

maintain a closely constant ratio of internal to external diameters and to be careful about burrs.

In their investigations Smith and Walker[35] also made use of this very simple technique developed by J. H. Preston[25]. The pressure measured by the totalhead tube in conjunction with the surface static pressure measured at the same location along the plate was calibrated in terms of local surface-shear stress. They used tubing having the ratio of internal to external diameter of 0.600, i.e. having the same proportions as used by Preston.

Brown and Joubert[2] during the measurements of boundary layer friction also used the Preston tube technique to compliment the measurements taken by a floating element. They found close agreement with their readings and noticed that poor alignment of the instrument with the wind tunnel floor gave negligible effects on their readings.

2.3.1. Deducing Shear Stress from Velocity Measurements - Indirect Method

(a) Pitot Tubes. By measuring the velocity of the fluid accurately it is possible to calculate its momentum and thus arrive at a value for the shear stress. Many experimenters used this technique, measuring the velocity by pitot tube also in conjunction with some other method such as hot-wire anemometers.

Schubauer and Klebanoff[31] in their investigation plotted mean velocity distributions using a combination of pitot tube traverses with hot wire anemometers. They mounted several measuring heads on various types of traversing equipment designed for convenience, rigidity and a minimum of interference at a point where a measurement was being made.

Klebanoff and Kiehl[20] also found that the pitot tube traverses gave good measurements of velocity. They also found that they could check their readings using a hot-wire anemometer.

(b) Hydrogen Bubbles. Many fluid dynamic investigations require determination of the velocity field over an extended region of space and single-point probe instruments (hot wires, pitot tubes and so on) cannot provide velocity information simultaneously over an extended region without the use of a large number of probes. Even the use of ten hot wires simultaneously is sometimes insufficient to resolve all the details needed in complicated time-dependent flow.

The velocity measurement technique using hydrogen bubbles was described by Schraub et al[32], but was refined for use in friction measurement by A. J. Grass[13]. The technique combines the hydrogen bubble generation and photography and Grass was able to photograph the flow pattern carrying the bubbles 30 mm out from the boundary.

A very high accuracy of velocity measurement can be obtained this way and the analysis of the films is relatively simple and not costly. An explanation of the experimental set up used is given in Chapter III and further detailed analysis in Appendix A.

CHAPTER III

THEORETICAL DESIGN OF NOZZLE OF CONSTANT SHEAR STRESS

3.1. Fully Developed Turbulent Flow

A fully developed turbulent flow may be defined as a flow where the velocity and the pressure at any point perform very irregular fluctuations of high frequency through the mixing of very small parcels of fluid (Dryden, 1939;, Hinze, 1959)[16].

The first mathematical attack on this motion is due to Osborne Reynolds (1895)[27], who separated the instantaneous motion at any point in the turbulent flow into two parts; a mean flow whose components are u, v, w, and a superposed fluctuating flow whose components are u', v', w', the mean values of which are zero. As a result of these fluctuations the fluid exhibits an apparent increase in the resistance to deformation through what is called "apparent shear stresses".

The methods available so far for the calculation of turbulent flows are based on hypotheses aimed at establishing a relationship between these apparent shear stresses and the mean values of the velocity components.

3.1.1. Momentum Transfer Theory

In the kinematic theory of gases as discussed by Roberts (Heat and Thermodynamics, 1933), viscosity is explained as a result of momentum transfer from one layer to another, through the thermal action of molecules. In turbulent fluid motion there is a similar process of transfer, though on a larger scale; the main difference being that the kinematic theory of gases concerns itself with the sub-microscopic motion of molecules, whereas for turbulent flows the concept deals with

microscopic motion of lumps of the fluid particles which results in momentum transfer from one layer of the fluid to another.

Prandtl (1925) in his theory for the transfer of momentum begins by neglecting the viscosity effect on the turbulent process on the basis that the additional turbulent stresses are much greater than those due to viscosity. Consequently the eddying motion as Reynolds showed will be controlled by such apparent shear stresses τ.

$$\tau = -\rho \, u \, v \tag{3.1.}$$

where ρ is the fluid density. If u and v and w = constant $\tau = 0$, but this formula gives τ = constant ($\tau_o \neq 0$).

In developing this concept, Prandtl considered an element of the fluid at a point A where the mean velocity is u as moving across the flow a distance L called "the mixing length" without any change of velocity and consequently without any change of momentum, to another point B where it mixes with the surrounding fluid. Continuity demands that such a mixing process takes place in both directions, and during the process, particles from faster layers of the flow will enter the slower layers accelerating them and vice versa, and the mutual action of this process is such as if friction were present.

If L is small, the velocity at point B will be $\left(u + L \frac{du}{dy}\right)$, where $\frac{du}{dy}$ is the velocity gradient in the direction y normal to the main flow, and consequently the displaced fluid element on arrival at B has a fluctuating velocity component u', equal to $- L \left(\frac{du}{dy}\right)$.

At this stage, to substitute for τ in equation (3.1.) some assumption about v' has to be made, and hence Prandtl assumes that v' may arise from the fact that two elements of the fluid having different velocities and occupying different positions in front of one another

may collide and move sideways from one another much in the manner of solid bodies. Consequently v' equation (3.1.) will vanish where $\frac{du}{dy}$ is equal to zero, i.e. at points of maximum of minimum velocities, and this actually is not the case because the turbulent mixing does not vanish at points of maximum velocities (Fage, 1936; Laufer, 1953; Klebanoff, 1954). To overcome this difficulty, Prandtl (1942) introduced an alternative approximation for τ in the form:

$$\tau = \rho L^2 \left[\left(\frac{du}{dy} \right)^2 + L_1^2 \left(\frac{d^2u}{dy^2} \right)^2 \right]^{\frac{1}{2}} \cdot \left(\frac{du}{dy} \right) \qquad (3.2.)$$

where L_1 is a new length to be determined experimentally. However, this form is inconvenient for analytical purposes, and is of interest only for problems in which equation (3.2.) would fail.

3.1.2. Vorticity Transfer Theory

In his theory for the vorticity transfer, Taylor[36], assumes that each element of the fluid retains the vorticity of the layer from which it parted and not the momentum as supposed in Prandtl's theory. This assumption realises the fact that, in two-dimensional motion, the local differences of pressure do not affect the vorticity of an element, whereas they may affect its momentum. Apart from that, Taylor's theory resembles Prandtl's[26] theory in that an element is supposed to move a distance L before mixing with the surrounding fluid.

For two-dimensional motion, the vorticity of the fluid ε at any point can be expressed as:

$$\varepsilon = \frac{1}{2} \left(\frac{\partial u_1}{dy} - \frac{\partial v_1}{dx} \right) \qquad (3.3.)$$

where u_1 and v_1 are the instantaneous components of the velocity in the

x and y directions respectively, and if the flow is uniform in the x - direction will equal $\frac{1}{2}\frac{du_1}{dy}$ which varies with time.

Neglecting the effect of viscosity, the equation of motion for a two-dimensional flow takes the form:

$$-\frac{1}{\rho}\frac{\partial p}{\partial x} = \frac{\partial u_1}{\partial t} + u_1\frac{\partial u_1}{\partial x} + v_1\frac{\partial v_1}{\partial y} \qquad (3.4.)$$

where $\frac{\partial p_1}{\partial x}$ is the pressure gradient causing the flow.

This equation can be written conveniently as:

$$-\frac{\partial}{\partial x}\left(\frac{P_1}{\rho} + \frac{u_1^2}{2} + \frac{v_1^2}{2}\right) = \frac{\partial u_1}{\partial t} + v_1\left(\frac{\partial u_1}{\partial y} - \frac{\partial v_1}{\partial x}\right)$$

or
$$-\frac{\partial}{\partial x}\left(\frac{P_1}{\rho} + \frac{u_1^2}{2} + \frac{v_1^2}{2}\right) = \frac{\partial u_1}{\partial t} + 2\,v_1\,\varepsilon \qquad (3.5.)$$

When the turbulent motion is uniform in the flow direction, the time mean values of $\frac{\partial u_1}{\partial t}$ and $\frac{\partial}{\partial x}(v_1^2 + u_1^2)$ will equal to zero; on the other hand the temporal averages of $\frac{\partial p_1}{\partial x_1}$ and of $2\,v_1\,.\,\varepsilon$ will be different from zero. Consequently equation (3.5.) takes the form:

$$-\frac{1}{\rho}\frac{\partial \bar{P}}{\partial x} = 2\overline{v\varepsilon} \qquad (3.6.)$$

where the bar denotes the time average values.

Now, an element of the fluid is transferred from one layer to another after travelling a distance L without any change in its vorticity until it mixes with the new layer. This element will possess a vorticity greater by an amount $-L\frac{d}{dy}\left(\frac{1}{2}\frac{d\bar{u}}{dy}\right)$ than that of the layer

with which it mixes. Taking v as the velocity fluctuation v', then:

$$\frac{1}{\rho}\frac{\partial \bar{P}}{\partial x} = \overline{v'L}\left(\frac{d^2\bar{u}}{dy^2}\right) \qquad (3.7.)$$

For uniform flow $\frac{\partial \bar{P}}{\partial x} = \frac{\partial \tau}{\partial y}$ thus:

$$\frac{\partial \tau}{\partial y} = \rho\, v'L\left(\frac{d^2\bar{u}}{dy^2}\right) \qquad (3.8.)$$

which is identical with Prandtl's equation (3.12.), only if $\overline{vL}$ is independent of y.

When the motion is not two-dimensional, the vorticity components are not conserved (Goldstein, pp. 211) and hence they are not transferable, but will change continuously due to the action of the three-dimensional turbulence field. To account for this, Taylor (1932) in his generalised vorticity transfer theory extended the original one to a three-dimensional case of flow, but the new expression became intractable for practical application. To gain simplicity, Taylor[36] modified the generalised theory by assuming that the vorticity remains conserved in a three-dimensional flow, an assumption justified when the turbulence is isotropic.

3.1.3. Von Karman's Similarity Hypothesis (1930)

According to this hypothesis, the turbulent fluctuations are similar at all points in the flow field, and they differ from point to point only by a length scale and a velocity scale. For the velocity scale, Von Karman uses the shear stress velocity V_* and for the length scale he uses the mixing length L due to Prandtl[26].

To establish the dependence of the mixing length on space coordinates, Karman assumed that it is independent of the magnitude of the velocity, and is a function of the velocity distribution only. To define this characteristic length scale, the ratio between the first and second derivatives of the mean velocity was chosen, thus:

$$L = \gamma \frac{\frac{du}{dy}}{\frac{d^2u}{dy^2}} \qquad (3.9.)$$

where γ is a constant to be determined experimentally. A mathematical argument to deduce equation (3.9.) is found in Schlichting's Boundary layer theory, 1955, pp. 392-393.

$$\tau = \rho \gamma \left(\frac{du}{dy}\right)^4 \Big/ \left(\frac{d^2u}{dy^2}\right)^2 \qquad (3.10.)$$

and this equation is clearly invalid in regions where $\frac{d^2u}{dy^2}$ is zero.

3.1.4. Comparison between the Theories

In order to test which of the two theories, the momentum transfer theory and the vorticity transfer theory, is most nearly correct, Fage and Falkner[8] conducted a series of velocity and temperature measurements in the wake behind a heated cylinder. These measurements gave support in this particular case of flow to the vorticity transfer theory, the predicted distributions of velocity and temperature agreeing closely with those obtained by direct measurements.

As indicated by Reynolds[27], the transport of heat by turbulent mixing is similar to the transport of momentum, and therefore the temperature and velocity distributions based on the momentum transfer theory will be similar. On the other hand, Fage (1932) has shown that

the vorticity transfer theory predicts different distributions for the temperature and the velocity. Therefore in flows where the distributions of temperature and velocity are similar, Prandtl's theory will offer a better approximation such as in the case of the flow along plates (Elias, 1929), whereas Taylor's[36] theory will offer a better representation where the distributions of temperature and velocity are not similar such as in the case of flow selected by Face and Falkner[8]. A detailed comparison between the two theories is contained in Goldstein[12].

3.2. Concept of The Boundary Layer

This concept was introduced by Prandtl[26] who showed that the flow near a solid surface can be divided into two regions; a thin region near the wall where the friction forces are of appreciable magnitude (boundary layer), and an outside region where the friction forces are negligible and where the theory of perfect fluids offers an exact solution (potential flow). While there is no sharp limit between these two regions, it is convenient for analytical purposes to assume there is, and that friction effects are wholly restricted to the layer whose thickness is δ.

Due to the retarding effect of the friction forces in the boundary layer, there is an energy gradient across the flow, and this is supposed to vanish outside the layer. The region of the retarded flow becomes thicker with distance in the downstream direction as more and more fluid become affected by the friction at the wall.

The equations of motion for two-dimensional incompressible viscous flow can be written in the form:

$$\frac{\partial u}{\partial t} + u\frac{\partial u}{\partial x} + v\frac{\partial u}{\partial y} = -\frac{1}{\rho}\frac{\partial P}{\partial x} + \left(\frac{\partial^2 u}{\partial x^2} + \frac{\partial^2 u}{\partial y^2}\right) \qquad (3.11.)$$

and

$$\frac{\partial v}{\partial t} + u\frac{\partial v}{\partial x} + v\frac{\partial v}{\partial y} = -\frac{1}{\rho}\frac{\partial P}{\partial y} + \nu\left(\frac{\partial^2 v}{\partial x^2} + \frac{\partial^2 v}{\partial y^2}\right) \qquad (3.11.)$$

where u and v are the mean velocity components in the x and y-directions respectively, P is the static pressure, and ρ and ν are the density and the kinematic viscosity of the fluid respectively. The accompanying equation of continuity is:

$$\frac{\partial u}{\partial x} + \frac{\partial v}{\partial y} = 0$$

Prandtl simplified these equations by dropping the small terms and finally he arrived at the form:

$$u\frac{\partial u}{\partial x} + v\frac{\partial u}{\partial y} = -\frac{1}{\rho}\frac{\partial P}{\partial x} + \nu\frac{\partial^2 u}{\partial y^2} \qquad (3.12.)$$

which together with the continuity equation:

$$\frac{\partial u}{\partial x} + \frac{\partial v}{\partial y} = 0 \qquad (3.13.)$$

and the boundary conditions at $y = 0$, $u = v = 0$ and at $y = \infty$, $u = U$ are suffient to describe the motion.

If we substitute for $\frac{du}{dy}$ by the shear stress τ, then equation (3.12.) can be reduced to:

$$u\frac{\partial u}{\partial x} + v\frac{\partial u}{\partial y} = -\frac{1}{\rho}\frac{\partial P}{\partial x} + \frac{1}{\rho}\frac{\partial \tau}{\partial y} \qquad (3.14.)$$

which is valid for both laminar and turbulent flows.

3.2.1. Boundary Layer, Displacement and Momentum Thicknesses

The definition of δ, the boundary layer thickness is to a certain extent arbitrary, because the velocity of the flow in the boundary layer approaches that of the main stream asymptotically. However it is often an advantage to have some numerical limit and an arbitrary value such as $u = 0.99\ U$ will serve.

To avoid such uncertainties in the definition of the boundary layer thickness, certain mathematical quantities which are more accurately defined are usually used, such as the displacement thickness δ_*, and the momentum thickness θ.

The displacement thickness is defined as:

$$\delta_* = \int_{y=0}^{y=\infty} \left(1 - \frac{u}{U}\right) dy \qquad (3.15.)$$

and it indicates the distance by which the external stream lines are shifted due to the formation of the boundary layer.

The momentum thickness on the other hand is defined by the integral:

$$\theta = \int_{y=0}^{y=\infty} \frac{u}{U}\left(1 - \frac{u}{U}\right) dy \qquad (3.16.)$$

and it is proportional to the loss of momentum in the boundary layer, since $\rho\ U^2\ \theta$ is the difference between the momentum of the mass inside the layer flowing with the potential velocity U, $\rho\ U_o \int_o^\infty u\ dy$ and between the actual momentum $\rho \int_o^\infty u^2\ dy$.

The quantities δ_* and θ have the advantage that they are independent of the upper limit of δ, since a negligible increase is obtained from the integrals when extending the integration beyond the thickness δ into the main stream.

3.2.2. Von Karman's Momentum Equation

The solution of the boundary layer equations (3.12. and 3.13.) for a given flow field is in many cases very difficult and time consuming. Therefore it becomes convenient to possess at least approximate methods of solution where an exact solution of the boundary layer equations cannot be obtained with a reasonable amount of work.

Most of these approximate methods are based on a momentum equation which can be derived from the equation of motion by integration. This momentum equation was introduced by Von Karman[18] and is valid both for laminar and for turbulent flows with or without a pressure gradient.

For a steady incompressible two-dimensional flow, upon integrating the boundary layer equation (3.14.) with respect to y to y = h (greater than δ) then:

$$\int_0^h \left(u \frac{\partial u}{\partial x} - v \frac{\partial u}{\partial y} - U \frac{dU}{dx} \right) dy = - \frac{\tau_o}{\rho}$$

where τ_o is the wall shear stress. Substituting for v the quantity $- \int_0^y \left(\frac{\partial u}{\partial x} \right) dy$ from the continuity equation, then:

$$\int_0^h \left(u \frac{\partial u}{\partial x} - \frac{\partial u}{\partial y} \int_0^y \frac{\partial u}{\partial x} dy - U \frac{dU}{dx} \right) dy = - \frac{\tau_o}{\rho}$$

Integrating by parts we get:

$$\int_0^h \frac{\partial}{\partial x}\,(u(U-u))\;dy + \frac{dU}{dx}\int_0^h (U-u)\;dy = \frac{\tau_o}{\rho} \qquad (3.17.)$$

which is the original form of the momentum equation. Since the values of the integrals in equation (3.17.) do not depend on the limit h as long as it is greater than the boundary layer thickness, h can be given any value short of ∞ provided it exceeds δ.

Now introducing the definitions of the displacement thickness and the momentum thickness (equations 3.15. and 3.16), equation (3.17.) can be reduced to:

$$\frac{\tau_o}{\rho} = \frac{d}{dx}\,(U^2\theta) + \delta_* U \frac{dU}{dx}$$

or

$$\frac{\tau_o}{\rho U^2} = \frac{d\theta}{dx} + \frac{\theta}{U}\frac{dU}{dx}\,(H+2) \qquad (3.18.)$$

where $H = \frac{\delta_*}{\theta}$ = a "shape" factor for the velocity profile. This is the form of the momentum equation given by Gruschwitz (1931).[14]

3.3. Universal Velocity Distribution Law

The velocity distribution in a pipe or a rectangular channel can be obtained from the mixing length hypotheses as follows:

According to Prandtl's momentum transfer theory, the turbulent shear stress τ is expressible as:

$$\tau = \rho L^2 \left(\frac{du}{dy}\right)^2$$

Assuming that τ remains constant with y in the immediate neighbourhood of the wall, then:

$$\tau = \tau_o = \rho L^2 \left(\frac{du}{dy}\right)^2 \qquad (3.19.)$$

At this stage, a statement about the mixing length L has to be made, and for that Prandtl introduces the experimental observation that L is unaffected by viscosity in which case the only length we have at our disposal on which L could depend, is the distance from the wall y. The only dimensionally correct formula for L is therefore:

$$L = \gamma y$$

where γ is a constant.

Substituting into equation (3.19.), we get:

$$\tau_o = \rho \gamma^2 y^2 \left(\frac{du}{dy}\right)^2 \qquad (3.20.)$$

or

$$\frac{du}{dy} = \frac{1}{\gamma}\sqrt{\frac{\tau_o}{\rho}} \cdot \frac{1}{y}$$

on integrating we get:

$$\frac{u}{V_*} = \frac{1}{\gamma} \log y + \text{constant} \qquad (3.21.)$$

where $V_* = \sqrt{\frac{\tau_o}{\rho}}$ = the shear stress velocity.

To evaluate the constant in equation (3.21.) the condition at the wall is used, namely u = 0 at a certain distance y_1 from the wall, thus:

$$\frac{u}{V_*} = \frac{1}{\gamma} (\ln y - \ln y_1)$$

or

$$\frac{u}{V_*} = \frac{1}{\gamma} \ln \frac{y}{y_1} \tag{3.22.}$$

For smooth walls, the viscosity becomes important in the immediate neighbourhood of the wall and therefore Prandtl suggests that:

$$y_1 = \frac{\beta\nu}{V_*}$$

which is dimensionally correct with β as a dimensionless constant. Accordingly equation (3.22.) takes the form:

$$\frac{u}{V_*} = \frac{1}{\gamma} \left[\log \frac{yV_*}{\nu} - \log \beta \right]$$

or

$$\frac{u}{V_*} = A \log \frac{yV_*}{\nu} + B \tag{3.23.}$$

which is called the universal velocity distribution law for smooth pipes with A and B as constants.

In the case of rough walls, to determine y_1, a second length is available here, namely the roughness height k, and the question is now whether the length $\frac{\nu}{V_*}$ is involved or not. The criterion is the ratio of these two lengths $\frac{kV_*}{\nu}$ which may be regarded as a Reynolds number characteristic of the single bump. If $\frac{kV_*}{\nu}$ is sufficiently large, $\frac{\nu}{V_*}$ becomes small in comparison with k and y_1 is taken as a fraction of the roughness height, thus:

$$y_1 = \alpha k$$

where α is a constant depending on the type, shape and arrangement of

the roughness elements. Substituting for y_1 into equation (3.22.), then:

$$\frac{u}{V_*} = \frac{1}{\gamma}\left(\ln\frac{y}{k} - \ln\alpha\right)$$

$$= A \log y/k + B_1 \qquad (3.24.)$$

where A and B_1 are constants. A detailed study of the variation of y_1 with wall conditions is found in a paper by C. M. White and C. F. Colebrook* (1937).

Von Karman's[18] formula for τ in the form:

$$\tau = \rho\,\gamma^2\left(\frac{du}{dy}\right)^4 \Big/ \left(\frac{d^2u}{dy^2}\right)^2 \qquad (3.25.)$$

will have an advantage over Prandtl's formula (equation 3.2.) only if τ proves to be constant with y. To check this we have at our disposal the experimental velocity distributions from the present test. From figures (3.5-3.8), the velocity distribution is logarithmic for most of the boundary layer thickness and as will be shown in Section (3.4.) can be represented by the equation:

$$\frac{u}{V_*} = 5.75 \log \frac{y}{k} + \text{constant}$$

Differentiating and substituting into (3.25.), then:

$$\tau = \rho\,\gamma^2\left(\frac{2.5V_*}{y}\right)^4 \Big/ \left(\frac{2.5\,V_*}{-y^2}\right)^2$$

* "Experiments with Fluid Friction with Roughened Pipes", Proc. Roy. Soc. of London, Ser. A, 161.

or

$$\frac{\tau}{\tau_o} = 6.25\ \gamma^2$$

here γ will remain constant only if $\frac{\tau}{\tau_o}$ does not vary with y, i.e. if $\frac{\partial \tau}{\partial y} = 0$ which actually is not the case, since the equation of motion is reduced to $\frac{\partial \tau}{\partial y} = \frac{\partial P}{\partial x}$ for the boundary layer under test as will be shown in Section (3.4.) and $\frac{\partial P}{\partial x}$ is in fact considerably different from zero.

Had we assumed a linear relationship for τ in the form:

$$\frac{\tau}{\tau_o} = \frac{R - y}{R}$$

where R is the pipe radius, equation (3.25.) can lead to a velocity distribution of the form:

$$\frac{U - u}{V_*} = -\frac{1}{\gamma}\left[\log\left(1 - \sqrt{1 + \frac{y}{R}} + \sqrt{1 - \frac{y}{R}}\right)\right] \qquad (3.26.)$$

which seems less easy than Prandtl's equation (equation 3.22.), and at the same time is in less agreement with the experimental results for pipes (Schlichting[30]), indeed a simple calculation of the value $\frac{U - u}{V_*}$ at, for example, y = 0.5 R, gives:

$$\frac{U - u}{V_*} = 1.298 \text{ according to Von Karman's} \qquad (3.26.)$$

and

$$\frac{U - u}{V_*} = 1.73 \text{ according to Prandtl's} \qquad (3.22.)$$

whereas experimental values of pipes range from 1.68-1.88. In the recent experiments the velocities in the boundary layer gave the following values:

k_{mm}	x/k	$\frac{U-u}{V_*}\ \frac{y}{R} = 0.50$
1.56	320	1.68
1.96	252	1.62
3.16	220	1.70
4.75	123	1.68

So it appears that the simpler form due to Prandtl better represents the facts.

3.4. Nozzle of Constant Drag

3.4.1. Concept of the Nozzle of Constant Drag

The concept of the nozzle of constant drag was originally introduced by C. M. White (1940) in his paper "The Equilibrium of Grains on the Bed of a Stream".* The nozzle was designed such as to ensure a constant shear stress along its bed, through accelerating the main flow nearly exponentially in the downstream direction. The turbulence

* Proceedings of the Royal Society of London, series A, 958, Vol. 174, pp. 322-338, February, 1940.

in this case was restricted to the boundary layer on the rough surface with the grains on the bed as the origin of turbulence, while the flow in the mainstream was steady and laminar.

In the theory, White assumes that the velocity distribution on the rough surface is like that near the wall of a rough pipe, where the longitudinal mean velocity component u may be described by the law:

$$u = 2.5\, V_* \ln \frac{y}{y_1} \qquad (3.27.)$$

where V_* is the shear velocity $= \sqrt{\frac{\tau_o}{\rho}}$ and y_1 is the shift of origin accounts for the turbulent mixing persists even where $u \to o$.

Now equation (3.27.) implies that, for a constant V_* and for values any smaller than the thickness of the boundary layer δ, the stream formation, is independent of x, and hence the stream lines will be parallel to the wall. Consequently there exists a certain discontinuity at the edge of the boundary layer, outside which the stream lines are somewhat inclined before entering the boundary layer, they turn through a small angle (Figure 3.1. p. 45)

Since the pressure increase across the boundary layer is very small or zero the pressure normal to the layer is practically constant, and the pressure inside the layer is determined by the outside flow. Thus from Figure 3.1., for the equilibrium of an element of the boundary layer, we have according to White:

$$\tau_o . x = \int_{y_1}^{\delta} (P - P_2)\, dy \qquad (3.28.)$$

where τ_o is the wall shear stress, and x is the distance from the leading edge of the wall.

Since P is determined by the irrotational motion outside the boundary layer, and since once it has entered the layer, the speed of a stream line remains unchanged, equation (3.28) may be written as:

$$V_*^2 \cdot x = \tfrac{1}{2} \int_{y_1}^{\delta} (U^2 - u^2)\, dy \qquad (3.29.)$$

where U is the velocity of the flow at the edge of the relevant boundary layer.

Substituting χ for $\dfrac{U}{2.5V_*}$ and z for $\dfrac{y}{y_1}$, the two limits z = 1.0 and $z = \dfrac{\delta}{y}$ correspond respectively to ln z = 0 and ln z = χ, and equation (3.29.) is thus reduced to:

$$\frac{x}{y_1} = \frac{6.25}{2} \int_{1}^{\chi} (\chi^2 - \ln^2 z)\, dz$$

or

$$\frac{x}{6.25y_1} = e^{\chi}(\chi - 1) - \frac{\chi^2}{2} + 1 \qquad (3.30.)$$

which is the general equation for the nozzle of constant drag.

To substitute for y, White (1940) used the value $y = \dfrac{k}{9}$ given by Schlichting (1936) for loosely packed spherical particles 1.50 diameters apart, since it more nearly represented the test conditions better than the value $y = \dfrac{k}{33}$ corresponding to Nikuradse's closely packed grains cemented to the wall of a pipe. Therefore equation (3.30.) takes the form:

$$1.5\, x/k = e^{\chi}(\chi - 1) - \frac{\chi^2}{2} + 1 \qquad (3.31.)$$

where k represents the mean diameter of the grains.

Strictly speaking, equation (3.31.) implies that each size of the sand requires a different nozzle, but the differences are small, and in erosion experiments when a nozzle is used with an inappropriate size of sand, the error is compensated by the bed adjusting itself in a slightly curved form.

To measure the average drag along the bed, White used a suspended metal strip mounted on a micrometer bar by two fine short cotton threads. The strip in this case was coated with sand grains similar in size and shape to those of the bed, and a travelling microscope was used to measure the displacement of the strip which has been related to the bed shear stress. On measuring the shear stress at $\frac{x}{k} = 45$, the hanging strip after allowing for the form drag, gave 19% greater drag than that predicted from theory.

3.5. Further Details of the Theory for Nozzle of Constant Drag

3.5.1. Boundary Layer Growth

Consider an element dx a distance x from the leading edge of the plate. The steady two-dimensional boundary will probably increase in thickness from δ at D to $\delta + \Delta\delta$. Assuming that the fluid motion near the surface of the plate is similar to that near the wall of a rough pipe according to Prandtl the velocity distribution within the boundary layer can be assumed to be $2.5\ V_* \log \frac{y}{y_1}$ (3.27.) where y_1 is a constant

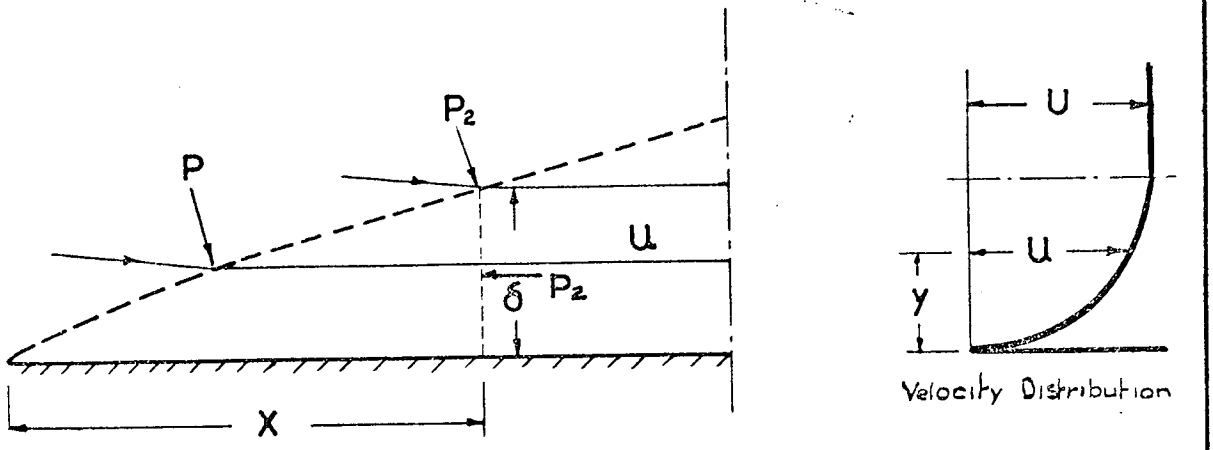

Boundary Layer near Rough Wall with Constant Drag after C.M. White (Vertical scale Exaggerated)

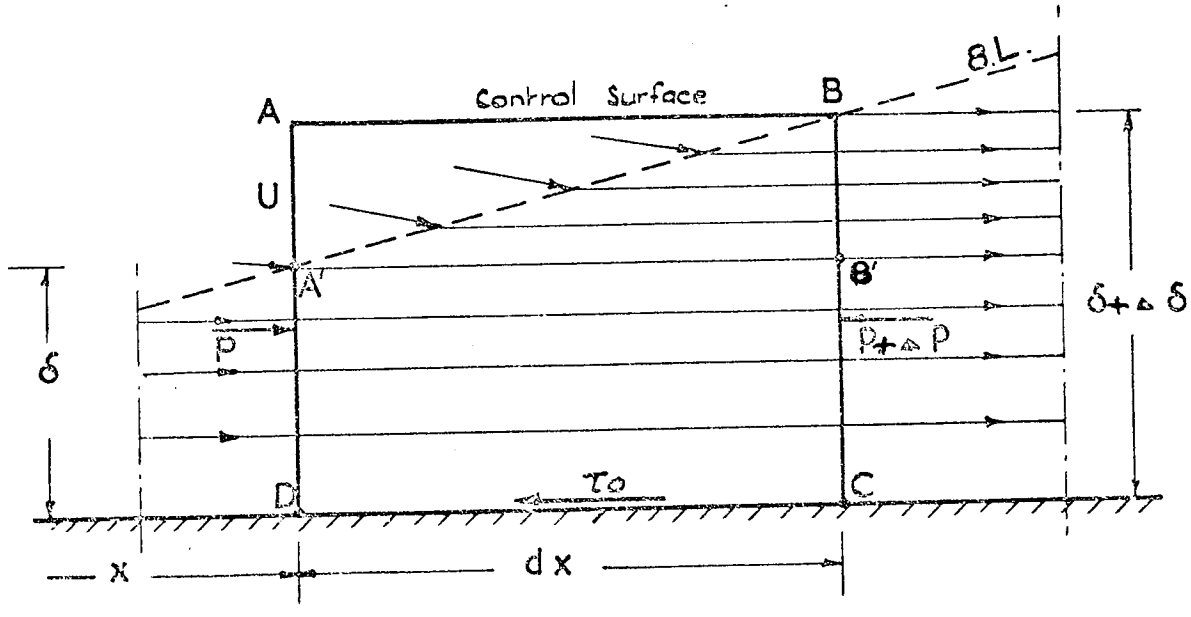

Modified Theory for Nozzle with Constant Drag.

Fig 3.1

and takes into account turbulent mixing which persists among the grains even when $u \to 0$. For constant wall shear stress V_* is a constant therefore u is a function of y only when $y = \delta$. This implies the stream function is independent of x. Therefore the stream lines are parallel to the plate.

The fluid motion within the control surface will be as shown in Figure 3.1. Using the Momentum Theorem for the control surface ABCD the rate of change of momentum flux must be equal to the externally applied forces

Flux of fluid leaving BC

$$dx\left[\frac{\partial}{\partial x}\int_{y_1}^{\partial} \rho u dy\right] + \int_{y_1}^{\partial} \rho u dy$$

Change in flux between A'D and BC

$$= dx\left[\frac{\partial}{\partial x}\int_{y_1}^{\partial} \rho u dy\right]$$

Since u is independent of x

$\therefore$ Flux across A'D = Flux across B'C

$\therefore$ Change in Flux = Fl across BB'

= Fl across AA' and AB

Flux across $AA' = \rho U (\Delta\delta)$

Flux across AB = Flux across BB' - Flux across AA'

$$= dx\left[\frac{\partial}{\partial x}\int_{y_1}^{\partial} \rho u dy\right] - \rho U (\Delta\delta)$$

Consider the change in momentum in the x direction for the control surface ABCD.

There is no change in momentum in the x direction between A'D and B'C. Within this control surface ABCD the change in momentum takes places through the surfaces AA', AB, and BB'. Therefore rate of change of momentum in x direction is equal to momentum across BB' - momentum across AA' - momentum across AB.

$$\text{Rate of change across BB'} = dx\left[\frac{\partial}{\partial x}\int_{y_1}^{\delta} \rho u^2 dy\right]$$

$$\text{Flux of momentum across AA'} = \rho U^2 \quad (\Delta\delta)$$

$$\text{Flux of momentum across AB} = U\left\{dx\left[\frac{\delta}{\delta x}\int_{y_1}^{\delta} \rho.udy\right] - \rho U\ (\Delta\delta)\right\}$$

$$= \left[U\ dx\ \frac{\partial}{\partial x}\int_{y_1}^{\delta} \rho udy - \rho U^2\ (\Delta\delta)\right]$$

Rate of change of momentum = force in x direction.

$$P\left[\delta + (\Delta\delta)\right] - \left(P + \frac{\partial p}{\partial x}dx\right)\left[\delta + (\Delta\delta)\right] - \tau_o\, dx$$

$$= dx\left[\frac{\partial}{\partial x}\int_{y_1}^{\delta} \rho u^2 dy\right] - \rho U^2\ (\Delta\delta) - Udx\left[\frac{\partial}{\partial x}\int_{y_1}^{\delta} \rho udy\right] - \rho U^2\ (\Delta\delta)$$

Simplifying and neglecting second order terms

$$-\frac{\partial P}{\partial x}\,.\,dx\,\delta - \tau_o\,dx = dx\left[\frac{\partial}{\partial x}\int_{y_1}^{\delta}\rho u^2\,dy\right] - \rho U^2\,(\Delta\delta)$$

$$-\left[Udx\left[\frac{\partial}{\partial x}\int_{y_1}^{\delta}\rho u\,dy\right] - \rho U^2\,(\Delta\delta)\right]$$

$$-\frac{\partial P}{\partial x}\,.\,dx\,\delta - \tau_o\,dx - dx\left[\frac{\partial}{\partial x}\int_{y_1}^{\delta}\rho u^2\,dy\right] + \rho U^2\,(\Delta\delta)$$

$$+\,Udx\left[\frac{\partial}{\partial x}\int_{y_1}^{\delta}\rho u\,dy\right] - \rho U^2\,(\Delta\delta) = 0$$

$$-\frac{\partial P}{\partial x}\,\delta - \tau_o - \frac{\partial}{\partial x}\int_{y_1}^{\delta}\rho u^2\,dy + U\,\frac{\partial}{\partial x}\int_{y_1}^{\delta}\rho u\,dy = 0$$

(3.32.)

Using Bernoulli's equation for mainstream flow

$$P + \tfrac{1}{2}\rho U^2 = \text{Constant}$$

$$\frac{\partial P}{\partial x} = -\rho U\,\frac{dU}{dx}$$

Substituting in above:

$$+ \rho U \delta \cdot \frac{dU}{dx} - \tau_o - \frac{\partial}{\partial x} \int_{y_1}^{\delta} \rho u^2 dy + U \frac{\partial}{\partial x} \int_{y_1}^{\delta} \rho u dy = 0 \qquad (3.33.)$$

Substituting for u from (3.27.) as $2.5 V_* \log \frac{y}{y_1}$ in (3.33.)

dividing throughout by ρ

$$\delta U \frac{dU}{dx} - \frac{\tau_o}{\rho} - \frac{\partial}{\partial x} \int_{y_1}^{\delta} (2.5V_*)^2 \ln^2 \frac{y}{y_1} dy$$

$$+ U \frac{\partial}{\partial x} \int_{y_1}^{\delta} 2.5V_* \ln \frac{y}{y_1} dy = 0 \qquad (3.34.)$$

Using White's transformation

$$\chi = \frac{U}{2.5V_*}, \quad Z = \frac{y}{y_1}$$

Substituting these in equation (3.27.) for the boundary condition

$y = \delta$, $u = U$

$$\delta = y_1 e^{\chi}$$

The limits of integration are now

$$Z = 1 \quad \text{and} \quad Z = \frac{\delta}{y_1} e^{\chi}$$

The equation (3.28.) reduces to

$$2.5V_* \, y_1 \, \chi e^{\chi} \frac{dU}{dx} - V_*^2 - 6.25V_*^2 \cdot y_1 \frac{\partial}{\partial x} \int_1^{\chi} \ln^2 Z \, dZ$$

$$+ 6.25V_*^2 \, \chi \, y_1 \cdot \frac{\partial}{\partial x} \int_1^{e^{\chi}} \ln Z \, dZ = 0$$

(3.35.)

Since V_* is independent of x the above is true.

Dividing through by $6.25 \, y_1$ and $\frac{dU}{dx} = 2.5V_* \frac{d\chi}{dx}$

i.e. $$V_*^2 \, \chi e^{\chi} \frac{d\chi}{dx} - \frac{V_*^2}{6.25 \, y_1} - V_* \frac{\partial}{\partial x} \int_1^{e^{\chi}} \ln^2 Z \, dZ$$

$$+ V_*^2 \, \chi \frac{\partial}{\partial x} \int_1^{e^{\chi}} \ln Z \, dZ = 0$$

This reduces to

$$\chi \, e_1 \frac{d\chi}{dx} - \frac{1}{6.25 \, y_1} - \frac{\partial}{\partial x} \int_1^{e^{\chi}} \ln^2 Z \, dZ + \chi \frac{\partial}{\partial x} \int_1^{e^{\chi}} \ln Z \, dZ = 0$$

(3.36.)

Integrating and substituting between the limits $Z = 1$ and $Z = e^{\chi}$, then:

$$- \frac{1}{6.25y} - \frac{\partial}{\partial x} (\chi^2 e^{\chi} - 2\chi e^{\chi} + 2e^{\chi} - 2) + \chi \frac{\delta}{\delta \chi} (\chi e^{\chi} - e^{\chi} + 1 \cdot \frac{d}{dx} = 0$$

on differentiating we get:

$$-\frac{1}{6.25y_1} - (\chi^2 e^{\chi} + 2\chi e^{\chi} - 2\chi e^{\chi} - 2e^{\chi} + 2e^{\chi})\frac{d\chi}{dx} + 2e\frac{d\chi}{dx} = 0$$

or

$$\frac{1}{6.25y_1} dx = (\chi^2 e^{\chi} - \chi e^{\chi}\chi d\chi)$$

By integrating this equation then:

$$\frac{x}{6.25y_1} = \chi^2 e^{\chi} - 3\chi e^{\chi} + 3e^{\chi} - \frac{\chi^2}{2} + e$$

at $x = 0$, $y = 0$ and hence $e = -3$, thus:

$$\frac{x}{6.25y_1} = \chi^2 e^{\chi} - 3\chi e^{\chi} + 3e^{\chi} \frac{\alpha^2}{2} \qquad (3.37.)$$

Substituting χ for $\frac{U}{2.5V_*}$ and Z for $\frac{y}{y_1}$, then $\delta = y\, e^{\chi}$ and the two limits $Z = 1$ and $Z = \frac{\delta}{y_1}$ correspond respectively to $\ln Z = 0$ and $\ln Z = \chi$, and thus equation (3.35.) is transformed to:

$$-V_*^2 - 6.25\frac{\delta}{\delta x}\int_1^{e^{\chi}} V_*^2 \ln^2 Z\, dZ + 6.25\, V_* \chi \cdot y_1 \cdot \frac{\delta}{\delta x}\int_1^{e^{\chi}} V_* \ln Z\, dZ$$

$$+ 2.5\, V_* y_1 e^{\chi}\frac{dU}{dx} = 0 \qquad (3.38.)$$

Since V_* is independent of x, then:

$$-\frac{V_*}{6.25\, y_1} - V_*^2\frac{\delta}{\delta x}\int_1^{e^{\chi}} \ln^2 Z\, dZ + \chi \cdot V_*^2\frac{\delta}{x}\int_1^{e^{\chi}} \ln Z\, dZ + V_*^2 \chi e^{\chi}\frac{d\chi}{dx} = 0$$

or

$$-\frac{1}{6.25\ y_1} - \frac{\delta}{\delta x}\int_1^{e^\chi} \ln^2 Z\, dZ + \chi \frac{\delta}{\delta x}\int_1^{e^\chi} \ln Z\, dZ + \chi e^\chi \frac{d\chi}{dx} = 0 \qquad (3.39.)$$

Integrating and substituting between the limits $Z = 1$ and $Z = e^\chi$, then:

$$-\frac{1}{6.25y_1} - \frac{\partial}{\partial x}(\chi^2 e^\chi - 2\chi e^\chi + 2e^\chi - 2) + \chi \frac{\delta}{\delta \chi}(\chi e^\chi - e^\chi + 1 \cdot \frac{d}{dx} = 0 \qquad (3.40.)$$

on differentiating we get:

$$-\frac{1}{6.25y_1} - (\chi^2 e^\chi + 2\chi e^\chi - 2\chi e^\chi - 2e^\chi + 2e^\chi)\frac{d\chi}{dx} + 2e^\chi \frac{d\chi}{dx} = 0$$

or

$$\frac{1}{6.25y_1} dx = (\chi^2 e^\chi - \chi e^\chi \chi d\chi) \qquad (3.41.)$$

By integrating this equation then:

$$\frac{x}{6.25y_1} = \chi^2 e^\chi - 3\chi e^\chi + 3e^\chi - \frac{\chi^2}{2} + c \qquad (3.42.)$$

at $x = 0$, $y = 0$ and hence $e = -3$, thus:

$$\frac{x}{6.25y_1} = \chi^2 e^\chi - 3\chi e^\chi + 3e^\chi \frac{\alpha^2}{2} \qquad (3.43.)$$

which takes into account the discontinuity of the stream on entering the boundary layer, and differs from the previous approximate formula (3.30.) by the small amount $\frac{\chi^2}{2}$.

For rough walls $\frac{V_* K}{\nu} > 60$ y_1 can be substituted by dk, where d is a fraction of the roughness height, depending on the type, shape and arrangement of the roughness and consequently equation (3.43) can be reduced to:

$$c \frac{x}{k} = e^{\chi} (\chi - 1) + 1 \qquad (3.44)$$

where c is a constant, which takes into account the discontinuity of the stream on entering the boundary layer, and differs from the previous approximate formula (3.36) by the small amount $\frac{\chi^2}{2}$.

For smooth walls on the other hand, equation (3.43) is still valid, and according to White and Colebrook (1937), y_1 can be substituted by $0.10 \frac{\nu}{V_*}$ and equation (3.43), then takes the form:

$$\frac{x}{0,625} \frac{\nu}{V_*} = e^{\chi} (\chi - 1) + 1 \qquad (3.45)$$

CHAPTER IV

APPARATUS

From the theory analysed in the previous Chapters II and III it can be seen that the proof of the theory depends on constant momentum along the flume and therefore velocity had to be measured very accurately at each of the points where pressure readings are to be taken. In the preliminary tests, photographic methods using Telcon particles was used but this method was later abandoned in favour of the Hydrogen Bubble technique. The change to this system was due to the fact that White's theory holds for two planes only and it was impossible to ensure this using a still camera.

The general layout of the preliminary apparatus is shown in Plate 5. The flume in this apparatus consisted of three parts, the smooth curved surface, the rough straight surface and the smooth sides.

The correct shape of the curve was important in this investigation, and special care was directed in its construction. The theoretical curve was calculated using White's theory on the calculation of the drag coefficient for various diameters of particle as given in the table below.

Table IV-1

$\frac{x}{k}$	χ	$\frac{\tau}{\rho U_*^2}$
5	2.07	0.037
10	2.43	0.027
20	2.82	0.020
50	3.45	0.0134
100	3.95	0.0102
300	4.76	0.0071

For each value of k, particle size, a new curve had to be designed and constructed. The point of entry is taken as the origin for the co-ordinates of x and y.

Table IV-2

Co-ordinates for Curves

x	y	y	y	y	y
	k = 3 mm	k = 2 mm	k = 1.5 mm	k = 1 mm	k = 0.5 mm
5	111.0	74.0	55.5	37.0	18.5
10	81.0	54.0	40.5	27.0	13.5
20	60.0	40.0	30.0	20.0	10.0
50	40.2	26.8	20.1	13.4	6.7
100	30.6	20.4	15.3	10.2	5.1
300	21.3	14.2	10.7	7.1	3.6
1000	14.7	9.8	7.4	4.9	2.5

After obtaining the co-ordinates of the curve, the curve was plotted full size on a template of cardboard which was used in cutting two symmetrical sides of perspex (1,100 × 920 × 12 mm) which were fixed together by spacers placed at convenient distances to form a supporting frame for the curve. A thin sheet of perspex 3 mm thick and 150 mm wide was fixed to this supporting frame thus forming a smooth clean boundary free from kinks and irregularities. This curve was extended at the upstream end tangent to the critical curve to avoid disturbing flow at entry. The supply tank was also supplied with a carefully designed bellmouthed entry to ensure undisturbed conditions at entry to the flume. The curve was provided with five sets of pressure tappings and five openings for total head measurement.

Two millimetre bore stainless steel hypodermic needle tubing was used both for the total head tubes and for the pressure tubes. The total head tubes were carefully bent at right angles so that their openings faced the line of flow. As it was essential to use fine diameter tubing so as not to disturb the flow, and also it was imperative not to collapse the walls of tube so they were gently heated before bending them at right angles. Specially made brass glands were fitted into previously threaded holes in the bottom and top of the channel, to ensure a water tight fit. Fine diameter stainless steel tubing was placed in the openings in the glands between the roof and the base and thus could act as anode when connected to the hydrogen bubble generator. A strip of brass 10 mm wide bent into a U shape was screwed into the end of the flume near the exist, acting as a cathode when connected to the hydrogen bubble generator.

From Plate 5 of the preliminary apparatus it can be seen that a mercury vapour lamp was used for lighting. This lamp flashed at 50 cycles per second thus giving a flash of light every 1/100th of a second. The light beam was passed through a condenser and series of focussing lenses before it was turned at right angles to cover a spot in the centre of the flume. From one side of the flume the camera, a 2¼ × 2¼ reflex Practisix was focussed through a telephoto lens held by a Novoflex extension tube at this spot in the centre. A millimetre grid made out of perspex was projected by a low wattage lamp through a series of lenses to the centre of the flume.

Sieved through a 1/10 mm opening sieve, small particles of white Telcon plastic, which has a specific gravity close to that of water were now fed through a plastic tube into the flume entry. An electrical stirrer kept the plastic particles agitated in the water as otherwise they were inclined to float on the surface of the feeding jar. As the particles move through the light beam across the millimetre grid they were

photographed and their velocities calculated. As Plate 6 shows the particles form a white tadpole shape on the print and the distance they have moved in 1/100th second is the distance from the front to the rear of this tadpole shape. By enlarging the negative to a known enlargement, with reference to the millimetre grid it is possible to calculate exactly the velocity of the particle. Focussing is very difficult and it is never possible to tell which particle one has focussed on and in which plane it is moving.

In the initial series of experiments pressure tappings were made in the wall of the flume and both the static pressure and the total head pressure were recorded on a single tube swivel arm manometer (made in Berlin by R. Fuess) with alcohol as metering fluid. (Plate 7.) The arm of the manometer could be set in any of five different inclinations having factors of 0.80, 0.40, 0.20, 0.10 or 0.05 to give the equivalent height of the vertical column of water in each case (based on 0.80 specific gravity for alcohol), the reading being the difference between the atmospheric pressure and the measured pressure in millimetres. The manometers were levelled frequently during the readings and the time average values for the pressures were recorded. This type of manometer has an advantage over a multi-tube manometer in eliminating errors resulting from slightly different inclinations of the individual tubes in the multi-tube case. The air lock in the polythene tubing attaching the manometers to the tapping points was found impossible to remove and no consistency could be found in the readings.

Due, therefore, to the difficulty of focussing on a particle moving only in one plane and also to the impossibility of obtaining consistent manometer readings, it was decided to give up this type of experimental procedure and proceed with an improved one using the hydrogen bubble technique.

The apparatus used in this type of experimental set up is shown in Plate 4. Due to the fact that electrolysis is being used to generate bubbles from stainless steel tubing of fine diameter it is necessary to improve the conductivity of the water by adding a reagent of sodium trichlorate. To maintain the conductivity of the water it is essential to make it a self contained system. This was done by using immersible pumps in the catcher tank and recirculating it to the feed tank. The three pumps were of Unit 5 construction, one being a 1 cubic metre per minute capacity and the other two being each of 2 cubic metre per minute capacity. At the low velocities only the smaller capacity pump was used whilst for high velocity test runs all pumps were switched on. (Plate 8.)

The velocity of the water was controlled not only by the regulation of the pumps but was also controlled by a valve fitted to the exhaust pipe at the end of the flume. By this dual control system tests could be carried out at a greater number of different values of velocity.

To facilitate the reading of pressure two banks of five open ended inclined manometers was constructed,(Plate 9.) The fact that they were open to the atmosphere eliminated air bubbles and allowed accurate pressure readings to be taken. Great care had to be taken in the reading of these manometers and it is essential to read from the same position as optical misalignment can cause distortion of readings.

When at the beginning of a test run the flow had been regulated to its required setting a period of time was allowed to elapse to ensure that it had reached steady conditions. After this condition of settled flow had been reached the two banks of inclined manometers were read. One bank giving the readings of static head whilst the other bank was connected to the velocity head tubes. When these readings had been recorded the hydrogen bubble generator was switched on and the bubbles began to "come off" the wire at the first measuring

position. The bubbles were allowed to discharge for some time to ensure an ample supply and when it appeared that optimum conditions had been reached the floodlight was carefully positioned to give the best background light for the bubbles. The bubbles given off the wire form a U shape which is the velocity profile and the movement of this profile is now filmed by a 16 mm Beaulieu movie camera.

The electrical supply which leads to the electrolysis of the stainless steel wire to give hydrogen bubbles is now transferred to the second position which is allowed to generate bubbles for about five minutes to ensure the profile is fully visible. The movie camera is now focussed for filming and about 3 metres of film are taken at the speed of 25 frames/sec. The process of moving the cathode to positions three, four and five is then carried out in consecutive steps and in each position about 3 metres of film are shot. When all five positions have been filmed the manometer levels are once more read, with the bubble generator switched off, to ensure that the readings are steady. The bubble generator is switched off as a precaution to ensure no hydrogen bubbles should enter the tubes connecting the manometers to the static and velocity head tappings.

The valve setting is now altered to give a different flow rate and after a reasonable time has elapsed, the manometer readings are again recorded. The hydrogen bubble generator is switched on and the filming procedure at the five measuring points is again repeated. Thus it can be seen that for a 100 foot movie film two series of velocity profiles for two different velocities can be recorded.

The developed film was then fed in an analysing projector and projected onto a wooden screen to which was pinned a millimetre grid graph paper. When the film had been properly focussed the path of one of the bubbles was traced for 25 frames, this being the film speed per second. A push lever allowed the film to be advanced one frame at

a time. In most cases the definition of each bubble was quite clear but in some cases it was difficult to follow their paths for a great distance. It was decided therefore to prevent any opportunity of interference of bubble velocity from the downstream station to plot only five frames, thus giving the distance travelled in 1/5th second.

From these plots on graph paper not only can the exact velocity of various bubbles in the profile be calculated but also the lift of the bubble can be measured. The theoretical analysis of this 'lift' of a hydrogen bubble is given in an ensuing chapter and it can be seen that this effect can be neglected.

The velocity profile for each position was thus drawn for various velocities and various bed materials. (Shown in Plates 2-3). As we now have a record of the velocity profile for each position at various flows it is possible by integration to calculate the momentum at these points. Momentum is directly proportional to the square of the velocity multiplied by a constant mass and as momentum is proportional to shear stress. Thus by integrating the velocity curve we can derive the momentum curve and if the momentum at all sections is constant then it is fair to state that the shear stress at each point is constant.

To obtain the results mentioned above and recorded on graphs shown in the following chapter (Appendix C) are a series of tests which had to be carried out using a variety of curves to suit the different bed material. It was decided to start off the test run using large and uniform bed material so applying White's theory the ordinates for a curve where k = 3 were plotted (shown in Table IV-2) on a piece of stiff cardboard which was used as a template for the base of the vertical walls. These walls were made of 12 mm thick perspex and 2 mm thick perspex bent to the shape of the curve was glued to the base using Special Tensol 132 Perspex cement.

To ensure uniformity of size of bed material 3 mm diameter glass spheres were used (Plate 10) and to ensure both ample cover over the base and also that they should not be carried down the exhaust pipe a 20 mm high perspex stop was fixed to the base of the channel. The pumps were then switched on and the water flow regulated by means of the valve. After the desired volume of flow had been obtained the water was allowed to flow for some time to ensure that the air pockets between the glass spheres had been eliminated and also to ensure that there were no small air bubbles on the perspex walls of the flume. The static head tubes were then primed by sucking out any air pockets and to ensure as little surface tension effect as possible, a drop of alcohol was run down the wall of each manometer tube. Everything was now ready for the pressure readings to be taken and the hydrogen bubble generator to be switched on as described earlier in the chapter.

To ensure sufficient illumination for the bubbles a 2 KW flood-light was used and its position was changed after the filming of each velocity profile at each position so that it gave the best illumination which occurred about 1.50 m from the profile being photographed. The photographs were taken against a black background to ensure extra sharpness. To facilitate the plotting of the paths of the separate bubbles in the U shaped profile (Plates 2-3) a negative process was used. This meant the bubbles appeared as black dots on the graph paper screen and were thus plotted with greater ease than if they had been positively printed resulting in white dots.

After the successful completion of this test the bed material was removed and replaced by 2 mm diameter glass spheres. This naturally meant redesigning and reconstructing the curve for the flume as k was now equal to 2 mm. (Plate 11.) The same procedure for constructing this curve was used as in the k = 3 mm curve.

On the completion of this test run the bed material was changed to 1 mm diameter glass spheres (Plate 12) and with the curve again changed the test procedure was repeated. Then natural bed material of 3 mm (Plate 13), 2 mm (Plate 14) and ½ mm diameter (Plate 15) were used for completing test runs.

CHAPTER V

CONCLUSIONS

5.1. Conclusions

The Theory derived in Chapter III shows that if the Momentum is constant the Total Force must be constant.

5.1.1. Total Force

The total force acting on the fluid body is the sum of the pressure force and the friction force. From the design of the flume we have ensured a constant pressure force therefore if the total force is constant then the friction force must also be constant.

5.1.2. Experimental Results

From the experimental results shown in Tables 1-9 of this Chapter we can see from column 3 that the rate of static pressure drop is constant. From the integration of the Velocity Profiles we arrive at the Momentum Curves and these have a constant value. It can therefore be concluded, that, as the rate of static pressure drop is constant and as also the value of momentum is constant, the shear stress is constant.

5.1.3. Preston Tube Results

From the theory enlarged upon in Appendix B, it can be concluded that if the difference of Static Head and Preston Tube readings is a constant then the shear stress is constant. The results obtained in column 5 of Tables 1-9 are of a constant value, and the shear stress has therefore been proven by two independent means to be constant.

5.1.4. Conclusions from Design

The theory on which the design of the nozzle is based gives a constant momentum because

(a) the rate of pressure drop along it is constant;

(b) the velocity is accelerated in such a manner that the momentum remains constant.

Therefore it is fair to assume that the design of this nozzle gives values of Shear Stress which are constant.

5.2. Graphical Results

5.2.1. Results from Graphs of Plot of Particle Reynolds Number against Bed Shear Stress

A series of graphs of particle Reynolds Number against Bed Shear Stress were plotted for a few values of velocity and Bed Shear Stress for each particle size. From the graphs shown in Appendix B it can be seen that there is a linear relationship between the Particle Reynolds Number and the Bed Shear Stress, but that in some cases at high velocity values, i.e. at high values of Reynolds Number, there is a drop-off in the curve. Similar results were obtained in tests on Flat Plates at the Göttingen Institute.

Owing to the experimental set up there were limits to the value to which the velocity could be increased; but it is a fair assumption that the shear stress can only increase linearly until a critical value of particle Reynolds Number is reached.

5.3. Bed Movement Due to Constant Shear

It seems a logical assumption that if the shear stress along the whole bed is constant then bed load movement would commence at all points along the bed at the same instant. To test this surmise it was proposed to film bed load movement, and a wide angle close up lens was fitted to the Beaulieu movie camera. Flow was started and filming commenced and gradually the velocity of flow was increased whilst filming was in progress. At a certain critical value of velocity instantaneous movement of bed load started and this was recorded on the movie film.

As the enlargement of 16 mm movie film to full plate size is nearly impossible it was decided to repeat the test using two motorised $2\frac{1}{4} \times 2\frac{1}{4}$ Hasselblad Reflex cameras fitted with close up lenses.

Plate 16 shows the flume just before motion was due to start whilst Plate 17 shows motion having started all along the bed of the flume. As Plate 17 was taken from approximately one metre range, so as to show the whole length of the flume, and therefore does not show the motion in great detail it was decided at the same time to take a more detailed view from closer range. The result of this close up photography is Plate 18 which shows distinctly the surface particles in motion.

Having thus proven that movement starts instantaneously along the bed when the shear stress is constant, another test with a different curve, not appropriate to the 1 mm diameter bed material, used in the test, was run. Again there was instantaneous bed load movement all along the bed of the flume.

5.3.1. Critical Shear Stress

Shields[34] proposed that bed load movement occurred when the value of the bed shear stress reached a critical value. If this theory is true then Plates 16 and 17 prove this. As there was no constancy of bed shear stress when the curve was changed it may be assumed that critical shear stress is not the only criterion for bed load movement.

TABLE OF RESULTS

Table 1

½ mm Diameter Sand

	Area under Velocity Curve mm^2	Area Under Momentum Curve mm^2	Static Tube Reading mm	Preston Tube Reading mm	Difference mm
1.	3,500	5,400	143	133	10
2.	3,550	5,480	145	136	9
3.	3,300	5,280	142	132	10
4.	2,750	5,400	143	133	10
5.	3,100	5,450	143	134	9
1.	3,910	5,510	133	130	3
2.	3,700	5,510	133	130	3
3.	3,250	5,710	133	129	4
4.	3,500	5,650	134	130	4
5.	3,300	6,150	134	130	4
1.	4,550	5,550	136	132	4
2.	4,570	5,520	137	133	4
3.	4,250	5,800	133	129	4
4.	4,410	5,380	134	130	4
5.	4,350	5,750	132	128	4
1.	3,000	7,280	133	127	6
2.	3,000	7,800	132	126	6
3.	2,850	7,450	133	127	6
4.	2,950	7,750	133	126	7
5.	3,070	7,850	134	128	6
1.	3,450	5,120	127	120	7
2.	3,350	5,240	128	121	7
3.	3,200	5,100	129	122	7
4.	3,100	5,180	129	121	8
5.	3,150	5,250	129	122	7
1.	3,450	5,100	144	135	9
2.	3,460	5,350	146	136	10
3.	3,250	5,020	144	134	10
4.	3,050	5,290	145	135	10
5.	3,120	5,380	144	135	9
1.	4,240	7,150	140	135	5
2.	4,150	7,180	141	136	5
3.	4,050	7,050	136	131	5
4.	4,300	6,950	137	132	5
5.	3,850	7,000	137	133	4

	Area under Velocity Curve mm^2	Area under Momentum Curve mm^2	Static Tube Reading mm	Preston Tube Reading mm	Difference mm
1.	4,020	6,400	136	132	4
2.	4,050	6,420	137	134	3
3.	4,000	6,500	133	129	4
4.	3,800	6,430	134	131	3
5.	3,850	6,550	132	129	3

Table 2

1 mm Diameter Glass Sphere

	Area under Velocity Curve mm^2	Area under Momentum Curve mm^2	Static Tube Reading mm	Preston Tube Reading mm	Difference mm
1.	8,440	16,840	123	116	7
2.	8,510	16,500	123	116	7
3.	8,680	16,100	125	118	7
4.	8,250	15,900	125	118	7
5.	8,350	16,250	125	118	7
1.	8,100	14,700	123	115	8
2.	7,900	14,710	123	115	8
3.	8,100	14,000	125	115	10
4.	8,200	12,400	125	117	8
5.	8,100	12,400	124	117	7
1.	6,830	11,690	123	116	7
2.	6,500	11,560	123	116	7
3.	6,600	12,400	125	117	8
4.	6,700	11,760	125	117	8
5.	6,800	11,640	124	117	7
1.	6,150	8,140	122	115	7
2.	6,080	8,400	122	115	7
3.	5,950	8,980	124	115	9
4.	5,850	8,450	124	116	8
5.	5,950	8,400	123	116	7
1.	3,910	8,040	129	121	8
2.	3,750	7,150	129	121	8
3.	3,850	7,850	132	123	9
4.	3,710	8,000	132	124	8
5.	3,550	7,700	131	123	8
1.	5,760	8,140	131	122	9
2.	5,540	8,460	131	122	9
3.	5,610	8,050	133	123	10
4.	5,550	8,420	133	123	10
5.	5,550	8,550	132	123	9

Table 3

1 mm Diameter Sand

	Area under Velocity Curve mm^2	Area under Momentum Curve mm^2	Static Tube Reading mm	Preston Tube Reading mm	Difference mm
1.	5,720	6,650	129	121	8
2.	5,310	6,850	129	121	8
3.	5,120	7,380	132	123	9
4.	5,110	7,180	132	123	9
5.	5,450	7,310	131	122	9
1.	5,510	9,650	131	122	9
2.	5,380	9,700	131	122	9
3.	5,400	9,700	133	123	10
4.	5,590	9,950	133	124	9
5.	5,450	9,810	132	123	9
1.	7,100	14,200	133	124	9
2.	7,050	14,310	133	124	9
3.	7,200	14,400	135	125	10
4.	7,020	14,390	135	126	9
5.	6,950	14,280	135	126	9
1.	4,200	8,000	125	121	4
2.	3,600	7,550	125	121	4
3.	3,600	7,880	126	121	5
4.	4,000	7,000	127	123	4
5.	3,800	6,900	127	124	3
1.	5,720	6,850	129	125	4
2.	5,450	6,930	129	124	5
3.	5,150	7,280	130	125	5
4.	5,100	7,180	130	125	5
5.	5,200	7,310	130	125	5
1.	5,410	6,650	129	125	4
2.	5,500	6,850	131	127	4
3.	5,350	7,380	132	128	4
4.	5,250	7,180	132	128	4
5.	5,300	7,310	132	127	5
1.	6,490	8,140	126	116	10
2.	6,380	8,460	127	116	9
3.	6,950	8,050	128	119	9
4.	5,900	8,420	128	118	10
5.	6,050	8,550	128	118	10

	Area under Velocity Curve mm^2	Area under Momentum Curve mm^2	Static Tube Reading mm	Preston Tube Reading mm	Difference mm
1.	6,100	8,140	131	128	3
2.	6,100	8,400	132	129	3
3.	6,160	8,480	134	131	3
4.	6,000	7,850	135	132	3
5.	5,850	8,480	134	131	3

Table 4

1½ mm Diameter Sand

	Area under Velocity Curve mm^2	Area under Momentum Curve mm^2	Static Tube Reading mm	Preston Tube Reading mm	Difference mm
1.	6,650	9,700	123	116	7
2.	6,600	9,250	123	116	7
3.	6,100	9,180	124	117	7
4.	6,100	9,200	125	117	8
5.	5,900	9,100	124	117	7
1.	8,520	18,800	139	131	8
2.	8,500	18,500	136	128	8
3.	8,800	19,000	139	131	8
4.	8,700	18,500	136	128	8
5.	7,800	17,700	137	130	7
1.	5,650	10,980	129	128	1
2.	5,630	11,350	129	127	2
3.	5,950	11,050	128	127	1
4.	5,380	10,500	128	127	1
5.	5,360	10,750	130	129	1
1.	8,350	16,700	128	126	2
2.	8,850	16,300	128	126	2
3.	8,700	16,550	129	126	3
4.	8,250	15,500	129	128	1
5.	8,400	16,500	130	128	2
1.	6,740	7,620	123	116	7
2.	6,800	7,500	123	116	8
3.	6,200	7,300	124	116	8
4.	6,400	7,500	125	118	7
5.	6,550	7,450	125	118	7
1.	3,500	9,200	129	123	6
2.	3,300	9,500	131	125	6
3.	3,500	9,800	132	125	7
4.	3,700	10,000	132	126	6
5.	4,000	10,200	132	126	6
1.	6,300	9,000	123	116	7
2.	6,200	8,900	123	116	7
3.	6,320	8,850	124	116	8
4.	6,100	8,700	125	117	8
5.	5,950	9,200	124	117	7

	Area under Velocity Curve mm^2	Area under Momentum Curve mm^2	Static Tube Reading mm	Preston Tube Reading mm	Difference mm
1.	3,740	11,500	131	122	9
2.	3,750	11,600	131	122	9
3.	3,600	11,500	132	123	9
4.	3,900	11,000	133	124	9
5.	3,950	12,000	132	123	9
1.	8,200	14,800	127	118	9
2.	7,400	15,100	127	118	9
3.	8,310	15,200	128	118	10
4.	7,200	15,000	128	119	9
5.	7,600	14,500	128	118	10
1.	3,720	11,750	125	121	4
2.	3,750	11,000	125	121	4
3.	3,650	11,000	126	121	5
4.	3,800	12,000	126	121	5
5.	3,750	11,900	125	121	4
1.	4,160	7,850	129	121	8
2.	4,900	8,400	129	121	8
3.	4,500	8,400	130	121	9
4.	4,500	8,600	131	122	9
5.	4,400	8,500	131	122	9
1.	4,690	6,650	139	131	8
2.	4,550	6,900	136	128	8
3.	4,500	6,820	136	128	8
4.	4,500	7,100	139	131	8
5.	4,600	7,300	137	128	9
1.	3,350	9,800	129	125	4
2.	3,420	9,900	129	124	5
3.	3,400	9,800	130	125	5
4.	3,400	10,000	131	126	5
5.	3,450	10,900	132	127	5

Table 5

1⅓ mm Diameter Glass Spheres

	Area under Velocity Curve mm^2	Area under Momentum Curve mm^2	Static Tube Reading mm	Preston Tube Reading mm	Difference mm
1.	6,220	12,200	148	138	10
2.	6,400	13,000	147	137	10
3.	6,350	12,400	147	137	10
4.	6,300	12,200	147	136	11
5.	6,100	11,800	145	135	10
1.	6,960	15,100	154	140	14
2.	6,940	15,200	152	138	14
3.	6,740	14,800	151	136	15
4.	6,840	14,600	150	137	13
5.	6,900	14,900	147	133	14
1.	5,310	12,700	144	135	9
2.	5,210	12,200	142	133	9
3.	5,110	11,000	142	132	10
4.	6,520	11,600	140	131	9
5.	5,240	11,520	140	131	9
1.	6,500	13,100	135	128	7
2.	6,320	13,900	133	126	7
3.	6,200	13,600	132	124	6
4.	6,240	13,240	131	124	7
5.	6,310	12,800	131	123	8
1.	6,840	13,880	139	134	5
2.	6,920	13,420	137	132	5
3.	6,860	13,800	135	130	5
4.	6,460	13,460	135	130	5
5.	6,500	12,900	134	129	5
1.	5,150	15,670	145	141	4
2.	5,100	15,600	142	139	3
3.	5,210	14,900	141	138	3
4.	5,100	15,000	138	134	4
5.	5,050	15,080	138	134	4
1.	7,450	18,100	135	130	5
2.	7,600	18,460	133	128	5
3.	7,220	16,200	130	126	4
4.	7,200	17,300	130	126	4
5.	7,250	16,800	130	125	5

	Area under Velocity Curve mm^2	Area under Momentum Curve mm^2	Static Tube Reading mm	Preston Tube Reading mm	Difference mm
1.	7,480	16,370	151	142	9
2.	8,000	16,400	140	132	8
3.	8,050	16,200	140	132	8
4.	7,800	15,550	140	132	8
5.	7,650	15,800	138	131	7
1.	7,190	13,370	132	127	5
2.	7,290	13,500	130	125	5
3.	7,310	13,300	127	121	6
4.	7,200	12,800	130	124	6
5.	6,600	12,600	128	124	4
1.	9,500	16,720	150	146	4
2.	9,700	17,100	149	146	3
3.	9,450	16,550	150	146	4
4.	9,150	15,950	150	146	4
5.	8,850	14,780	149	144	5
1.	6,660	15,200	145	140	5
2.	6,550	15,000	141	137	4
3.	6,500	15,000	141	137	4
4.	6,600	14,850	141	137	4
5.	6,200	14,600	141	136	5
1.	7,520	15,800	135	133	2
2.	7,150	15,000	135	132	3
3.	7,200	14,800	135	133	2
4.	7,400	14,950	136	134	2
5.	7,200	14,900	135	132	3

Table 6

2 mm Diameter Glass Spheres

	Area under Velocity Curve mm^2	Area under Momentum Curve mm^2	Static Tube Reading mm	Preston Tube Reading mm	Difference mm
1.	8,810	11,620	134	126	8
2.	8,620	11,890	131	124	7
3.	8,900	11,790	132	124	8
4.	8,650	11,960	134	125	9
5.	8,970	12,100	132	124	8
1.	6,910	15,360	148	140	8
2.	7,450	15,610	148	140	8
3.	6,840	15,210	147	139	8
4.	6,810	15,610	147	139	8
5.	6,450	15,690	146	138	8
1.	6,610	13,400	148	132	6
2.	6,450	13,500	146	131	5
3.	6,410	13,310	147	131	6
4.	6,410	13,300	147	131	6
5.	6,110	13,620	145	129	6
1.	6,050	11,300	149	133	16
2.	6,000	11,550	147	132	15
3.	5,980	11,750	147	132	15
4.	5,855	11,700	147	131	16
5.	6,185	11,680	146	130	16
1.	6,980	15,200	149	146	3
2.	6,990	15,500	147	144	3
3.	6,950	15,580	146	143	3
4.	6,780	15,380	146	142	4
5.	6,550	15,820	145	141	4
1.	5,710	11,850	146	144	2
2.	5,750	12,050	144	142	2
3.	5,830	12,210	143	141	2
4.	5,650	12,320	143	141	2
5.	5,720	12,200	142	140	2

Table 7

2 mm Diameter Sand

	Area under Velocity Curve mm^2	Area under Momentum Curve mm^2	Static Tube Reading mm	Preston Tube Reading mm	Difference mm
1.	4,620	10,360	147	139	8
2.	4,420	10,600	148	139	9
3.	4,350	10,750	147	139	8
4.	4,280	10,480	147	139	8
5.	4,300	10,710	146	138	8
1.	6,230	11,850	144	134	10
2.	6,180	12,050	144	134	10
3.	5,990	12,200	145	135	10
4.	5,950	13,320	144	133	11
5.	5,900	12,200	144	133	11
1.	5,810	11,300	143	132	11
2.	5,820	11,550	143	132	11
3.	5,900	11,800	143	133	10
4.	5,850	11,750	143	132	11
5.	5,780	11,700	140	129	11
1.	7,000	15,360	147	133	14
2.	7,000	14,500	147	133	14
3.	6,900	15,210	148	133	15
4.	7,100	15,600	147	134	13
5.	7,050	15,690	147	133	14
1.	8,400	11,620	139	134	5
2.	8,450	11,890	140	135	5
3.	8,450	11,790	141	136	5
4.	8,550	11,960	141	135	6
5.	8,480	12,000	140	135	5
1.	6,650	14,200	132	128	4
2.	6,510	14,310	132	128	4
3.	6,550	14,400	133	128	5
4.	6,490	14,390	133	129	4
5.	6,660	14,280	131	126	5
1.	6,550	13,400	125	122	3
2.	6,620	13,500	126	122	4
3.	6,560	13,300	126	122	4
4.	6,350	13,330	125	121	4
5.	6,480	13,620	124	120	4

	Area under Velocity Curve mm^2	Area under Momentum Curve mm^2	Static Tube Reading mm	Preston Tube Reading mm	Difference mm
1.	6,680	15,200	134	132	2
2.	6,780	15,500	135	133	2
3.	6,900	15,580	136	134	2
4.	6,800	15,380	135	133	2
5.	6,900	15,820	134	132	2
1.	5,350	9,650	128	124	4
2.	5,350	9,700	128	124	4
3.	5,330	9,700	129	125	4
4.	5,380	9,800	129	125	4
5.	5,380	9,810	128	124	4
1.	5,800	15,200	137	126	11
2.	6,900	15,500	135	124	11
3.	6,780	15,580	135	124	11
4.	6,880	15,380	138	127	11
5.	6,900	15,820	136	126	10

Table 8

3 mm Diameter Glass Spheres

	Area under Velocity Curve mm^2	Area under Momentum Curve mm^2	Static Tube Reading mm	Preston Tube Reading mm	Difference mm
1.	6,900	10,400	133	127	6
2.	6,000	9,700	134	128	6
3.	6,400	10,100	134	128	6
4.	6,200	10,100	134	127	7
5.	6,600	11,000	133	126	7
1.	10,920	14,750	132	129	3
2.	9,860	14,200	133	129	4
3.	10,700	15,600	135	131	4
4.	9,720	15,000	135	131	4
5.	10,000	14,900	134	130	4
1.	10,300	13,960	131	123	8
2.	9,800	13,300	132	124	8
3.	10,200	13,600	134	125	9
4.	9,700	14,100	133	124	9
5.	10,170	14,200	133	124	9
1.	10,500	14,650	132	125	7
2.	10,000	14,500	133	126	7
3.	10,000	14,950	135	127	8
4.	10,320	15,000	134	126	8
5.	9,850	15,000	135	127	8
1.	10,100	14,430	135	130	5
2.	10,500	14,100	134	129	5
3.	10,400	14,500	136	131	5
4.	10,300	14,100	136	131	5
5.	10,200	14,950	135	129	6
1.	6,630	16,470	127	122	5
2.	5,740	16,900	128	122	6
3.	5,570	17,400	129	123	6
4.	5,570	17,200	128	122	6
5.	6,050	17,400	129	123	6

Table 9

3 mm Diameter Sand

	Area under Velocity Curve mm^2	Area under Momentum Curve mm^2	Static Tube Reading mm	Preston Tube Reading mm	Difference mm
1.	6,410	16,800	127	123	4
2.	6,000	15,900	128	124	4
3.	5,900	17,100	129	125	4
4.	6,200	17,200	131	126	5
5.	6,250	17,100	130	126	4
1.	4,780	16,800	155	135	20
2.	4,760	17,100	153	132	21
3.	4,650	17,200	149	129	20
4.	4,550	17,800	150	130	20
5.	4,720	17,800	144	125	19
1.	6,300	14,500	139	131	8
2.	6,100	14,300	136	128	8
3.	6,300	14,700	139	131	8
4.	6,250	14,700	136	128	8
5.	6,250	14,700	137	130	7
1.	6,140	12,700	153	149	4
2.	6,000	12,900	151	147	4
3.	5,950	12,900	150	146	4
4.	5,850	12,900	151	146	5
5.	5,950	12,700	148	144	4
1.	5,640	11,400	148	138	10
2.	5,720	11,800	147	137	10
3.	5,800	11,600	147	136	11
4.	5,550	11,800	147	137	10
5.	5,750	12,000	145	135	10
1.	6,330	9,620	129	126	3
2.	5,650	9,370	129	125	4
3.	5,850	9,640	128	124	4
4.	5,930	9,850	128	124	4
5.	6,150	10,650	127	123	4
1.	6,410	9,800	130	124	6
2.	6,000	8,850	131	125	6
3.	6,000	8,950	132	126	6
4.	6,100	9,900	132	126	6
5.	6,510	9,950	132	126	6

	Area under Velocity Curve mm^2	Area under Momentum Curve mm^2	Static Tube Reading mm	Preston Tube Reading mm	Difference mm
1.	7,620	11,300	133	126	7
2.	7,250	11,600	134	127	7
3.	6,800	10,900	135	128	7
4.	7,100	11,900	134	127	7
5.	7,200	12,100	134	126	8
1.	6,120	14,350	154	140	14
2.	6,200	14,300	152	138	14
3.	6,180	14,700	151	136	15
4.	6,160	14,700	150	137	13
5.	6,190	14,700	147	133	14

APPENDIX A

HYDROGEN BUBBLE TECHNIQUE

A.1. Probe Manufacture and Operation

Bubble Formation

The power supply and controls needed are simple. Standard electrical circuits, timers and switch gear suffice. A complete hydrogen bubble generating set made by Armfield Hydraulic Engineering Company was used in these tests.

Voltage required is a function of electrolyte concentration, the distance between electrodes and geometry. It is best to supply a variable working - voltage supply from about 10-250 volts. To avoid undue operating hazard it is usually possible to limit voltage to less than 100 volts by the use of sufficient electrolyte. Usually in hard water no added electrolyte is needed. In softer waters, sodium sulphate has been found a satisfactory additive; its solubility is high, it forms many ions and its corrosion and toxicity are acceptable in most systems. About 0.15 g/l of Na_2SO_4 has been sufficient in most cases. Other electrolytes may work as well or better.

The d.c. voltage applied between the probe and some other location in the flow establishes an electrostatic field in the water.

The material used to make bubble - generation wire is not critical except with respect to corrosion, cost and frangibility: platinum, copper and stainless steel wire have all been used successfully. The stainless steel wires, used here, are stronger and easier to handle. Platinum is usually preferred because it does not corrode, and it appears to collect dirt less rapidly. Wires are usually best cleaned of dirt by squirting a small jet from a syringe (or other convenient tool) upstream of the wire.

The most difficult operating problem is control of "bubble quality". Large currents are needed to obtain sufficient optical density of the bubbles for good photography over appreciable distances. Under these conditions it is difficult to eliminate all over sized bubbles; some large bubbles are almost always formed and rise too acutely to give accurate traces. Since these are few in number they can be ignored in finding velocity patterns; they represent a very small flow disturbance based on total volume of generated bubbles and observed rise rates.

The bulk of the bubbles have diameters of the order of one half to one wire diameter 0.005 to 0.05 mm dia. Much more troublesome than the few larger bubbles is the lack of repeatability of bubble formation under apparently constant conditions. Most wires require "aging" under operating conditions for a few minutes before they will produce bubbles uniformly. Some wires produce more uniform and smaller bubbles than others for no known reason. Some water supplies give better, that is small and more uniform, bubbles than others. Sometimes a wire which has worked satisfactorily begins erratic bubble formation for no apparent reason. When this occurs, reversing the polarity on the wire for a few minutes, then returning to normal polarity and aging the wire anew, will often solve the difficulty. Standard probe cleaning methods, do not appear to improve these matters much. These problems of bubble control are not unsurmountable but make the technique somewhat "finicky". All these problems are related to the apparently complex combination of surface electro-chemistry and hydrodynamic actions that control the bubble formation and release from the wire. Full understanding of these effects would require extensive separate researches and, to date, it has been more expedient to deal with these problems on a purely empirical basis.

Since hydrogen is soluble in water, the bubbles generated at the wire rapidly dissolve; this has both advantages and disadvantages. The primary advantage is that no "return circuit interference" occurs in closed circuit flows. The disadvantage is that the bubble half-life is very short, a rough guide from experience of the bubbles used is a half-life of the order of three seconds.

A.2. Lighting

The production of acceptable light levels is strongly dependent on the angle of the incident light on the bubbles with respect to the line of sight of the camera or viewer. For best results this angle should be approximately 65 degrees. A sharply collimated sheet of light produced by two slots in series is usually best in order to prevent strong light scattering in the water. Dark backgrounds are necessary and in this experiment a black-board was used. Very strong light sources are necessary and in this case 2 KW flood lighting was employed.

A.3. Terminal Rise Rate

The terminal rise rate may be approximated by using Stokes' solution for solid spheres since the Reynolds numbers based on bubble diameter are less than one (see for example Lamb (1945)). The result is

$$\bar{v}_T = \frac{1}{18} \frac{\rho_{H_2O} - \rho_{H_2}}{\mu_{H_2O}} g d^2$$

For example, for bubbles of 0.02 mm diameter in water with kinetic viscosity of 1.2×10^{-6} m^2 sec^{-1} $= \nu = \frac{\mu}{\rho}$.

$$\bar{u} = 0.035 \text{ mm/s}$$

and the rise rate Reynolds number $= \frac{\bar{u}d}{\nu} = 0.058 << 1.0$ which is adequately low for use in Stokes' equation. Errors introduced by such low terminal velocity are usually small even though the estimate of d, the bubble diameter, is conservatively large.

A.4. Bubble Rise Rate Uncertainty

The terminal velocity for the use of the bubble of 0.02 mm diameter was given as 0.035 mm/s. However, if no velocity gradient exists the maximum rise rate should be 1/50th of the mean velocity. Thus with bubble sizes normally found mean speeds down to 18 mm/s can be measured without undue distortion due to bubble rise.

A.5. Velocity Defect Bubble Generating Wire

The disturbance to the overall flow pattern because of the existence of the bubble-generating wires is small. However, the local disturbance in the viscous wake of an infinite cylinder of the same diameter as the generating wires is not negligible. The velocity behind the wire is less than the free stream velocity value owing to the momentum losses associated with the drag on the wire. This velocity defect may be approximated closely in the Reynolds number range ($R_{e_d} = 1 \rightarrow 5$) by the asymptotic laminar-wake solution for an infinite cylinder. The solution of the boundary layer equation is obtained by assuming the wake profile to be similar at all downstream stations which are sufficiently removed from the wire. The solution in terms of the similarity parameter

$$\zeta = y\left(\frac{U_\infty}{\nu x}\right)^{\frac{1}{2}}$$

is given by Schlichting[30]. Hot wire data taken behind a 2 mm dia. generating wire which is not generating bubbles shows general agreement with the laminar wake solution. The defect is not negligible; even at 200 diameter downstream from the wire the centre line wake velocity is only 91 per cent of the free stream velocity.

The velocity defect, however, is markedly reduced when hydrogen bubbles are being generated from the wire. The bubble velocity reaches the free stream velocity in 70 wire diameters in test carried out by Schraub et al[32].

Precautions in Experimental Procedure

In all cases of the present experiments the messurements were taken beyond stations which were at least 150 diameters (76 mm) behind the wire. Wherever possible this critical distance was increased to 250 diameters and the working range of the distance was from 150 d. (or 250 d.) to 1000 d. In addition to this precaution, the 0.75 mm anode was kept in a position downstream of the cathode wire in all the cases. Hence even if there was an error due to the velocity defect behind the wire it would have been uniform in all the measurements.

APPENDIX B

DETERMINATION OF SKIN FRICTION WITH PRESTON TUBES

B.1. Theoretical Analysis

Ludwieg and Tillmann[23] have presented evidence which suggests that

$$\frac{u}{U_*} = f\left(\frac{U_* y}{\nu}\right) \qquad (1b)$$

is true in a limited region near the surface independent of pressure gradient and upstream disturbances. If this is so, then it seems likely that conditions in this region are functions only of the physical properties of the fluid ρ and ν, τ_o and a suitable length. If a total head tube placed on the wall measures a pressure p, the velocity u at this depth $\frac{d}{2}$ can be expressed by

$$u = \sqrt{\frac{(p - p_o)}{\rho}}$$

where p_o is the static pressure at this point.

R.H.S. of equation (1b) then becomes

$$\frac{u}{U_*} = \sqrt{\frac{p - p_o}{\rho}} \cdot \frac{1}{\sqrt{\frac{\tau_o}{\rho}}} = \sqrt{\frac{p - p_o}{\tau_o}} \qquad (2b)$$

L.H.S. of equation (1b)

$$\frac{U_* y}{\nu} = \frac{U_* d}{2\nu} \quad \text{and} \quad y = \frac{d}{2}$$

$$\frac{U_* y}{\nu} = \frac{1}{2}\sqrt{\frac{\tau_o}{\rho}} \cdot \frac{d^2}{\nu} \qquad (3b)$$

$\frac{\tau_o d^2}{\rho\nu^2}$ is dimensionless therefore τ_o can be looked upon as having dimensions of $\frac{\rho\nu^2}{d^2}$, i.e.

$$\left[\tau_o\right] \equiv \left[\frac{\rho\nu^2}{d^2}\right] \qquad (4b)$$

Substituting (4b) in (2b)

$$\frac{p - p_o}{\tau_o} = \frac{(p - p_o)}{\nu^2} d^2 \qquad (5b)$$

So equation (1b) can be expressed using equations (3b) and (5b), i.e.

$$\left(\frac{p - p_o}{\nu^2}\right) d^2 = \phi \frac{\tau_o d^2}{\rho\nu^2}$$

This is equation (5b) OR from 1b, 2b & 3b $\sqrt{\frac{p-p_o}{\tau_o}} = f\left\{\frac{1}{2}\sqrt{\frac{\tau_o}{\rho}}\,\frac{d}{\nu}\right\}$

$$\tau_o = \phi\,(p - p_o) \qquad (6b)$$

B.2. Description of Apparatus

As the theoretical derivation given in the preceding paragraph is based on Preston's[25] experimental work it is therefore necessary to use instrumentation of the same order as he used.

B.2.1. Pitot Tubes

The geometrically similar circular pitot tubes were chosen to have as nearly as possible a ratio of internal to external diameter of 0.600. This was done because not only did Preston[25] use this ratio but Young and Mass[39] have determined the displacement of the effective

centre, for conditions which are equivalent to those obtaining in a boundary layer several pitot diameters from the wall, and for this ratio of internal to external diameter.

Secondly, the large sizes of hypodermic tubing in stock have approximately this ratio. Thirdly, this type of tube is very robust - any thinner would be difficult to machine and liable to damage. Great care was taken in bending the tube and getting rid of burrs.

B.2.2. Manometers

Two banks of sensitive open ended water manometers were connected so as to read $(p_1 - p_2)$ and $(p - p_o)$ respectively. Readings of $(p - p_o)$ against $(p_1 - p_2)$ were then taken for all five pitots, the speed of flow in the flume being varied from the lowest to the highest and an accuracy of about one per cent can be expected at the lower range.

B.3. Conclusions

(a) A simple and accurate method has been developed by Preston[25] for deducing the skin friction from the readings of geometrically similar round pitot tubes located on the surface.

(b) In the development of this method it has been established that there is a region near the wall of the order of 1/10th of the boundary layer thickness in which conditions depend only on τ_o, ρ, ν and a suitable length.

REFERENCES

(1) Blasius, H., Grenzschichten in Flüssigkeiten mit kleiner, Reibung, Z. Math. u Phys. 56, 1 (1908).

(2) Brown, K. C. and Joubert, P. N., The Measurement of Turbulent Boundary Layers with Adverse Pressure Gradients, Journal of Fluid Mechs., Vol. 35, (1969).

(3) Clauser, F. H., Turbulent Boundary Layers in Adverse Pressure Gradients, Journal of Aero. Sciences, February (1954).

(4) Coles, D., Measurement in the Boundary Layer on a Smooth Flat Plate, Ph.D. Thesis, California Institute of Technology, (1963).

(5) Dhawan S., Direct Measurement of Skin Friction, Report 1121, California Institute of Technology, (1962).

(6) Durand W. F., Aerodynamic Theory, Vol. III, Div. G. L. Prandtl - The Mechanics of Viscous Fluids, (1938).

(7) Einstein, H. A. and Li, H., The Viscous sub-layer along a Smooth Boundary, A.S.C.E. Proc., 82, (1956).

(8) Fage, A and Falkner, V. M., Proc. Roy. Soc., A. 129, (1930).

(9) Falkner, V. M., A New Law for Calculating Drag, Douglas Aircraft, Engineering Vol. XV, No. 169, (1943).

(10) Falkner, V. M. and Skan, S. W., Some Approximate Solutions of the boundary layer equation, Phil. Mag 12, 865 (1936).

(11) Ferrari, C., "Wall Turbulence", N.A.C.A. Republication, ER-2-8-59 W, (1959).

(12) Goldstein, S., ed. Modern Developments in Fluid Dynamics, Clarendon Press (Oxford), (1938).

(13) Grass, A. J., Turbulent Flow over Smooth and Rough Boundaries, Journal of Fluid Mechs., Vol. 8, (1969).

(14) Gruschwitz, E., The Turbulent Boundary Layer in Plane Flow with Pressure Rise and Pressure Fall, Ing.-Arch. 2, 821, (1931).

(15) Hakkinen, R. J., Skin Friction Measurements at High Velocities, N.A.C.A. T.N. 3486, (1955).

(16) Hinze, J. O., Turbulence, McGraw-Hill Book Co. Inc. (New York), (1959).

(17) Kemf, S. G., Neue Ergebnisse der Widerstandsformschung, Werft, Reederei, Hafen, Vol. 10, (1929).

(18) Karman von Theodore, Progress in the Statistical Theory of Turbulence, Proc. Nat. Acad. Sci., Vol. 34, No. 11, (1948), also Laminare und Turbulente Reibung, N.A.C.A. T.N., 1092, (1946).

(19) Klebanoff, P. S., Characteristics of Turbulence in a Boundary Layer with Zero Pressure Gradient, N.A.C.A. Rept. 1247, (1955).

(20) Klebanoff, P. S. and Diehl, Z. W., Some Features of Artificially Thickened Fully Developed Turbulent Boundary Layers with Zero Pressure Gradient, N.A.C.A. Report 110, (1951).

(21) Laufer, J., The Structure of Turbulence in a Two-Dimensional Channel, N.A.C.A. Report 1033, (1954).

(22) Ludwieg, H., Instrument for Measuring the Wall Shearing Stress of Turbulent Boundary Layers, N.A.C.A. T.N., 1284, (1950).

(23) Ludwieg, H. and Tillmann, W., Investigations of the Wall Shearing Stress in Turbulent Boundary Layers, N.A.C.A. T.N. 1285, (1950).

(24) Polhausen, K., Zur näherungsweisen Integration der Differential Gleichung der Grenzschicht, ZAMM1, 252, (1921).

(25) Preston, J. H., The Determination of Turbulent Skin Friction by Means of Pitot Tubes, Journal of Roy. Aero. Soc., February (1954).

(26) Prandtl, L., Recent Results of Turbulence Research, N.A.C.A. T.M. 720, (1933).

(27) Reynolds, O., Phil. Trans. Roy. Soc., (London), (1883).

(28) Sandborn, V. A. and Braun, W. H., Turbulent Shear Spectra and Local Isotropy in the Lay Speed Boundary Layer, N.A.C.A. T.M. 3761, (1956).

(29) Sandborn, V. A. and Slogan, R. J., Study of the Momentum Distribution of Turbulent Boundary Layers in Adverse Pressure Gradients, N.A.C.A. T.M. 3264, (1953).

(30) Schliching, H., Boundary Layer Theory, McGraw-Hill Book Co. Inc., New York, (1960).

(31) Schubauer, G. B. and Klebanoff, P. S., Investigations of Separation of the Turbulent Boundary Layer, N.A.C.A. Report 1030, (1950).

(32) Schraub, F. A., Kline, S. J., Henry J. and Rundstatler, P., Use of Hydrogen Bubbles for Quantiative Determination of Time Dependent Velocity Fields in Low Speed Water Flows, Journal of Basic Engineering, June, (1965).

(33) Schultz-Grunow, F., New Frictional Reistance Law for Smooth Plates, N.A.C.A. T.M. 986, (1953).

(34) Shields, A., Applications of Similarity Principles and Turbulence Research to Bed Load Movement. Translated from German. California Institute of Technology, (1936).

(35) Smith, D. and Walker, J., Skin Friction Measurements in Incompressible Flow, N.A.C.A. T.M. 4231, (1957).

(36) Taylor, C. I., Statistical Theory of Turbulence, Part 1, Proc. Roy. Soc. (London) Ser. A, Vol. 151, No. 873, September, (1935).

(37) Townsend, A. A., The Structure of Turbulent Shear Flow, Cambridge University Press, (1956).

(38) White, C. M., The Equilibrium of a Grain on the Bed of a Stream, Proc. Roy. Soc. (London) Ser. A. Vol. 174, February, (1940).

(39) Young, A. D. and Mass, J. N., The Behaviour of the Pitot Tube in a Transverse Total Pressure Gradient, R.A.E., R and M, 1770 (1937).

Pages 103 missing

Missing page(s) from the bound copy

APPENDIX C

VELOCITY PROFILE AND MOMENTUM CURVES

3 mm Diameter Glass Spheres

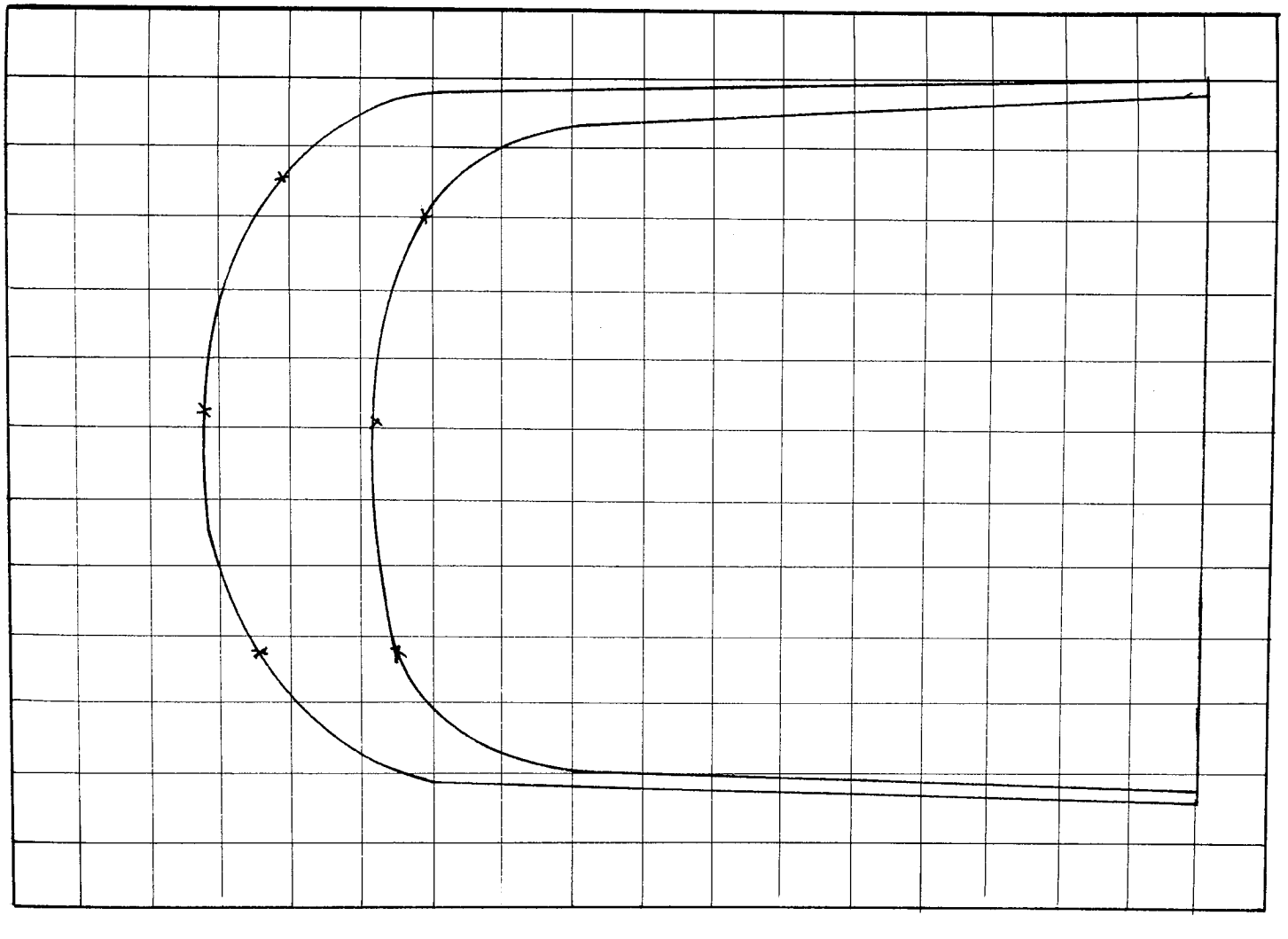

POSITION 1 Scales: Velocity: 1 mm = $\frac{1}{5}$ mm/s Area under Velocity Curve = 10,920 mm^2

Momentum: 1 mm^2 = $\frac{1}{25}$ kgmm/s Area under Momentum Curve = 14,750 mm^2

BED MATERIAL: 3 mm Diameter Glass Spheres

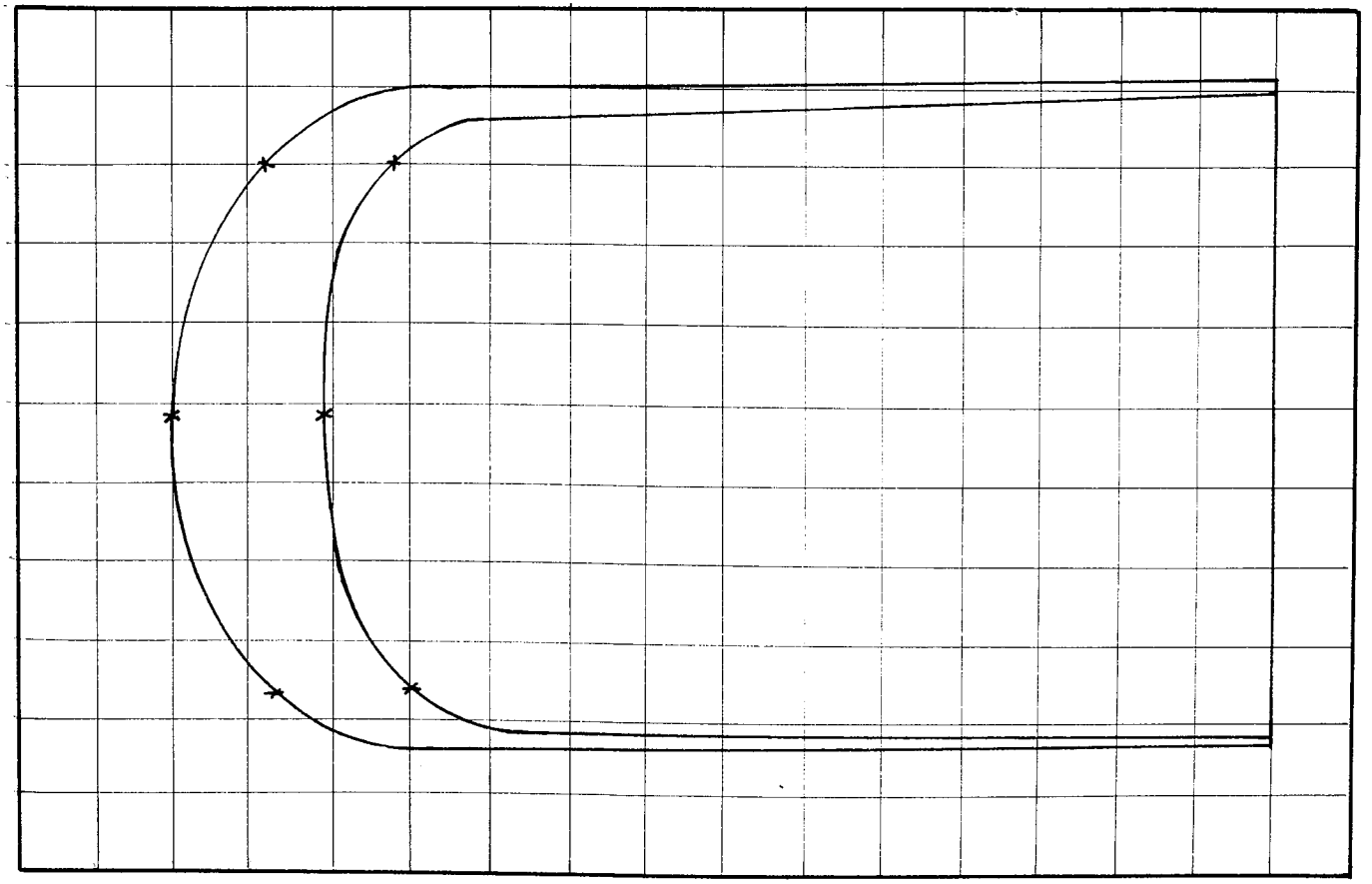

POSITION 2 Scales: Velocity: 1 mm = $\frac{1}{5}$ mm/s Area under Velocity Curve = 9,860 mm^2

Momentum: 1 mm^2 = $\frac{1}{25}$ kgmm/s Area under Momentum Curve = 14,200 mm^2

BED MATERIAL: 3 mm Diameter Glass Spheres

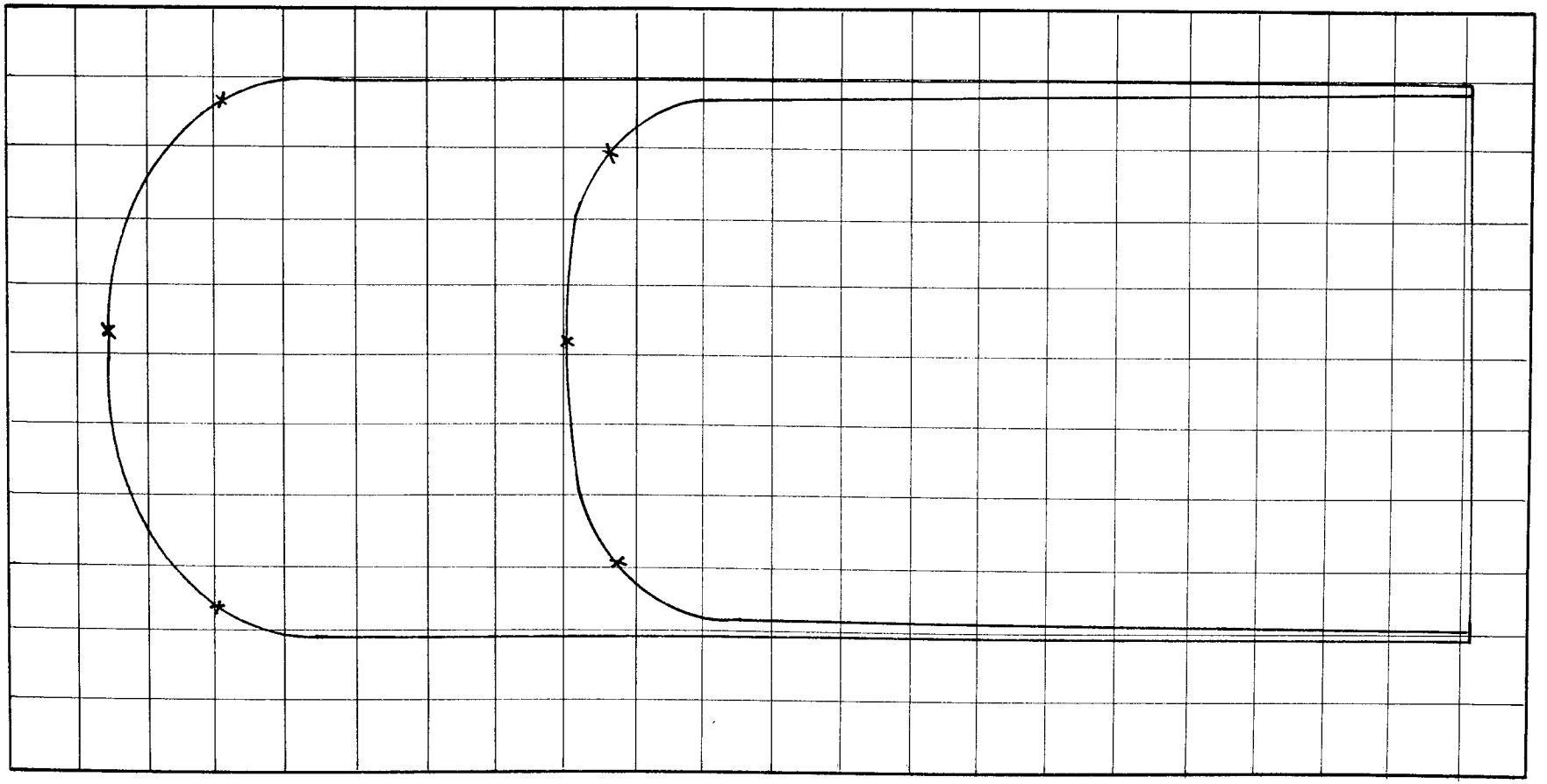

POSITION 3 Scales: Velocity: 1 mm = $\frac{1}{5}$ mm/s Area under Velocity Curve = 10,700 mm^2

Momentum: 1 mm^2 = $\frac{1}{25}$ kgmm/s Area under Momentum Curve = 15,600 mm^2

BED MATERIAL: 3 mm Diameter Glass Spheres

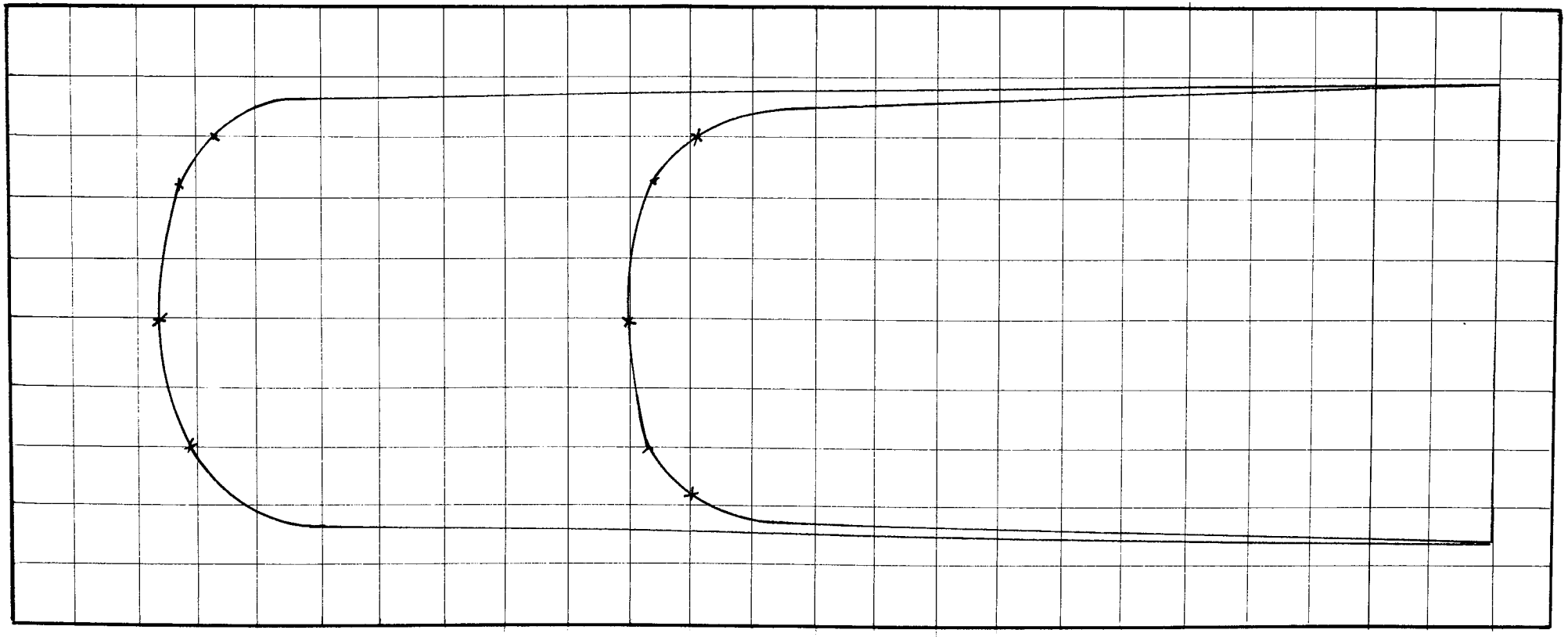

POSITION 4 Scales: Velocity : 1 mm = $\frac{1}{5}$ mm/s Area under Velocity Curve = 9,720 mm^2

Momentum: 1 mm^2 = $\frac{1}{25}$ kgmm/s Area under Momentum Curve = 15,000 mm^2

BED MATERIAL: 3 mm Diameter Glass Spheres

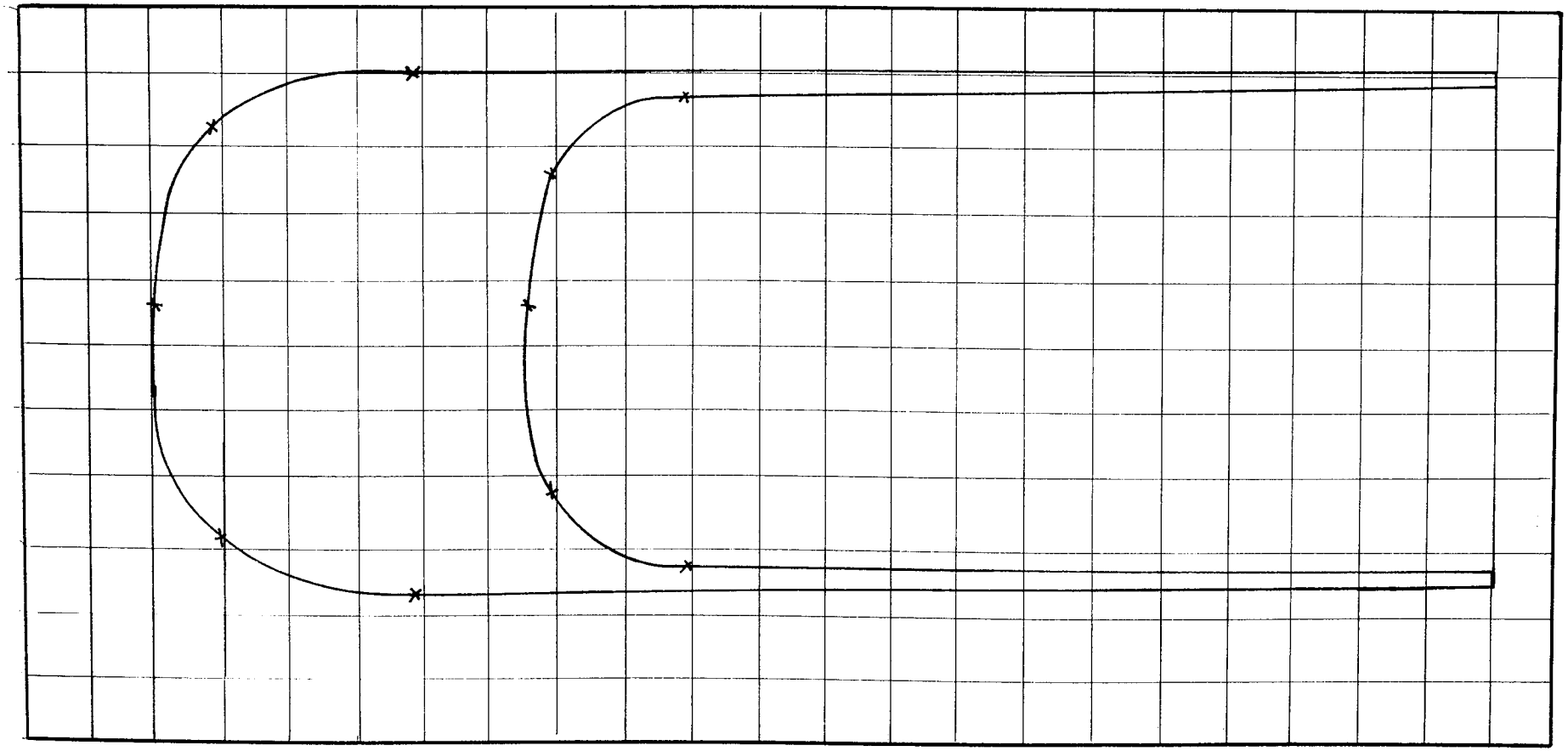

POSITION 5 Scales: Velocity: 1 mm = $\frac{1}{5}$ mm/s Area under Velocity Curve = 10,100 mm^2

Momentum: 1 mm^2 = $\frac{1}{25}$ kgmm/s Area under Momentum Curve = 14,900 mm^2

BED MATERIAL: 3 mm Diameter Glass Spheres

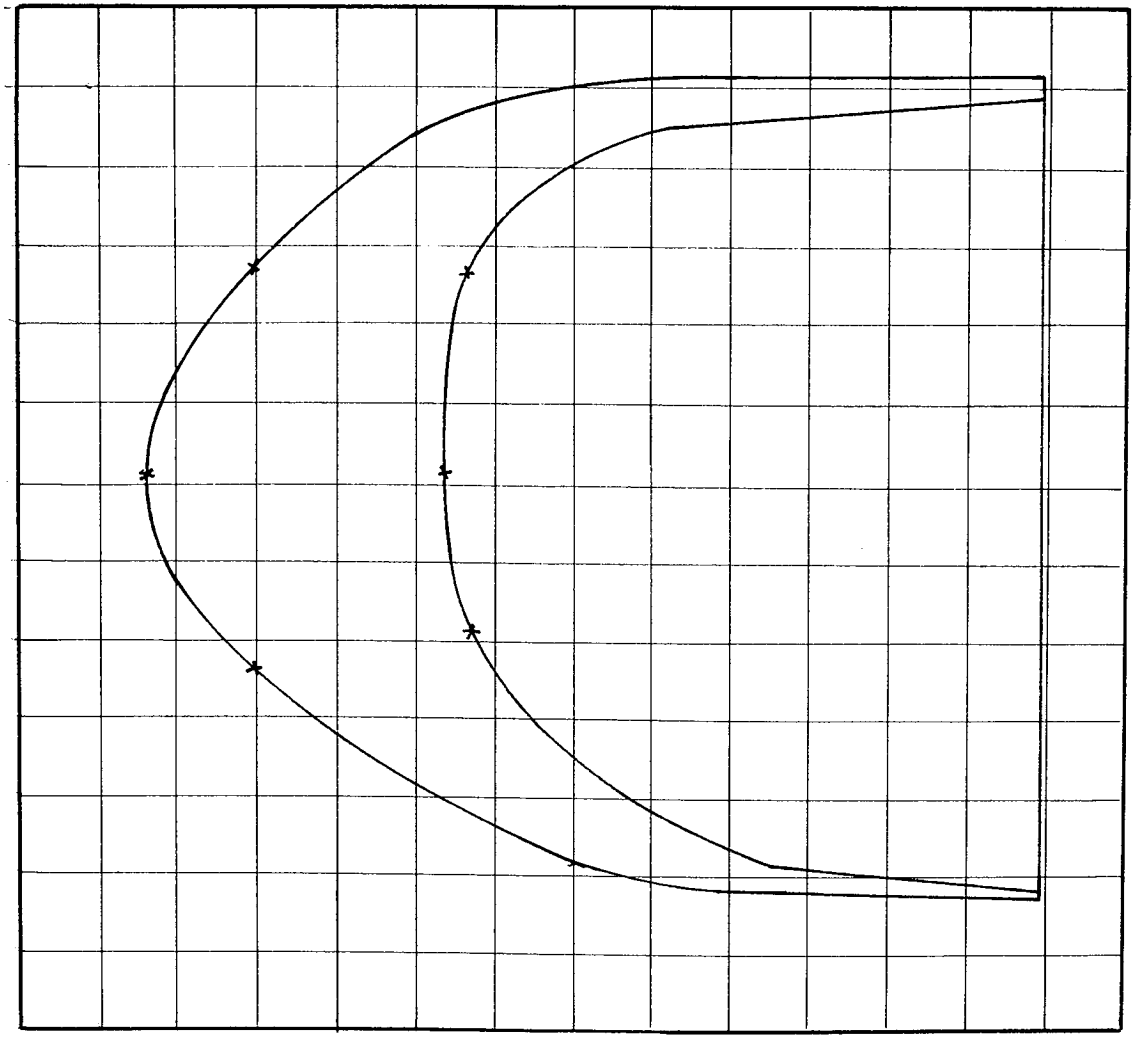

POSITION 1 Scales: Velocity: 1 mm = $\frac{1}{5}$ mm/s Area under Velocity Curve = 6,900 mm^2

Momentum: 1 mm^2 = $\frac{1}{25}$ kgmm/s Area under Momentum Curve = 10,400 mm^2

BED MATERIAL: 3 mm Diameter Glass Spheres

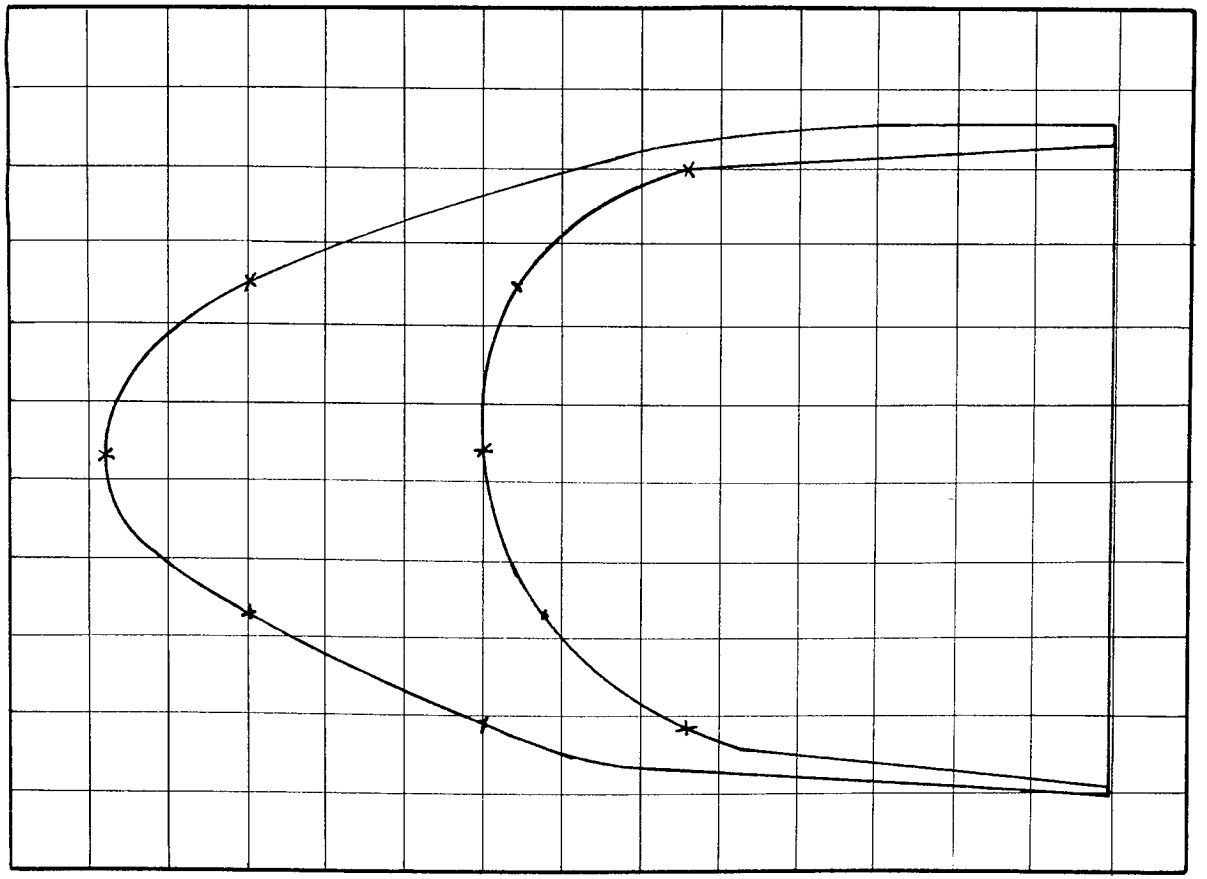

POSITION 2 Scales: Velocity: 1 mm = $\frac{1}{5}$ mm/s

Momentum: 1 mm^2 = $\frac{1}{25}$ kgmm/s

Area under Velocity Curve = 6,000 mm^2

Area under Momentum Curve = 9,700 mm^2

BED MATERIAL: 3 mm Diameter Glass Spheres

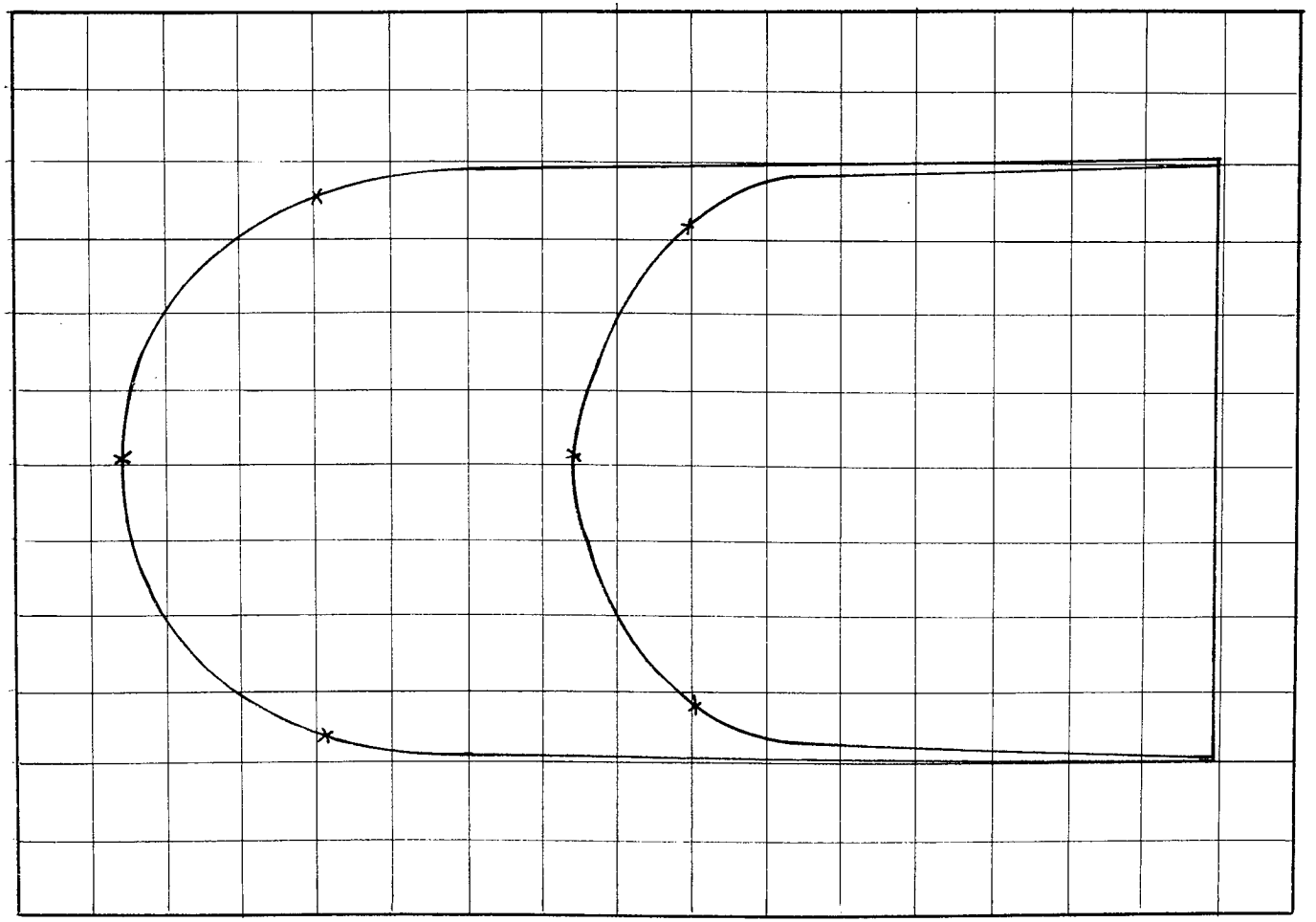

POSITION 3 Scales: Velocity: 1 mm = $\frac{1}{5}$ mm/s Area under Velocity Curve = 6,400 mm^2

Momentum: 1 mm^2 = $\frac{1}{25}$ kgmm/s Area under Momentum Curve = 10,100 mm^2

BED MATERIAL: 3 mm Diameter Glass Spheres

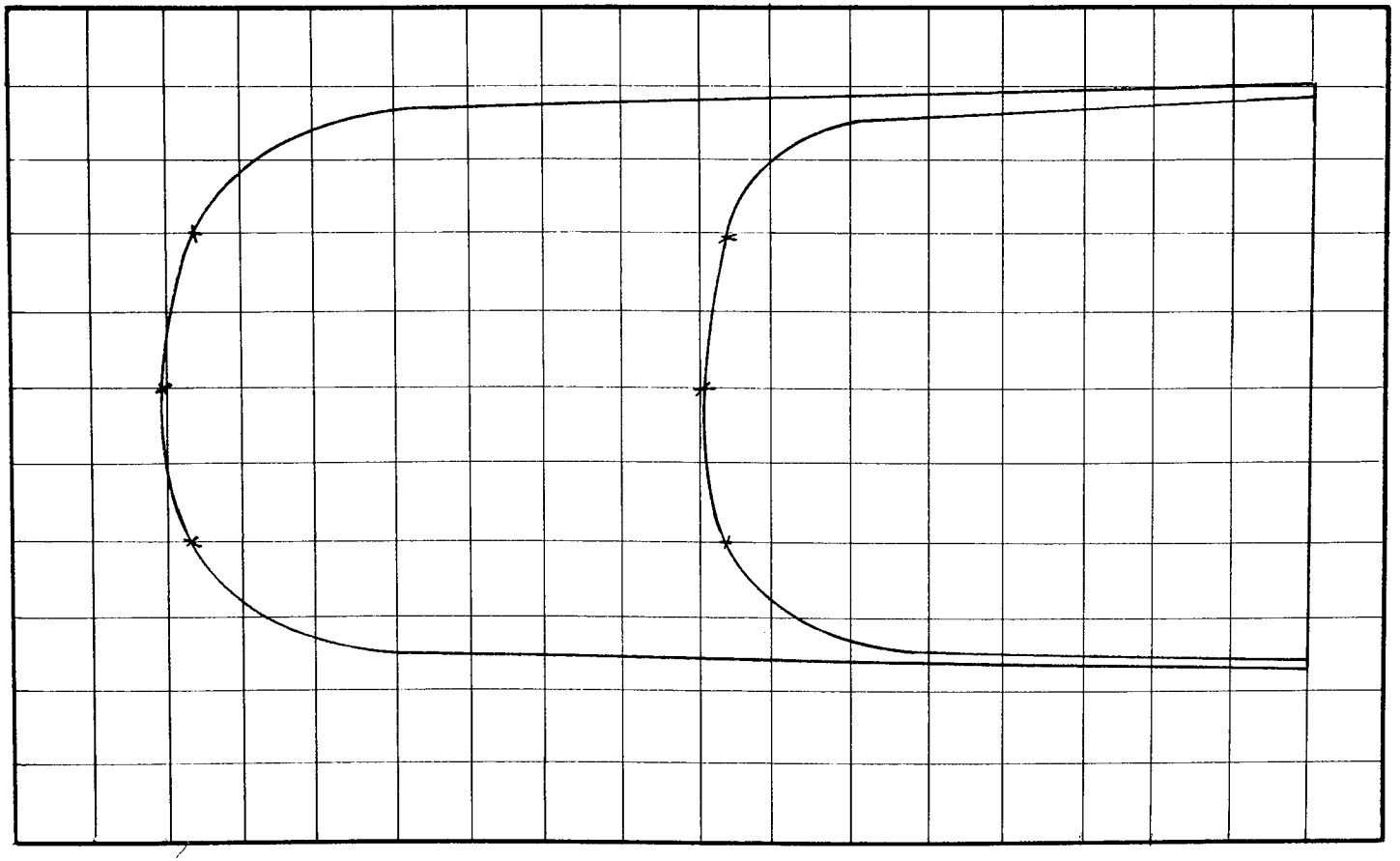

POSITION ' Scales: Velocity: 1 mm = $\frac{1}{5}$ mm/s Area under Velocity Curve = 6,200 mm^2

Momentum: 1 mm^2 = $\frac{1}{25}$ kgmm/s Area under Momentum Curve = 10,100 mm^2

BED MATERIAL: 3 mm Diameter Glass Spheres

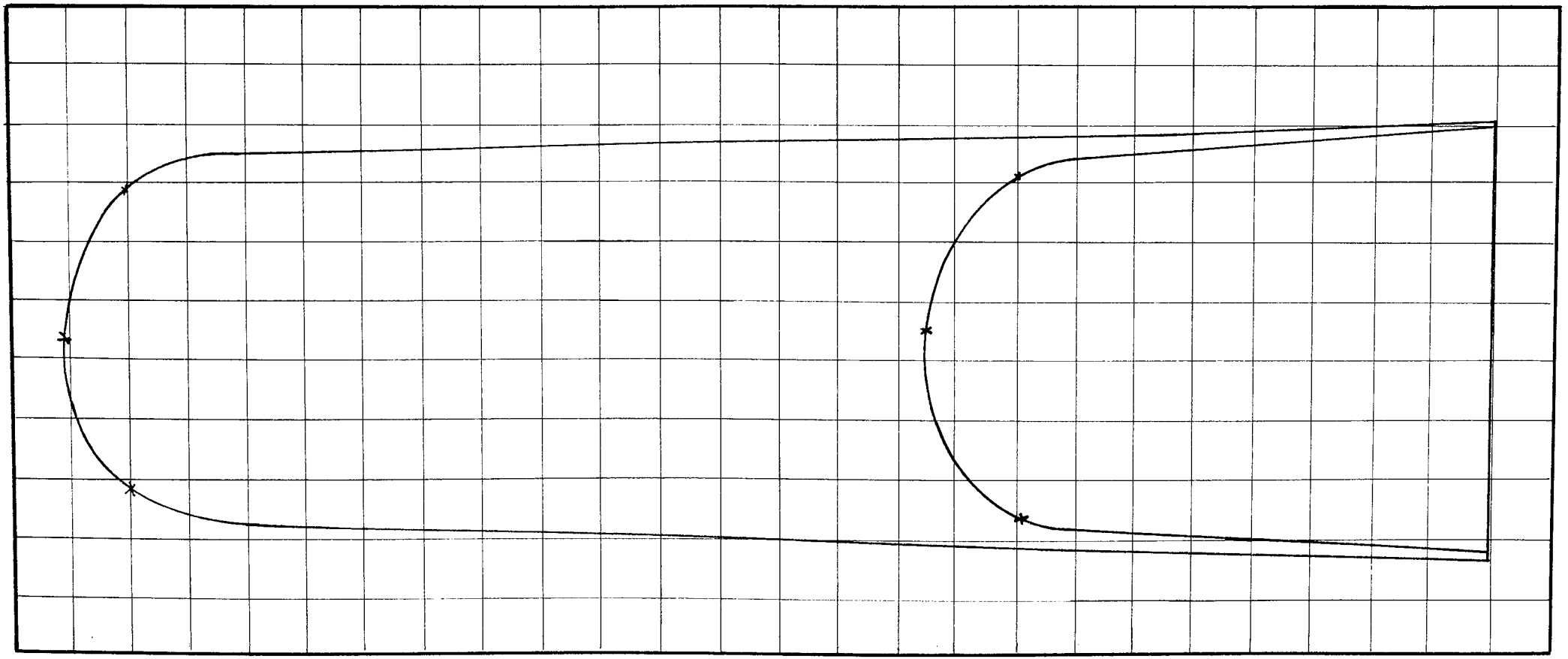

POSITION 5 Scales: Velocity: 1 mm = $\frac{1}{5}$ mm/s Area under Velocity Curve = 6,600 mm^2

Momentum: 1 mm^2 = $\frac{1}{25}$ kgmm/s Area under Momentum Curve = 11,000 mm^2

BED MATERIAL: 3 mm Diameter Glass Spheres

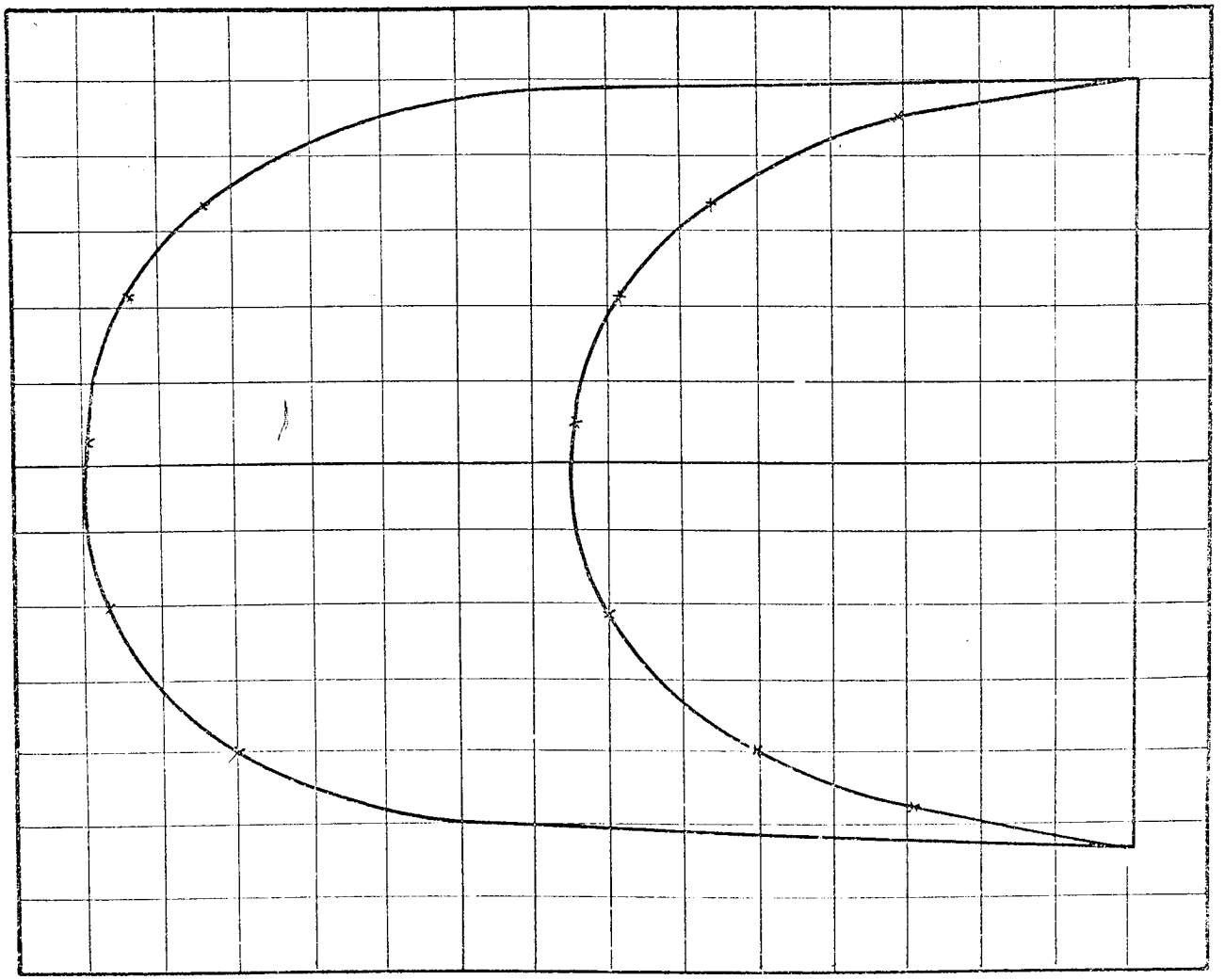

POSITION 1 Scales: Velocity: 1 mm = 1 mm/s Area under Velocity Curve = 6,110 mm^2

Momentum: 1 mm^2 = $\frac{1}{3}$ kgmm/s Area under Momentum Curve = 12,700 mm^2

BED MATERIAL: 3 mm Diameter Sand

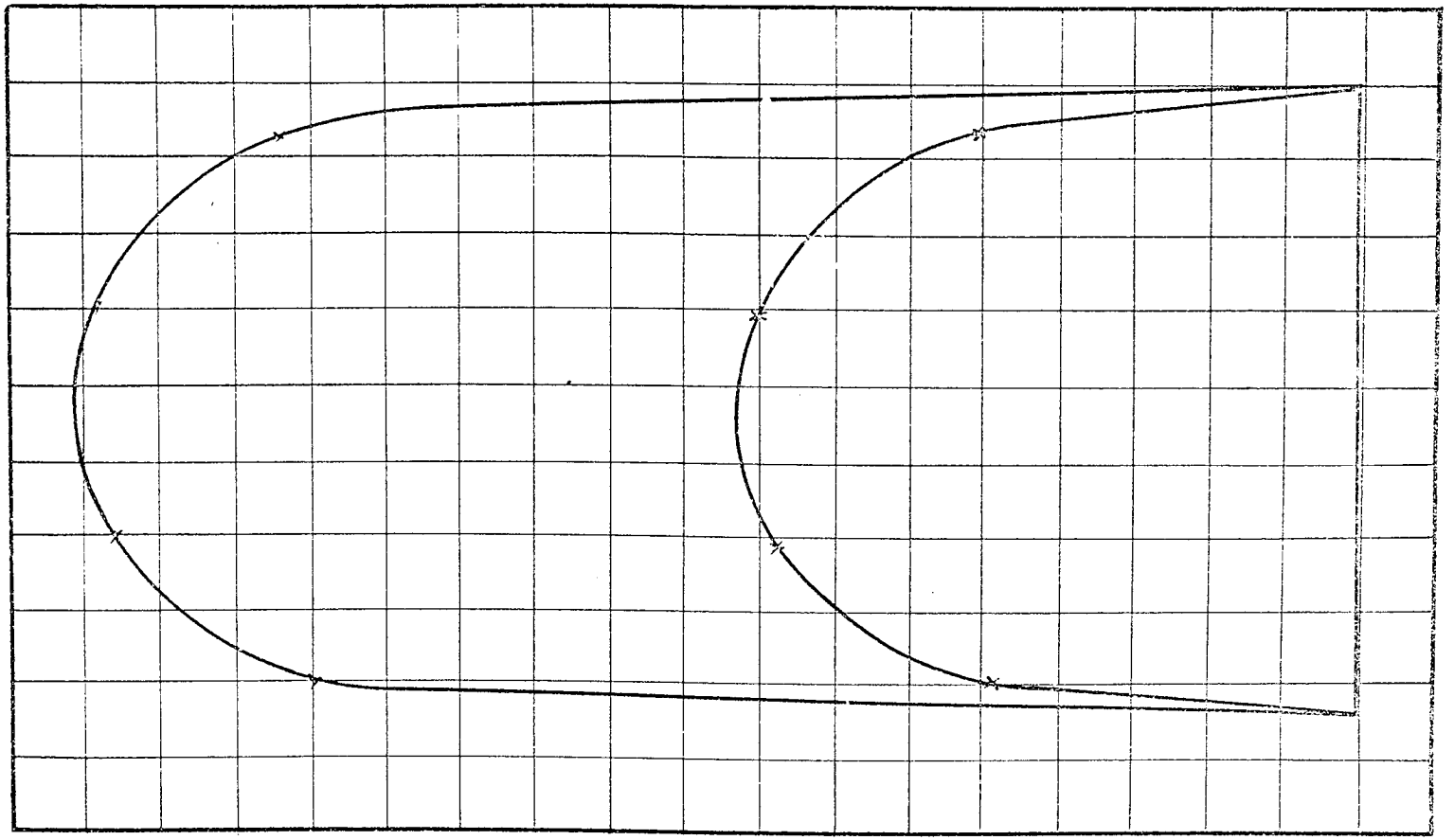

POSITION 2 Scales: Velocity: 1 mm = 1 mm/s Area under Velocity Curve = 6,000 mm^2

Momentum: 1 mm^2 = $\frac{1}{3}$ kgmm/s Area under Momentum Curve = 12,000 mm^2

BED MATERIAL : 3 mm Diameter Sand

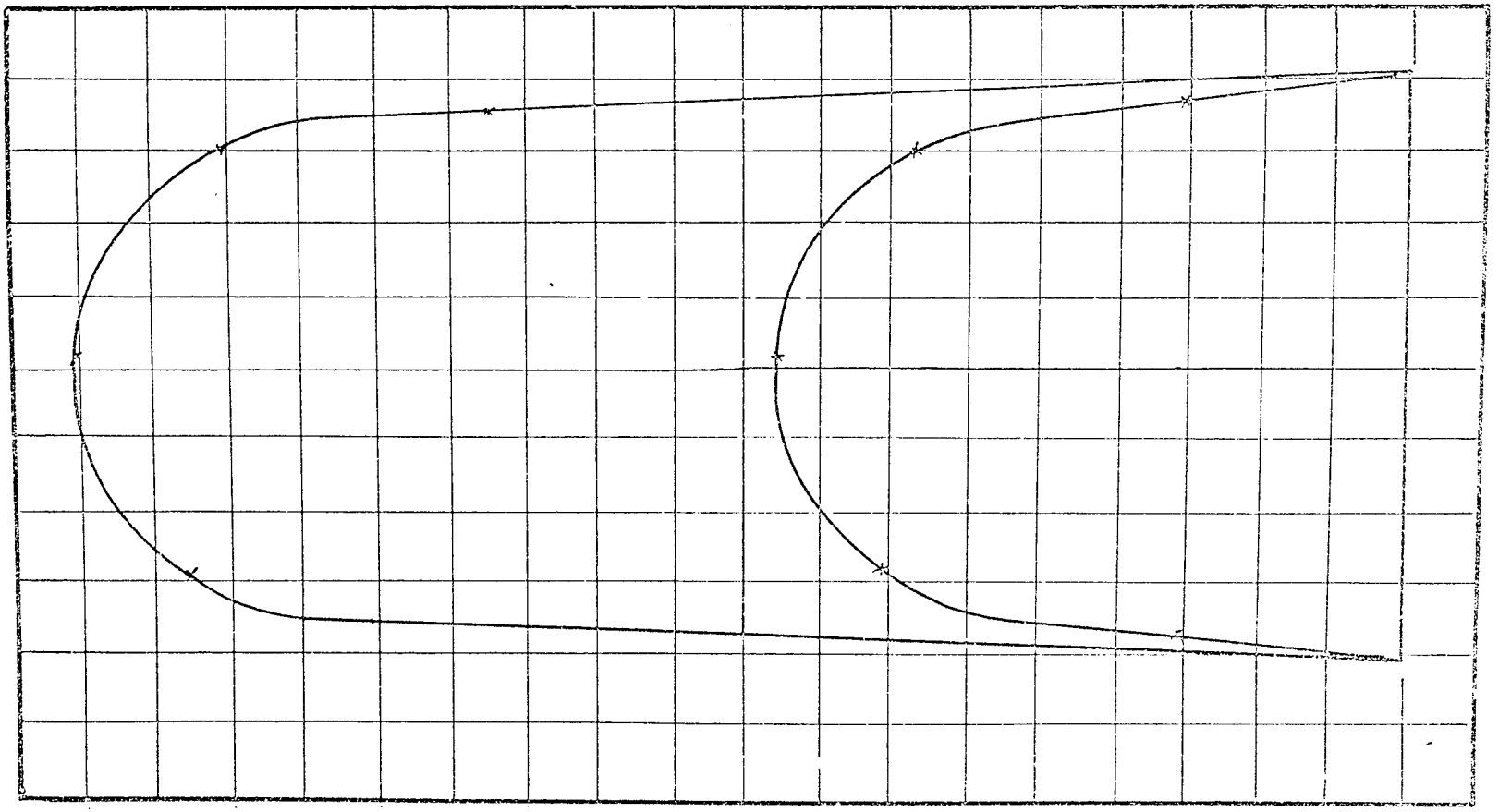

POSITION 3 Scales: Velocity: 1 mm = 1 mm/s Area under Velocity Curve = 5,950 mm^2

Momentum: 1 mm^2 = $\frac{1}{3}$ kgmm/s Area under Momentum Curve = 12,900 mm^2

BED MATERIAL: 3 mm Diameter Sand

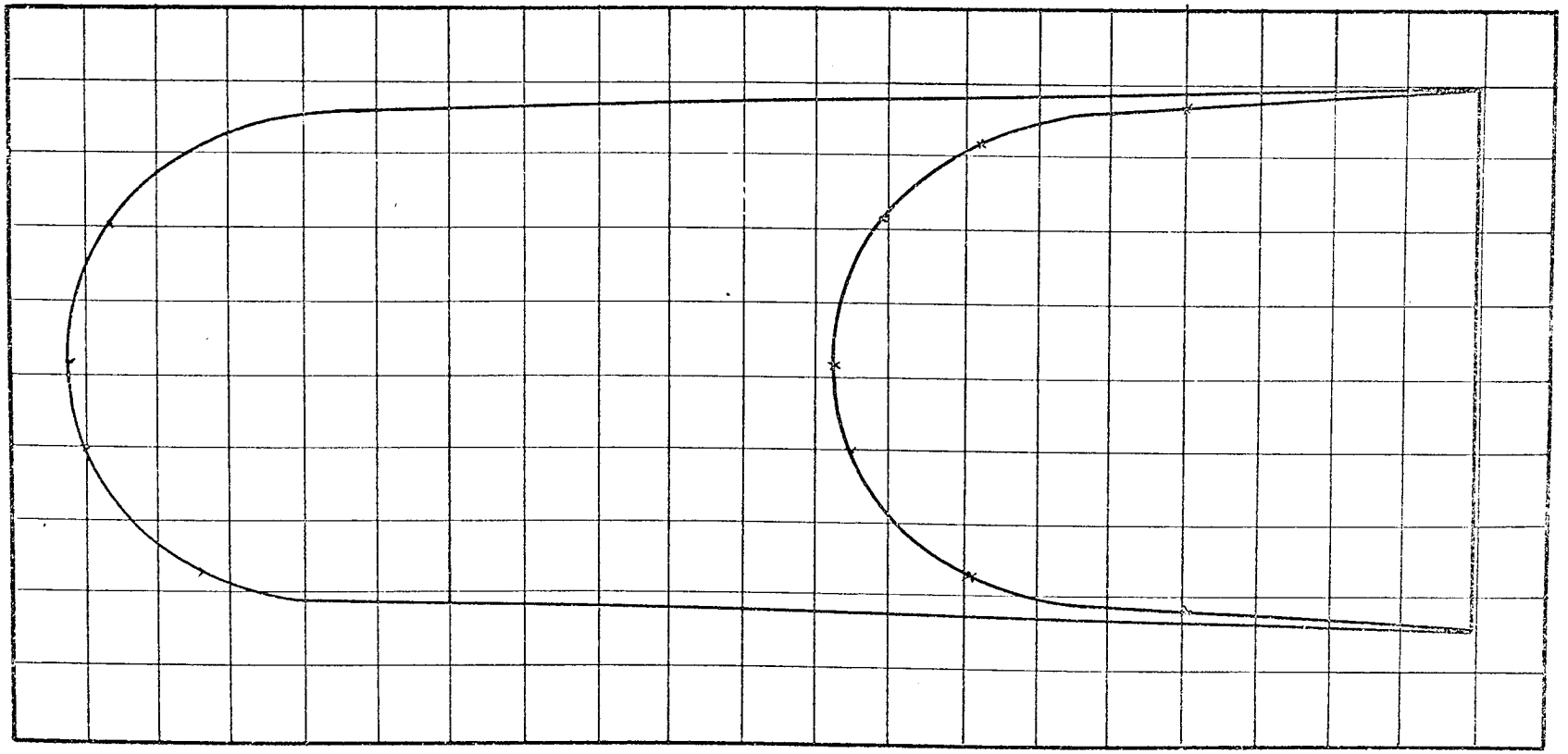

POSITION 4 Scales: Velocity: 1 mm = 1 mm/2 Area under Velocity Curve = 5,850 mm^2

Momentum: 1 mm^2 = $\frac{1}{5}$ kgmm/s Area under Momentum Curve = 12,900 mm^2

BED MATERIAL: 3 mm Diameter Sand

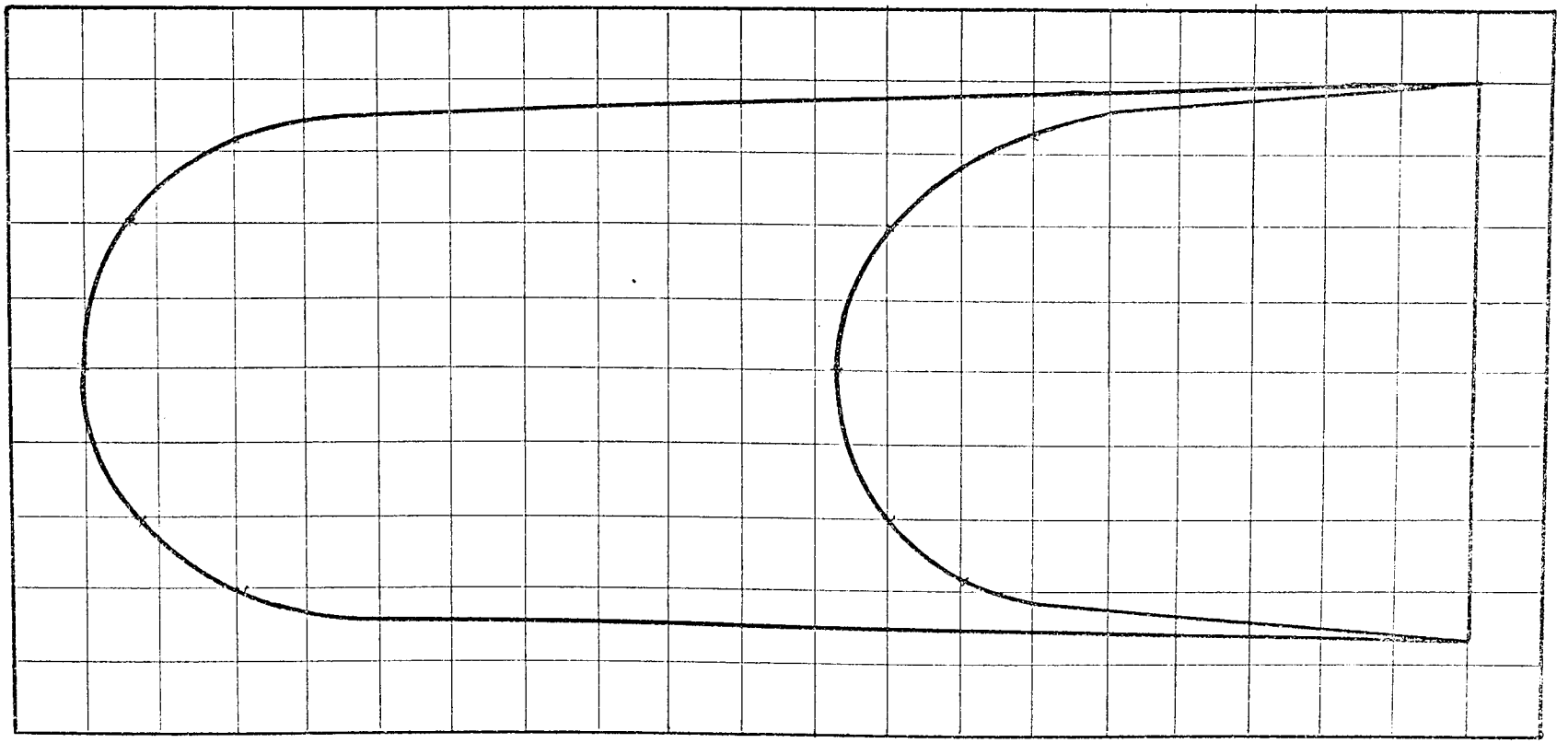

POSITION 5 Scales: Velocity: 1 mm = 1 mm/s Area under Velocity Curve = 5,550 mm^2

Momentum: 1 mm^2 = $\frac{1}{3}$ kgmm/s Area under Momentum Curve = 12,700 mm^2

BED MATERIAL: 3 mm Diameter Sand

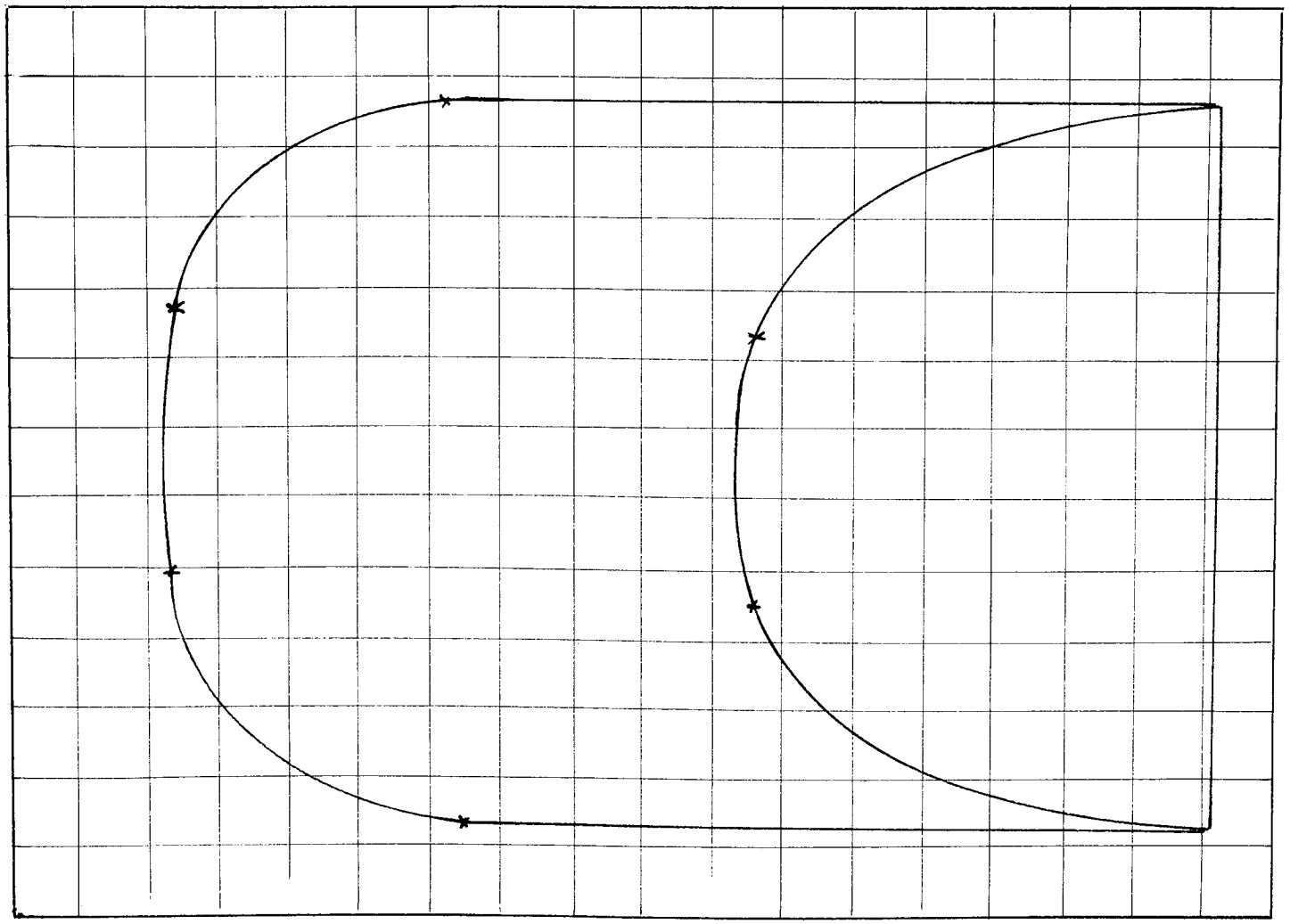

POSITION 1 Scales: Velocity: 1 mm = $\frac{1}{5}$ mm/s Area under Velocity Curve = 6,300 mm^2

Momentum: 1 mm^2 = $\frac{1}{25}$ kgmm/s Area under Momentum Curve = 14,500 mm^2

BED MATERIAL: 3 mm Diameter Sand

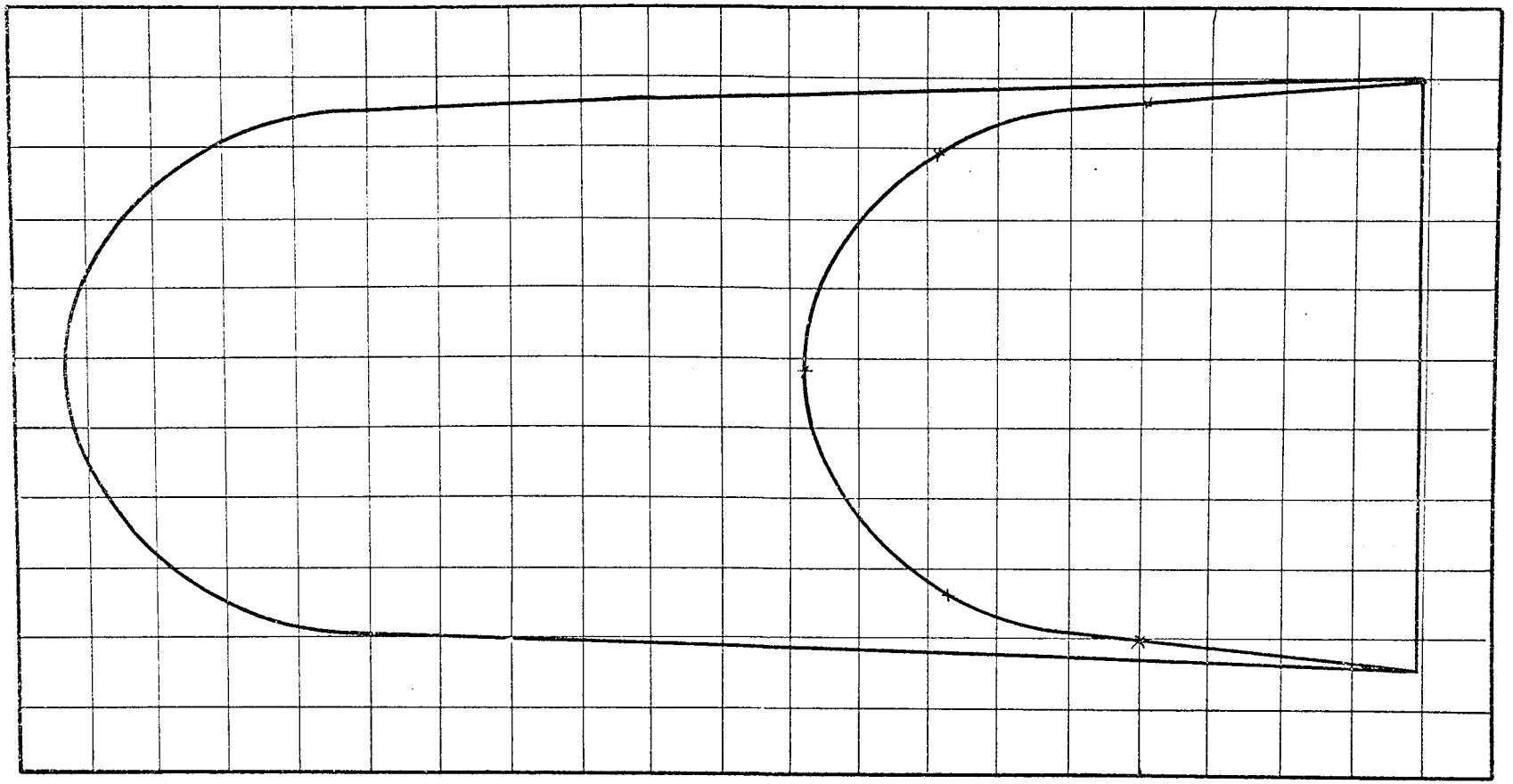

POSITION 2 Scales: Vertical: 1 in = 1/3 ft Area of Vertical Cross Section = 6,10 in²

Horizontal: 1 in = 1/3 ft Area of Horizontal Cross Section = 14, 22 in²

BED MATERIAL: 3 mm Diameter Sand

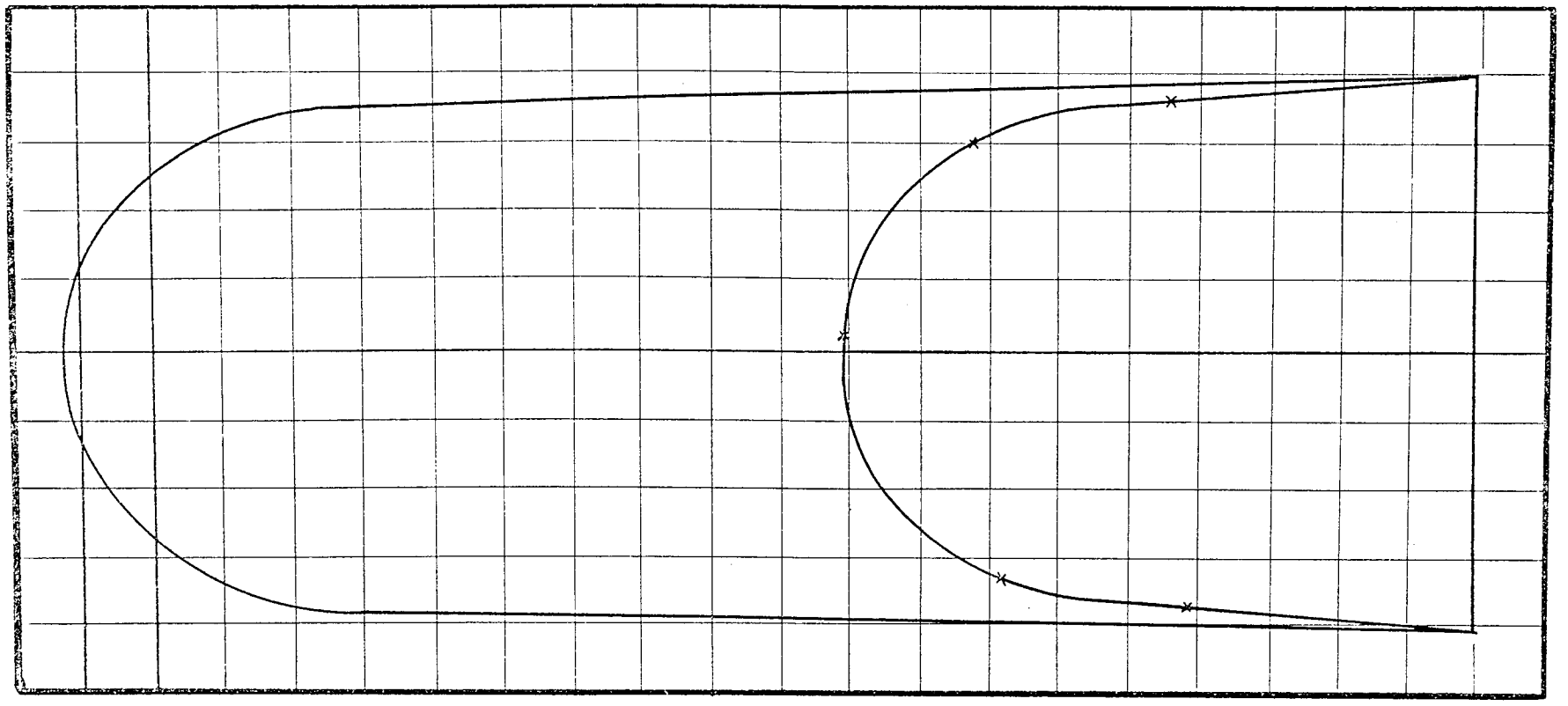

POSITION : Scale : Velocity : 1 = 1 /s Area under Velocity Curve = , ft²

Moment : 1 ft² = 1 ft/s Area under Moment Curve = 1, ft²

BED MATERIAL: Dia Sand

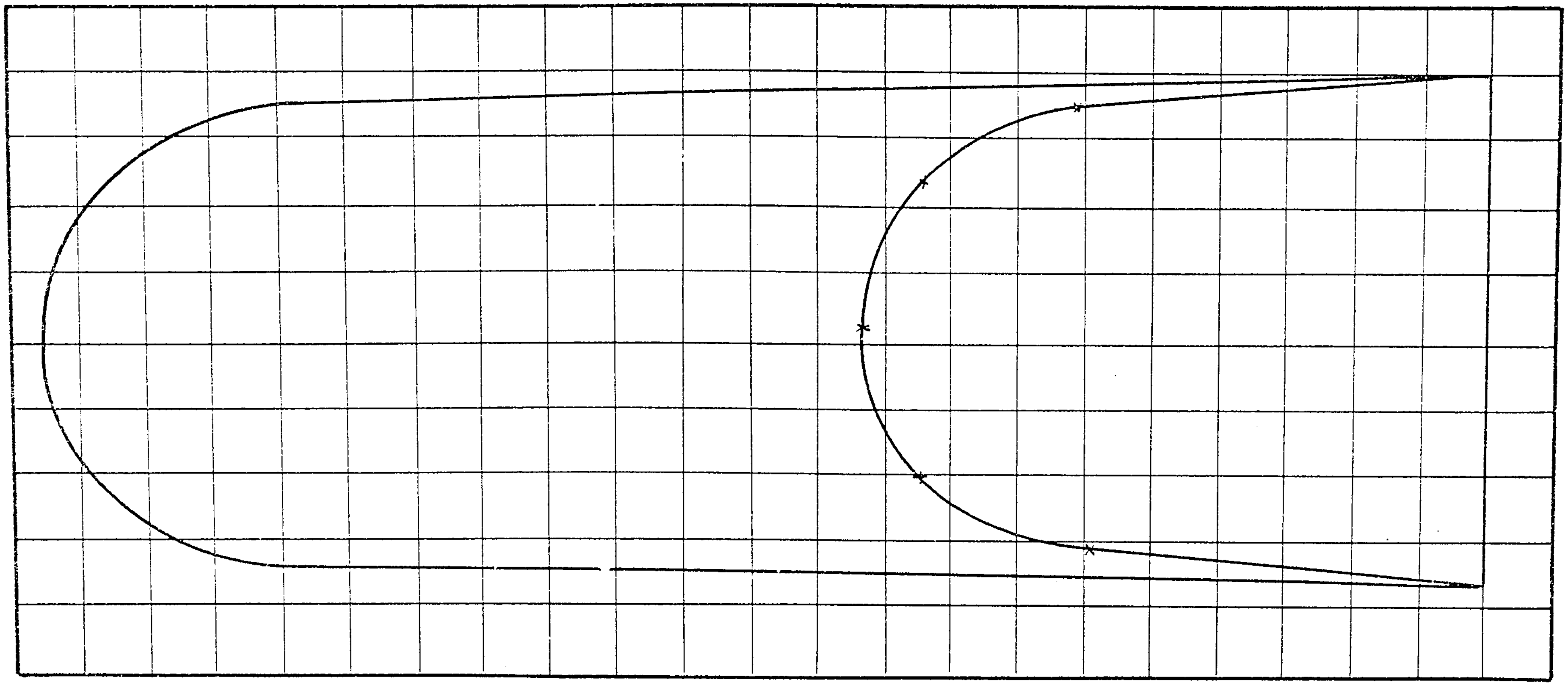

POSITION 4 S[illegible]: V[illegible]: 1 [illegible] / [illegible] A[illegible] V[illegible] C[illegible] ,25[illegible]

M[illegible] : 1 [illegible] m/[illegible] A[illegible] M[illegible] C[illegible] 1,72[illegible]

BED MATERIAL: D[illegible] S[illegible]

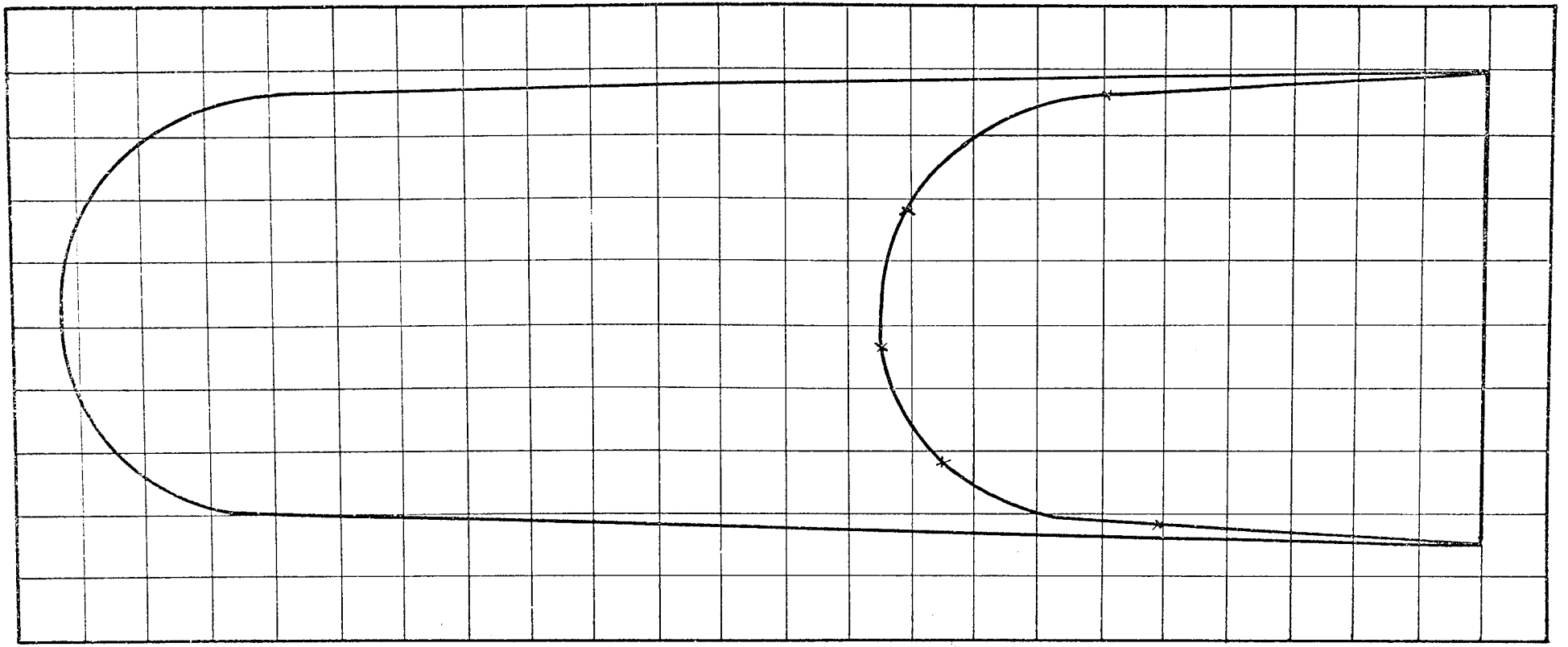

POSITION 5 Scale : V [illegible] : 1 [illegible] / A [illegible] V [illegible] C [illegible]

M [illegible] : 1 [illegible] A [illegible] M [illegible] C [illegible]

BED MATERIAL: [illegible] D [illegible] S [illegible]

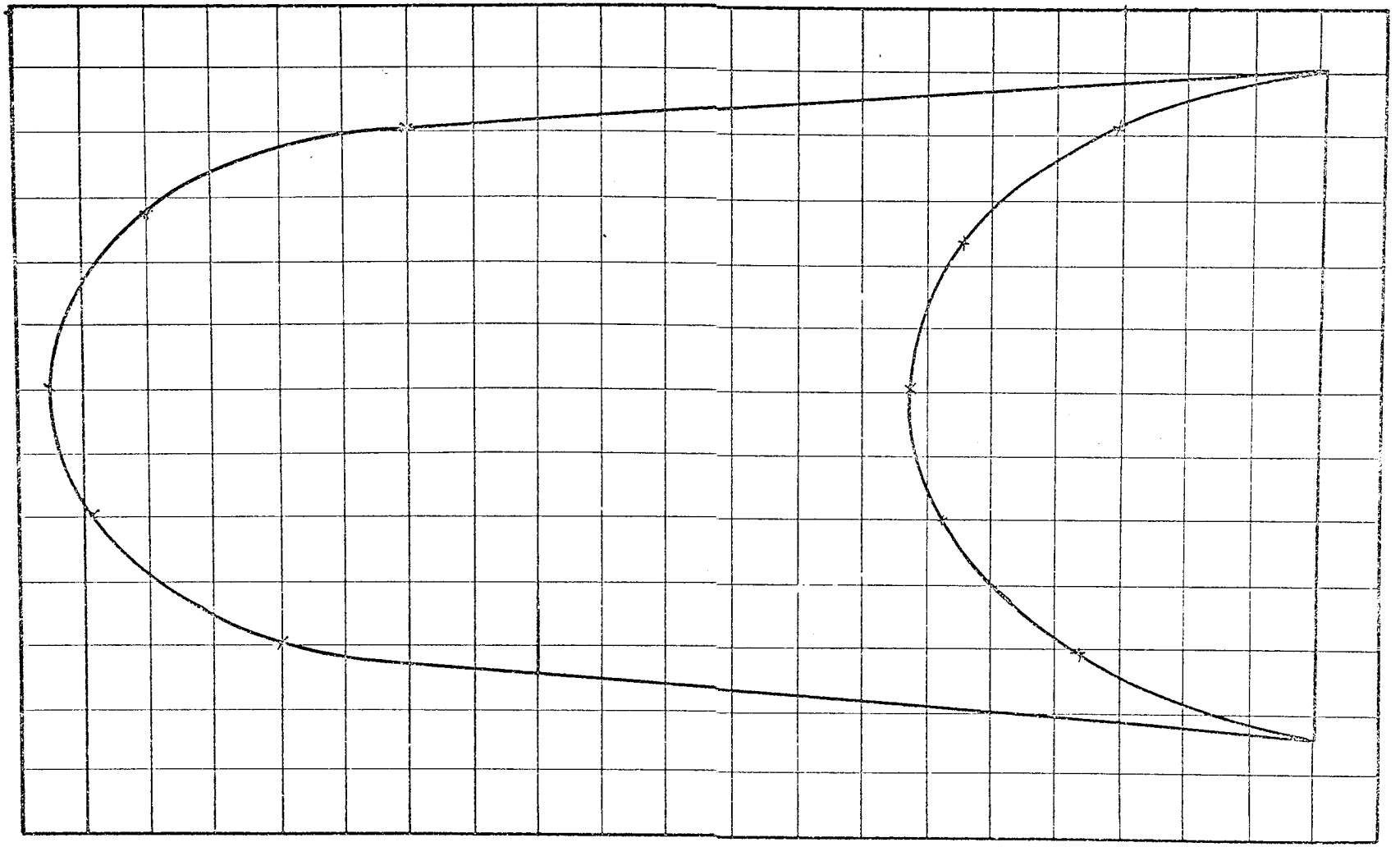

POSITION 1 Scales: Velocity : 1 mm = 1mm/s Area under Velocity Curve = 4,700 mm^2

Momentum : 1 mm^2 = $\frac{1}{2}$ kgmm/s Area under Momentum Curve = 16,000 mm^2

BED MATERIAL: 3 mm Diameter Sand

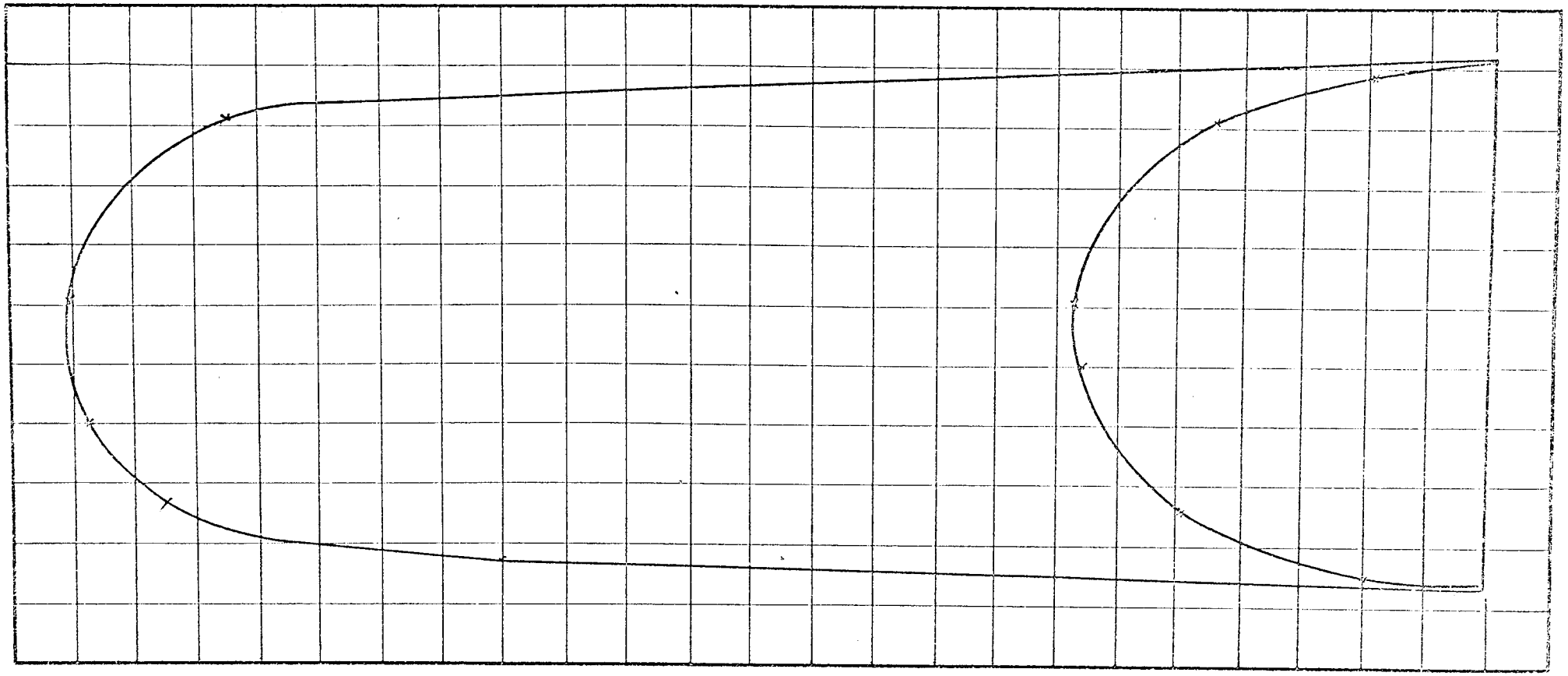

POSITION 2 Scales: Velocity: 1 mm = 1 mm/s Area under Velocity Curve = 4,760 mm^2

Momentum: 1 mm^2 = $\frac{1}{2}$ kgmm/s Area under Momentum Curve = 17,100 mm^2

BED MATERIAL: 3 mm Diameter Sand

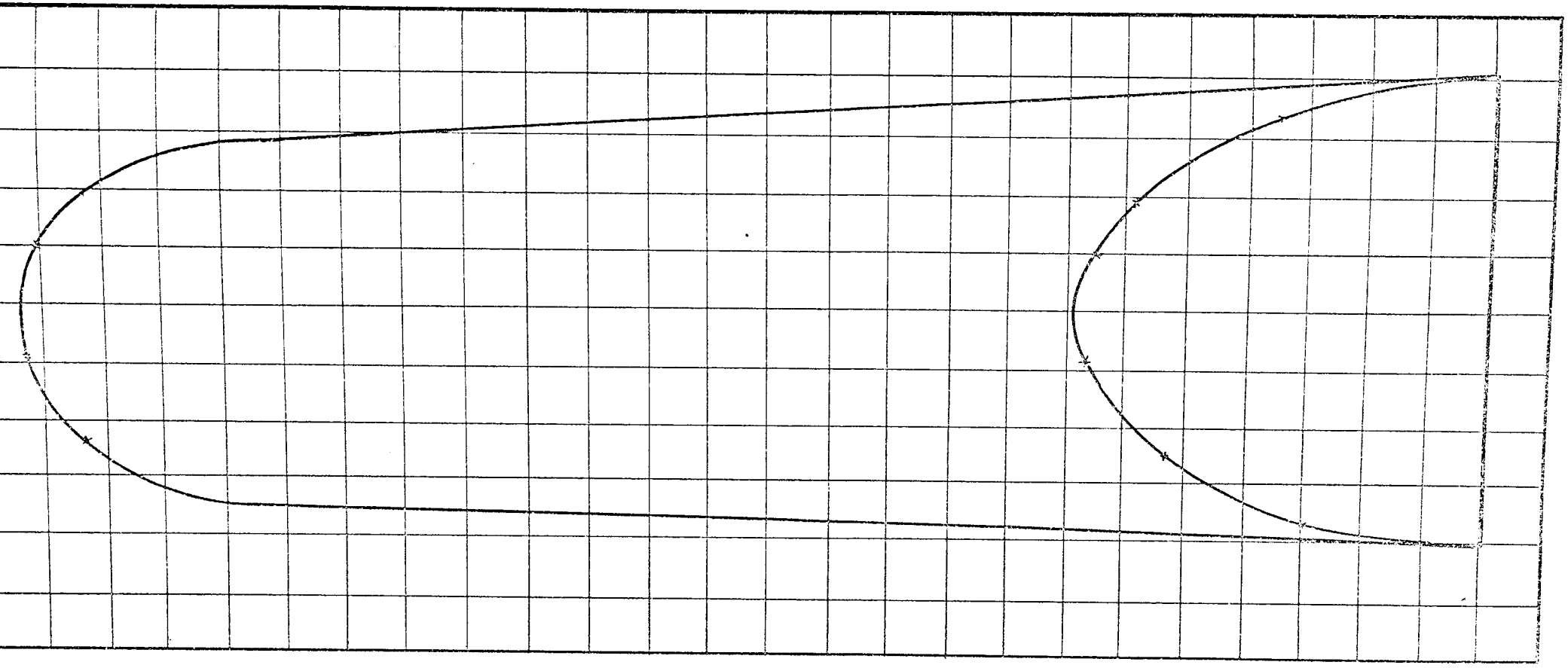

POSITION 3 Scales: Velocity : 1 mm = 1 mm/s Area under Velocity Curve = [illegible],650 mm^2

Momentum: 1 mm^2 = $\frac{1}{2}$ kgmm/s Area under Momentum Curve = 17,200 mm^2

BED MATERIAL: 3 mm Diameter Sand

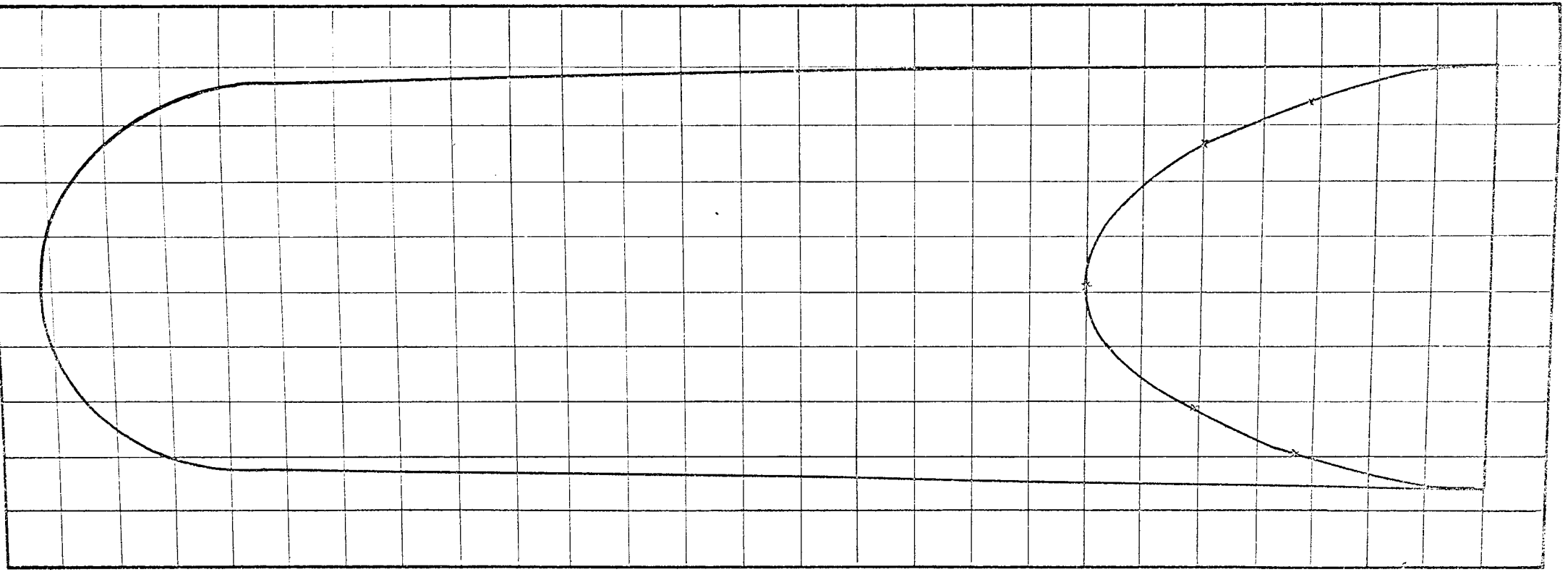

POSITION / Scales: Velocity: 1 mm = 1 mm/s Area under Velocity Curve = ,550 mm^2

Momentum: 1 mm^2 = $\frac{1}{3}$ kgmm/s Area under Momentum Curve = 17,500 mm^2

BED MATERIAL: 3 mm Diameter Sand

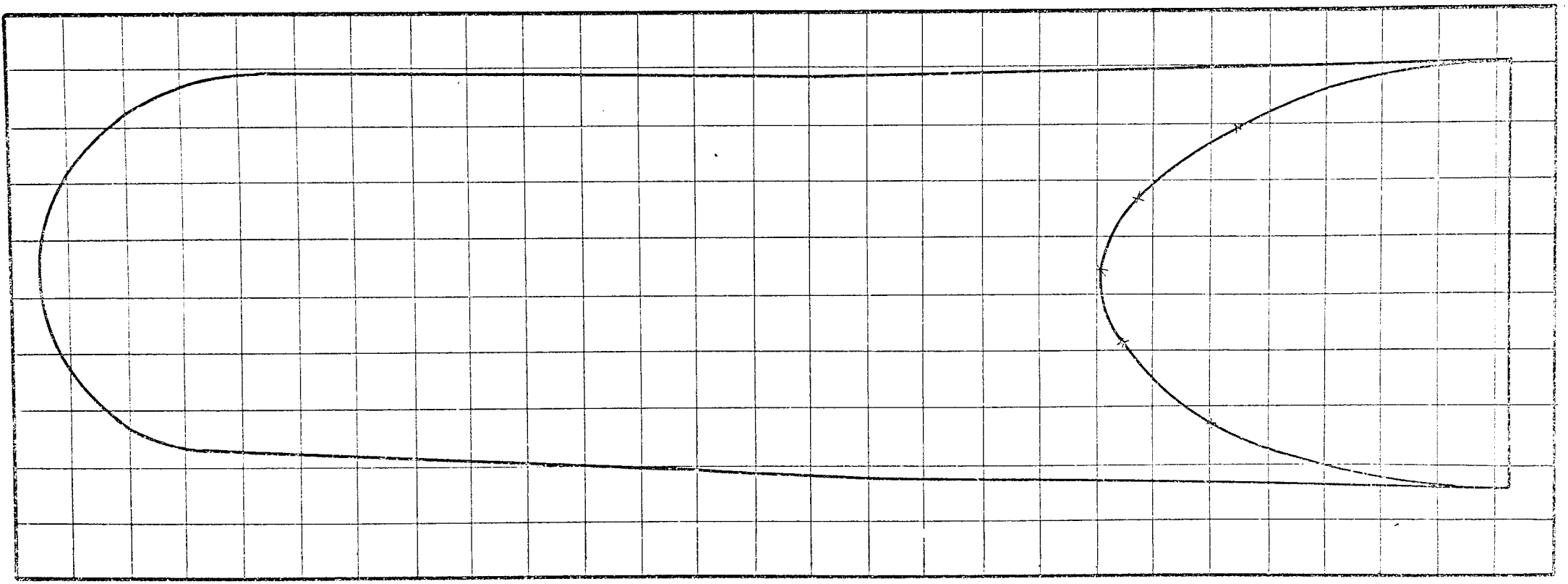

POSITION 5 Scales: Velocity: 1 mm = 1 mm/s Area under Velocity Curve = ,720 mm^2

Momentum: 1 mm^2 = $\frac{1}{2}$ kgmm/s Area under Momentum Curve = 17,[illegible]00 mm^2

BED MATERIAL: 3 mm Diameter Sand

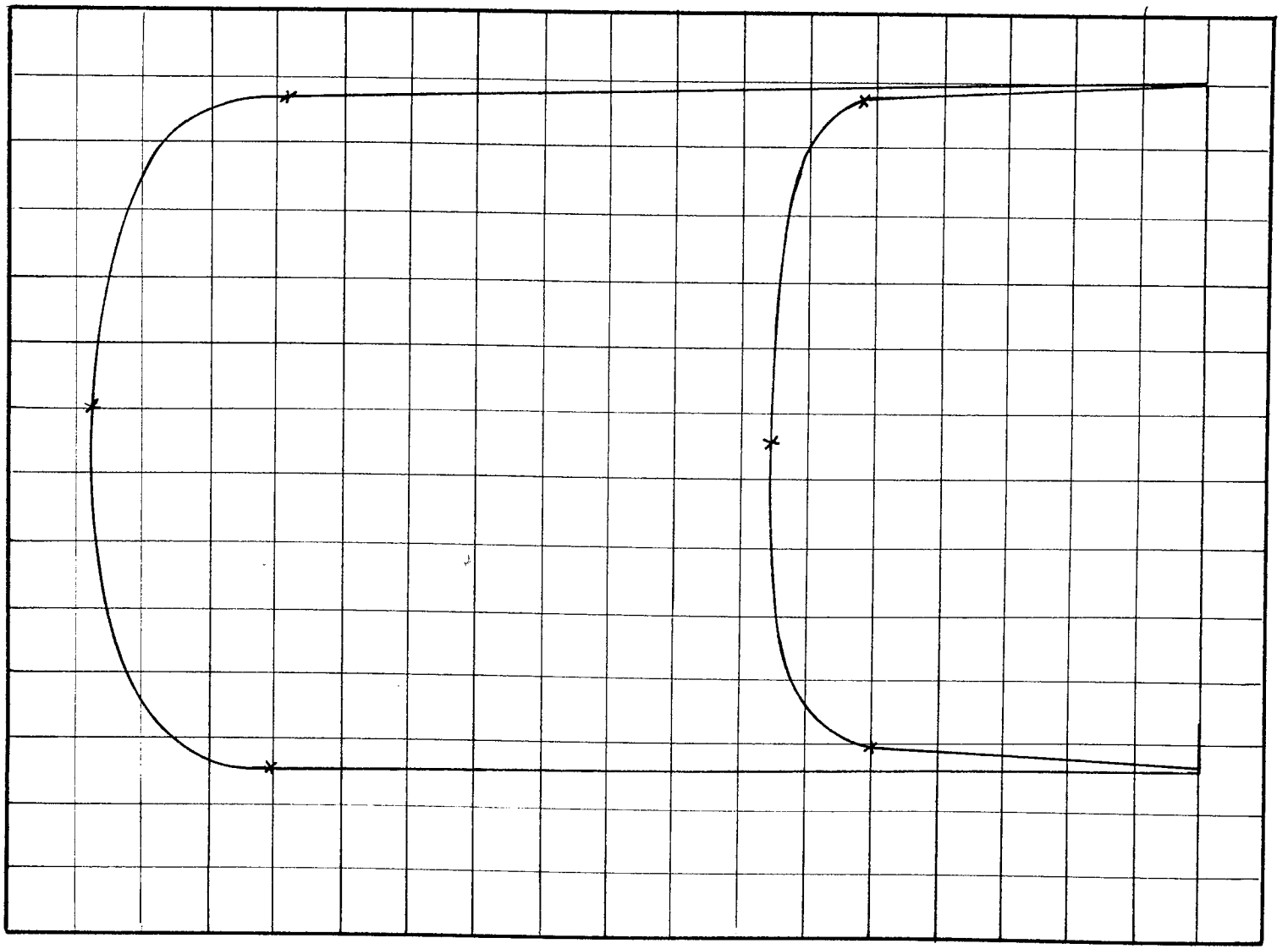

POSITION 1 Scales: Velocity: 1 mm = 1 mm/s

Momentum: 1 mm^2 = $\frac{1}{3}$ kgmm/s

Area under Velocity Curve = 6,410 mm^2

Area under Momentum Curve = 16,800 mm^2

BED MATERIAL: 3 mm Diameter Sand

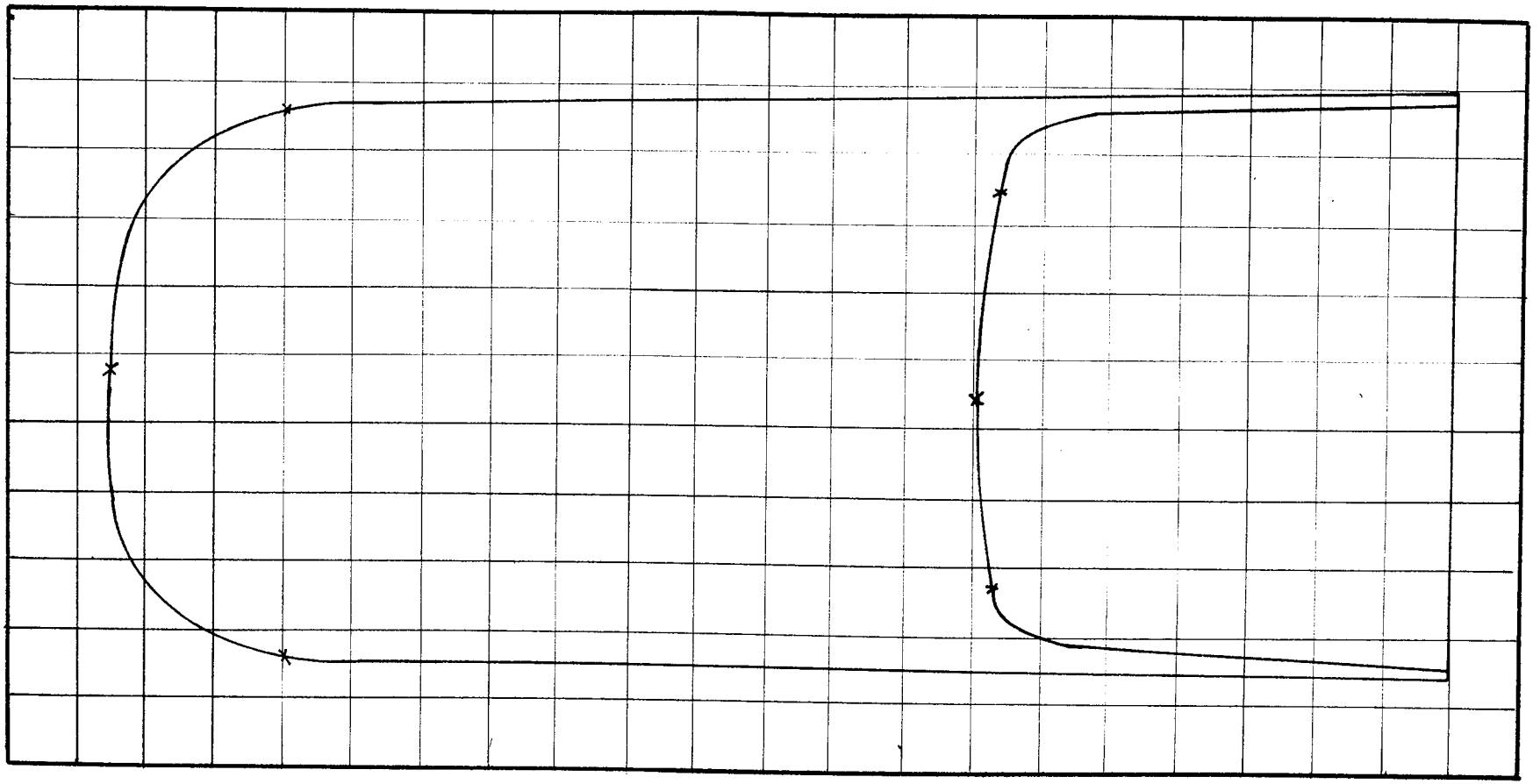

POSITION 2 Scales: Velocity: 1 mm = 1 mm/s

Momentum: 1 mm^2 = $\frac{1}{5}$ kgmm/s

Area under Velocity Curve = 6,000 mm^2

Area under Momentum Curve = 15,900 mm^2

BED MATERIAL: 3 mm Diameter Sand

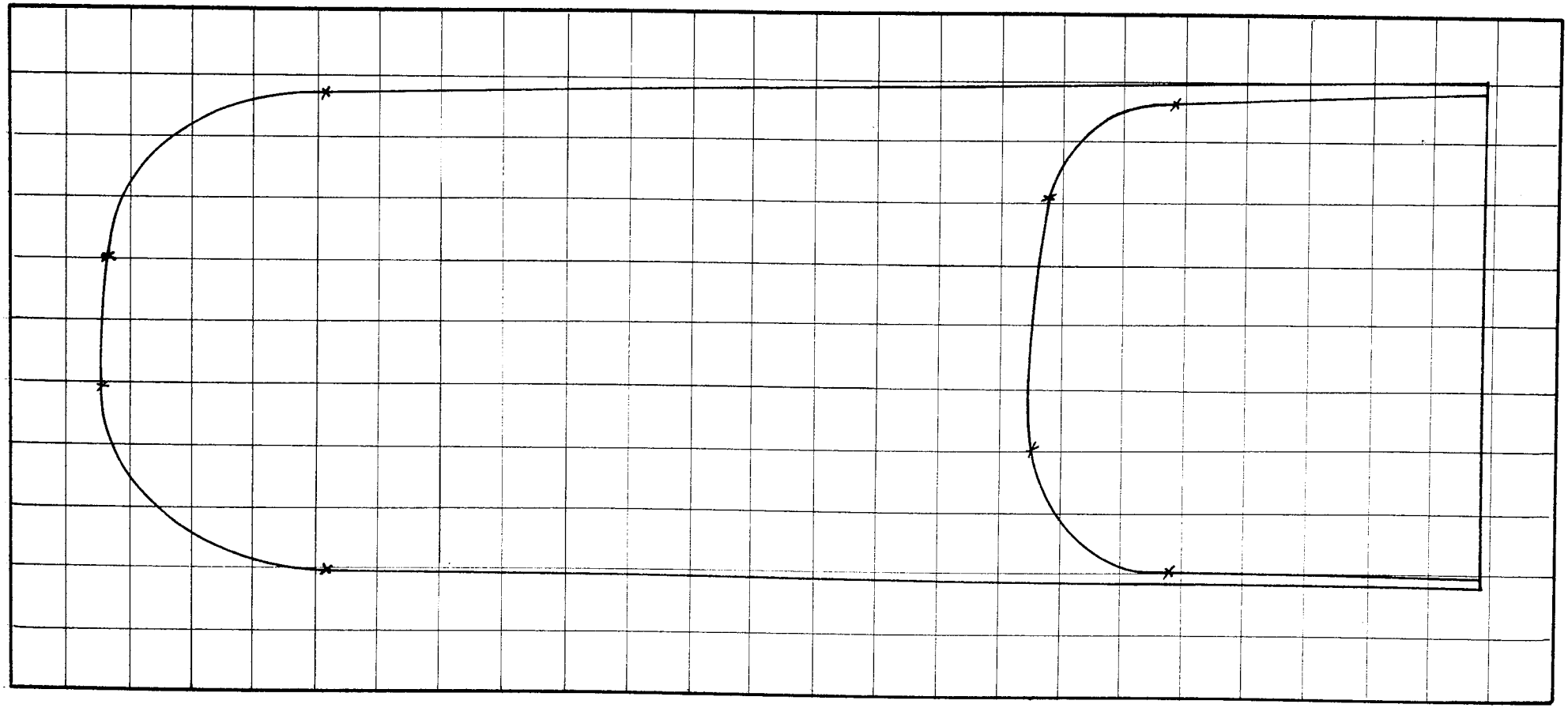

POSITION 3 Scales: Velocity: 1mm = 1 mm/s

Momentum: 1 mm^2 = $\frac{1}{3}$ kgmm/s

Area under Velocity Curve = 5,900 mm^2

Area under Momentum Curve = 17,100 mm^2

BED MATERIAL: 3 mm Diameter Sand

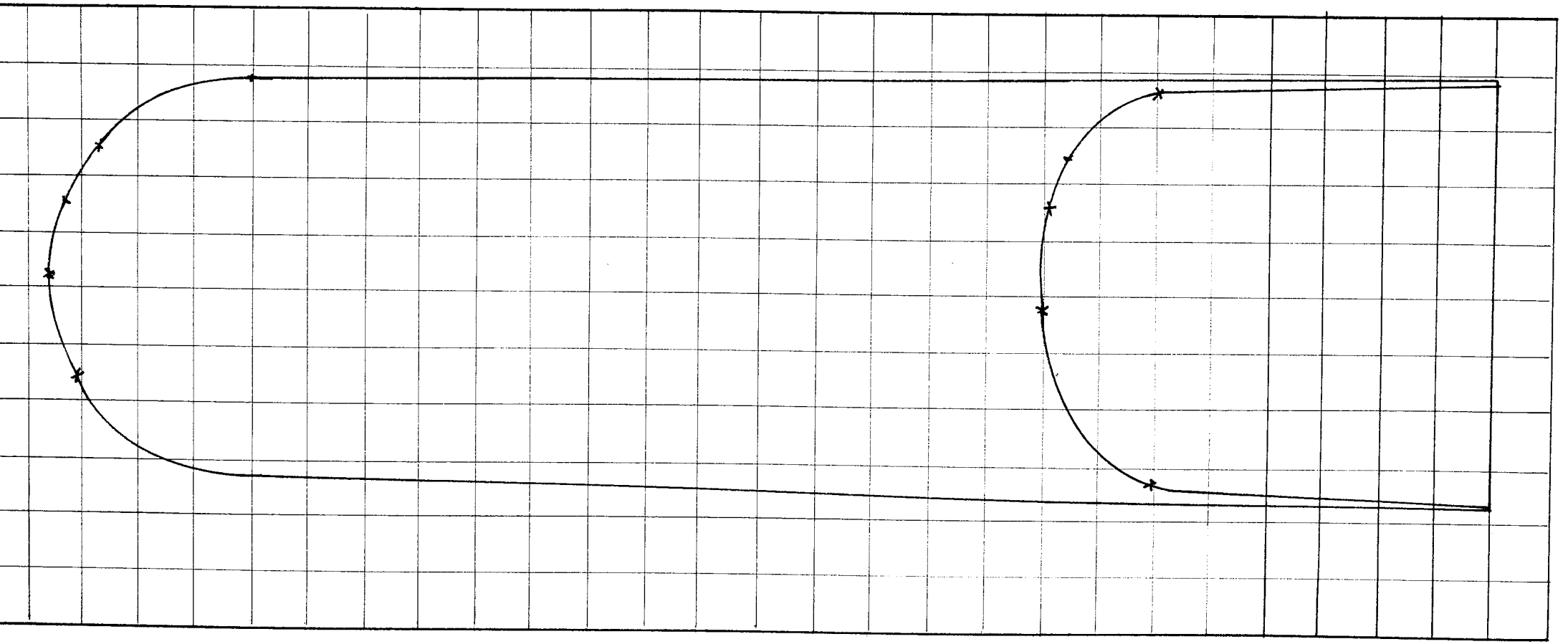

POSITION 4 Scales: Velocity: 1 mm = 1 mm/s Area under Velocity Curve = 6,200 mm^2

Momentum: 1 mm^2 = $\frac{1}{3}$ kgmm/S Area under Momentum Curve = 17,200 mm^2

BED MATERIAL: 3 mm Diameter Sand

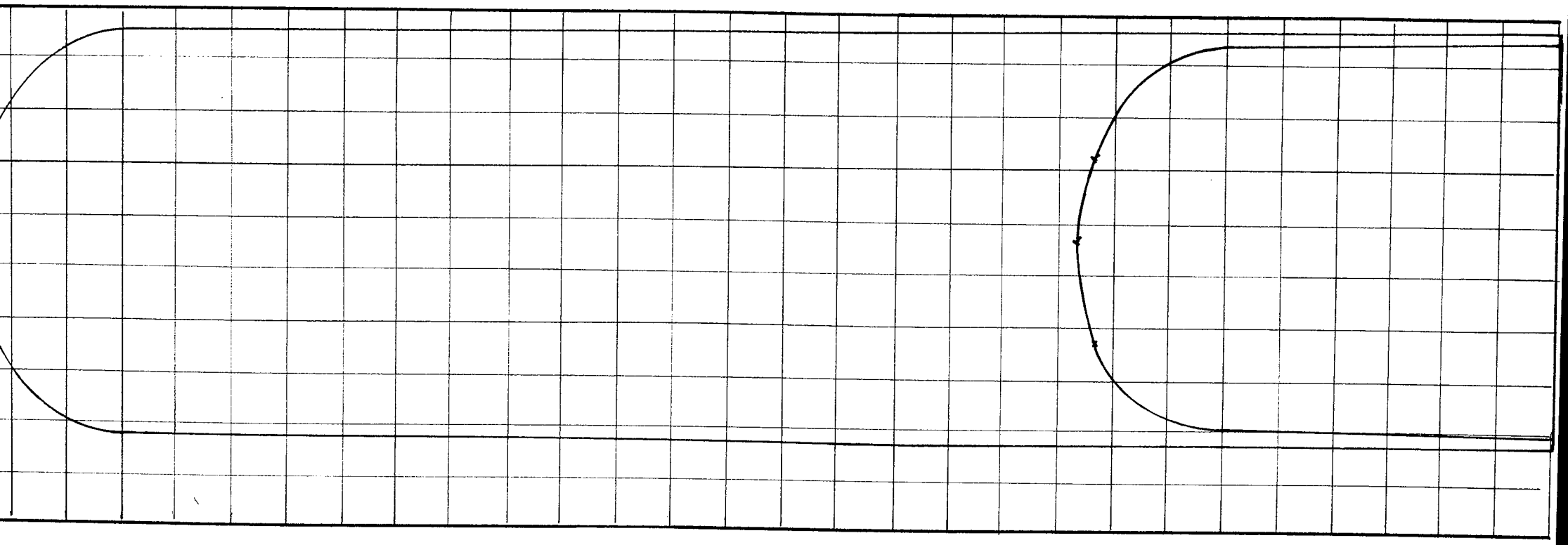

POSITION 5 Scales: Velocity: 1 mm = 1 mm/s

Momentum: 1 mm^2 = $\frac{1}{3}$ kgmm/s

Area under Velocity Curve = 6,250 mm^2

Area under Momentum Curve = 17,100 mm^2

BED MATERIAL: 3 mm Diameter Sand

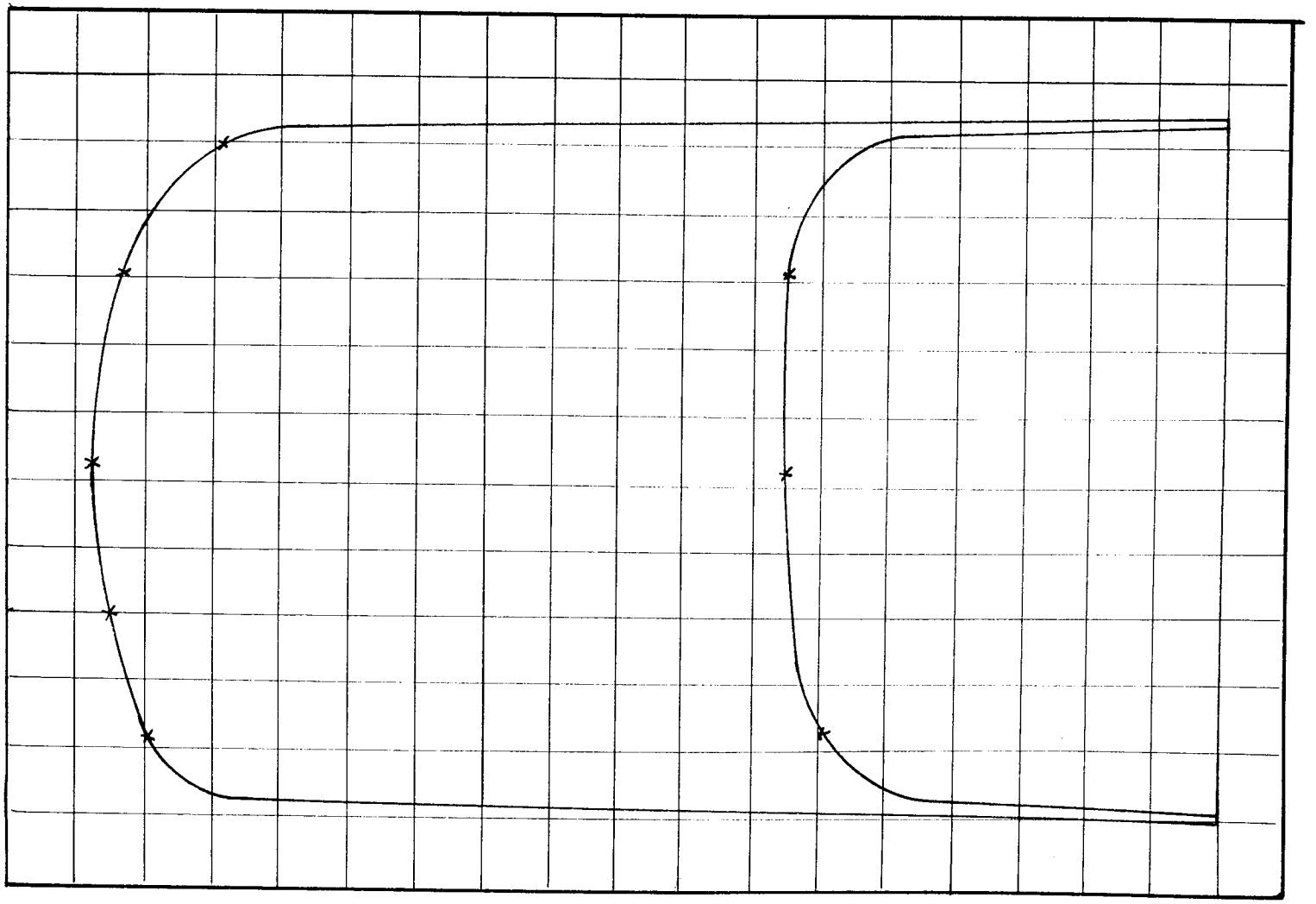

POSITION 1 Scales: Velocity: 1 mm = $\frac{1}{10}$ mm/s

Momentum: 1 mm^2 = $\frac{1}{25}$ kgmm/s

Area under Velocity Curve = 6,630 mm^2

Area under Momentum Curve = 16,170 mm^2

BED MATERIAL: 3 mmDiameter Sand

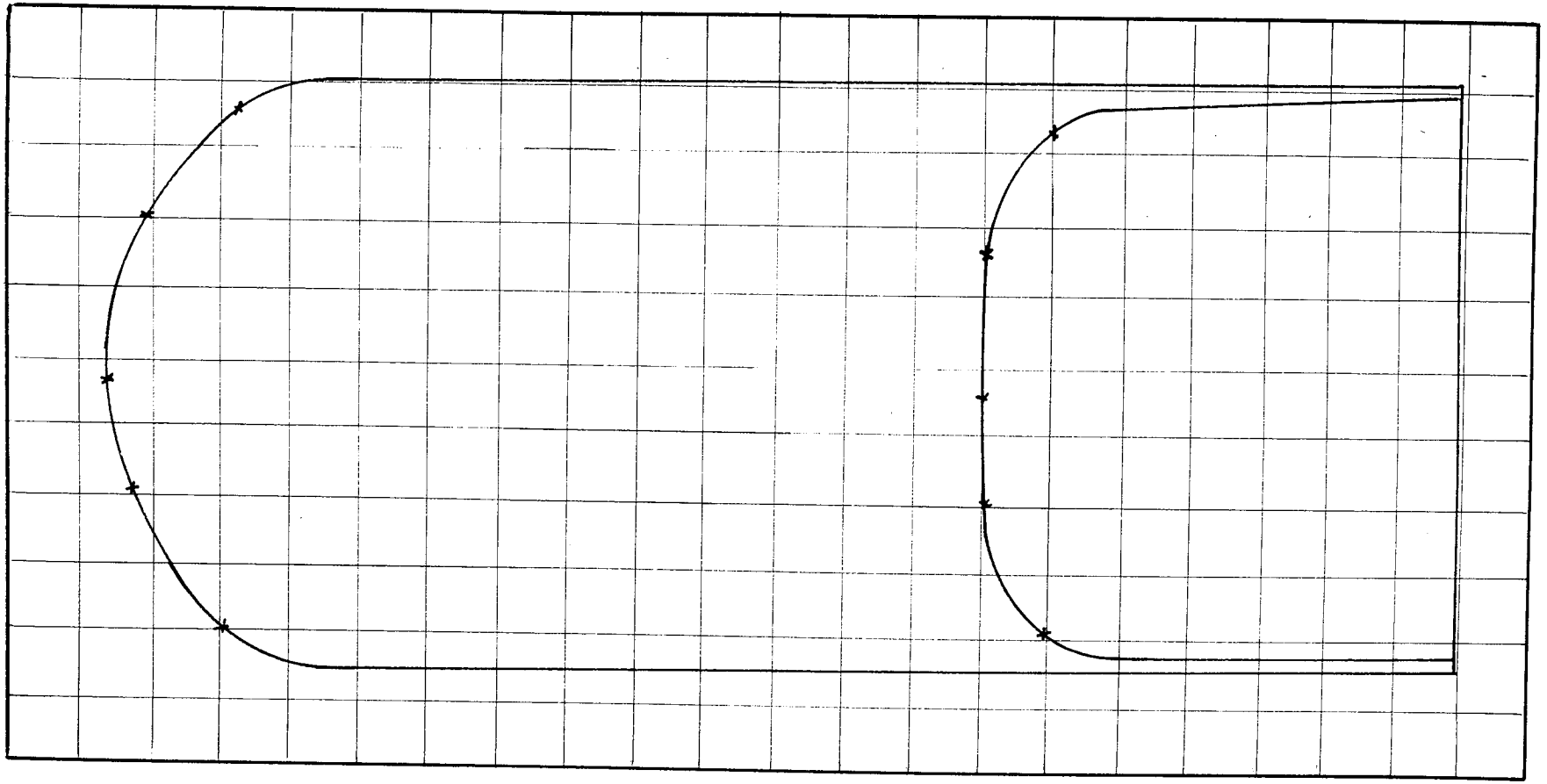

POSITION 2 Scales: Velocity: 1 mm = $\frac{1}{10}$ mm/s Area under Velocity Curve = 5,740 mm^2

Momentum: 1 mm^2 = $\frac{1}{25}$ kgmm/s Area under Momentum Curve = 16,900 mm^2

BED MATERIAL: 3 mm Diameter Sand

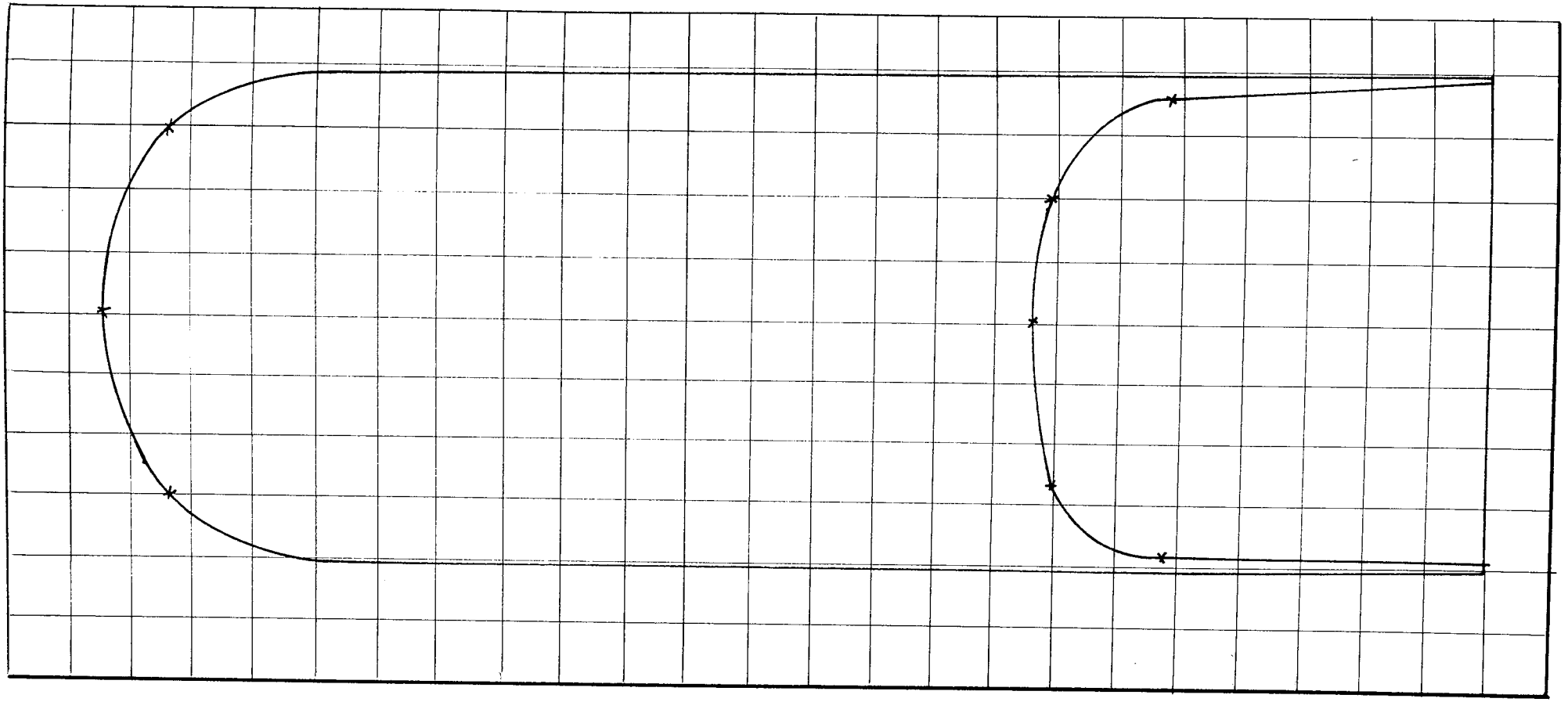

POSITION 3 Scales: Velocity: 1 mm = $\frac{1}{10}$ mm/s Area under Velocity Curve = 5,570 mm^2

Momentum: 1 mm^2 = $\frac{1}{25}$ kgmm/s Area under Momentum Curve = 17,400 mm^2

BED MATERIAL: 3 mm Diameter Sand

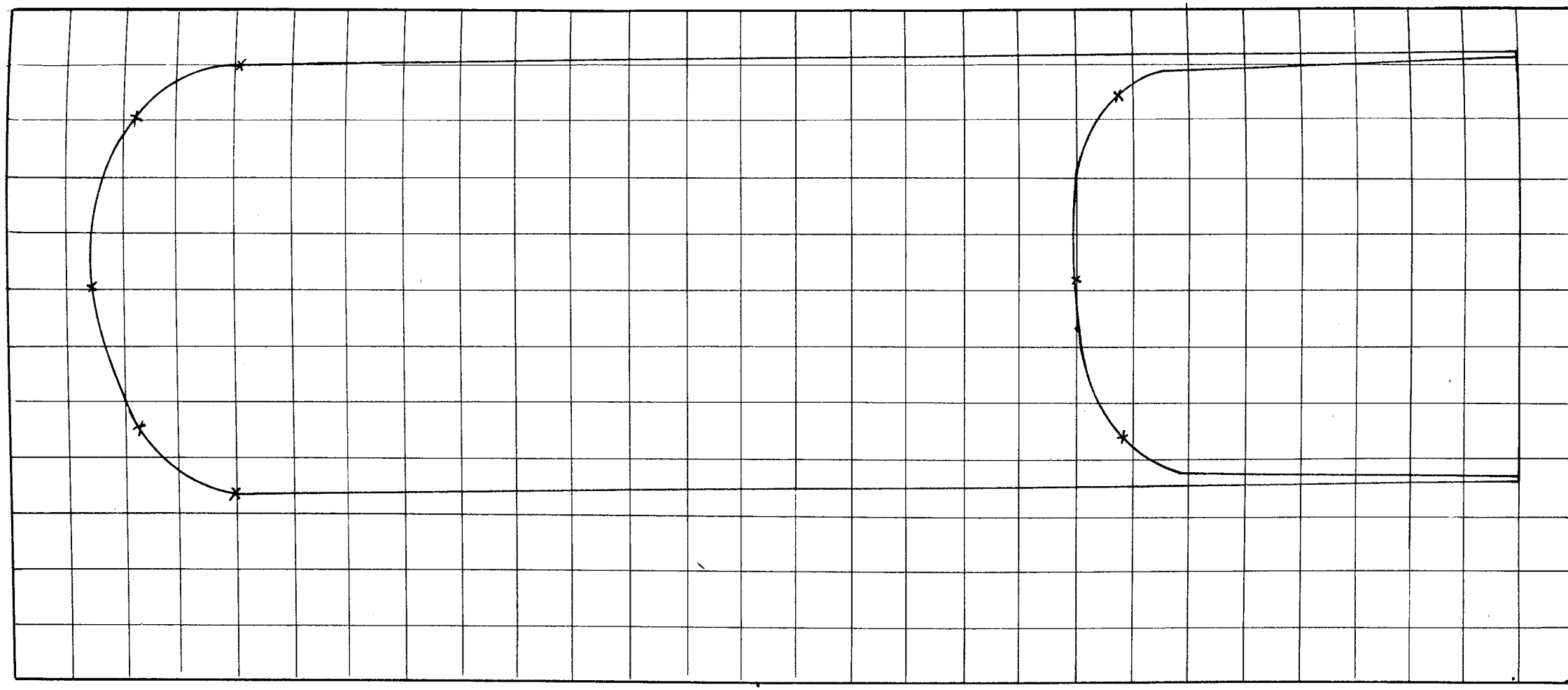

POSITION 4 Scales: Velocity: 1 mm = $\frac{1}{10}$ mm/s Area under Velocity Curve = 5,570 mm^2

Momentum: 1 mm^2 = $\frac{1}{25}$ kgmm/s Area under Momentum Curve = 17,200 mm^2

BED MATERIAL: 3 mm Diameter Sand

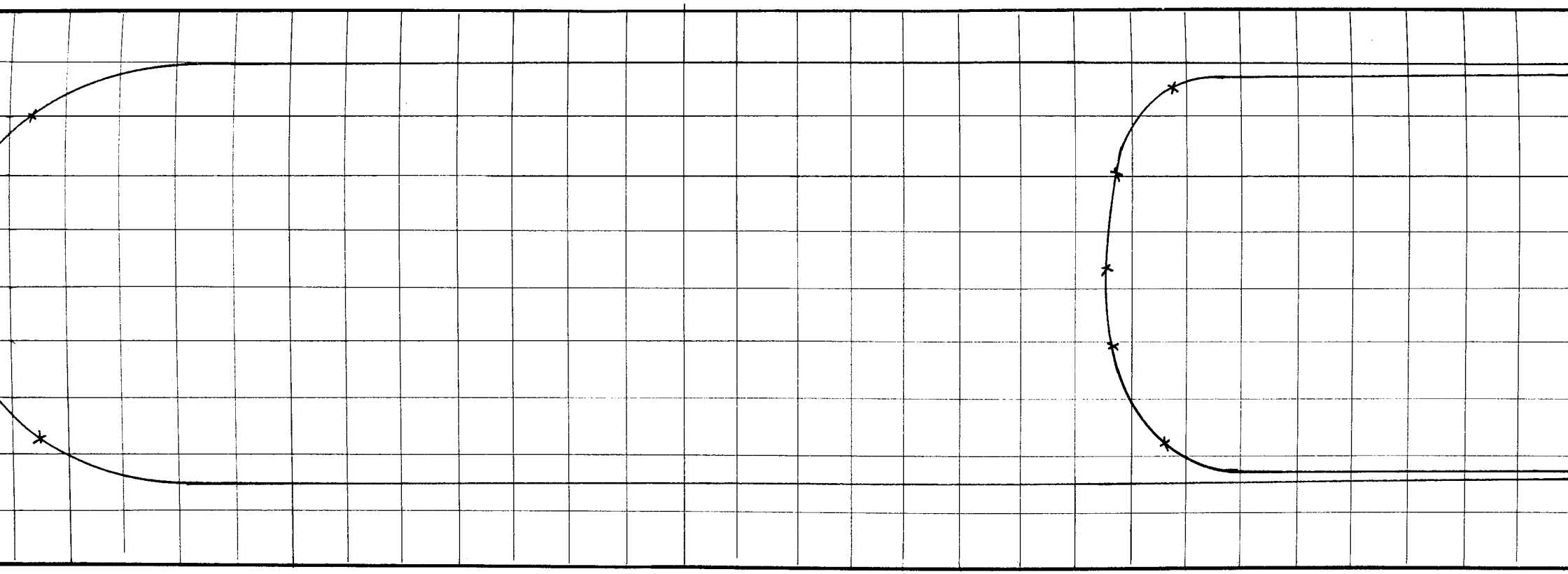

POSITION 5 Scales: Velocity: 1 mm = $\frac{1}{10}$ mm/s Area under Velocity Curve = 6,050 mm^2

Momentum: 1 mm^2 = $\frac{1}{25}$ kgmm/s Area under Momentum Curve = 17,400 mm^2

BED MATERIAL: 3 mm Diameter Sand

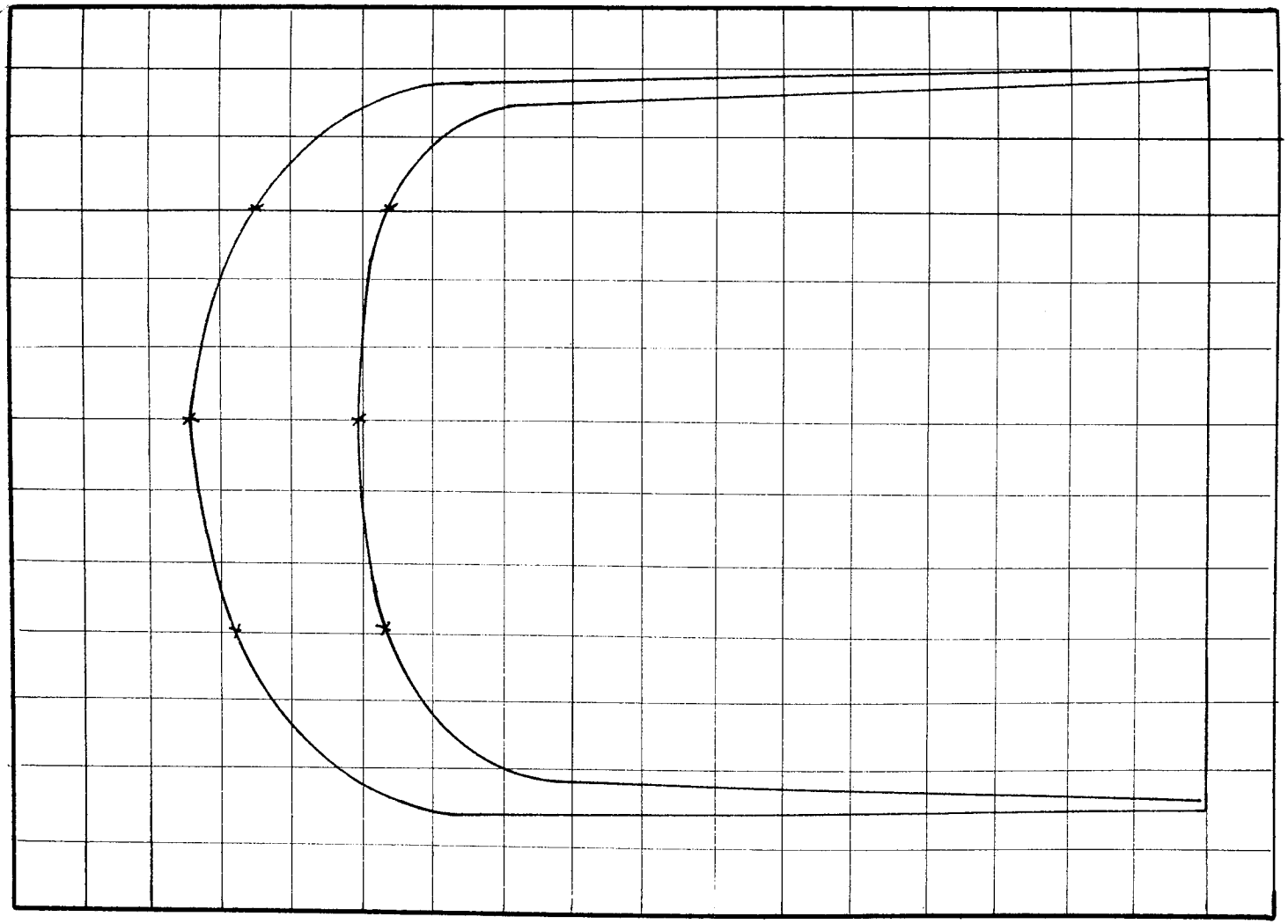

POSITION 1 Scales: Velocity: 1 mm = $\frac{1}{5}$ mm/s Area under Velocity Curve = 14,130 mm^2

Momentum: 1 mm^2 = $\frac{1}{25}$ kgmm/s Area under Momentum Curve = 10,100 mm^2

BED MATERIAL: 3 mm Diameter Sand

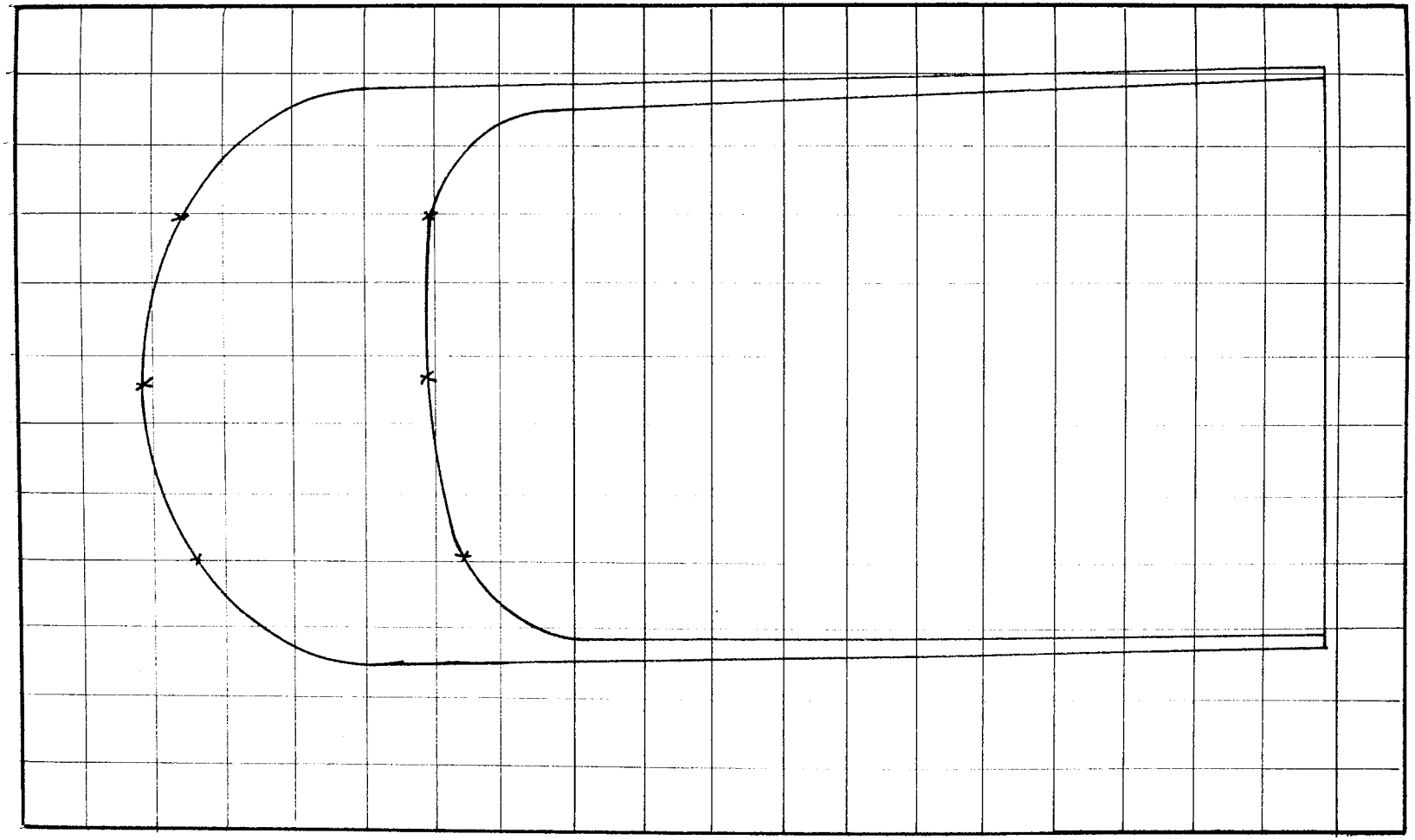

POSITION 2 Scales: Velocity: 1 mm = $\frac{1}{5}$ mm/s Area under Velocity Curve = 10,500 mm^2

Momentum: 1 mm^2 = $\frac{1}{25}$ kgmm/s Area under Momentum Curve = 14,100 mm^2

BED MATERIAL: 3 mm Diameter Sand

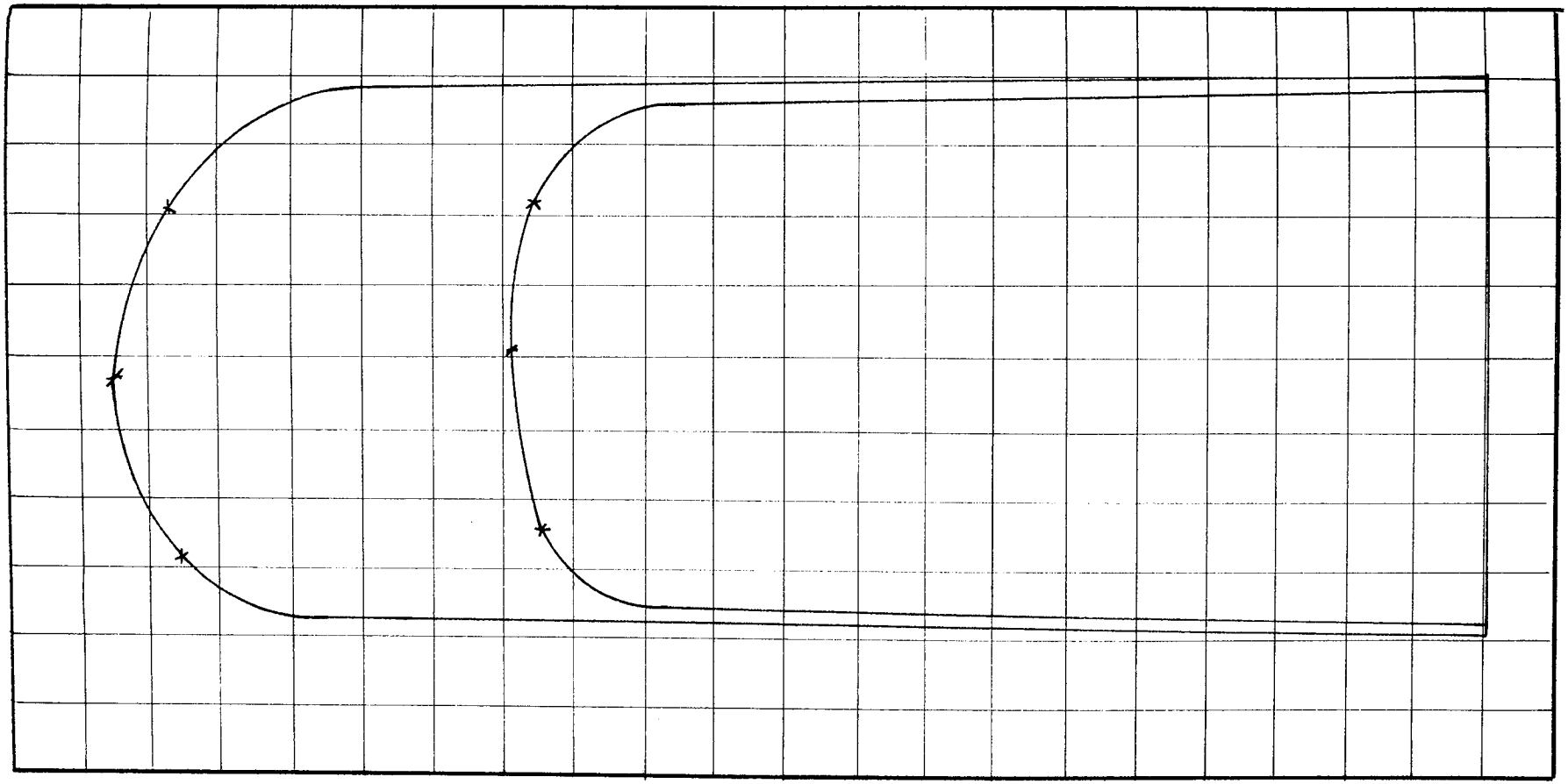

POSITION 3 Scales: Velocity: 1 mm = $\frac{1}{5}$ mm/s Area under Velocity Curve = 10,400 mm^2

Momentum: 1 mm^2 = $\frac{1}{25}$ kgmm/s Area under Momentum Curve = 14,500 mm^2

BED MATERIAL: 3 mm Diameter Sand

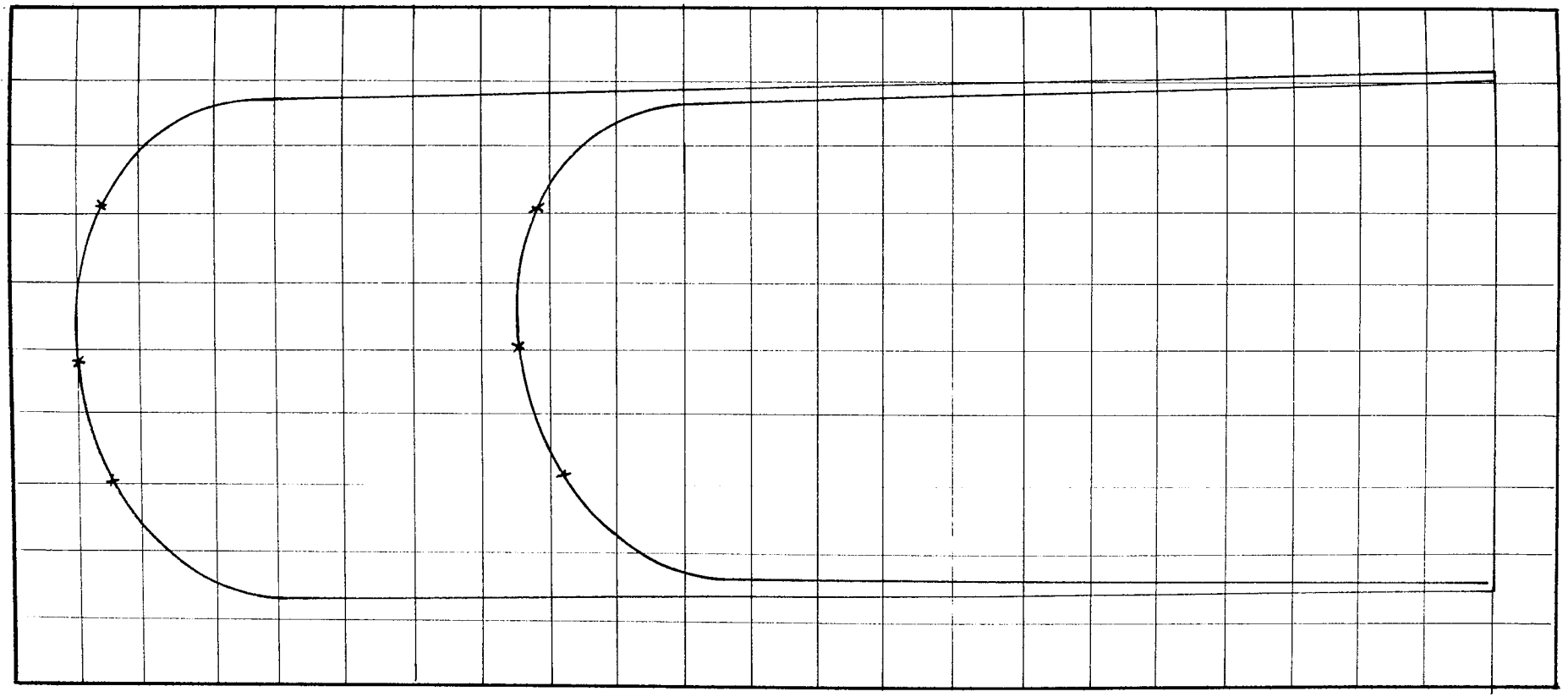

POSITION 4 Scales: Velocity: 1 mm = $\frac{1}{5}$ mm/s Area under Velocity Curve = 10,300 mm^2

Momentum: 1 mm^2 = $\frac{1}{25}$ kgmm/s Area under Momentum Curve = 14,100 mm^2

BED MATERIAL: 3 mm Diameter Sand

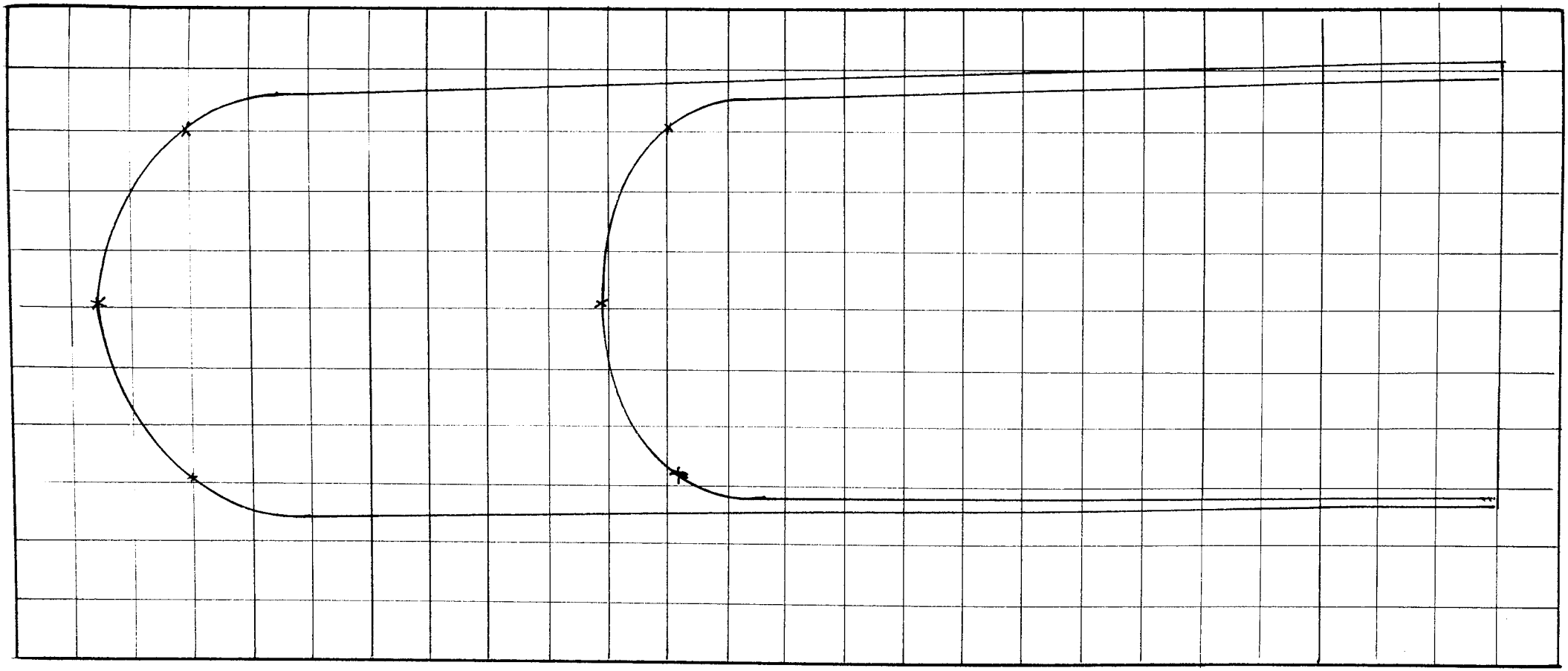

POSITION 5 Scales: Velocity: 1mm = $\frac{1}{5}$ mm/s Area under Velocity Curve = 10,200 mm^2

Momentum: 1 mm^2 = $\frac{1}{25}$ kgmm/s Area under Momentum Curve = 14,950 mm^2

BED MATERIAL: 3 mmDiameter Sand

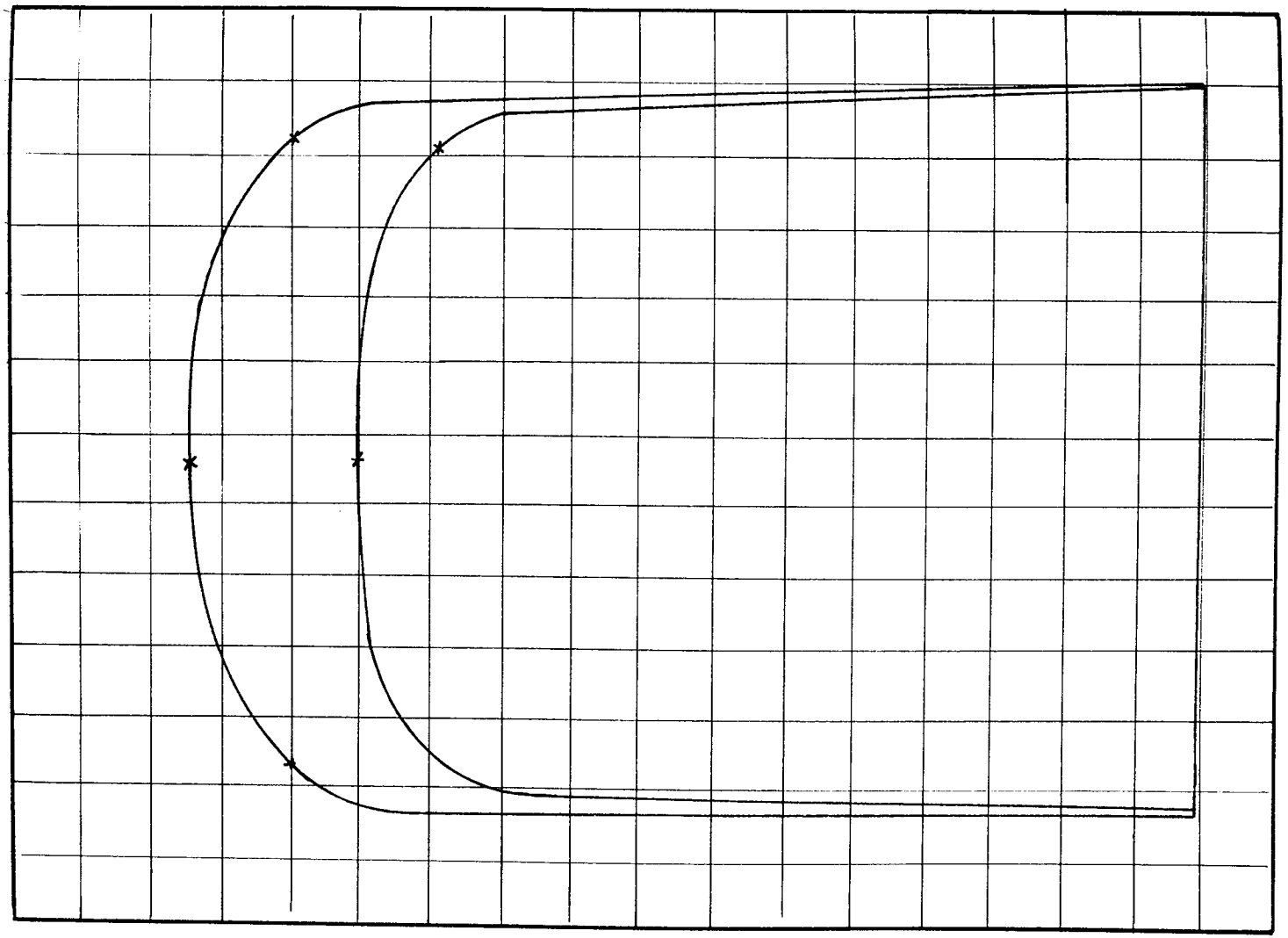

POSITION 1 Scales: Velocity: 1 mm = $\frac{1}{5}$ mm/s Area under Velocity Curve = 10,500 mm^2

Momentum: 1 mm^2 = $\frac{1}{25}$ kgmm/s Area under Momentum Curve = 14,650 mm^2

BED MATERIAL: 3 mm Diameter Sand

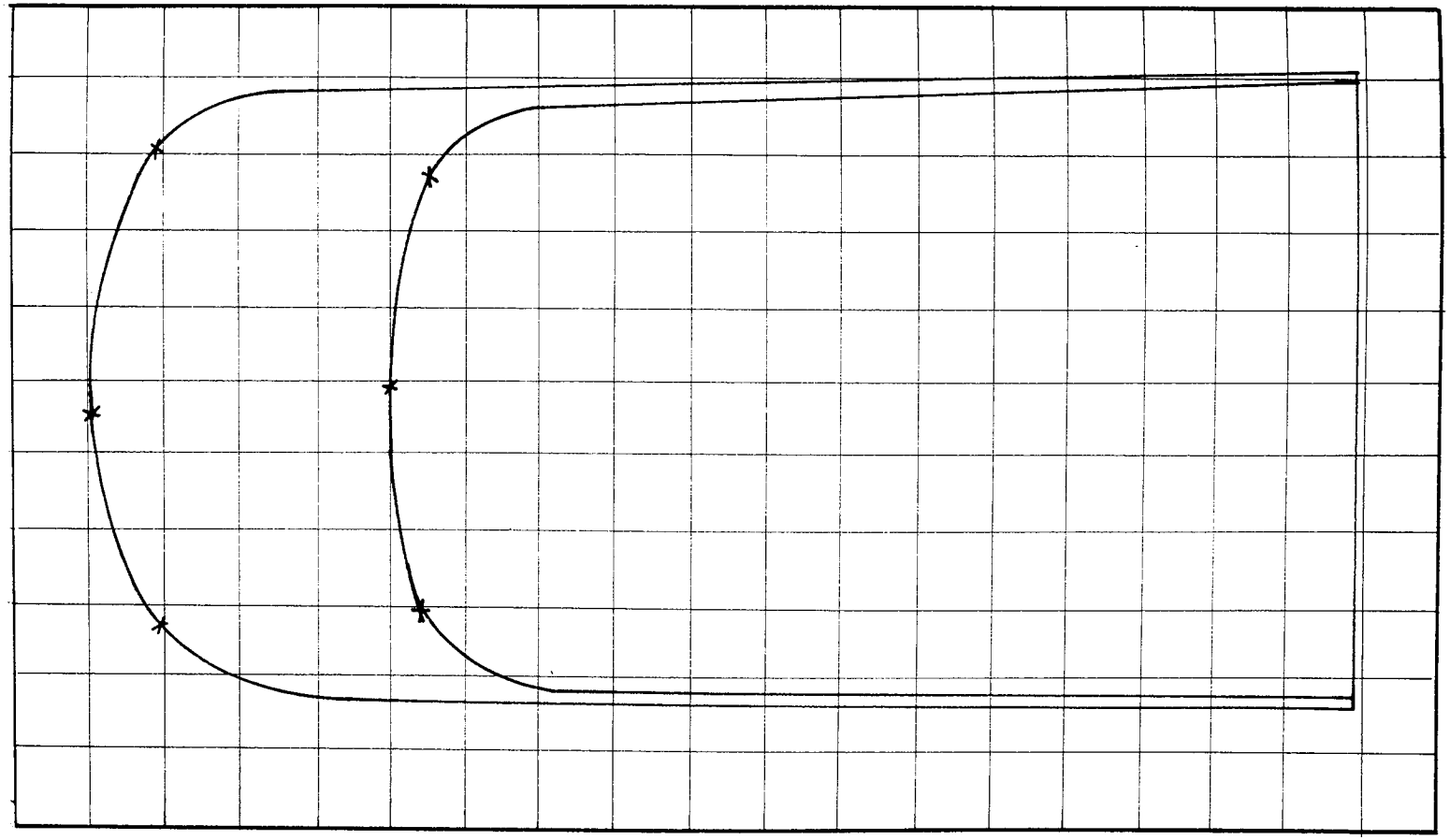

POSITION 2 Scales: Velocity: 1 mm = $\frac{1}{5}$ mm/s Area under Velocity Curve = 10,000 mm^2

Momentum: 1 mm^2 = $\frac{1}{25}$ kgmm/s Area under Momentum Curve = 14,500 mm^2

BED MATERIAL: 3 mm Diameter Sand

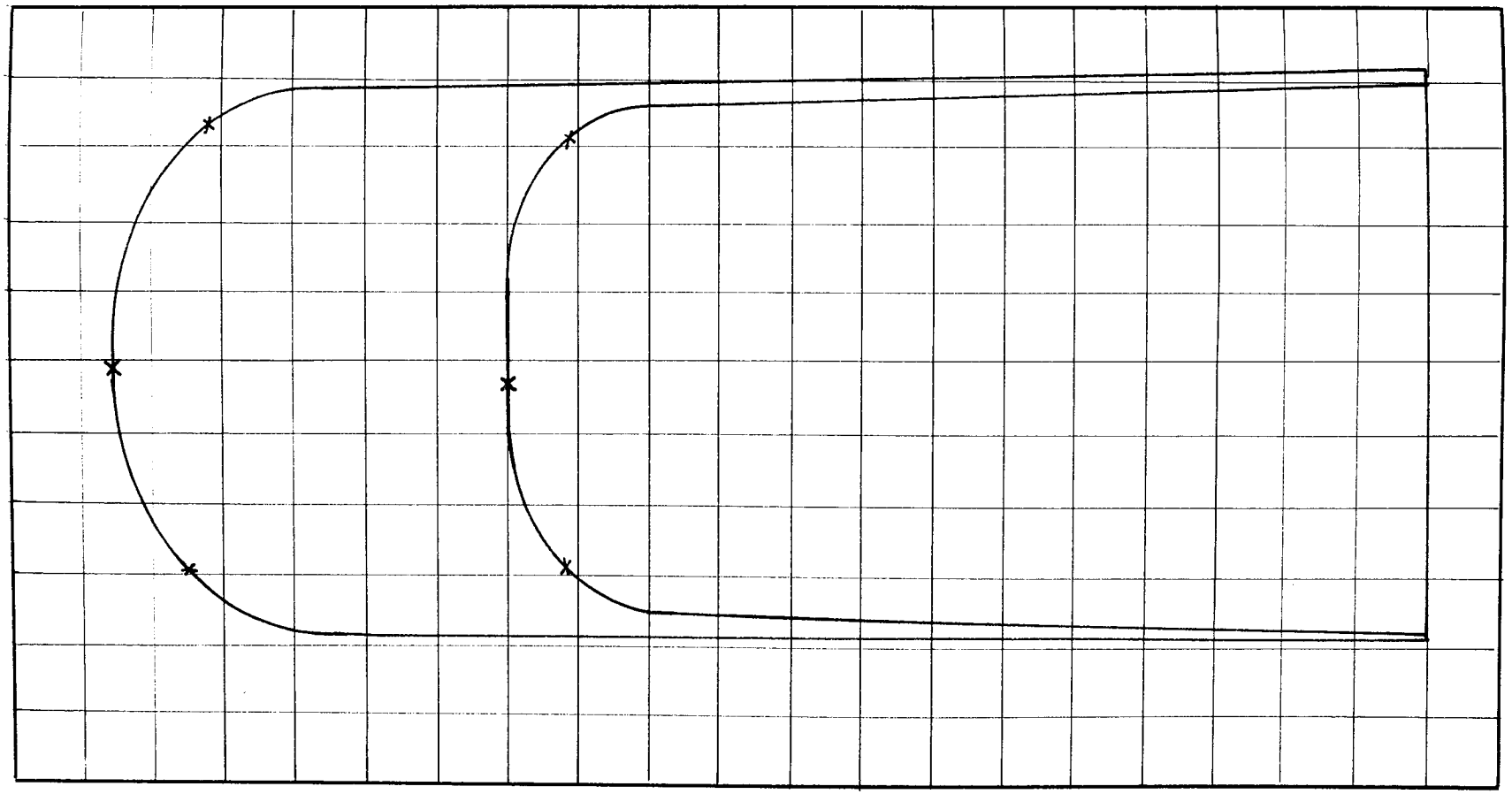

POSITION 3 Scales: Velocity: 1 mm = $\frac{1}{5}$ mm/s

Momentum: 1 mm^2 = $\frac{1}{25}$ kgmm/s

Area under Velocity Curve = 10,000 mm^2

Area under Momentum Curve = 14,950 mm^2

BED MATERIAL: 3 mm Diameter Sand

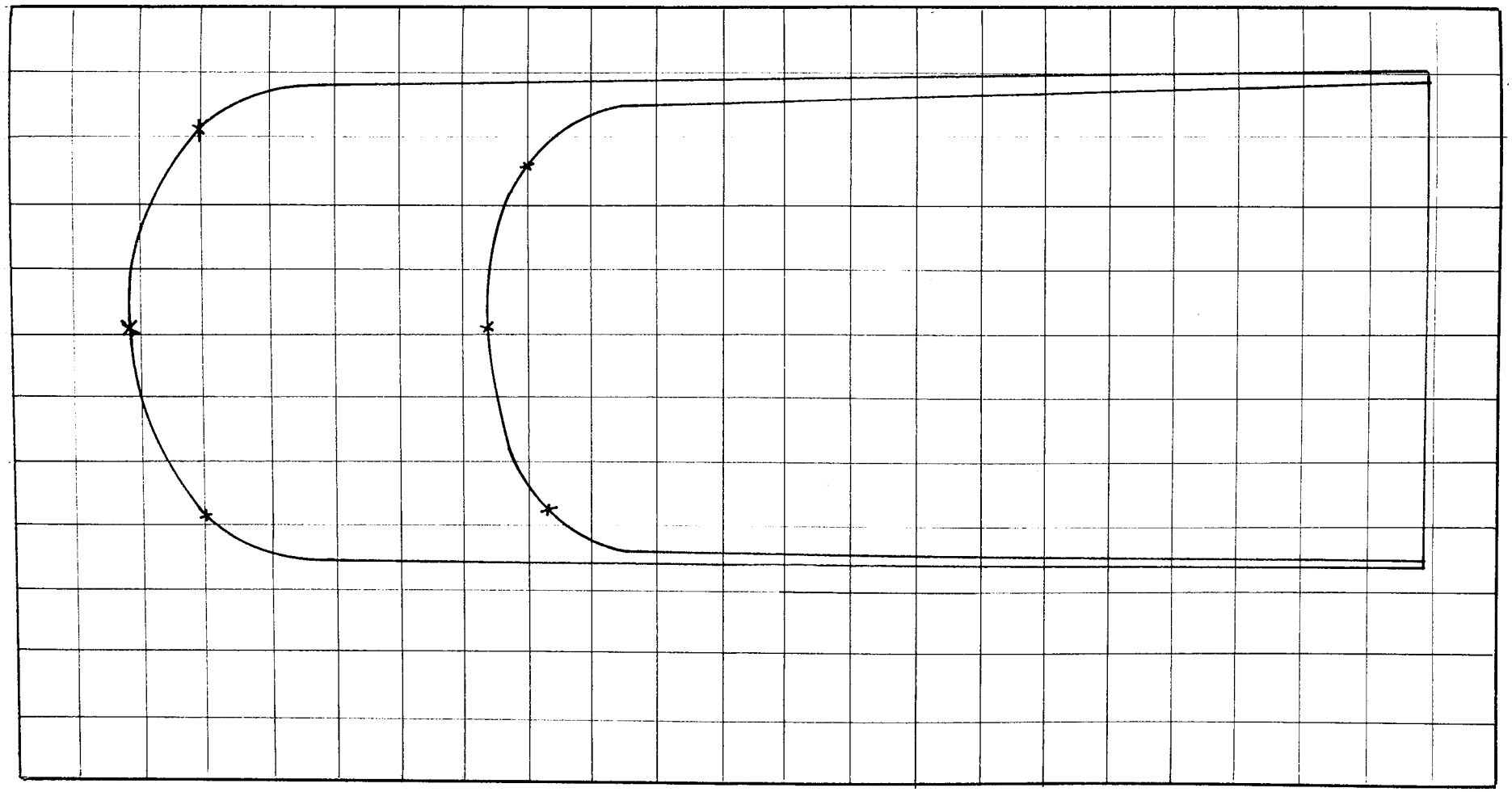

POSITION 4 Scales: Velocity: 1 mm = $\frac{1}{5}$ mm/s Area under Velocity Curve = 10,320 mm^2

Momentum: 1 mm^2 = $\frac{1}{25}$ kgmm/s Area under Momentum Curve = 15,000 mm^2

BED MATERIAL: 3 mm Diameter Sand

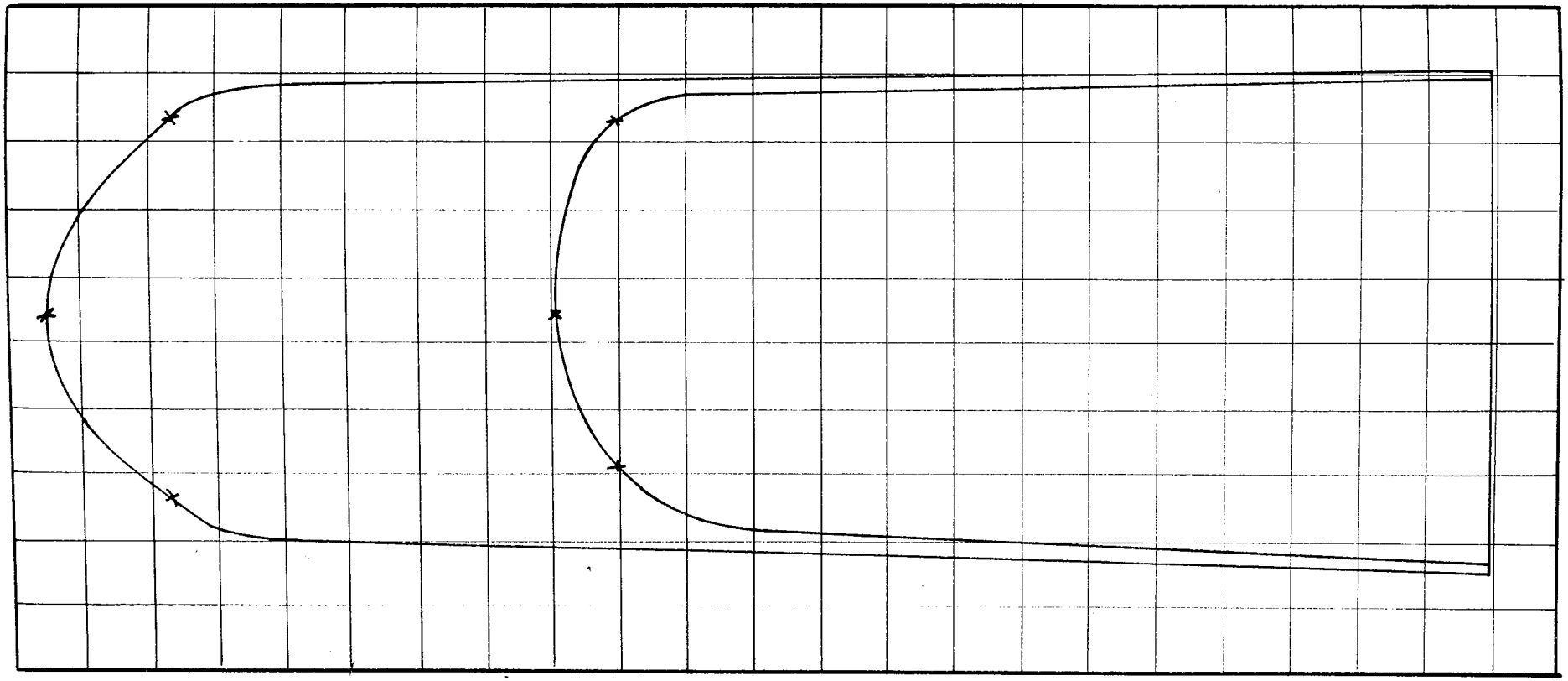

POSITION 5 Scales: Velocity: 1 mm = $\frac{1}{5}$ mm/s Area under Velocity Curve = 9,850 mm^2

Momentum: 1 mm^2 = $\frac{1}{25}$ kgmm/s Area under Momentum Curve = 15,000 mm^2

BED MATERIAL: 3 mm Diameter Sand

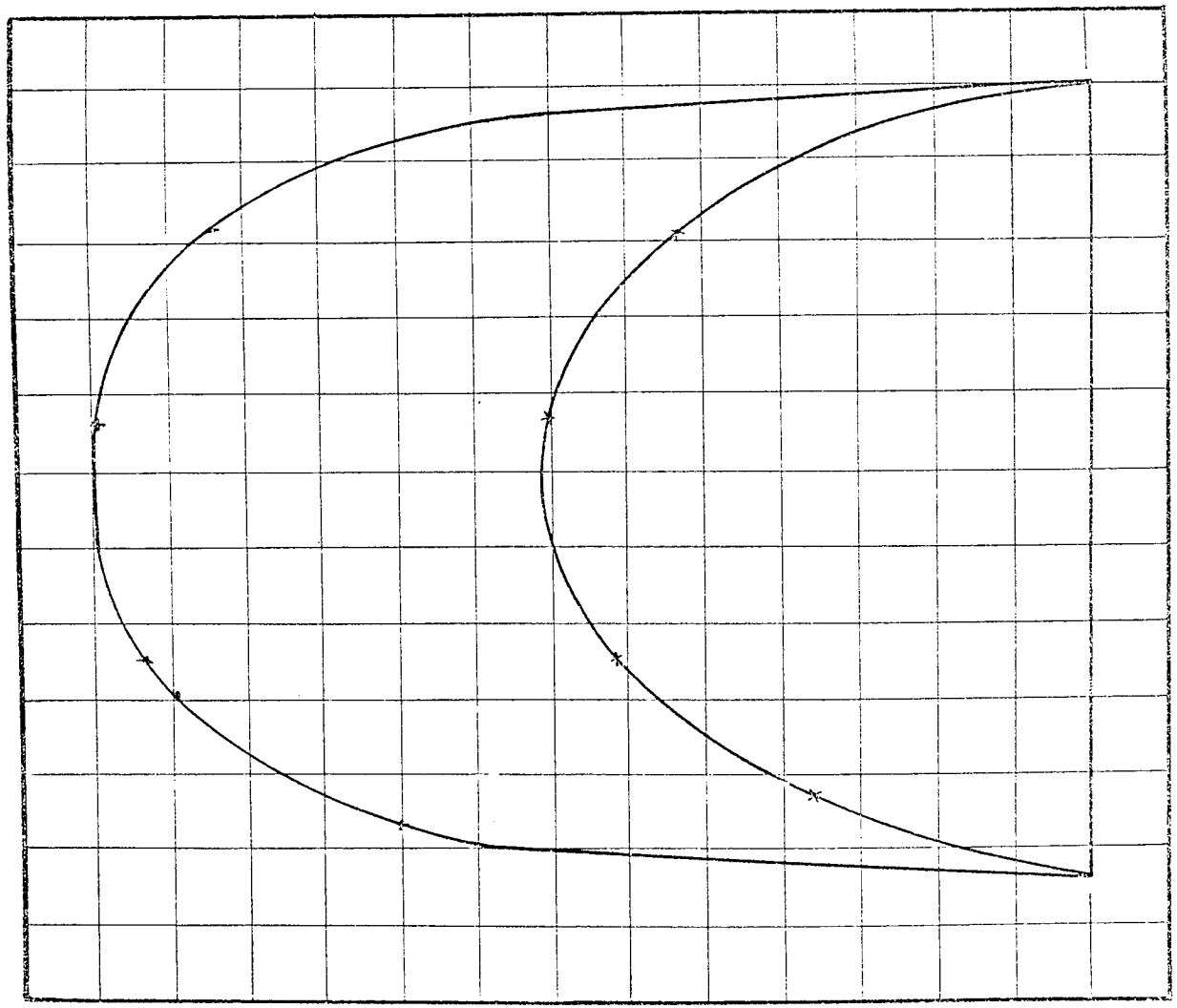

POSITION 1 Scales: Velocity: 1 mm = 1 mm/s Area under Velocity Curve = 5,640 mm^2

Momentum: 1 mm^2 = $\frac{1}{3}$ kgmm/s Area under Momentum Curve = 11, 00 mm^2

BED MATERIAL: 3 mm Diameter Sand

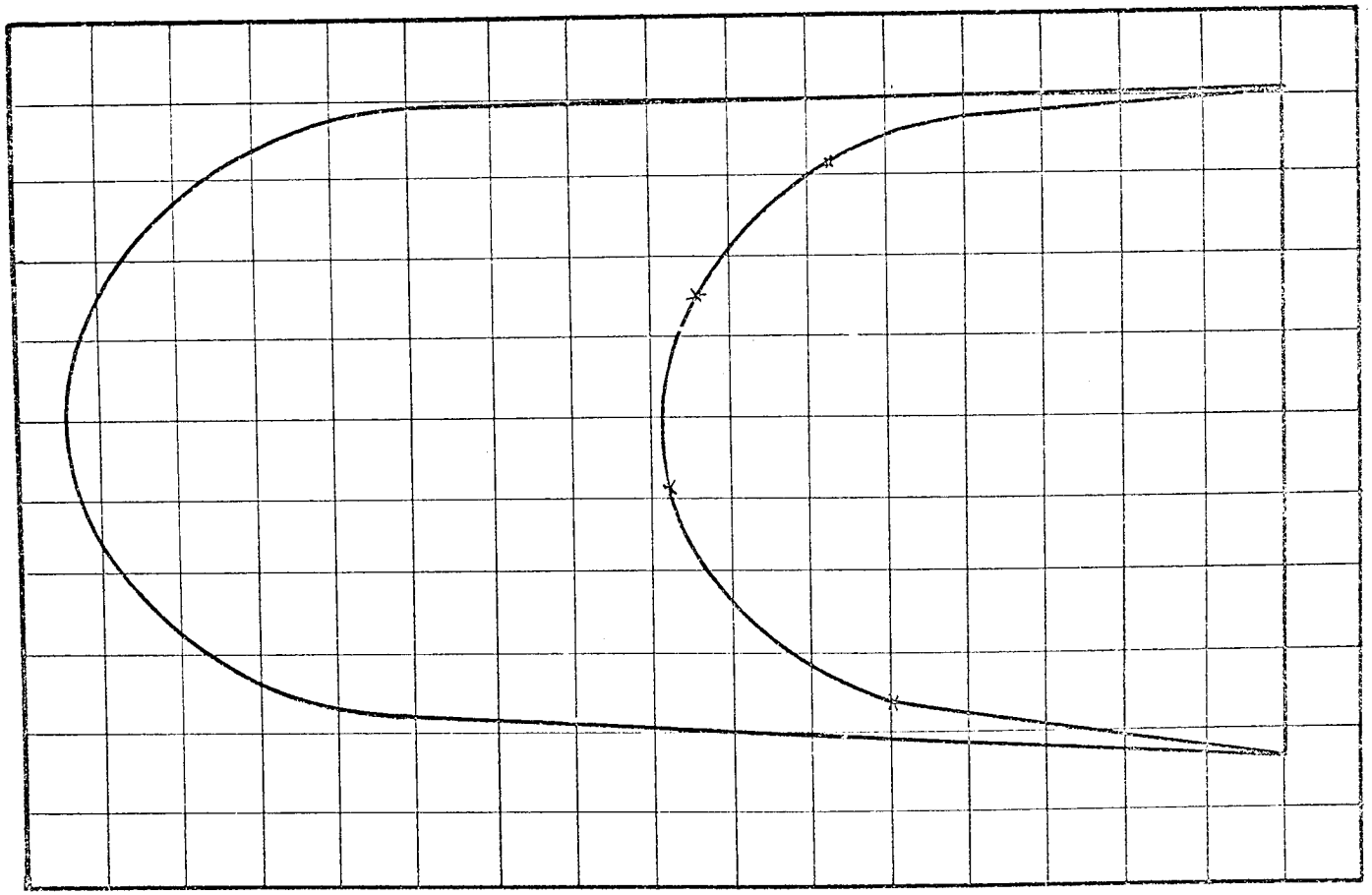

POSITION 2 Scales: Velocity: 1 mm = 1 mm/s Area under Velocity Curve = 5,720 mm^2

Momentum: 1 mm^2 = $\frac{1}{3}$ kgmm/s Area under Momentum Curve = 11,900 mm^2

BED MATERIAL : 3 mm Diameter Sand

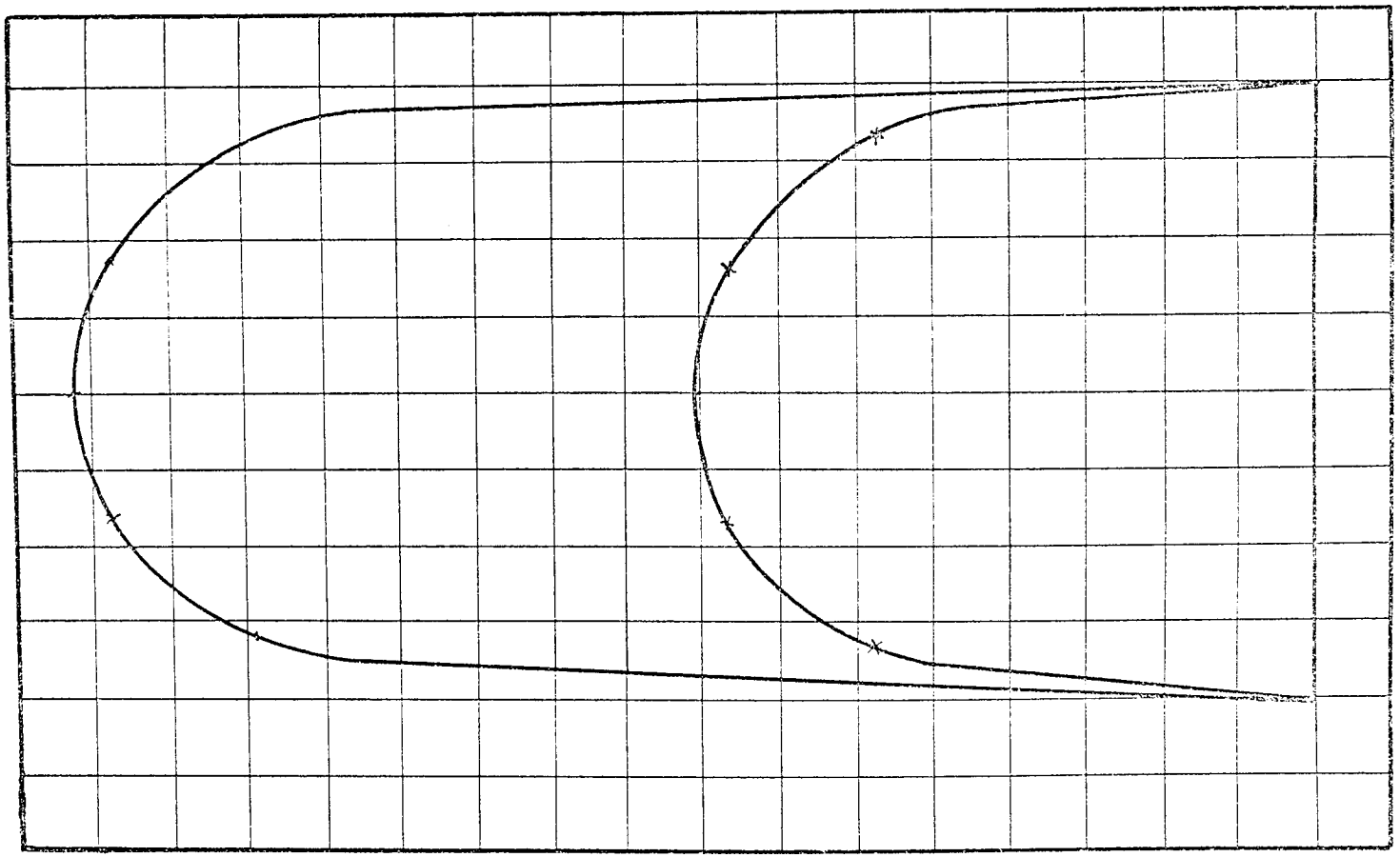

POSITION 3 Scales: Velocity: 1 mm = 1 mm/s Area under Velocity Curve = 5,300 mm^2

Momentum: 1 mm^2 = $\frac{1}{3}$ kgmm/s Area under Momentum Curve = 11,600 mm^2

BED MATERIAL: 3 mm Diameter Sand

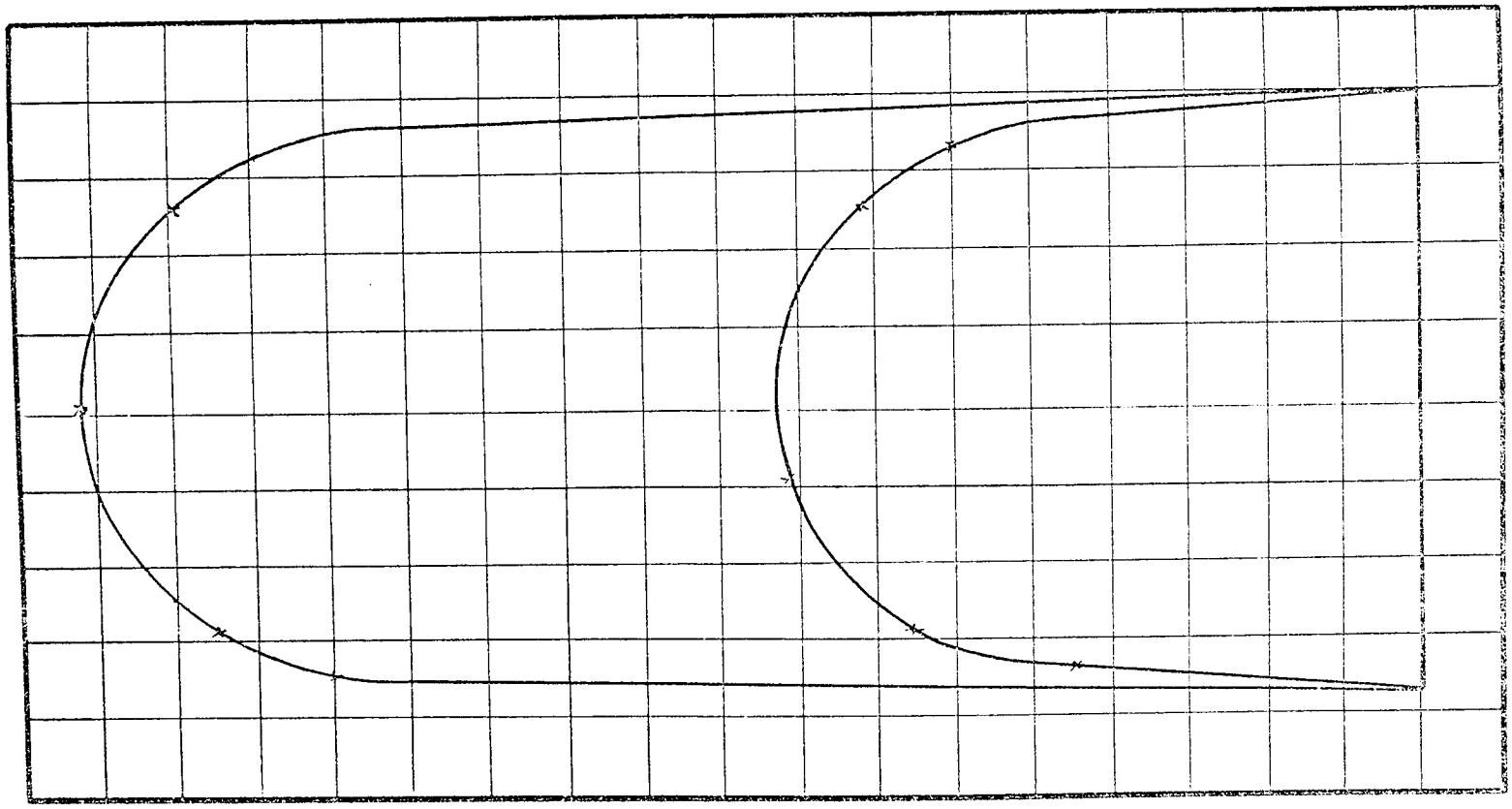

POSITION 4 Scales: Velocity: 1 mm = 1 mm/s Area under Velocity Curve = 5,550 mm^2

Momentum: 1 mm^2 = $\frac{1}{3}$ kgmm/s Area under Momentum Curve = 11,700 mm^2

BED MATERIAL: 3 mm Diameter Sand

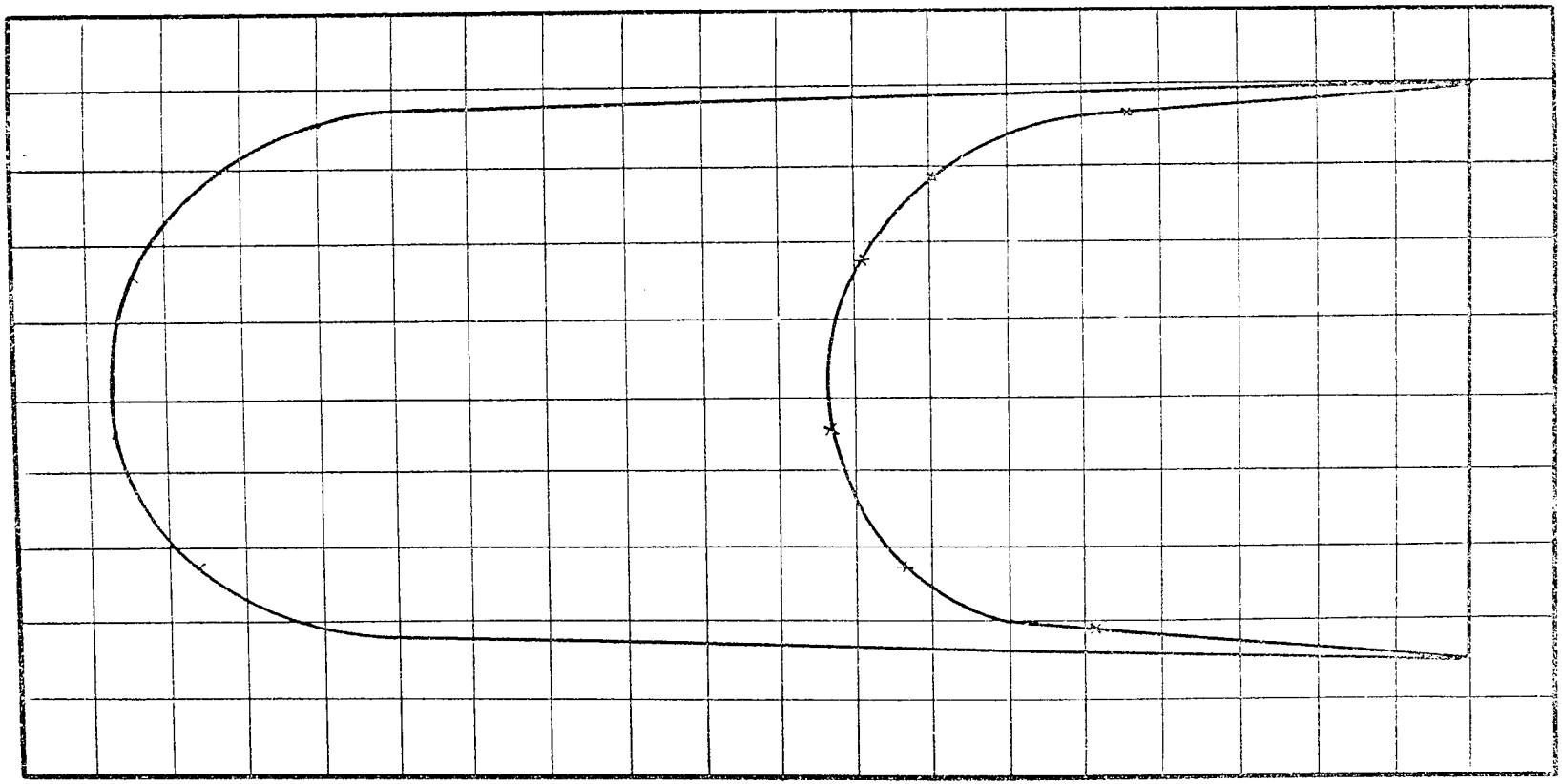

POSITION 5 Scales: Velocity : 1 mm = 1 mm/s Area under Velocity Curve = 5,750 mm^2

Momentum : 1 mm^2 = $\frac{1}{3}$ kgmm/s Area under Momentum Curve = 12,000 mm^2

BED MATERIAL: 3 mm Diameter Sand

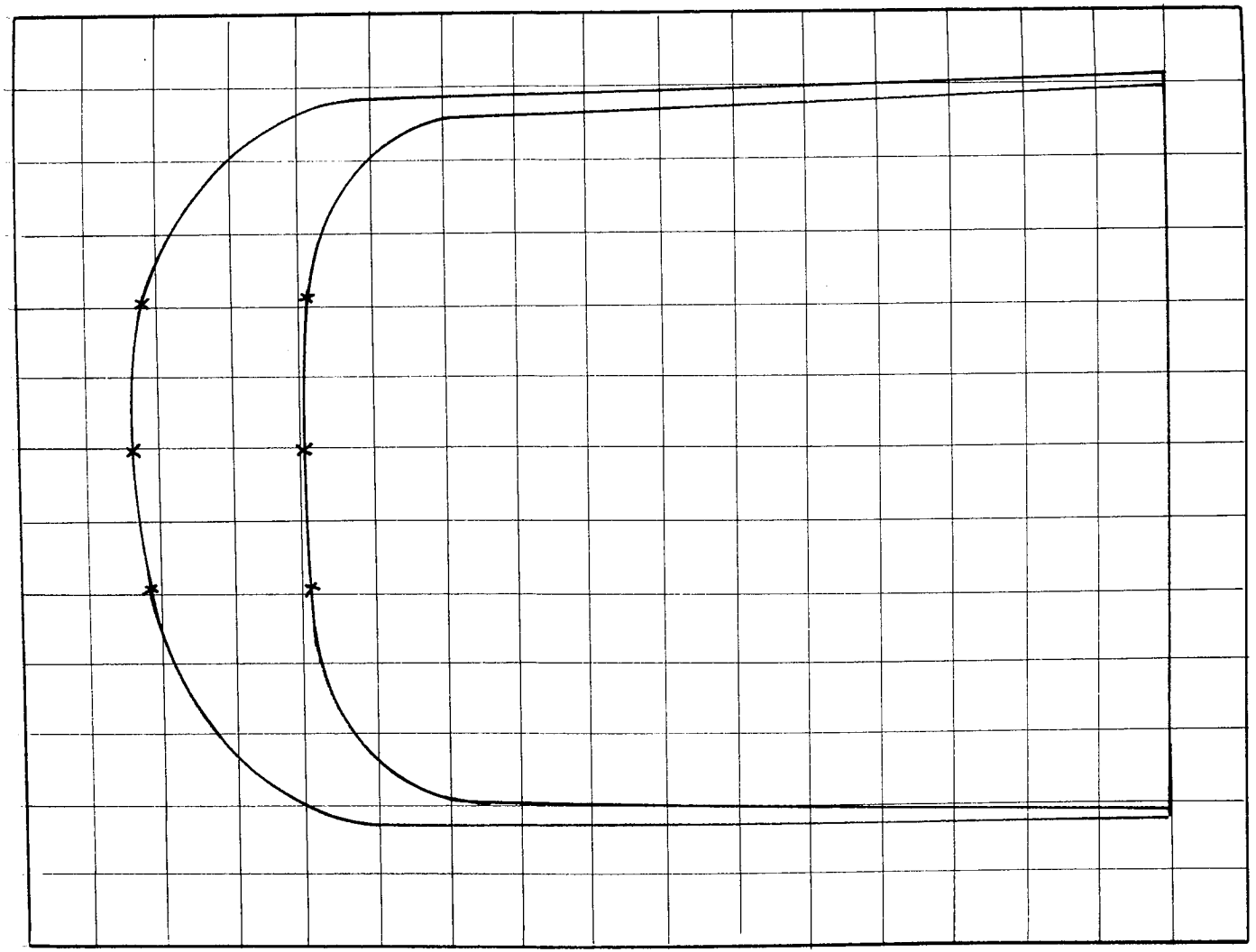

POSITION 1 Scales: Velocity: 1 mm = $\frac{1}{5}$ mm/s Area under Velocity Curve = 10,300 mm^2

Momentum: 1 mm^2 = $\frac{1}{25}$ kgmm/s Area under Momentum Curve = 13,960 mm^2

BED MATERIAL 3 mm Diameter Sand

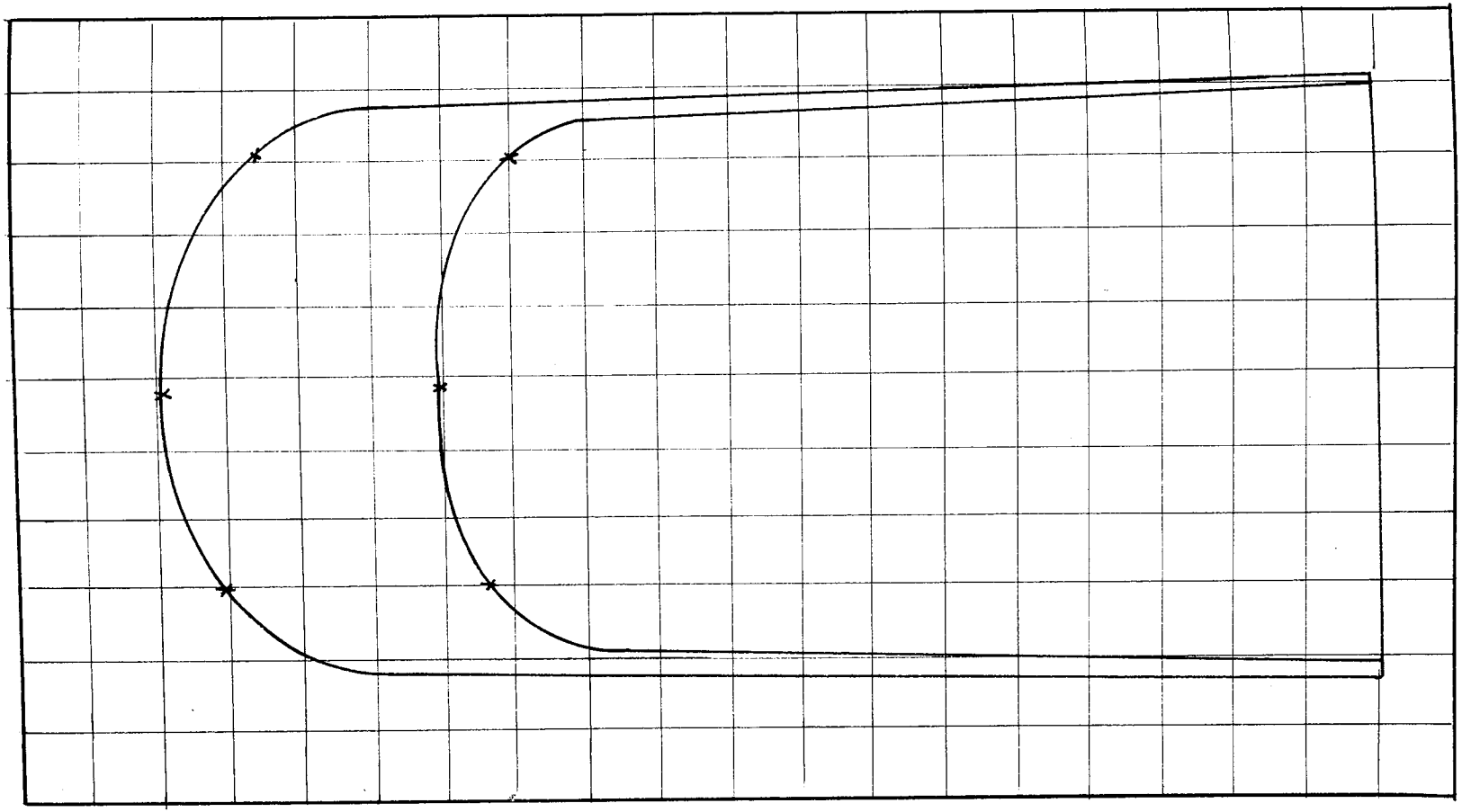

POSITION 2 Scales: Velocity: 1 mm = $\frac{1}{5}$ mm/s Area under Velocity Curve = 9,800 mm^2

Momentum: 1 mm^2 = $\frac{1}{25}$ kgmm/s Area under Momentum Curve = 13,300 mm^2

BED MATERIAL 3 mm Diameter Sand

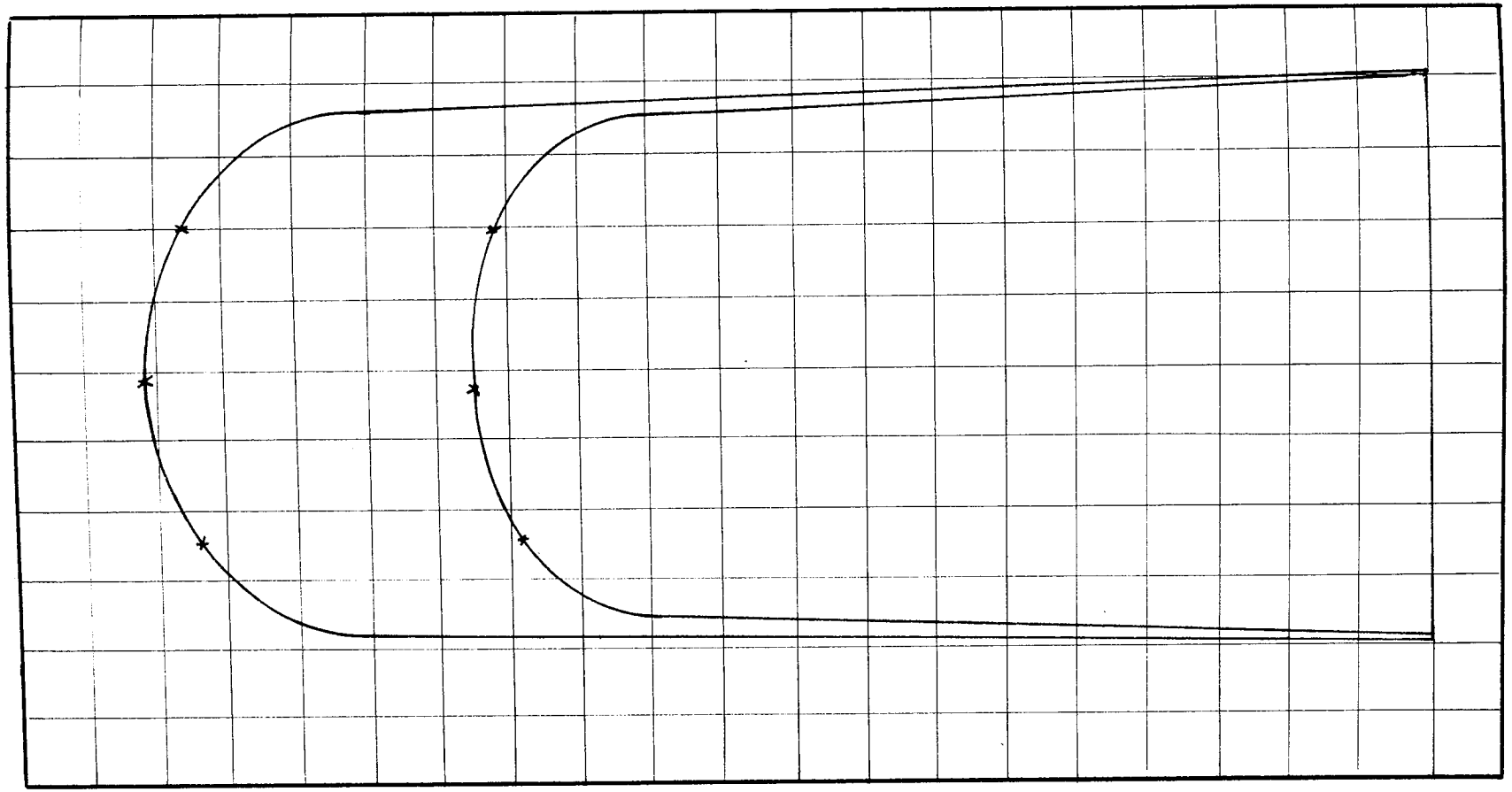

POSITION 3 Scales: Velocity: 1 mm = $\frac{1}{5}$ mm/s Area under Velocity Curve = 10,200 mm^2

Momentum: 1 mm^2 = $\frac{1}{25}$ kgmm/s Area under Momentum Curve = 13,600 mm^2

BED MATERIAL: 3 mm Diameter Sand

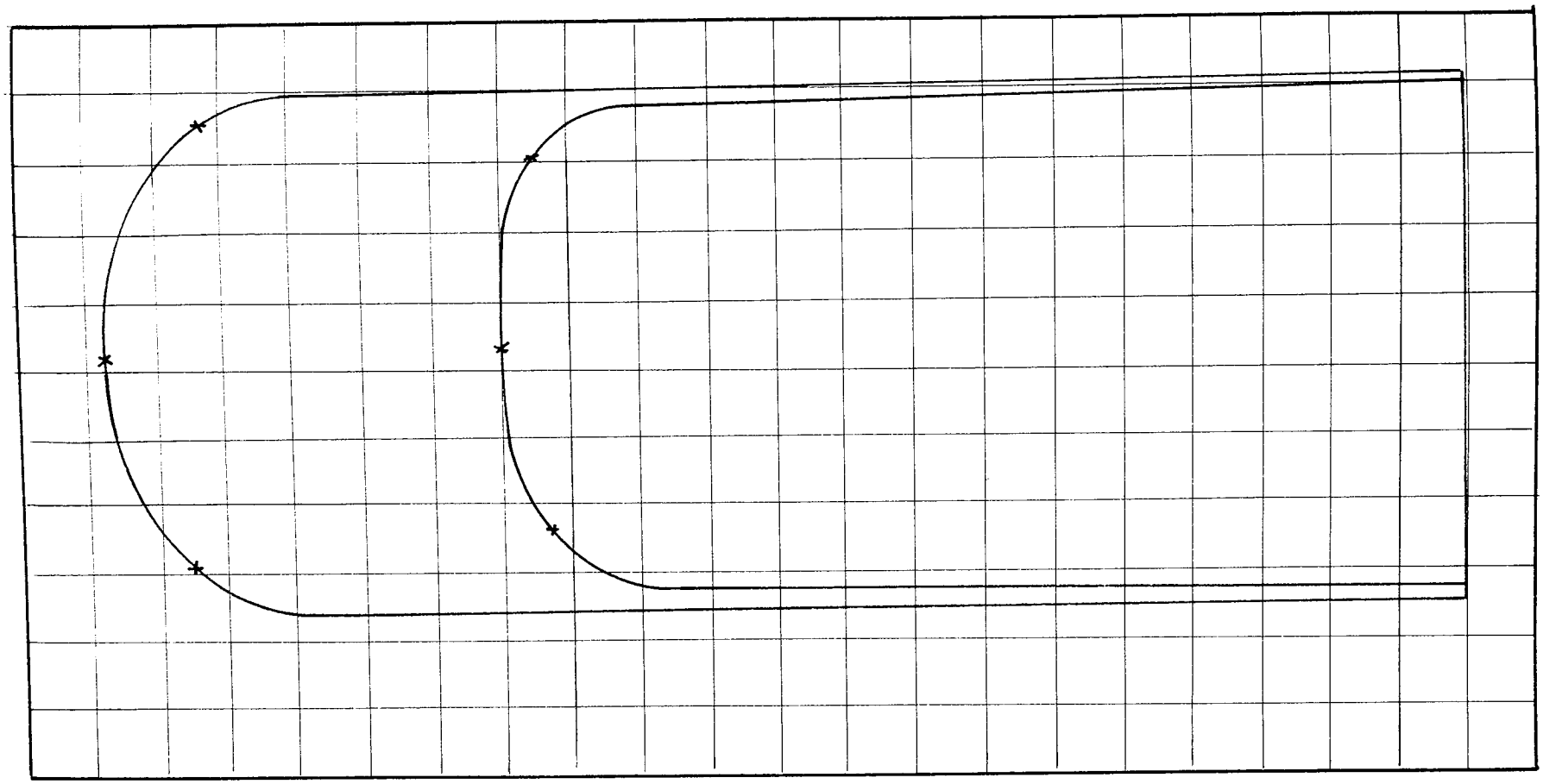

POSITION 4 Scales: Velocity: 1 mm = $\frac{1}{5}$ mm/s Area under Velocity Curve = 9,700 mm^2

Momentum: 1 mm^2 = $\frac{1}{25}$ kgmm/s Area under Momentum Curve = 14,100 mm^2

BED MATERIAL: 3 mm Diameter Sand

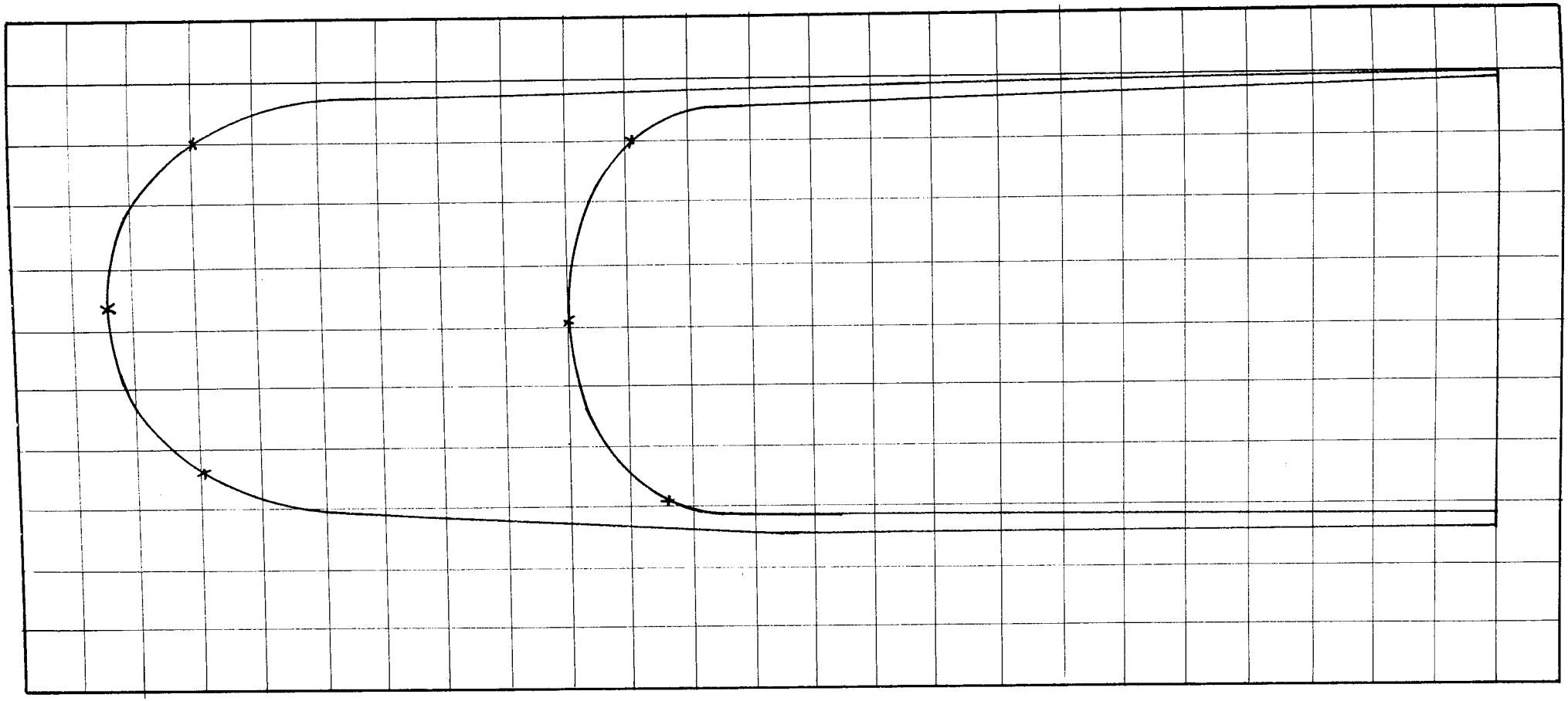

POSITION 5 Scales: Velocity; 1 mm = $\frac{1}{5}$ mm/s Area under Velocity Curve = 10,170 mm^2

Momentum: 1 mm^2 = $\frac{1}{25}$ kgmm/s Area under Momentum Curve = 14,200 mm^2

BED MATERIAL: 3 mm Diameter Sand

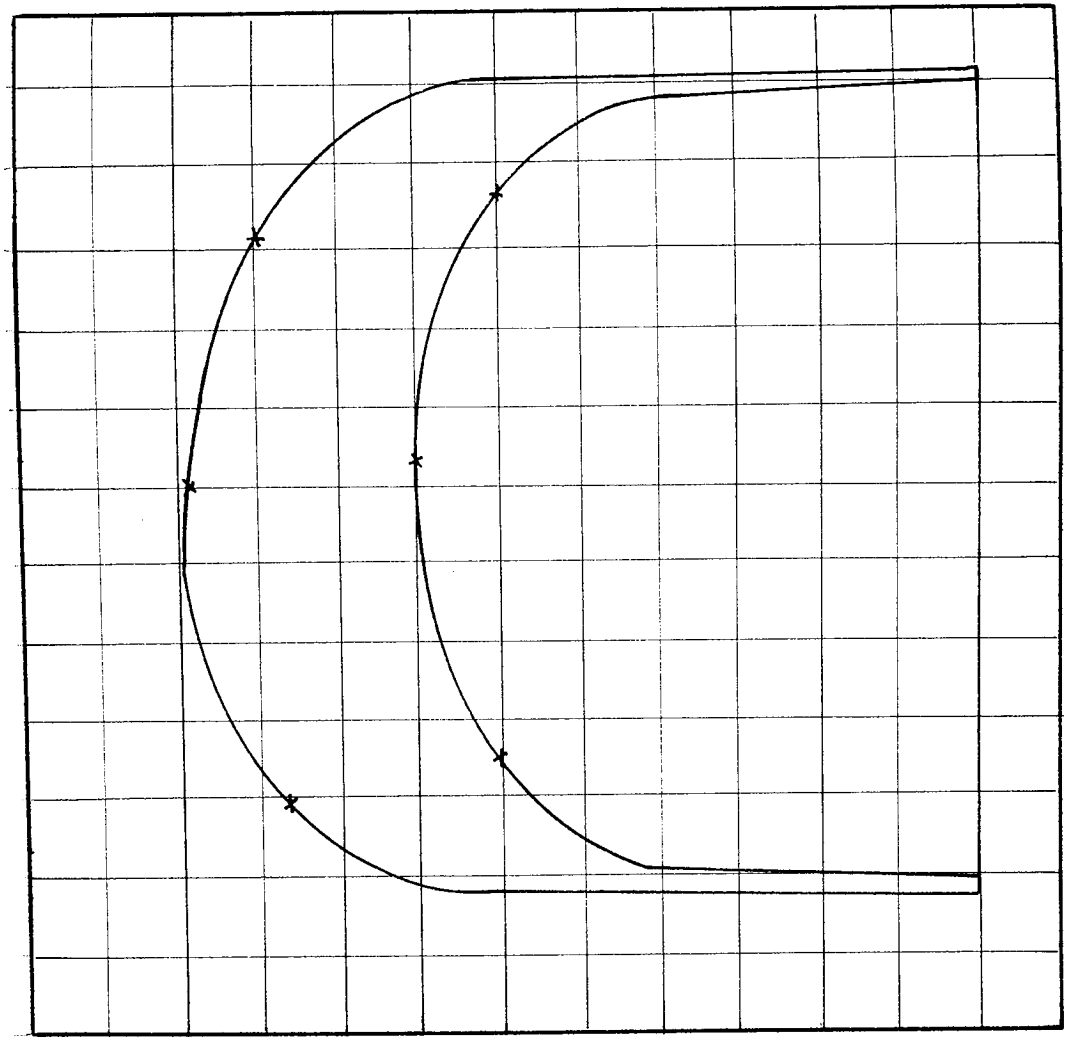

POSITION 1 Scales: Velocity: 1 mm = $\frac{1}{5}$ mm/s Area under Velocity Curve = 6,410 mm^2

Momentum: 1 mm^2 = $\frac{1}{25}$ kgmm/s Area under Momentum Curve = 9,800 mm^2

BED MATERIAL: 3 mm Diameter Glass Spheres

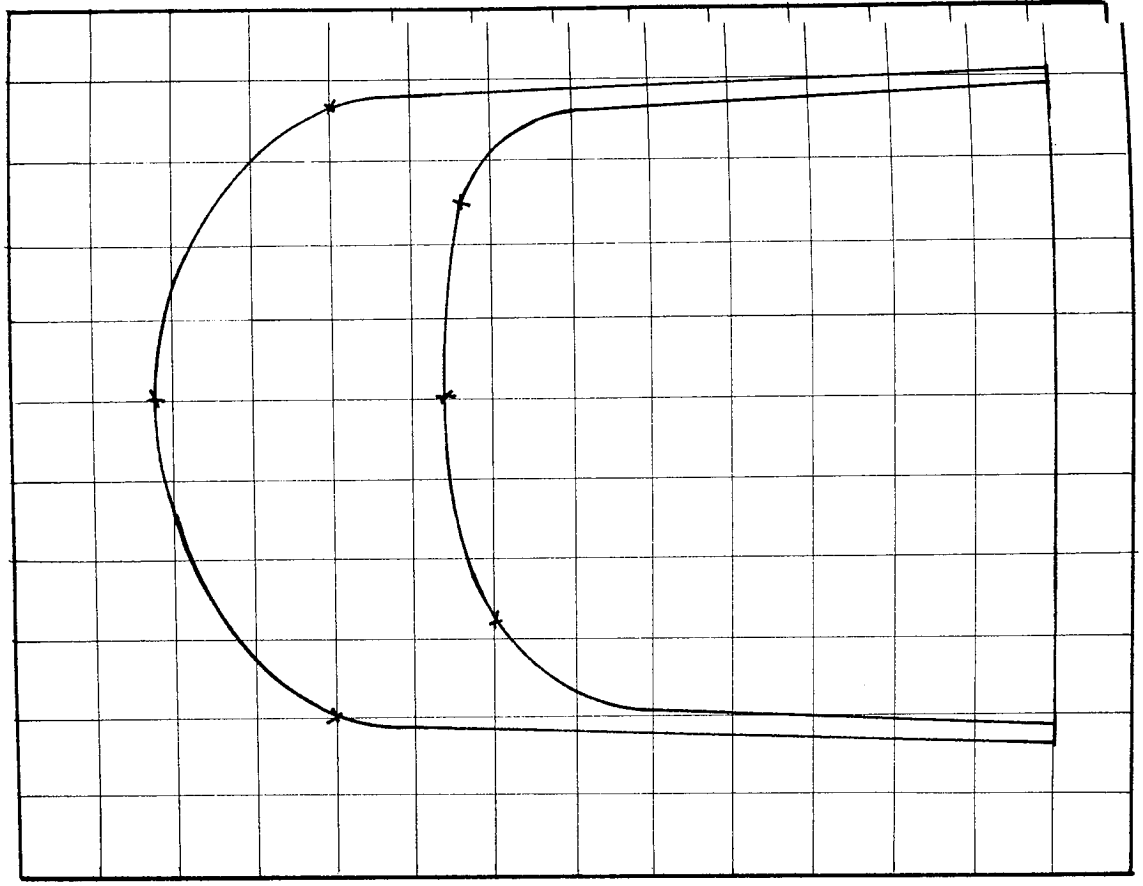

POSITION 2 Scales: Velocity: 1 mm = $\frac{1}{5}$ mm/s Area under Velocity Curve = 6,000 mm^2

Momentum: 1 mm^2 = $\frac{1}{25}$ kgmm/s Area under Momentum Curve = 8,850 mm^2

BED MATERIAL: 3 mm Diameter Glass Spheres

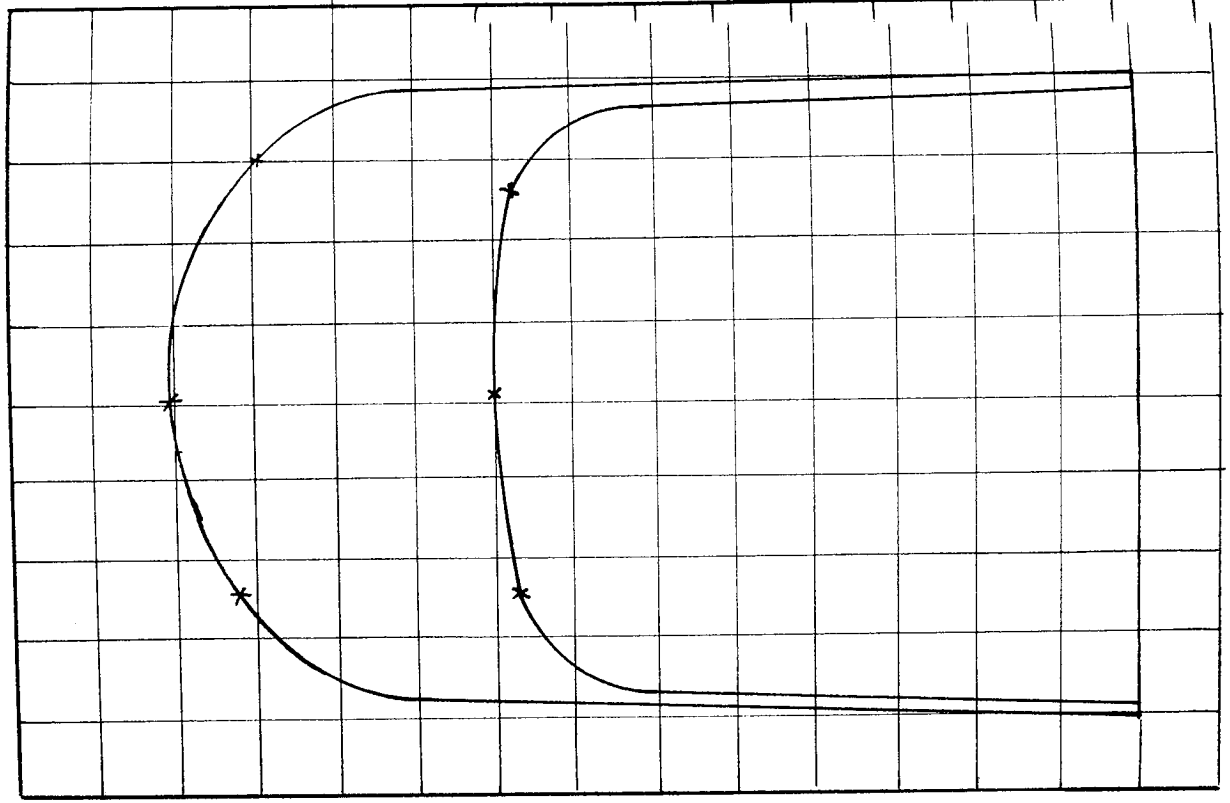

POSITION 3 Scales: Velocity: 1 mm = $\frac{1}{5}$ mm/s Area under Velocity Curve = 6,000 mm^2

Momentum: 1 mm^2 = $\frac{1}{25}$ kgmm/s Area under Momentum Curve = 8,950 mm^2

BED MATERIAL: 3 mm Diameter Glass Spheres

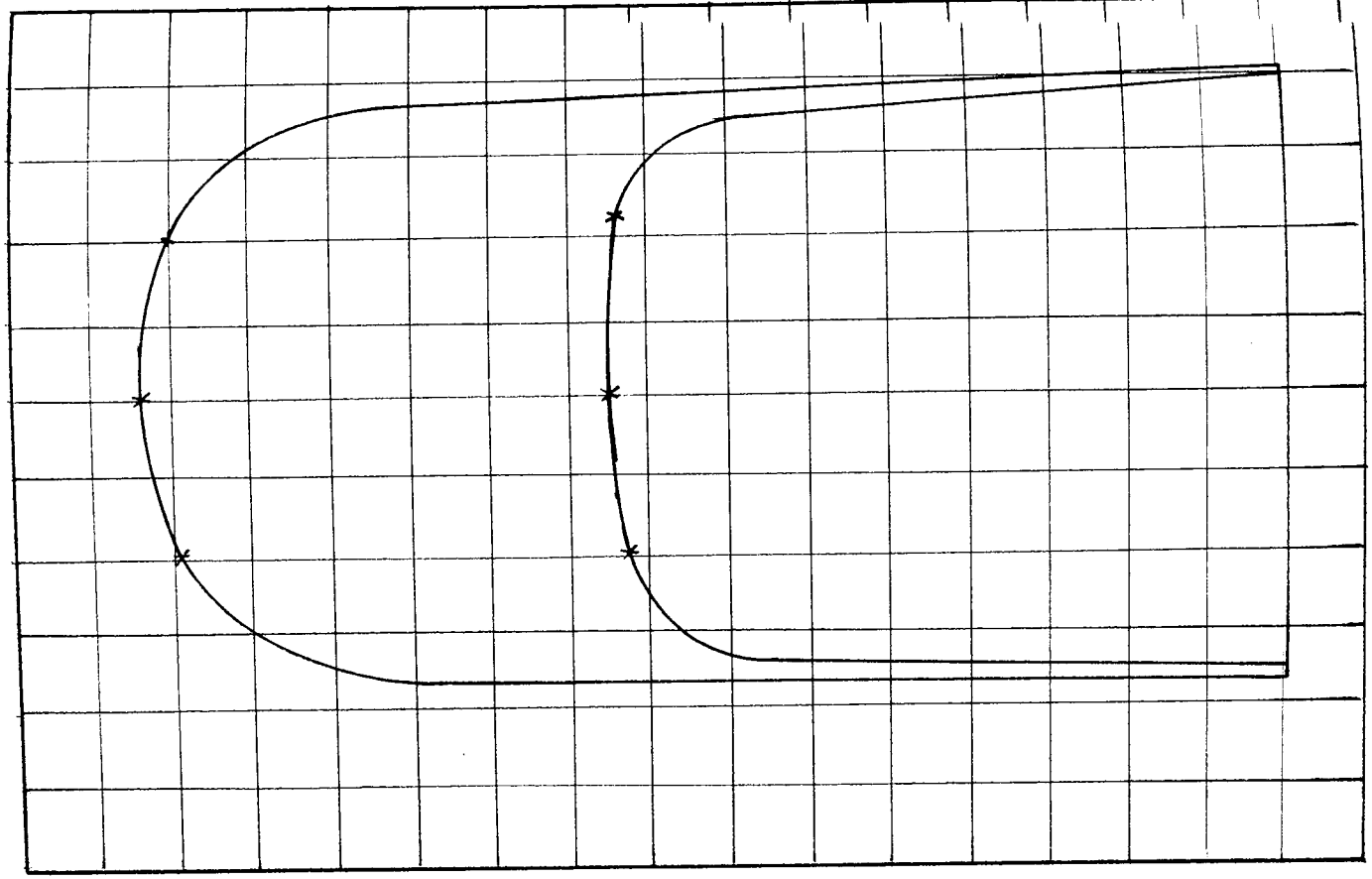

POSITION 4 Scales: Velocity: 1 mm = $\frac{1}{5}$ mm/s Area under Velocity Curve = 6,100 mm^2

Momentum: 1 mm^2 = $\frac{1}{25}$ kgmm/s Area under Momentum Curve = 9,900 mm^2

BED MATERIAL: 3 mm Diameter Glass Spheres

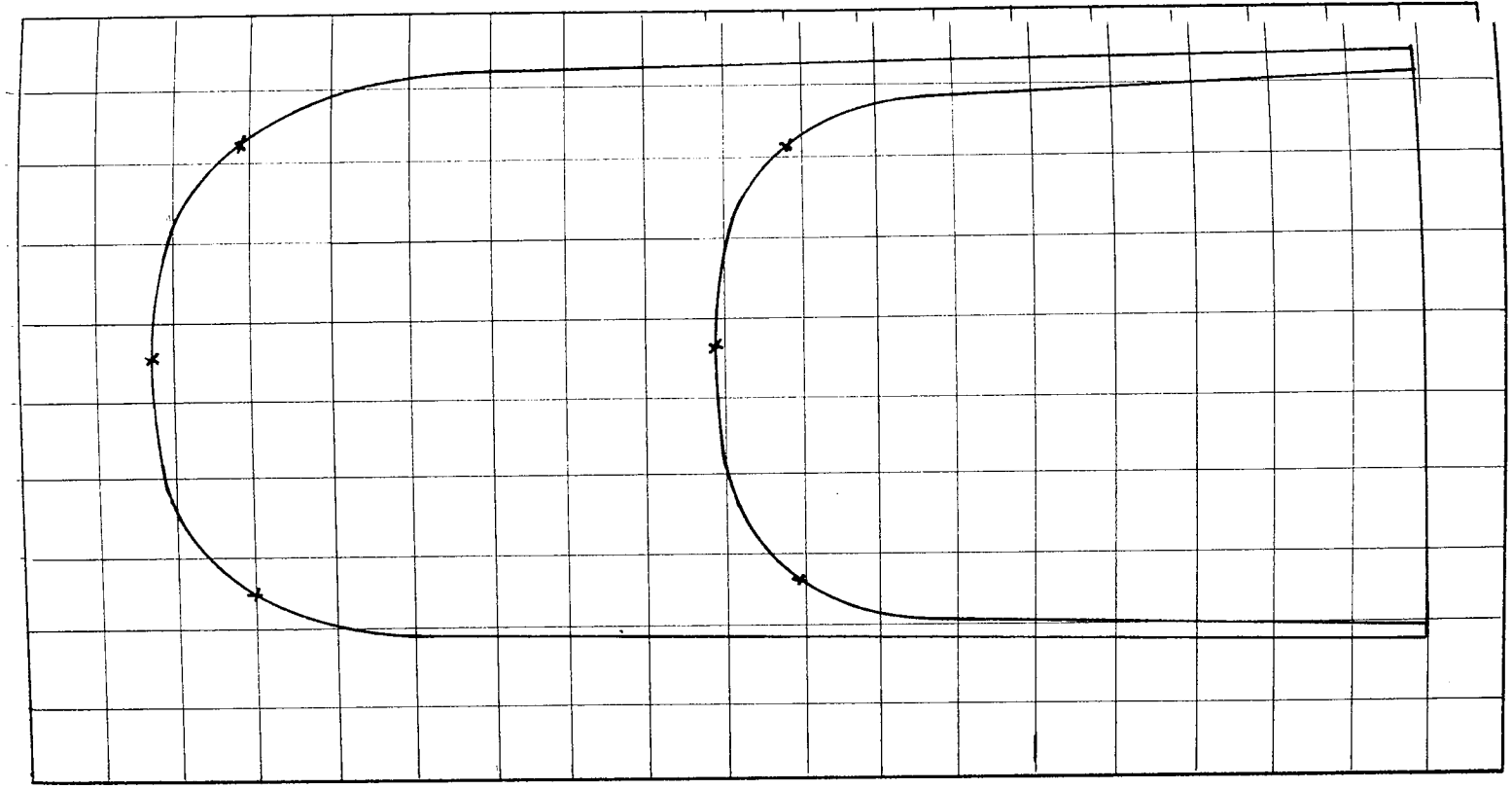

POSITION 5 Scales: Velocity: 1 mm = $\frac{1}{5}$ mm/s Area under Velocity Curve = 6,510 mm^2

Momentum: 1 mm^2 = $\frac{1}{25}$ kgmm/s Area under Momentum Curve = 9,950 mm^2

BED MATERIAL: 3 mm Diameter Glass Spheres

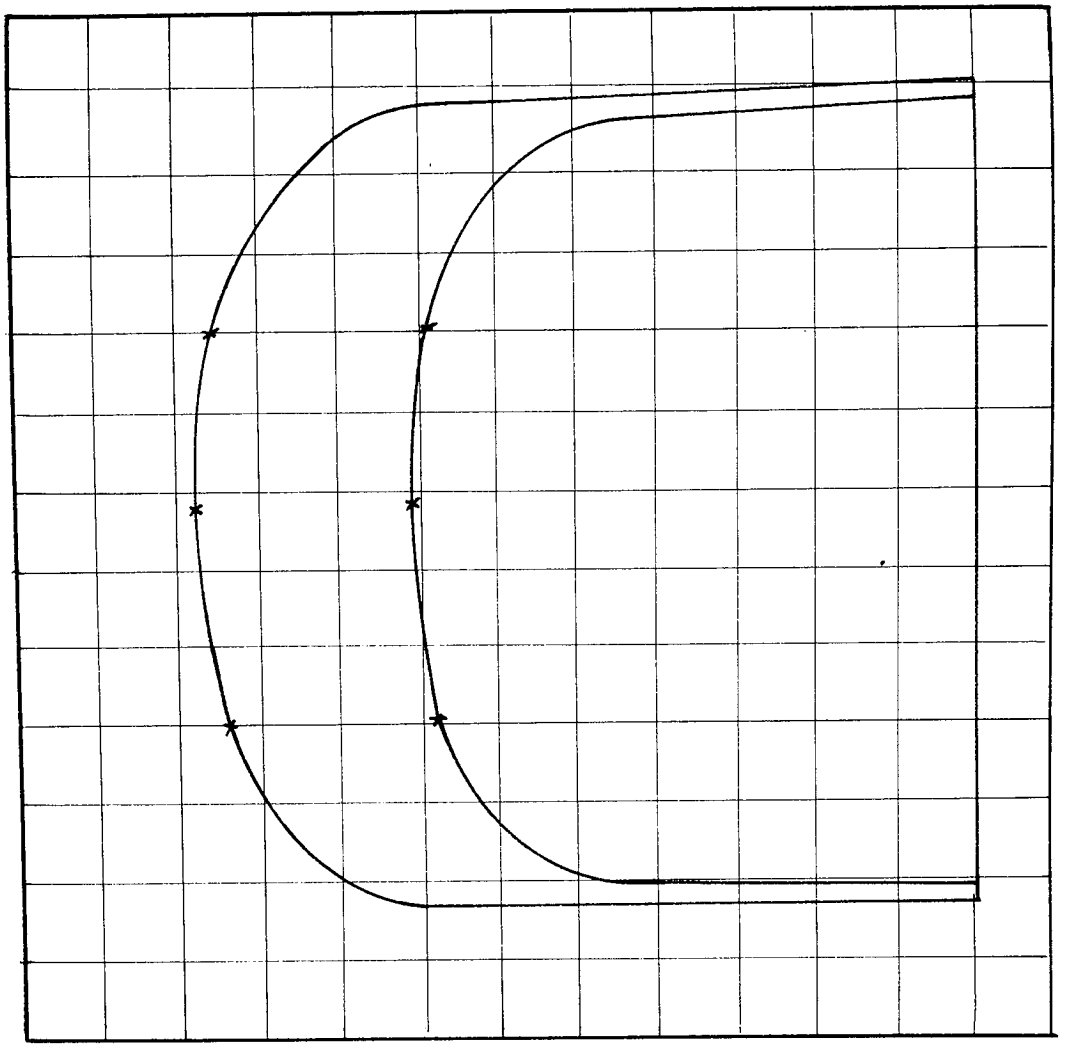

POSITION 1 Scales: Velocity: 1 mm = $\frac{1}{5}$ mm/s Area under Velocity Curve = 6,330 mm^2

Momentum: 1 mm^2 = $\frac{1}{25}$ kgmm/s Area under Momentum Curve = 9,620 mm^2

BED MATERIAL: 3 mm Diameter Glass Spheres

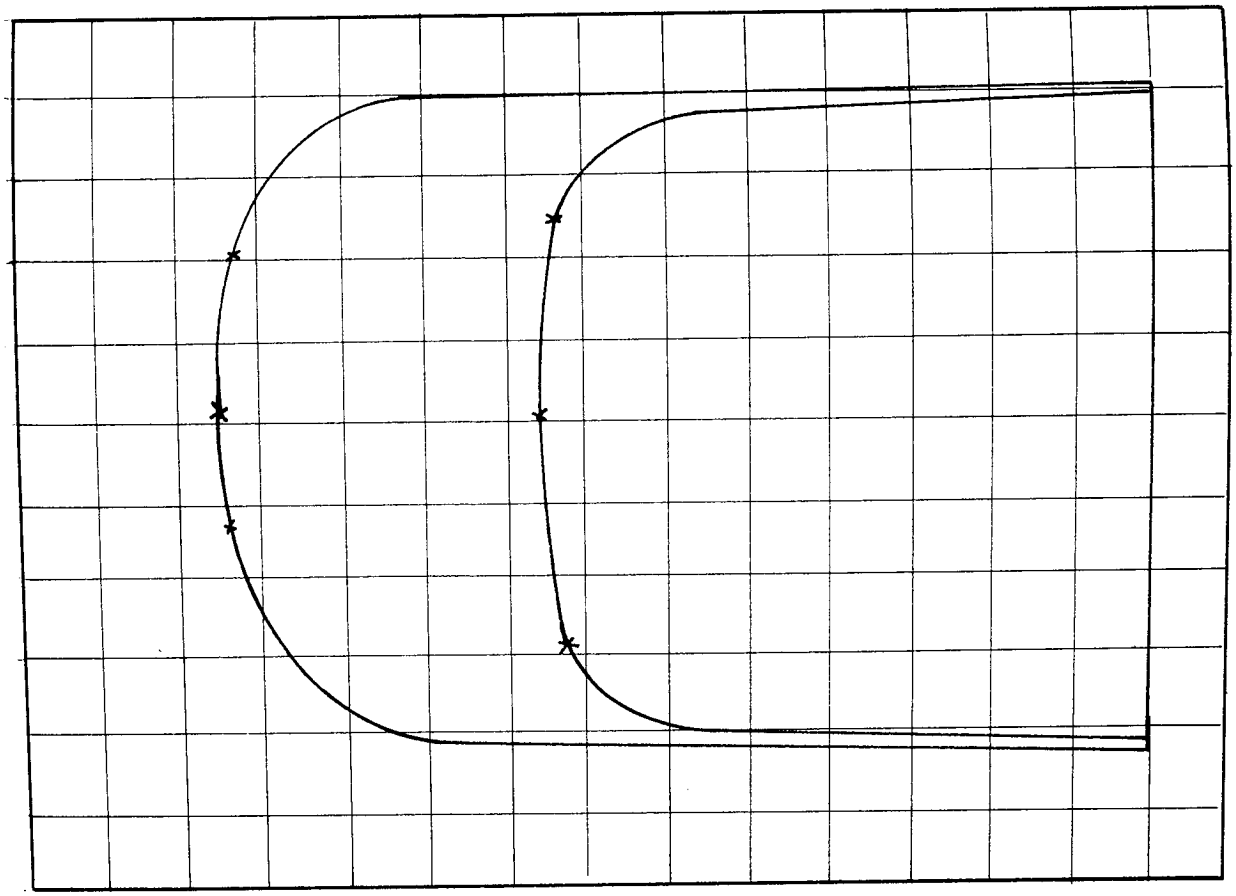

POSITION 2 Scales: Velocity: 1 mm = $\frac{1}{5}$ mm/s Area under Velocity Curve = 5,650 mm^2

Momentum: 1 mm^2 = $\frac{1}{25}$ kgmm/s Area under Momentum Curve = 9,370 mm^2

BED MATERIAL: 3 mm Diameter Glass Spheres

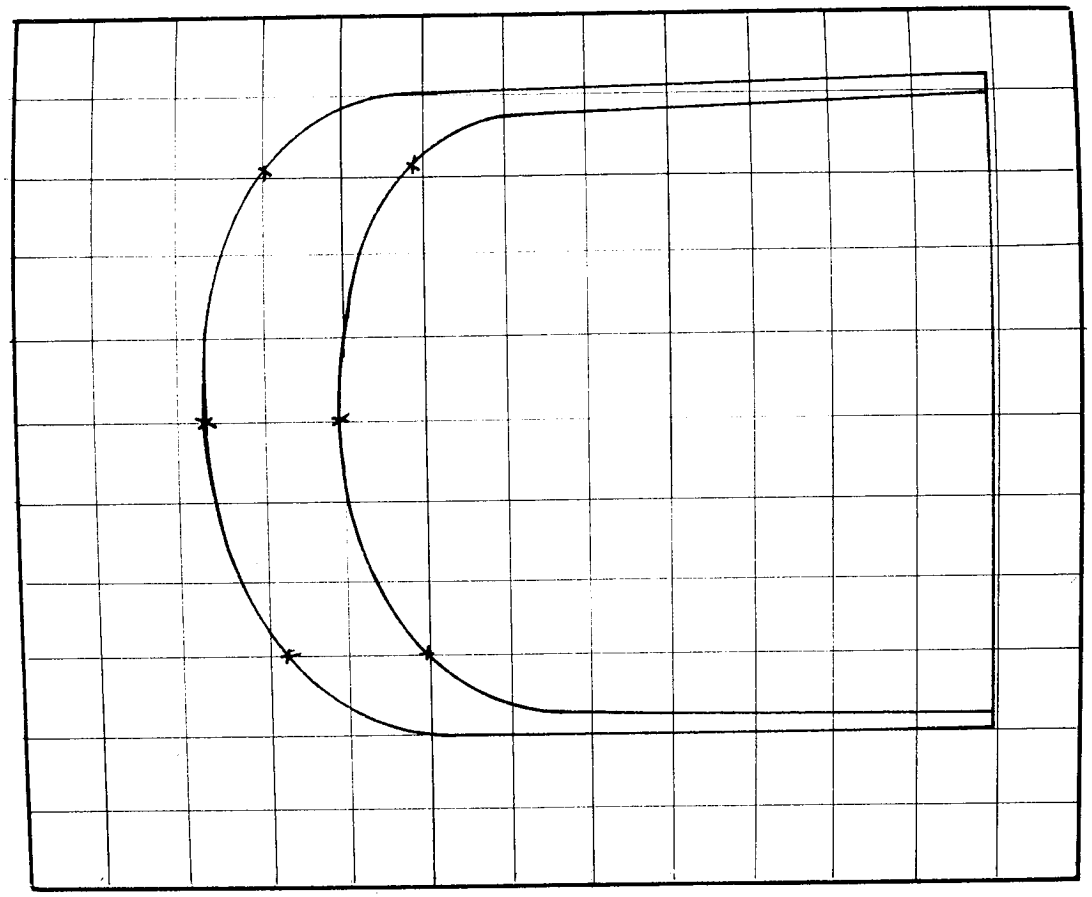

POSITION 3 Scales: Velocity: 1 mm = $\frac{1}{5}$ mm/s

Momentum: 1 mm^2 = $\frac{1}{25}$ kgmm/s

Area under Velocity Curve = 5,850 mm^2

Area under Momentum Curve = 9,640 mm^2

BED MATERIAL: 3 mm Diameter Glass Spheres

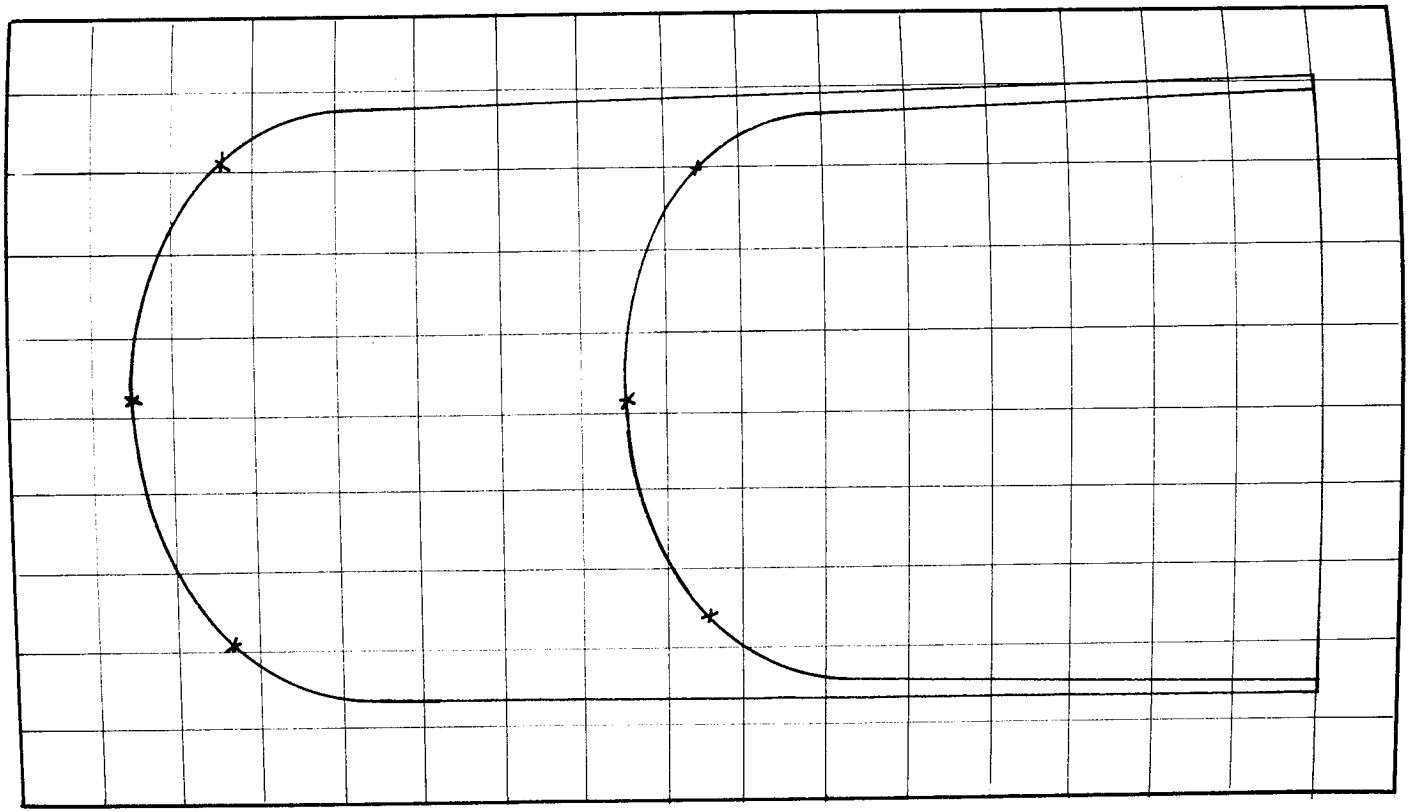

POSITION 4 Scales: Velocity: 1 mm = $\frac{1}{5}$ mm/s Area under Velocity Curve = 5,930 mm^2

Momentum: 1 mm^2 = $\frac{1}{25}$ kgmm/s Area under Momentum Curve = 9,850 mm^2

BED MATERIAL: 3 mm Diameter Glass Spheres

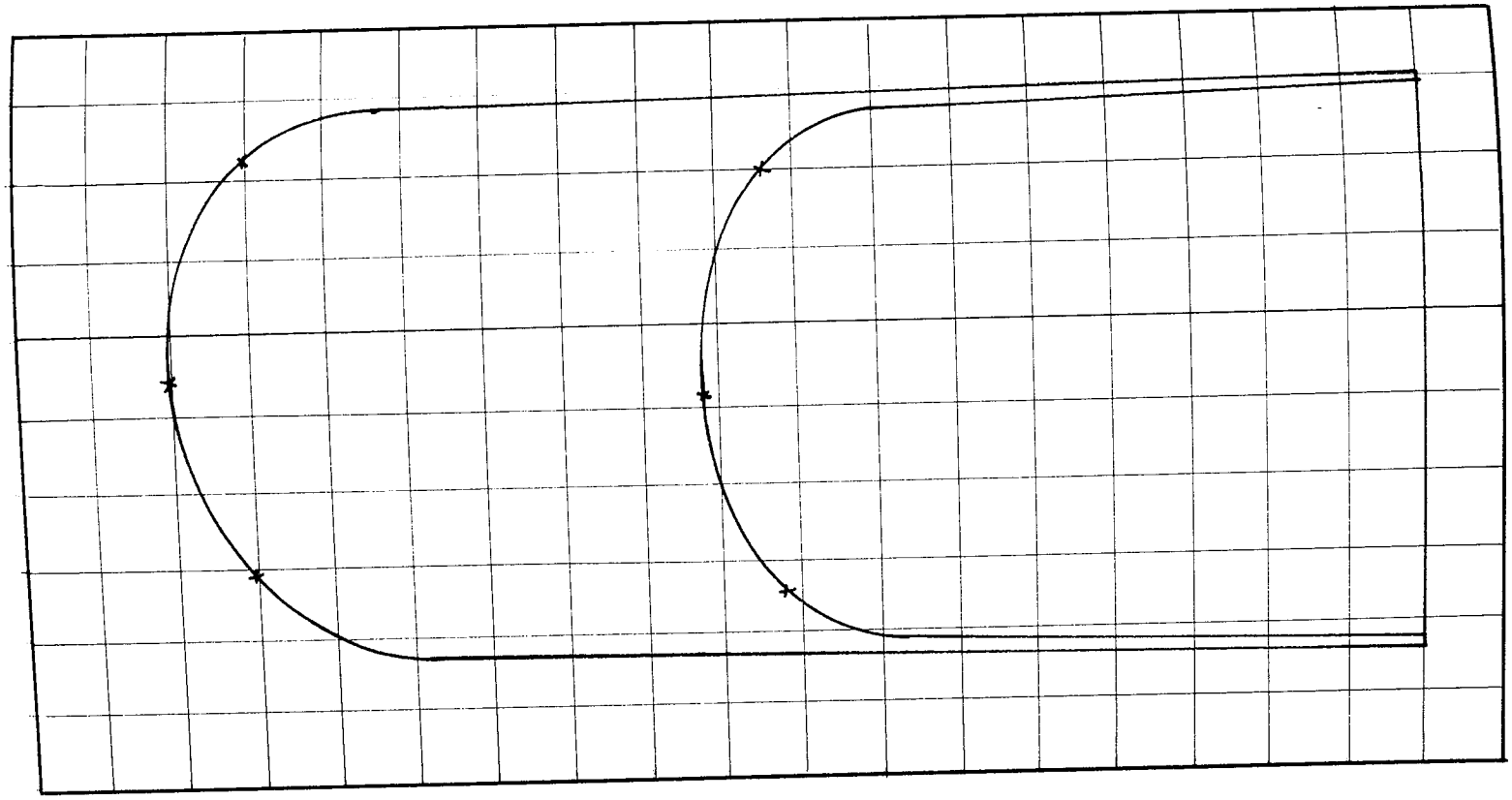

POSITION 5 Scales: Velocity: 1 mm = $\frac{1}{5}$ mm/s

Momentum: 1 mm^2 = $\frac{1}{25}$ kgmm/s

Area under Velocity Curve = 6,150 mm^2

Area under Momentum Curve = 10,650 mm^2

BED MATERIAL: 3 mm Diameter Glass Spheres

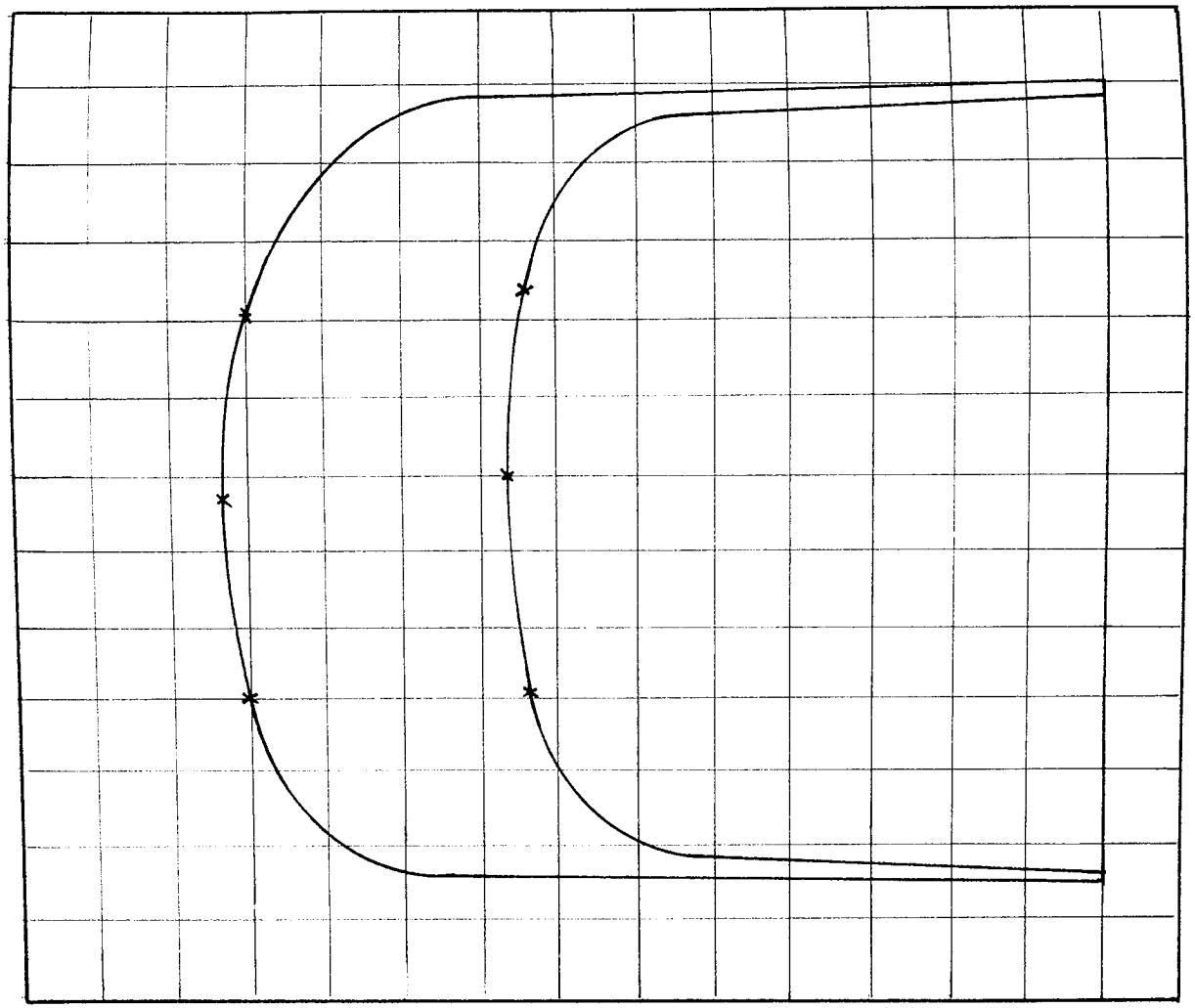

POSITION 1 Scales: Velocity: 1 mm = $\frac{1}{5}$ mm/s Area under Velocity Curve = 7,620 mm^2

Momentum: 1 mm^2 = $\frac{1}{25}$ kgmm/s Area under Momentum Curve = 11,300 mm^2

BED MATERIAL: 3 mm Diameter Glass Spheres

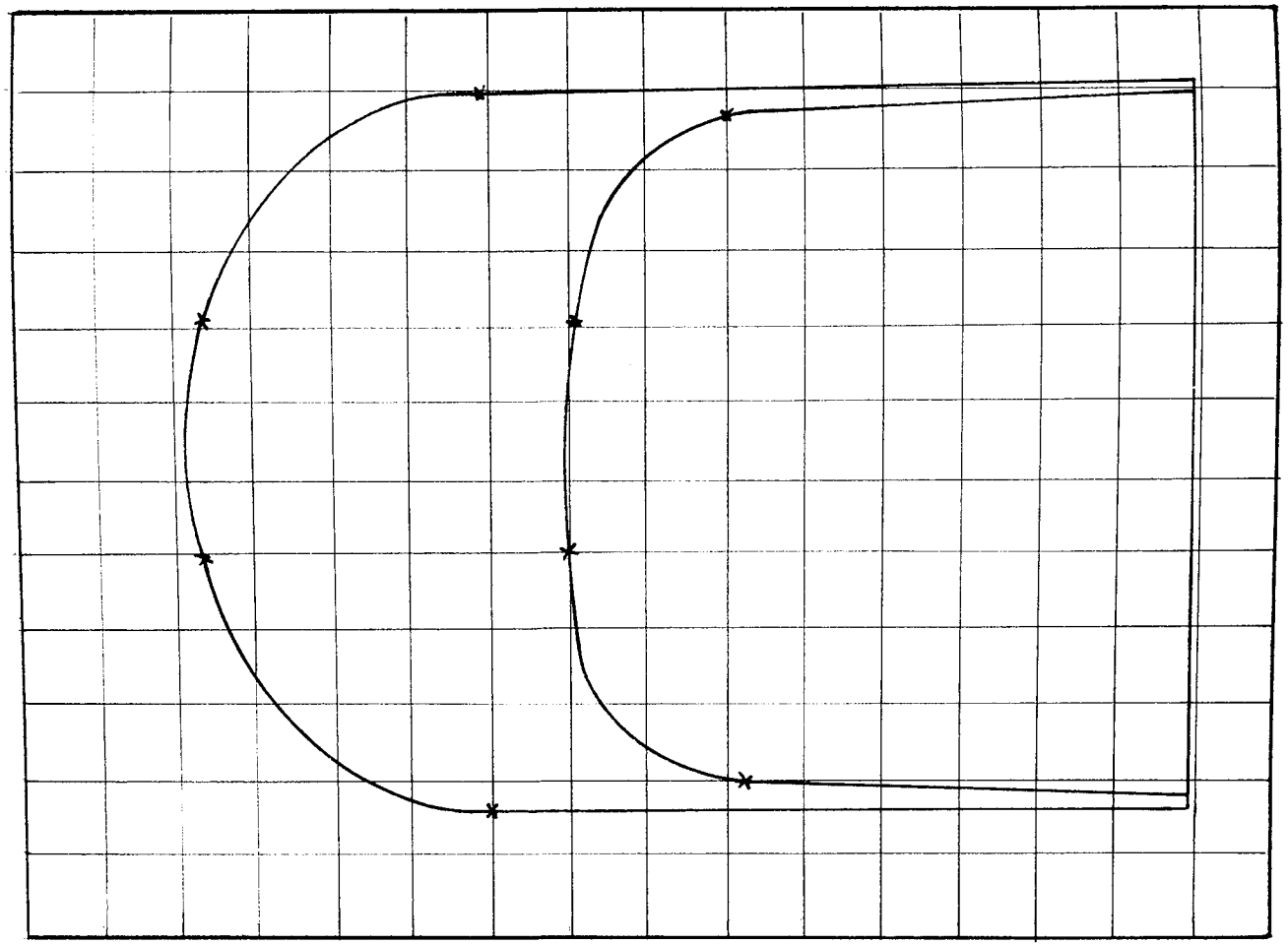

POSITION 2 Scales: Velocity: 1 mm = $\frac{1}{5}$ mm/s Area under Velocity Curve = 7,250 mm^2

Momentum: 1 mm^2 = $\frac{1}{25}$ kgmm/s Area under Momentum Curve = 11,600 mm^2

BED MATERIAL: 3 mm Diameter Glass Spheres

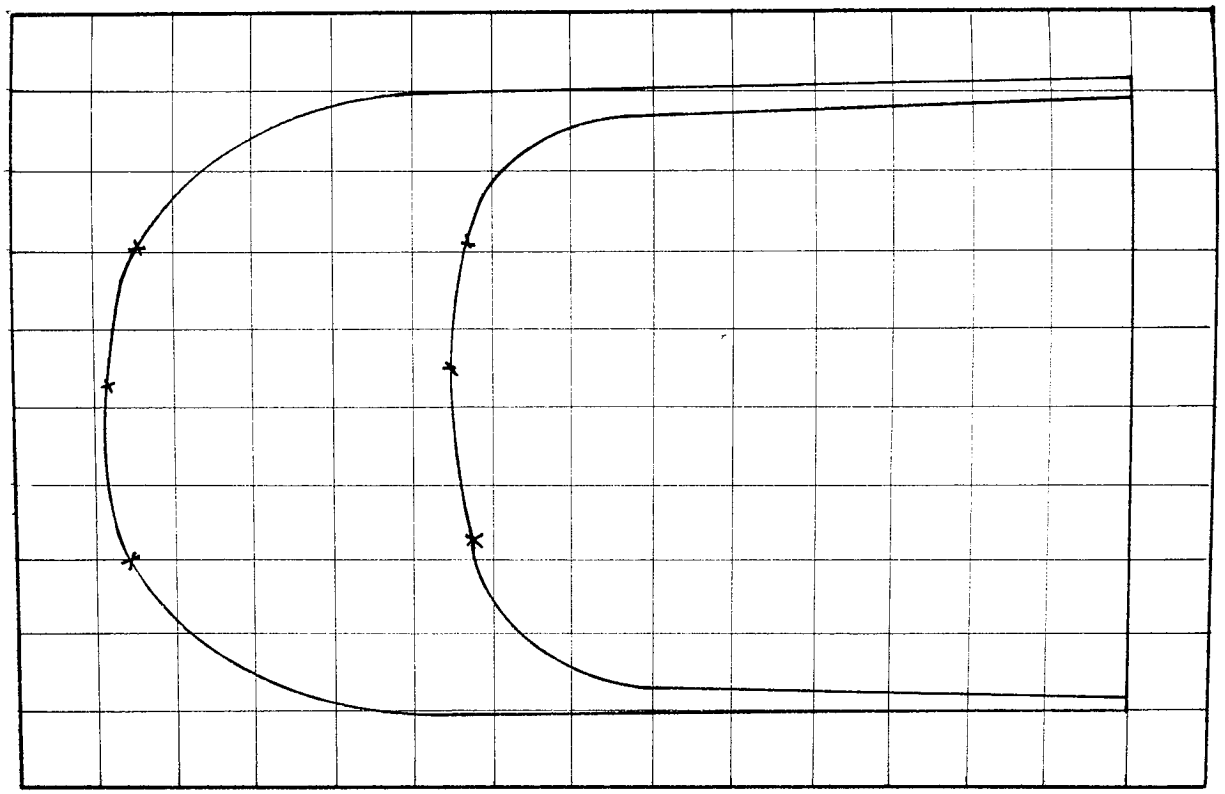

POSITION 3 Scales: Velocity: 1 mm = $\frac{1}{5}$ mm/s Area under Velocity Curve = 6,800 mm^2

Momentum: 1 mm^2 = $\frac{1}{25}$ kgmm/s Area under Momentum Curve = 10,900 mm^2

BED MATERIAL : 3 mm Diameter Glass Spheres

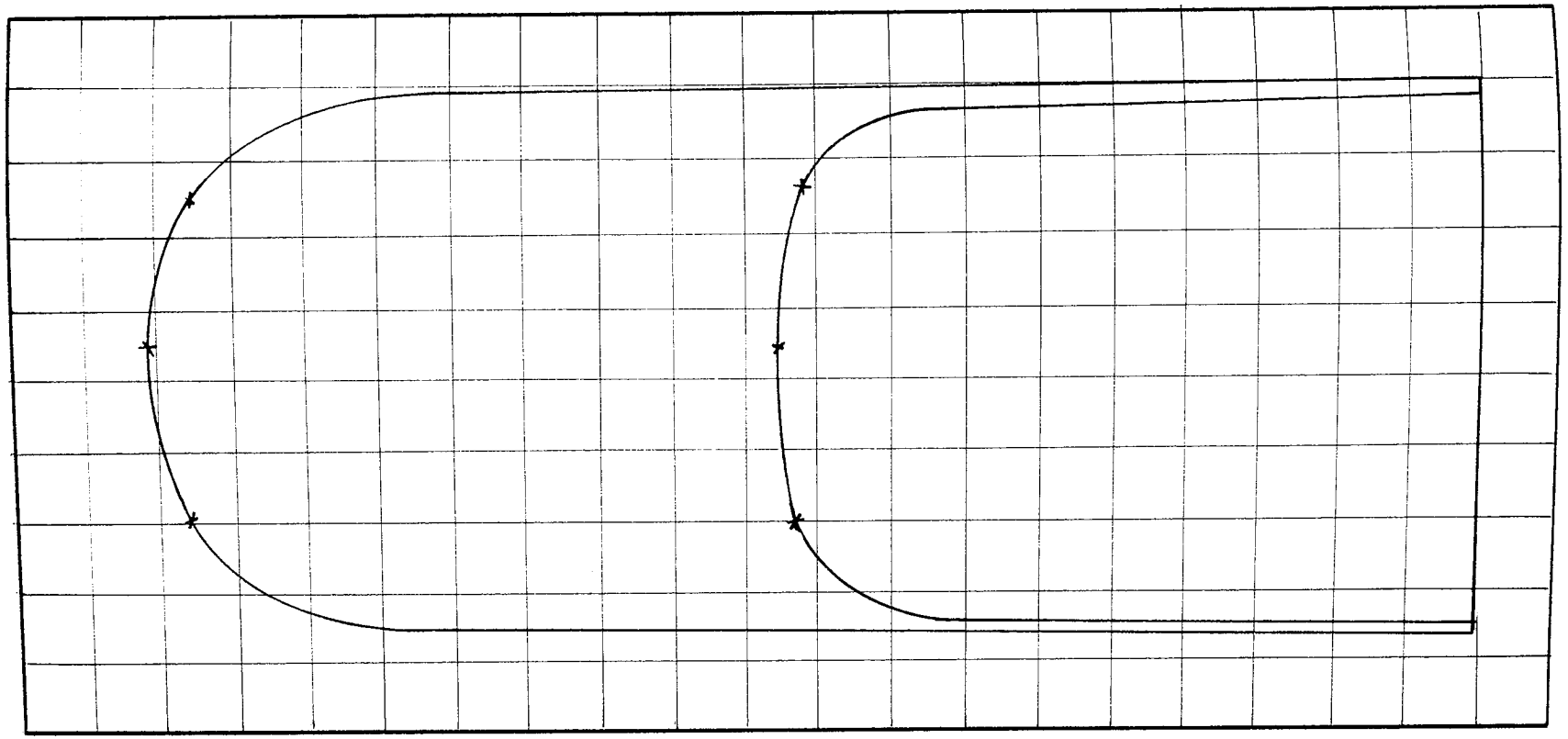

POSITION 4 Scales: Velocity: 1 mm = $\frac{1}{5}$ mm/s Area under Velocity Curve = 7,100 mm^2

Momentum: 1 mm^2 = $\frac{1}{25}$ kgmm/s Area under Momentum Curve = 11,900 mm^2

BED MATERIAL: 3 mm Diameter Glass Spheres

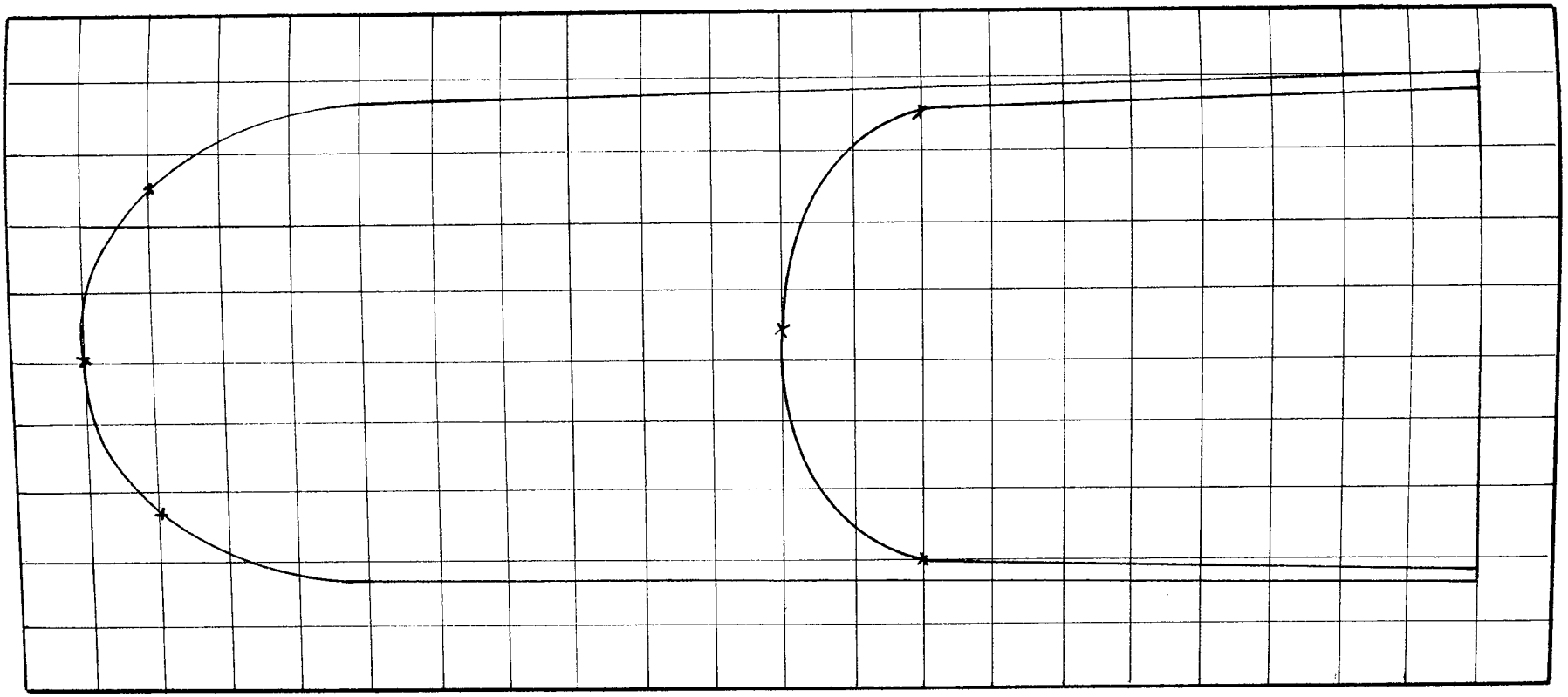

POSITION 5 Scales: Velocity: 1 mm = $\frac{1}{5}$ mm/s Area under Velocity Curve = 7,200 mm^2

Momentum: 1 mm^2 = $\frac{1}{25}$ kgmm/s Area under Momentum Curve = 12,100 mm^2

BED MATERIAL: 3 mm Diameter Glass Spheres

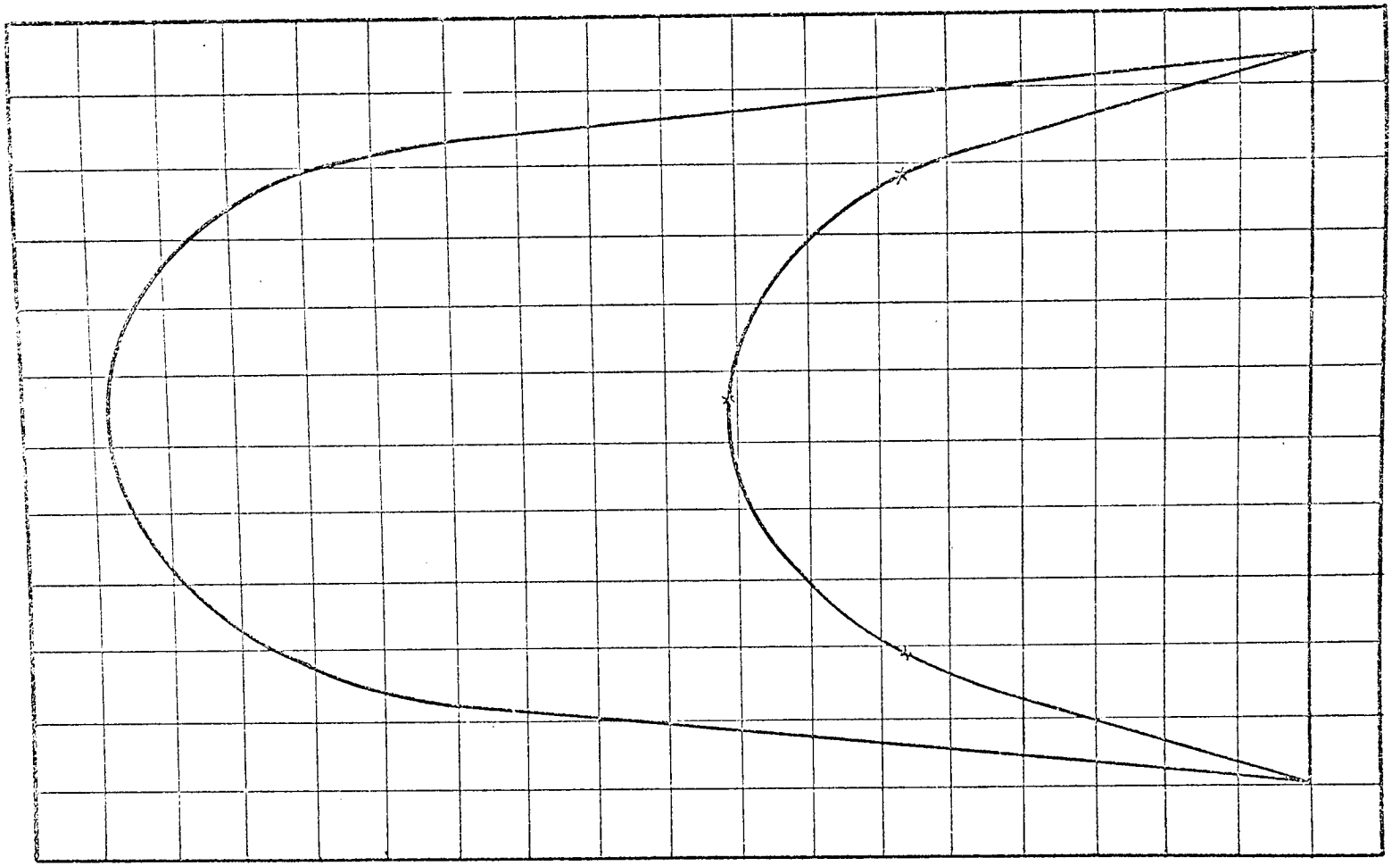

POSITION 1 Scales: Velocity: 1 mm = 1 mm/s Area under Velocity Curve = 6,120 mm^2

Momentum: 1 mm^2 = $\frac{1}{25}$ gmm/s Area under Momentum Curve = 1,350 mm^2

BED MATERIAL: 3 mm Diameter Glass Spheres

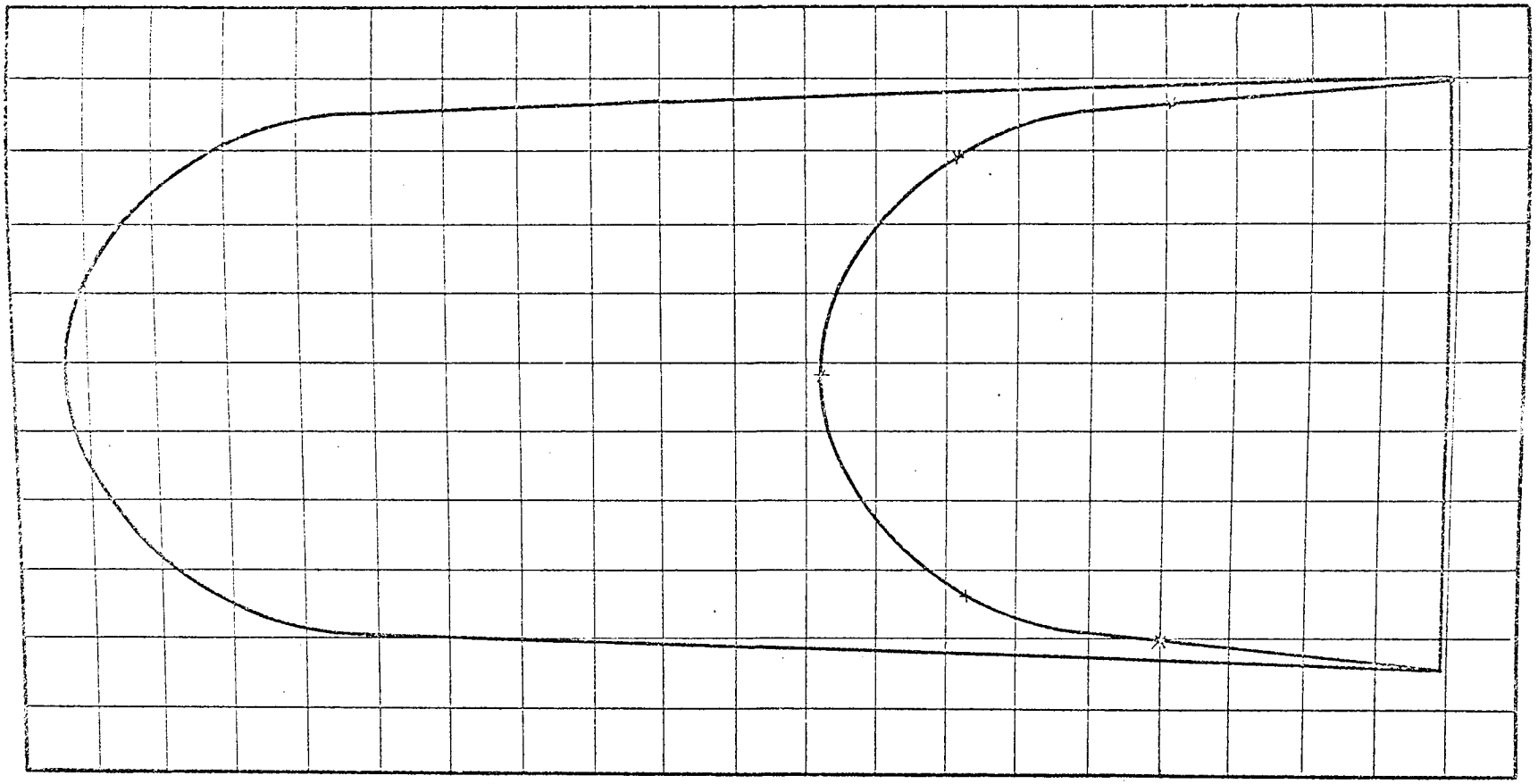

POSITION 2 Scales: Velocity: 1 mm = 1 mm/s Area under Velocity Curve = 6,200 mm^2

Momentum: 1 mm^2 = $\frac{1}{25}$ kgmm/s Area under Momentum Curve = 1[illegible],200 mm^2

BED MATERIAL: [illegible] mm Diameter Glass Spheres

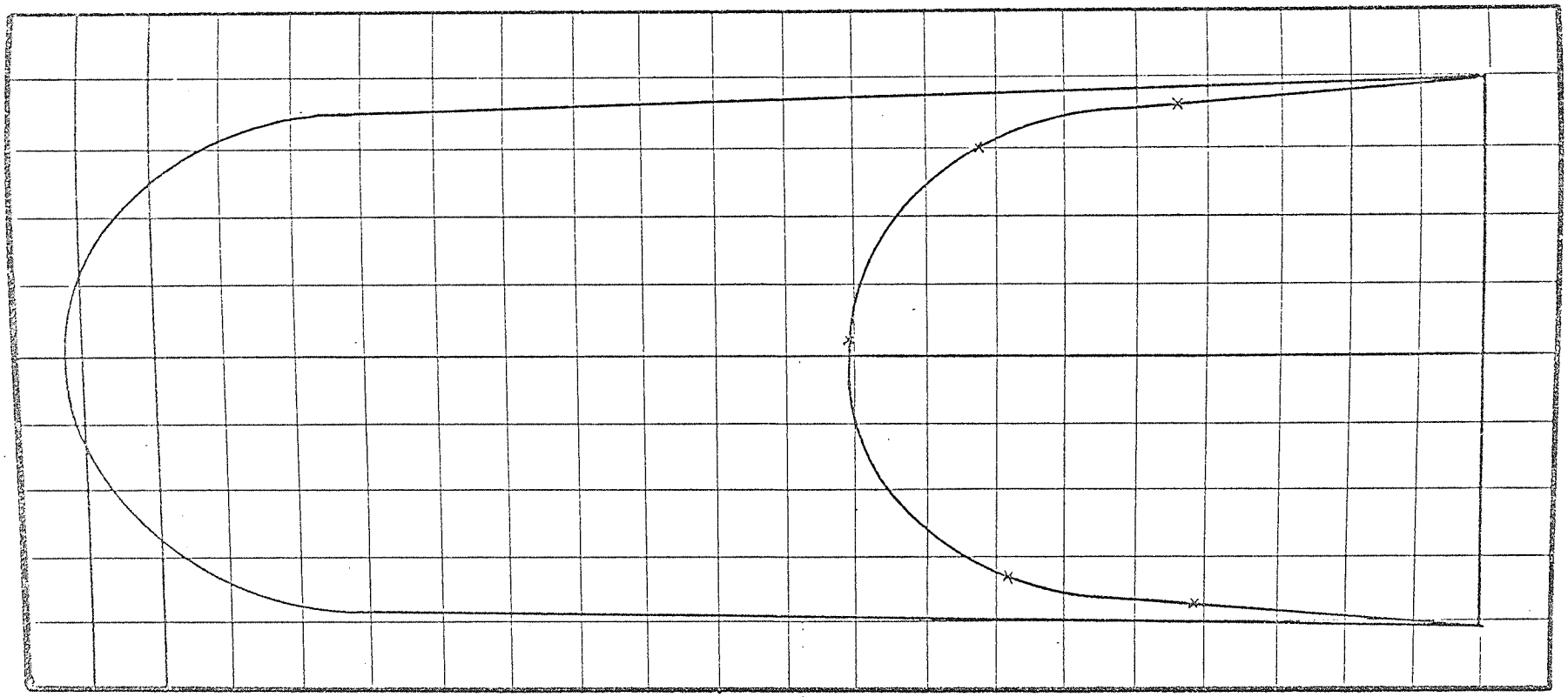

POSITION 3 Scales: Velocity: 1 mm = 1 mm/s Area under Velocity Curve = 6,180 mm^2

Momentum: 1 mm^2 = $\frac{1}{25}$ kgmm/s Area under Momentum Curve = 14,700 mm^2

BED MATERIAL: 3 mm Diameter Glass Spheres

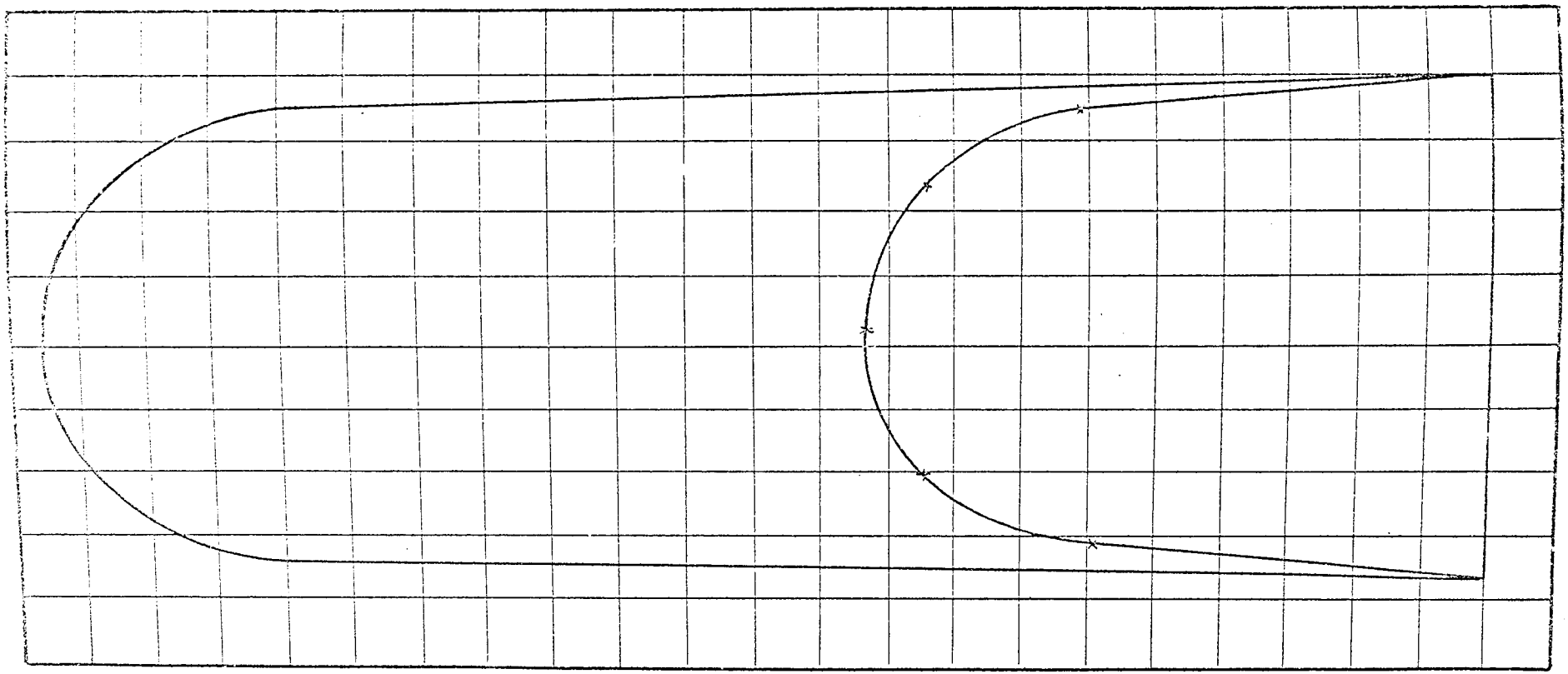

POSITION ' Scales: Velocity: 1 mm = 1 mm/s Area under Velocity Curve = 6,160 mm^2

Momentum: 1 mm^2 = $\frac{1}{25}$ kgmm/s Area under Momentum Curve = 1[illegible],700 mm^2

BED MATERIAL: [illegible] mm Diameter Glass Spheres

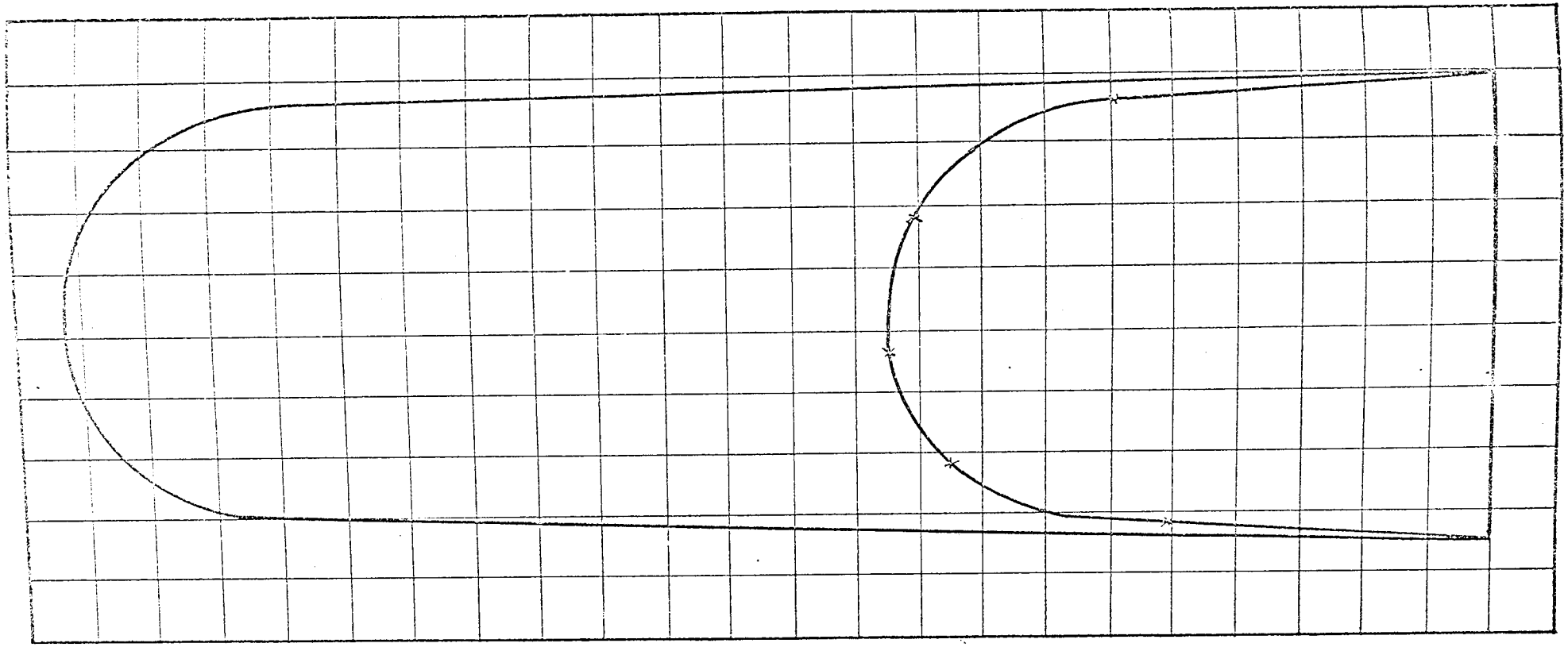

POSITION 5 Scales: Velocity: 1 mm = 1 mm/s Area under Velocity Curve = 6,190 mm^2

Momentum: $1mm^2 = \frac{1}{25}$ kgmm/s Area under Momentum Curve = 14,700 mm^2

BED MATERIAL: 3 mm Diameter Glass Spheres

1½ mm Diameter Sand

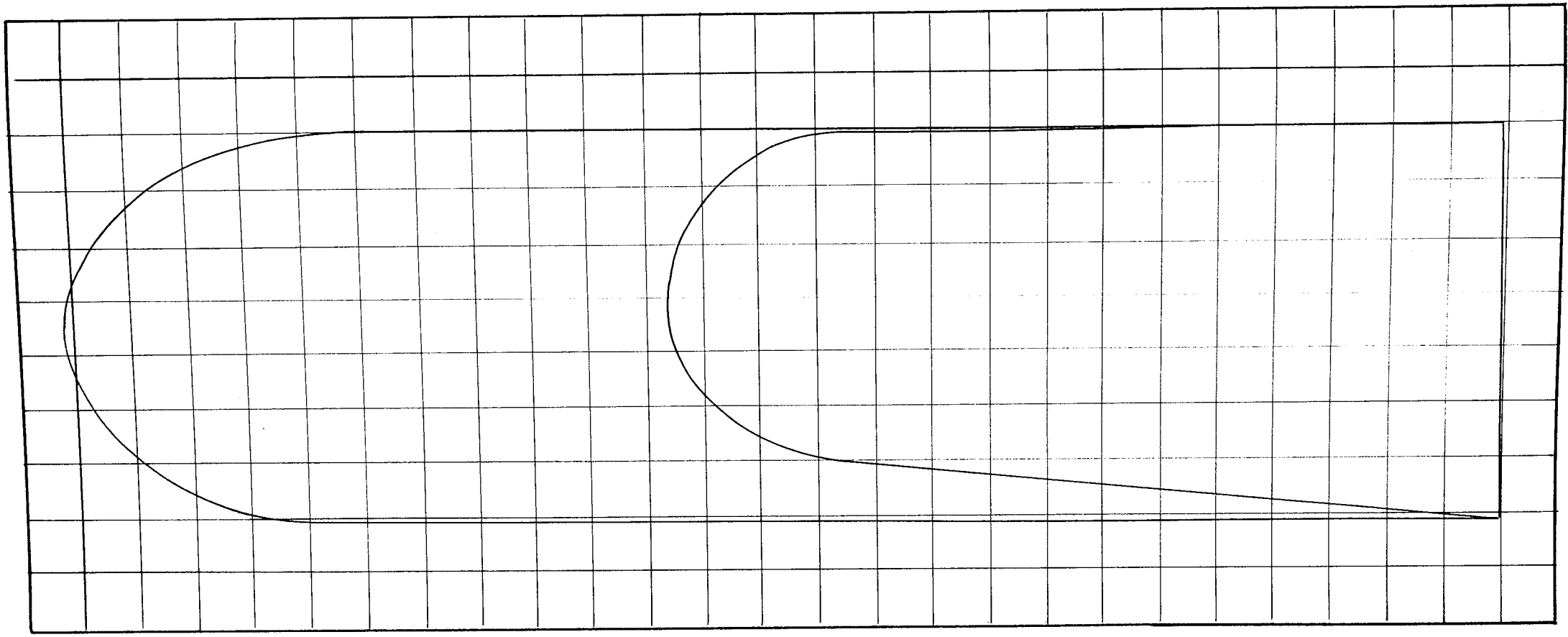

Scales:- Velocity 1 mm = 1 mm/s Area Velocity Curve 8100 mm^2

Momentum 1 mm = $\frac{1}{25}$ kgmm/s Momentum Curve 1'700 mm^2

POSITION 1

BED MATERIAL $1\frac{1}{2}$ mm Diameter Glass Spheres

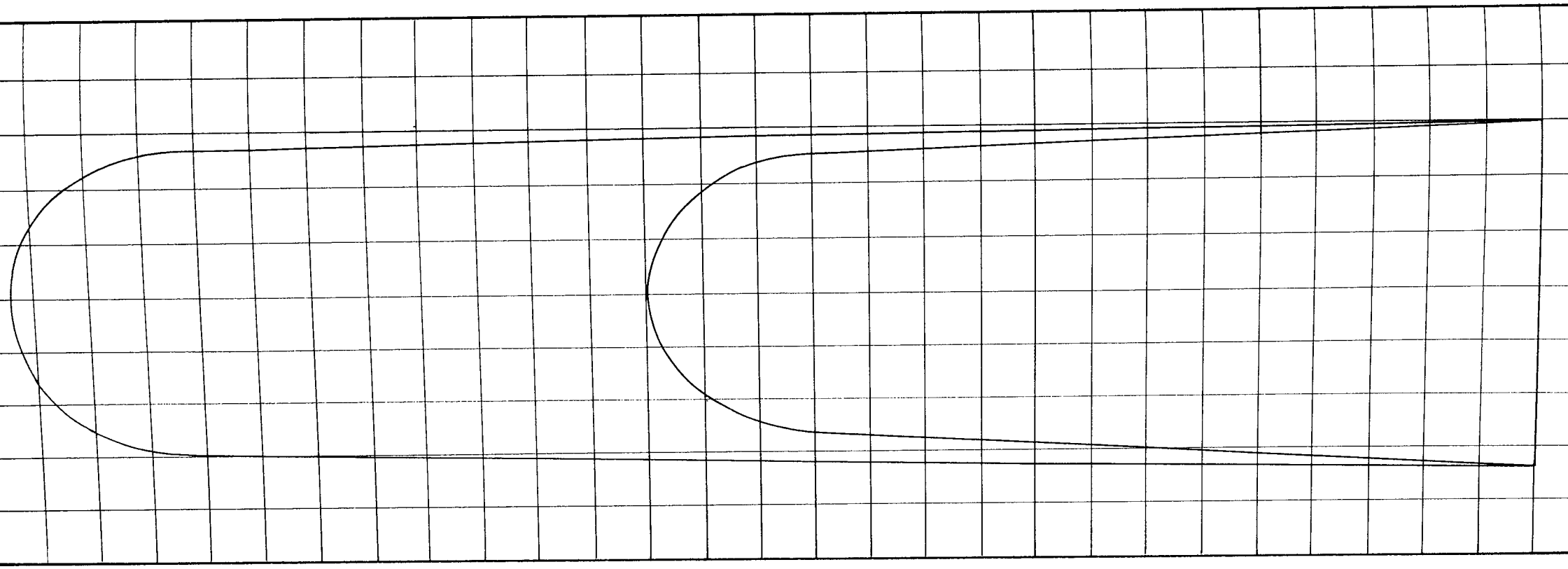

POSITION 2

Scales:- Velocity 1 mm = 1 mm/s

Momentum 1 mm = 1 kgmm/s

Area Velocity Curve = 7900 mm^2

Area Momentum = 14710 mm^2

BED MATERIAL $1\frac{1}{2}$ mm Diameter Glass Spheres

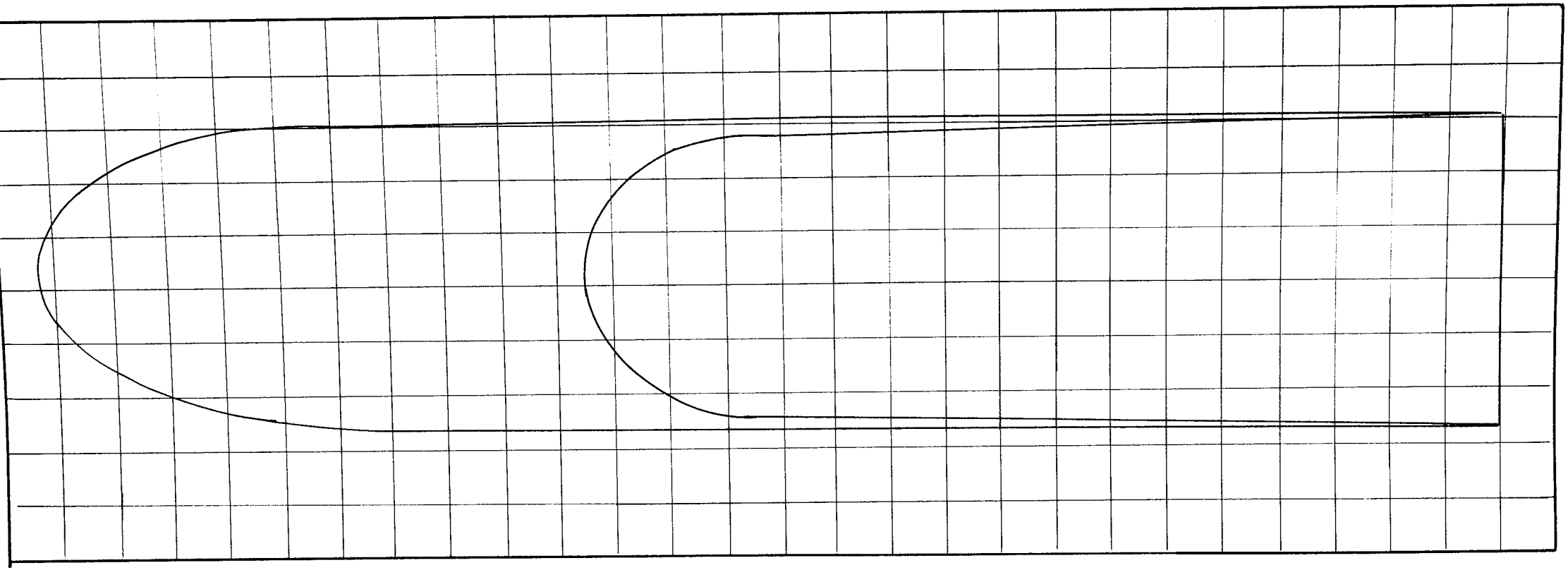

POSITION 3

Scales:- Velocity 1 mm = 1 mm/s Area Velocity Curve = 8100 mm^2
Momentum 1 mm = $\frac{1}{25}$ kgmm/s Momentum = 14000 mm

BED MATERIAL $1\frac{1}{2}$ mm Diameter Glass Spheres

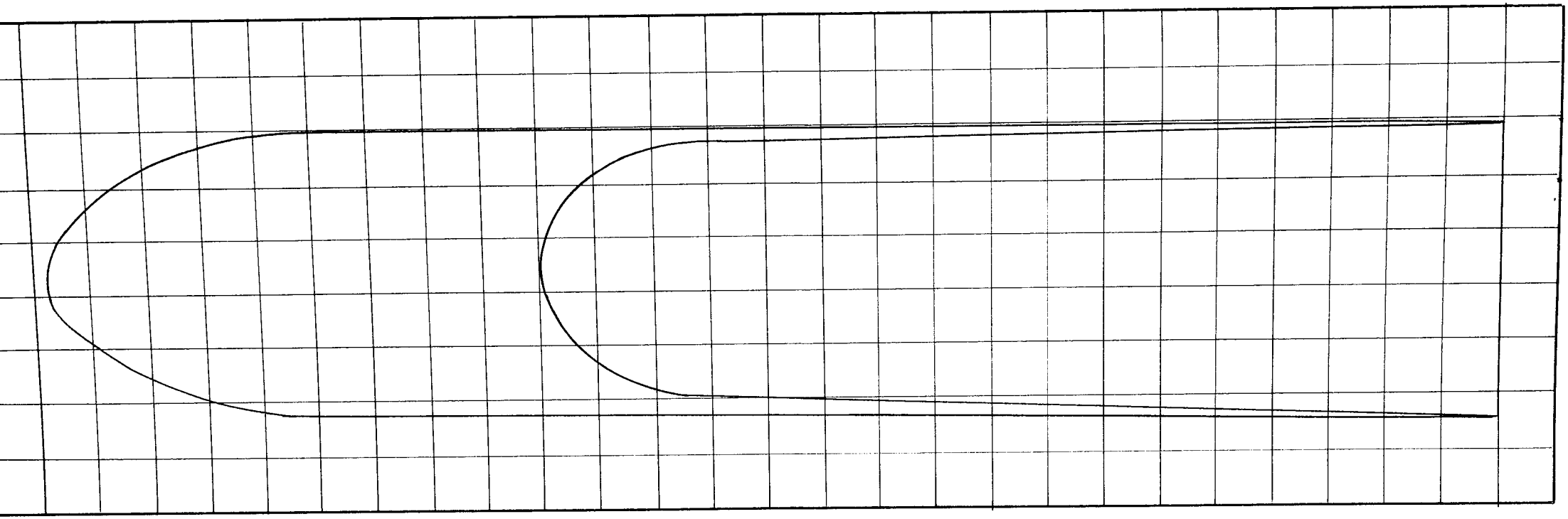

POSITION 4

Scales:- Velocity 1 mm = 1 mm/s

Momentum 1 mm = $\frac{1}{25}$ kgmm/s

Area Velocity Curve = 3200 mm^2

Momentum Curve = 12,000 mm^2

BED MATERIAL $1\frac{1}{2}$ mm Diameter Glass Spheres

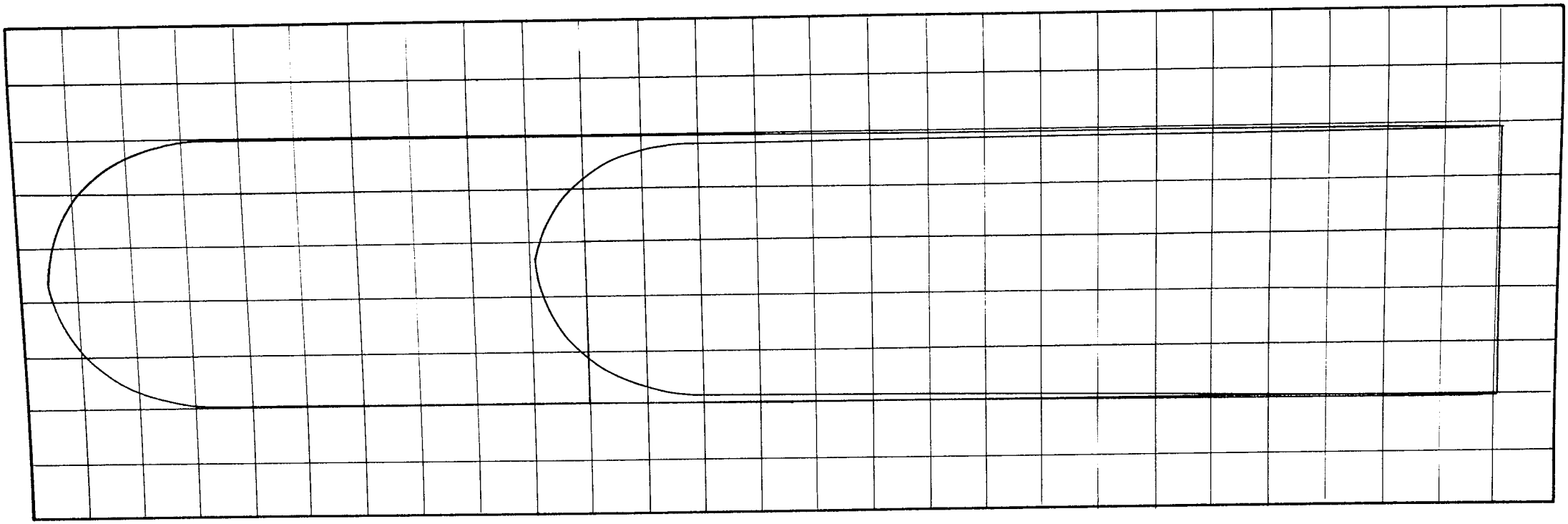

POSITION 5

Scale:- Velocity 1 mm = 1 mm/s

Momentum 1 mm = $\frac{1}{25}$ kgmm/s

Area Velocity Curve = 8100 mm^2

Momentum Curve = 124000 mm^2

BED MATERIAL $1\frac{1}{2}$ mm Diameter Glass Spheres

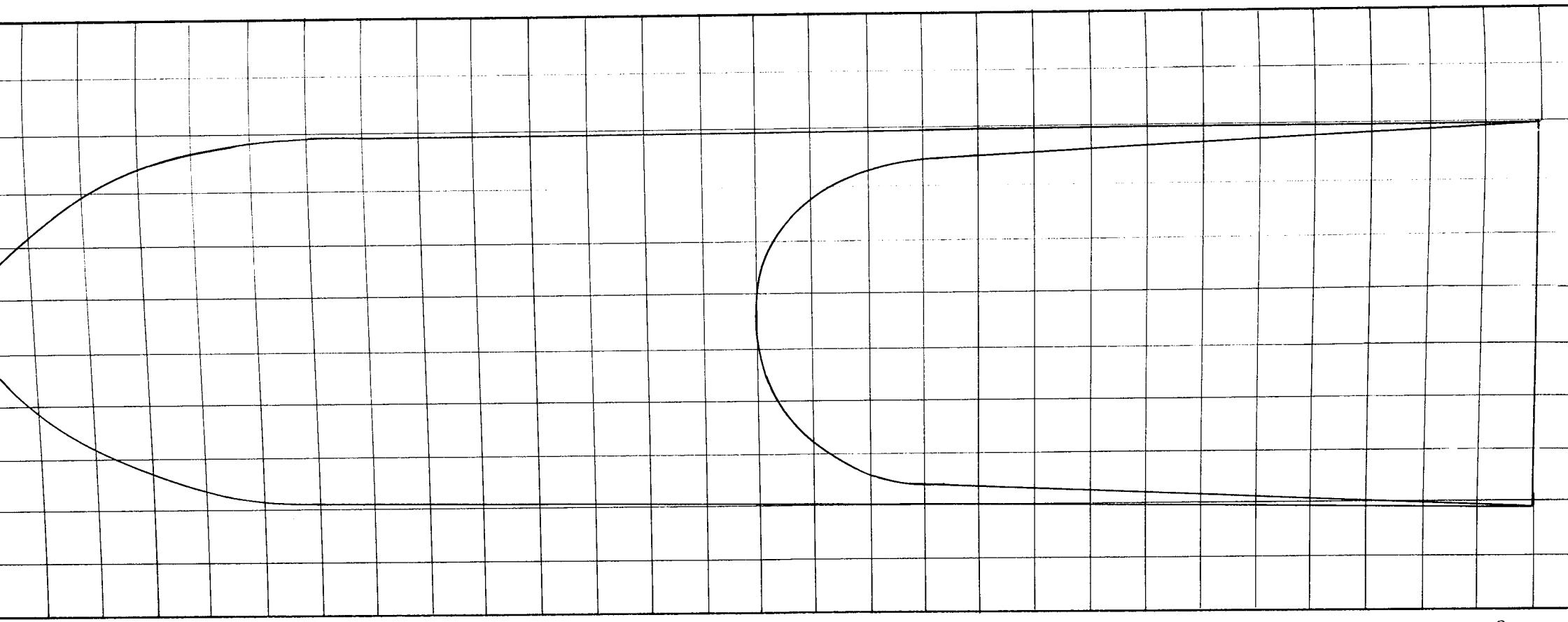

OSITION 1

Scales:- Velocity: 1 mm = 1mm/s

Momentum: 1 mm = 1kg mm/s

Area under velocity curve = 8440mm^2

Momentum = 16840mm^2

BED MATERIAL:- $1\frac{1}{2}$ mm Diameter Glass Spheres

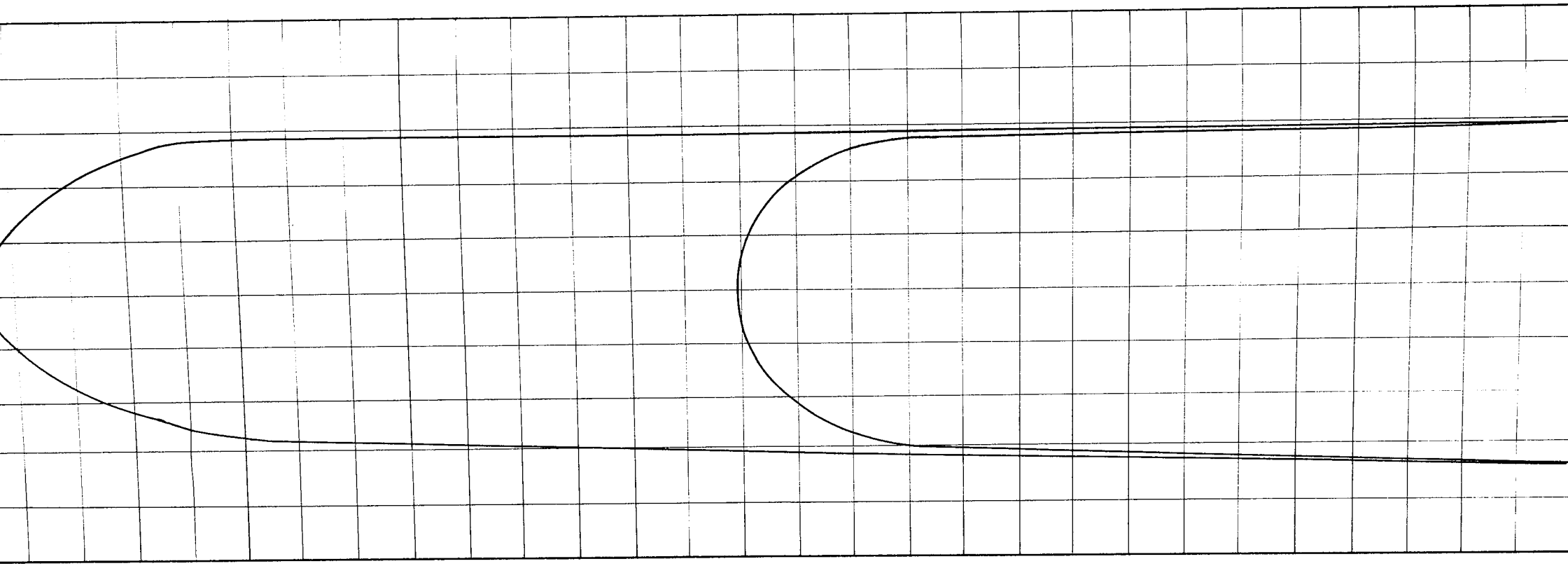

Scales:- Velocity 1 mm = 1 mm/s Area under velocity curve = 8510mm^2

Momentum 1 mm = 1 kg mm/s Momentum = 16500mm^2

POSITION 2

BED MATERIAL = $1\frac{1}{2}$ mm Diameter Glass Spheres

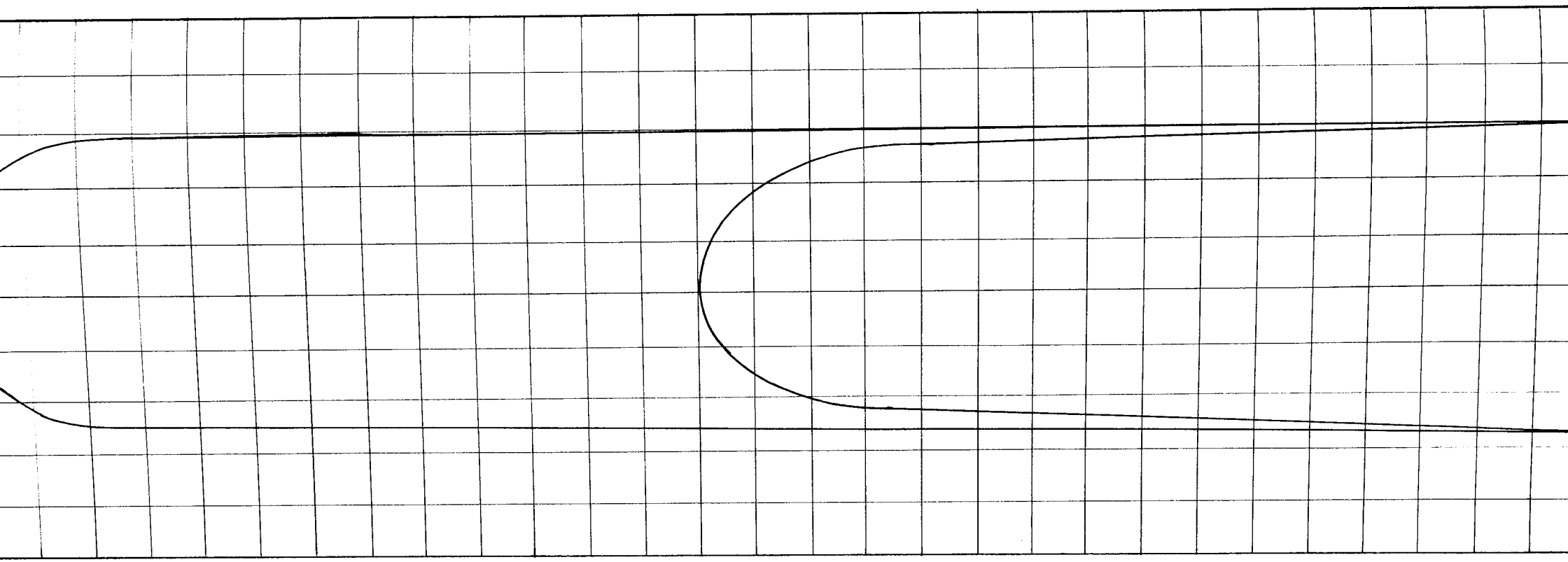

POSITION 3

Scales:- Velocity: 1 mm = 1mm/s

Momentum: 1 mm = kg mm/s

Area under velocity curve = 8680mm^2

Momentum = 16100 mm^2

BED MATERIAL $1\frac{1}{2}$ mm Diameter Glass Spheres

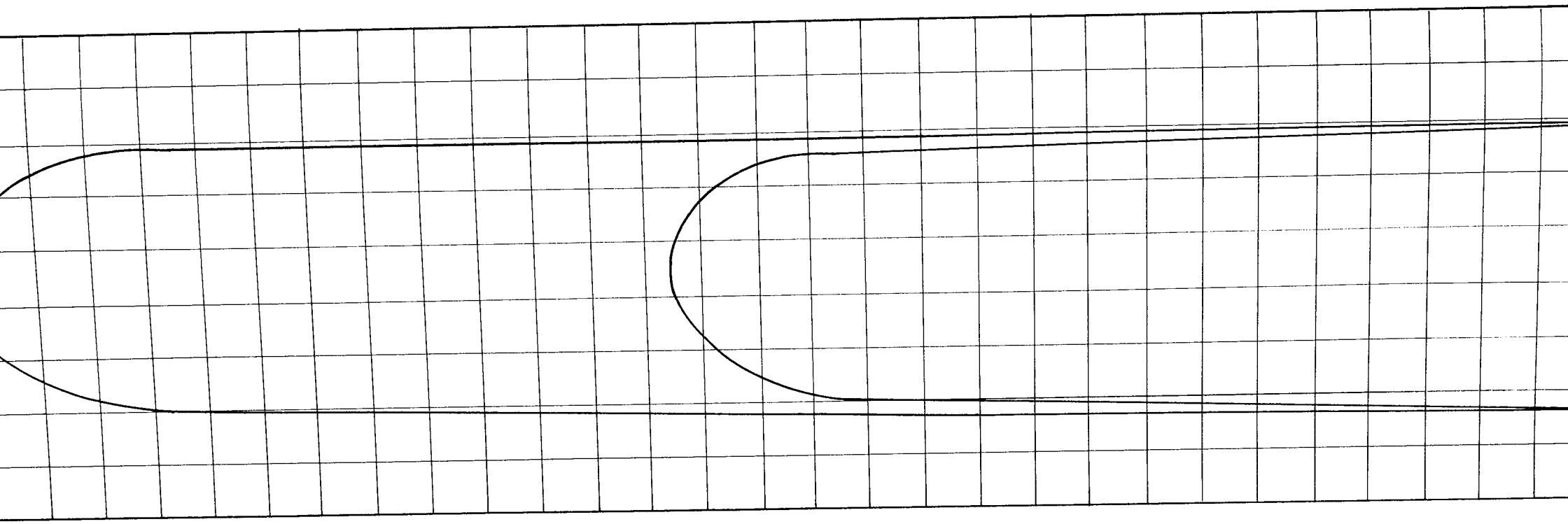

POSITION 4

Scales:- Velocity: 1 mm = 1 mm/s

Momentum: 1 mm = 1 kg.mm/s

Area under Velocity Curve = 8250mm^2

Momentum = 15190mm^2

BED MATERIAL $1\frac{1}{2}$ mm Diameter Glass Spheres

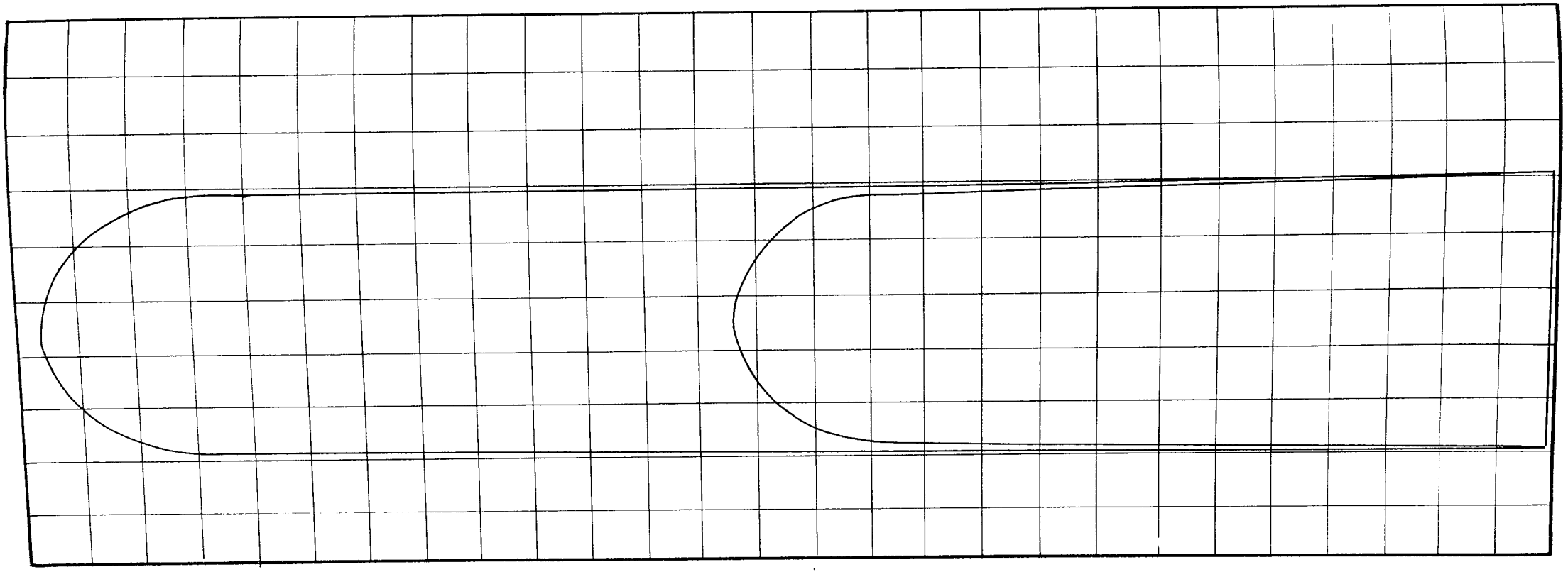

POSITION 5

Scales:- Velocity: 1 mm = 1 mm/s

Momentum: 1 mm = 1 kg mm/s

Area under velocity curve = 8350 mm^2

Momentum = 16,250 mm^2

BED MATERIAL $1\frac{1}{2}$ Diameter Glass Spheres

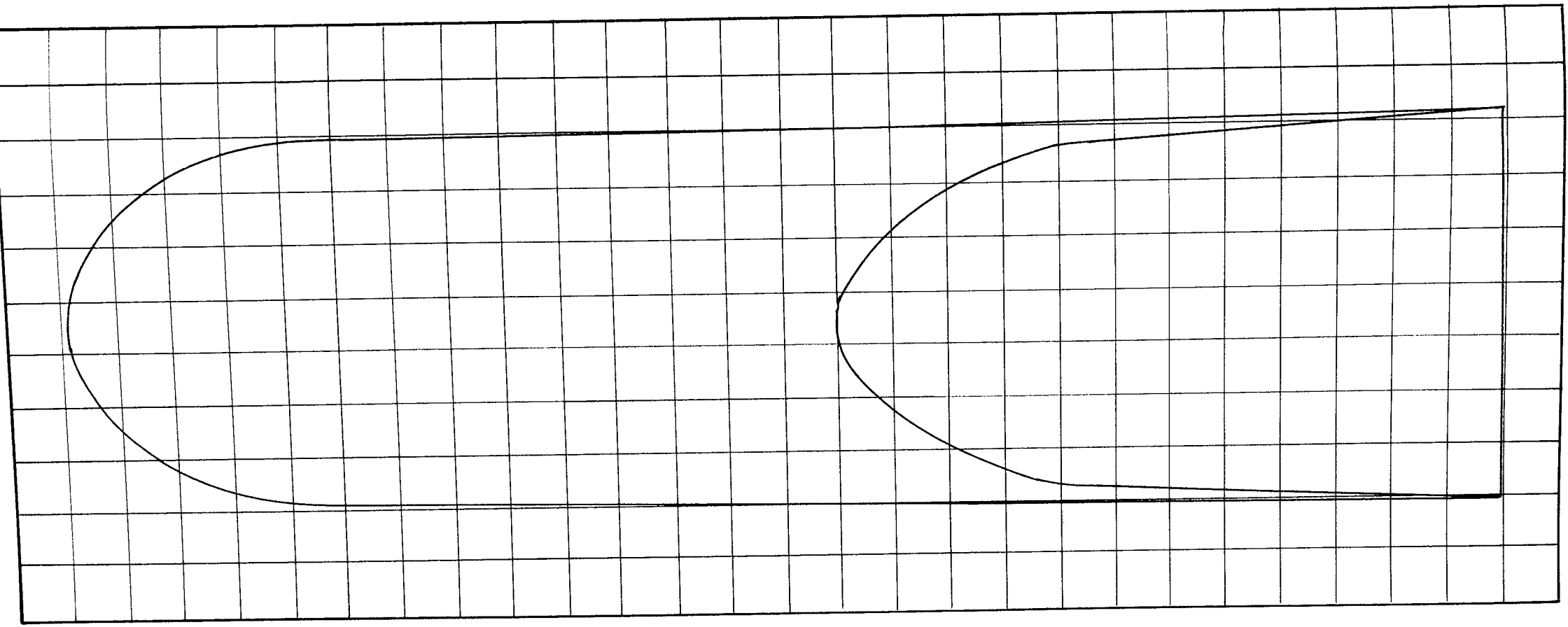

POSITION 1

Scales:- Velocity: 1 mm = 1mm/s

Momentum: $1mm^2 = \frac{1kg}{25}\ mm/s$

Area under Velocity Curve = $6960mm^2$

Momentum = $15100\ mm^2$

BED MATERIAL $1\frac{1}{2}$ mm Diameter Glass Spheres

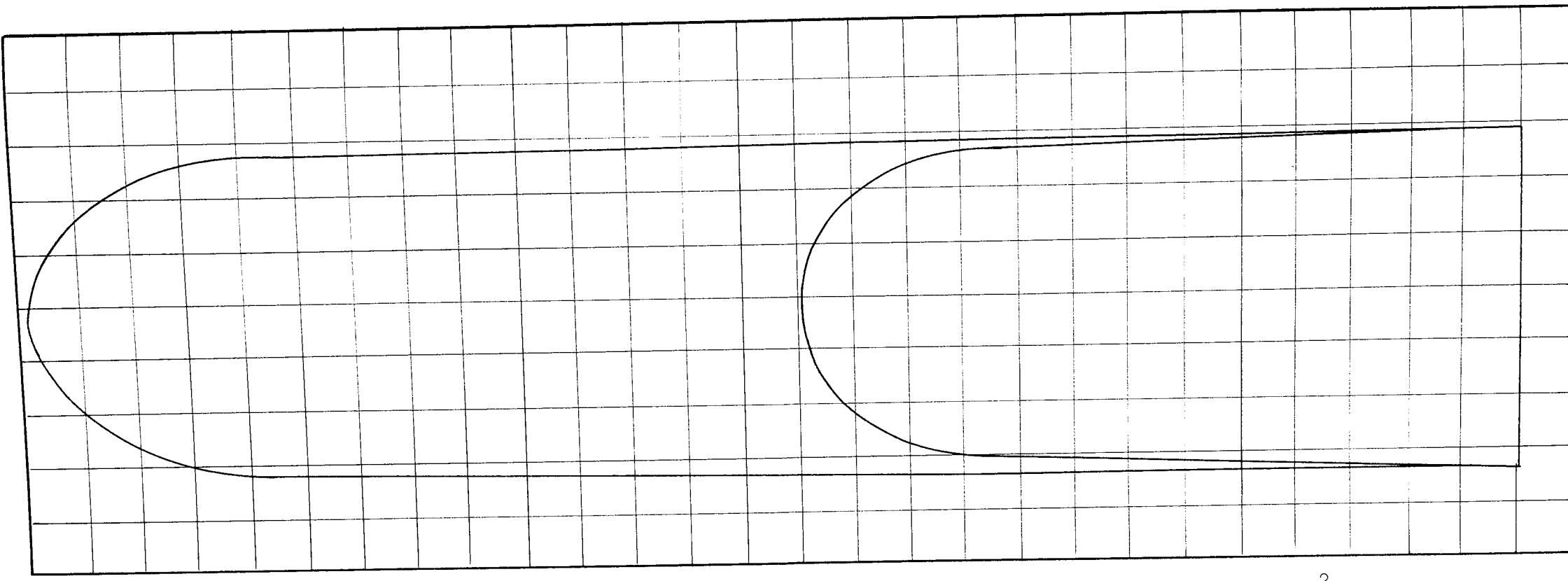

POSITION 2

Scales:- Velocity: 1 mm = 1 mm/s

Momentum: 1 mm^2 = $\frac{1}{25}$ kg mm/s

Area under Velocity Curve = 6940 mm^2

Momentum = 64900 mm^2

BED MATERIAL $1\frac{1}{2}$ mm Diameter Glass Spheres

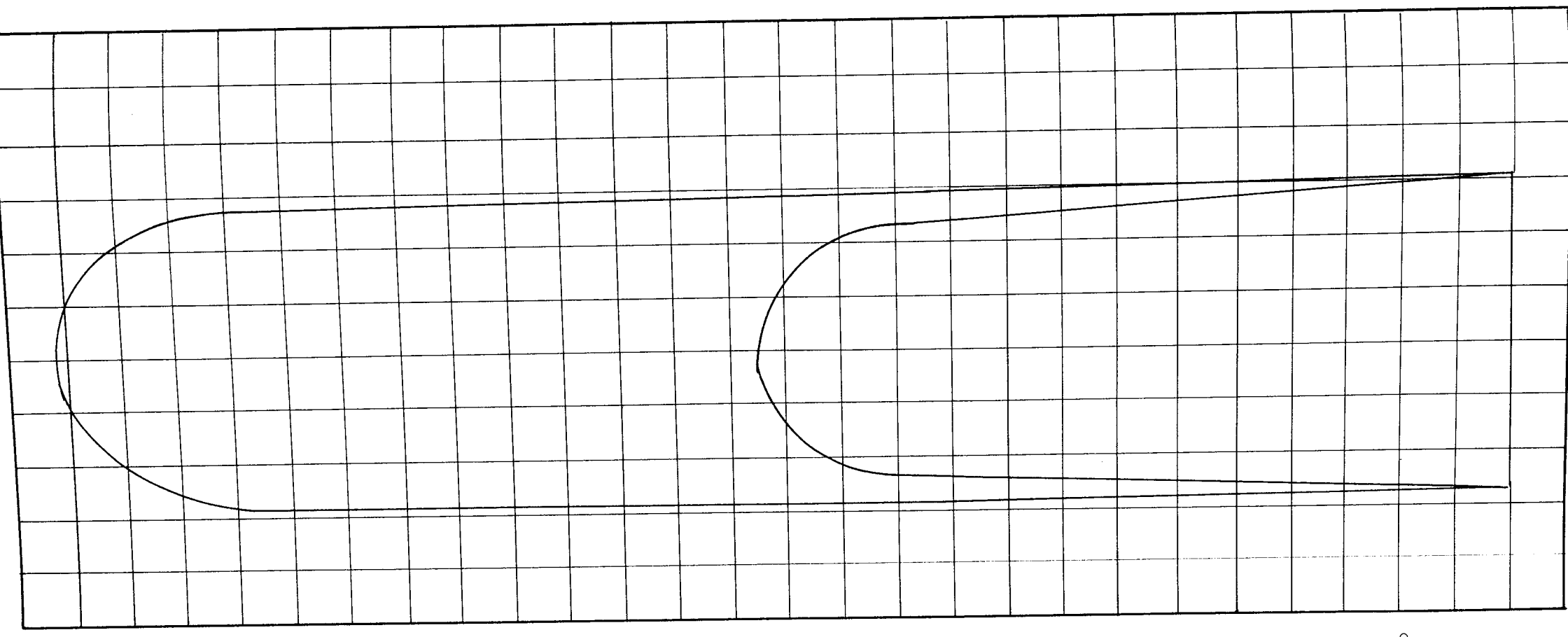

Scales:- Velocity: 1 mm = 1 mm/s

Momentum: $1mm^2 = \frac{1}{25}$ kg mm/s

Area under Velocity Curve = $674 0mm^2$

Momentum = $14800\ mm^2$

POSITION 3

BED MATERIAL $1\frac{1}{2}$ mm Diameter Glass Spheres

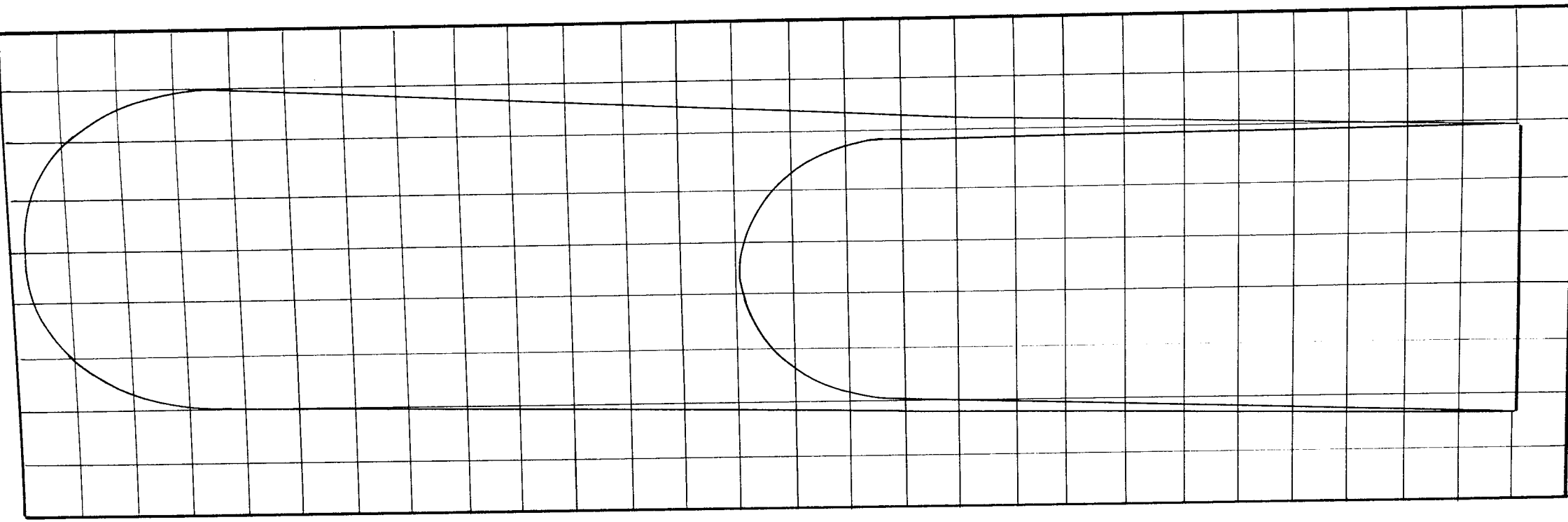

Scales:- Velocity: 1 mm = 1mm/s

Momentum: $1mm^2 = \frac{1}{25}$ kg mm/s

Area under Velocity Curve = $6840mm^2$

Momentum = $14600\ mm^2$

POSITION 4

BED MATERIAL $1\frac{1}{2}$ mm Diameter Glass Spheres

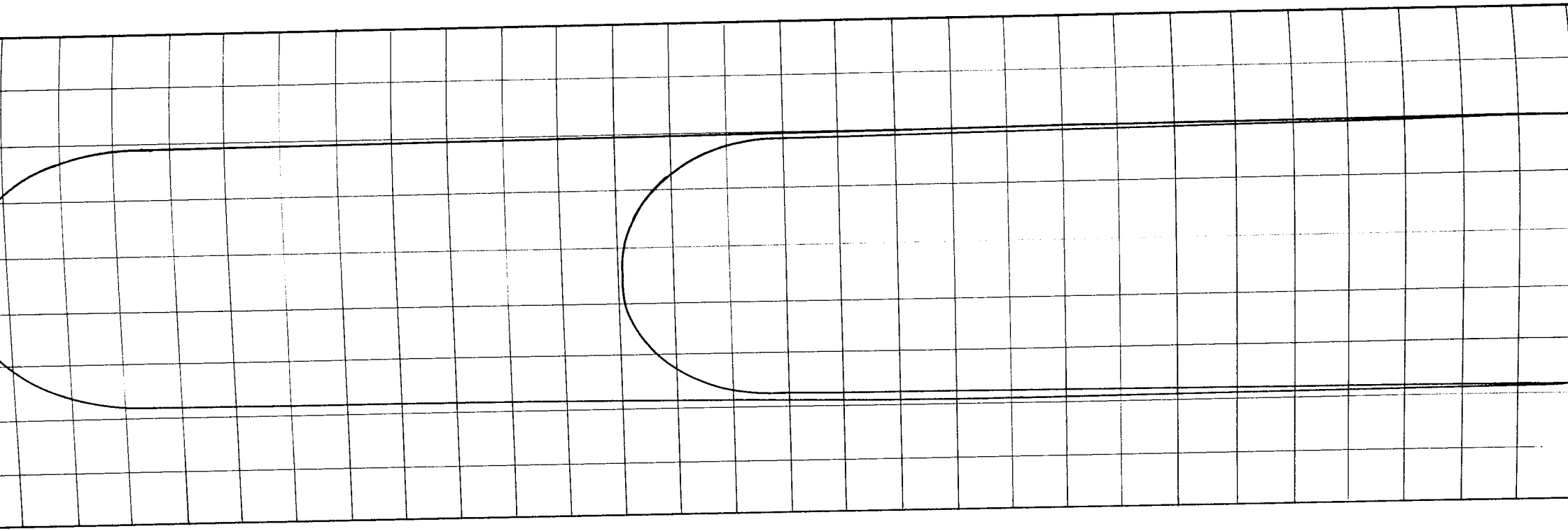

Scales:- Velocity: 1 mm = 1 mm/s

Momentum: 1 mm^2 = $\frac{1}{25}$ kg mm/s

Area under Velocity Curve = 6900 mm^2

Momentum = 14900 mm^2

POSITION 5

BED MATERIAL $1\frac{1}{2}$ mm Diameter Glass Spheres

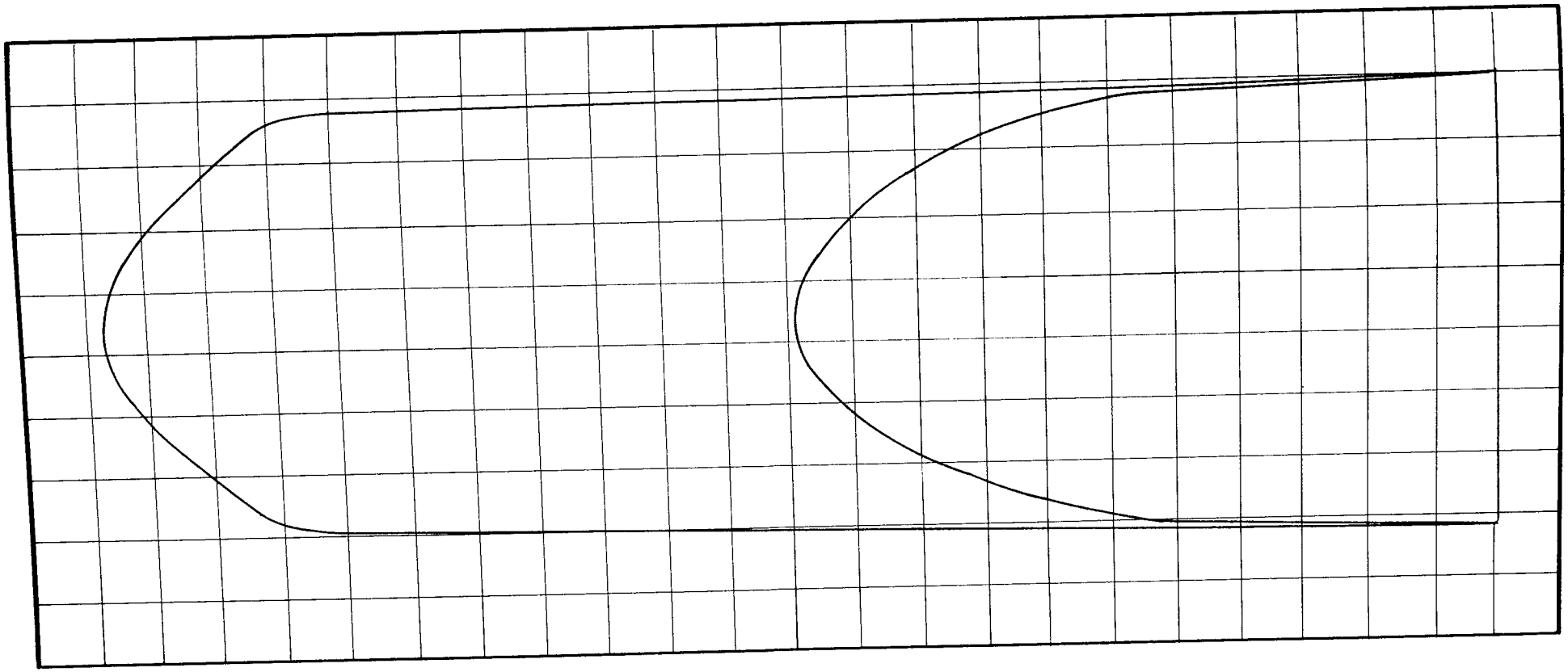

POSITION 1 Scales: Velocity: 1 mm = $\frac{1}{5}$ mm/s

Momentum: 1 mm^2 = $\frac{1}{25}$ kgmm/s

Area under Velocity Curve = 6,220 mm^2

Area under Momentum Curve = 12,220 mm^2

BED MATERIAL: $\frac{11}{2}$ mm Diameter Glass Spheres

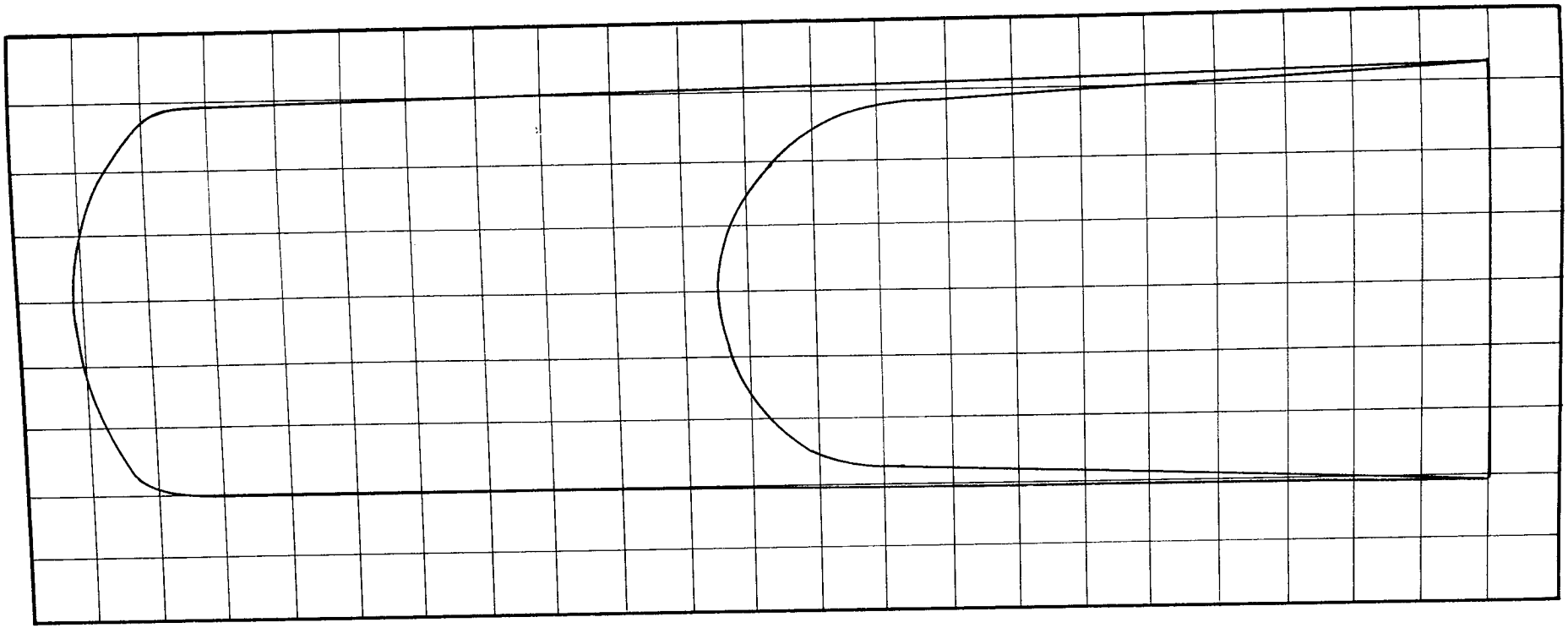

POSITION 2 Scales: Velocity: 1 mm = $\frac{1}{5}$ mm/s Area under Velocity Curve = 6400mm^2

Momentum: 1 mm^2 = $\frac{1}{25}$ kgmm/s Area under Momentum Curve = 13000mm^2

BED MATERIAL; 1 $\frac{1}{2}$ mm Diameter Glass Spheres

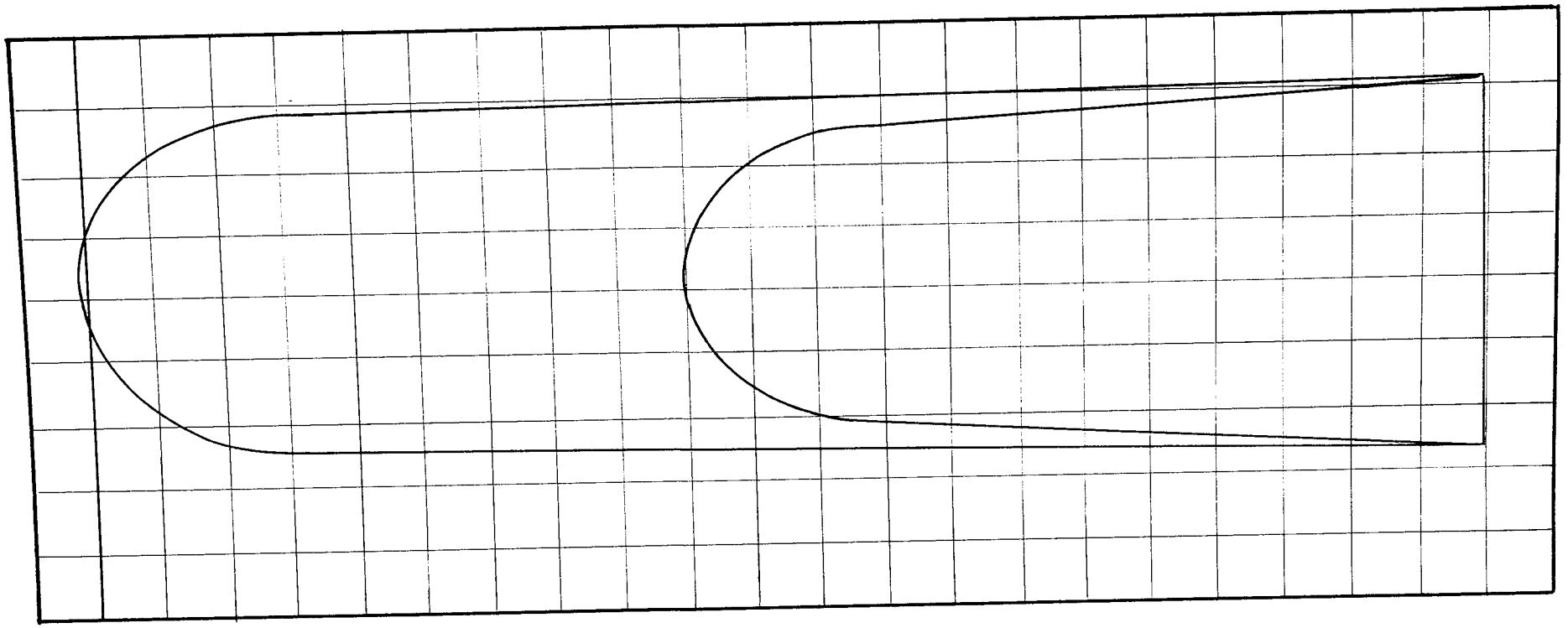

POSITION 3 Scales: Velocity : 1 mm = $\frac{1}{5}$ mm/s Area under Velocity Curve = 635 mm^2

Momentum: 1 mm^2 = $\frac{1}{25}$ kgmm/s Area under Momentum Curve = 1240 mm^2

BED MATERIAL: $1\frac{1}{2}$ mm Diameter Glass Spheres

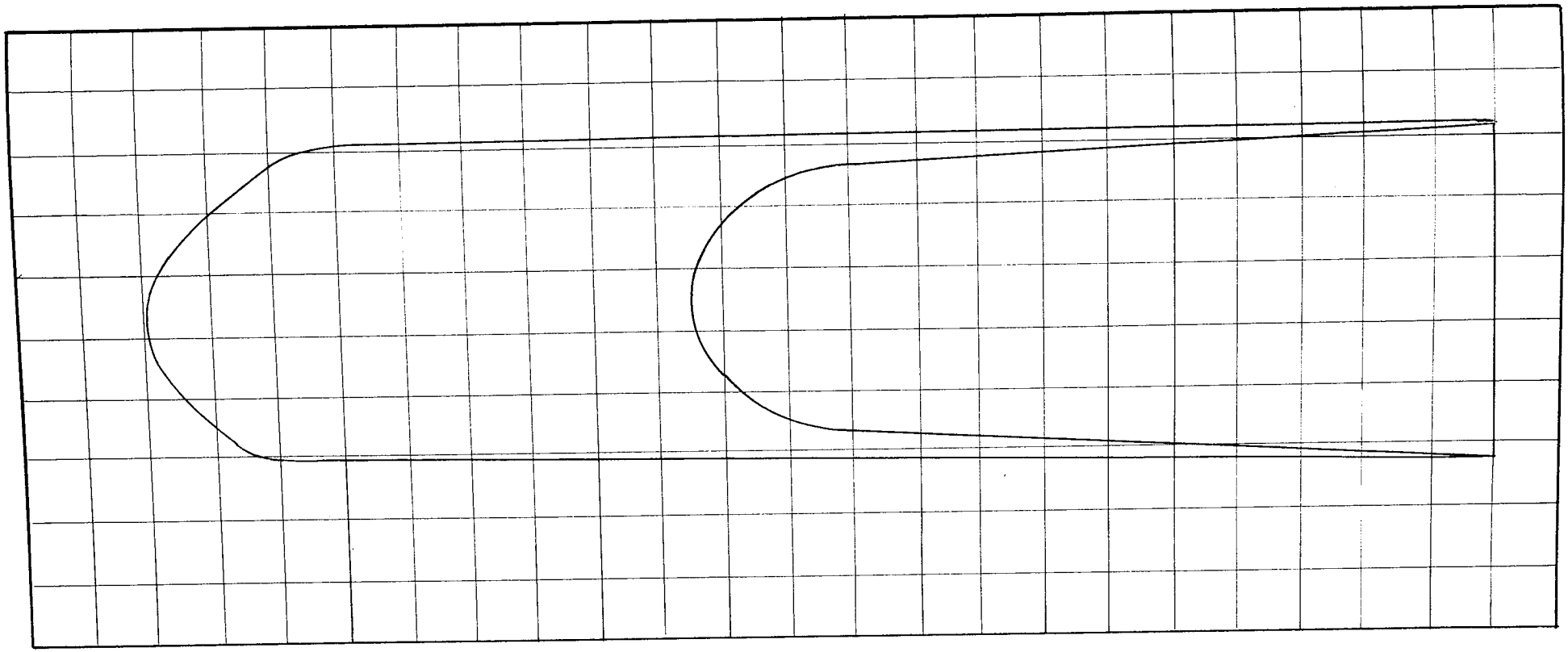

POSITION 4 Scales: Velocity 1 mm = $\frac{1}{5}$ mm/s Area under Velocity Curve = 6300 mm^2

Momentum 1 mm^2 = $\frac{1}{25}$ kgmm/s Area under Momentum Curve = 12,200 mm^2

BED MATERIAL: $1\frac{1}{2}$ mm Diameter Glass Spheres

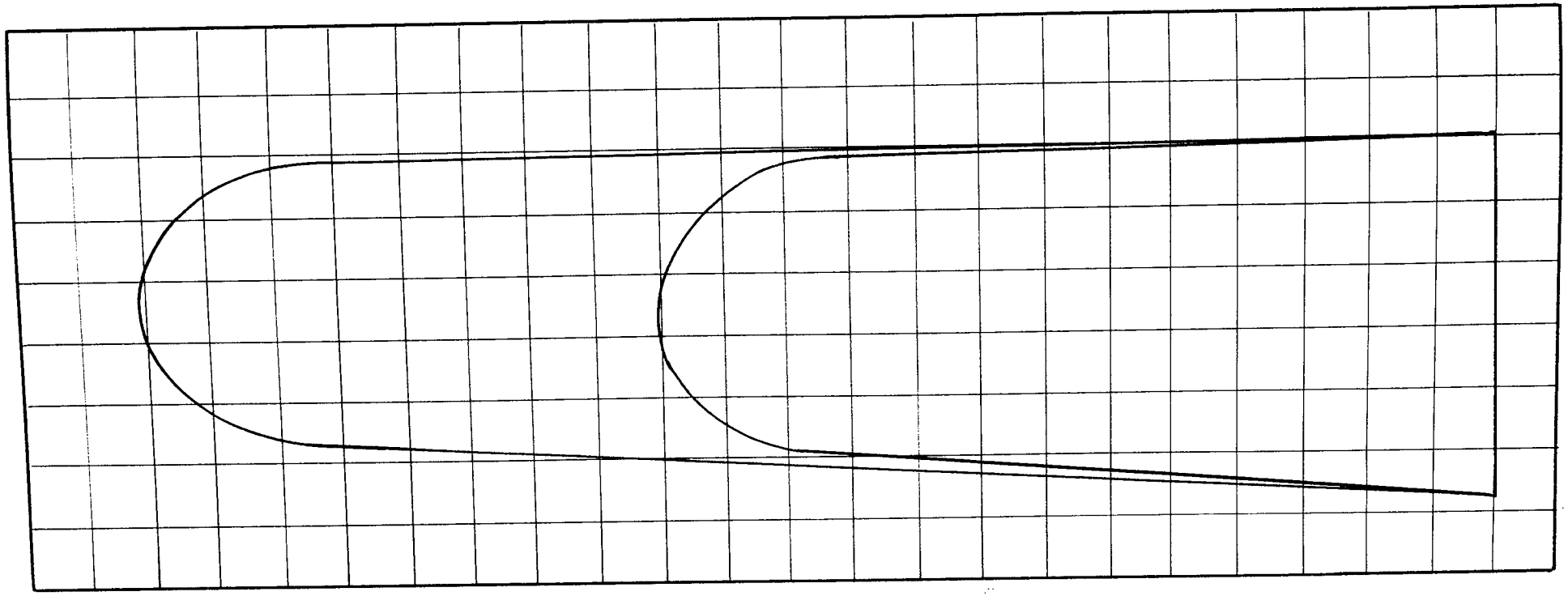

POSITION 5 Scales: Velocity: 1 mm = $\frac{1}{5}$ mm/s Area under Velocity Curve = 6,100 mm^2

Momentum: 1 mm^2 = $\frac{1}{25}$ kgmm/s Area under Momentum Curve = 11,800 mm^2

BED MATERIAL: $1\frac{1}{2}$ mm Diameter Glass Spheres

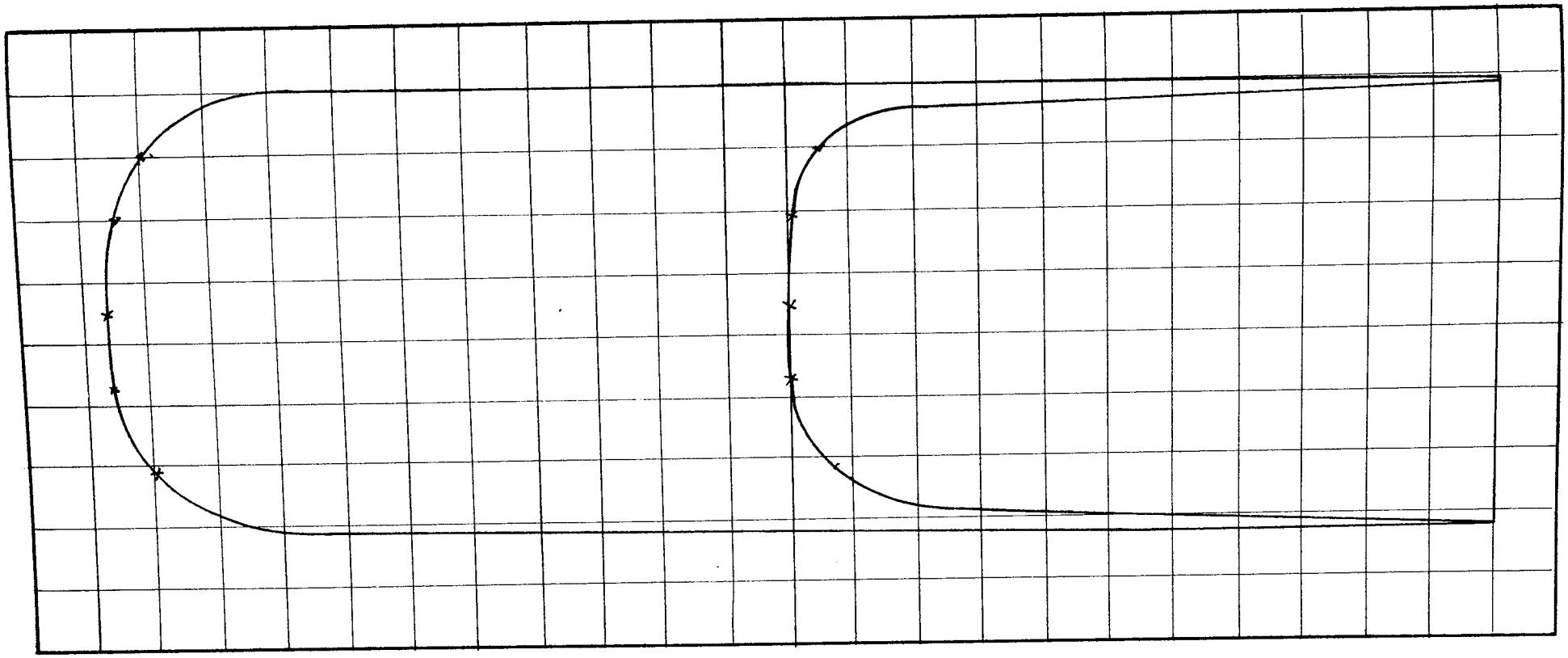

POSITION 1 Scales: Velocity: 1 mm = 1 mm/s

Momentum: 1 mm^2 = $\frac{1}{4}$ kgmm/s

Area under Velocity Curve = 7,190 mm^2

Area under Momentum Curve = 13,370 mm^2

BED MATERIAL: $1\frac{1}{2}$ mm Diameter Glass Spheres

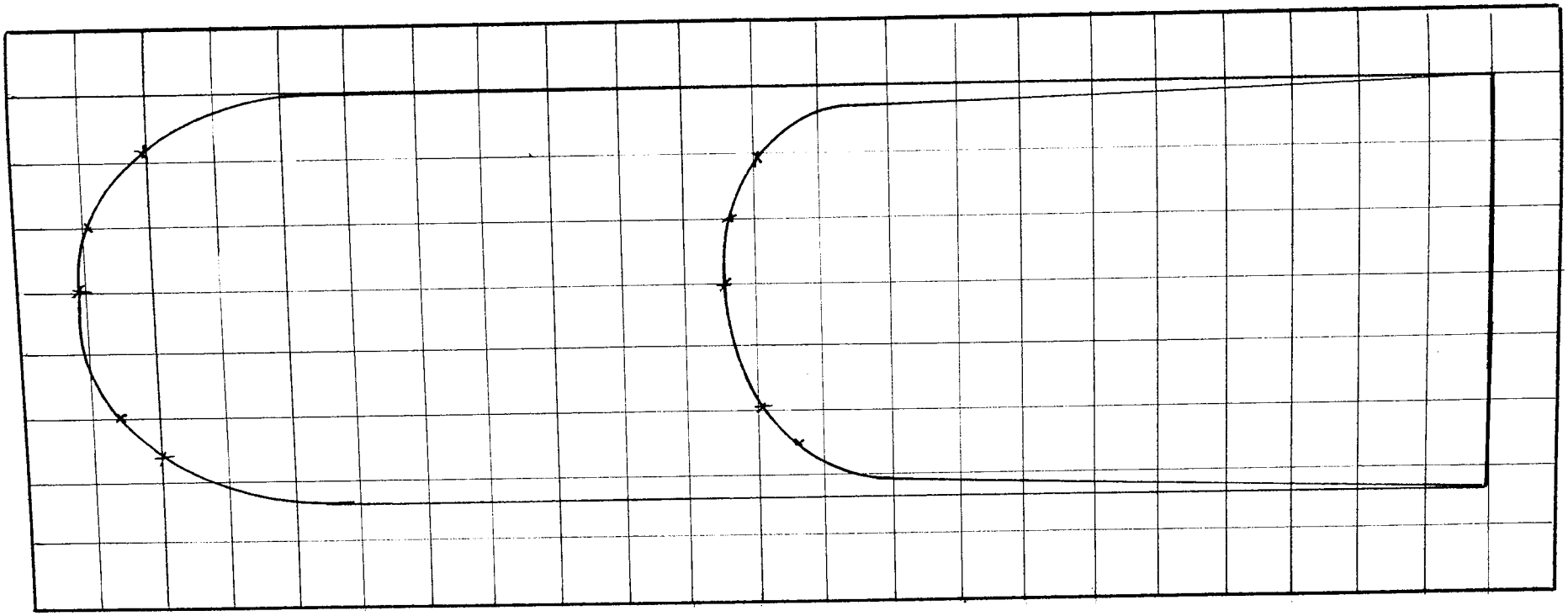

POSITION 2 Scales: Velocity: 1 mm = 1 mm/s
Momentum: 1 mm ^{2} = $\frac{1}{4}$ kgmm/s

Area under Velocity Curve = 7,290 mm^2
Area under Momentum Curve = 13,500 mm^2

BED MATERIAL: $1\frac{1}{2}$ mm Diameter Glass Spheres

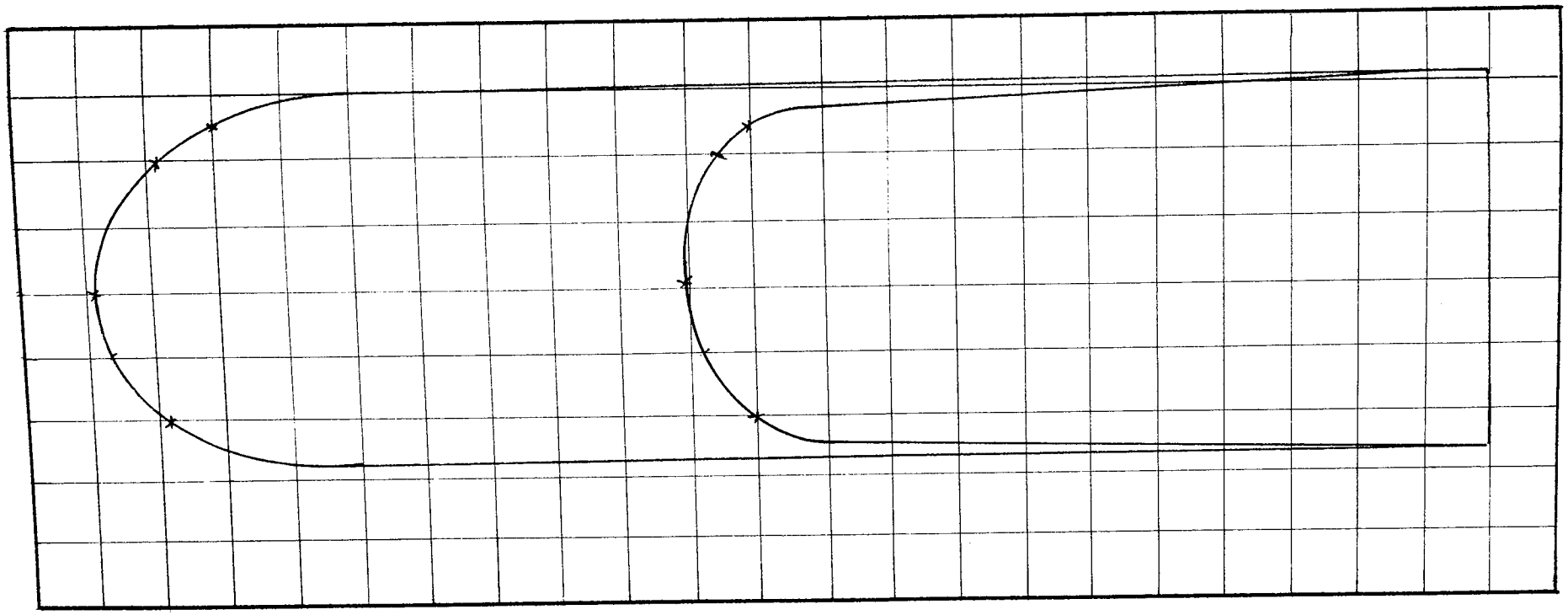

POSITION 3: Scales: Velocity: 1 mm = 1 mm/s Area under Velocity Curve = 7,310 mm^2

Momentum: 1 mm^2 = $\frac{1}{4}$ kgmm/s Area under Momentum Curve = 13,300 mm^2

BED MATERIAL: $1\frac{1}{2}$ mm Diameter Glass Spheres

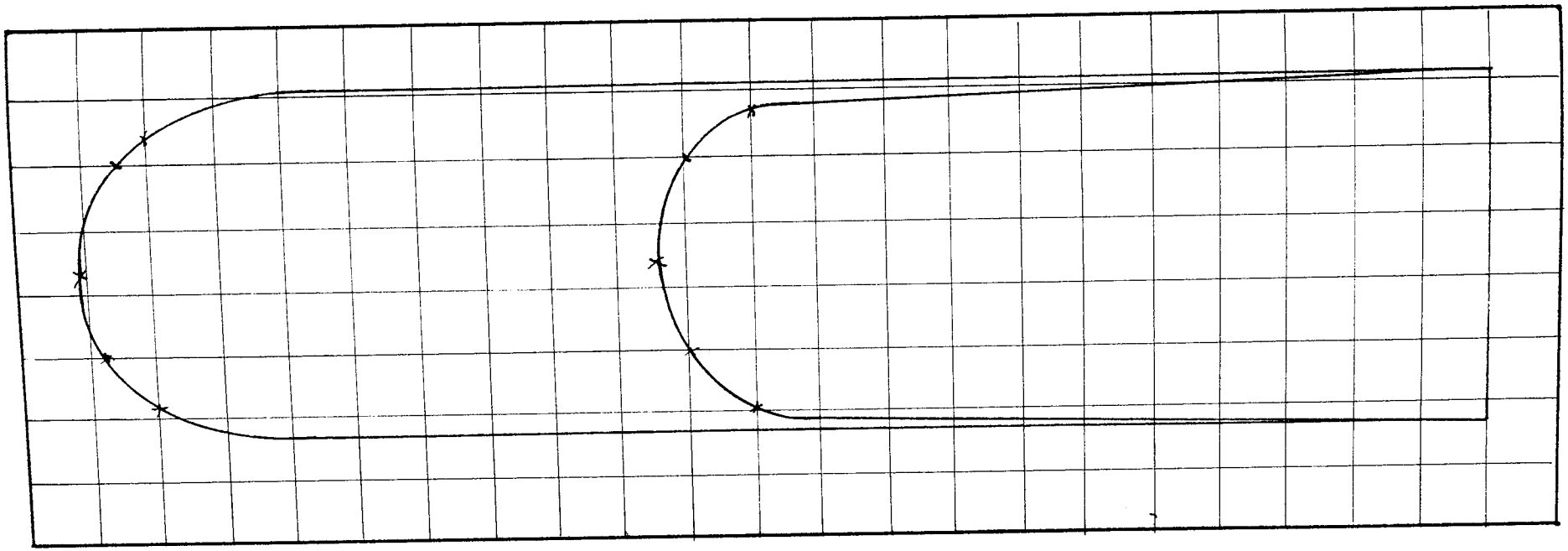

POSITION 4 Scale: Velocity: 1 mm = 1 mm/s Area under Velocity Curve = 7,200 mm^2

Momentum: 1 mm^2 = $\frac{1}{4}$ kgmm/s Area under Momentum Curve = 12,800 mm^2

BED MATERIAL: $1\frac{1}{2}$ mm Diameter Glass Spheres

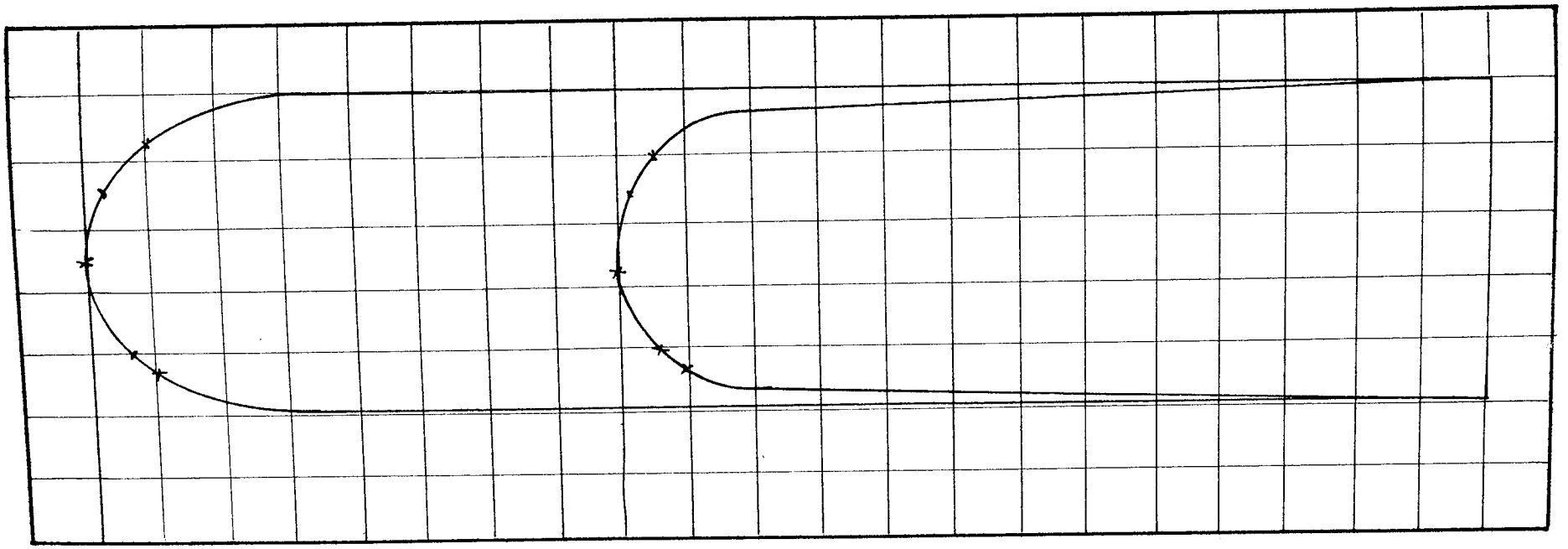

POSITION 5 Scales: Velocity: 1 mm = 1 mm/s Area under Velocity Curve = 6,600 mm^2

Momentum: 1 mm^2 = $\frac{1}{4}$ kgmm/s Area under Momentum Curve = 12,600 mm^2

BED MATERIAL: $1\frac{1}{2}$ mm Diameter Glass Spheres

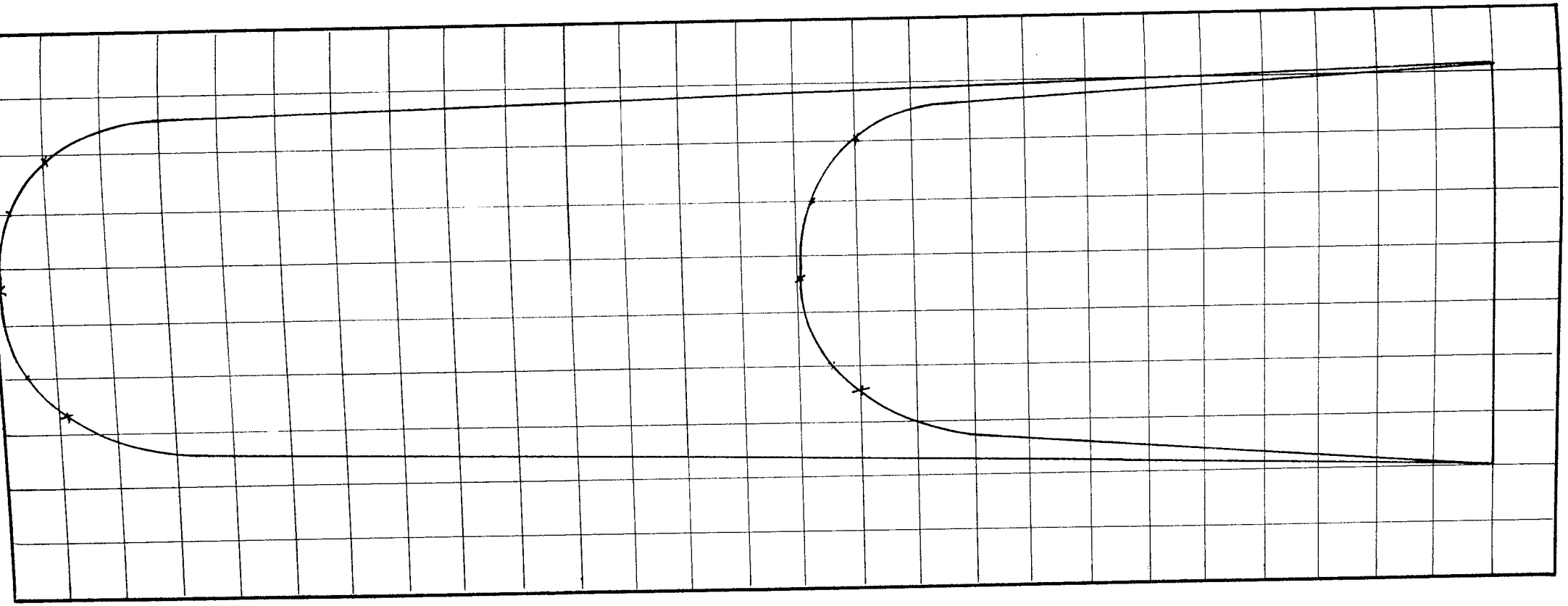

POSITION 1 Scales: Velocity: 1 mm = 1 mm/s Area under Velocity Curve = 7,480 mm^2

Momentum: 1 mm^2 = $\frac{1}{4}$ kgmm/s Area under Momentum Curve = 16,370 mm^2

BED MATERIAL: $1\frac{1}{2}$ Diameter Glass Spheres

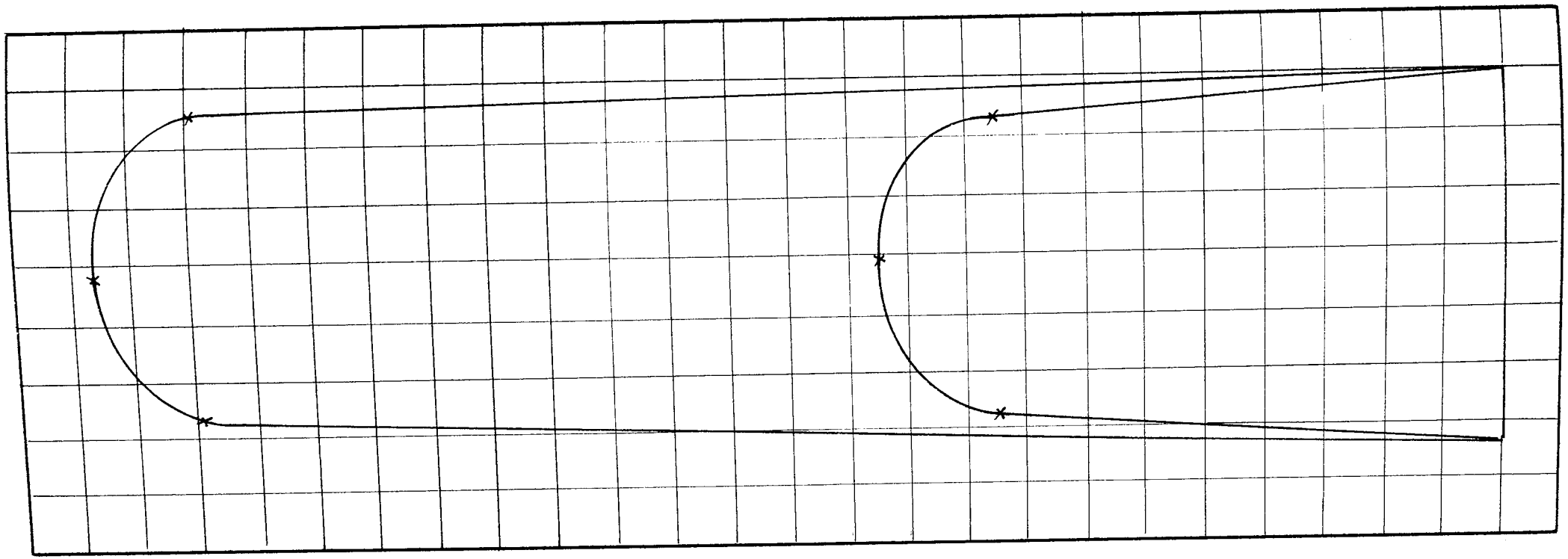

POSITION 2 Scales: Velocity: 1 mm = 1 mm/s Area under Velocity Curve = 6,550 mm^2

Momentum: 1 mm^2 = $\frac{1}{25}$ kgmm/s Area under Momentum Curve = 15,000 mm^2

BED MATERIAL: $1\frac{1}{2}$ mm Diameter Glass Spheres

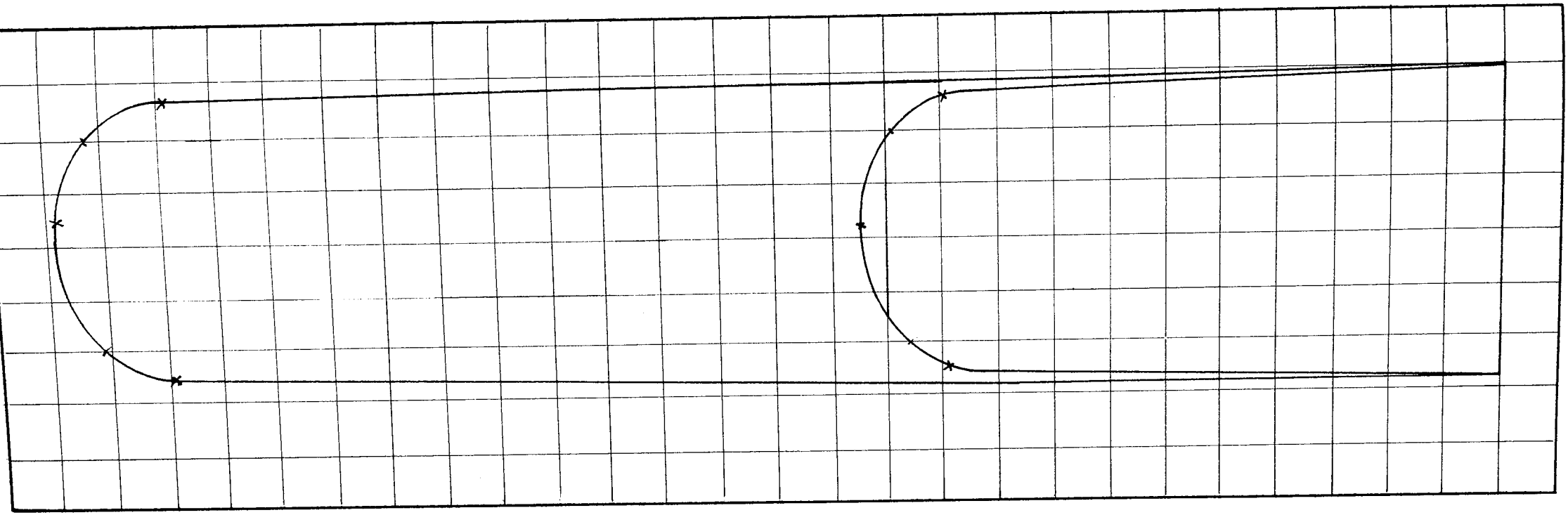

POSITION 3 Scales: Velocity: 1 mm = 1 mm/s Area under Velocity Curve = 6,500 mm^2

Momentum: 1 mm^2 = $\frac{1}{25}$ kgmm/s Area under Momentum Curve = 15,000 mm^2

BED MATERIAL: $1\frac{1}{2}$ mm Diameter Glass Spheres

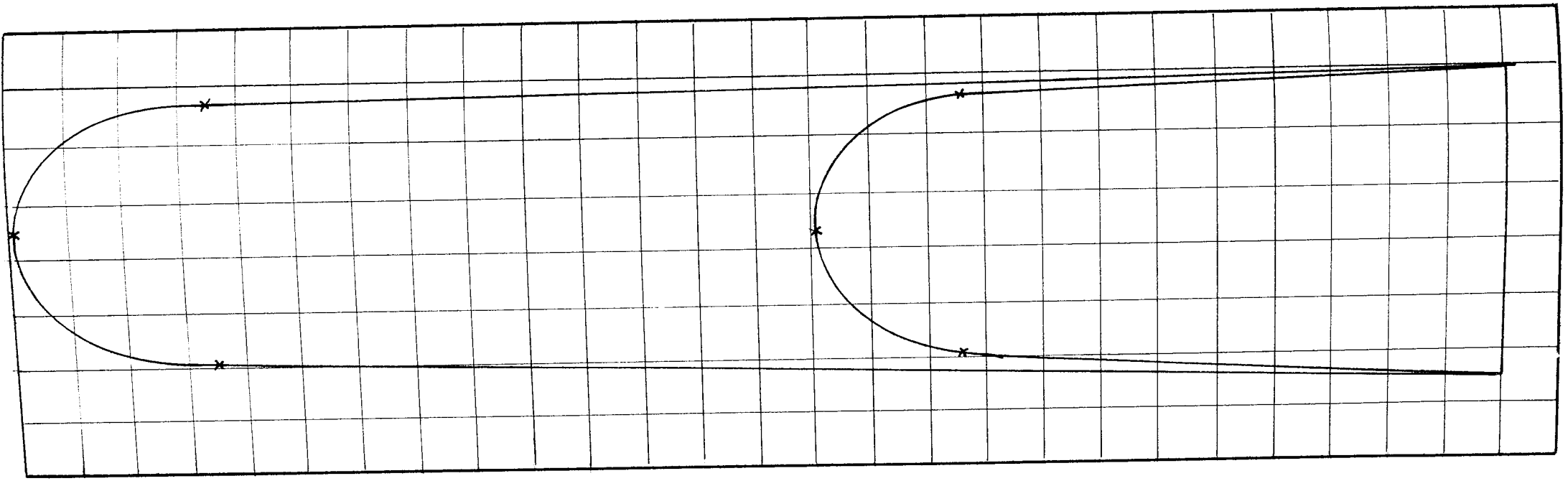

POSITION 4 Scales Velocity: 1 mm = 1 mm/s Area under Velocity Curve = 6,600 mm^2

Momentum: 1 mm^2 = $\frac{1}{25}$ kgmm/s Area under Momentum Curve = 14,850 mm^2

BED MATERIAL: $1\frac{1}{2}$ mm Diameter Glass Spheres

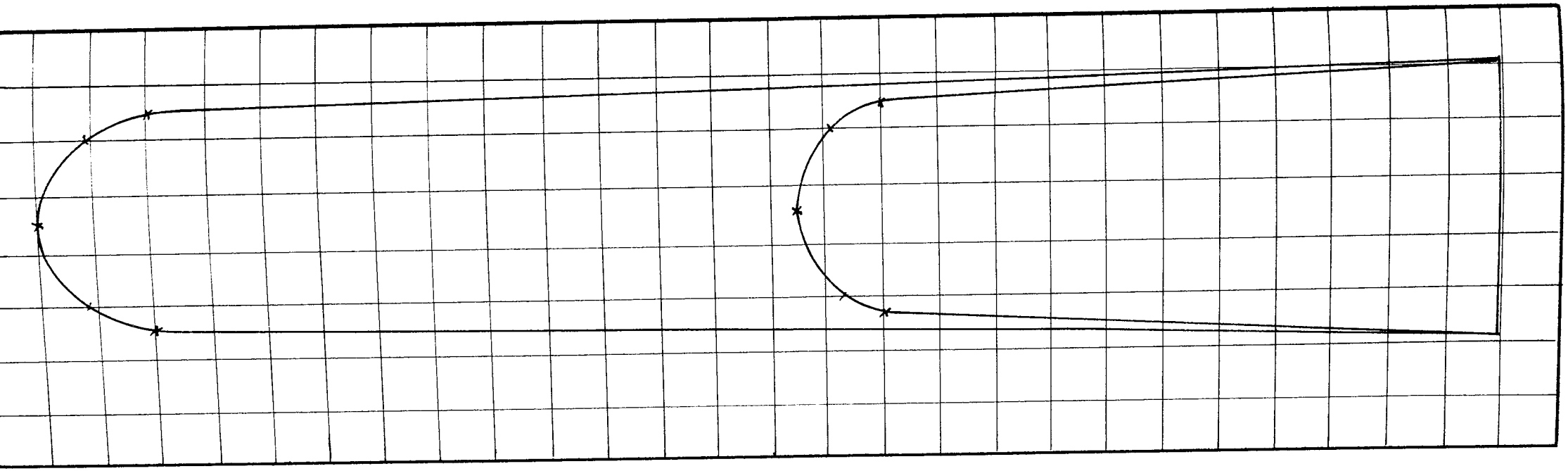

POSITION 5 Scale: Velocity: 1 mm = 1 mm/s Area under Velocity Curve = 6,200 mm^2

Momentum: 1 mm^2 = $\frac{1}{25}$ kgmm/s Area under Momentum Curve = 14,600 mm^2

BED MATERIAL: $1\frac{1}{2}$ mm Diameter Glass Spheres

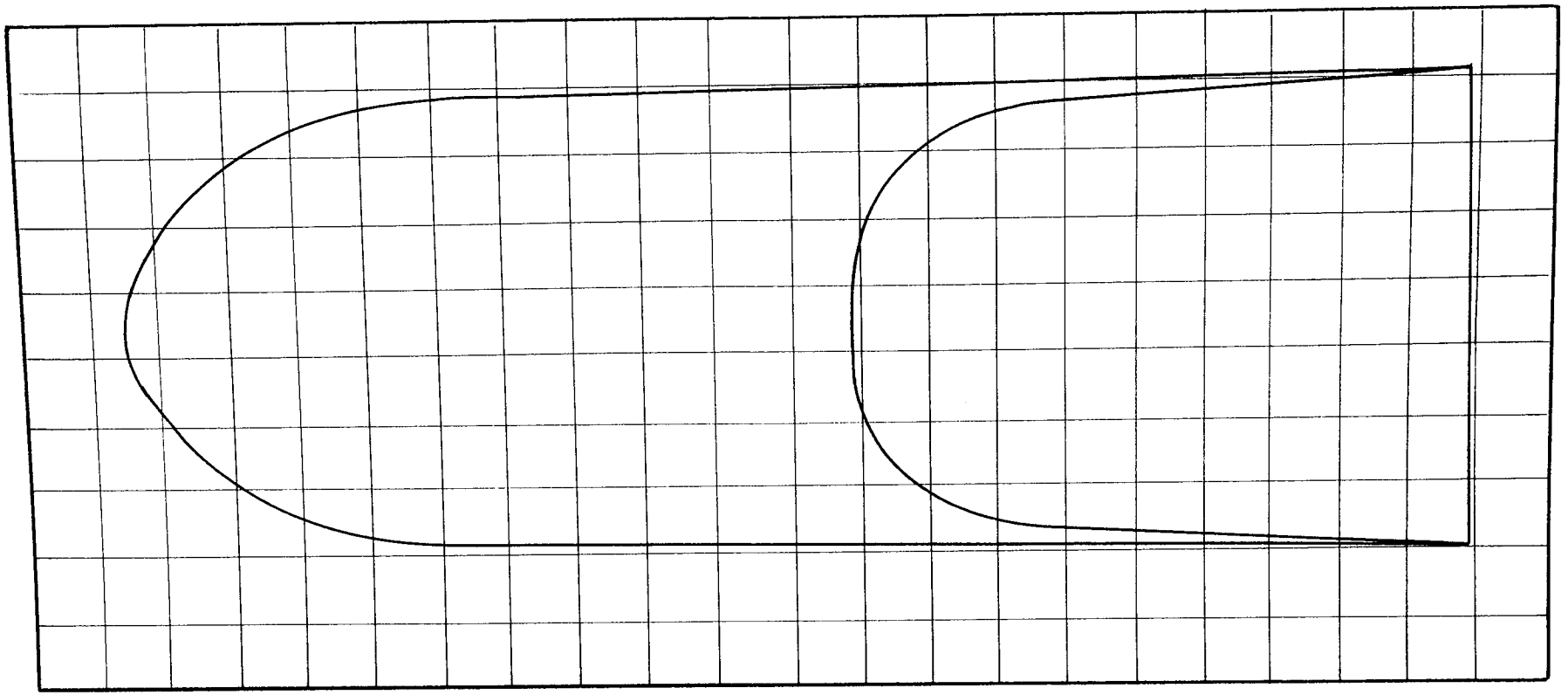

POSITION 1

Scales: Velocity = 1 mm = $\frac{1}{5}$ mm/s

1 mm^2 = $\frac{1}{100}$ kgmm/s

Area under Velocity Curve = 5310mm^2

Area under Momentum Curve = 12700mm^2

BED MATERIAL: $1\frac{1}{2}$ mm Diameter Glass Spheres

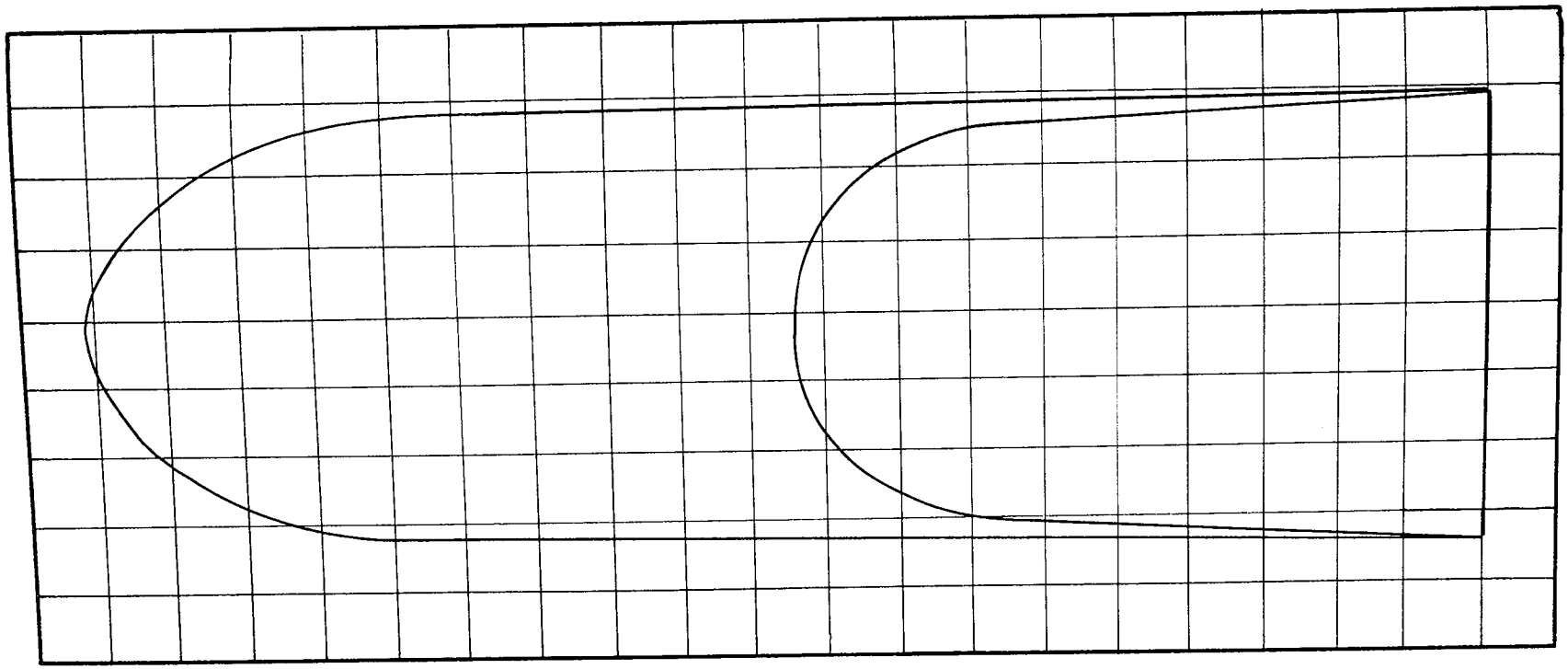

POSITION 2 Scales: Velocity = 1 mm = $\frac{1}{5}$ mm/s

1 mm^2 = $\frac{1}{100}$ kgmm/s

Area under Velocity Curve = 5210mm^2

Area under Momentum Curve = 12200mm^2

BED MATERIAL: $1\frac{1}{2}$ mm Diameter Glass Spheres

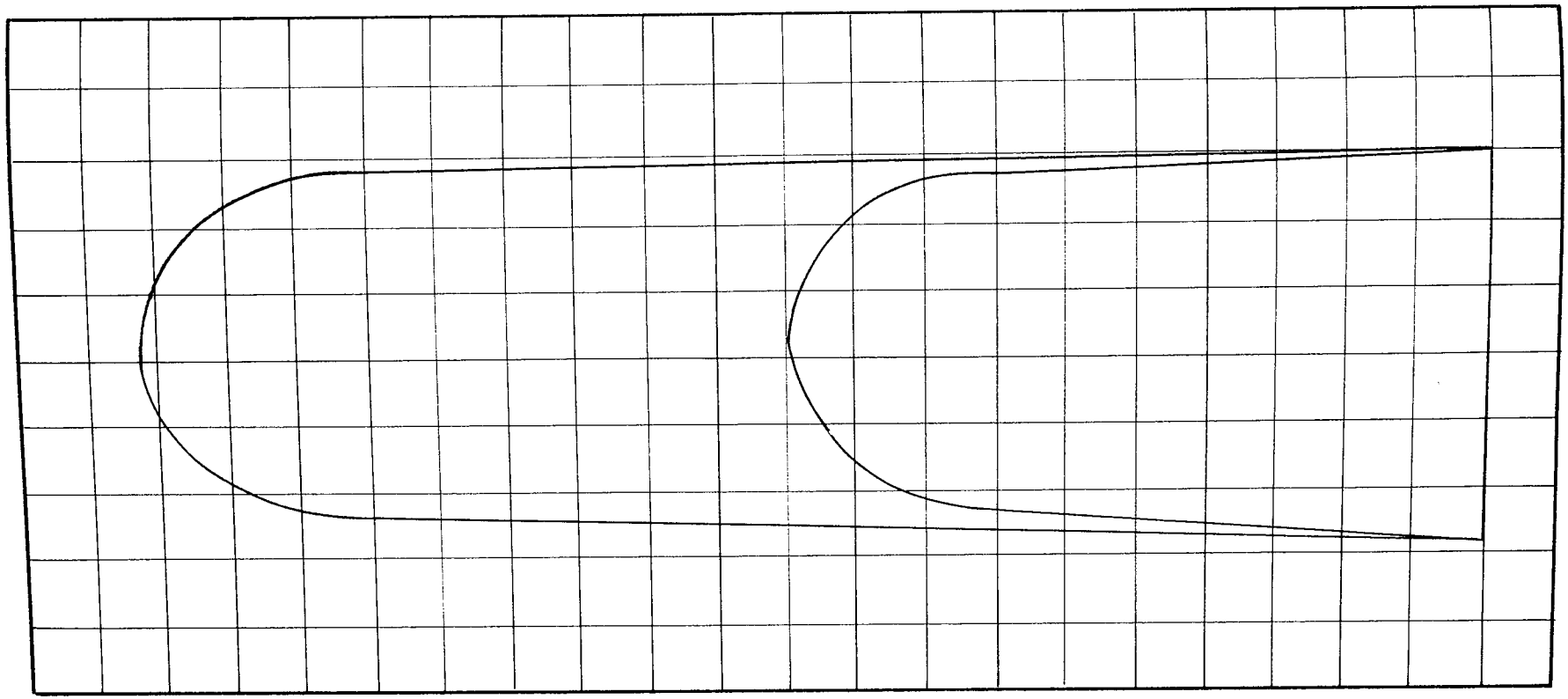

POSITION 3 Scales: Velocity = 1 mm = $\frac{1}{5}$ mm/s Area under Velocity Curve = 5110 mm^2

1 mm^2 = $\frac{1}{100}$ kgmm/s Area under Momentum Curve = 11000mm^2

BED MATERIAL: $1\frac{1}{2}$ mm Diameter Glass Spheres

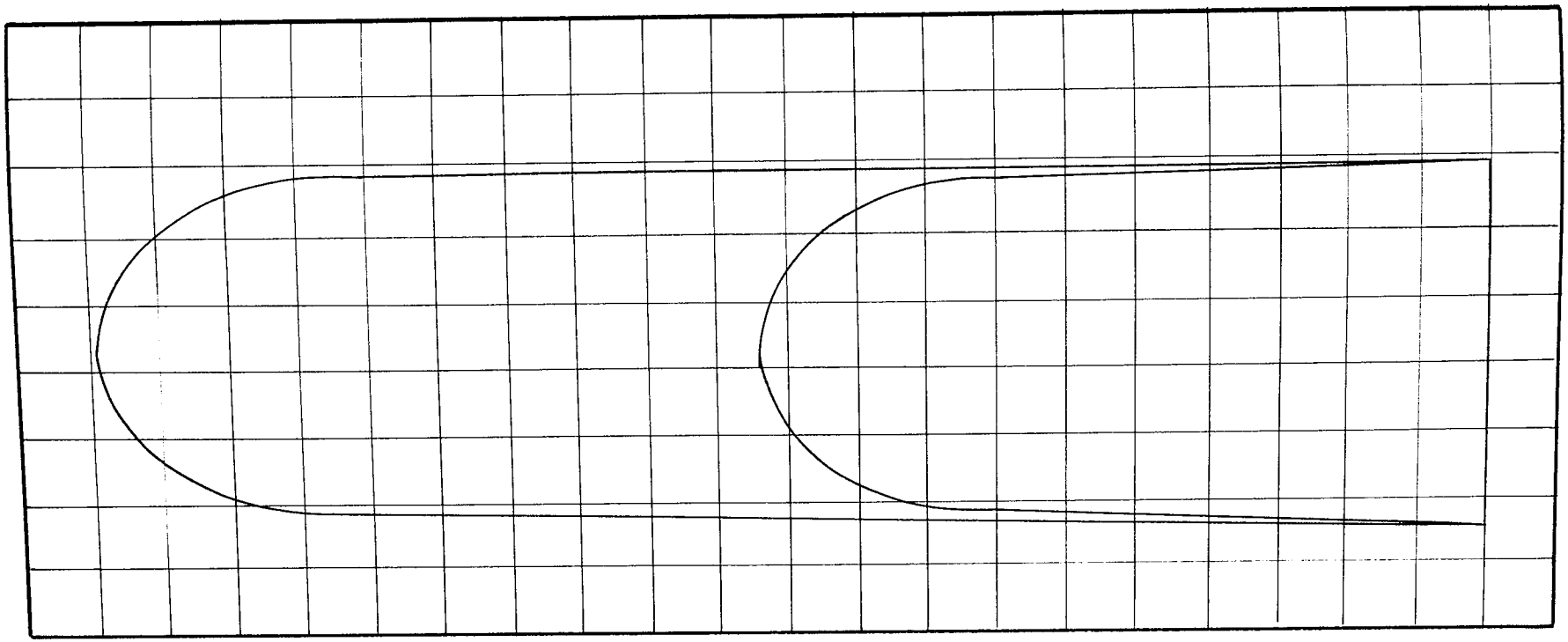

POSITION 4 Scales: Velocity = 1 mm = $\frac{1}{5}$ mm/s

$1\ mm^2 = \frac{1}{100}$ kgmm/s

Area under Velocity Curve = $5620 mm^2$

Area under Momentum Curve = $11600 mm^2$

BED MATERIAL: 1 $\frac{1}{2}$ mm Diameter Glass Spheres

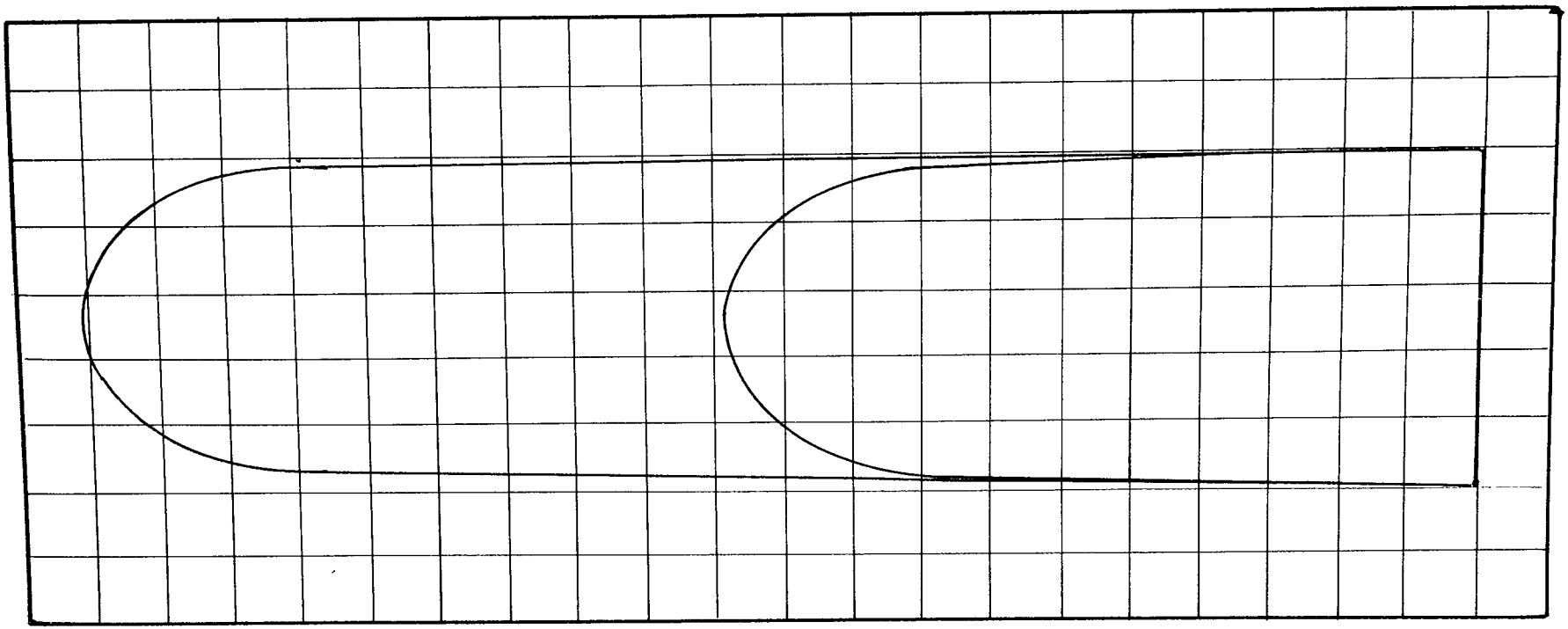

POSITION 5 Scales: Velocity = 1 mm = $\frac{1}{5}$ mm/s Area under Velocity Curve = 5240mm^2

1 mm^2 = $\frac{1}{100}$ kgmm/s Area under Momentum Curve = 11520mm^2

BED MATERIAL: $1\frac{1}{2}$ mm Diameter Glass Spheres

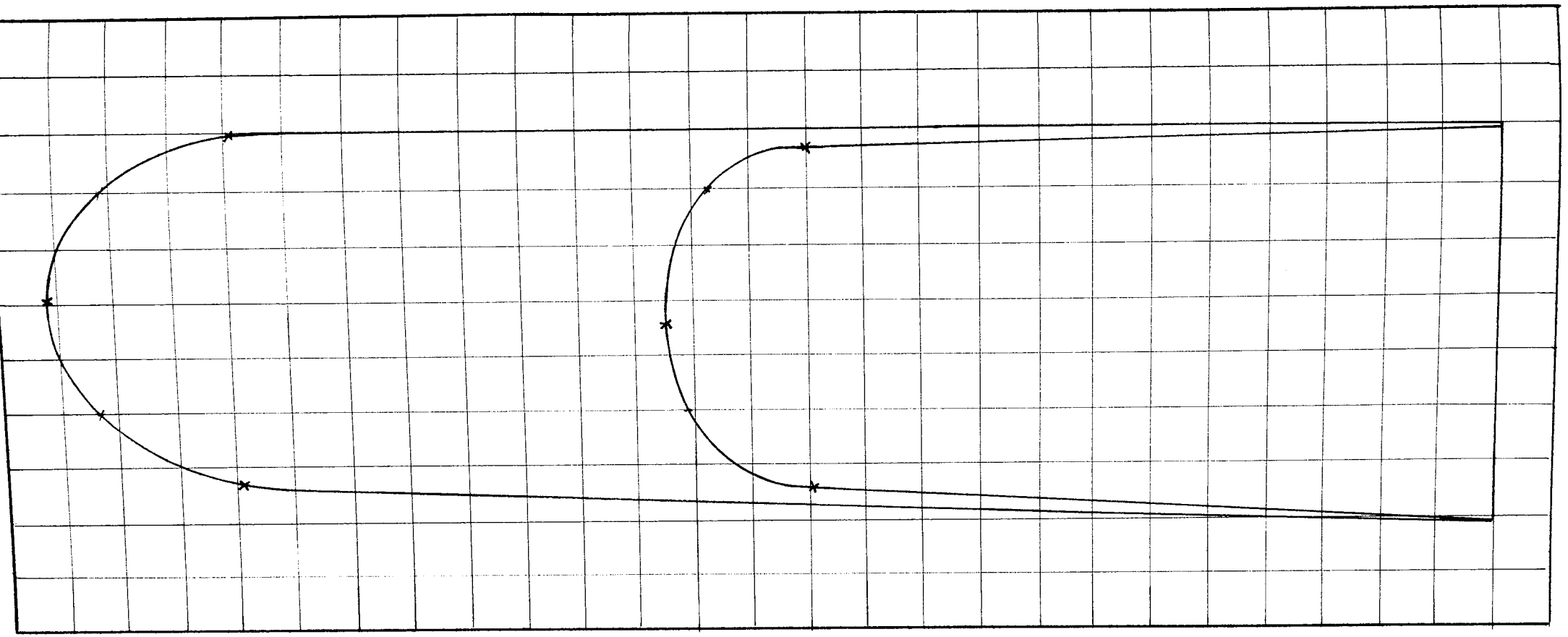

POSITION 1 Scales: Velocity: 1 mm = 1 mm/s

Momentum: 1 mm^2 = $\frac{1}{6}$ kgmm/s

Area under Velocity Curve = 9,500 mm^2

Area under Momentum Curve = 16,720 mm^2

BED MATERIAL: $1\frac{1}{2}$ mm Diameter Glass Spheres

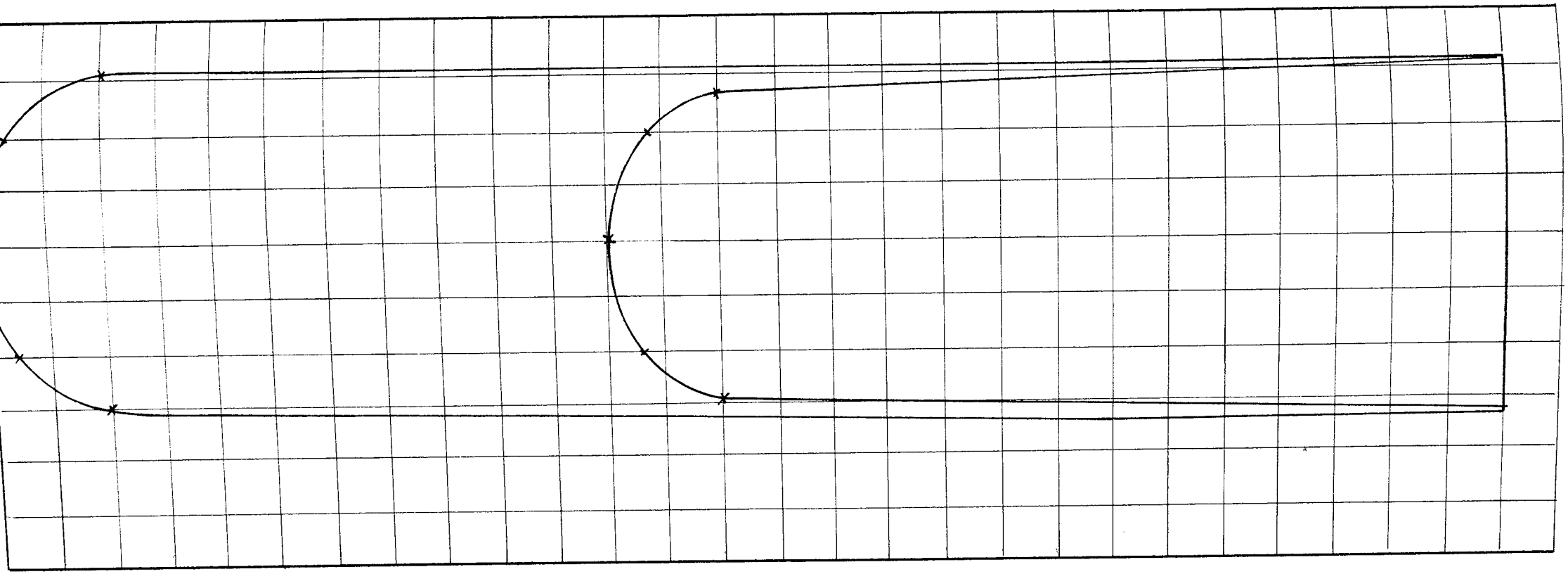

POSITION 2 Scales: Velocity: 1 mm = 1 mm/s Area under Velocity Curve = 9,700 mm^2

Momentum: 1 mm^2 = $\frac{1}{6}$ kgmm/s Area under Momentum Curve = 17,100 mm^2

BED MATERIAL: $1\frac{1}{2}$ mm Diameter Glass Spheres

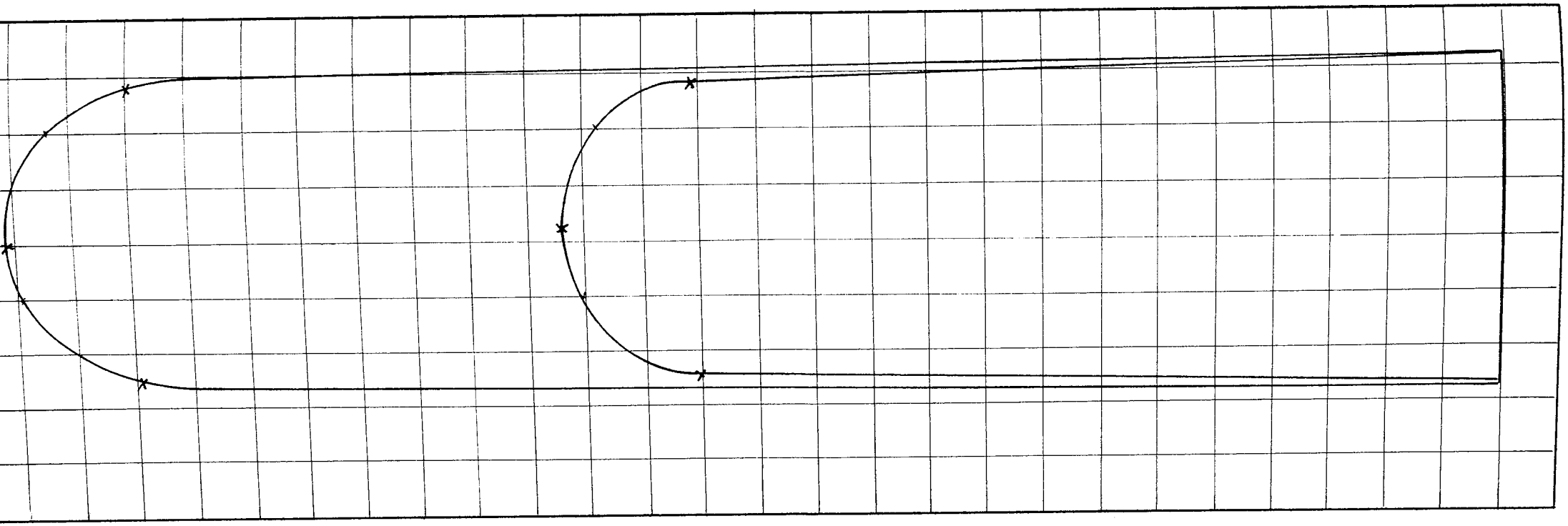

POSITION 3 Scales: Velocity: 1 mm = 1 mm/s Area under Velocity Curve = 9,450 mm^2

Momentum: 1 mm^2 = $\frac{1}{6}$ kgmm/s Area under Momentum Curve = 16,550 mm^2

BED MATERIAL: $1\frac{1}{2}$ mm Diameter Glass Spheres

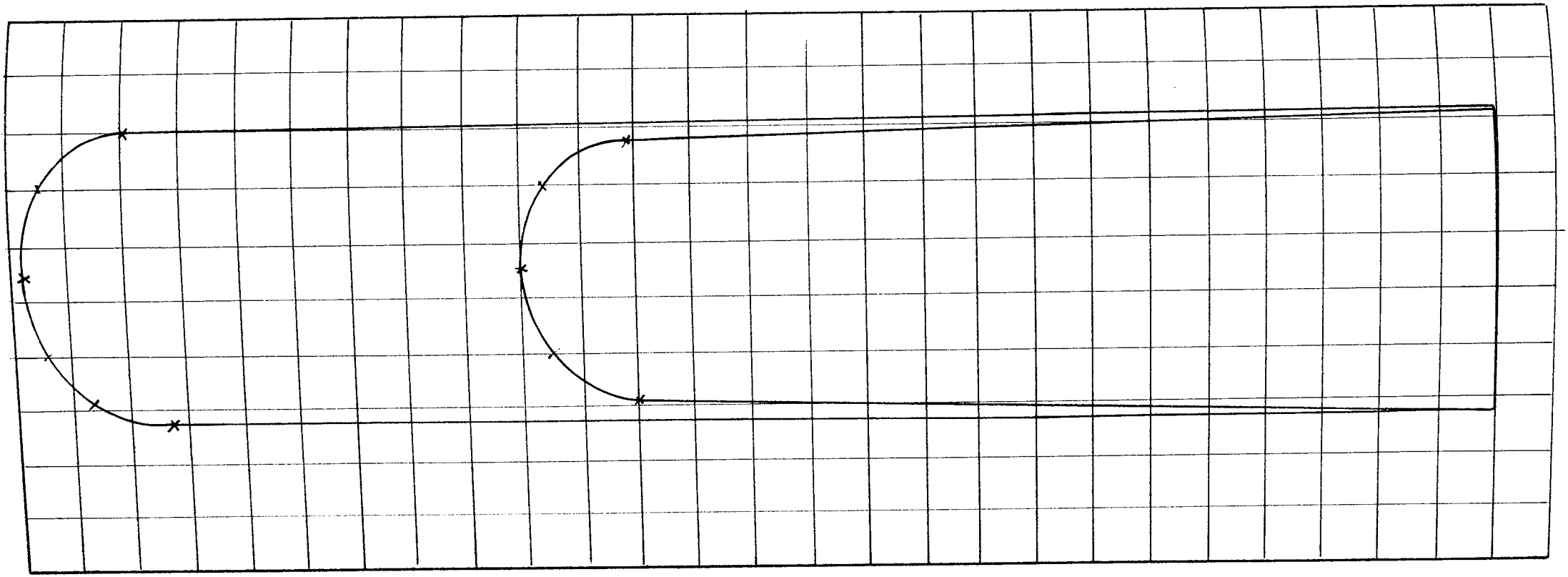

POSITION 4 Scales: Velocity: 1 mm = 1 mm/s Area under Velocity Curve = 9,150 mm^2

Momentum: 1 mm^2 = $\frac{1}{6}$ kgmm/s Area under Momentum Curve = 15,950 mm^2

BED MATERIAL: $1\frac{1}{2}$ mm Diameter Glass Spheres

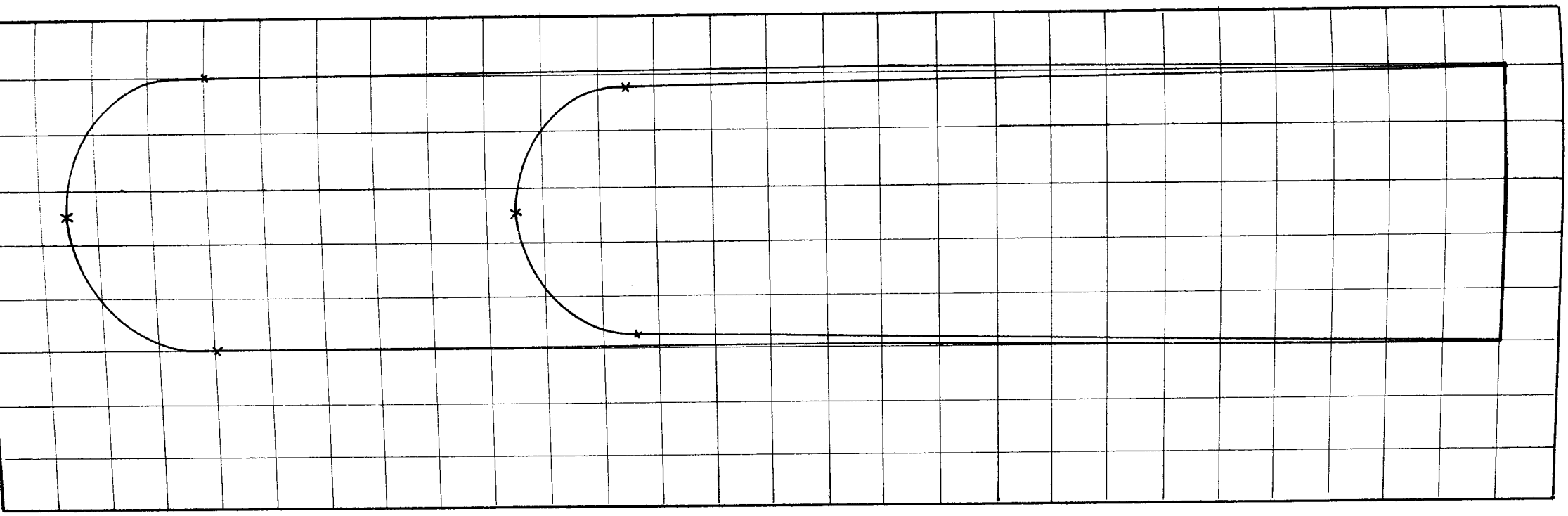

POSITION 5 Scales: Velocity: 1 mm = 1 mm/s Area under Velocity Curve = 8,850 mm^2

Momentum: 1 mm^2 = $\frac{1}{6}$ kgmm/s Area under Momentum Curve = 14,780 mm^2

BED MATERIAL: $1\frac{1}{2}$ mm Diameter Glass Spheres

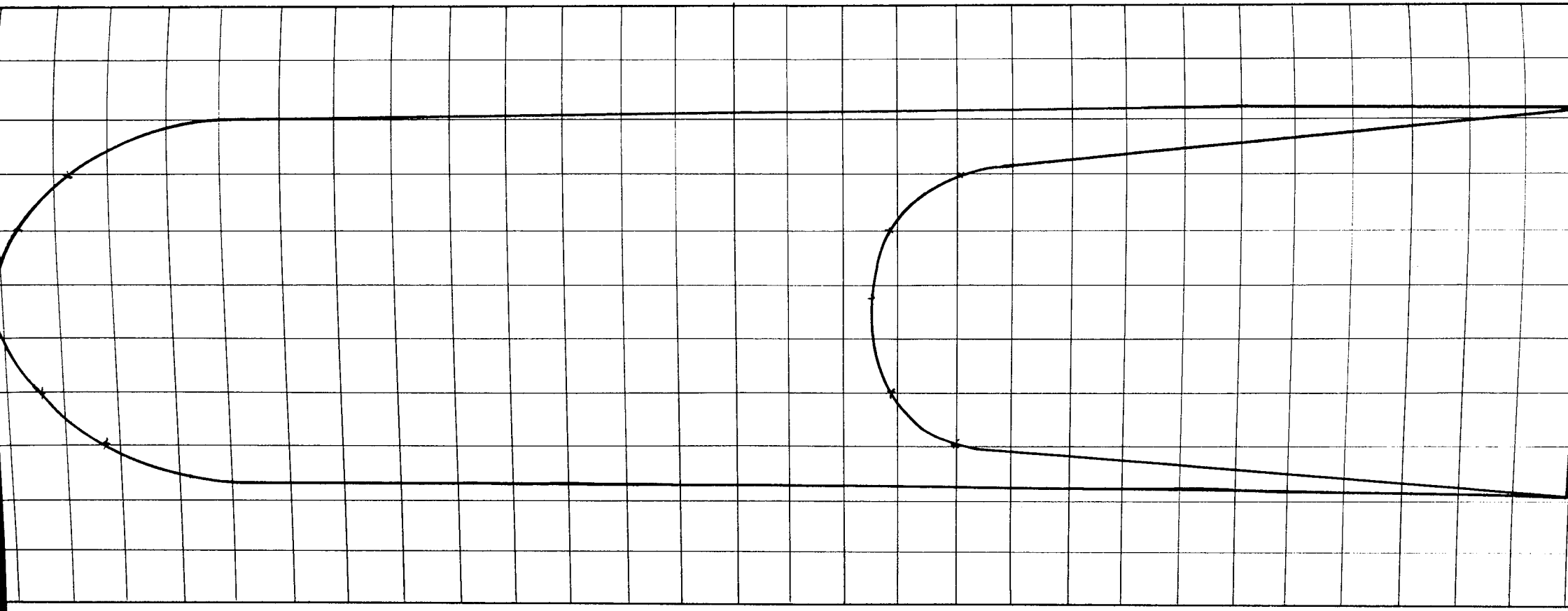

POSITION 1 Scales; Velocity: 1 mm = 1 mm/s

Momentum: 1 mm^2 = $\frac{1}{25}$ kgmm/s

Area under Velocity Curve = 7,450 mm^2

Area under Momentum Curve = 18,100 mm^2

BED MATERIAL: $1\frac{1}{2}$ mm Diameter Glass Spheres

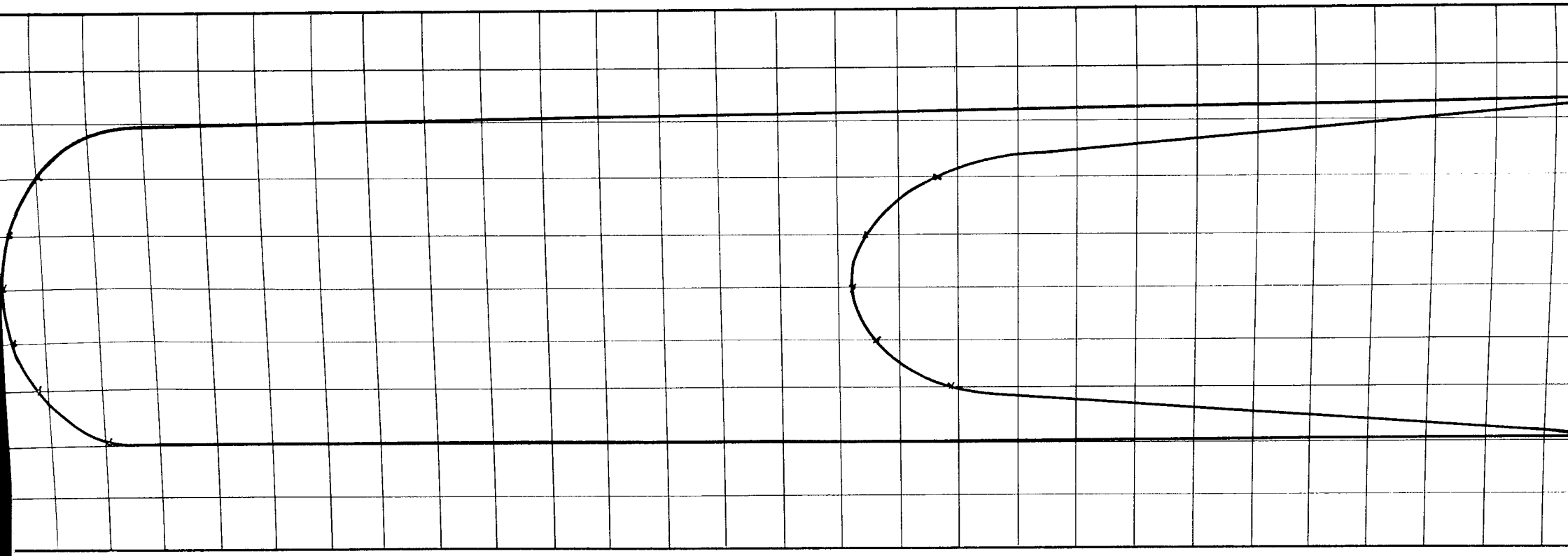

POSITION 2 Scales: Velocity: 1 mm = 1 mm/s Area under Velocity Curve = 7,600 mm^2

Momentum: 1 mm^2 = $\frac{1}{25}$ kgmm/s Area under Momentum Curve = 13,460 mm^2

BED MATERIAL: $1\frac{1}{2}$ mm Diameter Glass Spheres

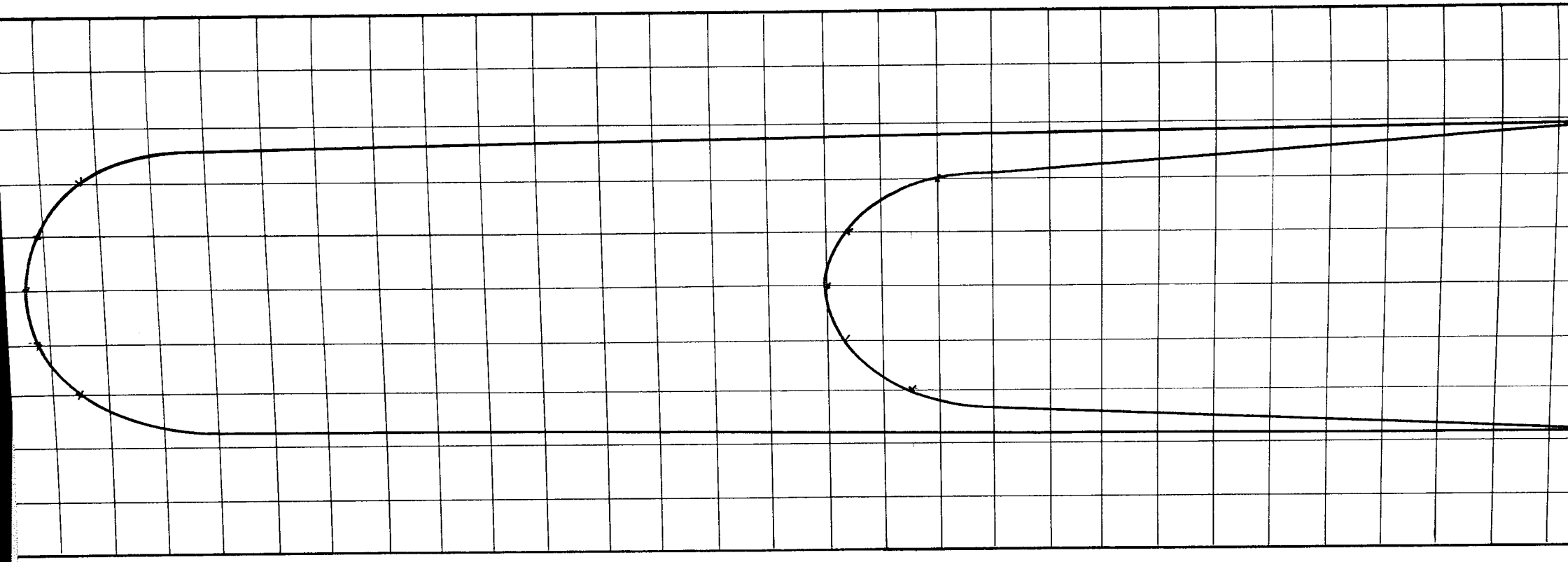

POSITION 3 Scales: Velocity: 1 mm = 1 mm/s Area under Velocity Curve = 7,220

Momentum: 1 mm^2 = $\frac{1}{25}$ kgmm/s Area under Momentum Curve = 16,200 mm^2

BED MATERIAL: $1\frac{1}{2}$ mm Diameter Glass Spheres

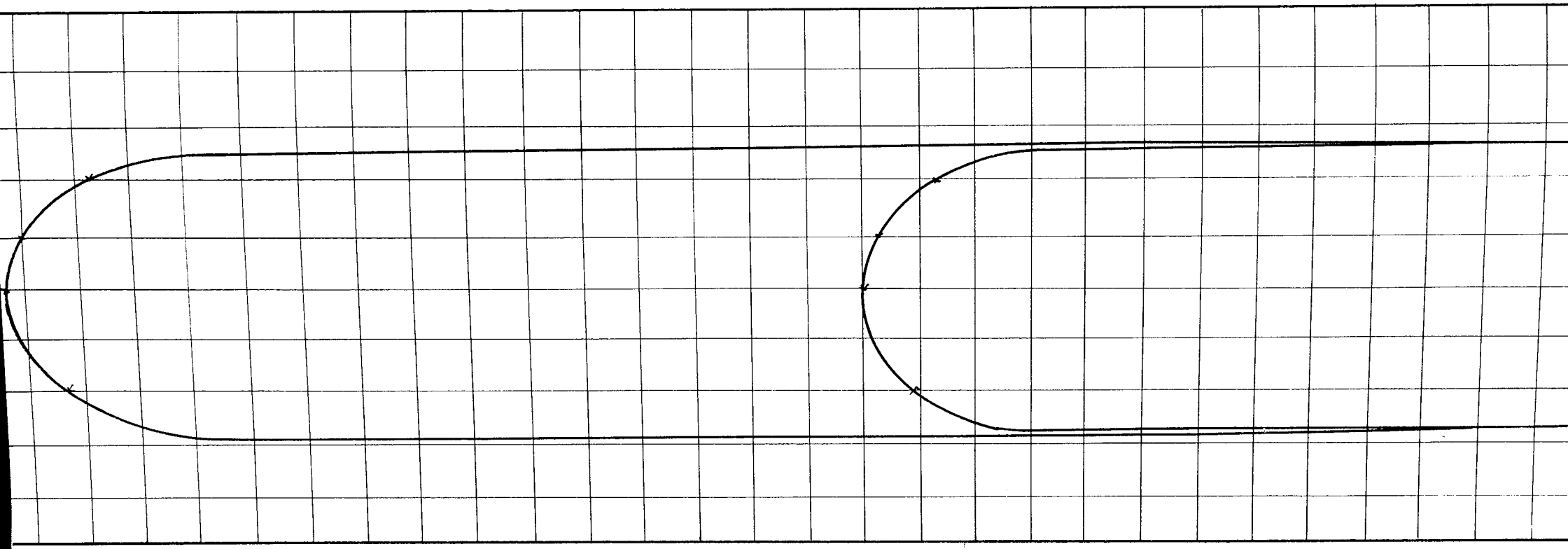

POSITION 4 Scales: Velocity: 1 mm = 1 mm/s Area under Velocity Curve = 7,200 mm^2

Momentum: 1 mm^2 = $\frac{1}{25}$ kgmm/s Area under Momentum Curve = 17,300 mm^2

BED MATERIAL: $1\frac{1}{2}$ mm Diameter Glass Spheres

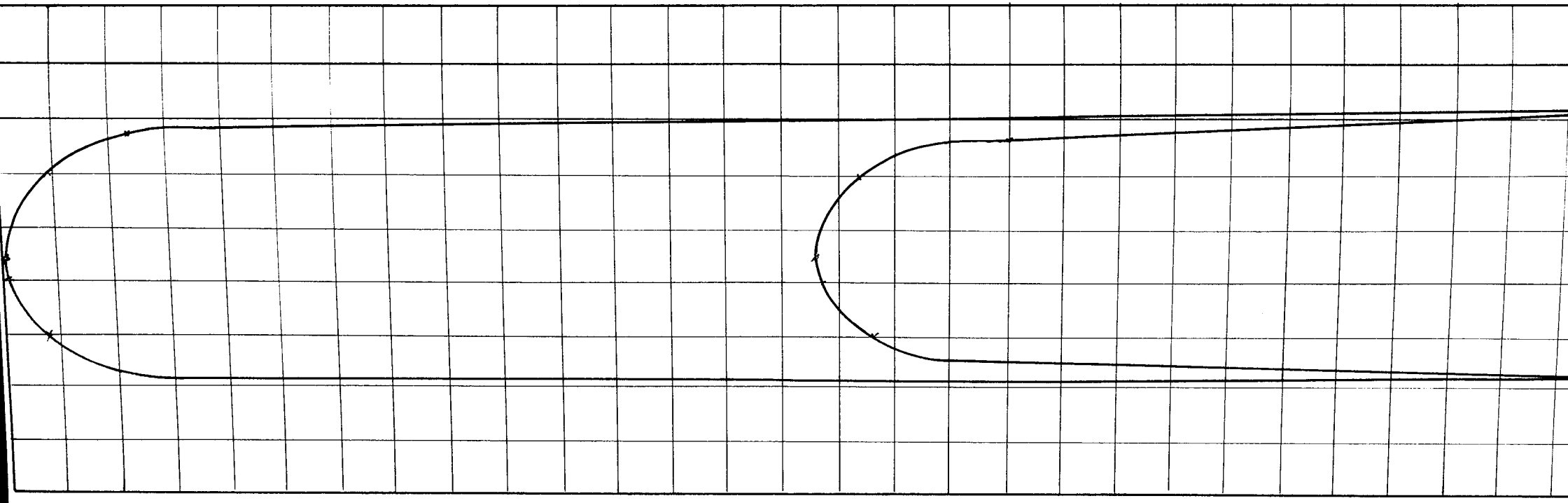

POSITION 5 Scales: Velocity: 1 mm = 1 mm/s Area under Velocity Curve = 7,250 mm^2

Momentum: 1 mm^2 = $\frac{1}{25}$ kgmm/s Area under Momentum Curve = 16,800 mm^2

BED MATERIAL: $1\frac{1}{2}$ mm Diameter Glass Spheres

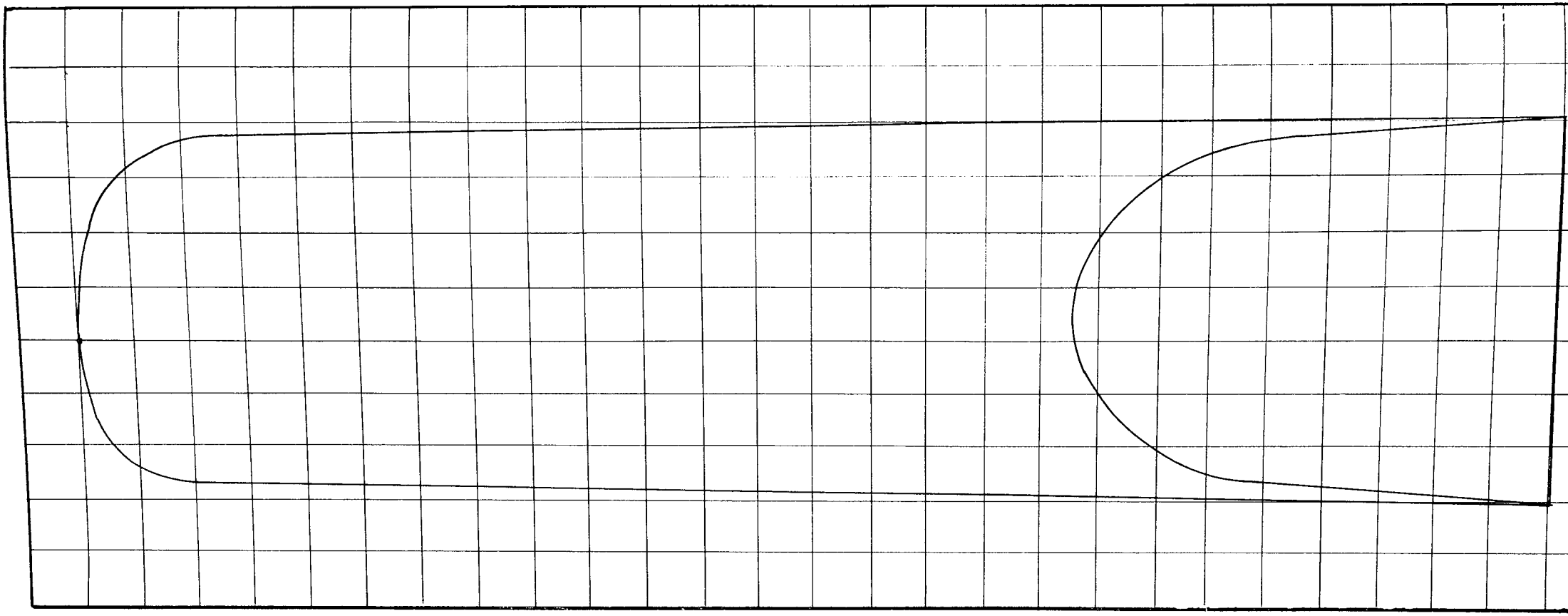

POSITION 1 Scales: Velocity: 1 mm = 1 mm/s Area under Velocity Curve = 5150 mm^2

Momentum: 1 mm^2 = $\frac{1}{25}$ gm mm/s Area under Momentum Curve = 15670 mm^2

BED MATERIAL 1½ mm Diameter Glass Spheres

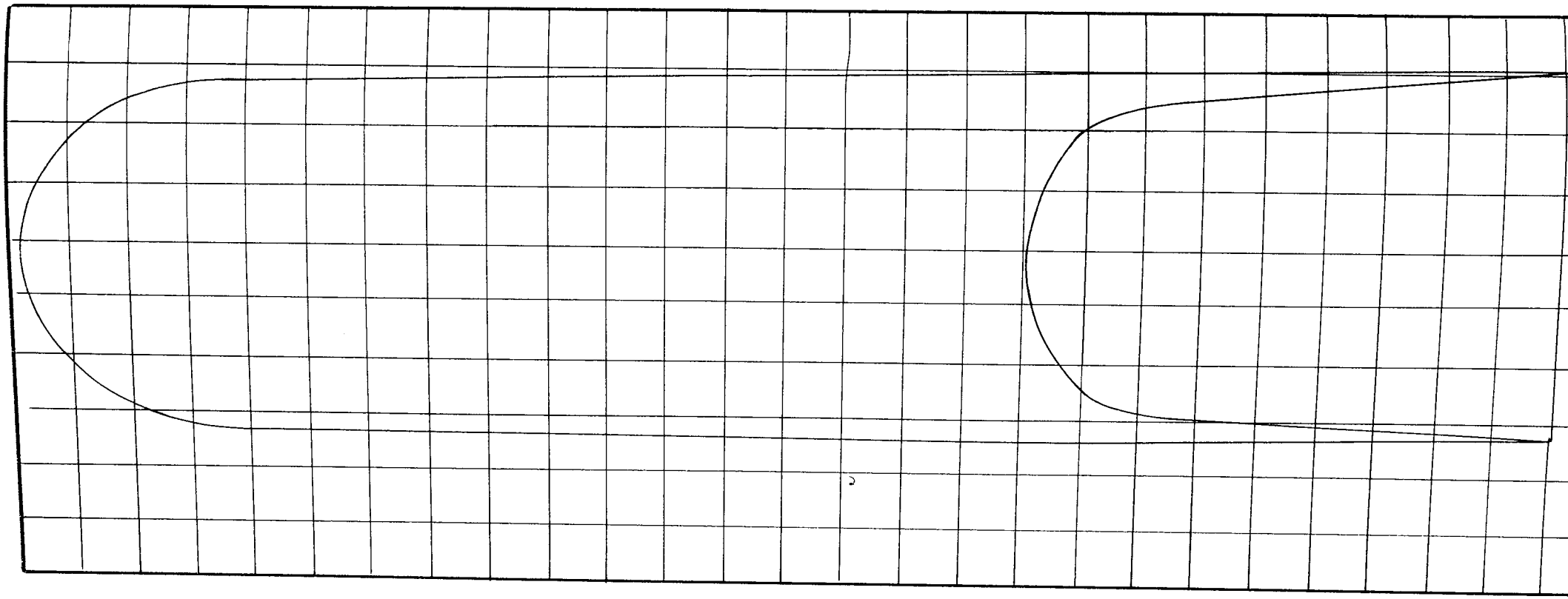

POSITION 2 Scales: Velocity: 1 mm = 1 mm/s

Momentum: 1 mm^2 = $\frac{1}{25}$ kgmm/s

Area under Velocity Curve = 5,100 mm^2

Area under Momentum Curve = 15,600 mm^2

BED MATERIAL: $1\frac{1}{2}$ mm Diameter Glass Spheres

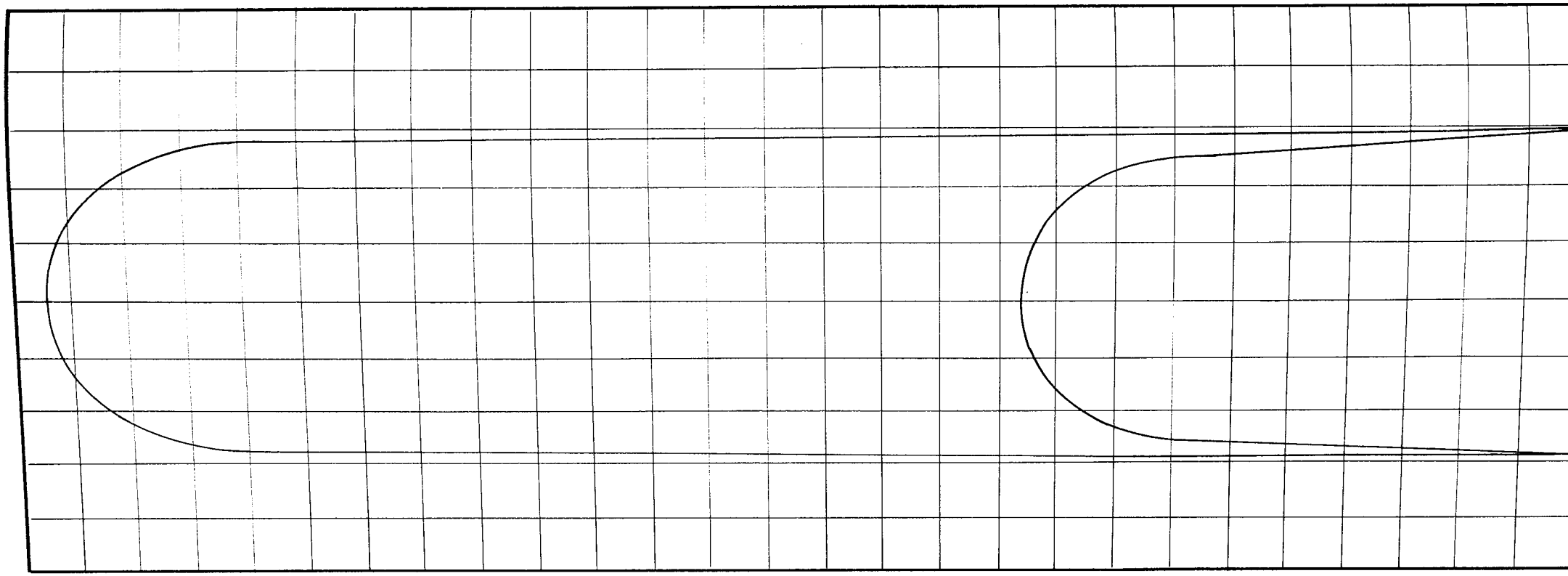

POSITION 3 Scales: Velocity : 1 mm = 1 mm/s

Momentum : 1 mm^2 = $\frac{1}{25}$ kgmm/s

Area under Velocity Curve = 5,210 mm^2

Area under Momentum Curve = 1[illegible],900 mm^2

BED MATERIAL : $1\frac{1}{2}$ mm Diameter Glass Spheres

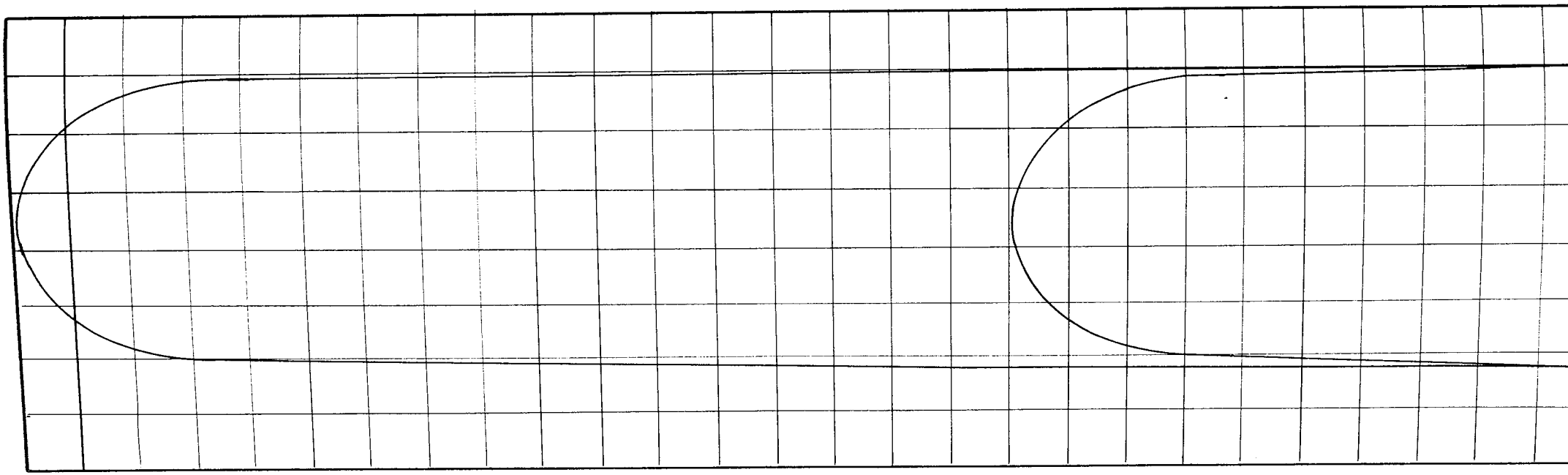

POSITION 4 Scales: Velocity: 1 mm = 1 mm/s Area under Velocity Curve = 5,100 mm^2

Momentum: 1 $mm^2 = \frac{1}{25}$ kgmm/s Area under Momentum Curve = 15,000 mm^2

BED MATERIAL: $1\frac{1}{2}$ mm Diameter Glass Spheres

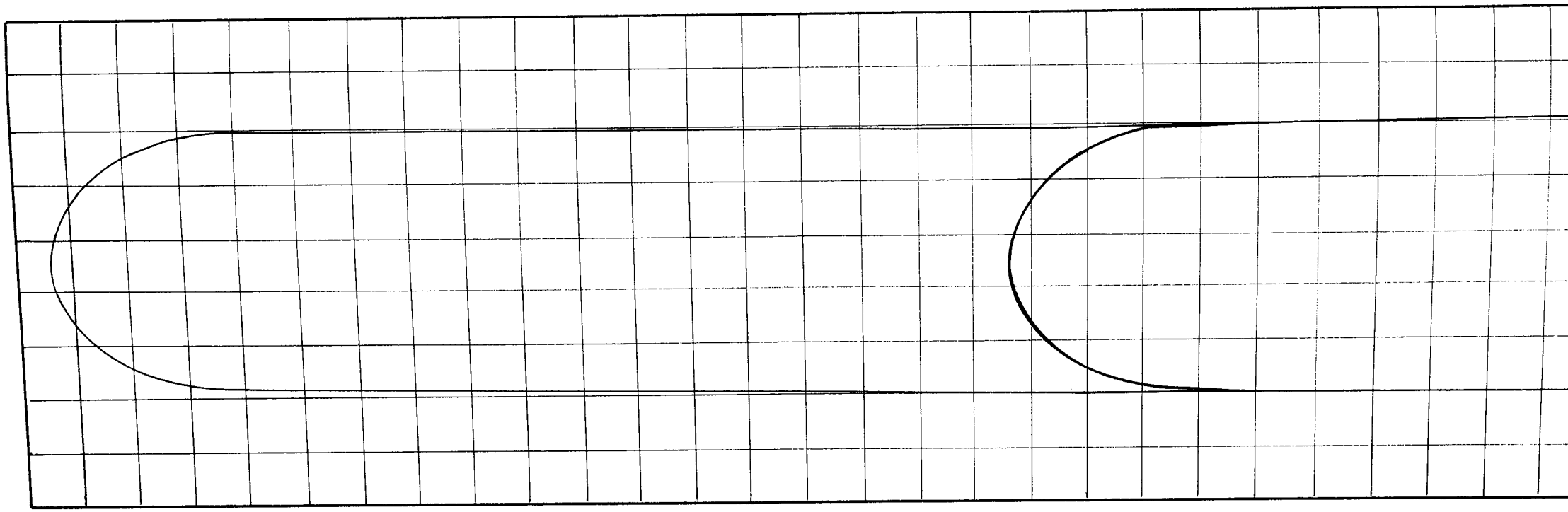

POSITION 5 Scales: Velocity: 1 mm = 1 mm/s Area under Velocity Curve = 5,050 mm^2

Momentum: 1 mm^2 = $\frac{1}{25}$ kgmm/s Area under Momentum Curve = 15,080 mm^2

BED MATERIAL: $1\frac{1}{2}$ mm Diameter Glass Spheres

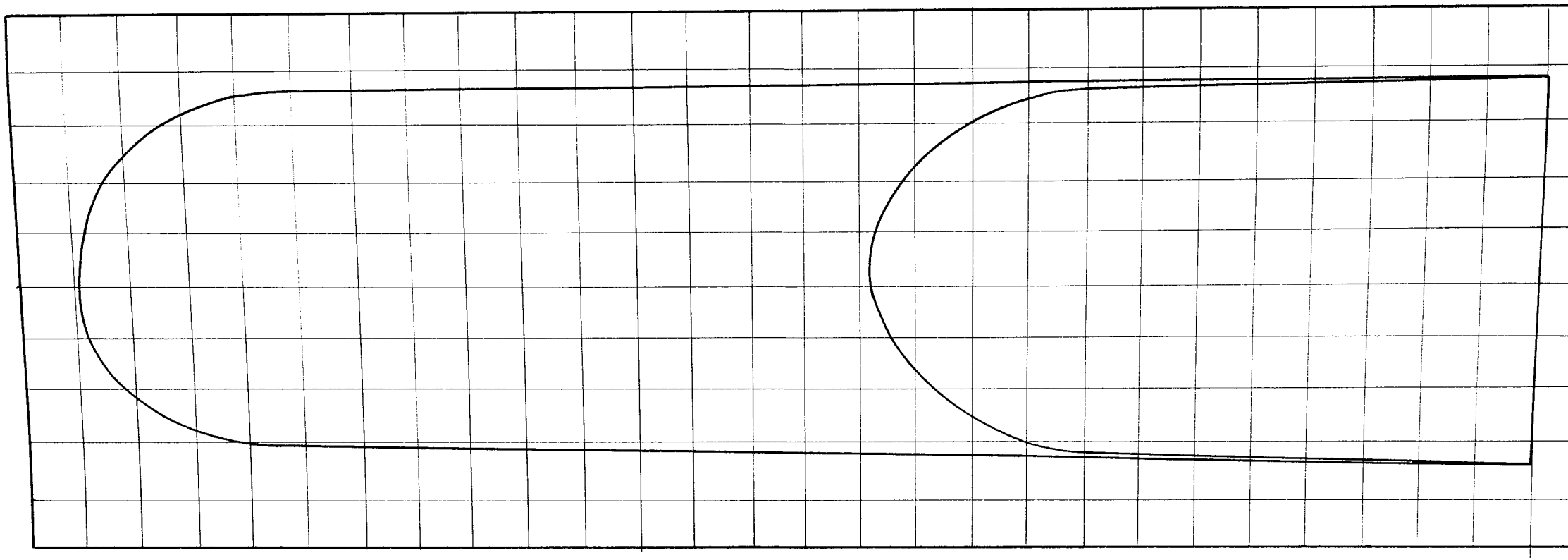

POSITION 1 Scales: Velocity: 1 mm = 1 mm/s Area under Velocity Curve = 6,840 mm^2

Momentum: 1 mm^2 = $\frac{1}{25}$ kgmm/s Area under Momentum Curve = 13,880 mm^2

BED MATERIAL: $1\frac{1}{2}$ mm Diameter Glass Spheres

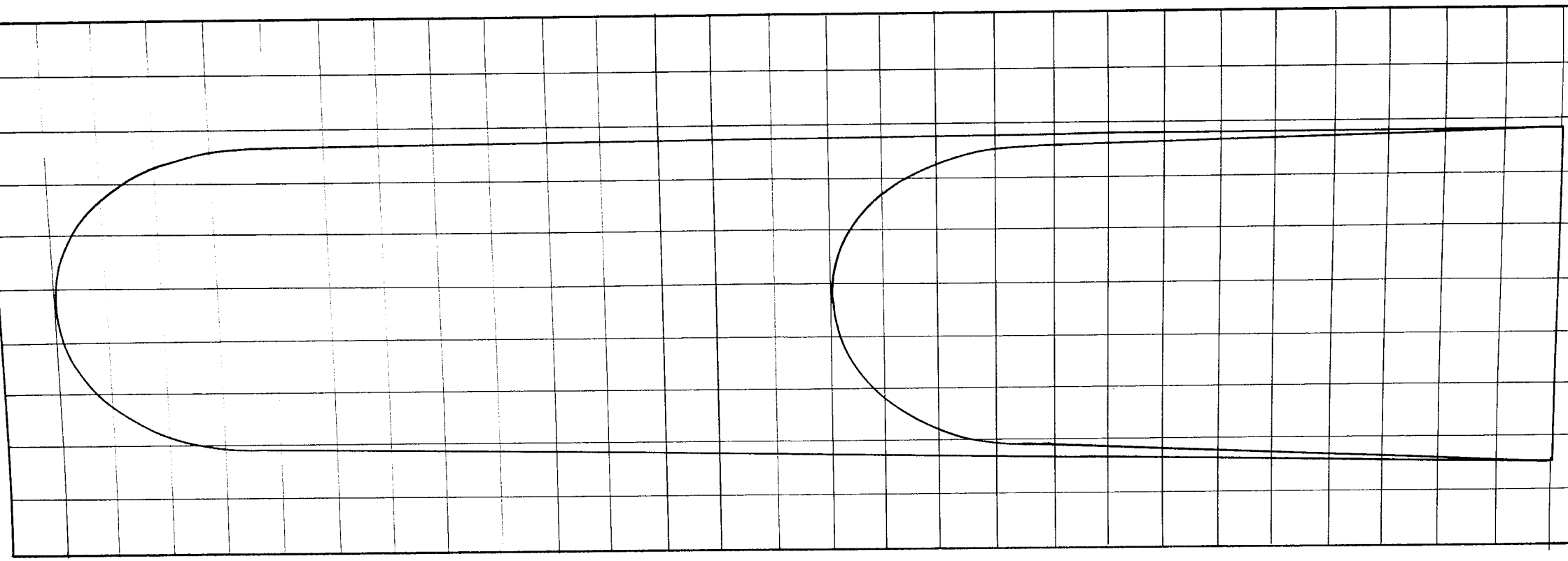

POSITION 2 Scales: Velocity: 1 mm = 1 mm/s Area under Velocity Curve = 1,420 mm^2

Momentum: 1 mm^2 = $\frac{1}{25}$ kgmm/s Area under Momentum Curve = 6,920

BED MATERIAL: $1\frac{1}{2}$ mm Diameter Glass Spheres

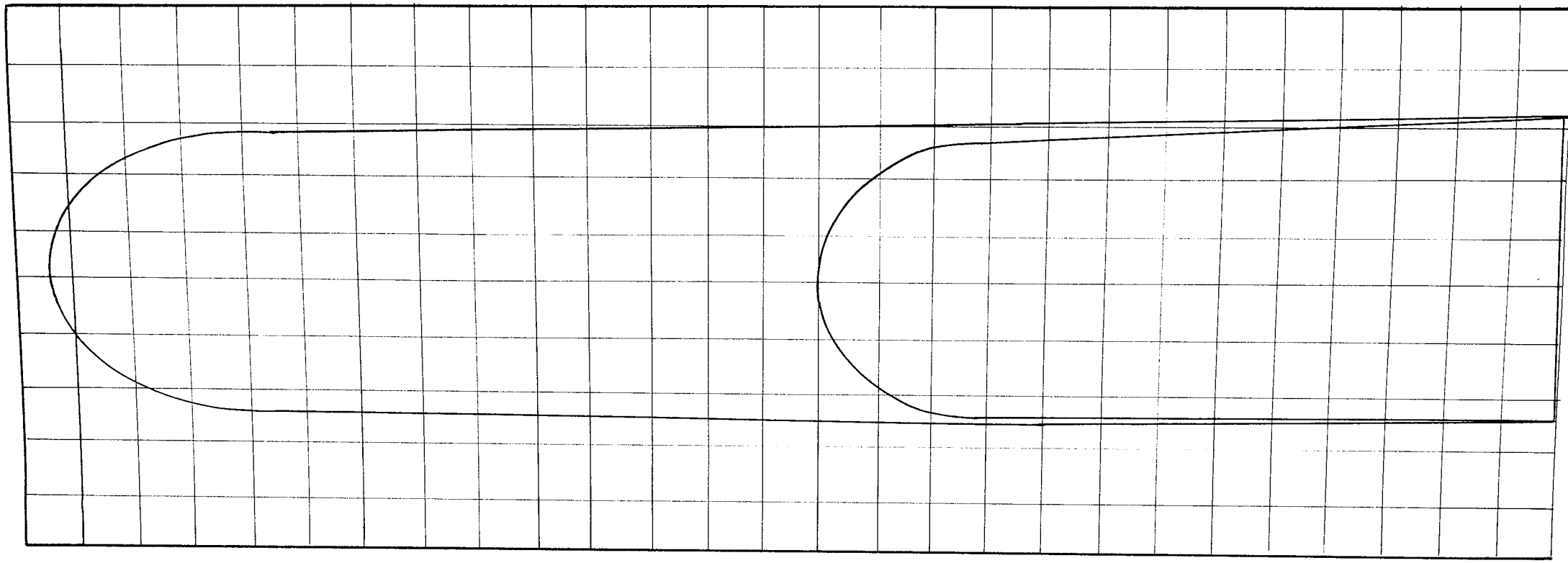

POSITION 3 Scales: Velocity: 1 mm = 1mm/s Area under Velocity Curve = 6,860 mm^2

Momentum: 1 mm^2 = $\frac{1}{25}$ kgmm/s Area under Momentum Curve = 13,800 mm^2

BED MATERIAL: $1\frac{1}{2}$ mm Diameter Glass Spheres

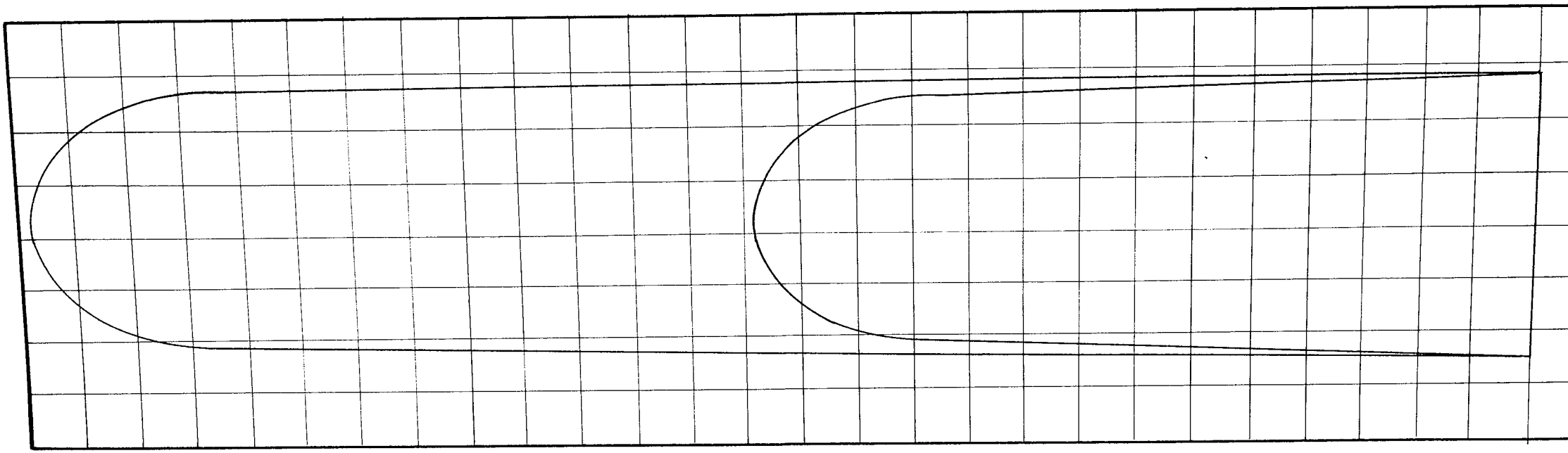

POSITION 4 Scales: Velocity: 1 mm = 1 mm/s Area under Velocity Curve = 6,460 mm^2

Momentum: 1 mm^2 = $\frac{1}{25}$ kgmm/s Area under Momentum Curve= 13,460 mm^2

BED MATERIAL: $1\frac{1}{2}$ mm Diameter Glass Spheres

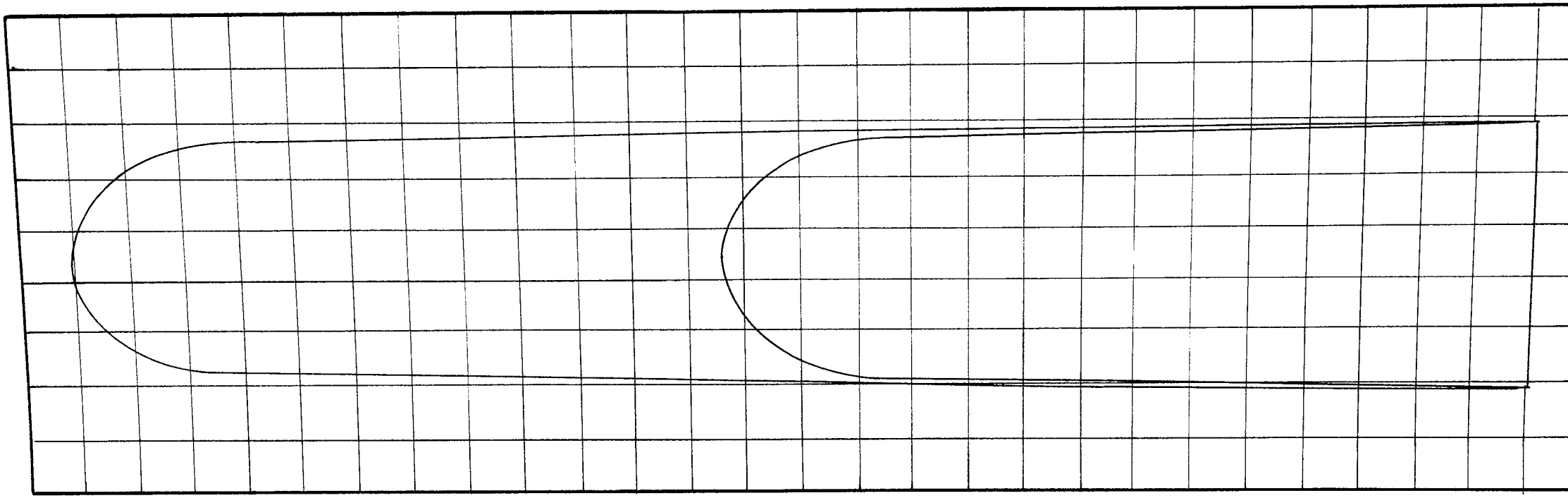

POSITION 5 Scales: Velocity: 1 mm = 1 mm/s Area under Velocity Curve = 6,500 mm^2

Momentum: 1 mm^2 = $\frac{1}{25}$ kgmm/s Area under Momentum Curve = 12,900 mm^2

BED MATERIAL: $1\frac{1}{2}$ mm Diameter Glass Spheres

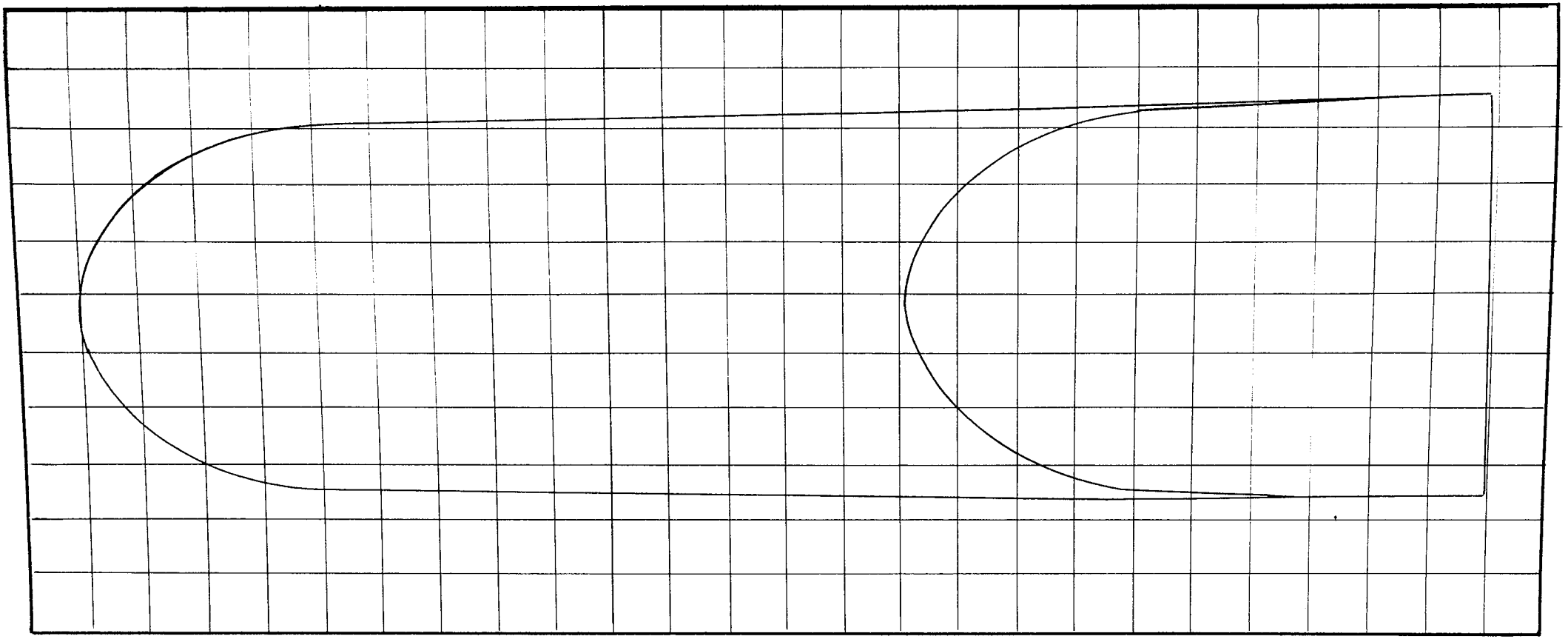

POSITION 1

Scales: Velocity : 1 mm $\frac{1}{5}$ mm/s

Momentum: 1 mm^2 $\frac{5}{}$ = $\frac{1}{100}$ kgmm/s

Area under Velocity Curve = 6500mm^2

Area under Momentum Curve = 13100mm^2

BED MATERIAL: $1\frac{1}{2}$ mm Diameter Glass Spheres

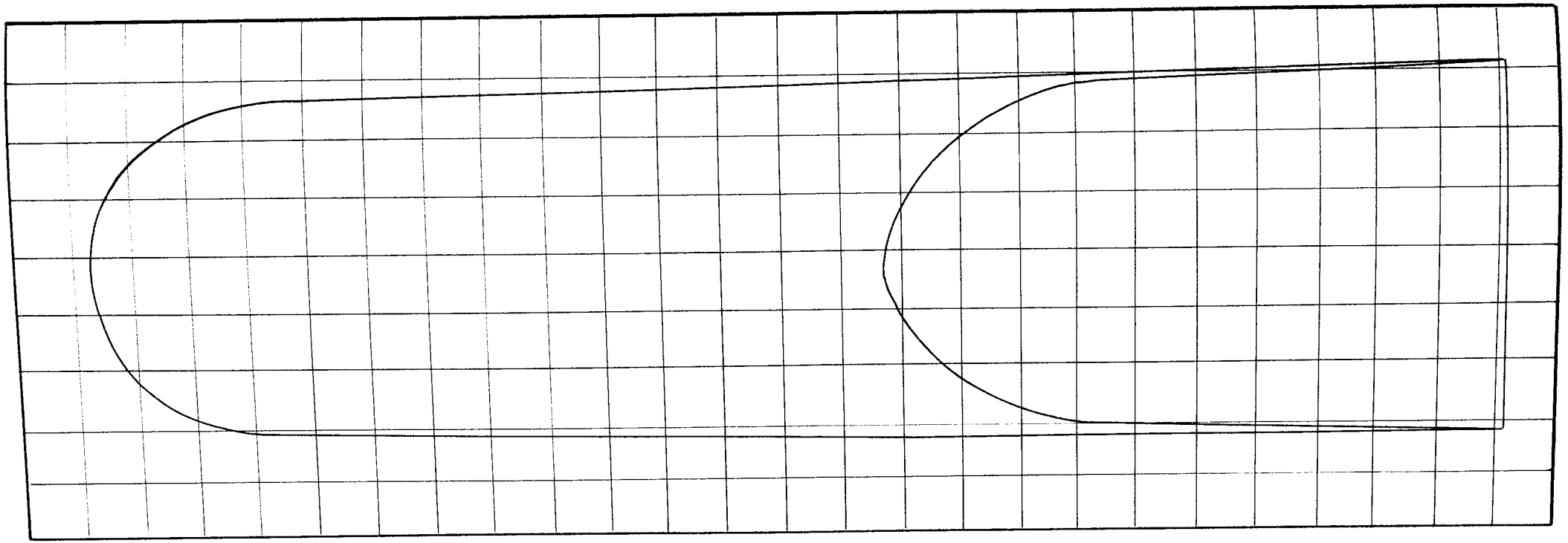

POSITION 2

Scales: Velocity : 1 mm $\frac{1}{5}$ mm/s

Momentum : 1 mm^2 = $\frac{1}{100}$ kgmm/s

Area under Velocity Curve = 6320mm^2

Area under Momentum Curve = 13900mm^2

BED MATERIAL: $1\frac{1}{2}$mm Diameter Glass Spheres

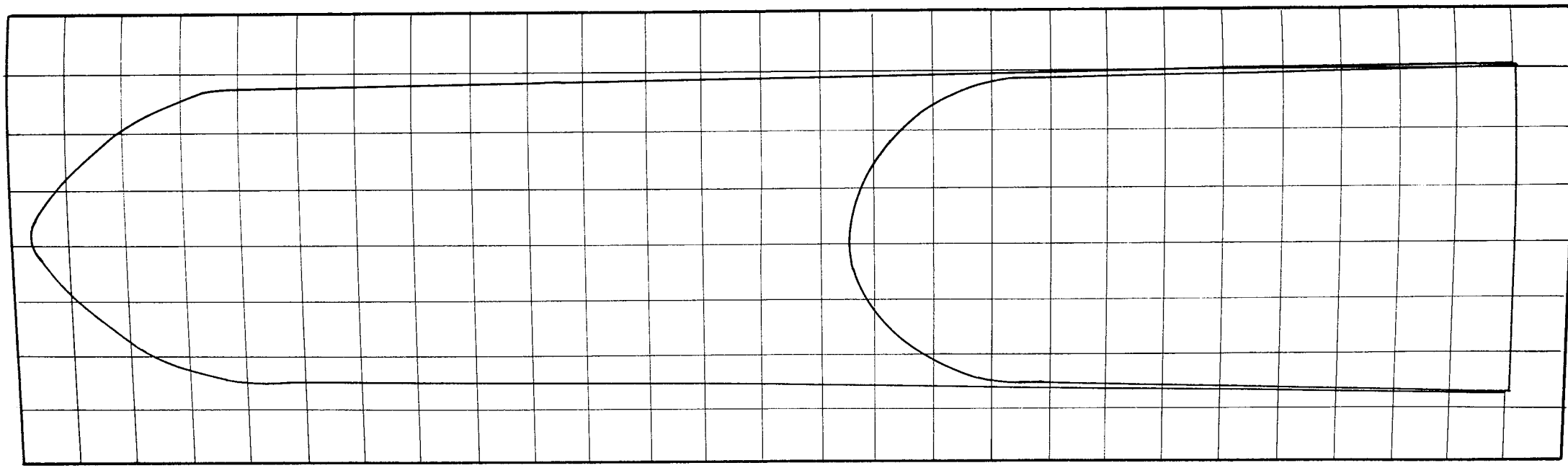

POSITION 3 Scales: Velocity : 1 mm $\frac{1}{5}$ mm/s Area under Velocity Curve = 6200mm^2

Momentum : 1 mm^2 = $\frac{1}{100}$ kgmm/s Area under Momentum Curve = 13600mm^2

BED MATERIAL: 1 $\frac{1}{2}$ mm Diameter Glass Spheres

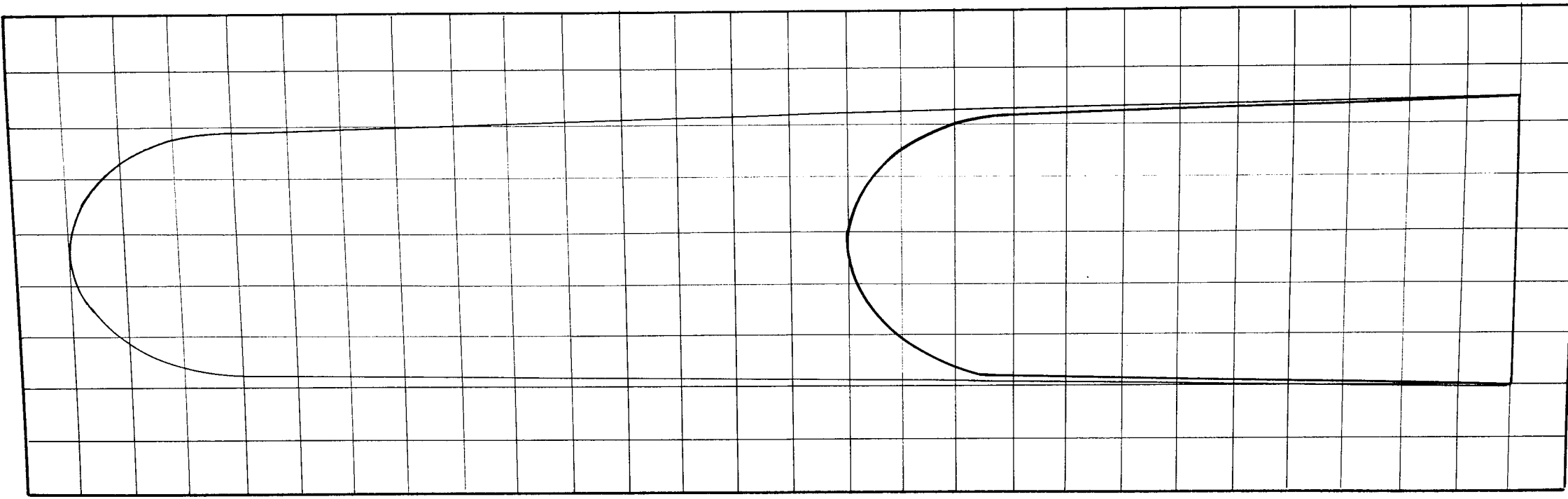

POSITION 4 Scales: Velocity : 1 mm $\frac{1}{5}$ mm/s Area under Velocity Curve = 6240mm^2

Momentum : 1 mm^2 = $\frac{1}{100}$ kgmm/s Area under Momentum Curve = 13240mm^2

BED MATERIAL: 1$\frac{1}{2}$ mm Diameter Glass Spheres

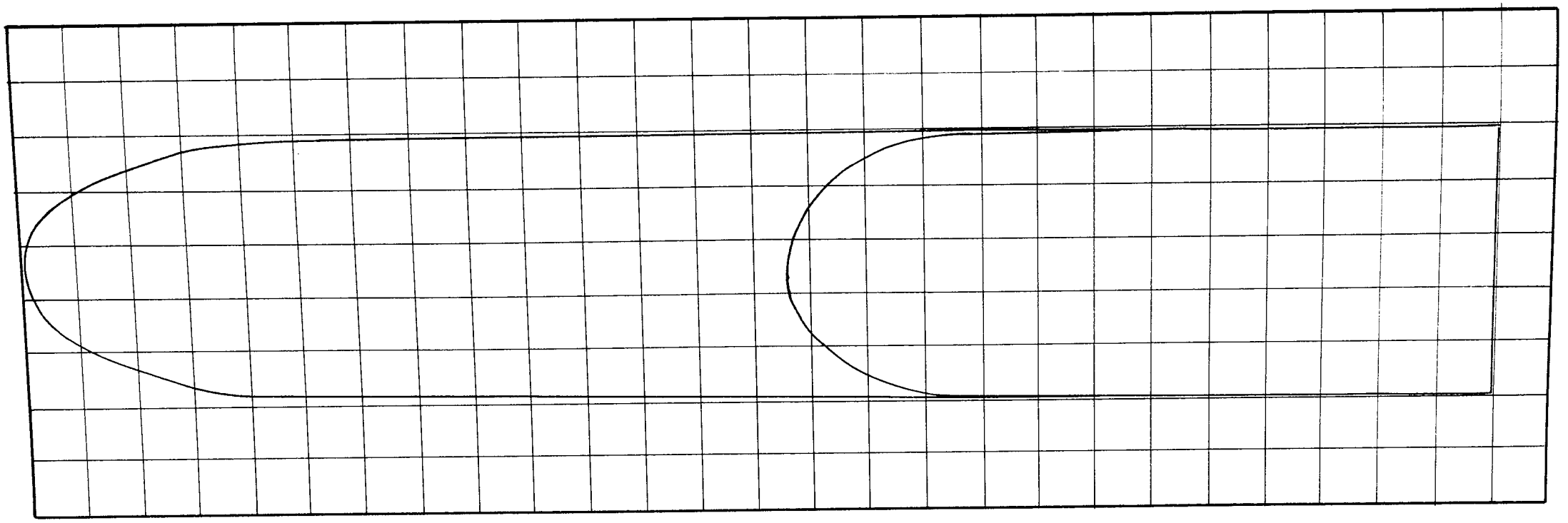

POSITION 5

Scales: Velocity : 1 mm $\frac{1}{5}$ mm/s

Momentum : 1 mm^2 = $\frac{1}{100}$ kgmm/s

Area under Velocity Curve = 6310mm^2

Area under Momentum Curve = 12800mm^2

BED MATERIAL: $1\frac{1}{2}$ mm Diameter Glass Spheres

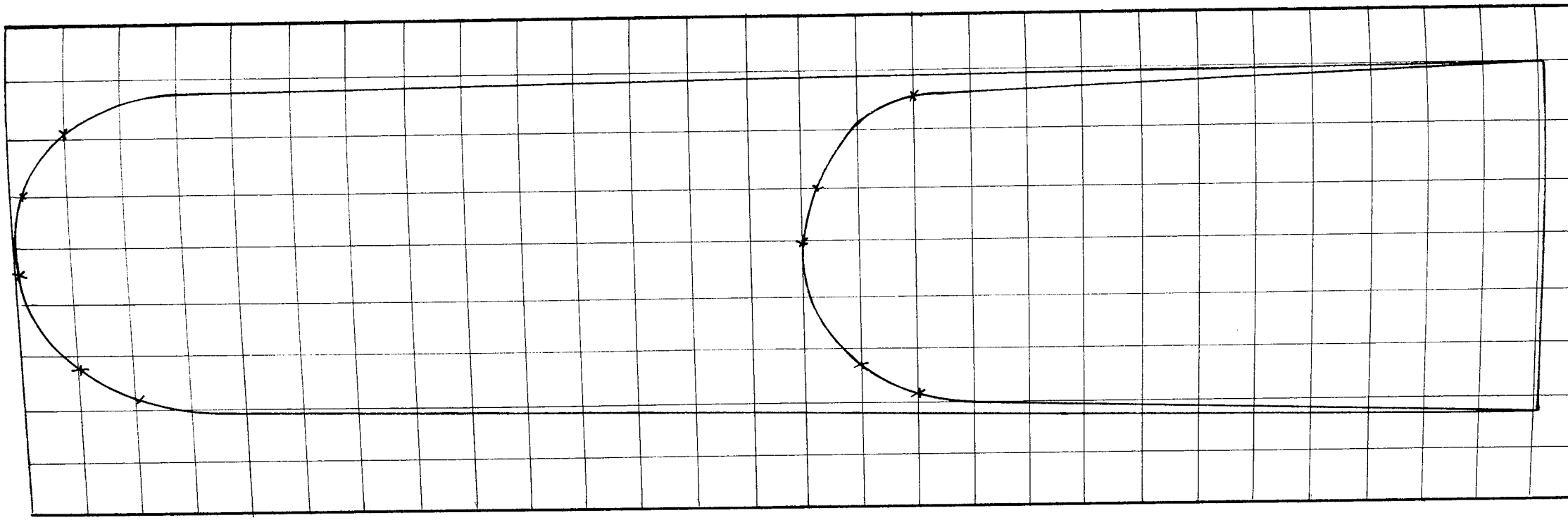

POSITION 2 Scale: Velocity: 1 mm = 1 mm/s Area under Velocity Curve = 8,000 mm^2

Momentum: 1 mm^2 = $\frac{1}{4}$ kgmm/s Area under Momentum Curve = 16,400 mm^2

BED MATERIAL: $1\frac{1}{2}$ Diameter Glass Spheres

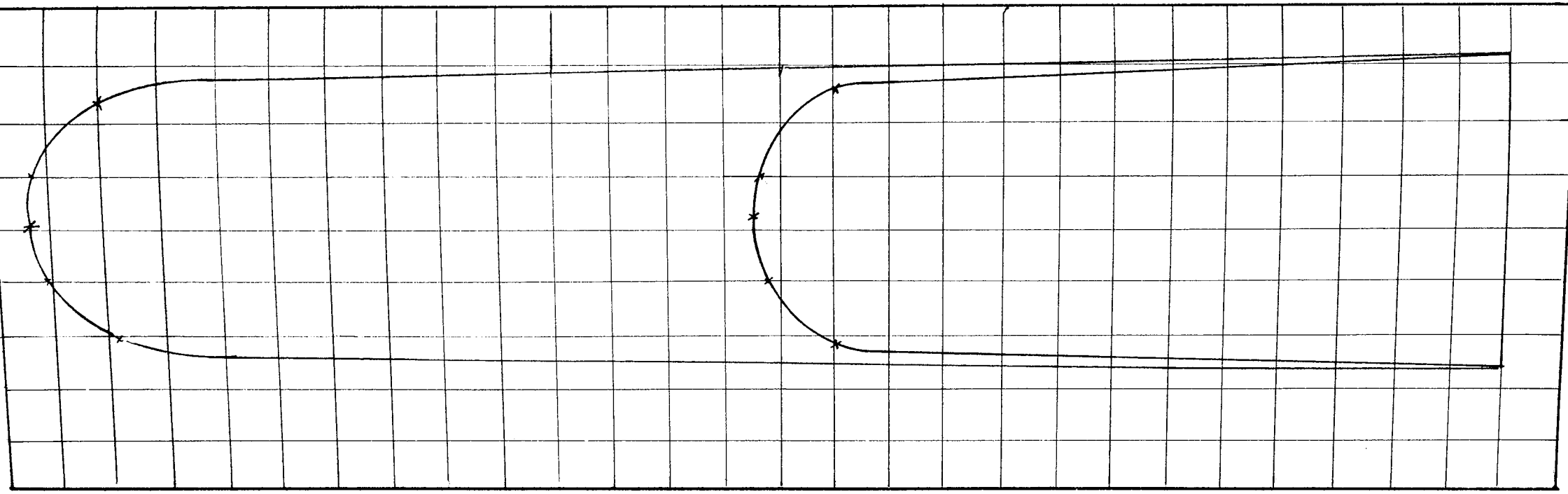

POSITION 3 Scales: Velocity: 1 mm = 1 mm/s Area under Velocity Curve = 8050 mm^2

Momentum: 1 mm^2 = $\frac{1}{4}$ kgmm/s Area under Momentum Curve = 16,200 mm^2

BED MATERIAL: $1\frac{1}{2}$ mm Diameter Glass Spheres

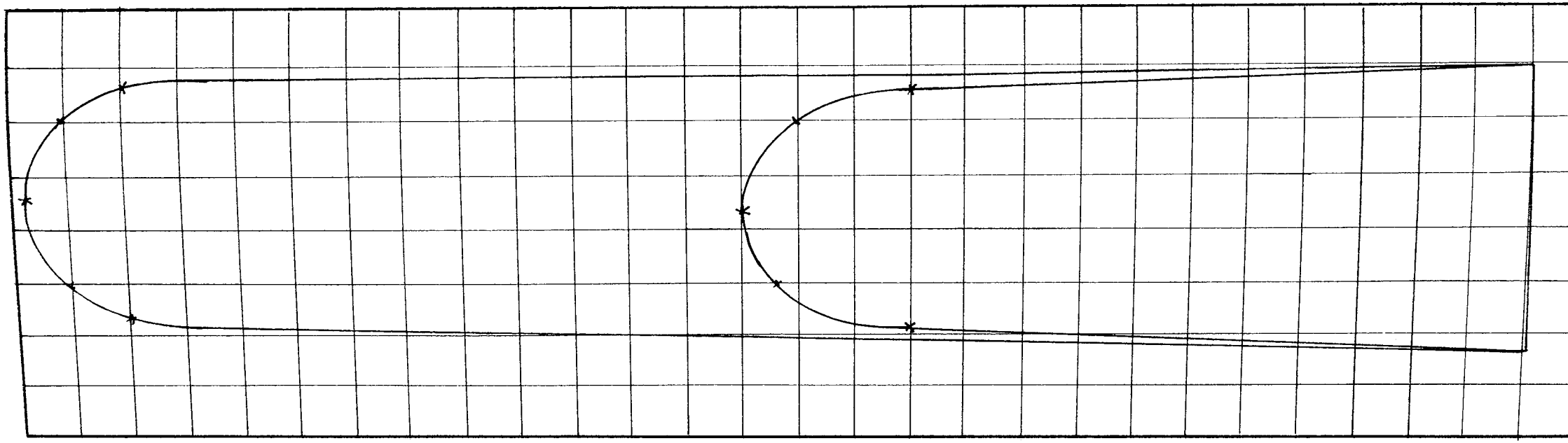

POSITION 4 Scales: Velocity: 1 mm = 1 mm/s Area under Velocity Curve = 7,800 mm^2

Momentum: 1 mm^2 = $\frac{1}{4}$ kgmm/s Area under Momentum Curve = 15,550 mm^2

BED MATERIAL: $1\frac{1}{2}$ mm Diameter Glass Spheres

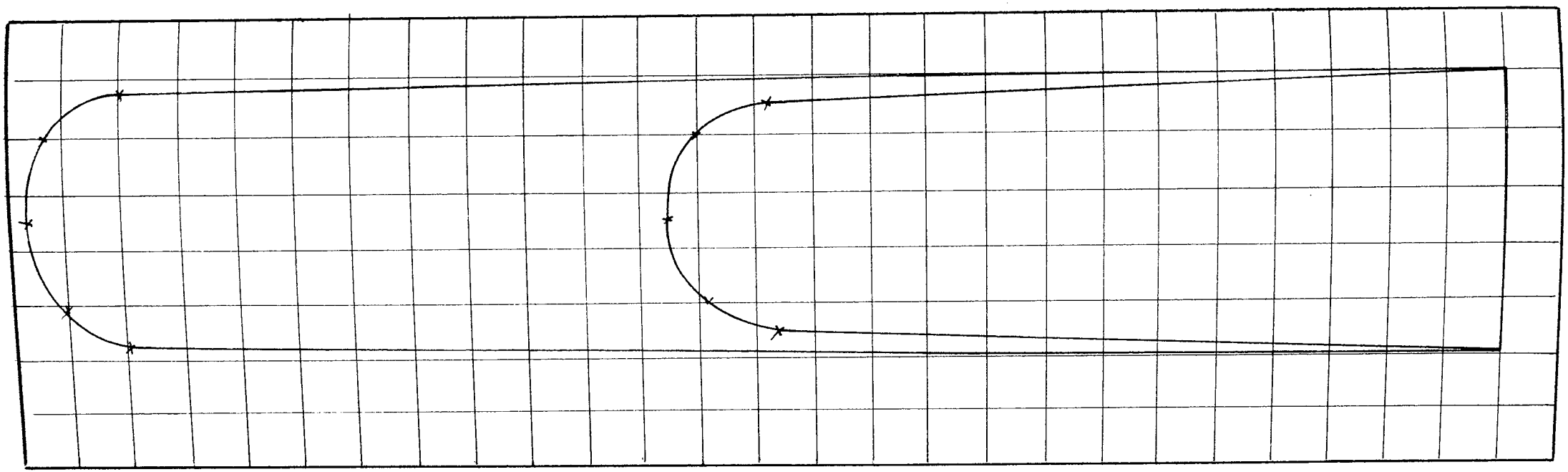

POSITION 5 Scales: Velocity: 1 mm = 1 mm/s Area under Velocity Curve = 7,650 mm^2

Momentum: 1 mm = $\frac{1}{4}$ kgmm/s Area under Momentum Curve = 15,800 mm^2

BED MATERIAL: $1\frac{1}{2}$ mm Diameter Glass Spheres

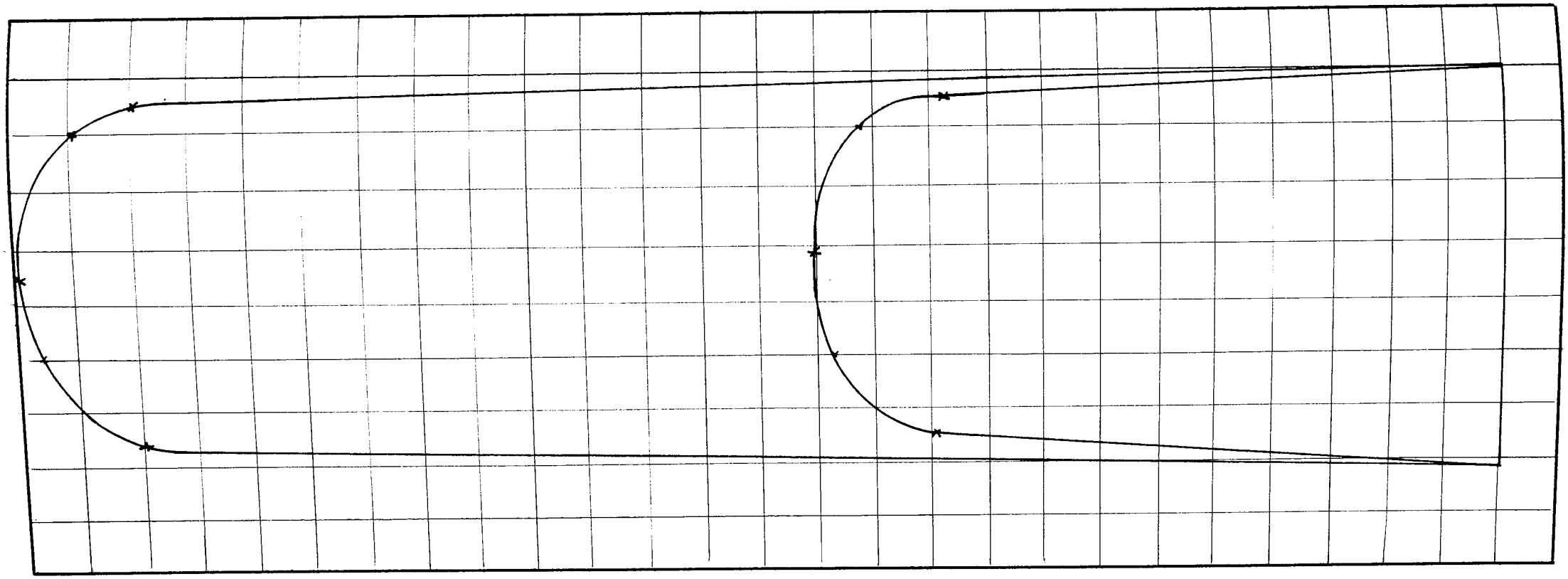

POSITION 1 Scales: Velocity: 1 mm = 1 mm/s

Momentum: 1 mm^2 = $\frac{1}{4}$ kgmm/s

Area under Velocity Curve = 7,520 mm^2

Area under Momentum Curve = 15,800 mm^2

BED MATERIAL: $1\frac{1}{2}$ mm Diameter Glass Spheres

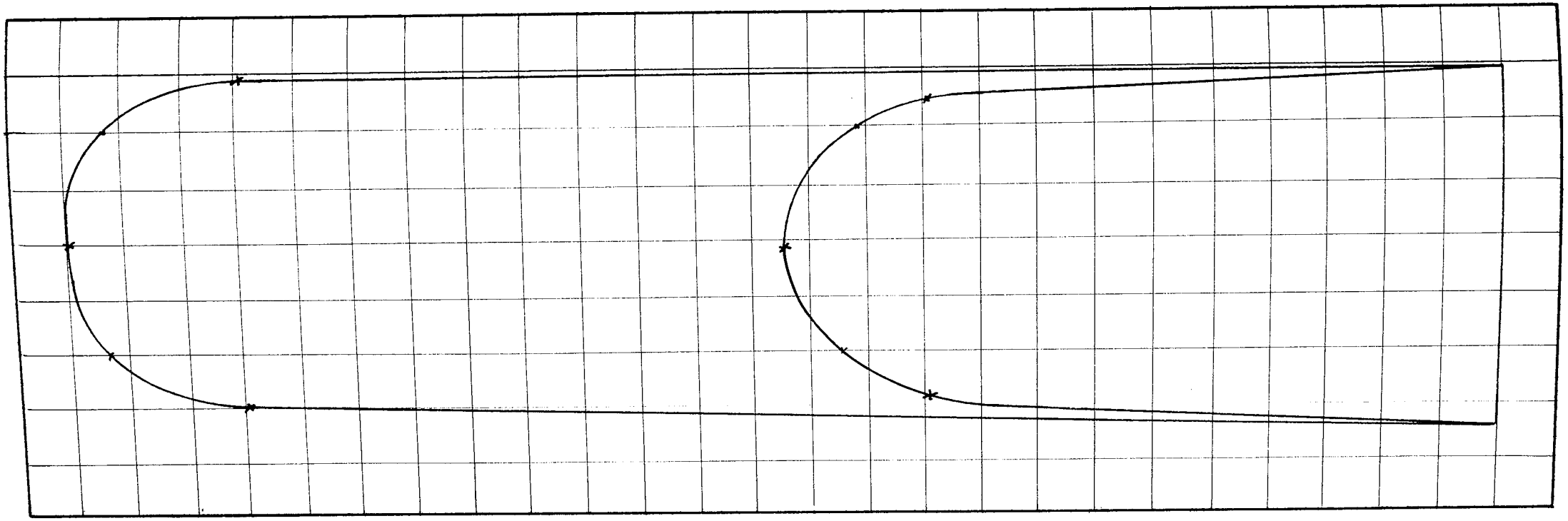

POSITION 2 Scales: Velocity: 1 mm = 1 mm/s Area under Velocity Curve = 7,150 mm^2

Momentum: 1 mm^2 = $\frac{1}{4}$ kgmm/s Area under Momentum Curve = 15,000 mm^2

BED MATERIAL 1 $\frac{1}{2}$ mm Diameter Glass Spheres

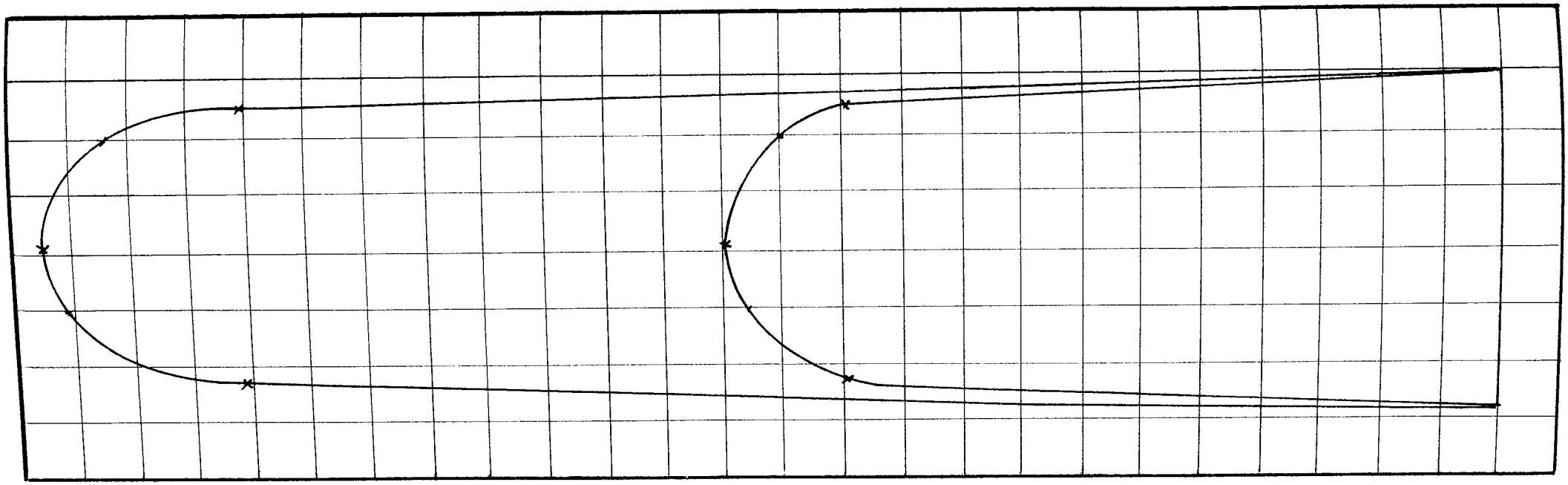

POSITION 3 Scales: Velocity : 1mm = 1 mm/s Area under Velocity Curve = 7,200 mm^2

Momentum : 1 mm^2 = $\frac{1}{4}$ kgmm/s Area under Momentum Curve = 14,800 mm^2

BED MATERIAL: $1\frac{1}{2}$ mm Diameter Glass Spheres

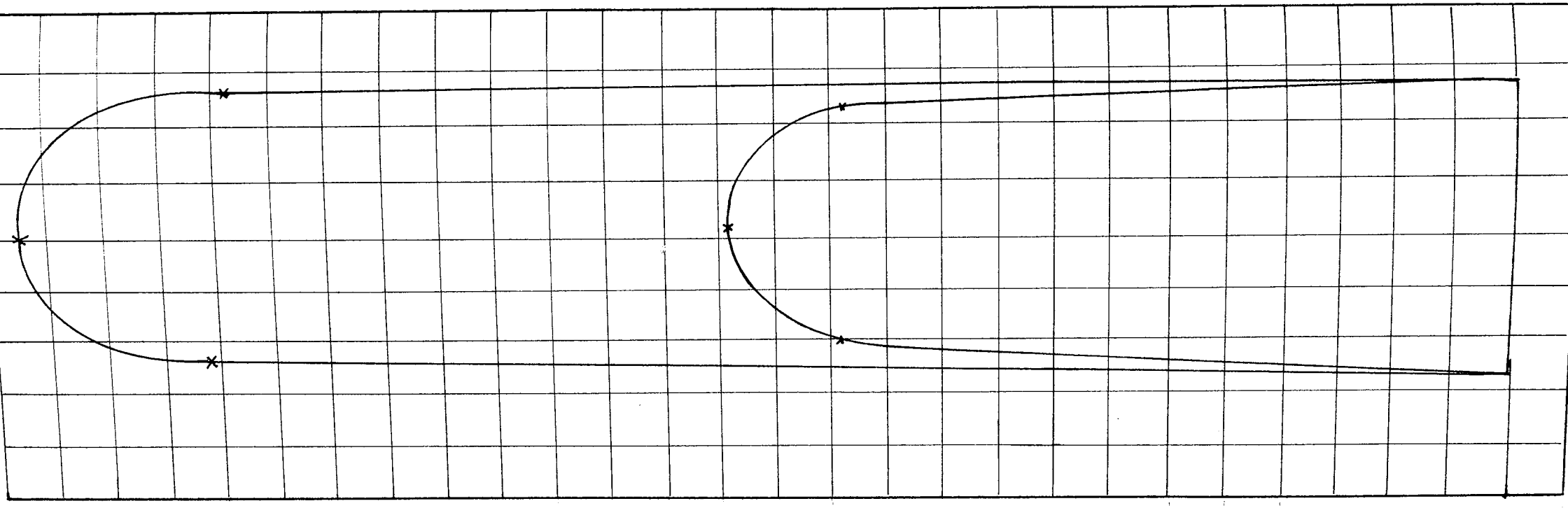

POSITION 4 Scales: Velocity: 1 mm = 1 mm/s Area under Velocity Curve = 7,400 mm^2

Momentum: 1 mm^2 = $\frac{1}{4}$ kgmm/s Area under Momentum Curve = 14,950 mm^2

BED MATERIAL: $1\frac{1}{2}$mm Diameter Glass Spheres

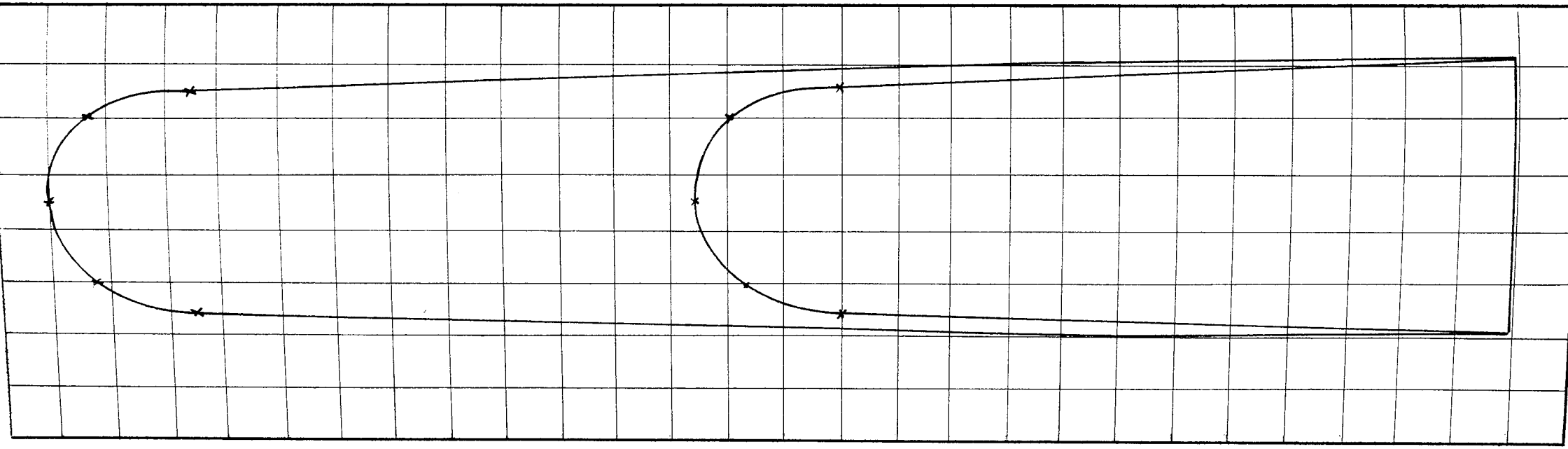

POSITION 5 Scales: Velocity: 1 mm = 1 mm/s Area under Velocity Curve = 7,200 mm^2

Momentum : 1 mm^2 = $\frac{1}{4}$ kgmm/s Area under Momentum Curve = 14,900 mm^2

BED MATERIAL: $1\frac{1}{2}$ mm Diameter Glass Spheres

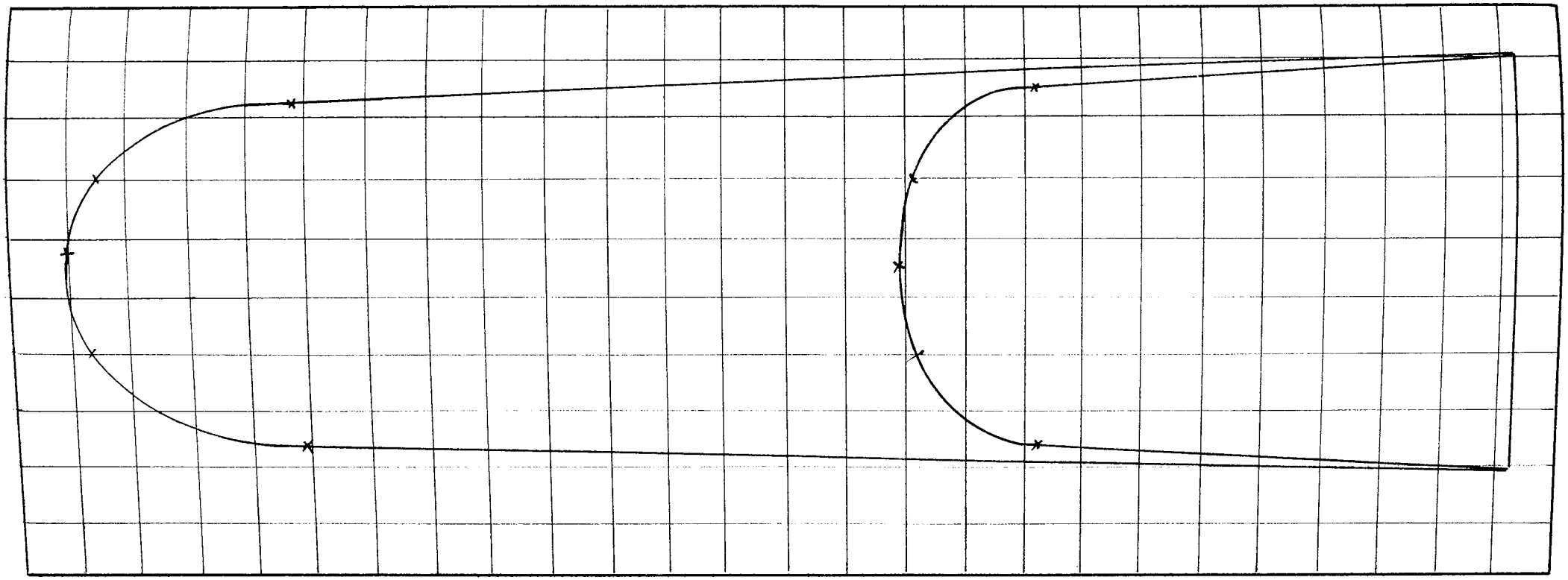

POSITION 1 Scales: Velocity: 1 mm = 1mm/s Area under Velocity Curve = 6,660 mm^2

Momentum : 1 mm^2 = $\frac{1}{25}$ kgmm/s Area under Momentum Curve = 15,200 mm^2

BED MATERIAL: $1\frac{1}{2}$ mm Diameter Glass Spheres

1½ mm Diameter Glass Spheres

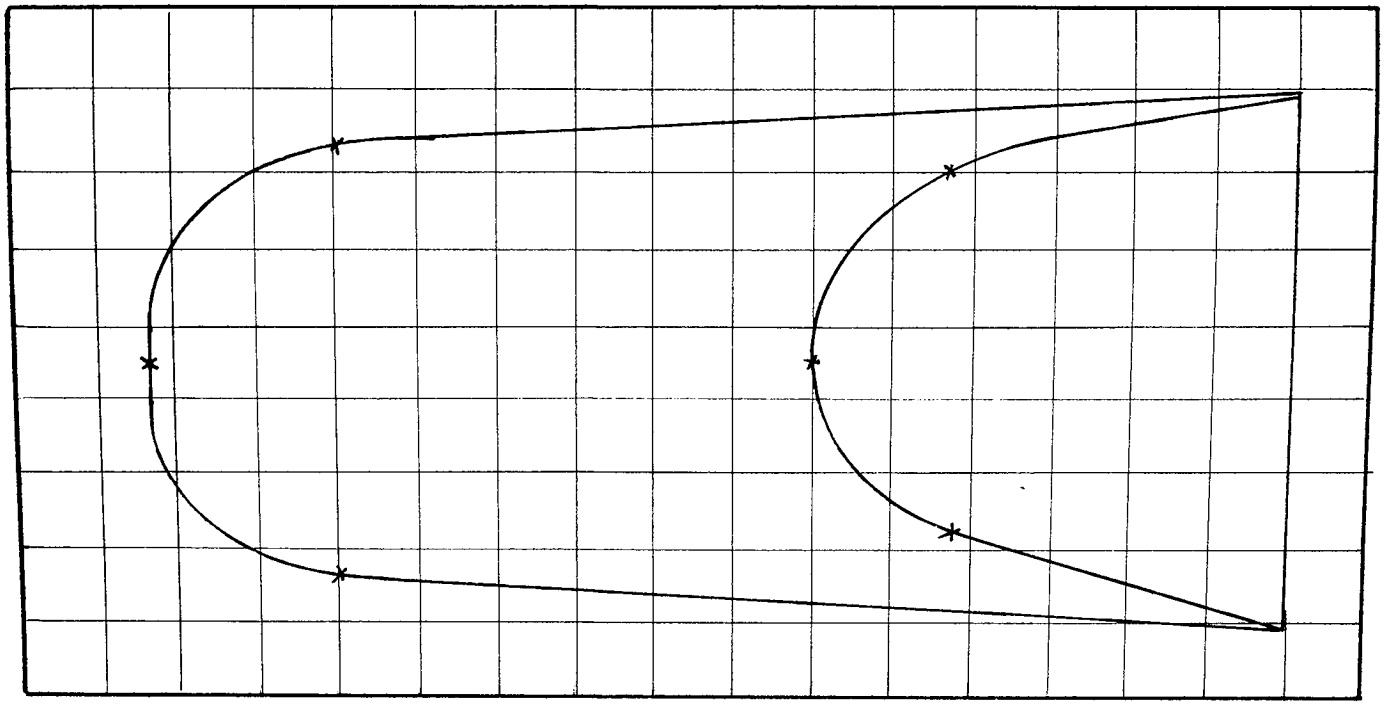

POSITION 1 Scales: Velocity: 1 mm = 1 mm/s Area under Velocity Curve = 3,350 mm^2

Momentum: 1 mm^2 = $\frac{1}{250}$ kgmm/s Area under Momentum Curve = 9,320 mm^2

BED MATERIAL: 1½ mm Diameter Sand

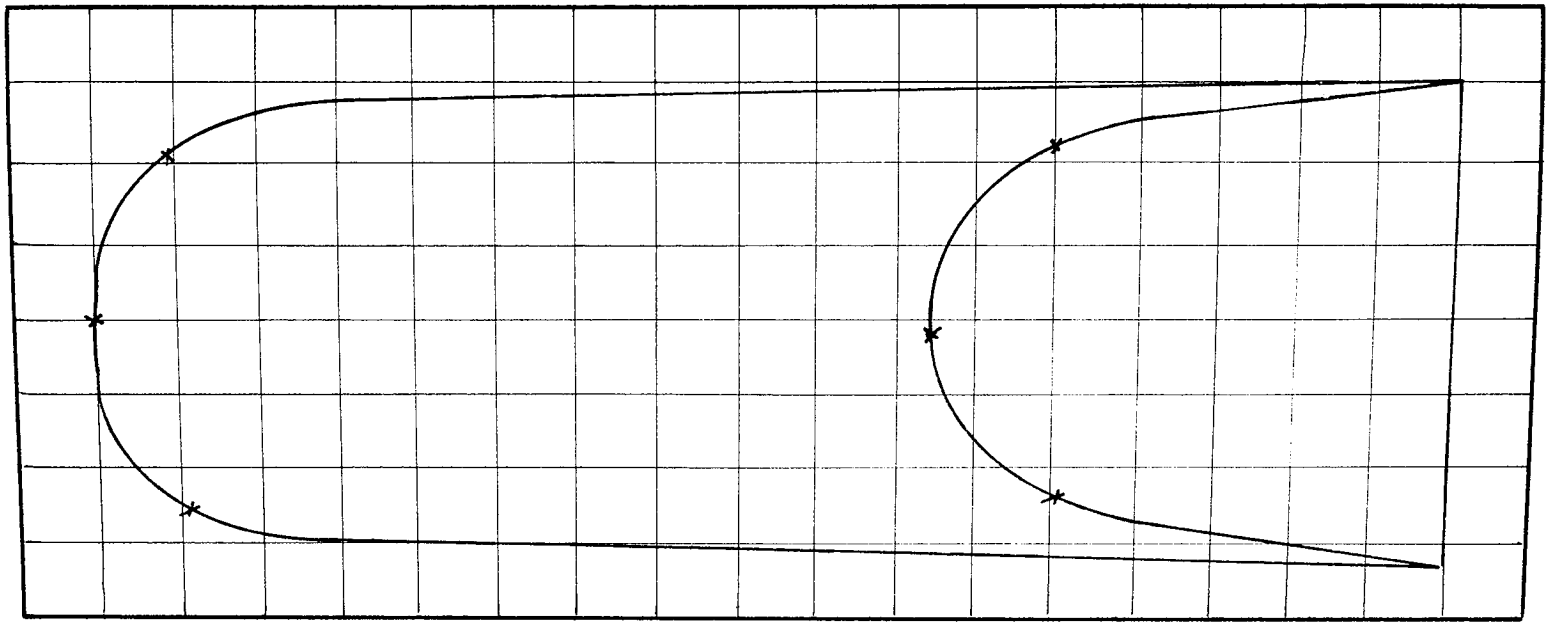

POSITION 2 Scales: Velocity: 1 mm = 1 mm/s Area under Velocity Curve = 3,420 mm^2

Momentum: $1mm^2 = \frac{1}{250}$ kgmm/s Area under Momentum Curve = 9,900 mm^2

BED MATERIAL: $1\frac{1}{2}$ mm Diameter Sand

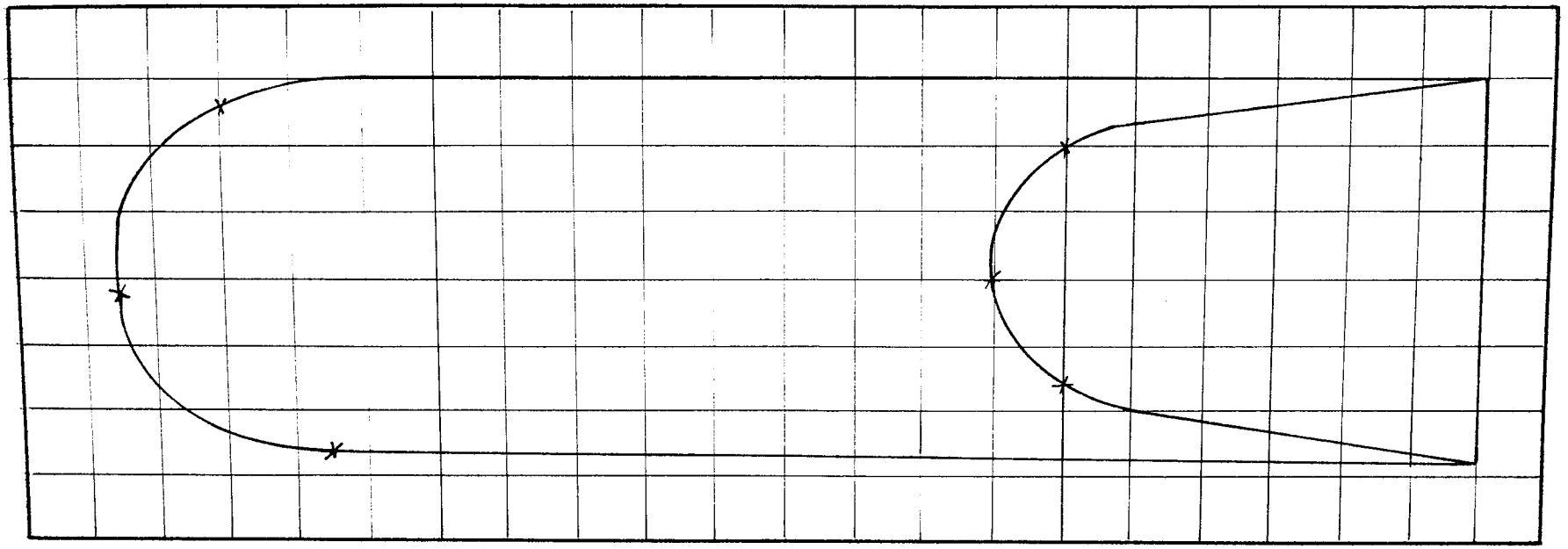

POSITION 3 Scales: Velocity: 1 mm = 1 mm/s

Momentum: 1 mm^2 = $\frac{1}{250}$ kgmm/s

Area under Velocity Curve = 3,400 mm^2

Area under Momentum Curve = 9,800 mm^2

BED MATERIAL: $1\frac{1}{2}$ mm Diameter Sand

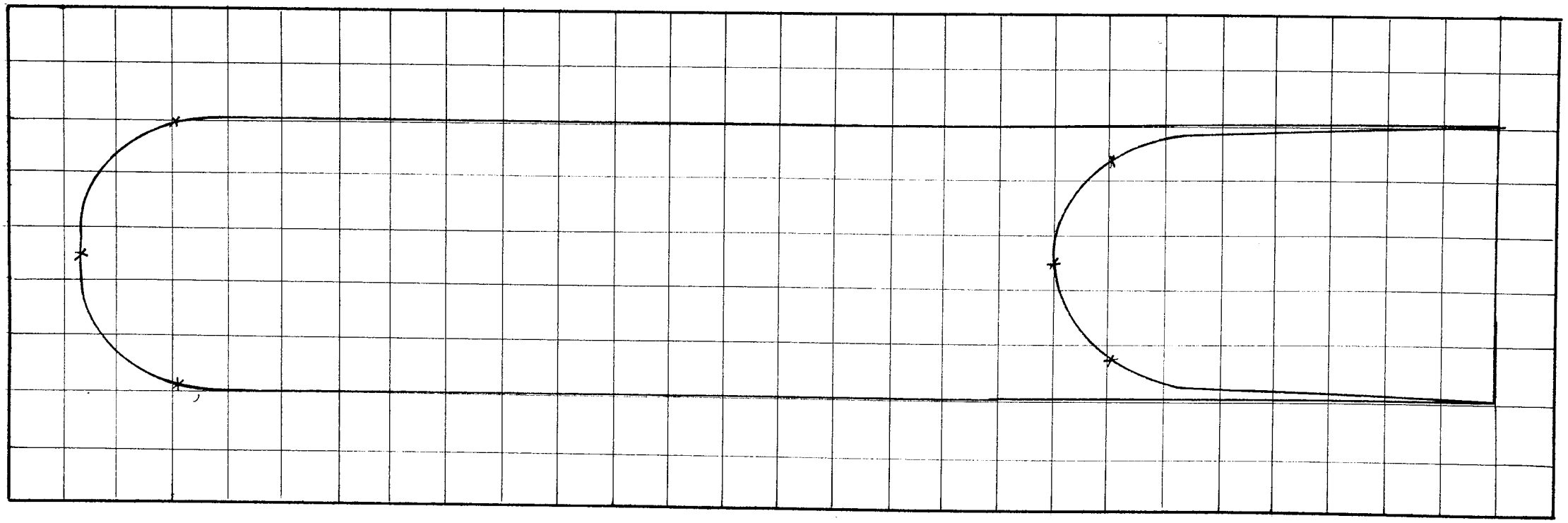

POSITION 5 Scale: Velocity: 1 mm = 1 mm /s

Momentum: 1 mm^2 = $\frac{1}{250}$ kgmm/s

Area under Velocity Curve = 3,450 mm^2

Area under Momentum Curve = 10,900 mm^2

BED MATERIAL: $1\frac{1}{2}$ mm Diameter Sand

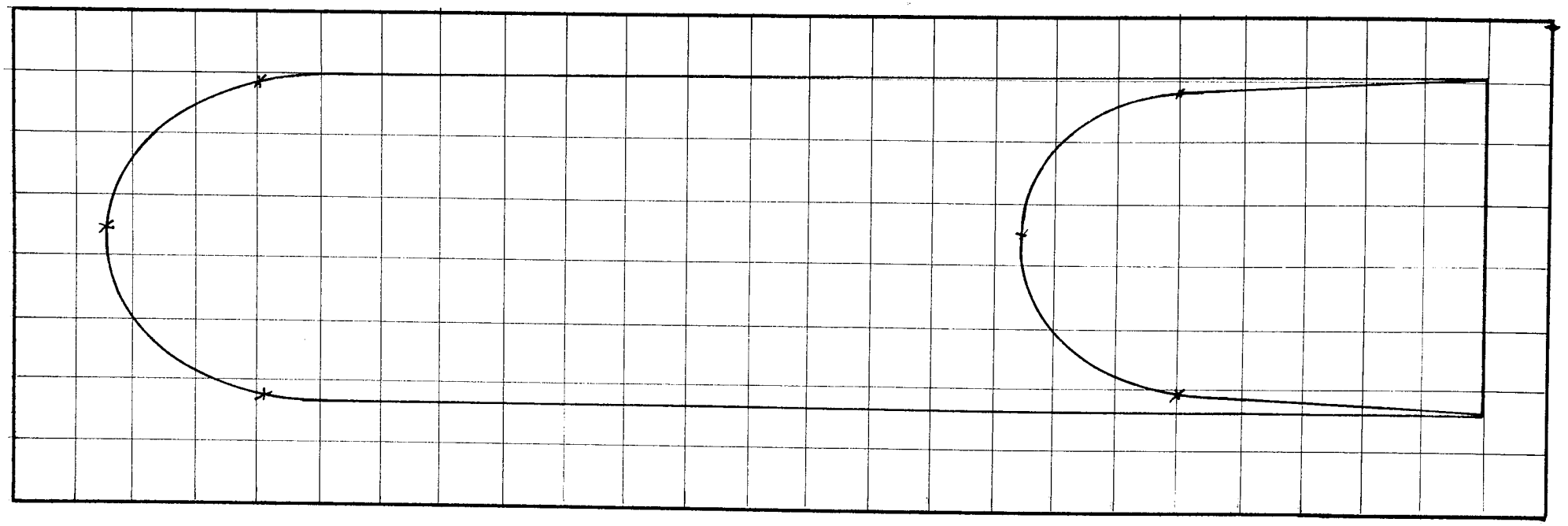

POSITION 4 Scales: Velocity : 1 mm = 1 mm/s Area under Velocity Curve = 3,400 mm^2

Momentum : 1 mm^2 = $\frac{1}{250}$ kgmm/s Area under Momentum Curve = 10,000 mm^2

BED MATERIAL: $1\frac{1}{2}$ mm Diameter Sand

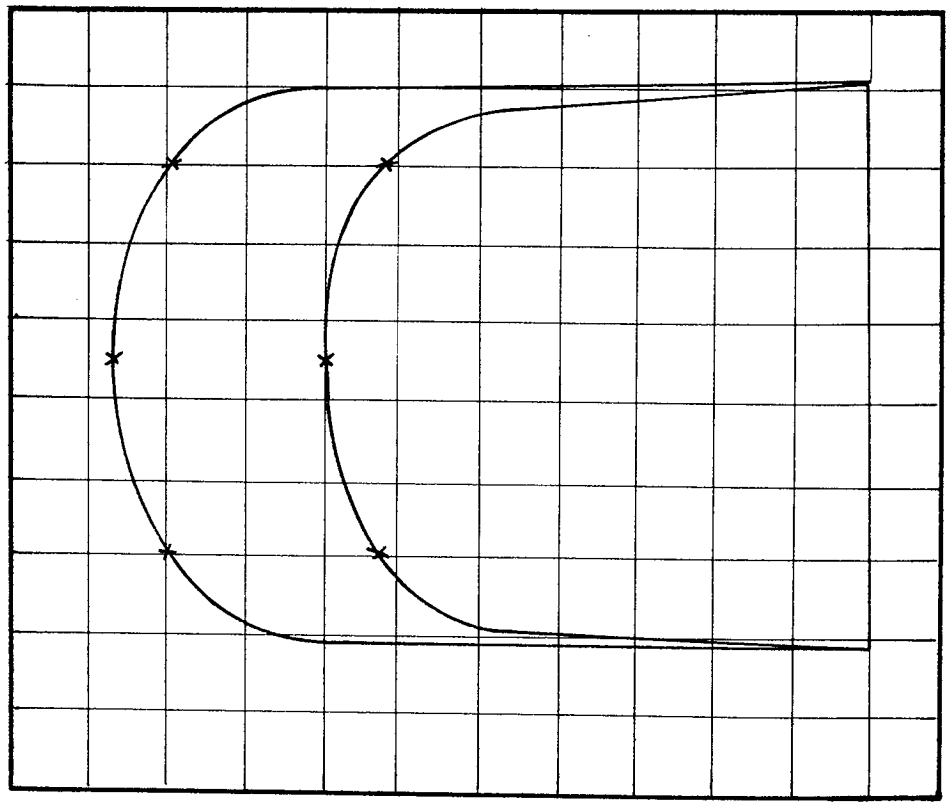

POSITION 1 Scales: Velocity : 1 mm = 1 mm/s Area under Velocity Curve = 4,690 mm^2

Momentum: 1 mm^2 = $\frac{1}{500}$ kgmm/s Area under Momentum Curve = 6,650 mm^2

BED MATERIAL: $1\frac{1}{2}$ mm Diameter Sand

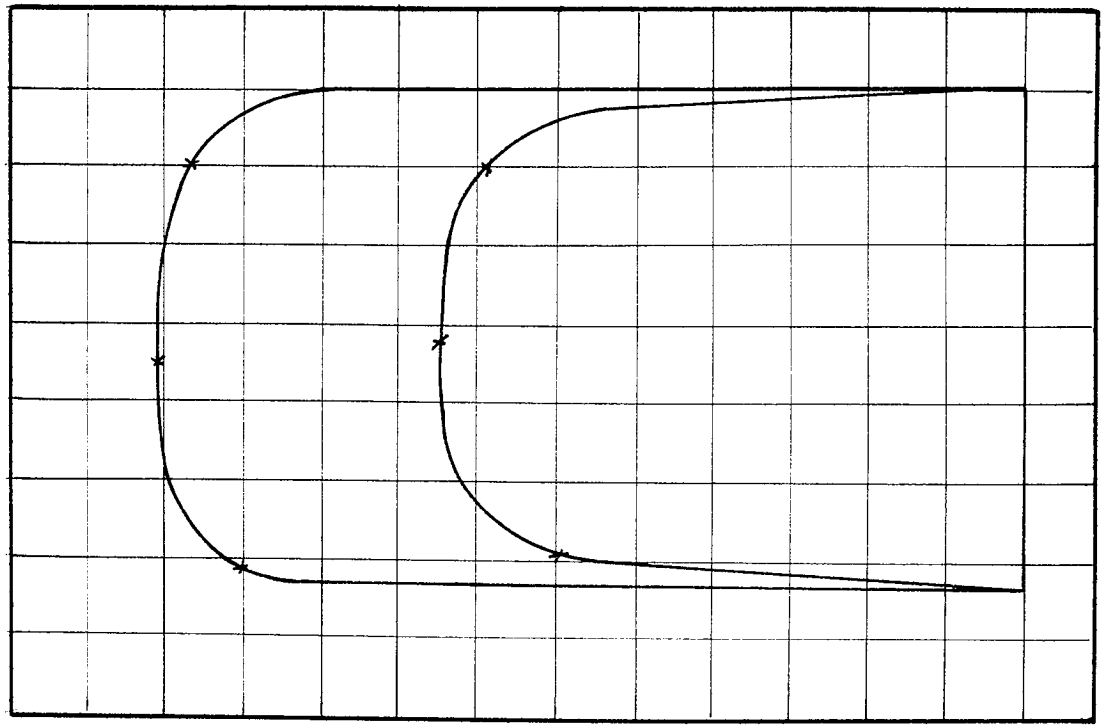

POSITION 2 Scales: Velocity: 1 mm = 1 mm/s Area under Velocity Curve = 4,550 mm^2

Momentum: 1 mm^2 = $\frac{1}{500}$ kgmm/s Area under Momentum Curve = 6,900 mm^2

BED MATERIAL: $1\frac{1}{2}$ mm Diameter Sand

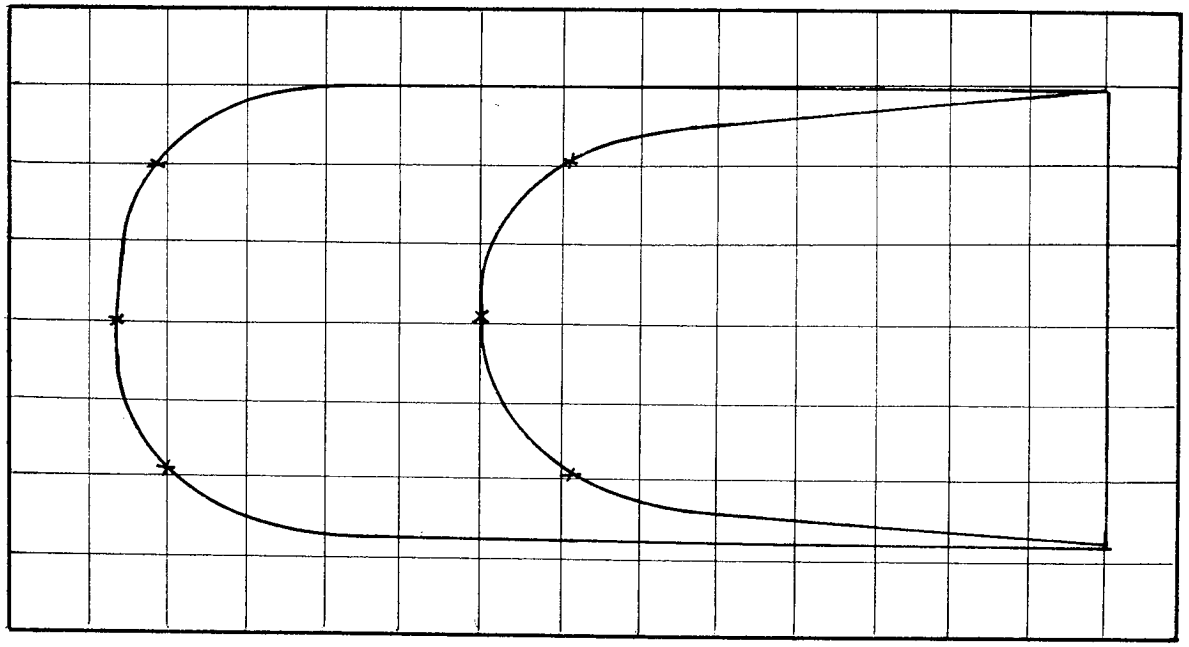

POSITION 3 Scales: Velocity: 1 mm = 1 mm/ s

Momentum: 1 mm^2 = $\frac{1}{500}$ kgmm/s

Area under Velocity Curve = 4,500 mm^2

Area under Momentum Curve = 6,820 mm^2

BED MATERIAL: $1\frac{1}{2}$ mm Diameter Sand

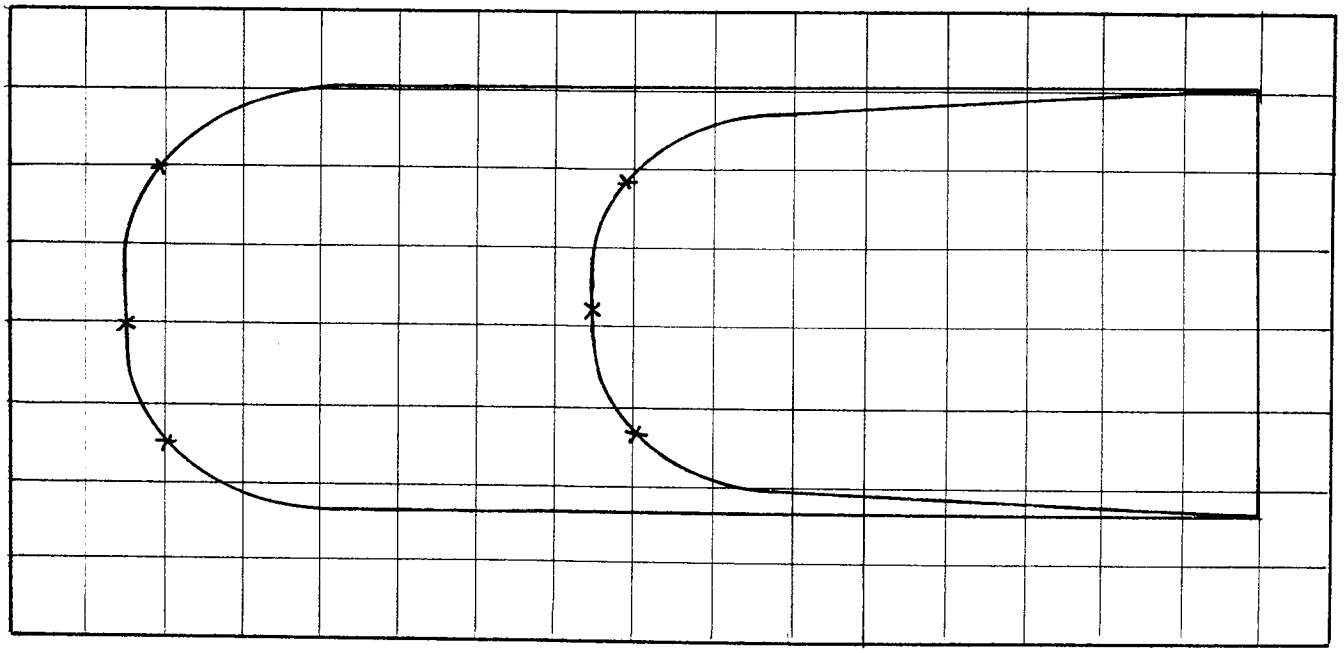

POSITION 4 Scales: Velocity : 1 mm = 1 mm/s Area under Velocity Curve = 4,500 mm^2

Momentum: 1 mm^2 = $\frac{1}{500}$ kgmm/s Area under Momentum Curve = 7,100 mm^2

BED MATERIAL: $1\frac{1}{2}$ mm Diameter Sand

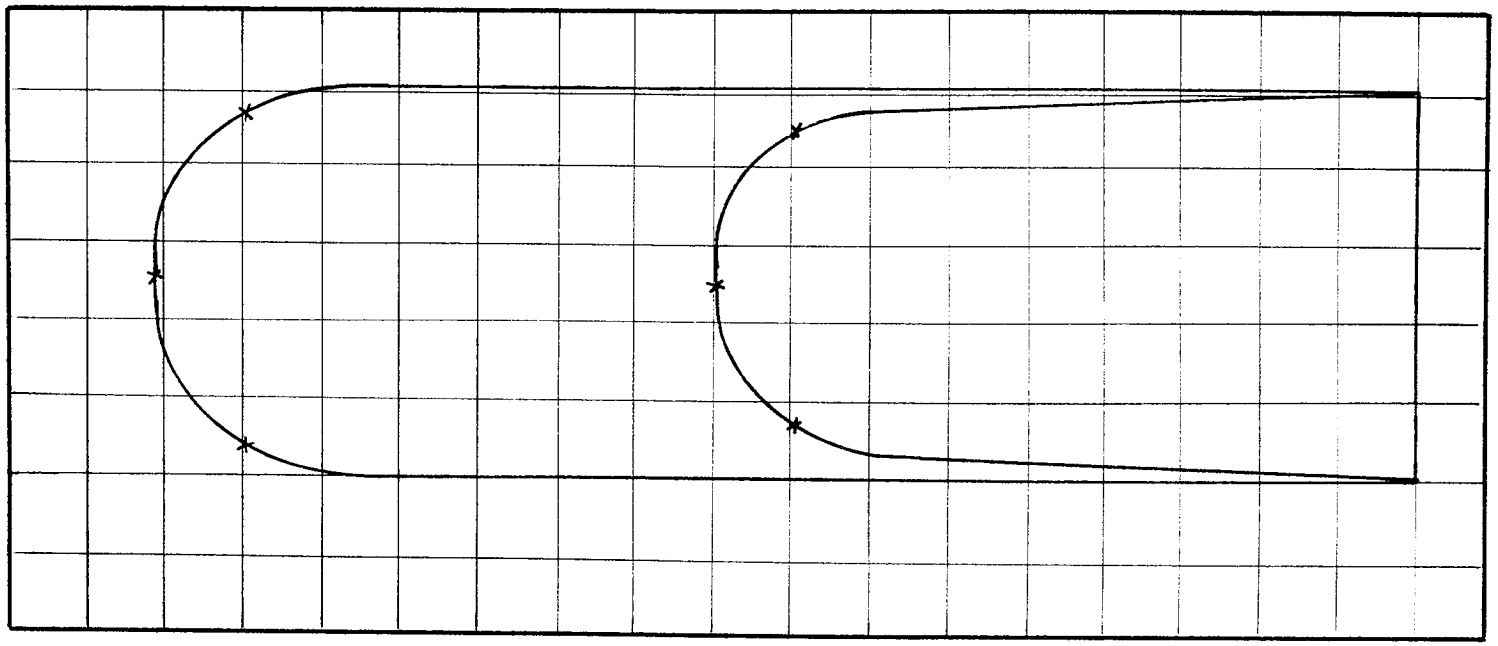

POSITION 5 Scales: Velocity : 1 mm = 1 mm/s Area under Velocity Curve = 4,600 mm^2

Momentum: 1 mm^2 = $\frac{1}{500}$ kgmm/s Area under Momentum Curve = 7,300 mm^2

BED MATERIAL: $1\frac{1}{2}$ mm Diameter Sand

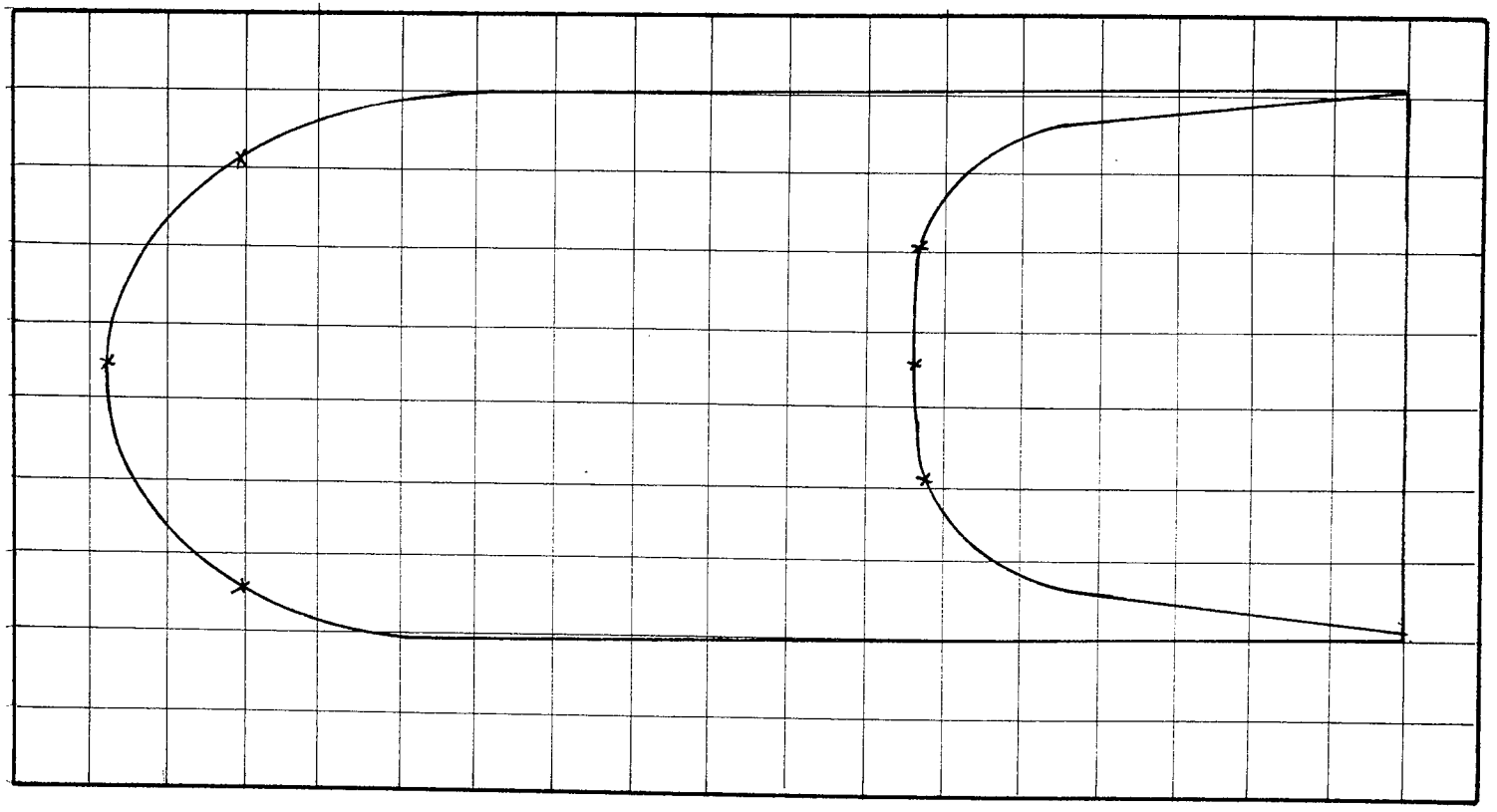

POSITION 1 Scales: Velocity: 1 mm = 1 mm/s

Momentum: 1 mm^2 = $\frac{1}{250}$ kgmm/s

Area under Velocity curve = 3,600 mm^2

Area under Momentum curve = 11,500 mm^2

BED MATERIAL : $1\frac{1}{2}$ mm Diameter Sand

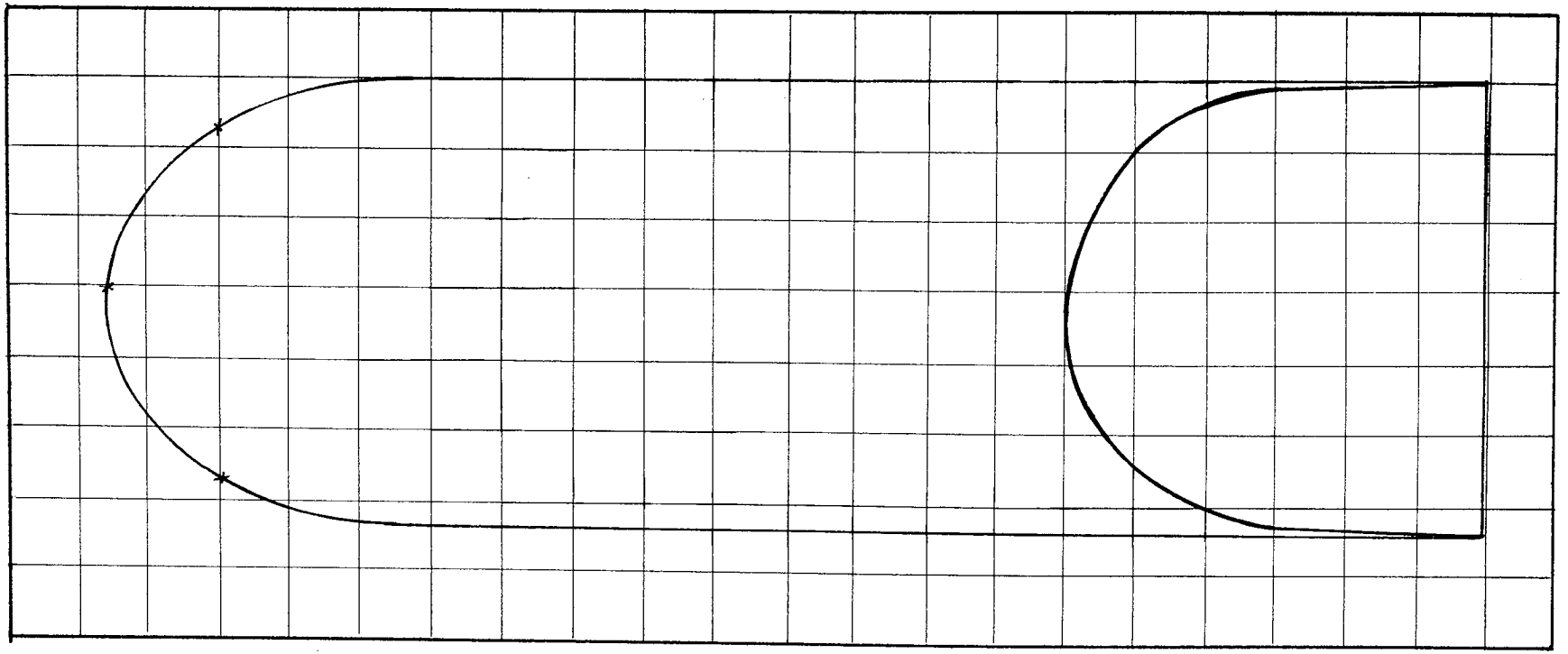

POSITION 2 Scales: Velocity: 1 mm = 1 mm/s Area under Velocity Curve = 3,750 mm^2

Momentum: 1 mm^2 = $\frac{1}{250}$ kgmm/s Area under Momentum Curve = 11,600 mm^2

BED MATERIAL: $1\frac{1}{2}$ mm Diameter Sand

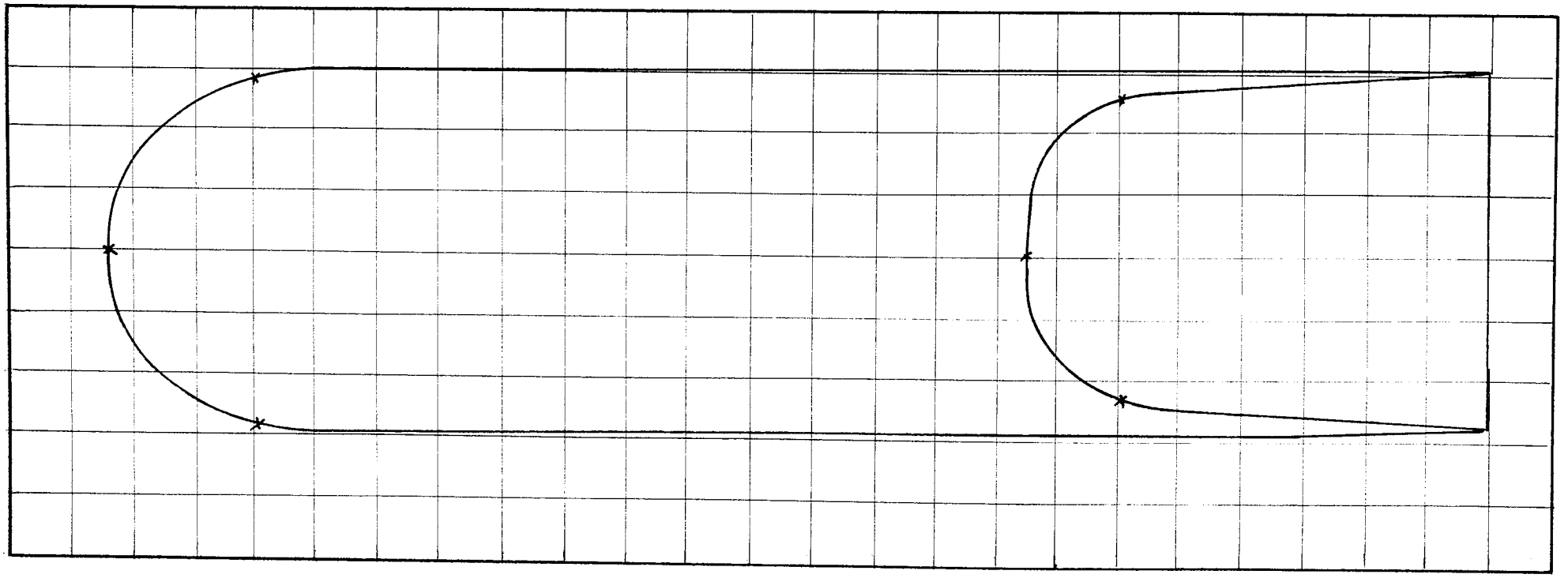

POSITION 3 Scales: Velocity: 1 mm = 1 mm/s Area under Velocity Curve = 3,600 mm^2

Momentum: $1mm^2 = \frac{1}{250}$ kgmm/s Area under Momentum Curve = 11,500 mm^2

BED MATERIAL: $1\frac{1}{2}$ mm Diameter Sand

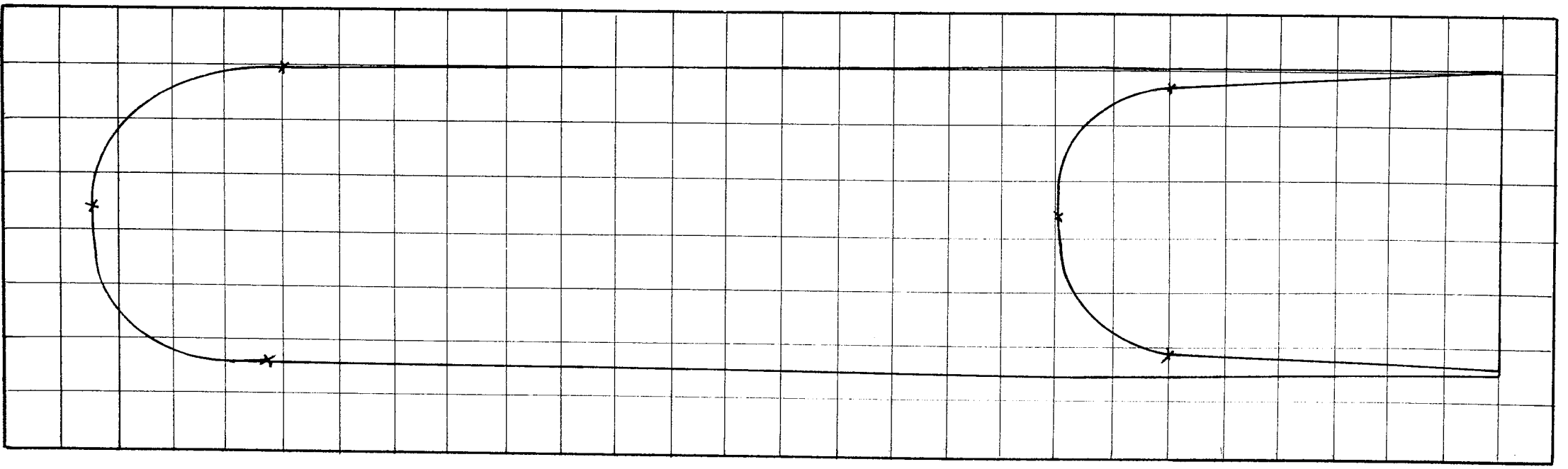

POSITION 4 Scales: Velocity: 1mm = 1 mm/s Area under Velocity Curve = 3,900 mm^2

Momentum: 1 mm^2 = $\frac{1}{250}$ kgmm/s Area under Momentum Curve = 11,000 mm^2

BED MATERIAL: $1\frac{1}{2}$ mm Diameter Sand

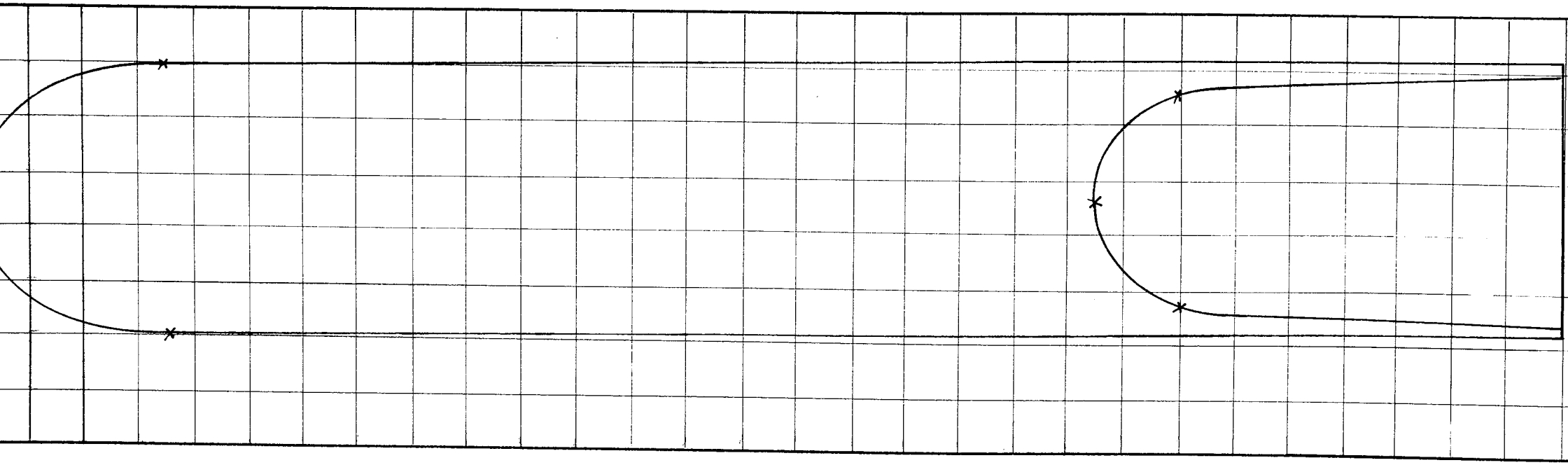

POSITION 5 Scales: Velocity: 1 mm = 1 mm/s Area under Velocity Curve = 3,950 mm^2

Momentum: 1 mm^2 = $\frac{1}{250}$ kgmm/s Area under Momentum Curve = 12,000mm^2

BED MATERIAL: $1\frac{1}{2}$ mm Diameter Sand

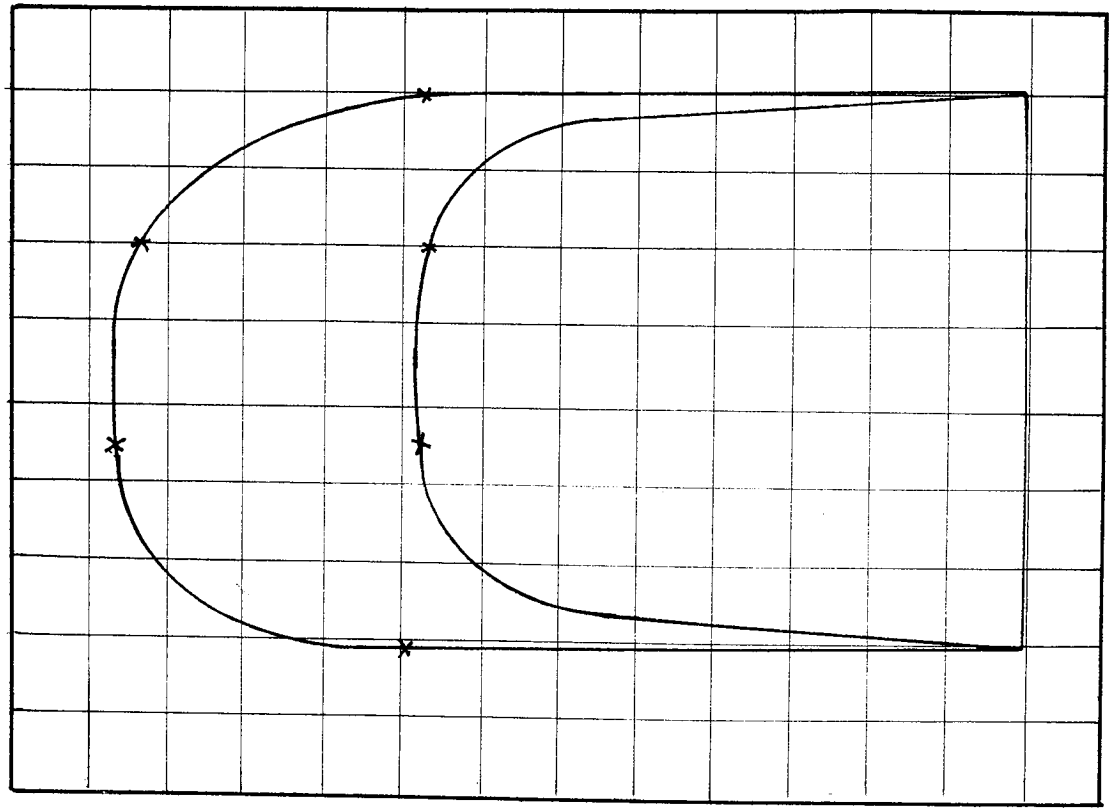

POSITION 1 Scales: Velocity: 1 mm = 1 mm/s Area under Velocity Curve = 4,160 mm^2

Momentum: 1 mm^2 = $\frac{1}{250}$ kgmm/s Area under Momentum Curve = 7,850 mm^2

BED MATERIAL: $1\frac{1}{2}$ mm Diameter Sand

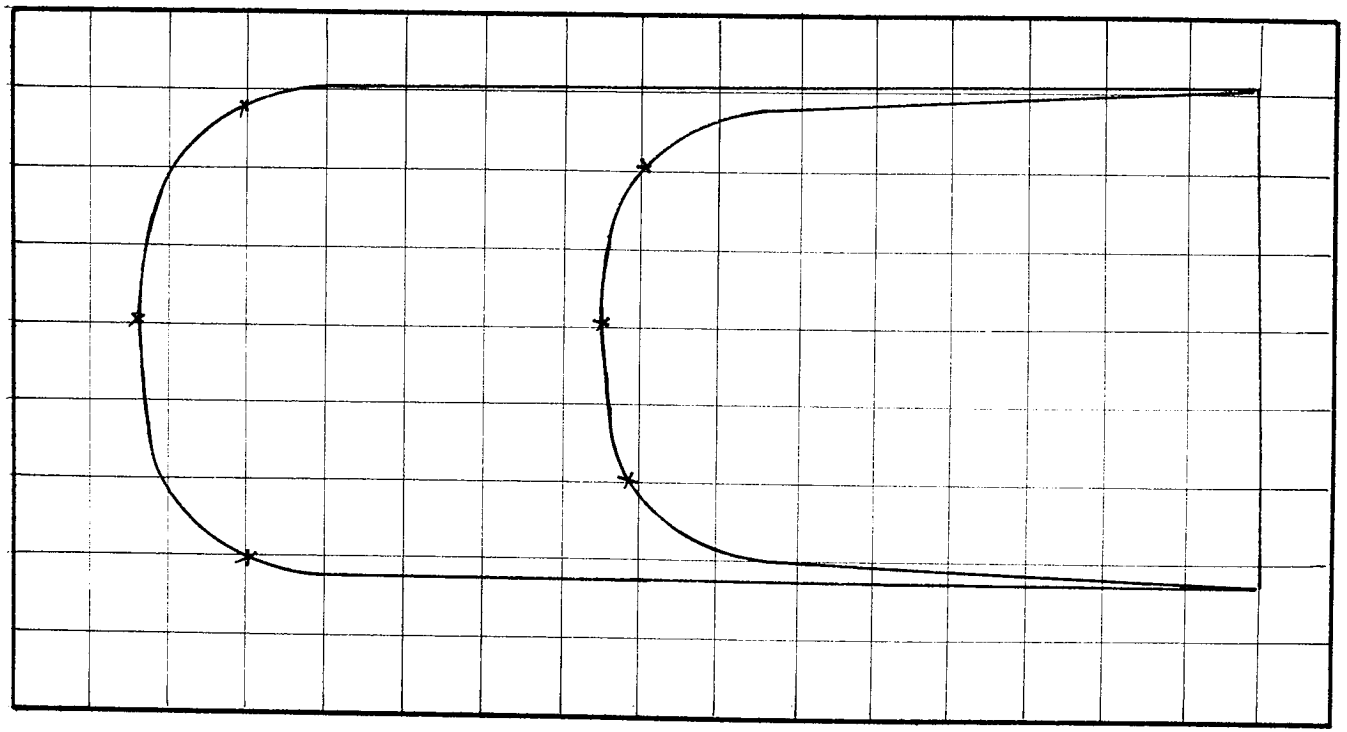

POSITION 2 Scales : Velocity: 1 mm = 1 mm/s Area under Velocity Curve = 4,900 mm^2

Momentum: 1 mm^2 = $\frac{1}{250}$ kgmm/s Area under Momentum Curve = 8,400 mm^2

BED MATERIAL: $1\frac{1}{2}$ mm Diameter Sand

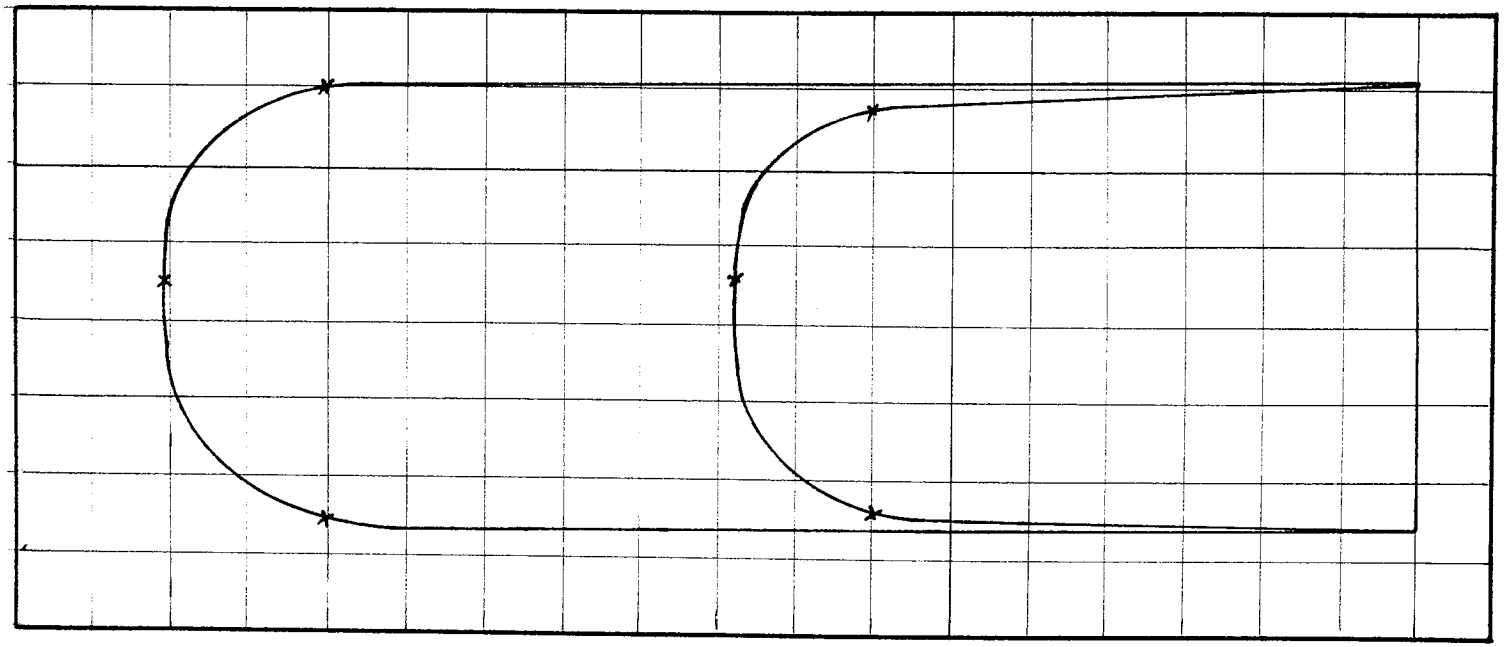

POSITION 3 Scales: Velocity: 1mm = 1 mm/s Area under Velocity Curve = 4,500 mm^2

Momentum: 1 mm^2 = $\frac{1}{250}$ kgmm/s Area under Momentum Curve = 8,400 mm^2

BED MATERIAL: $1\frac{1}{2}$ mm Diameter Sand

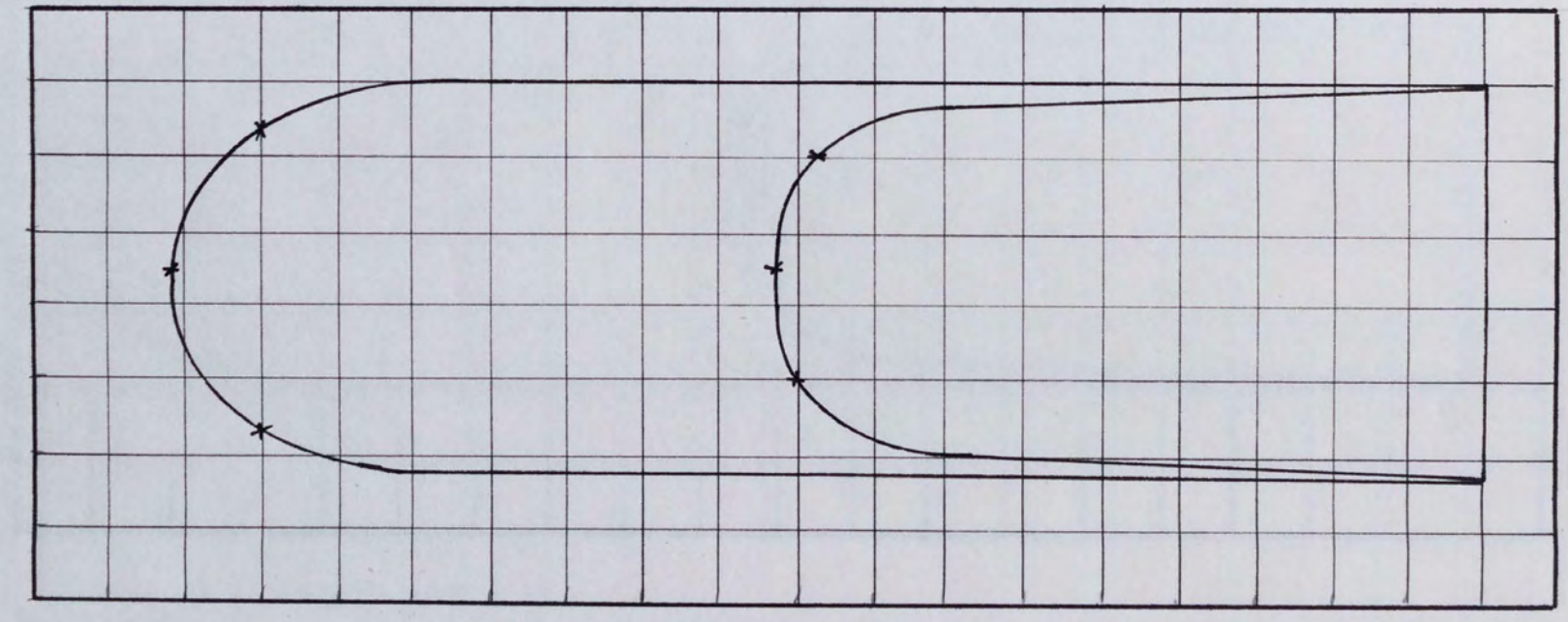

POSITION 4 Scales: Velocity: 1 mm = 1 mm/s Area under Velocity Curve = 4,500 mm^2

Momentum: 1 mm^2 = $\frac{1}{250}$ kgmm/s Area under Momentum Curve = 8,600 mm^2

BED MATERIAL: $1\frac{1}{2}$ mm Diameter Sand

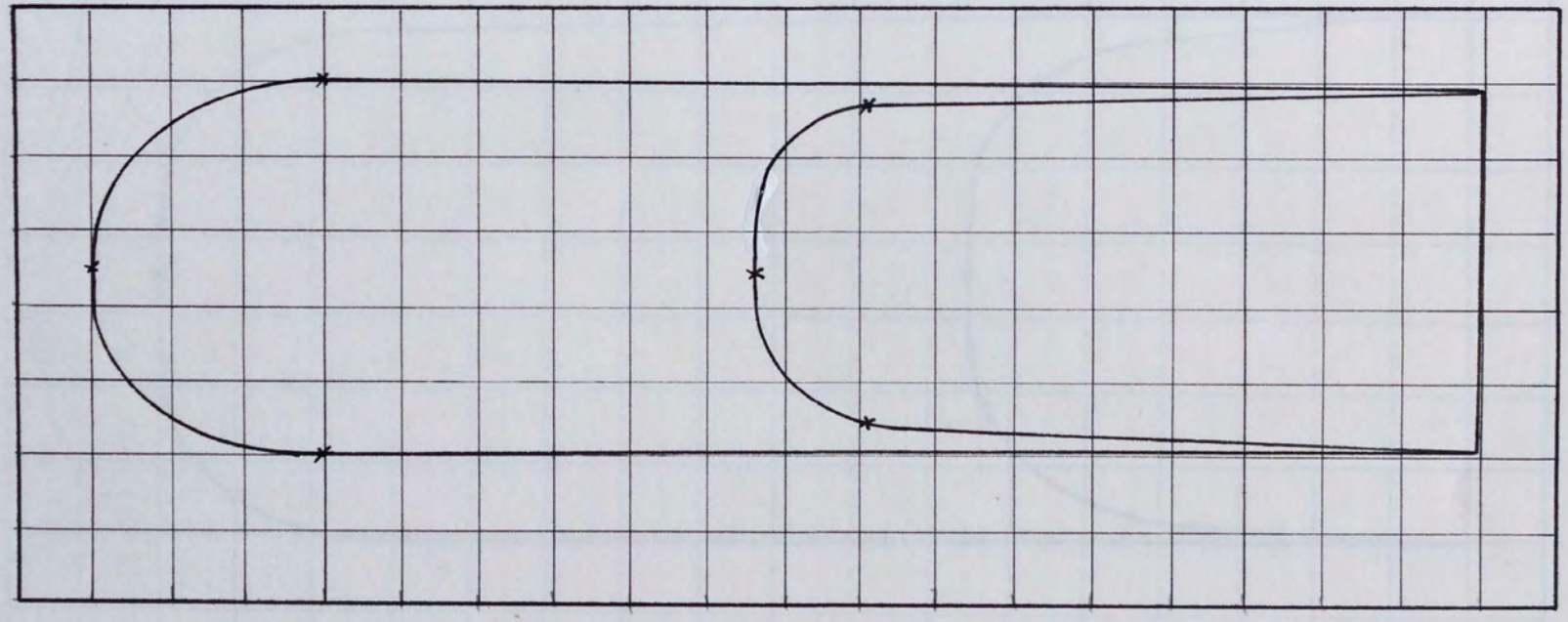

POSITION 5 Scales: Velocity: 1 mm = 1 mm/s Area under Velocity Curve = 4,400 mm^2

Momentum: 1 mm^2 = $\frac{1}{250}$ kgmm/s Area under Momentum Curve = 8,500mm^2

BED MATERIAL: $1\frac{1}{2}$ mm Diameter Sand

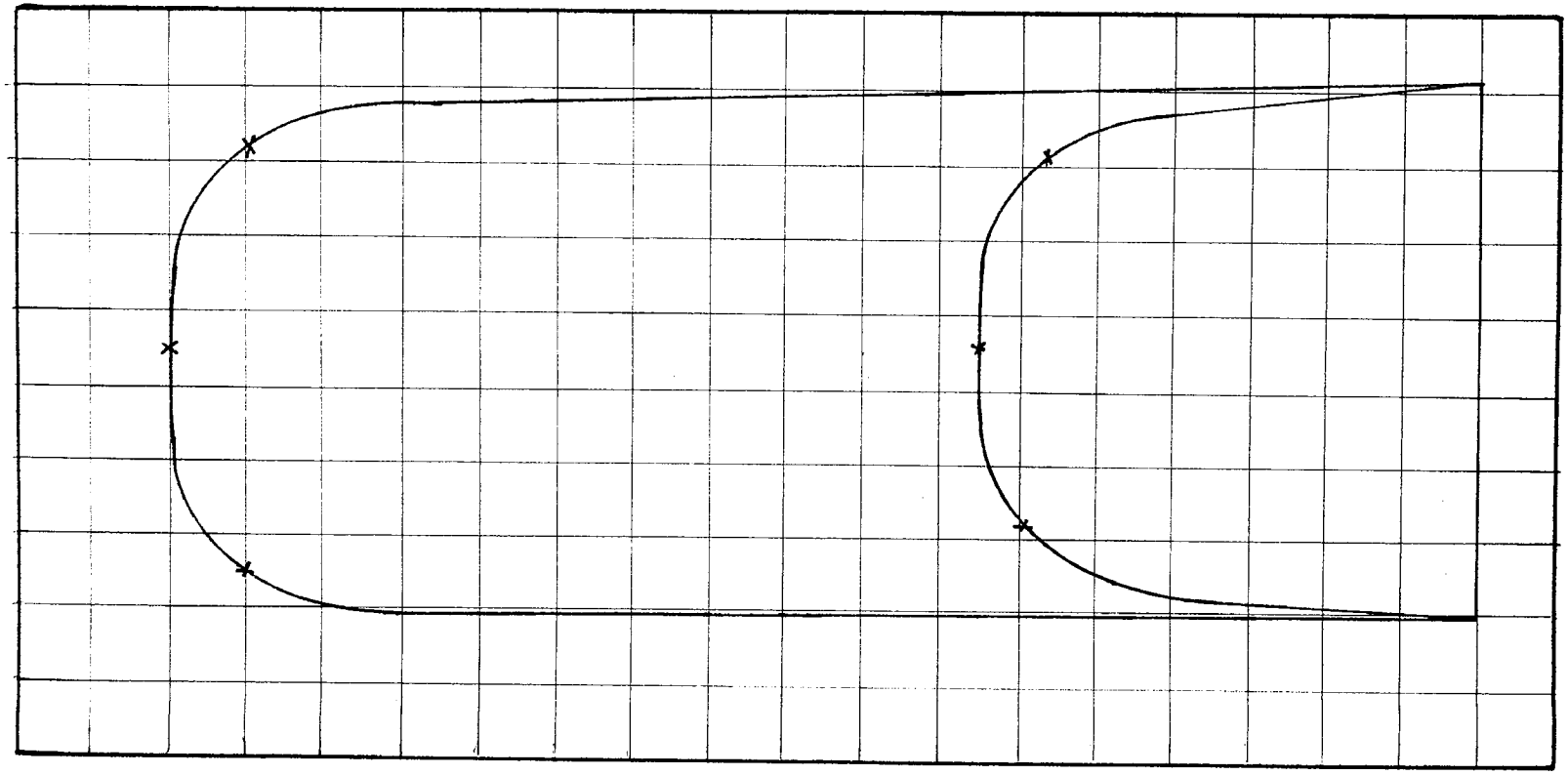

POSITION 1 Scales: Velocity: 1 mm = 1 mm/s Area under Velocity Curve = 3,720 mm^2

Momentum: 1 mm^2 = $\frac{1}{25}$ kgmm/s Area under Momentum Curve = 11,750 mm^2

BED MATERIAL: $1\frac{1}{2}$ mm Diameter Sand

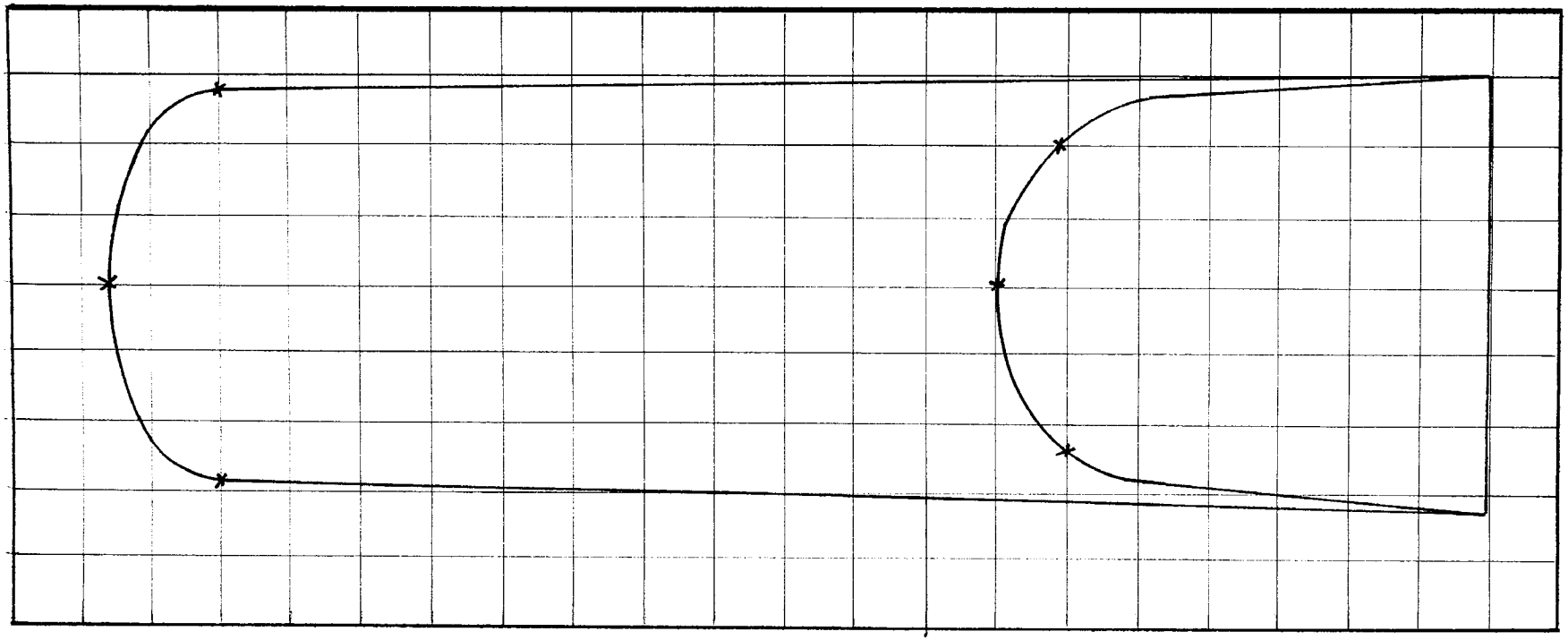

POSITION 2 Scales: Velocity: 1 mm = 1 mm/s Area under Velocity Curve = 3,750 mm^2

Momentum: 1 mm^2 = $\frac{1}{25}$ kgmm/s Area under Momentum Curve = 11,000 mm^2

BED MATERIAL: $1\frac{1}{2}$ mm Diameter Sand

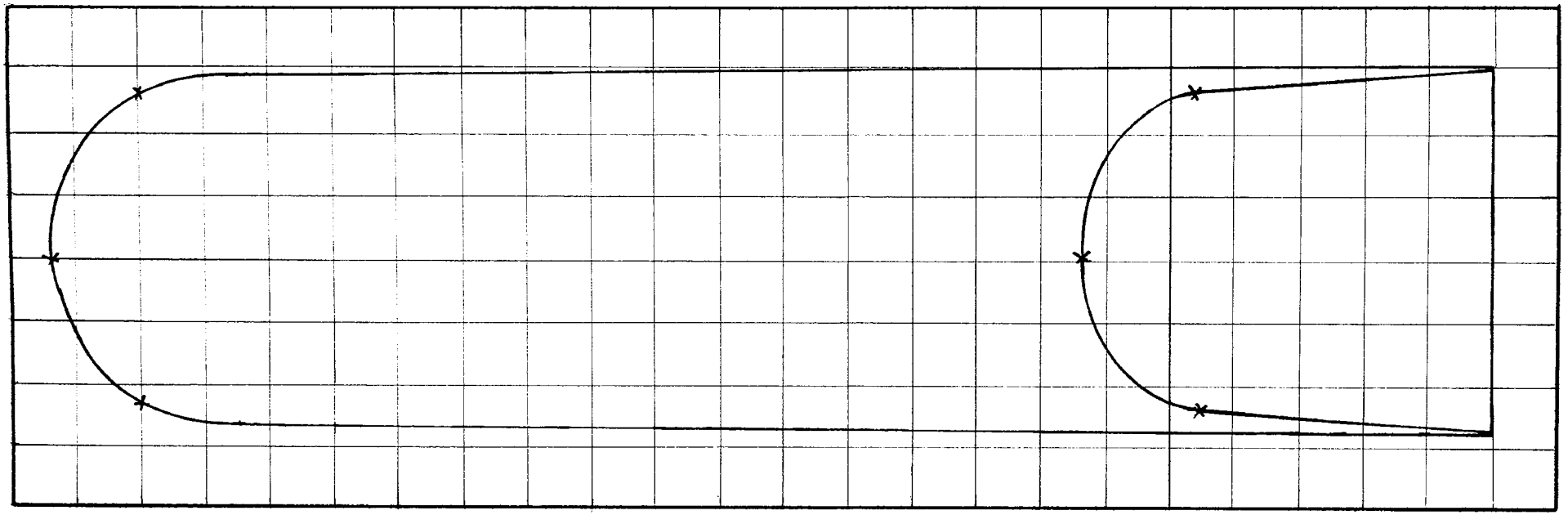

POSITION 3 Scales: Velocity 1 mm = 1 mm/s Area under Velocity Curve = 3,650 mm^2

Momentum: 1 mm^2 = $\frac{1}{25}$ kgmm/s Area under Momentum Curve = 11,000 mm^2

BED MATERIAL: $1\frac{1}{2}$ mm Diameter Sand

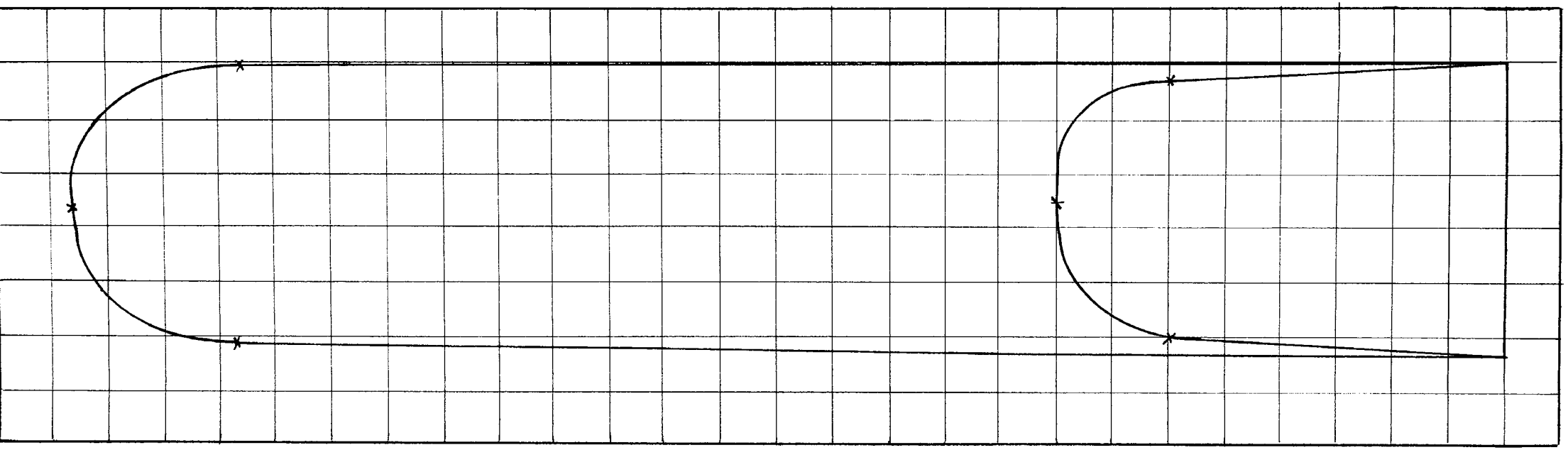

POSITION 4 Scales: Velocity: 1 mm = 1 mm/s Area under Velocity Curve = 3,800 mm^2

Momentum: 1 mm^2 = $\frac{1}{25}$ kgmm/s Area under Momentum Curve = 12,000 mm^2

BED MATERIAL: $1\frac{1}{2}$ mm Diameter Sand

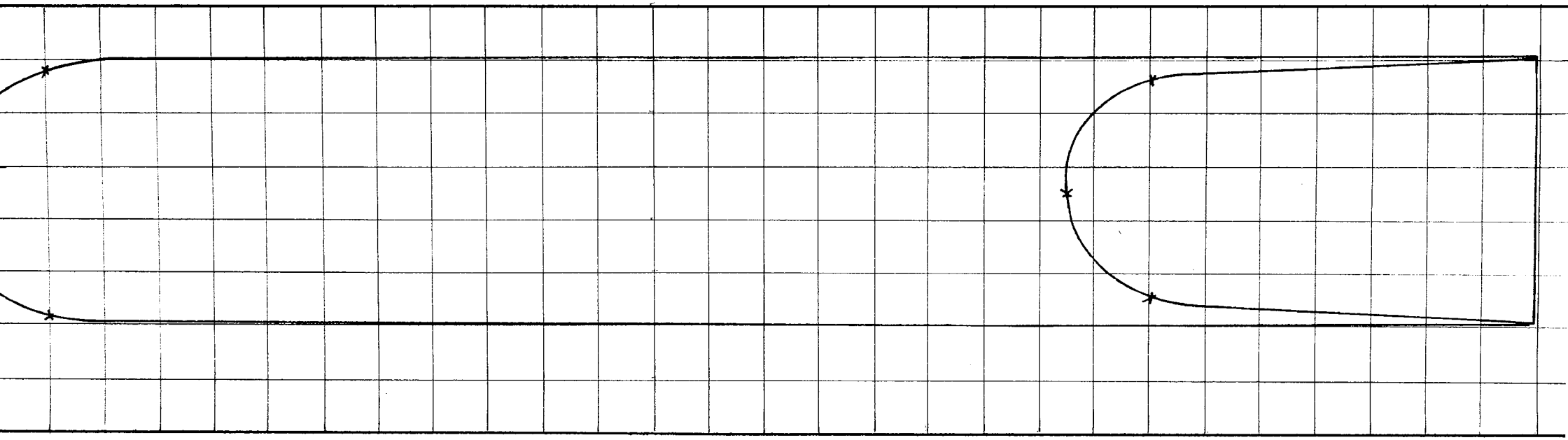

POSITION 5 Scales: Velocity : 1 mm = 1 mm/s Area under Velocity Curve = 3,750 mm^2

Momentum: 1 mm^2 = $\frac{1}{25}$ kgmm/s Area under Momentum Curve = 11,900 mm^2

BED MATERIAL: $1\frac{1}{2}$ mm Diameter Sand

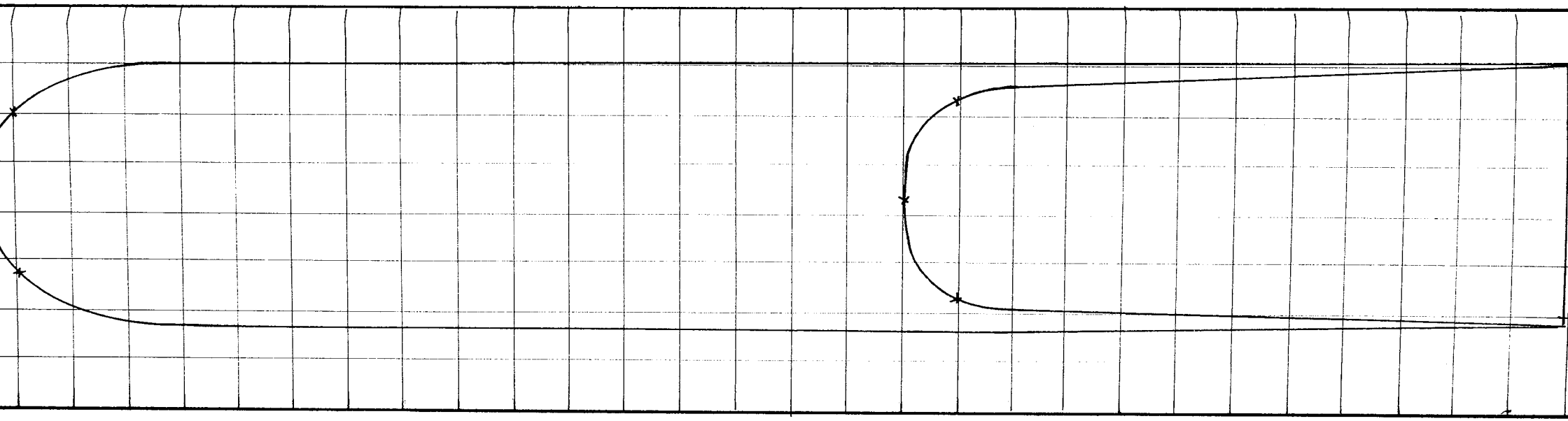

POSITION 4 Scales: Velocity: 1 mm = 1 mm/s Area under Velocity Curve = 7,200 mm^2

Momentum: 1 $mm^2 = \frac{1}{25}$ kgmm/s Area under Momentum Curve = 15,000 mm^2

BED MATERIAL: $1\frac{1}{2}$ mm Diameter Sand

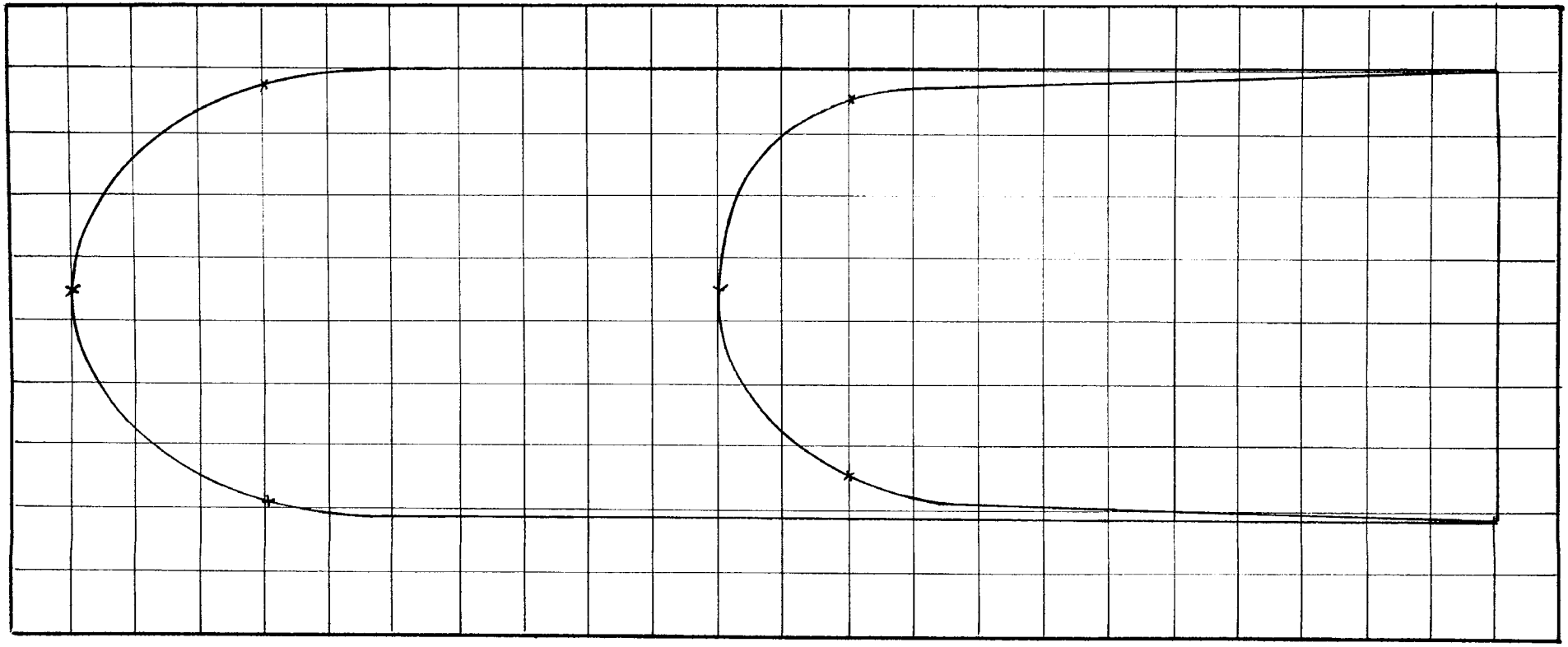

POSITION 1 Scales: Velocity: 1 mm = 1 mm/s Area under Velocity Curve = 8,200 mm^2

Momentum: 1 mm^2 = $\frac{1}{25}$ kgmm/s Area under Momentum Curve = 14,800 mm^2

BED MATERIAL: $1\frac{1}{2}$ mm Diameter Sand

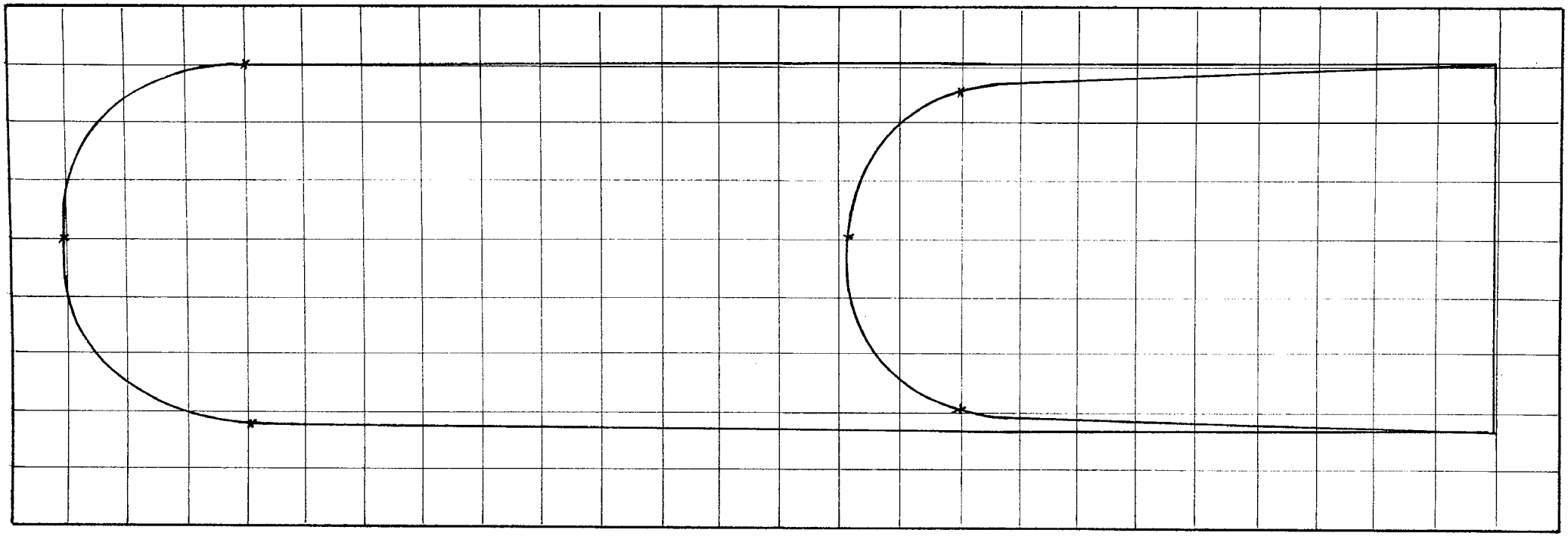

POSITION 2 Scales: Velocity: 1mm = 1 mm/s Area under Velocity Curve = 7,400 mm^2

Momentum: 1 mm^2 = $\frac{1}{24}$ kgmm/s Area under Momentum Curve = 15,100 mm^2

BED MATERIAL: $1\frac{1}{2}$ mm Diameter Sand

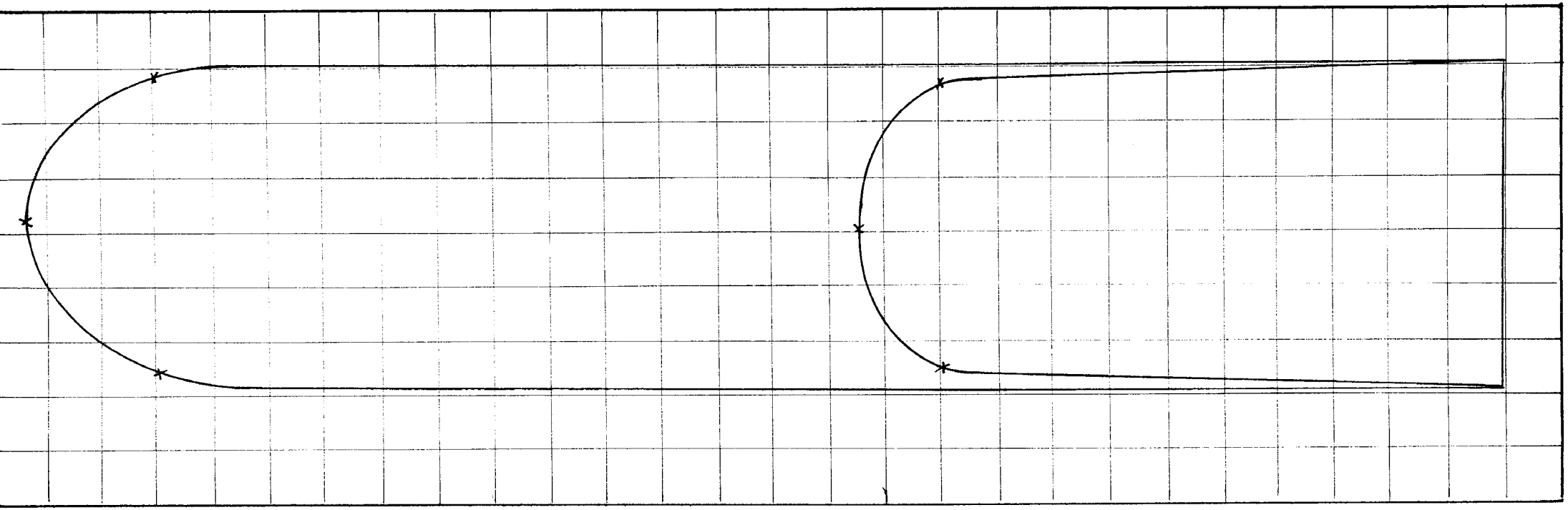

POSITION 3 Scales: Velocity: 1 mm = 1 mm/s Area under Velocity Curve = 8,310 mm^2

Momentum: 1 $mm^2 = \frac{1}{25}$ kgmm/s Area under Momentum Curve = 15,200 mm^2

BED MATERIAL: $1\frac{1}{2}$ mm Diameter Sand

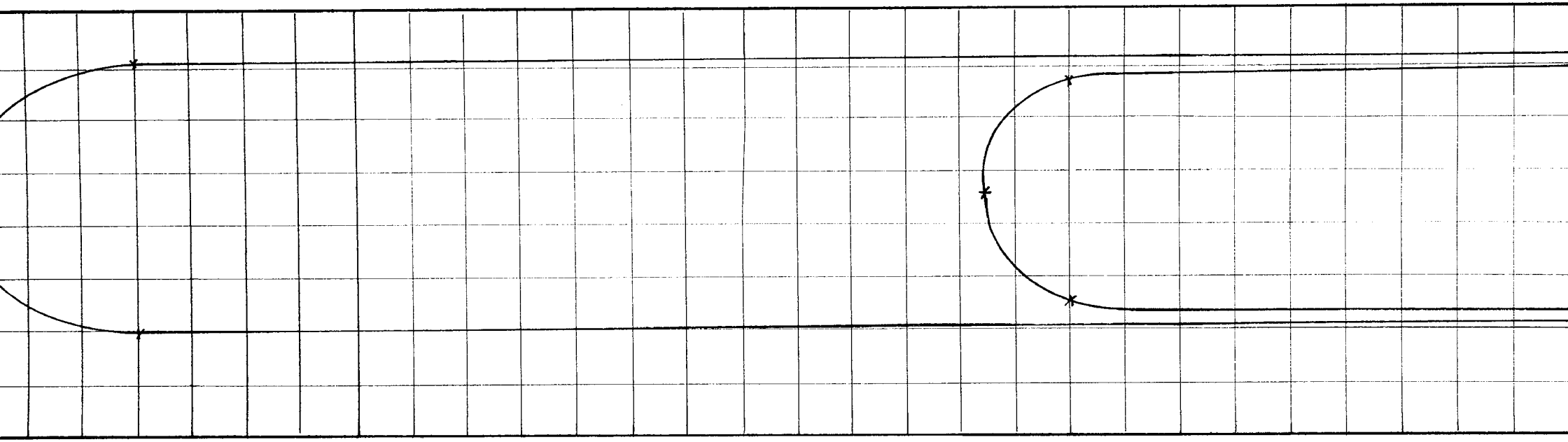

POSITION 5 Scales: Velocity: 1 mm = 1 mm/s Area under Velocity Curve = 7,600 mm^2

Momentum: 1 mm^2 = $\frac{1}{25}$ kgmm/s Area under Momentum Curve = 14,500 mm^2

BED MATERIAL: $1\frac{1}{2}$ mm Diameter Sand

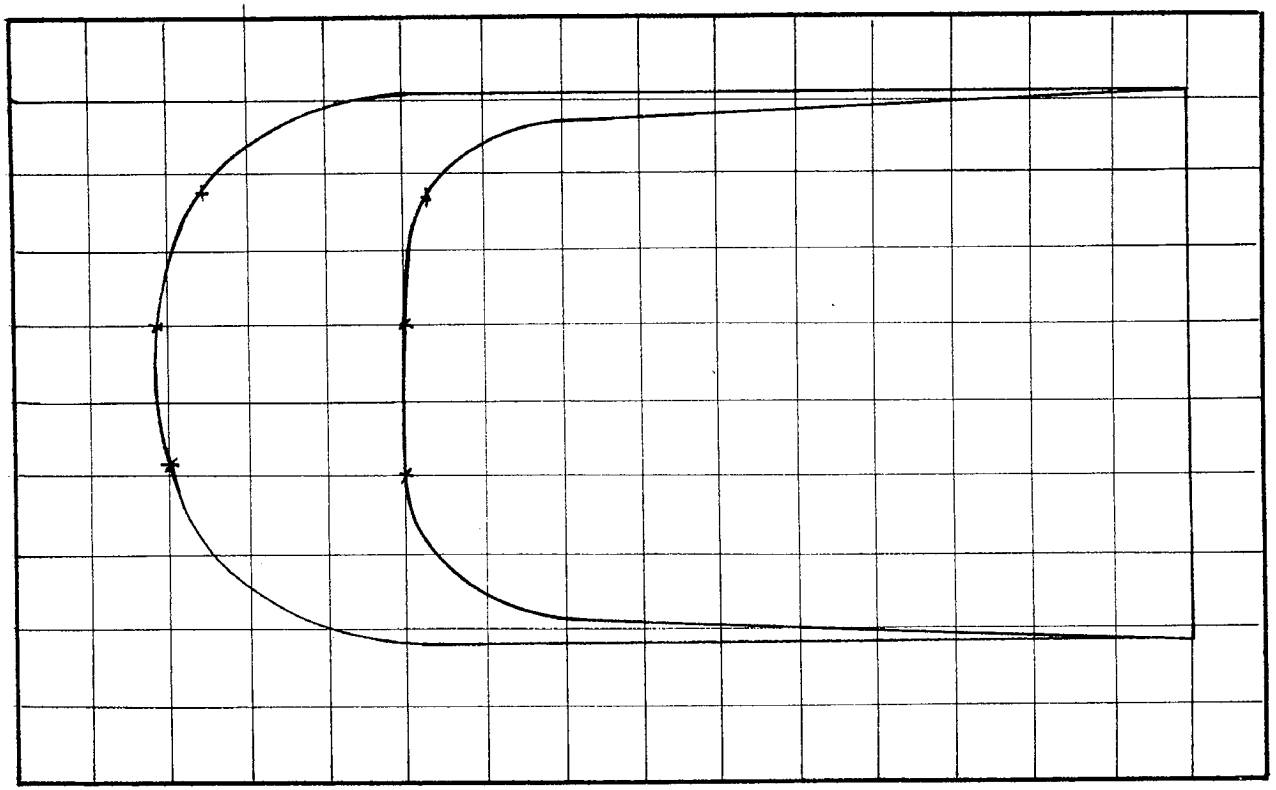

POSITION 1 Scales: Velocity: 1 mm. = 1 mm/s

Momentum: 1 mm^2 = $\frac{1}{75}$ kgmm/s

Area under Velocity Curve = 6,300 mm^2

Area under Momentum Curve = 9,000 mm^2

BED MATERIAL: $1\frac{1}{2}$ mm Diameter Sand

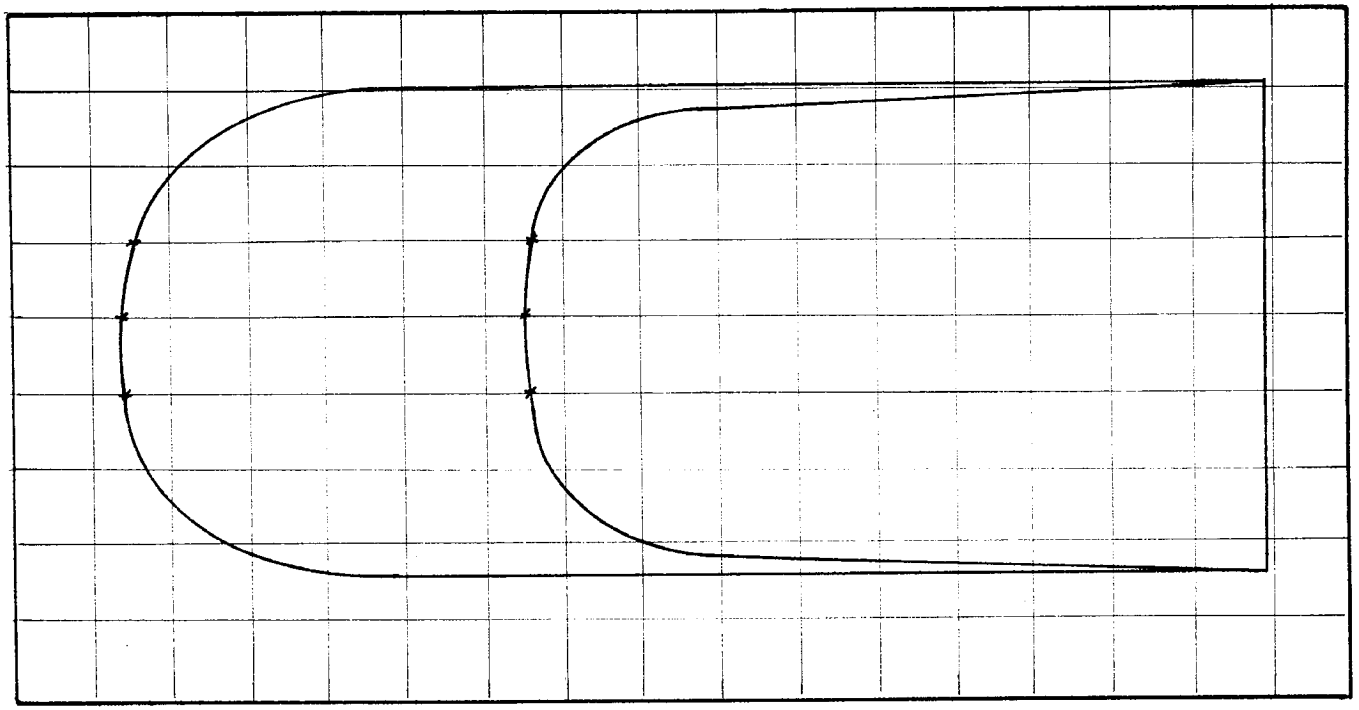

POSITION 2 Scales: Velocity: 1 mm = 1 mm/s Area under Velocity Curve = 6,200 mm^2

Momentum: 1 mm^2 = $\frac{1}{75}$ kgmm/s Area under Momentum Curve = 8,900 mm^2

BED MATERIAL: $1\frac{1}{2}$ mm Diameter Sand

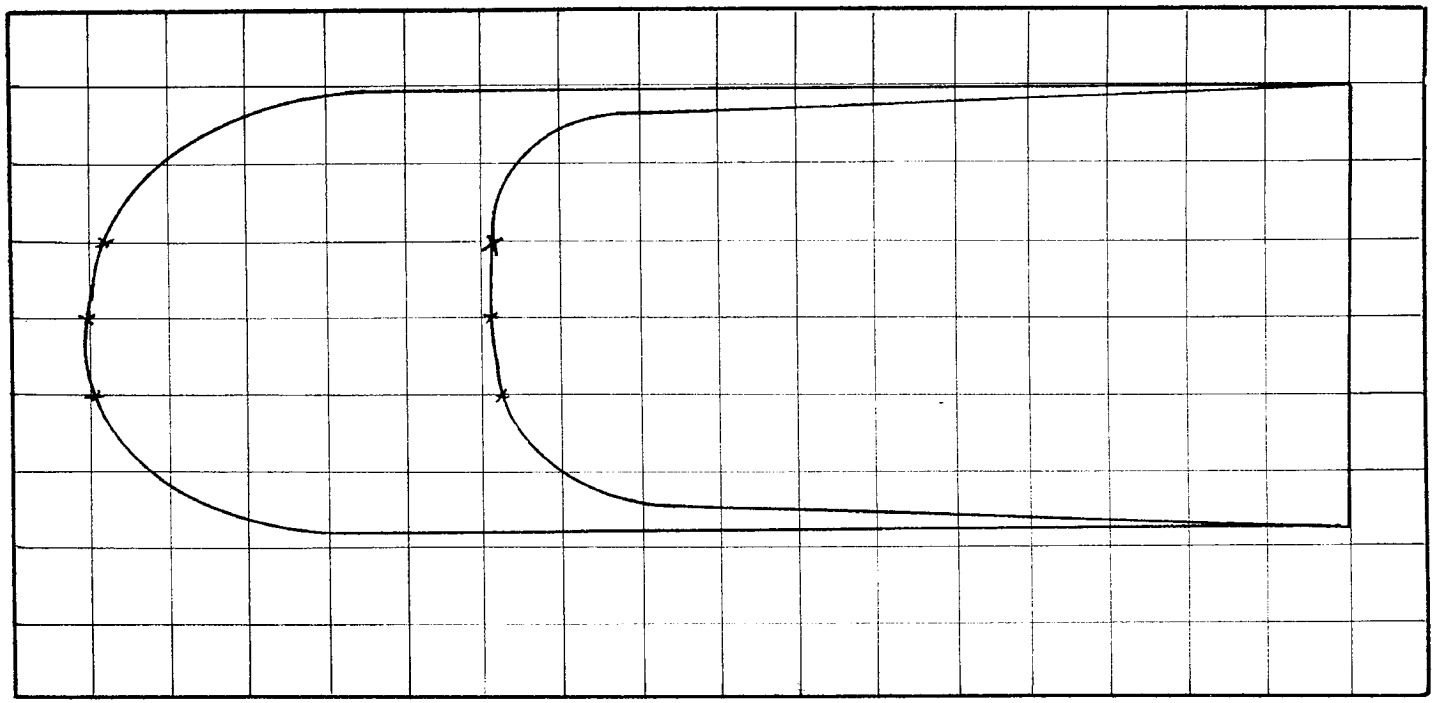

POSITION 3 Scales: Velocity: 1 mm = 1 mm/s Area under Velocity Curve = 6,320 mm^2

Momentum: 1 mm^2 = $\frac{1}{75}$ kgmm/s Area under Momentum Curve = 8,850 mm^2

BED MATERIAL: $1\frac{1}{2}$ mm Diameter Sand

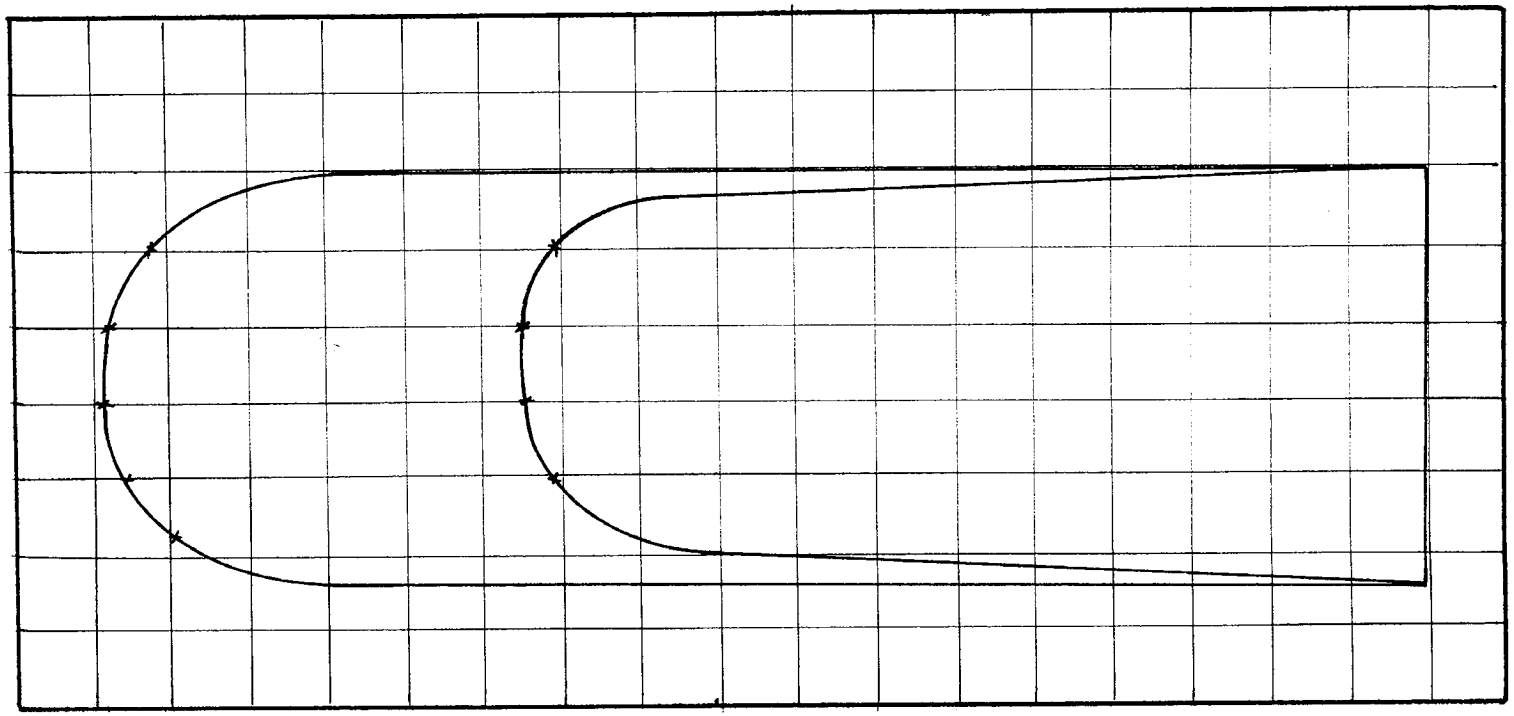

POSITION 4 Scales: Velocity: 1 mm = 1 mm/s Area under Velocity Curve = 6,100 mm^2

Momentum: 1 mm^2 = $\frac{1}{75}$ kgmm/s Area under Momentum Curve = 8,700 mm^2

BED MATERIAL: $1\frac{1}{2}$ mm Diameter Sand

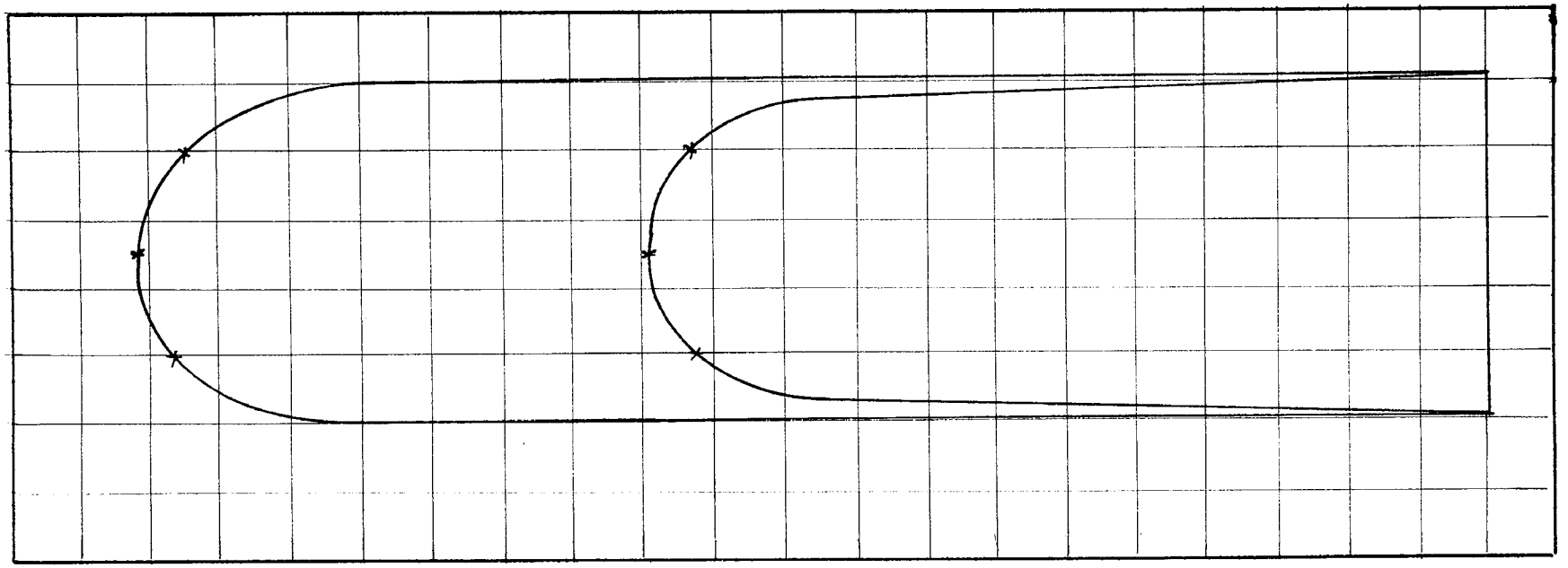

POSITION 5 Scales: Velocity: 1 mm = 1 mm/s Area under Velocity Curve = 5,950 mm^2

Momentum: 1 mm^2 = $\frac{1}{75}$ kgmm/s Area under Momentum Curve = 9,200 mm^2

BED MATERIAL: $1\frac{1}{2}$ mm Diameter Sand

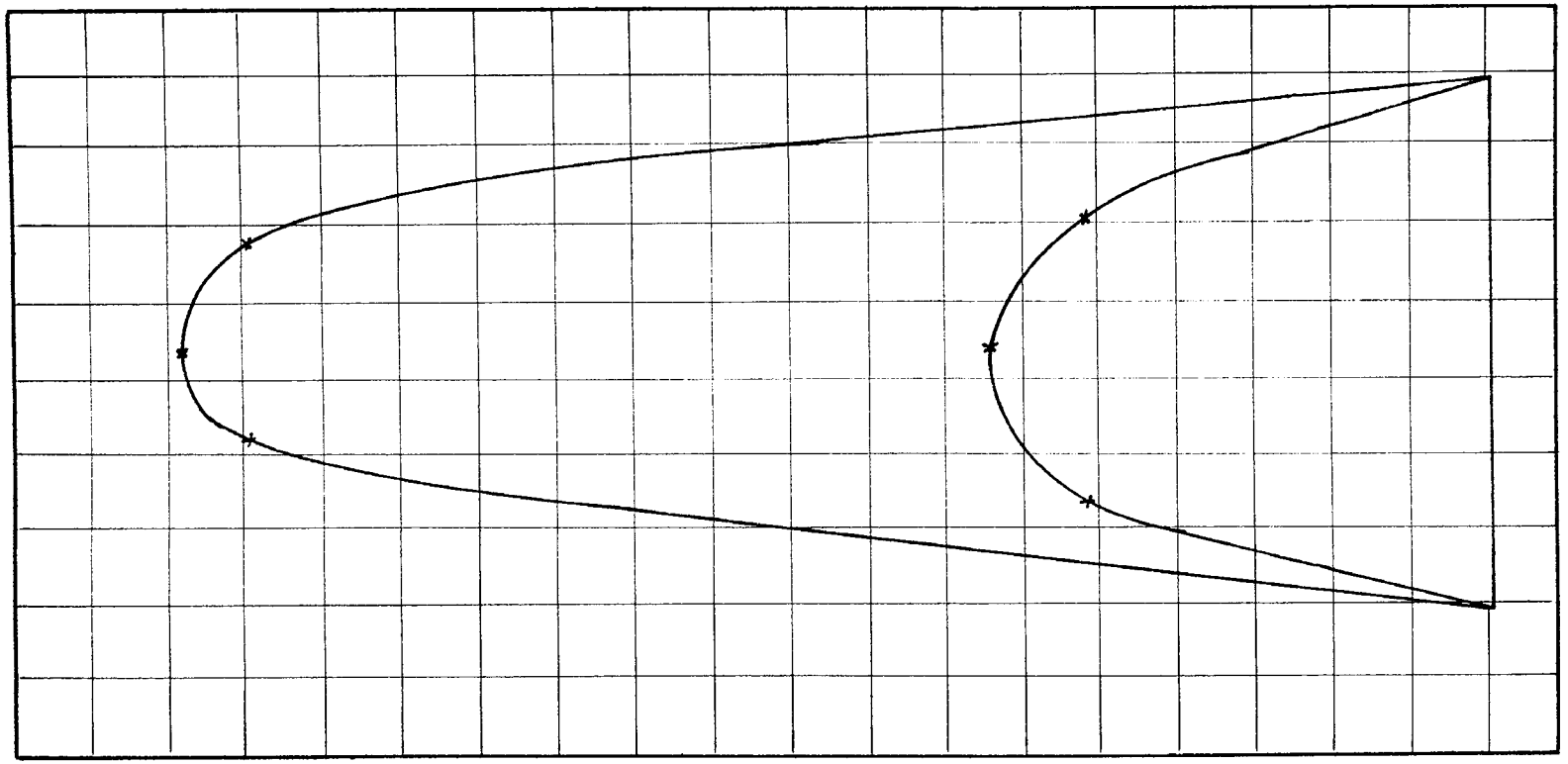

POSITION 1 Scales: Velocity: 1 mm = 1 mm/s Area under Velocity Curve = 3,500 mm^2

Momentum: $1mm^2 = \frac{1}{25}$ kgmm/s Area under Momentum Curve = 9,200 mm^2

BED MATERIAL: $1\frac{1}{2}$ mm Diameter Sand

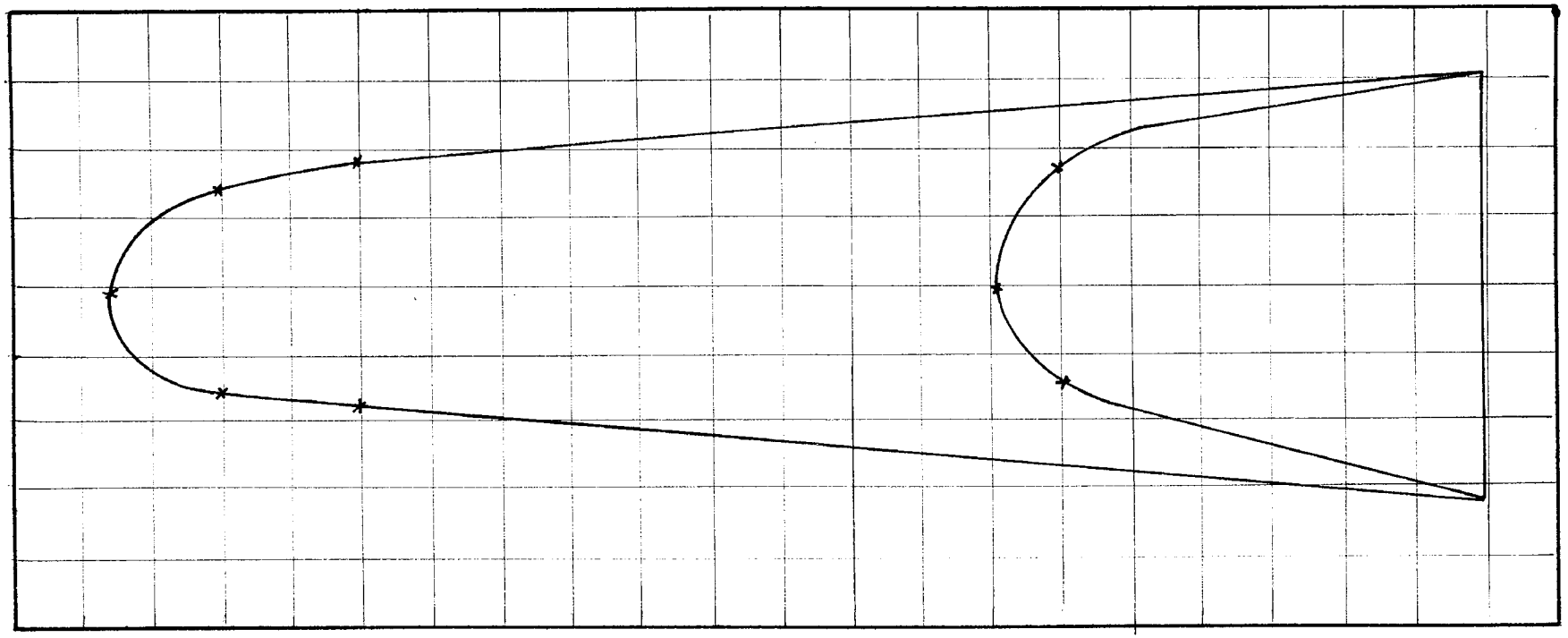

POSITION 2 Scales: Velocity: 1 mm = 1 mm/s Area under Velocity Curve = 3,300 mm^2

Momentum: 1 mm^2 = $\frac{1}{25}$ kgmm/s Area under Momentum Curve = 9,500 mm^2

BED MATERIAL: $1\frac{1}{2}$ mm Diameter Sand

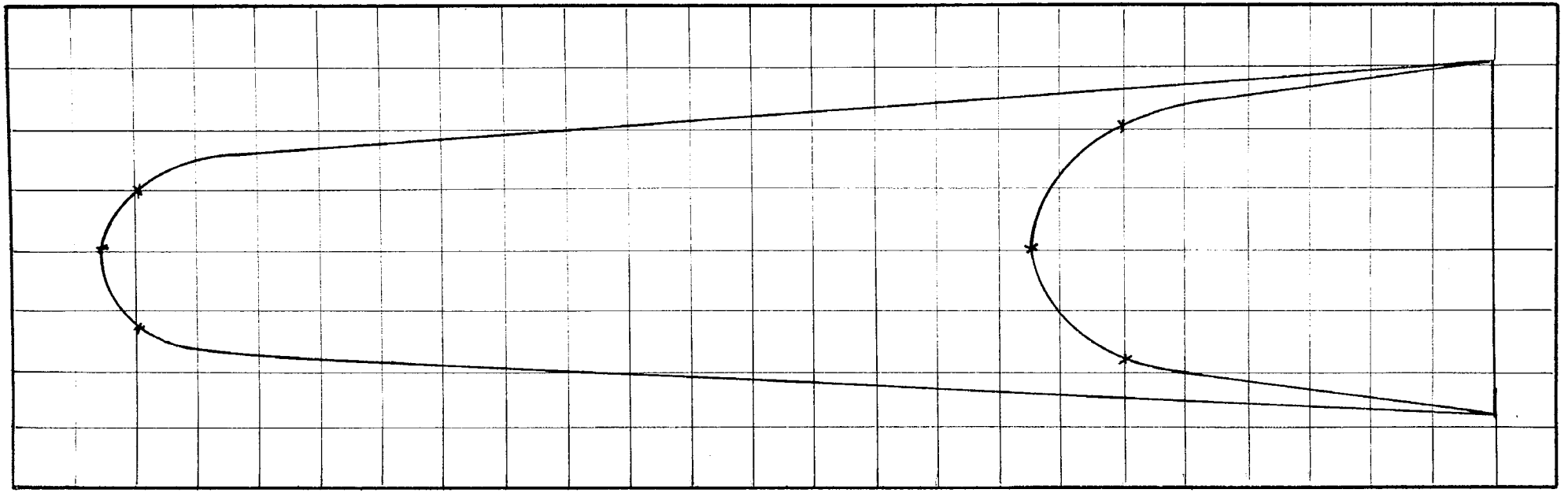

POSITION 3 Scales: Velocity: 1 mm = 1 mm/s Area under Velocity Curve = 3,500 mm^2

Momentum: 1 mm^2 = $\frac{1}{25}$ kgmm/s Area under Momentum Curve = 9,800 mm^2

BED MATERIAL: $1\frac{1}{2}$ mm Diameter Sand

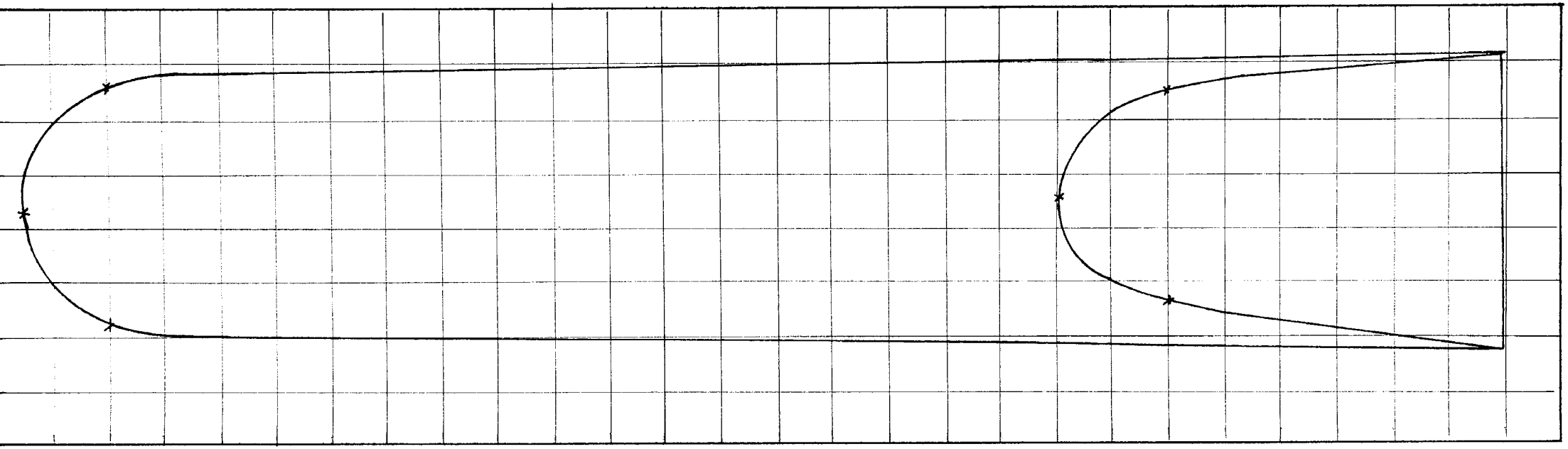

POSITION 4 Scales: Velocity: 1 mm = 1 mm/s Area under Velocity Curve = 3,700 mm^2

Momentum: 1 mm^2 = $\frac{1}{25}$ kgmm/s Area under Momentum Curve = 10,000 mm^2

BED MATERIAL: $1\frac{1}{2}$ mm Diameter Sand

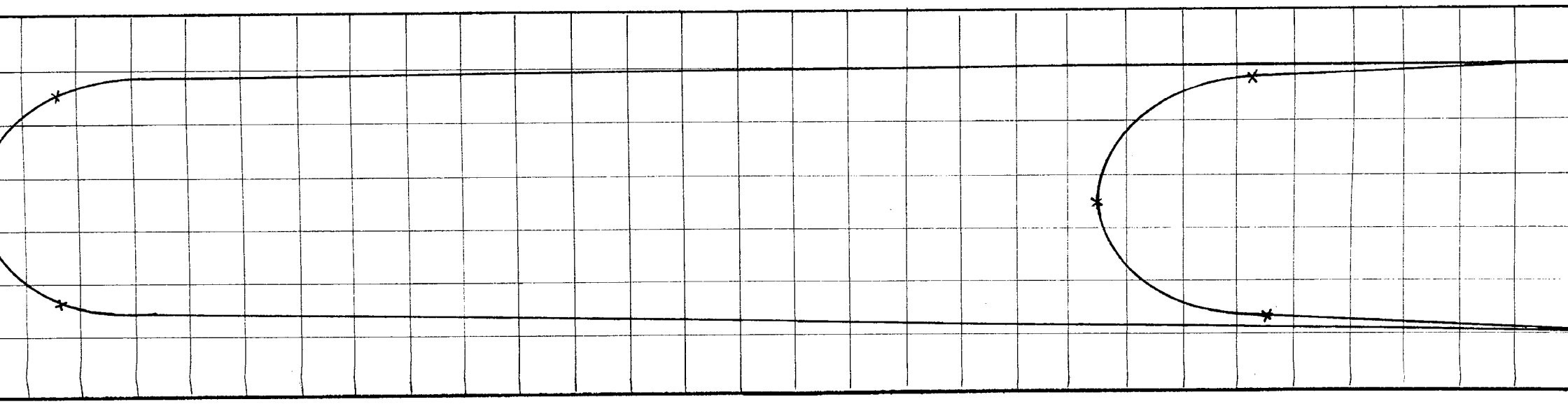

POSITION 5 Scales: Velocity: 1 mm = 1 mm/s Area under Velocity Curve = 4,000 mm^2

Momentum: 1 mm^2 = $\frac{1}{25}$ kgmm/s Area under Momentum Curve = 10,700 mm^2

BED MATERIAL: $1\frac{1}{2}$ mm Diameter Sand

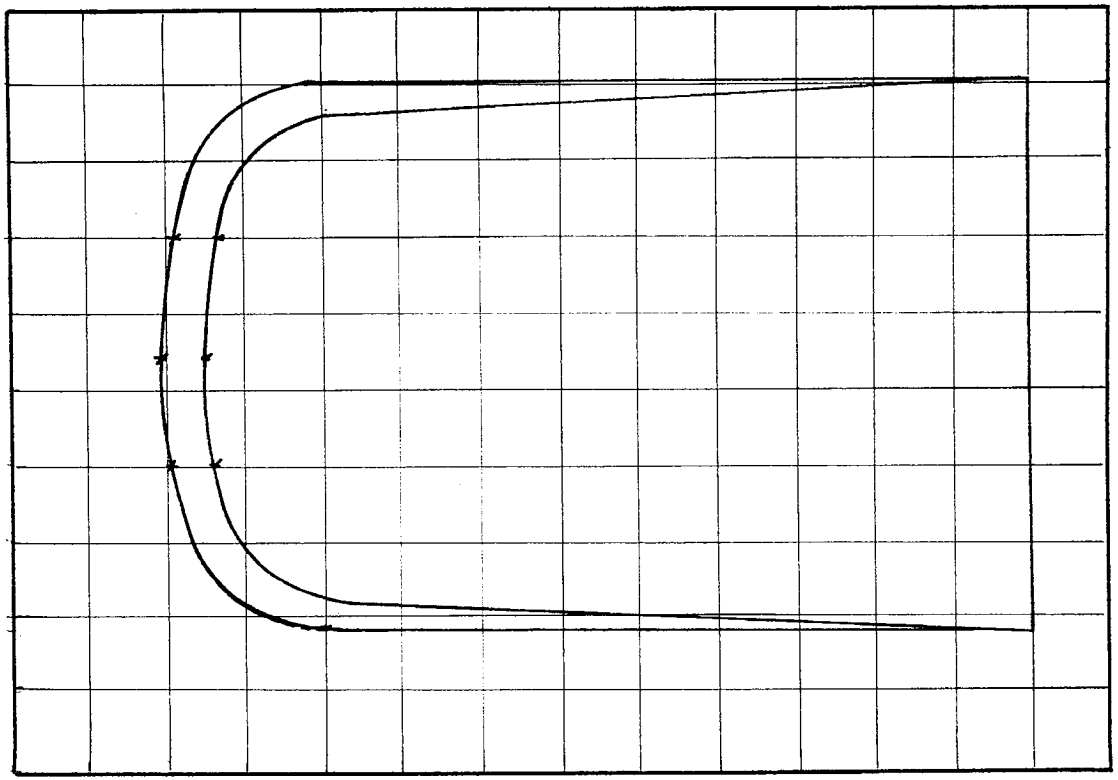

POSITION 1 Scales: Velocity: 1 mm = 1 mm/s Area under Velocity Curve = 6,740 mm^2

Momentum: 1 mm^2 = $\frac{1}{100}$ kgmm/s Area under Momentum Curve = 7,620 mm^2

BED MATERIAL: $1\frac{1}{5}$ mm Diameter Sand

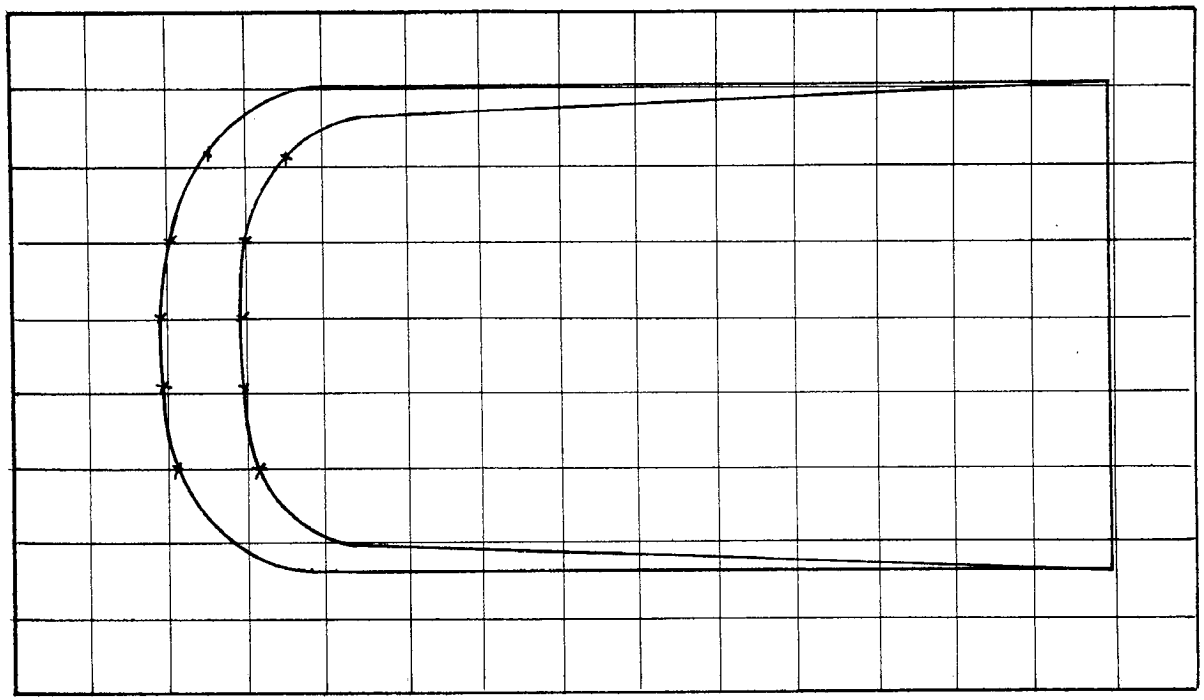

POSITION 2 Scales: Velocity: 1 mm = 1 mm/s Area under Velocity Curve = 6,800 mm^2

Momentum: 1 mm^2 = $\frac{1}{100}$ kgmm/s Area under Momentum Curve = 7,500 mm^2

BED MATERIAL: $1\frac{1}{2}$ mm Diameter Sand

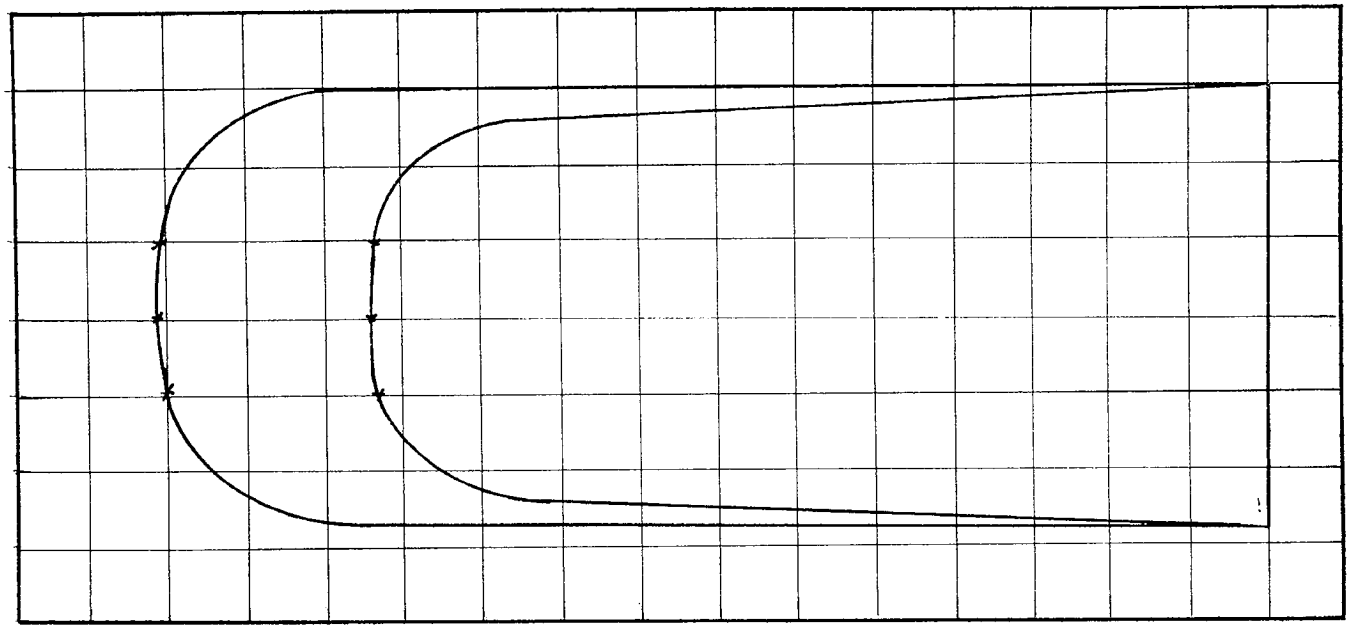

POSITION 3 Scales: Velocity: 1 mm = 1 mm/s Area under Velocity Curve = 6,200 mm^2

Momentum: 1 mm^2 = $\frac{1}{100}$ kgmm/s Area under Momentum Curve = 7,300 mm^2

BED MATERIAL: $1\frac{1}{2}$ mm Diameter Sand

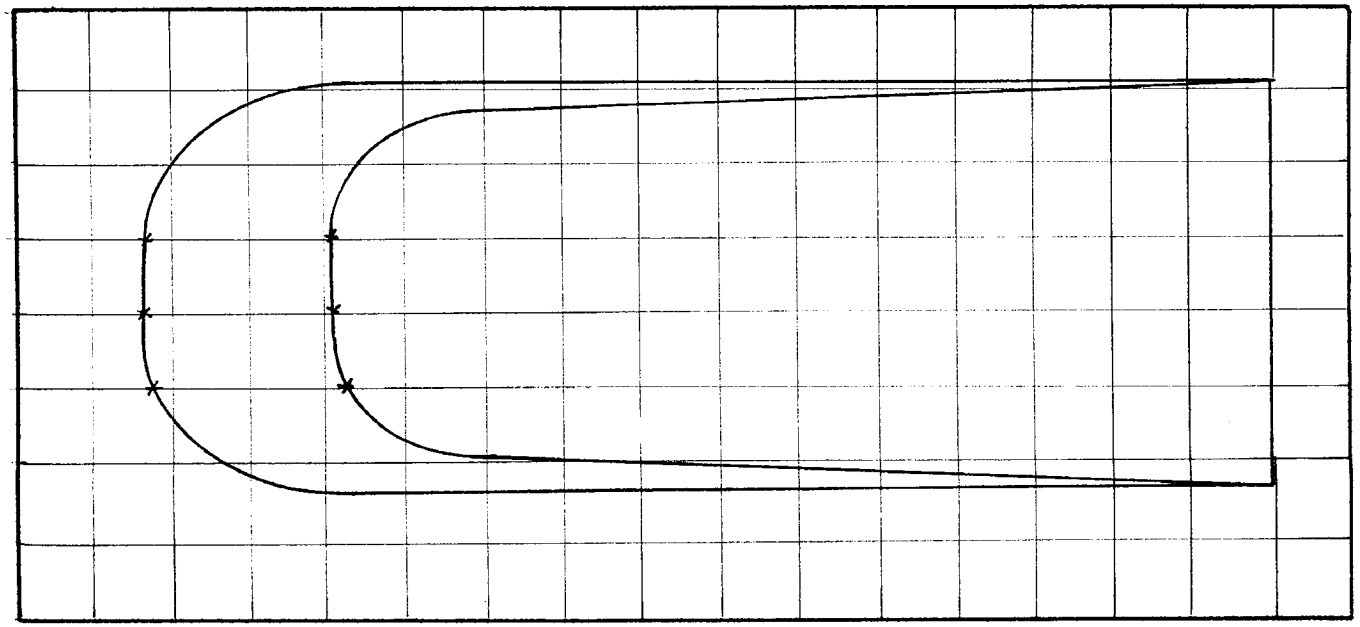

POSITION 4 Scales: Velocity: 1 mm = 1 mm/s Area under Velocity Curve = 6,400 mm^2

Momentum: 1 mm^2 = $\frac{1}{100}$ kgmm/s Area under Momentum Curve = 7,500 mm^2

BED MATERIAL: $1\frac{1}{2}$ mm Diameter Sand

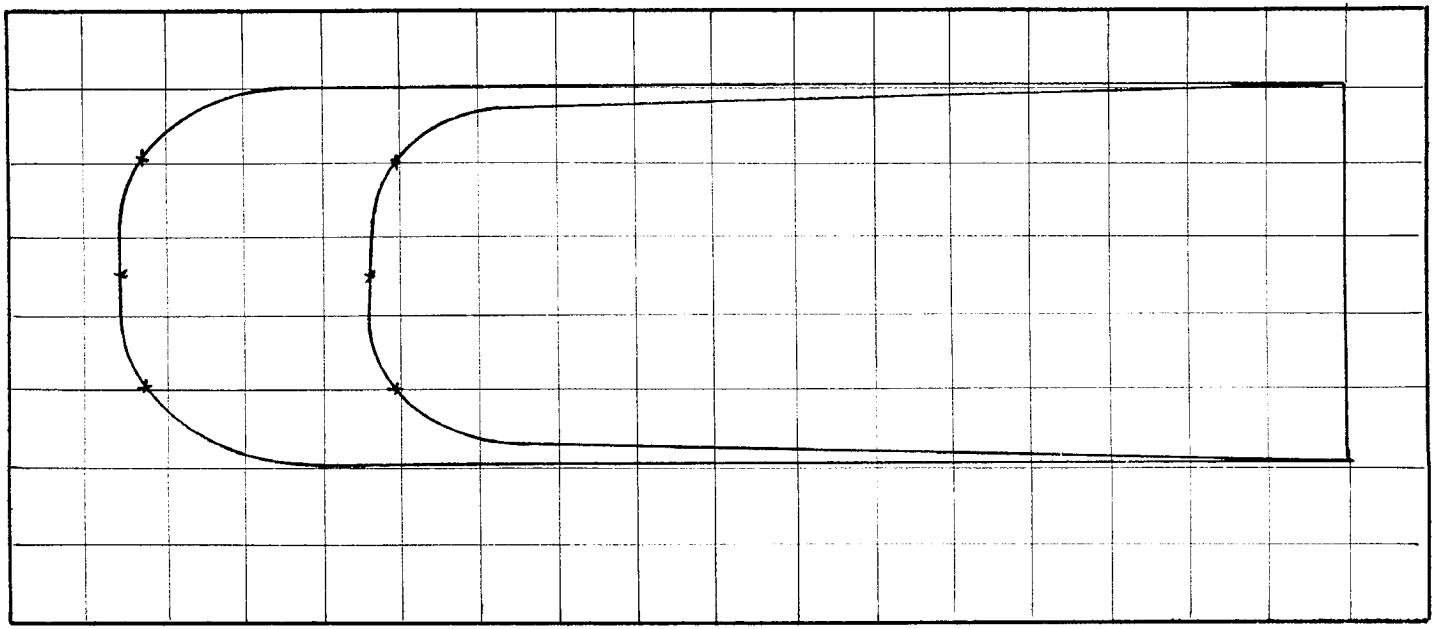

POSITION 5 Scales; Velocity: 1 mm = 1 mm/s Area under Velocity Curve = 6,550 mm^2

Momentum: 1 mm^2 = $\frac{1}{100}$ kgmm/s Area under Momentum Curve = 7,450 mm^2

BED MATERIAL: $1\frac{1}{2}$ mm Diameter Sand

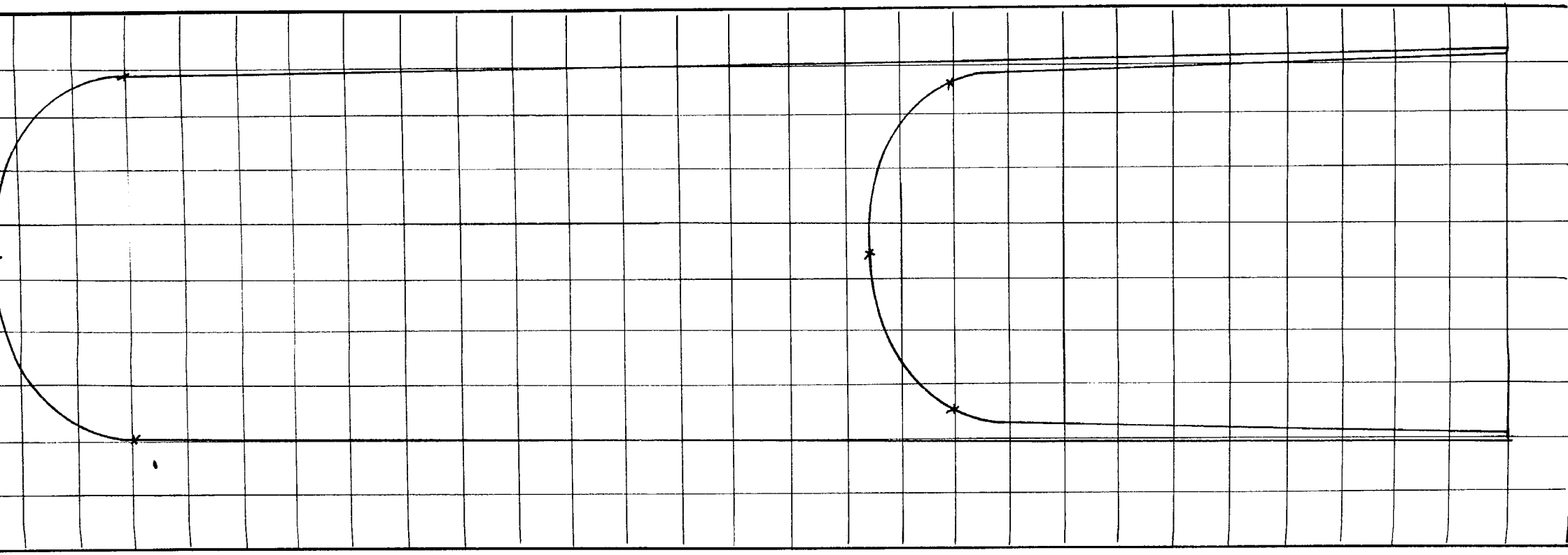

POSITION 1 Scales: Velocity: 1 mm = 1 mm/s Area under Velocity Curve = 8,350 mm^2

Momentum: 1 mm^2 = $\frac{1}{5}$ kgmm/s Area under Momentum Curve = 16,700 mm^2

BED MATERIAL : $1\frac{1}{2}$ mm Diameter Sand

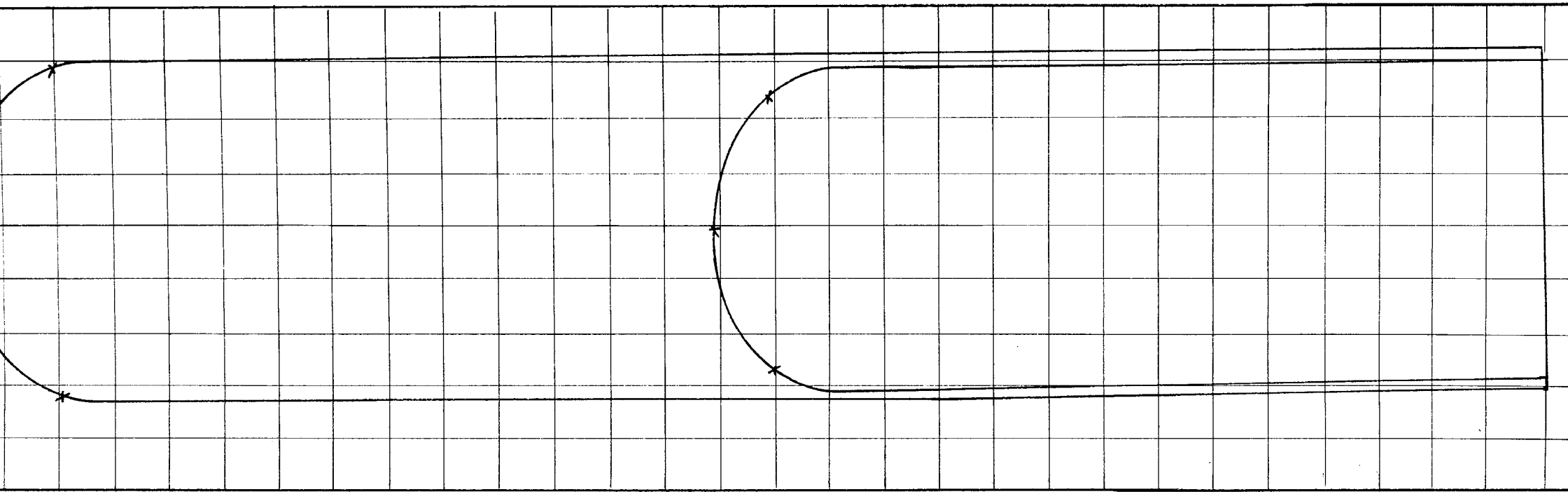

POSITION 2 Scales: Velocity: 1 mm = 1 mm/s Area under Velocity Curve = 8,850 mm^2

Momentum: 1 mm^2 = $\frac{1}{5}$ kgmm/s Area under Momentum Curve = 16,300 mm^2

BED MATERIAL: $1\frac{1}{2}$ mm Diameter Sand

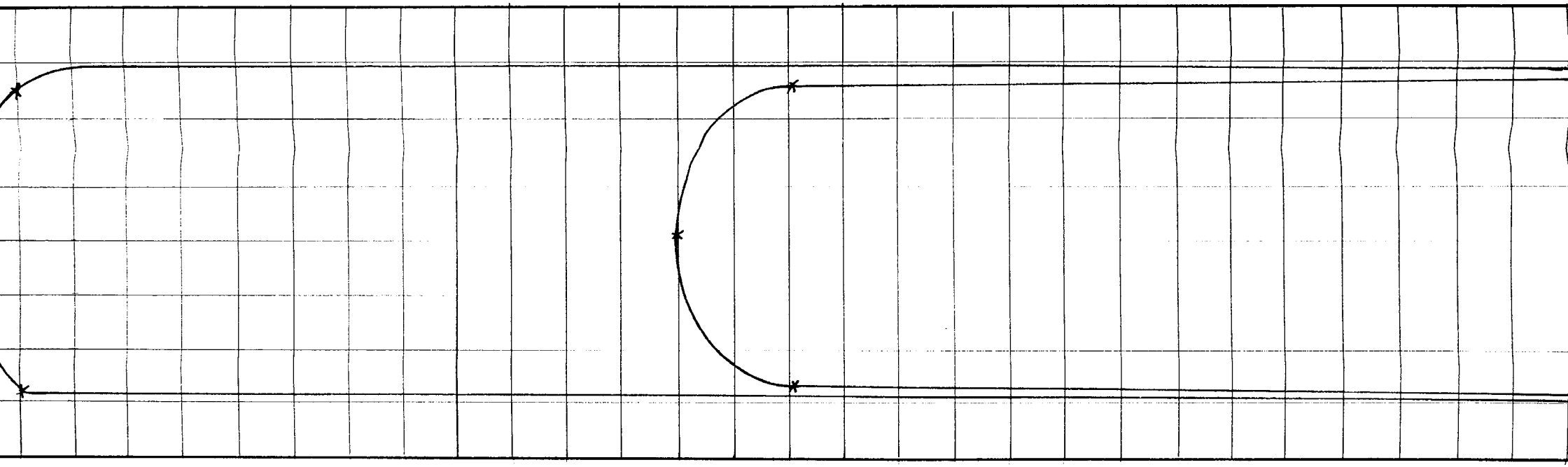

POSITION 3 Scales: Velocity: 1 mm = 1 mm/s Area under Velocity Curve = 8,700 mm^2

Momentum: 1 mm^2 = $\frac{1}{5}$ kgmm/s Area under Momentum Curve = 16,550 mm^2

BED MATERIAL: $1\frac{1}{2}$ mm Diameter Sand

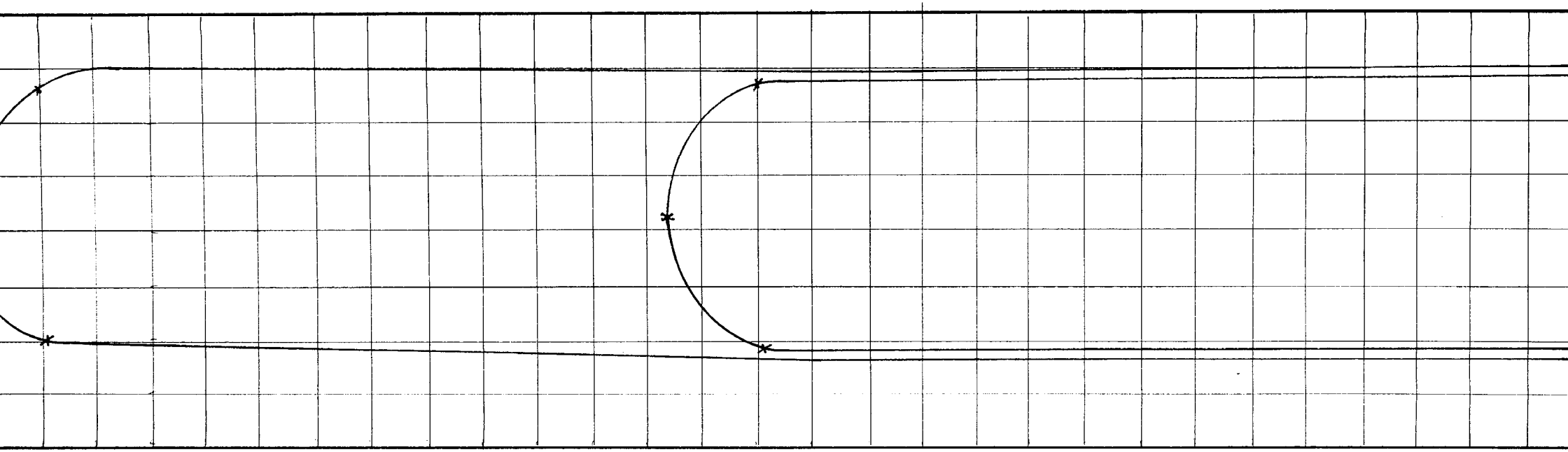

POSITION 4 Scales: Velocity: 1 mm = 1 mm/s Area under Velocity Curve = 8,250 mm^2

Momentum: 1 mm^2 = $\frac{1}{5}$ kgmm/s Area under Momentum Curve = 15,500 mm^2

BED MATERIAL: $1\frac{1}{2}$ mm Diameter Sand

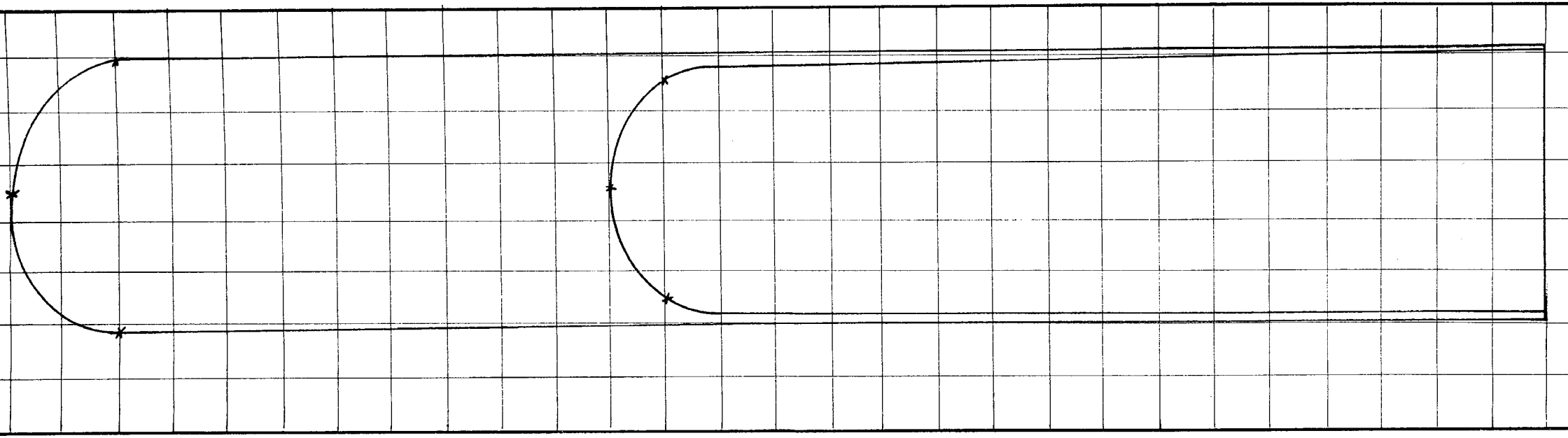

POSITION 5 Scales: Velocity: 1 mm = 1 mm/s Area under Velocity Curve = 3,400 mm^2

Momentum: 1 mm^2 = $\frac{1}{5}$ kgmm/s Area under Momentum Curve = 16,500 mm^2

BED MATERIAL: $1\frac{1}{2}$ mm Diameter Sand

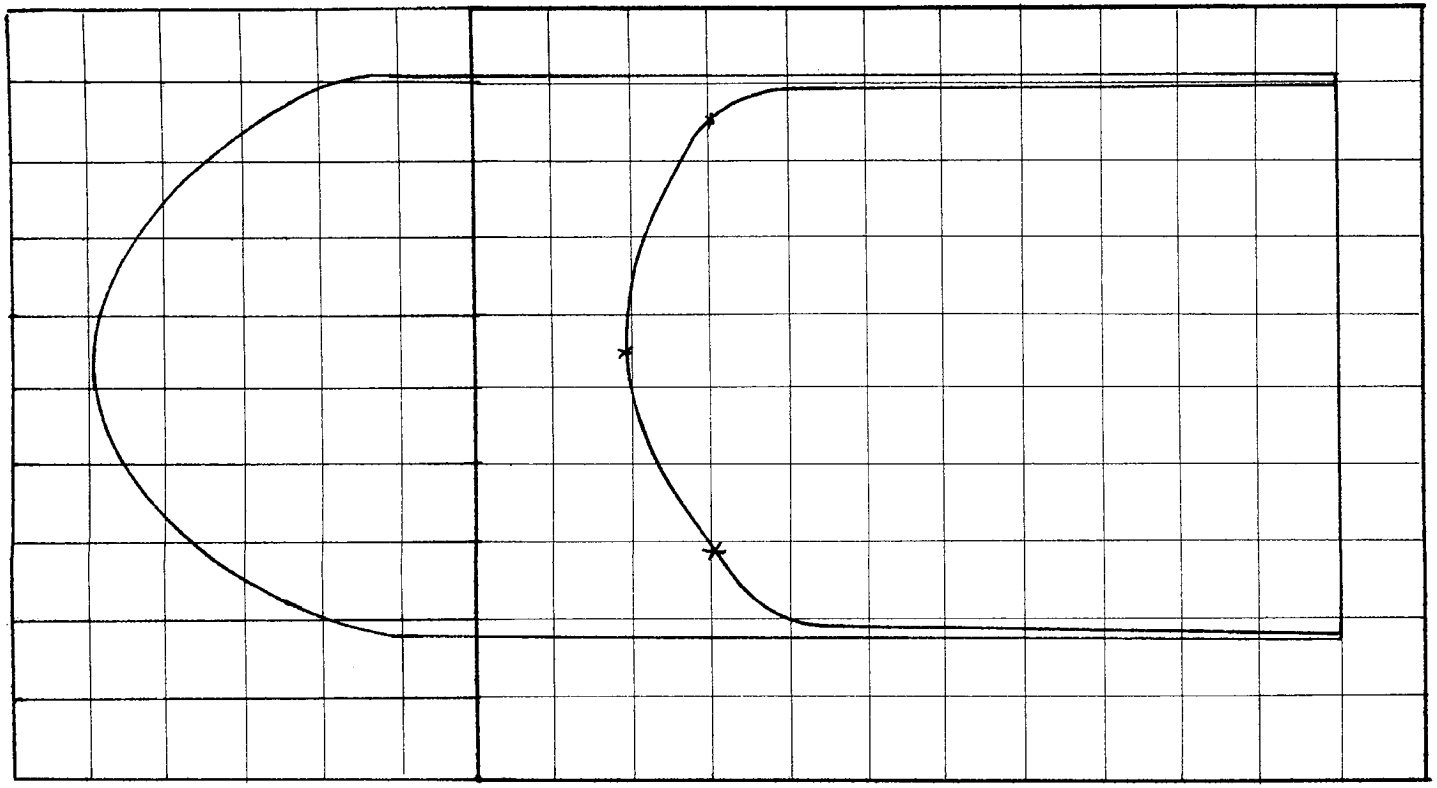

POSITION 1 Scales: Velocity: 1 mm = 1 mm/s Area under Velocity Curve = 5,650 mm^2

Momentum: 1 mm^2 = $\frac{1}{3}$ kgmm/s Area under Momentum Curve = 10,980 mm^2

BED MATERIAL: $1\frac{1}{2}$ mm Diameter Sand

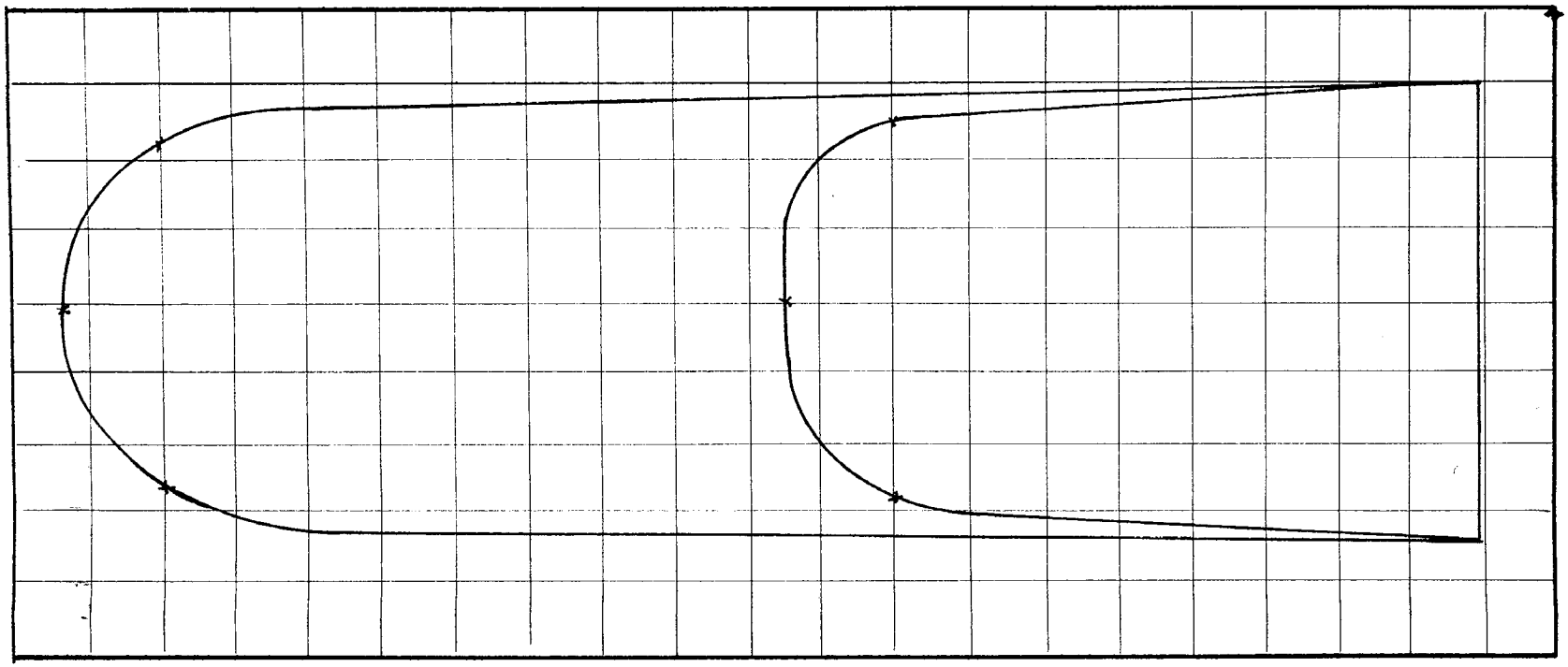

POSITION 2 Scales: Velocity: 1 mm = 1 mm/s Area under Velocity Curve = 5,630 mm^2

Momentum: 1 mm^2 = $\frac{1}{3}$ kgmm/s Area under Momentum Curve = 11,350 mm^2

BED MATERIAL: $1\frac{1}{2}$ mm Diameter Sand

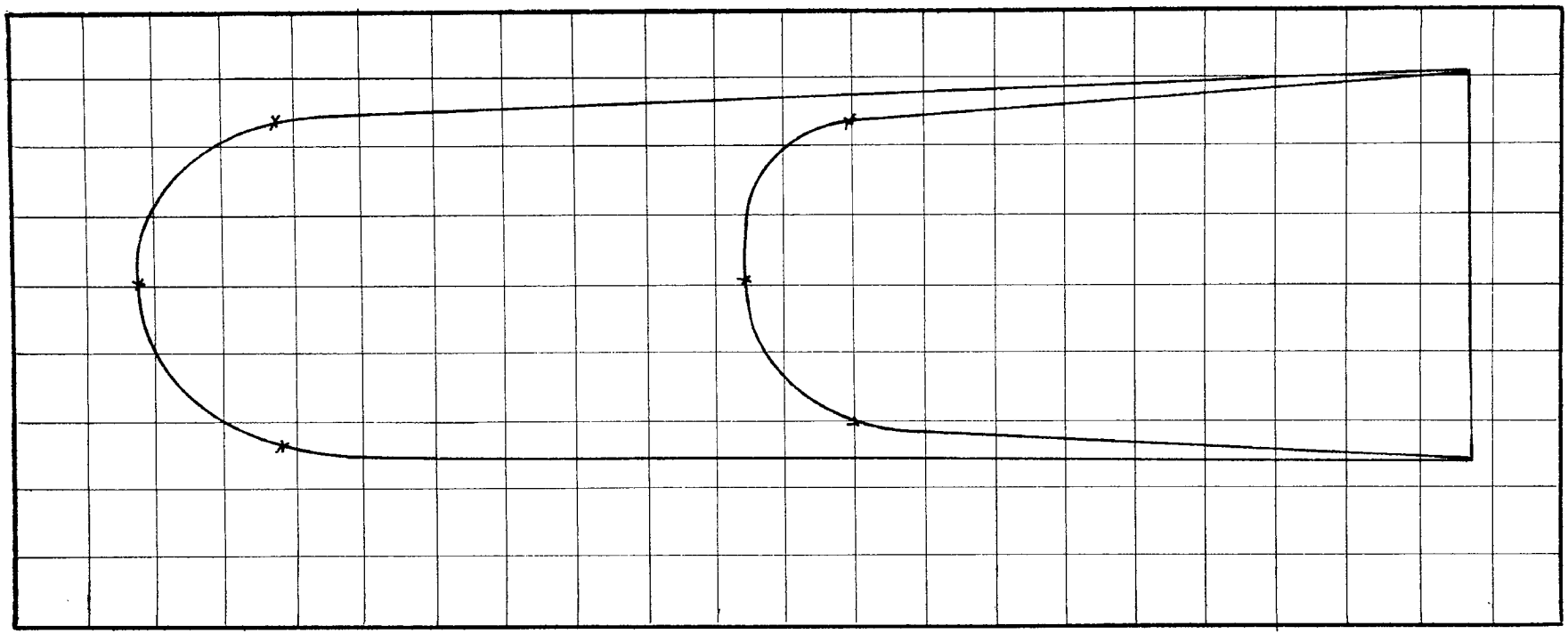

POSITION 3 Scales: Velocity: 1 mm = 1 mm/s Area under Velocity Curve = 5,950 mm^2

Momentum: 1 mm^2 = $\frac{1}{3}$ kgmm/s Area under Momentum Curve = 11,050 mm^2

BED MATERIAL: $1\frac{1}{2}$ mm Diameter Sand

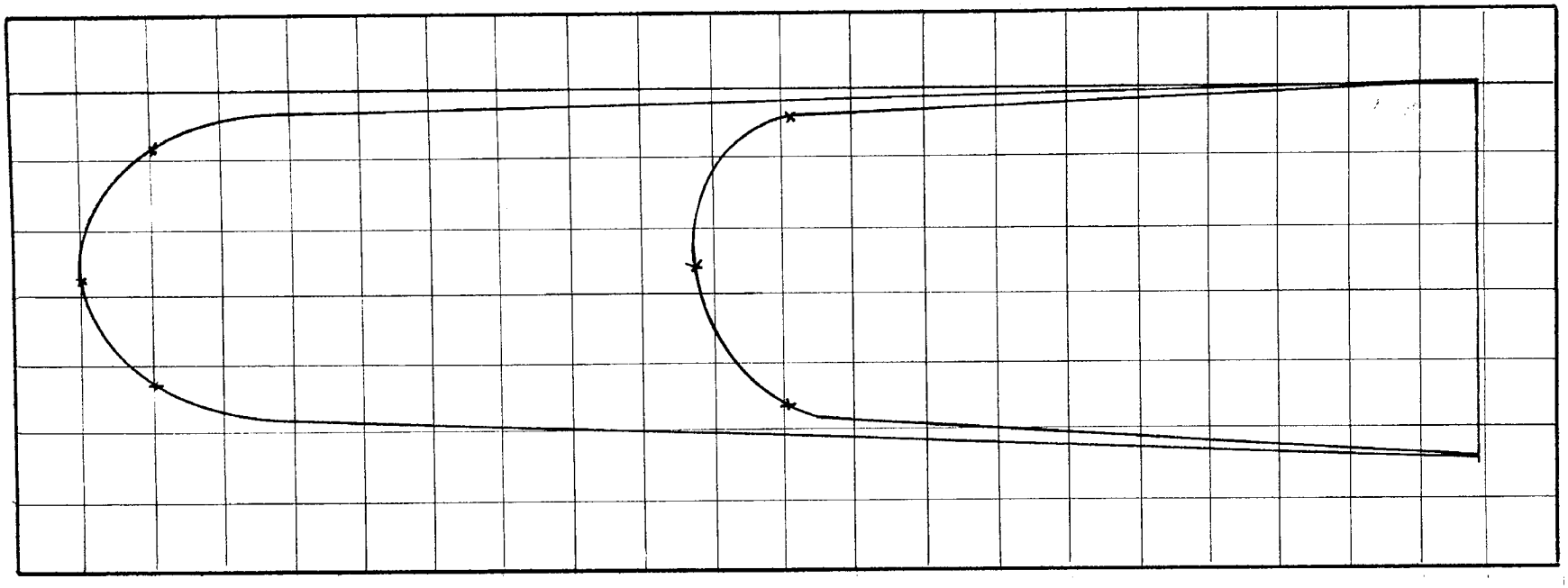

POSITION 4 Scales: Velocity : 1 mm = 1 mm/s Area under Velocity Curve = 5,380 mm^2

Momentum: 1 mm^2 = $\frac{1}{3}$ kgmm/s Area under Momentum Curve = 10,500 mm^2

BED MATERIAL: $1\frac{1}{2}$ mm Diameter Sand

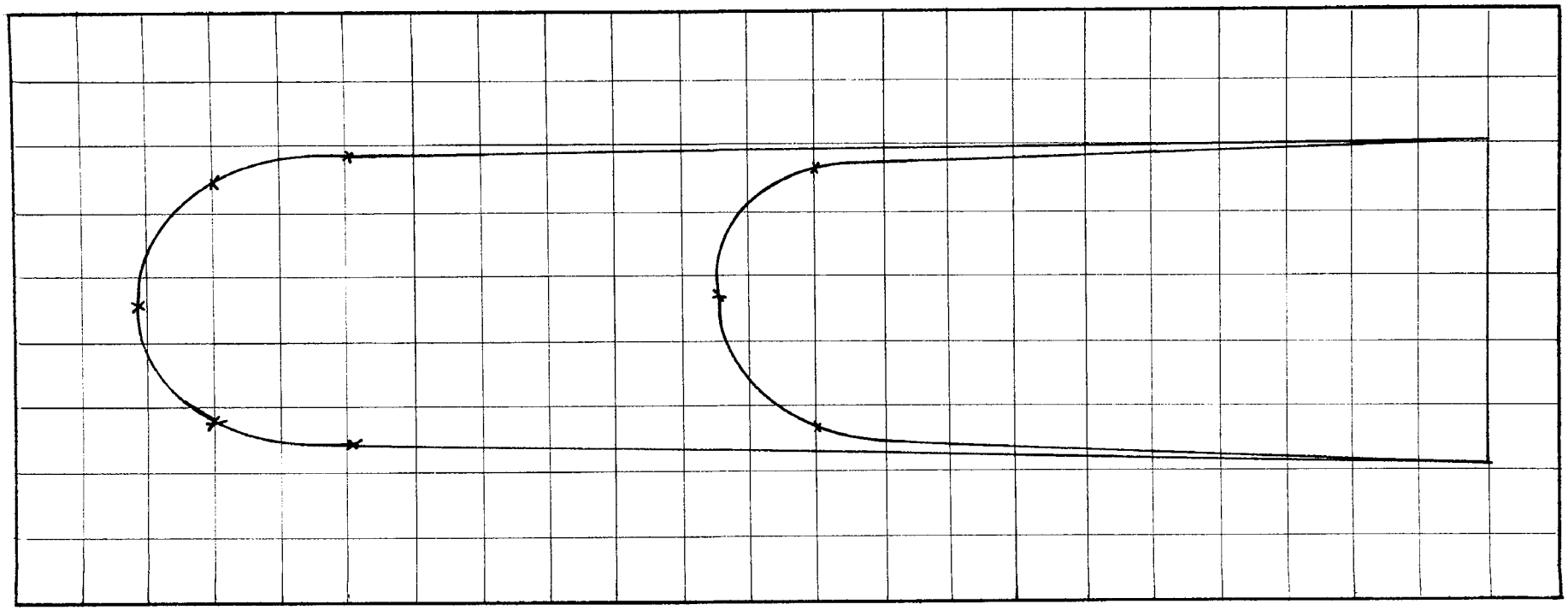

POSITION 5 Scales: Velocity: 1 mm = 1 mm/s Area under Velocity Curve = 5,360 mm^2

Momentum: 1 mm^2 = $\frac{1}{3}$ kgmm/s Area under Momentum Curve = 10,750 mm^2

BED MATERIAL: $1\frac{1}{2}$ mm Diameter Sand

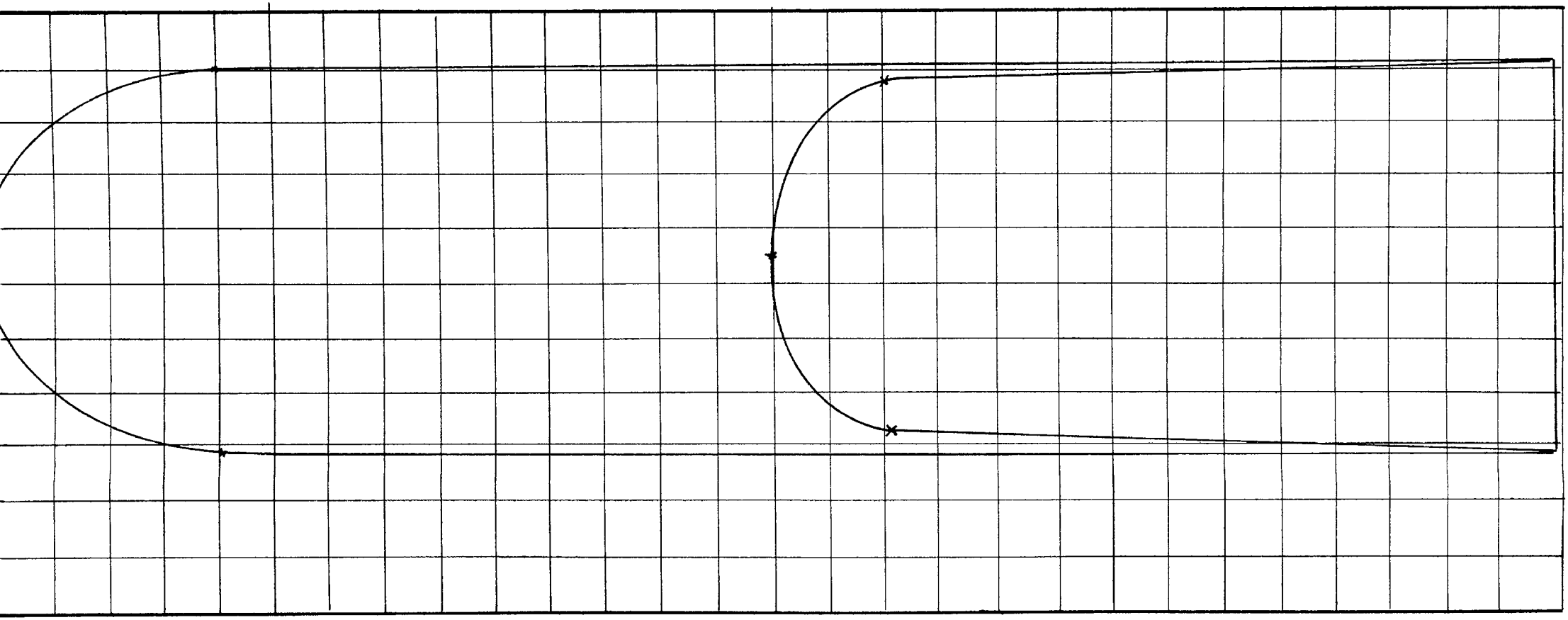

POSITION 1 Scales: Velocity: 1 mm = 1 mm/s Area under Velocity Curve = 8,520 mm^2

Momentum: 1 mm^2 = $\frac{1}{5}$ kgmm/s Area under Momentum Curve = 18,800 mm^2

BED MATERIAL: $1\frac{1}{2}$ mm Diameter Sand

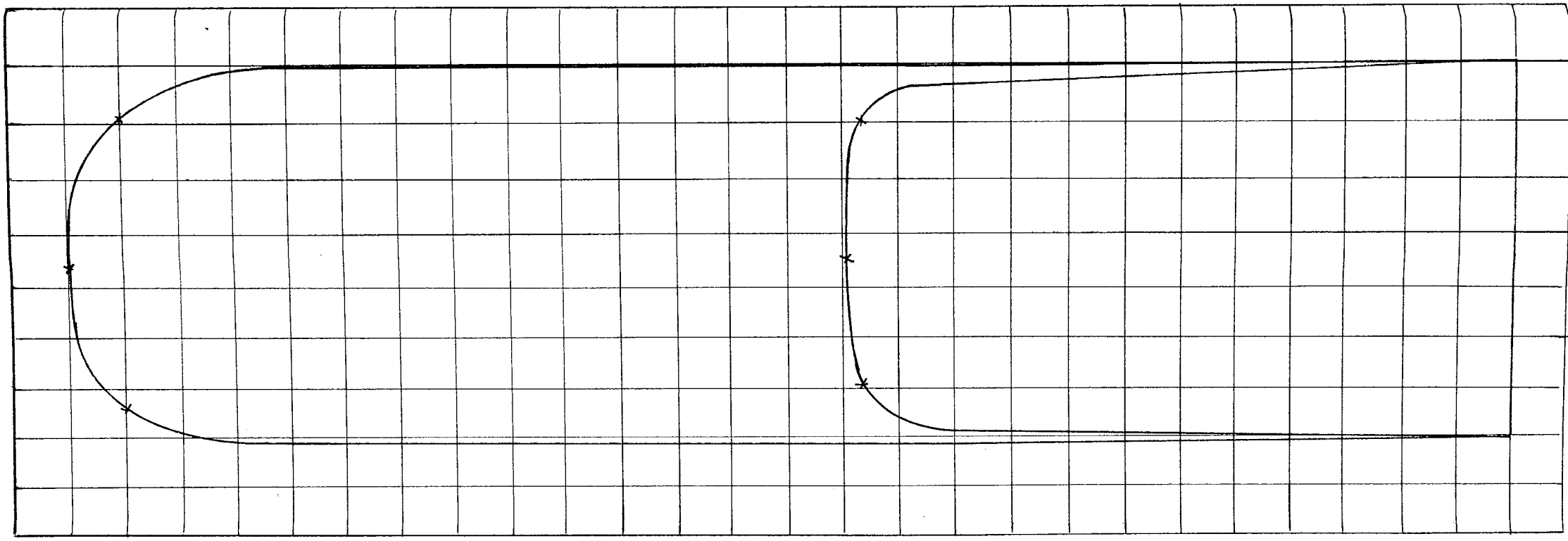

POSITION 2 Scales: Velocity: 1 mm = 1 mm/s Area under Velocity Curve = 8,500 mm^2

Momentum: 1 mm^2 = $\frac{1}{5}$ kgmm/s Area under Momentum Curve = 18,500 mm^2

BED MATERIAL: $1\frac{1}{2}$ mm Diameter Sand

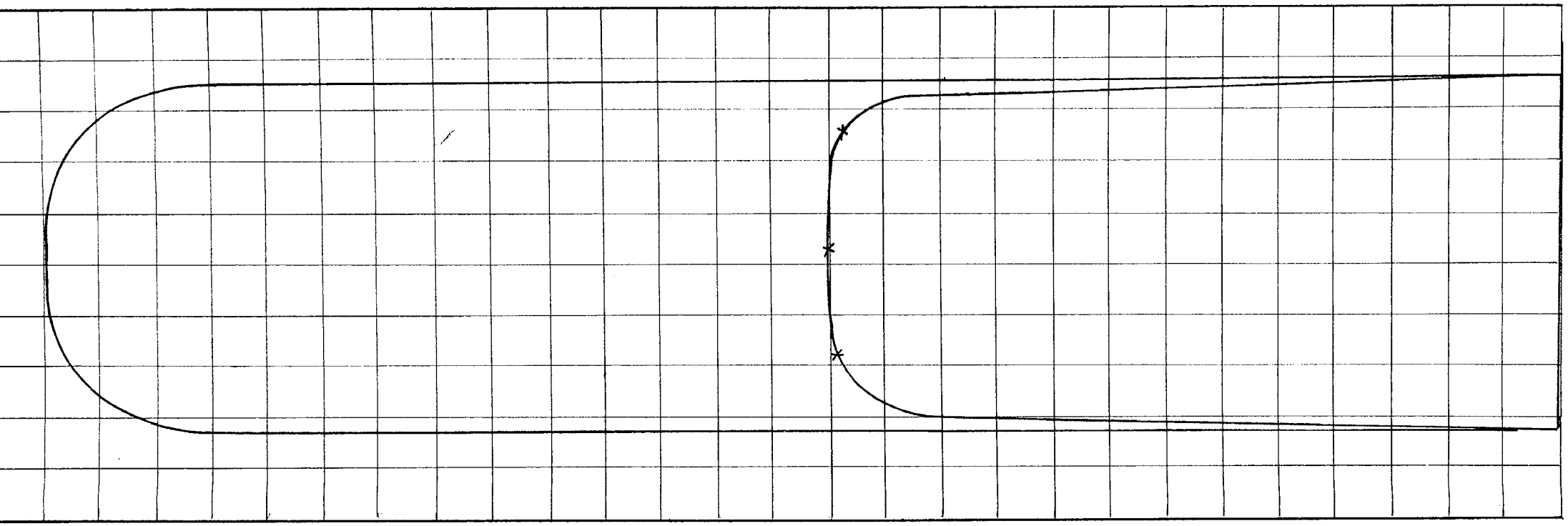

POSITION 3 Scales: Velocity: 1 mm = 1mm/s Area under Velocity Curve = 8,800 mm^2

Momentum: 1 mm^2 = $\frac{1}{5}$ kgmm/s Area under Momentum Curve = 19,000 mm^2

BED MATERIAL: $1\frac{1}{2}$ mm Diameter Sand

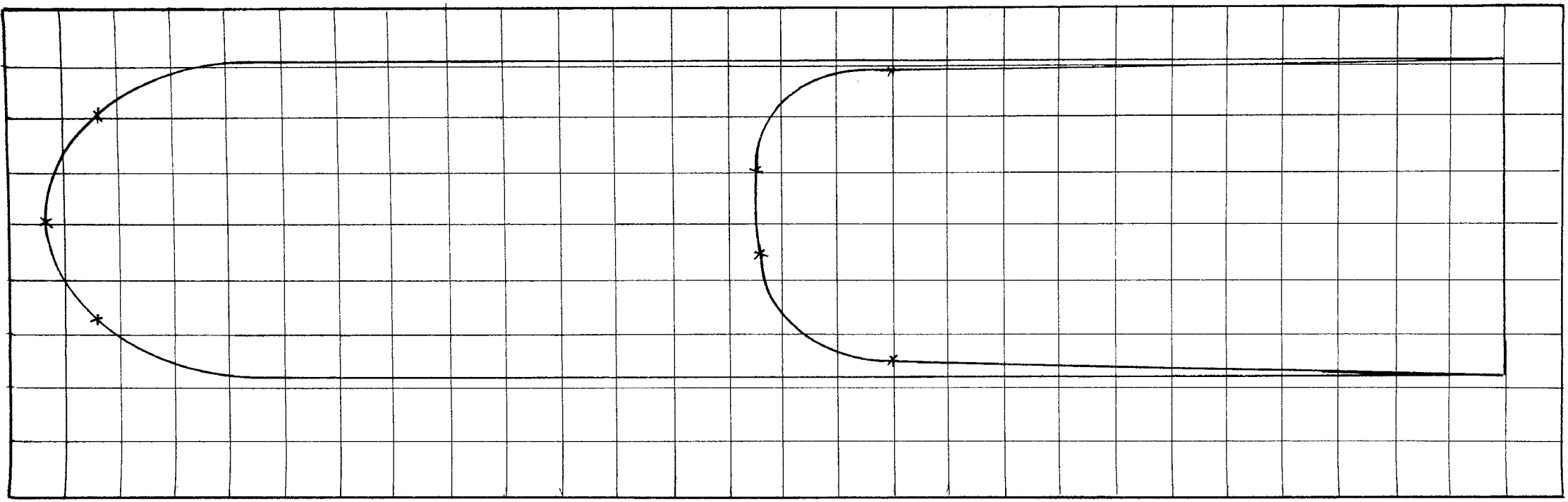

POSITION 4 Scales: Velocity: 1 mm = 1 mm/s Area under Velocity Curve = 8700 mm^2

Momentum: 1 mm^2 = $\frac{1}{5}$ kgmm/s Area under Momentum Curve = 18,500 mm^2

BED MATERIAL: $1\frac{1}{2}$ mm Diameter Sand

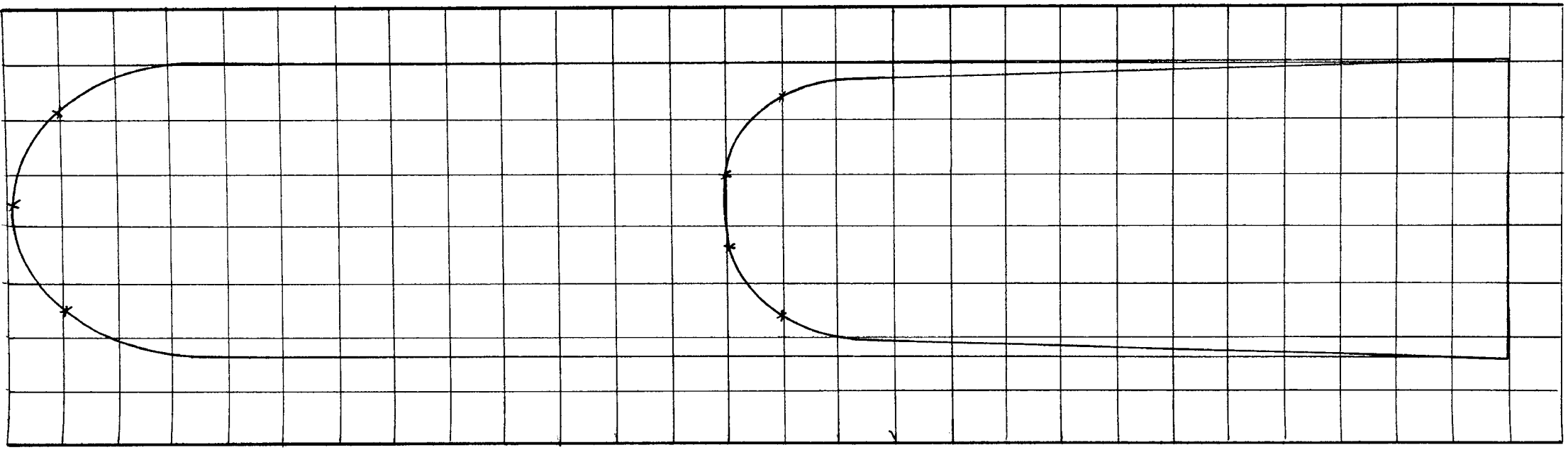

POSITION 5 Scales: Velocity: 1mm = 1 mm/s Area under Velocity Curve = 7,800 mm^2

Momentum: 1 mm^2 = $\frac{1}{5}$ kgmm/s Area under Momentum Curve = 17,700 mm^2

BED MATERIAL: $1\frac{1}{2}$ mm Diameter Sand

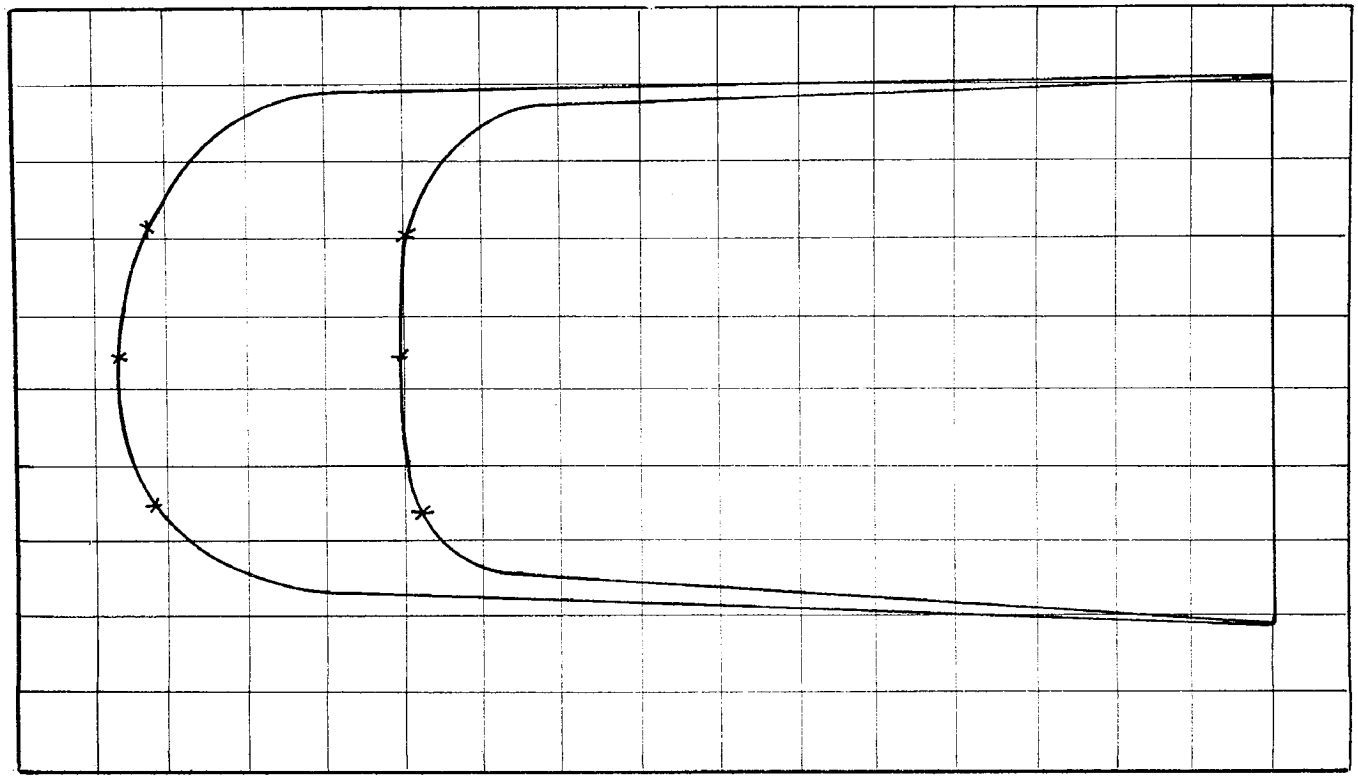

POSITION 1 Scales: Velocity: 1 mm = 1 mm/s Area under Velocity Curve = 6,650 mm^2

Momentum: 1 mm^2 = $\frac{1}{3}$ kgmm/s Area under Momentum Curve = 9,700 mm^2

BED MATERIAL: $1\frac{1}{2}$ mm Diameter Sand

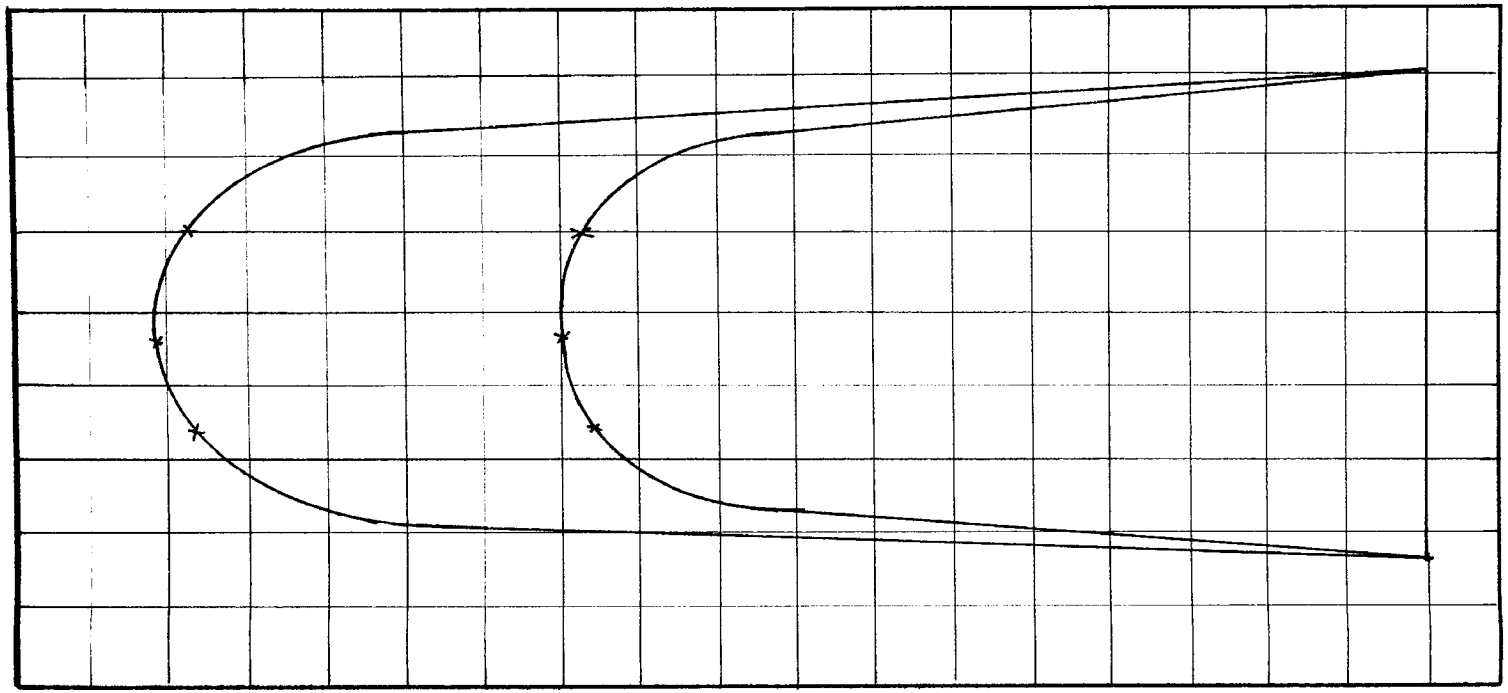

POSITION 2 Scales: Velocity: 1 mm = 1 mm/s Area under Velocity Curve = 6,600 mm^2

Momentum: 1 mm^2 = $\frac{1}{3}$ kgmm/s Area under Momentum Curve = 9,250 mm^2

BED MATERIAL: $1\frac{1}{2}$ mm Diameter Sand

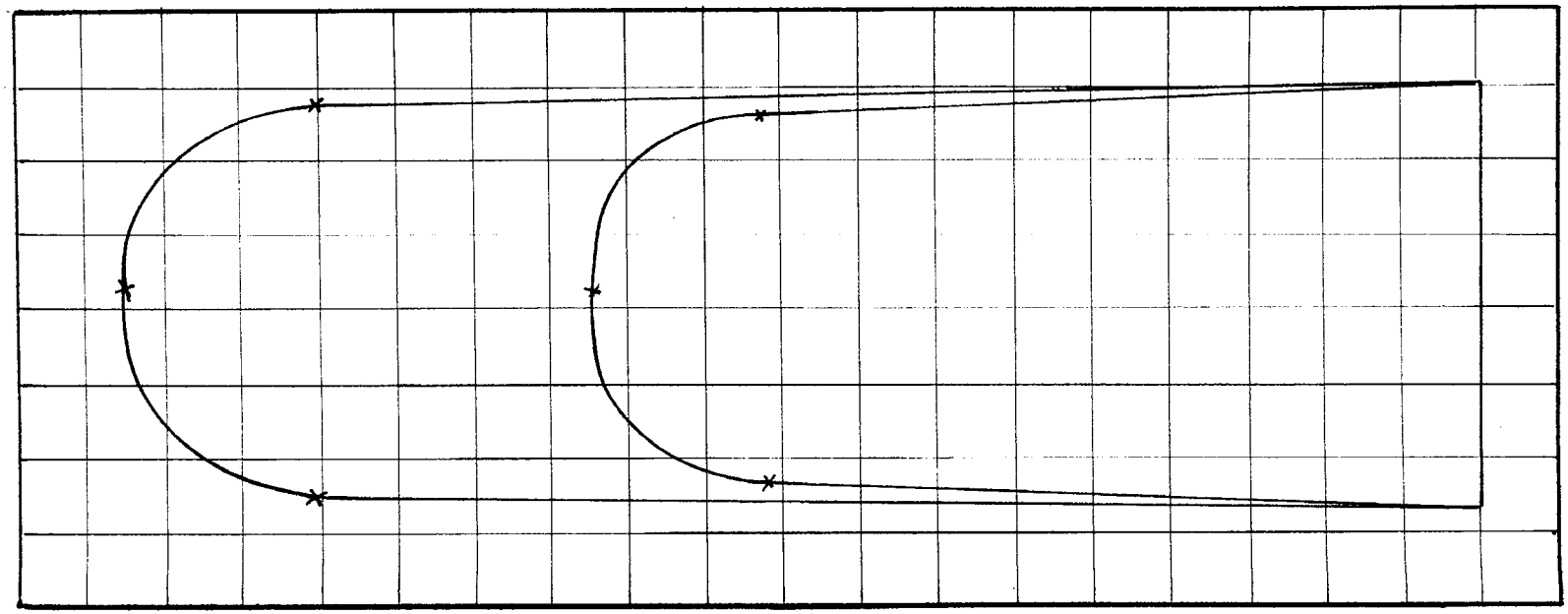

POSITION 3 Scales: Velocity: 1 mm = 1 mm/s Area under Velocity Curve = 6,100 mm^2

Momentum: 1 mm^2 = $\frac{1}{3}$ kgmm/s Area under Momentum Curve = 9,180 mm^2

BED MATERIAL: $1\frac{1}{2}$ mm Diameter Sand

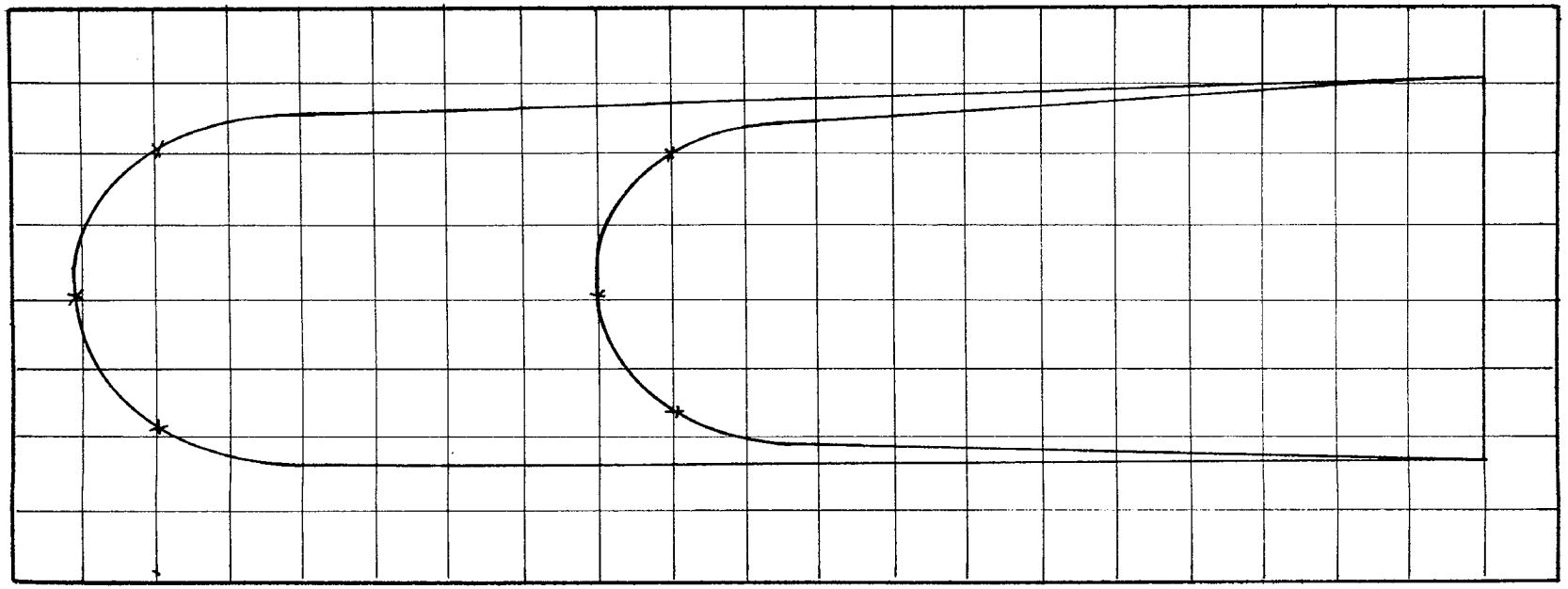

POSITION 4 Scales: Velocity: 1 mm = 1 mm/s Area under Velocity Curve = 6,100 mm^2

Momentum: 1 mm^2 = $\frac{1}{3}$ kgmm/s Area under Momentum Curve = 9,200 mm^2

BED MATERIAL: $1\frac{1}{2}$ mm Diameter Sand

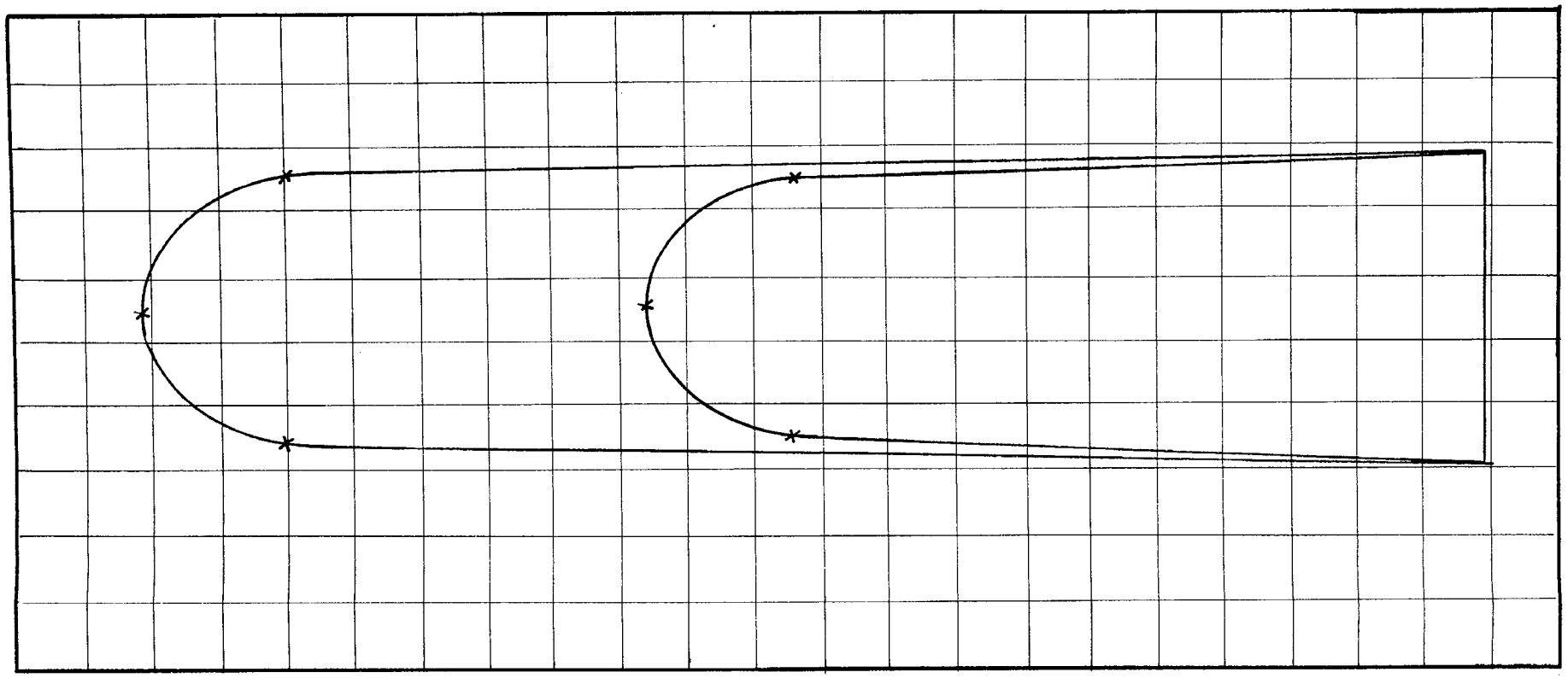

POSITION 5 Scales: Velocity: 1 mm = 1 mm/s Area under Velocity Curve = 5,900 mm^2

Momentum: 1 mm^2 = $\frac{1}{3}$ kgmm/s Area under Momentum Curve = 9,100 mm^2

BED MATERIAL: $1\frac{1}{2}$ mm Diameter Sand

½ mm Diameter Sand

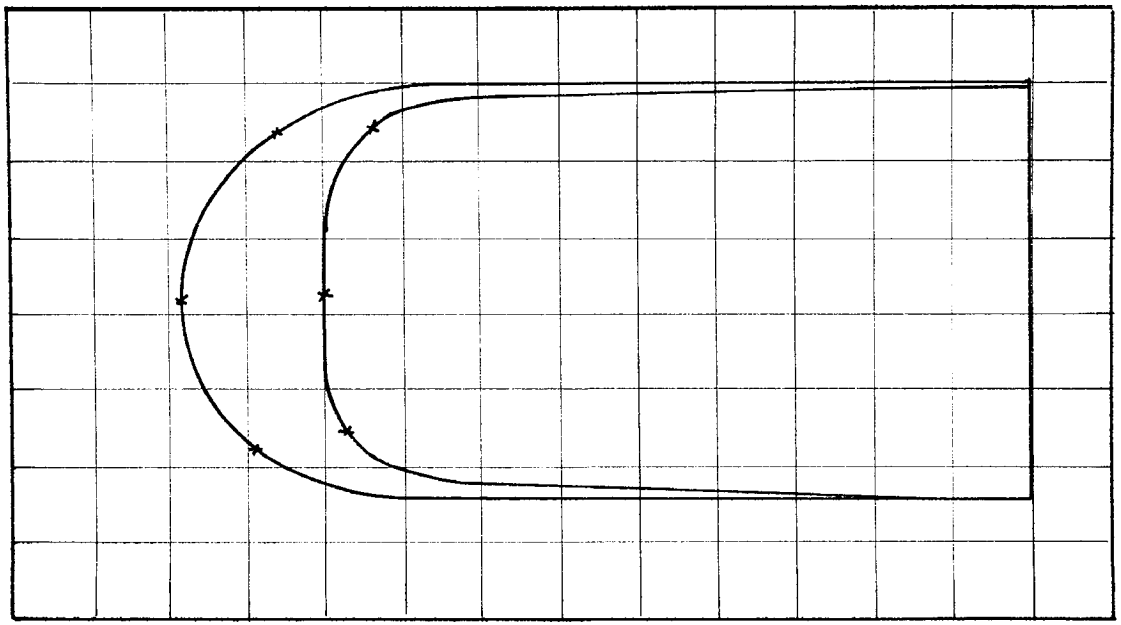

POSITION 1 Scales: - Velocity: = 1 mm = 1 mm/s

Momentum: = 1 mm^2 = $\frac{1}{50}$ kgmm/s

Area under Velocity Curve = 4,550 mm^2

Area under Momentum Curve = 5,550 mm^2

BED MATERIAL: $\frac{1}{2}$ mm Diameter Sand

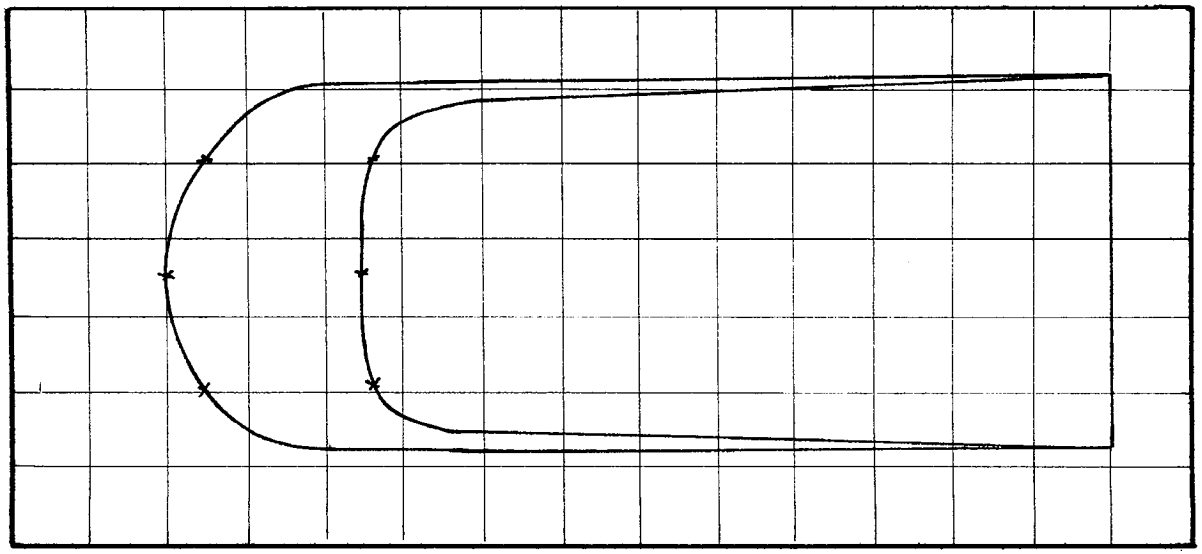

POSITION 2 Scales: - Velocity: = 1 mm = 1 mm/s Area under Velocity Curve = 4,570 mm^2

Momentum: = 1 mm^2 = $\frac{1}{50}$ kgmm/s Area under Momentum Curve = 5,520 mm^2

BED MATERIAL: $\frac{1}{2}$ mm Diameter Sand

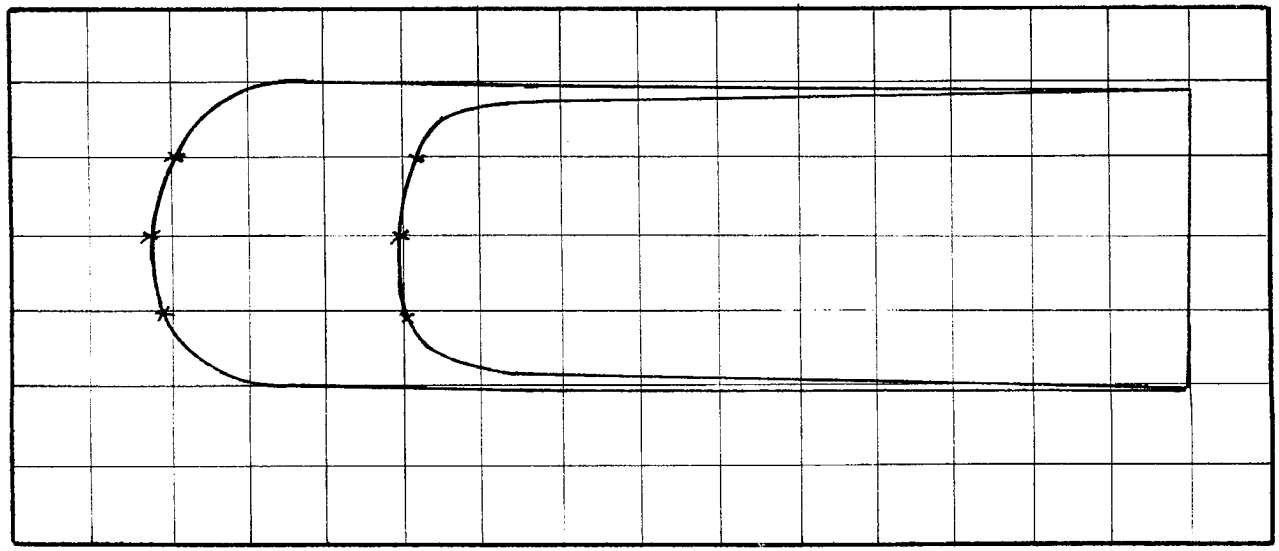

POSITION 3 Scales: – Velocity = 1 mm = 1 mm/s Area under Velocity Curve = 1,250 mm^2

Momentum = 1 mm^2 = $\frac{1}{50}$ kgmm/s Area under Momentum Curve = 5,300 mm^2

BED MATERIAL: $\frac{1}{2}$ mm Diameter Sand

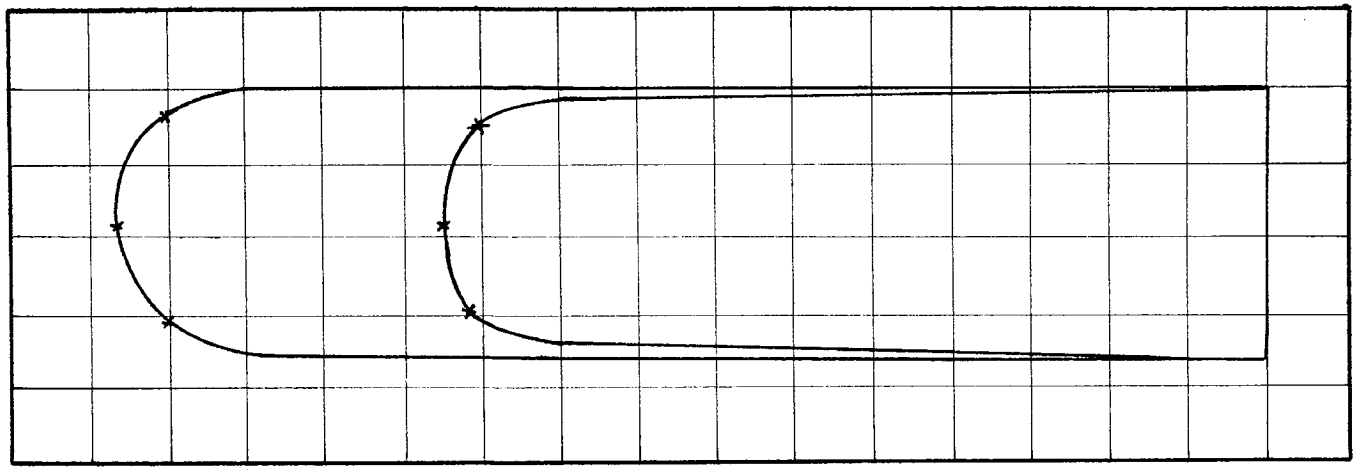

POSITION 4 Scales:- Velocity: = 1 mm = 1 mm/s Area under Velocity Curve = 4,110 mm^2

Momentum: = 1 mm^2 = $\frac{1}{50}$ kgmm/s Area under Momentum Curve = 5,380 mm^2

BED MATERIAL: $\frac{1}{2}$ mm Diameter Sand

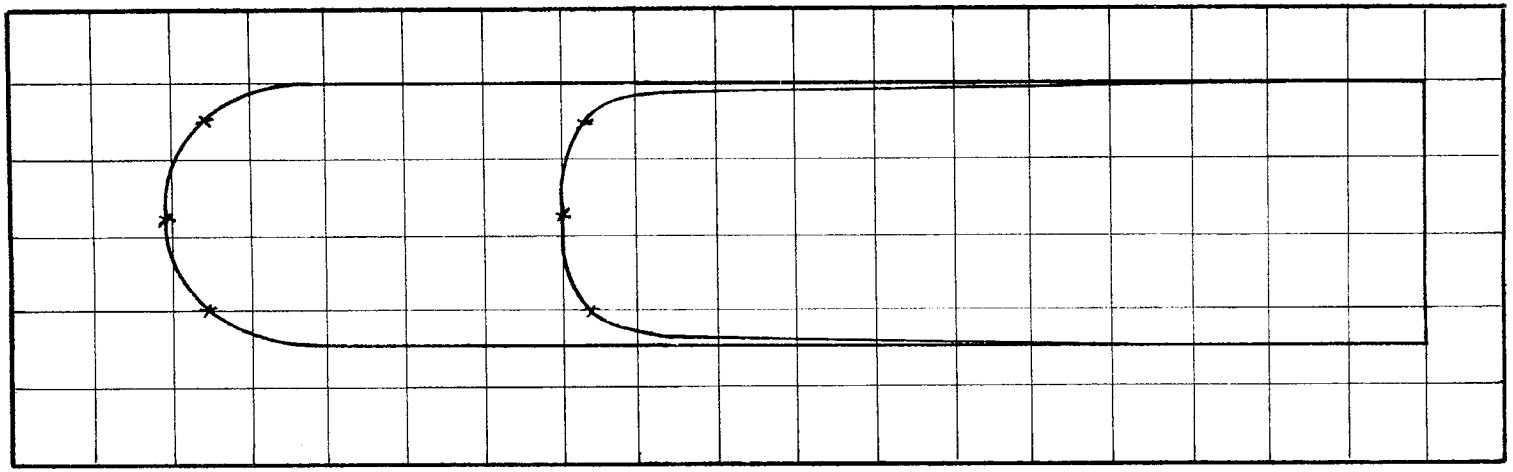

POSITION 5 Scales: – Velocity: = 1 mm = 1 mm/s Area under Velocity Curve = 4,350 mm^2

Momentum: = 1 mm^2 = $\frac{1}{50}$ kgmm/s Area under Momentum Curve = 5,750 mm^2

BED MATERIAL: $\frac{1}{2}$ mm Diameter Sand

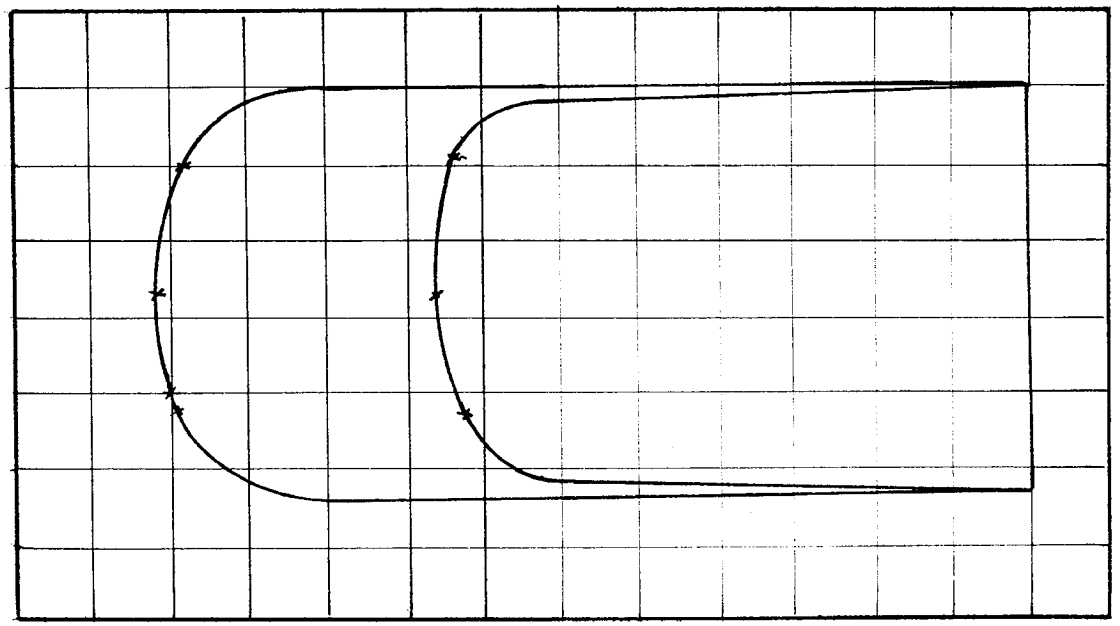

POSITION 1 Scales: Velocity 1 mm = 1 mm/s
Momentum 1 mm^2 = $\frac{1}{50}$ kgmm/s

Area under Velocity Curve = 3910 mm^2
Area under Momentum Curve = 5510 mm^2

BED MATERIAL: $\frac{1}{2}$ mm Diameter Sand

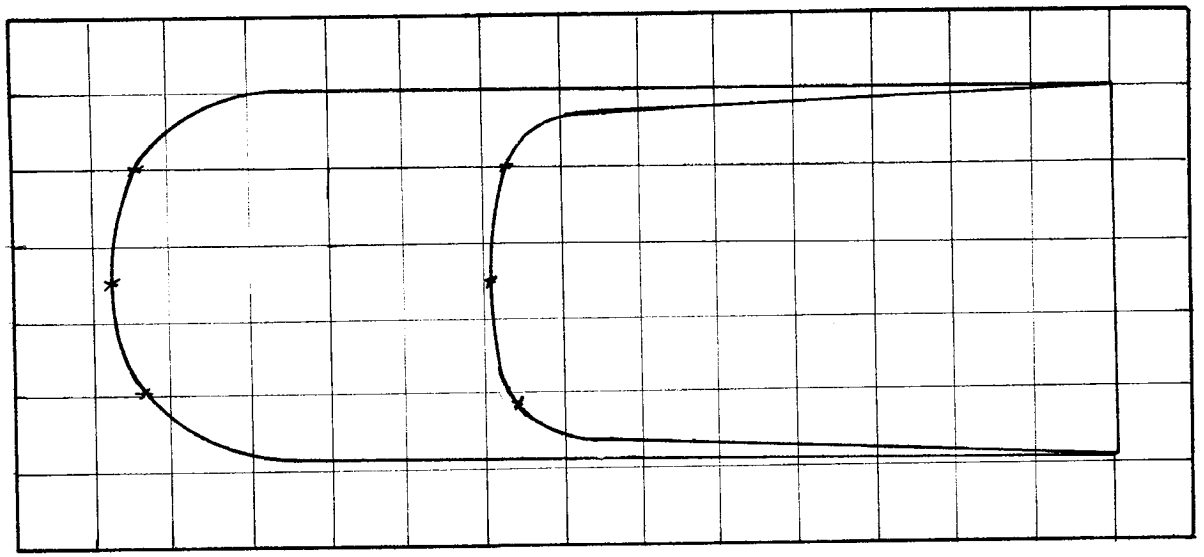

POSITION 2 Scales: Velocity: 1 mm = 1 mm/s

Momentum: 1 mm^2 = $\frac{1}{50}$ kgmm/s

Area under Velocity Curve=3,700 mm^2

Area under Momentum Curve=5,510 mm^2

BED MATERIAL: $\frac{1}{2}$ mm Diameter Sand

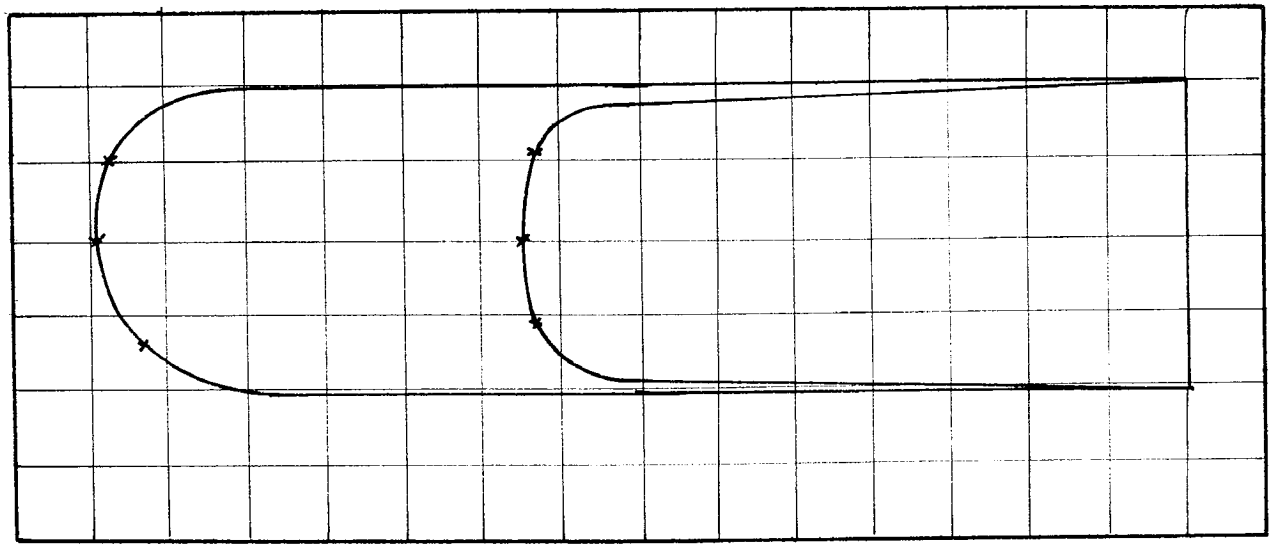

POSITION 3 Scales: Velocity : 1 mm = 1 mm/s Area under Velocity Curve = 3,250 mm^2

Momentum : 1 mm^2 = $\frac{1}{50}$ kgmm/s Area under Momentum Curve = 5,710 mm^2

BED MATERIAL: $\frac{1}{2}$ mm Diameter Sand

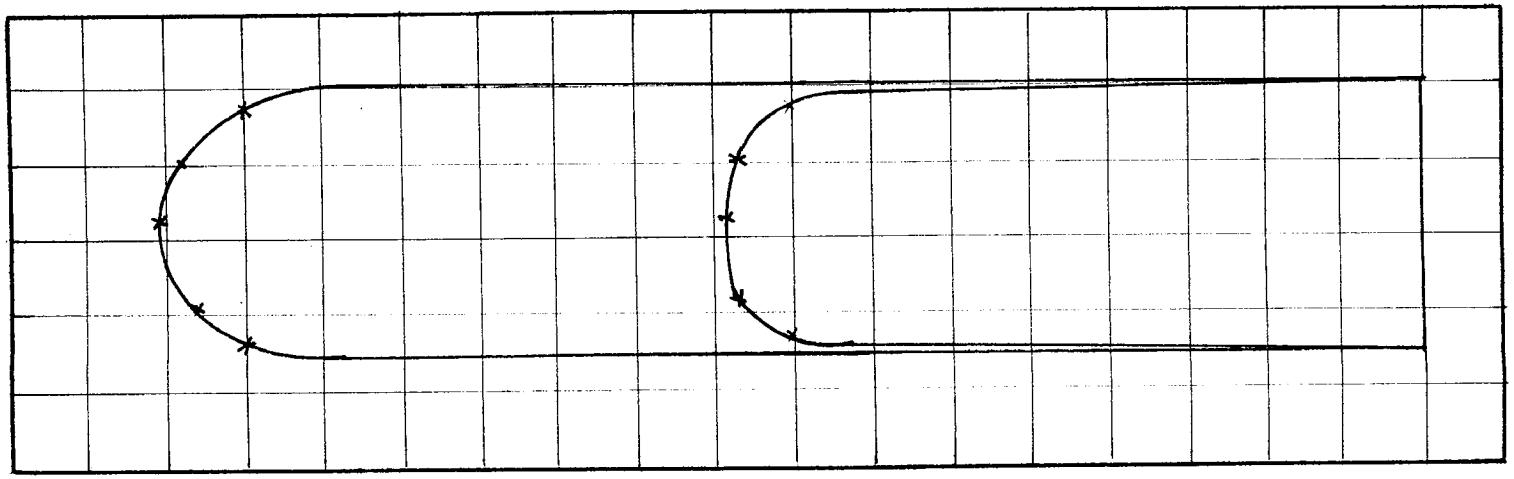

POSITION 4 Scales: Velocity 1 mm = 1 mm/s Area under Velocity Curve = 33,500 mm^2

Momentum 1 mm^2 = $\frac{1}{50}$ kgmm/s Area under Momentum Curve = 5,650 mm^2

BED MATERIAL: $\frac{1}{2}$ mm Diameter Sand

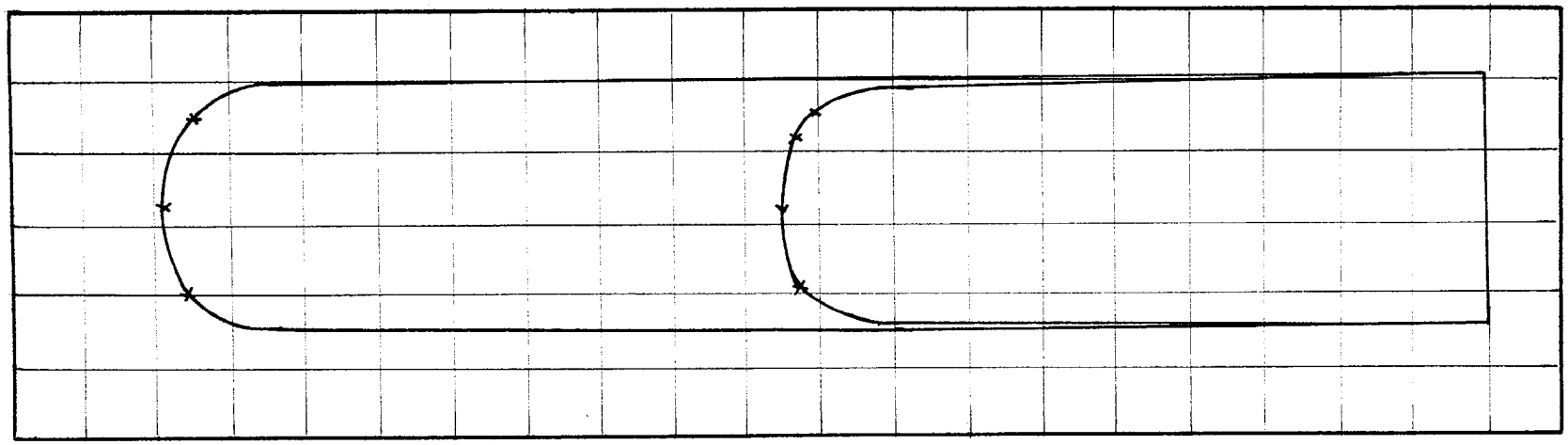

POSITION 5 Scales: Velocity 1 mm = 1 mm/s

Momentum 1 mm^2 = $\frac{1}{50}$ kgmm/s

Area under Velocity Curve = 330 mm^2

Area under Momentum Curve = 6,150 mm^2

BED MATERIAL: $\frac{1}{2}$ mm Diameter Sand

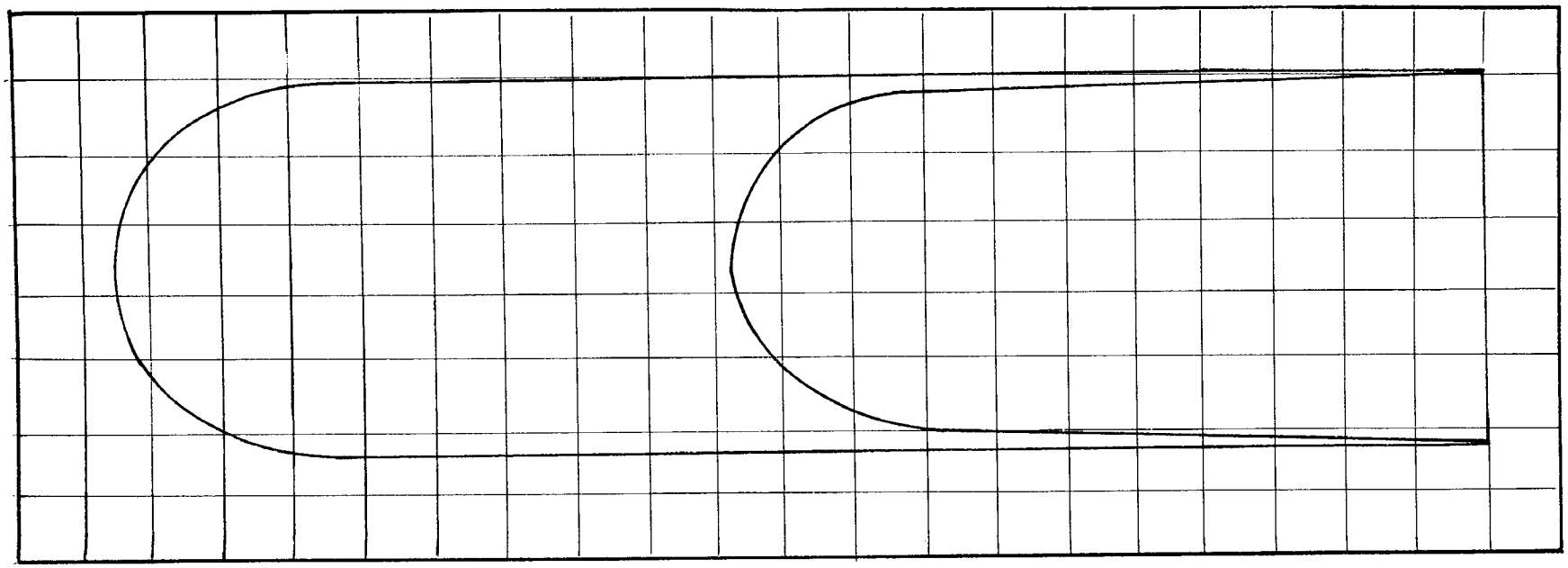

POSITION 1 Scales: Velocity: 1 mm = 1 mm/s

Momentum: 1 mm^2 = $\frac{1}{50}$ kgmm/s

Area under Velocity Curve = 3,500 mm^2

Area under Momentum Curve = 5,400 mm^2

BED MATERIAL: $\frac{1}{2}$ mm Diameter Sand

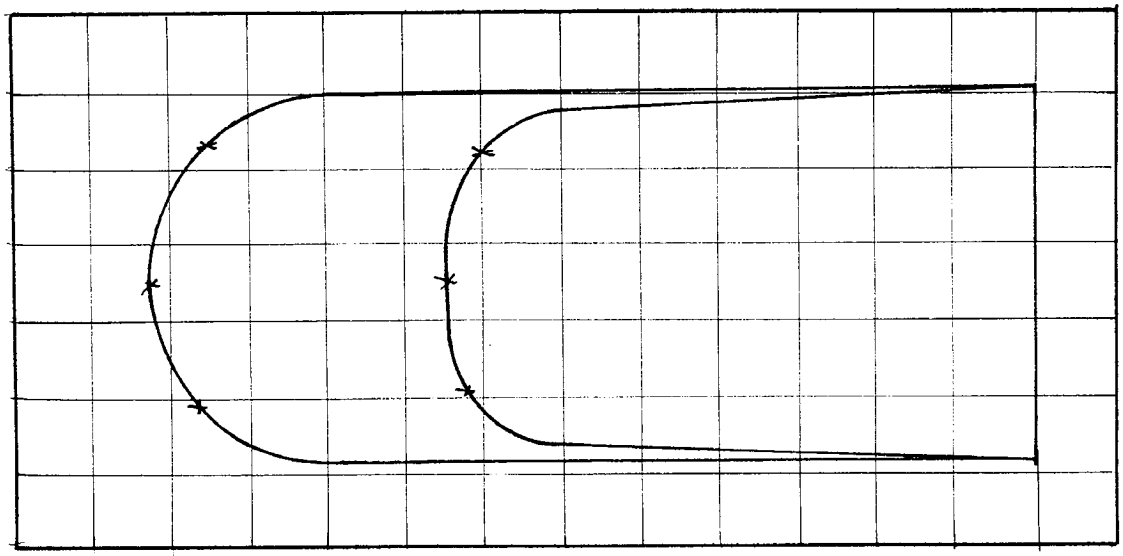

POSITION 2 Scales: Velocity: 1 mm = 1 mm/s Area under Velocity Curve = 3,550 mm^2

Momentum: 1 mm^2 = $\frac{1}{50}$ kgmm/s Area under Momentum Curve = 5,480 mm^2

BED MATERIAL: $\frac{1}{2}$ mm Diameter Sand

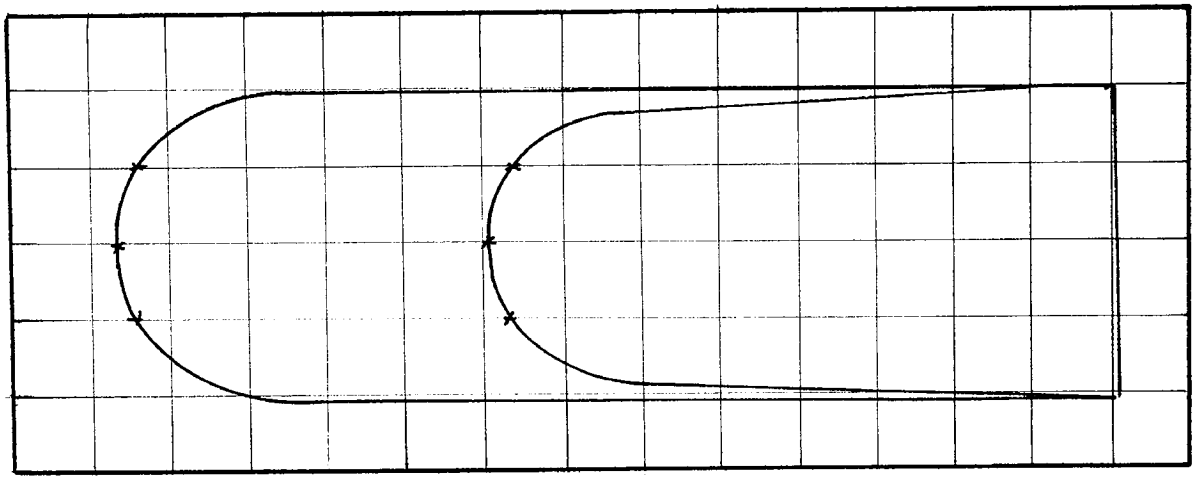

POSITION 3 Scales: Velocity: 1 mm = 1 mm/s Area under Velocity Curve = 3,300 mm^2

Momentum: 1 mm^2 = $\frac{1}{50}$ kgmm/s Area under Momentum Curve = 5,280 mm^2

BED MATERIAL: $\frac{1}{2}$ mm Diameter Sand

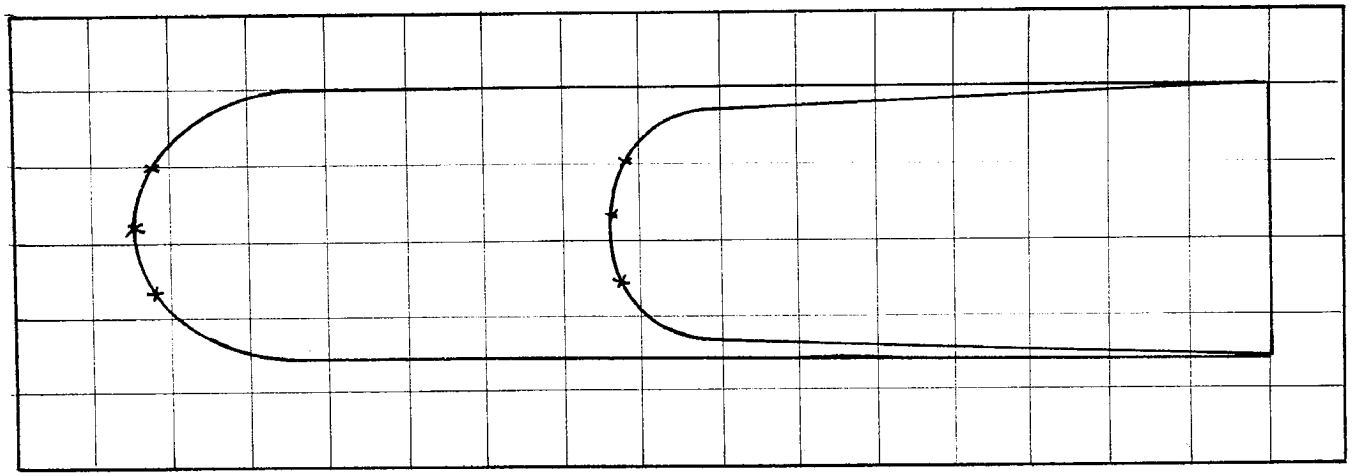

POSITION 4 Scales: Velocity: 1 mm = 1 mm/s

Momentum: 1 mm^2 = $\frac{1}{50}$ kgmm/s

Area under Velocity Curve = 2,750 mm^2

Area under Momentum Curve = 5,400 mm^2

BED MATERIAL: $\frac{1}{2}$ mm Diameter Sand

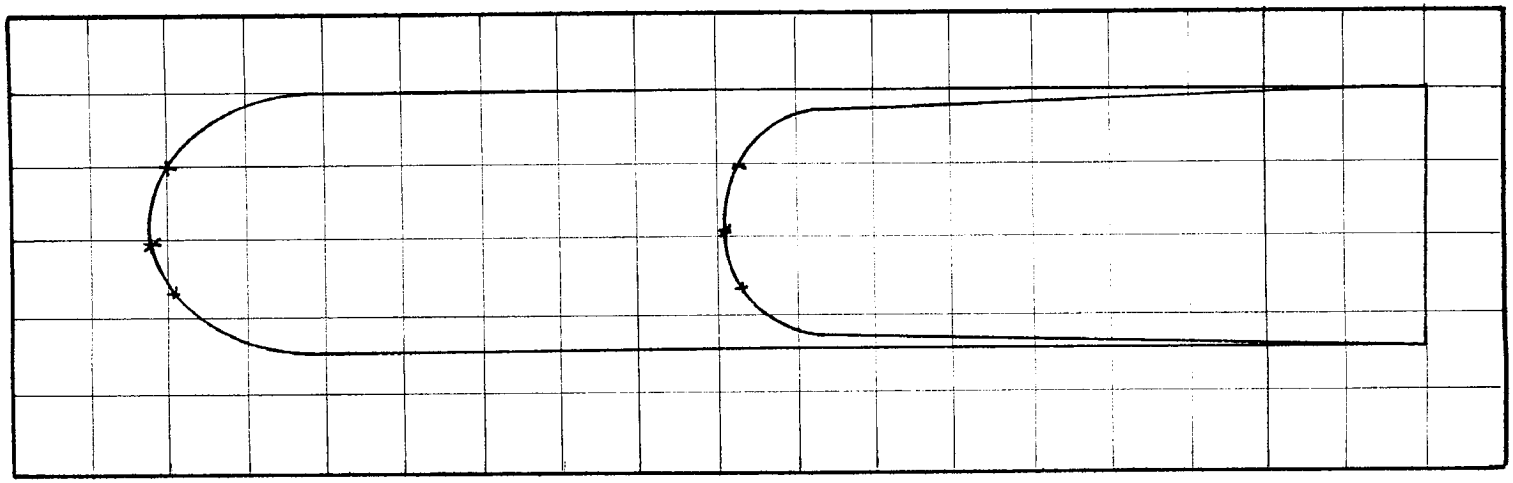

POSITION 5 Scales: Velocity: 1 mm = 1 mm/s Area under Velocity Curve = 3,100 mm^2

Momentum: 1 mm^2 = $\frac{1}{50}$ kgmm/s Area under Momentum Curve = 5,450 mm^2

BED MATERIAL: $\frac{1}{2}$ mm Diameter Sand

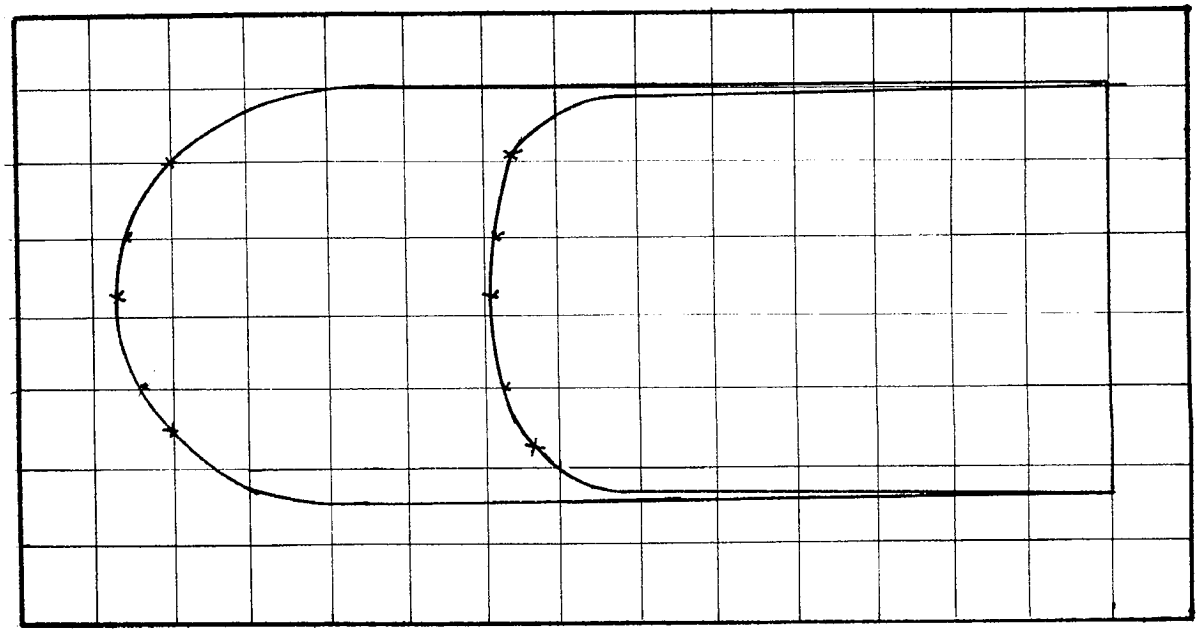

POSITION 1 Scale: Velocity: 1 mm = 1 mm/s

Momentum: 1 mm^2 = $\frac{1}{50}$ kgmm/s

Area under Velocity Curve = 4,240 mm^2

Area under Momentum Curve = 7,150 mm^2

BED MATERIAL: $\frac{1}{2}$ mm Diameter Sand

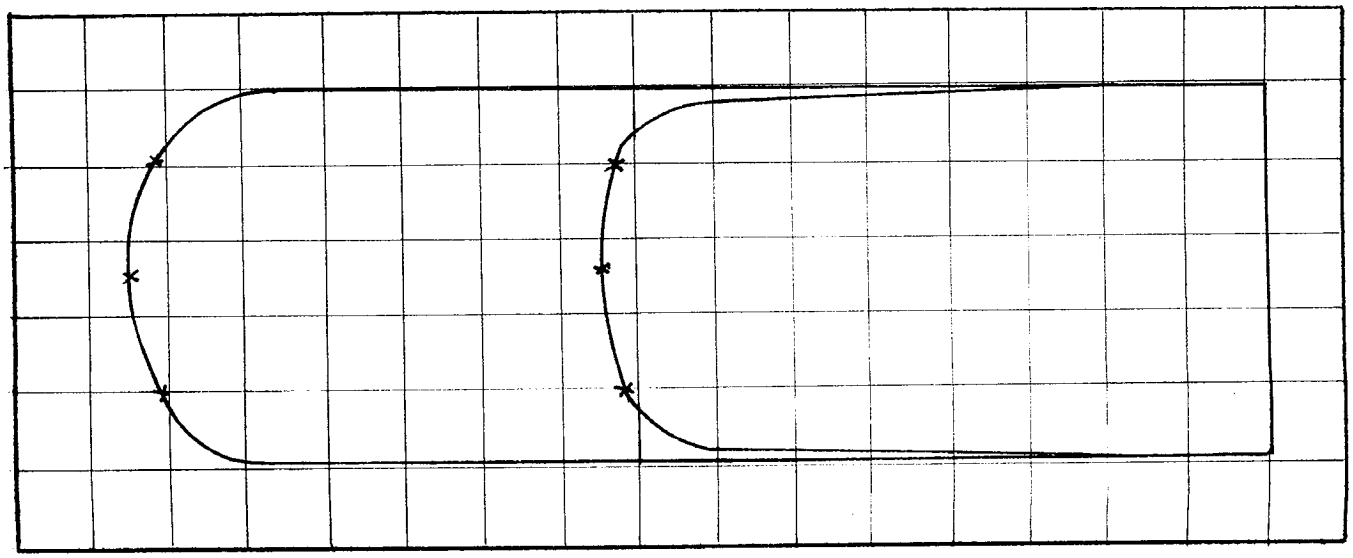

POSITION 2 Scale: Velocity: 1 mm = 1 mm/s Area under Velocity Curve = 4,150 mm^2

Momentum: 1 mm^2 = $\frac{1}{50}$ kgmm/s Area under Momentum Curve = 7,180 mm^2

BED MATERIAL: $\frac{1}{2}$ mm Diameter Sand

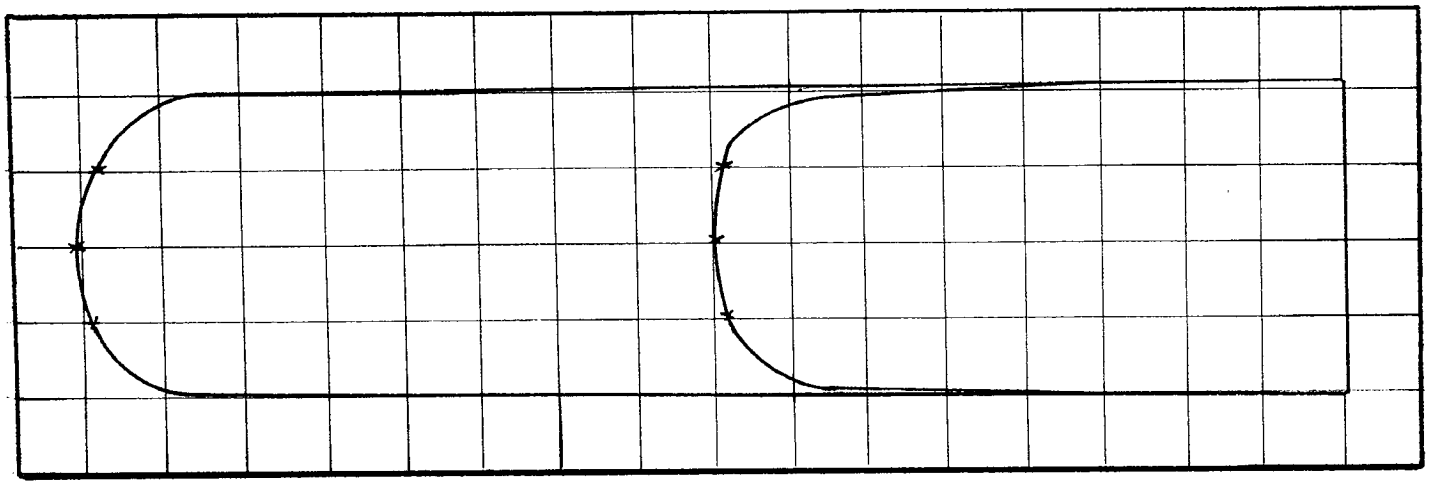

POSITION 3 Scale: Velocity: 1mm = 1 mm/s Area under Velocity Curve = 4,050 mm^2

Momentum: 1 mm^2 = $\frac{1}{50}$ kgmm/s Area under Momentum Curve = 7,050 mm^2

BED MATERIAL: $\frac{1}{2}$ mm Diameter Sand

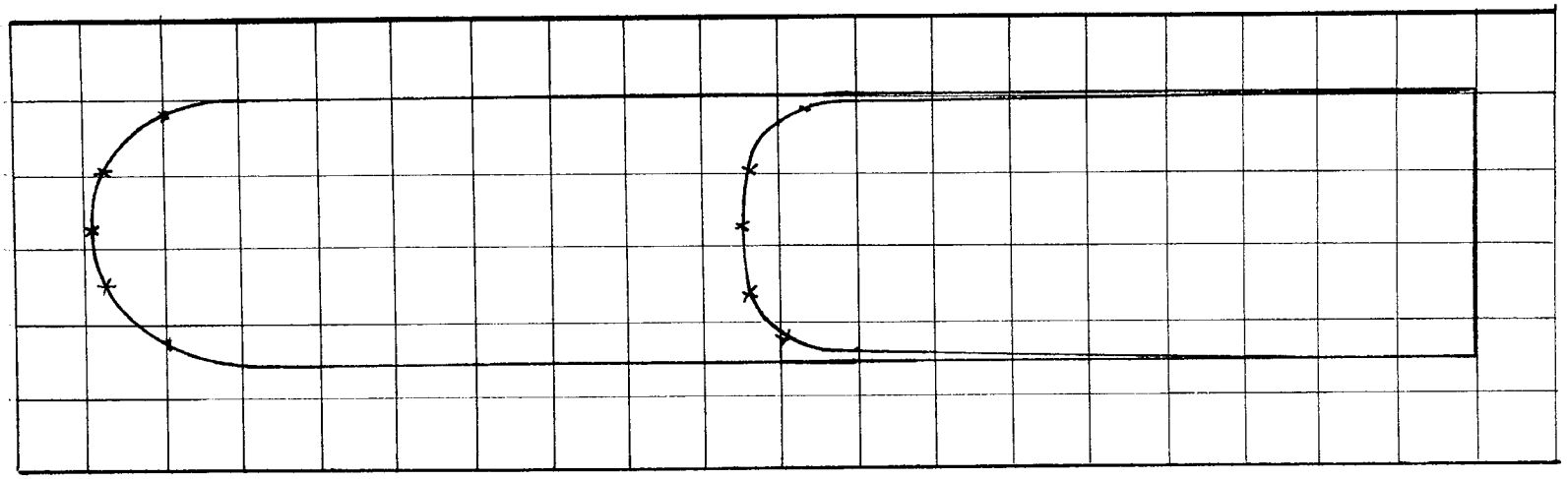

POSITION 4 Scale: Velocity: 1 mm = 1 mm/s Area under Velocity Curve = 4,300 mm^2

Momentum: 1 mm^2 = $\frac{1}{50}$ kgmm/s Area under Momentum Curve = 6,950 mm^2

BED MATERIAL: $\frac{1}{2}$ mm Diameter Sand

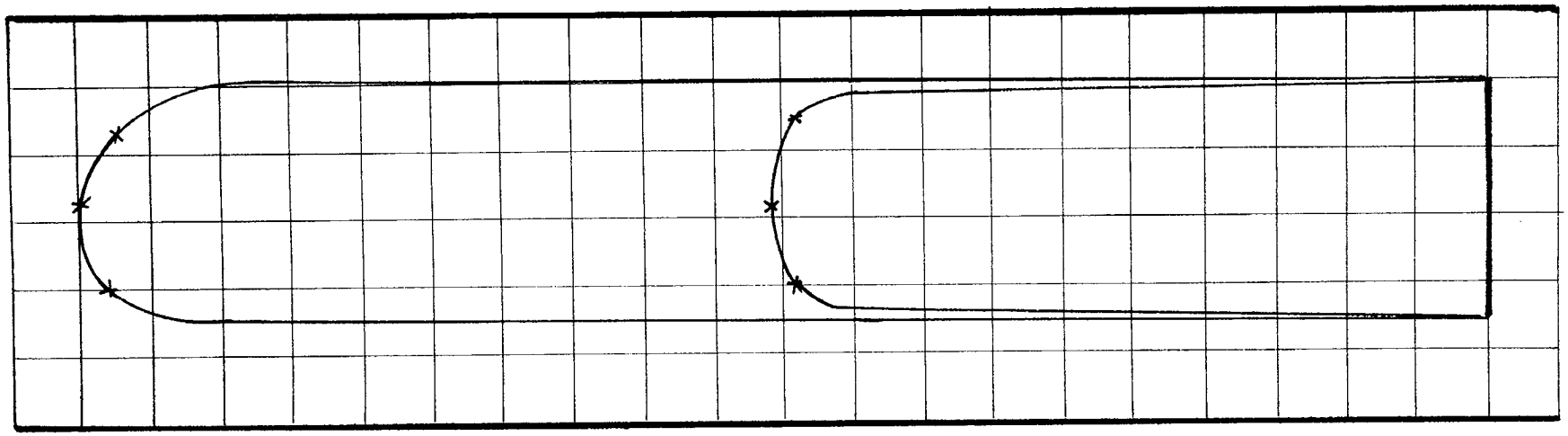

POSITION 5 Scale: Velocity: 1 mm = 1 mm/s Area under Velocity Curve = 3,850 mm^2

Momentum: 1 mm^2 = $\frac{1}{50}$ kgmm/s Area under Momentum Curve = 7,000 mm^2

BED MATERIAL: $\frac{1}{2}$ mm Diameter Sand

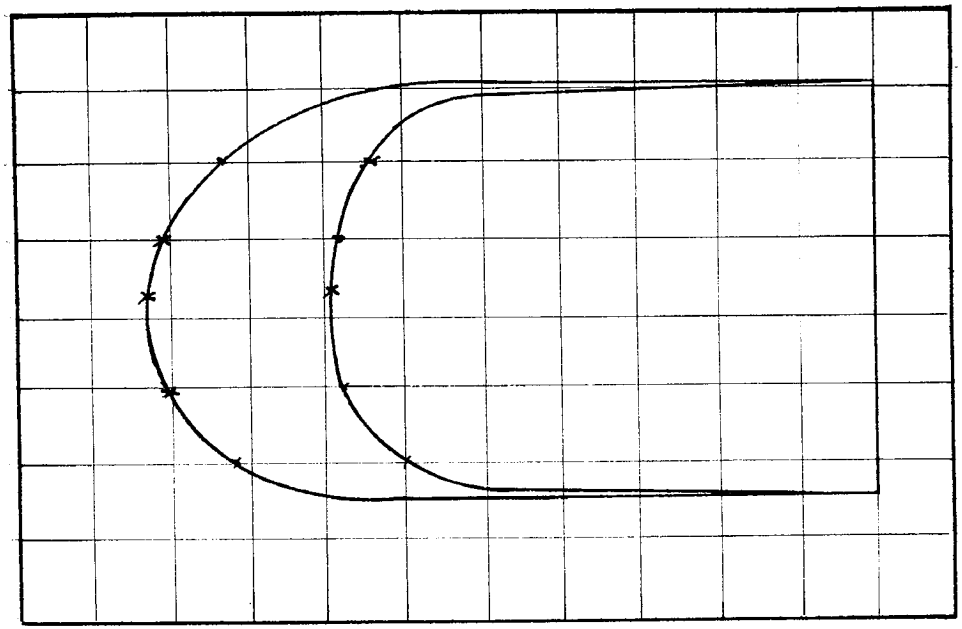

POSITION 1 Scale: Velocity: 1 mm ≙ 1 mm/s

Momentum: 1 mm^2 = $\frac{1}{50}$ kgmm/s

Area under Velocity Curve = 3,750 mm^2

Area under Momentum Curve = 5,100 mm^2

BED MATERIAL: $\frac{1}{2}$ mm Diameter Sand

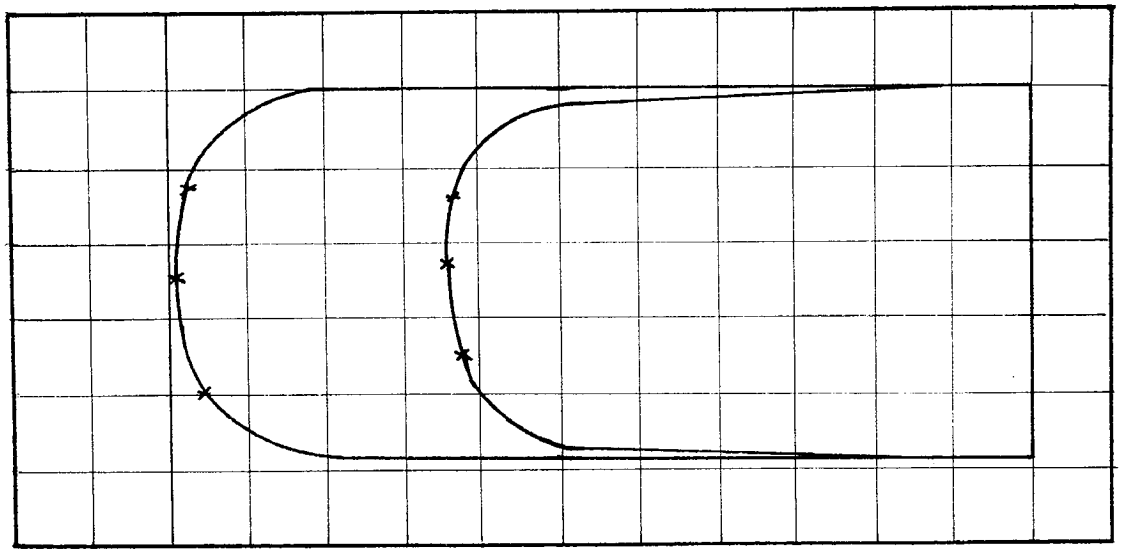

POSITION 2 Scale: Velocity: 1 mm = 1 mm/s Area under Velocity Curve = 3,460 mm^2

Momentum: 1 mm^2 = $\frac{1}{50}$ kgmm/s Area under Momentum Curve = 5,350 mm^2

BED MATERIAL: $\frac{1}{2}$ mm Diameter Sand

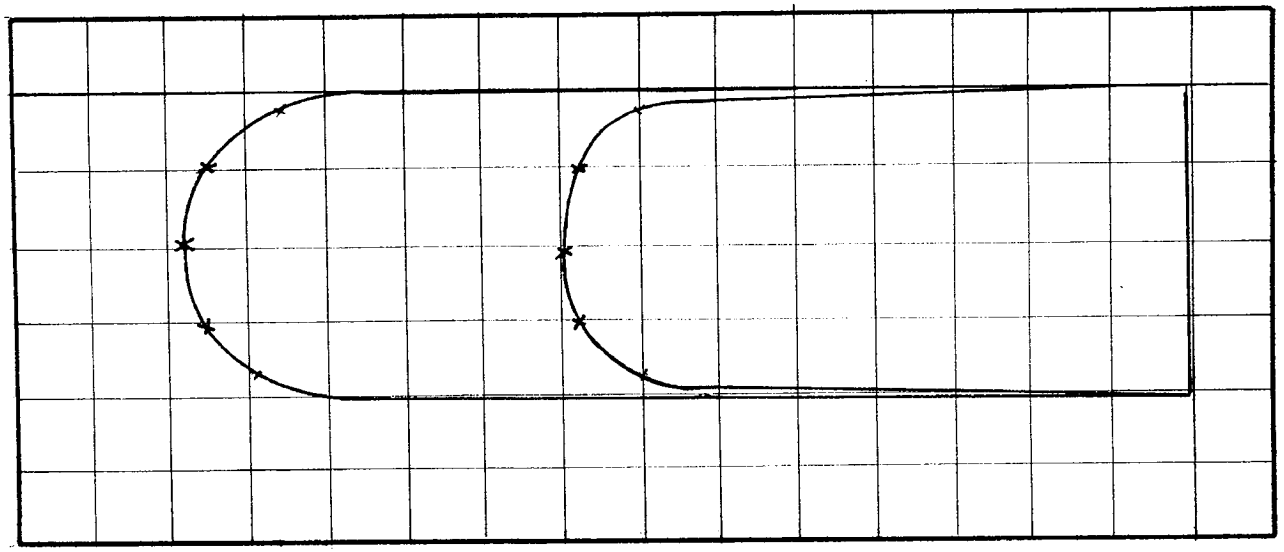

POSITION 3 Scale: Velocity: 1 mm = 1 mm/s Area under Velocity Curve = 3,250 mm^2

Momentum: 1 mm^2 = $\frac{1}{50}$ kgmm/s Area under Momentum Curve = 5,020 mm^2

BED MATERIAL: $\frac{1}{2}$ mm Diameter Sand

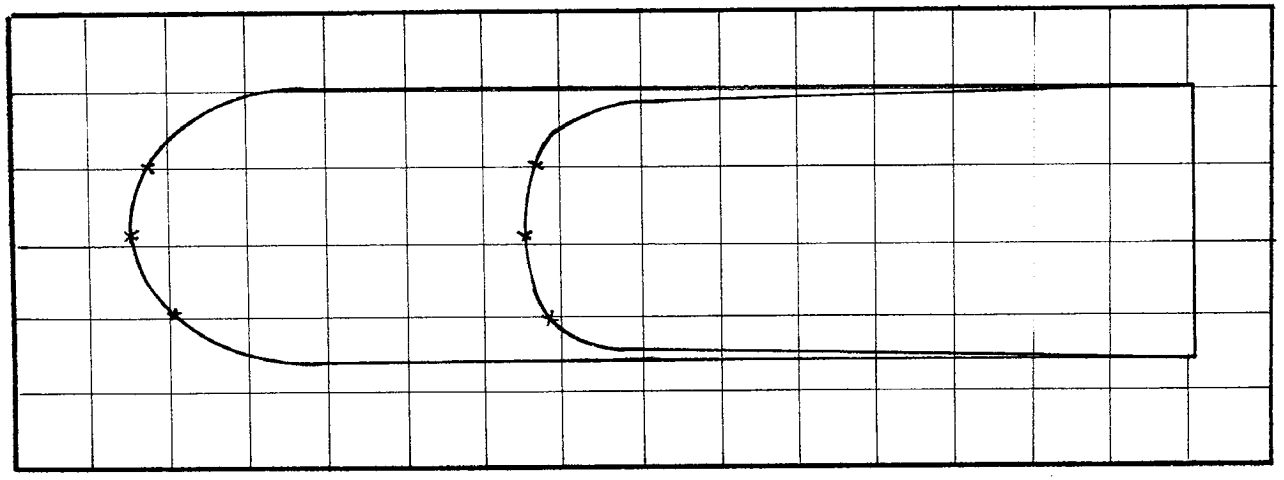

POSITION 4 Scale: Velocity: 1 mm = 1 mm/s Area under Velocity Curve = 3,050 mm^2

Momentum: 1 $mm^2 = \frac{1}{50}$ kgmm/s Area under Momentum Curve = 5,290 mm^2

BED MATERIAL : $\frac{1}{2}$ mm Diameter Sand

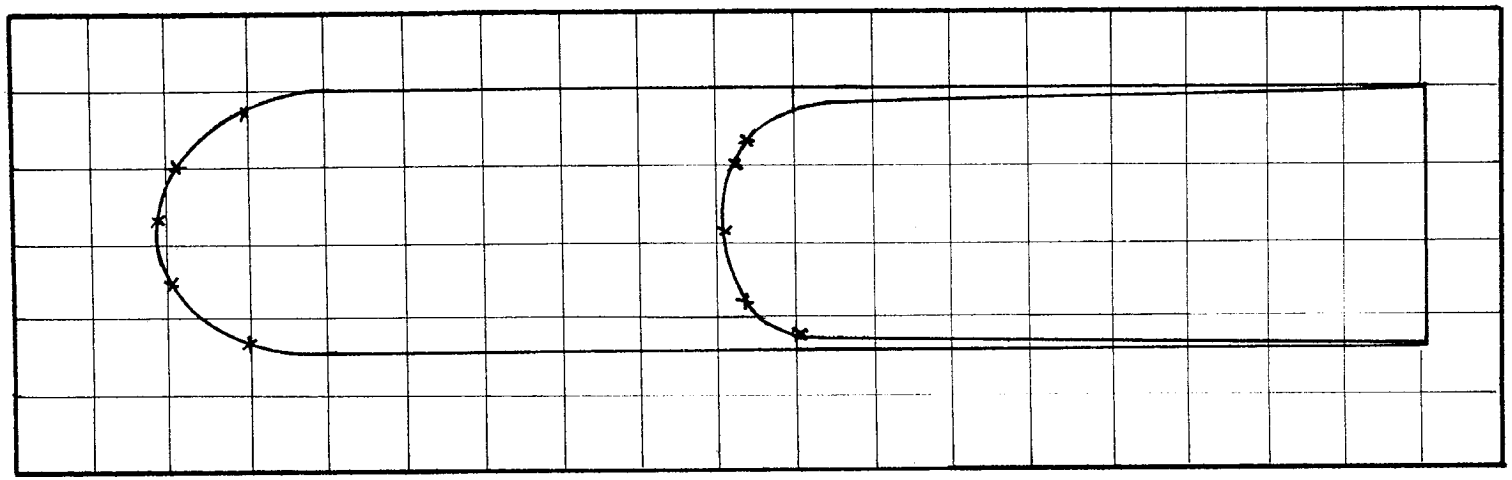

POSITION 5 Scale: Velocity: 1 mm = 1 mm/s Area under Velocity Curve = 3,120 mm^2

Momentum: 1 mm^2 = $\frac{1}{50}$ kgmm/s Area under Momentum Curve = 5,380 mm^2

BED MATERIAL: $\frac{1}{2}$ mm Diameter Sand

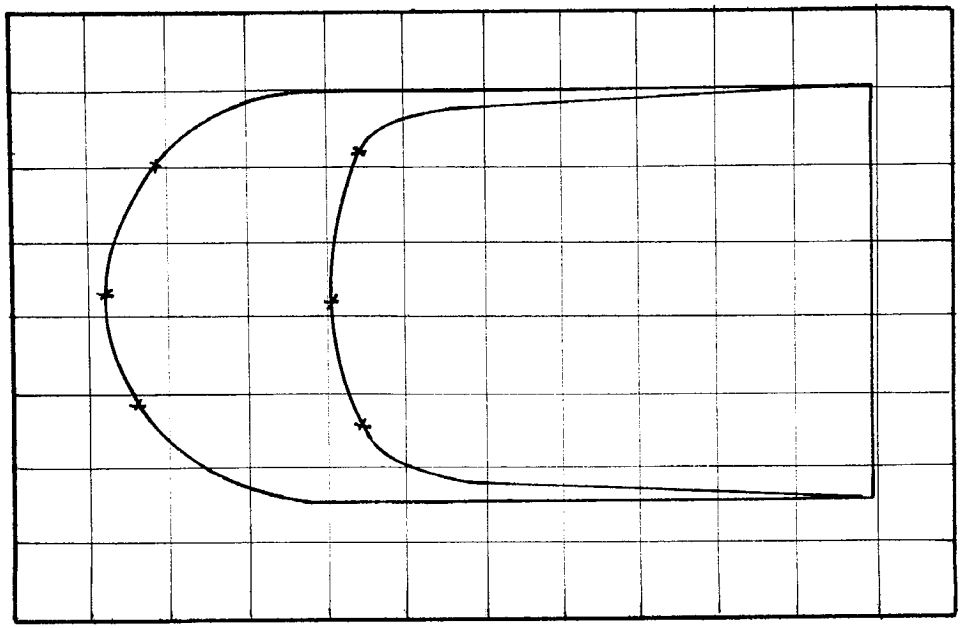

POSITION 1 Scale: Velocity: 1 mm = 1 mm/s Area under Velocity Curve = 3,450 mm^2

Momentum: 1 mm^2 = $\frac{1}{50}$ kgmm/s Area under Momentum Curve = 5,120 mm^2

BED MATERIAL: $\frac{1}{2}$ mm Diameter Sand

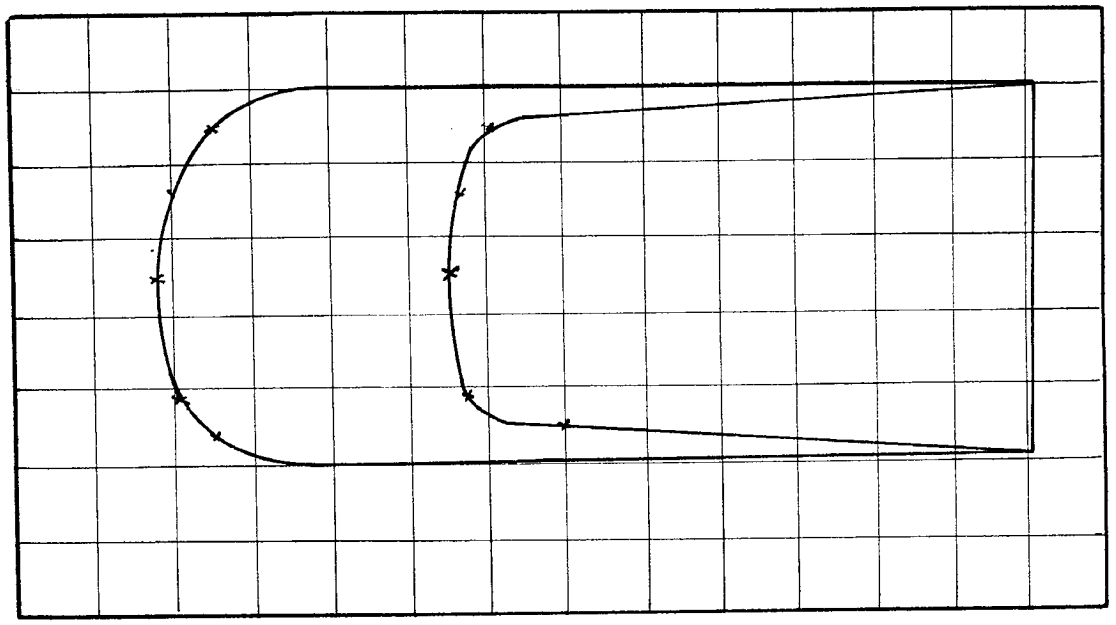

POSITION 2

Scale: Velocity: 1 mm = 1 mm/s Area under Velocity Curve = 3,350 mm^2

Momentum: 1 mm^2 = $\frac{1}{50}$ kgmm/s Area under Momentum Curve = 5,240 mm^2

BED MATERIAL: $\frac{1}{2}$ mm Diameter Sand

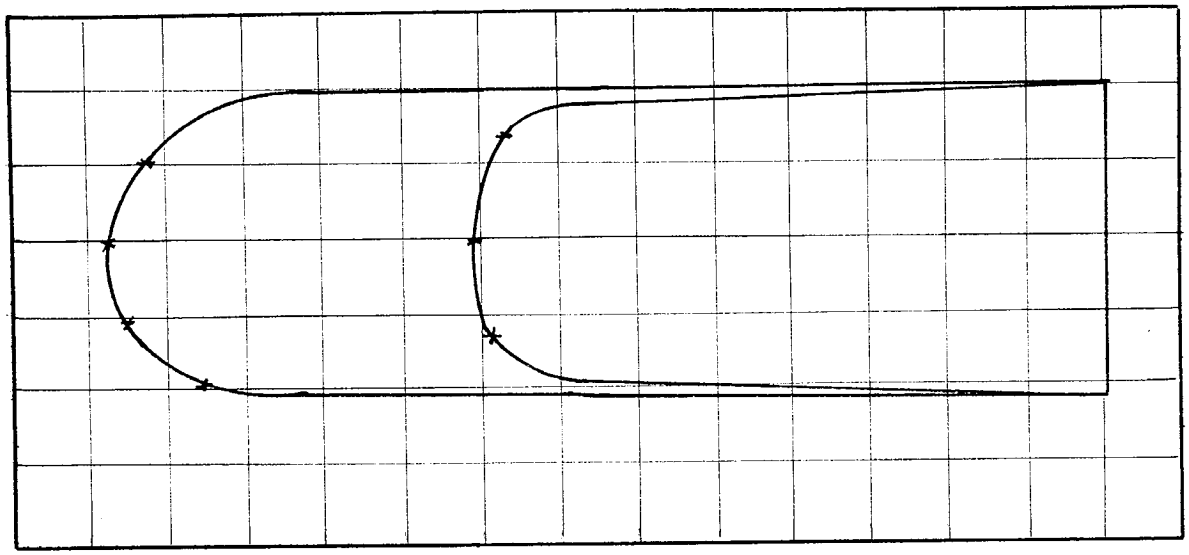

POSITION 3 Scale: Velocity: 1 mm = 1 mm/s

Momentum: 1 mm^2 = $\frac{1}{50}$ kgmm/s

Area under Velocity Curve = 3,200 mm^2

Area under Momentum Curve = 5,100 mm^2

BED MATERIAL: $\frac{1}{2}$ mm Diameter Sand

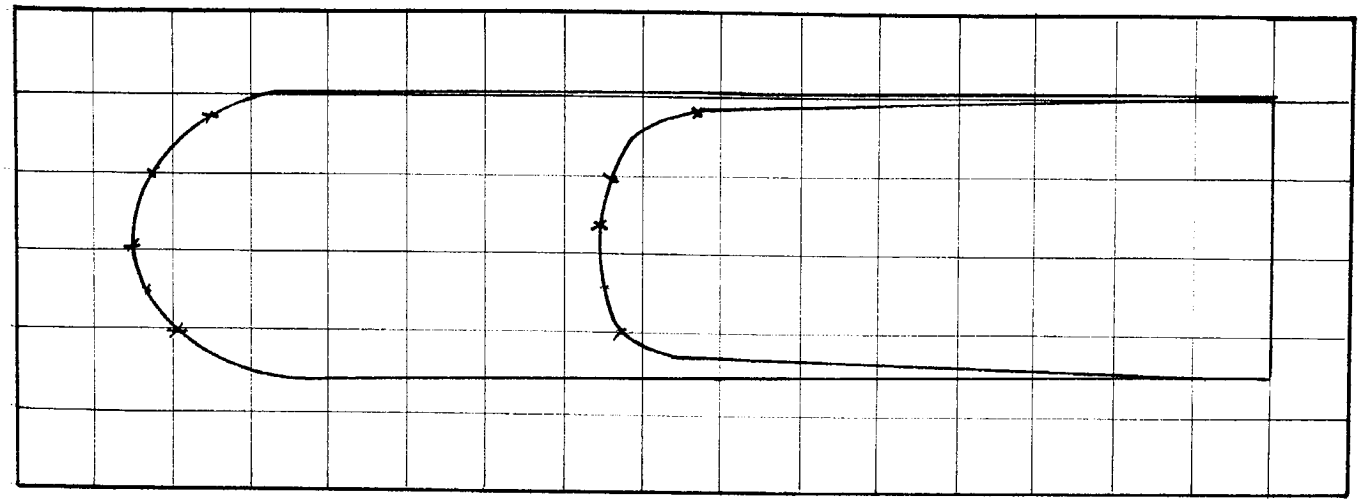

POSITION 4 Scale: Velocity: 1 mm = 1 mm/s

Momentum: 1 mm^2 = $\frac{1}{50}$ kgmm/s

Area under Velocity Curve = 3,100 mm^2

Area under Momentum Curve = 5,180 mm^2

BED MATERIAL: $\frac{1}{2}$ mm Diameter Sand

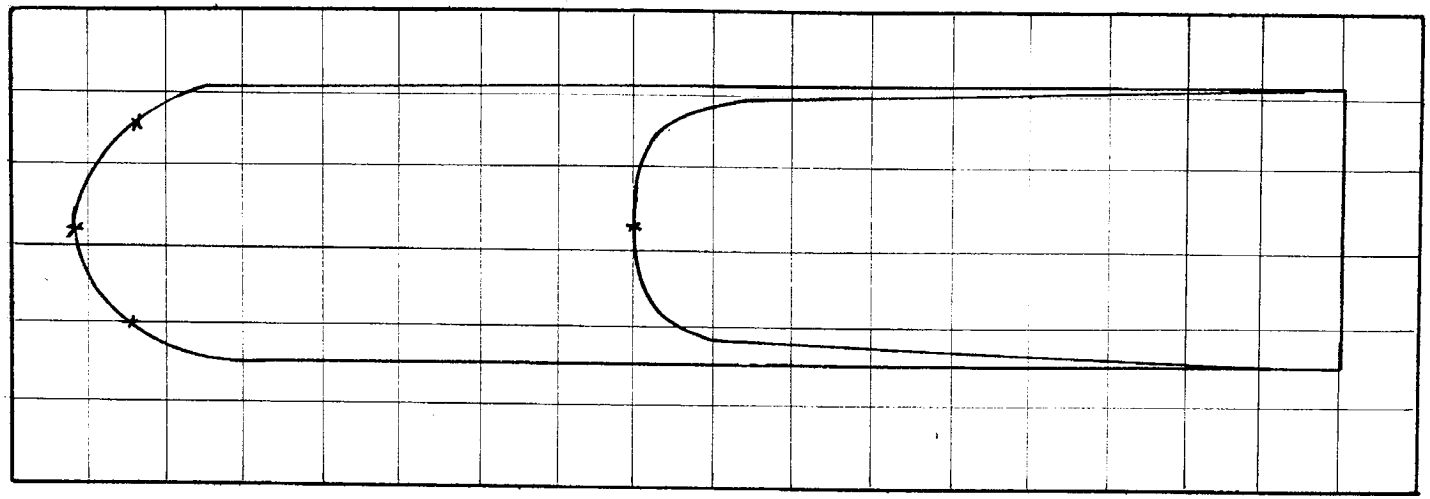

POSITION 5 Scale: Velocity: 1 mm = 1 mm/s Area under Velocity Curve = 3,150 mm^2

Momentum: 1 mm^2 = $\frac{1}{50}$ kgmm/s Area under Momentum Curve = 5,250 mm^2

BED MATERIAL: $\frac{1}{2}$ mm Diameter Sand

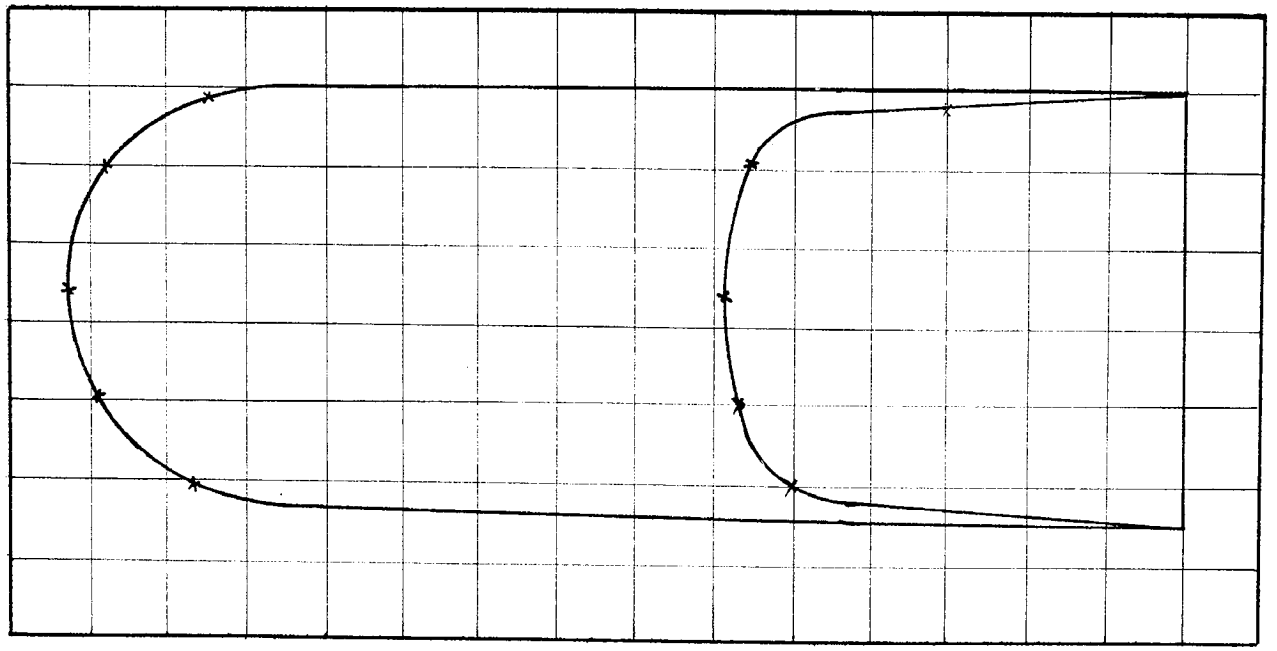

POSITION 1 Scales: Velocity : 1 mm = 1 mm/s Area under Velocity Curve = 3,000 mm^2

Momentum : 1 mm^2 = $\frac{1}{50}$ kgmm/s Area under Momentum Curve = 7,280 mm^2

BED MATERIAL: $\frac{1}{2}$ mm Diameter Sand

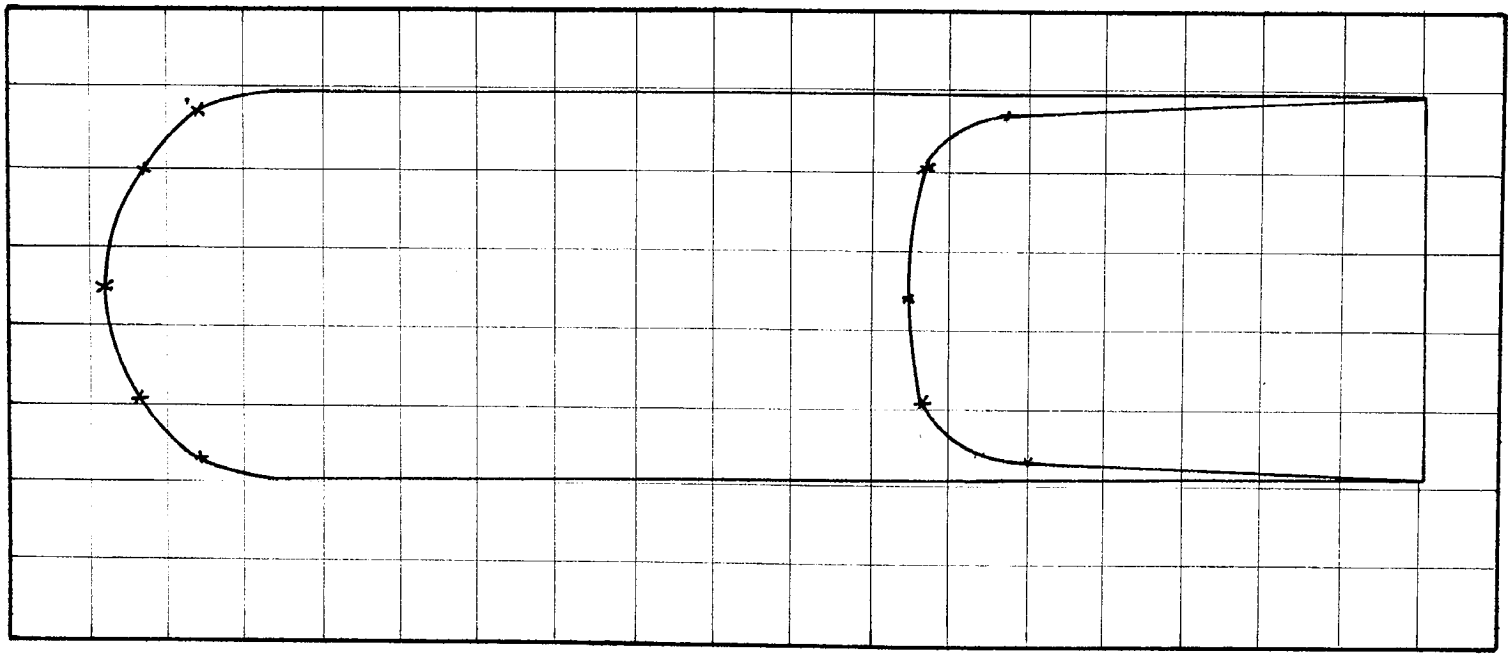

POSITION 2 Scale: Velocity: 1 mm = 1 mm/s Area under Velocity Curve = 3,000 mm^2

Momentum: 1 mm^2 = $\frac{1}{50}$ kgmm/s Area under Momentum Curve = 7,300 mm^2

BED MATERIAL: $\frac{1}{2}$ mm Diameter Sand

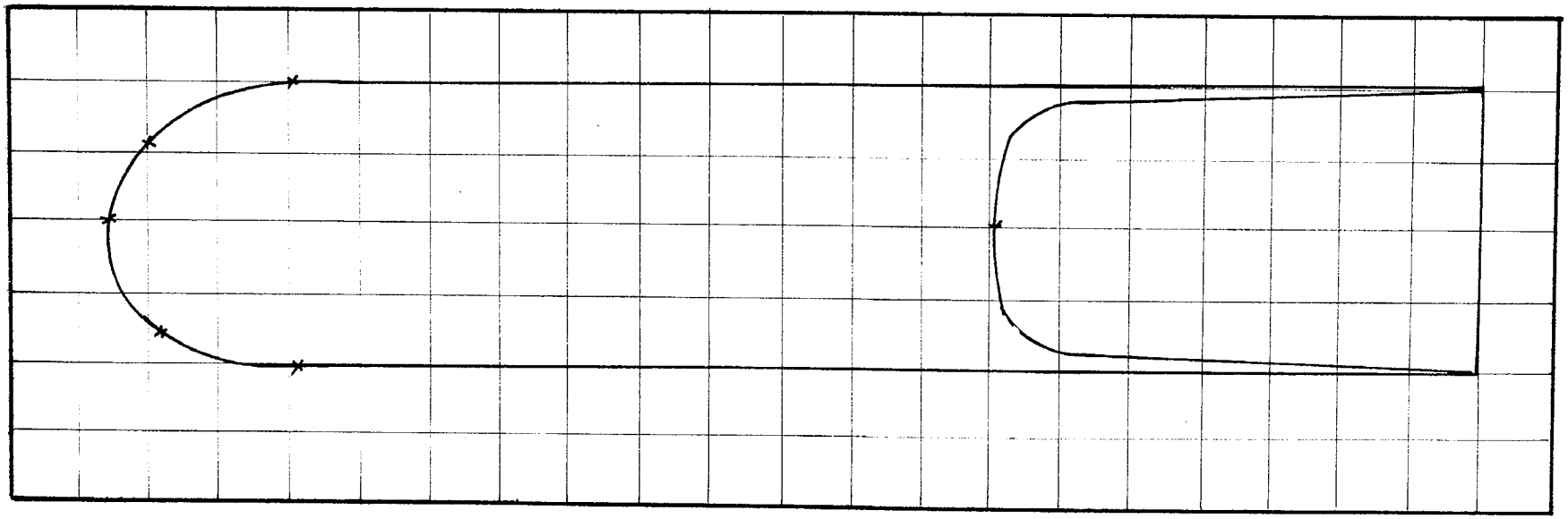

POSITION 3 Scale: Velocity: 1mm = 1mm/s Area under Velocity Curve = 2,850 mm^2

Momentum: 1 mm^2 = $\frac{1}{50}$ kgmm/s Area under Momentum Curve = 7,450 mm^2

BED MATERIAL: $\frac{1}{2}$ mm Diameter Sand

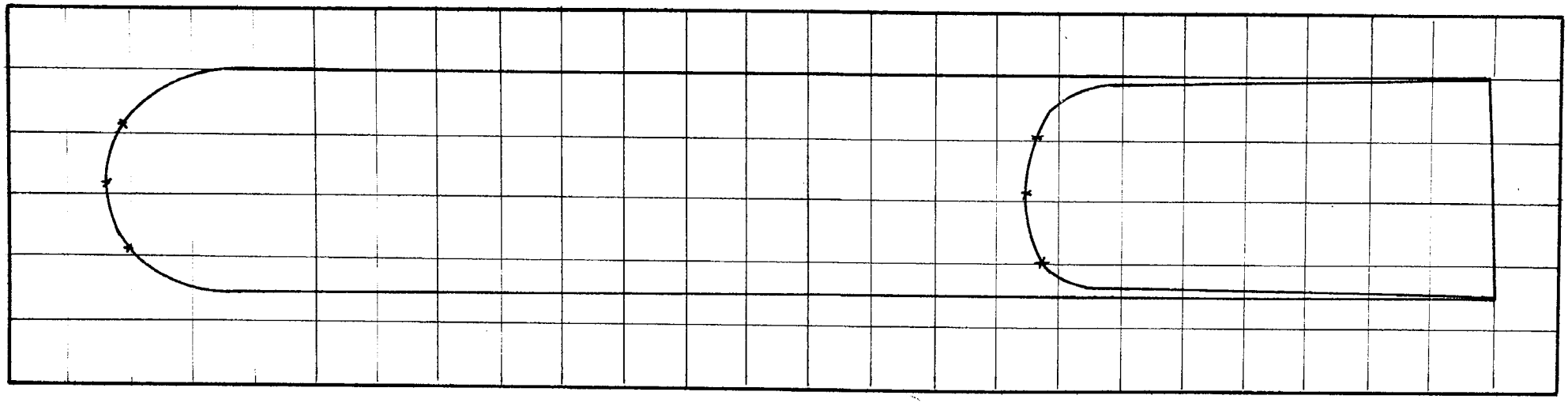

POSITION 4 Scales: Velocity: 1 mm = 1mm/s Area under Velocity Curve = 2,950 mm^2

Momentum: 1 mm^2 = $\frac{1}{50}$ kgmm/s Area under Momentum Curve = 7,750 mm^2

BED MATERIAL: $\frac{1}{2}$ mm Diameter Sand

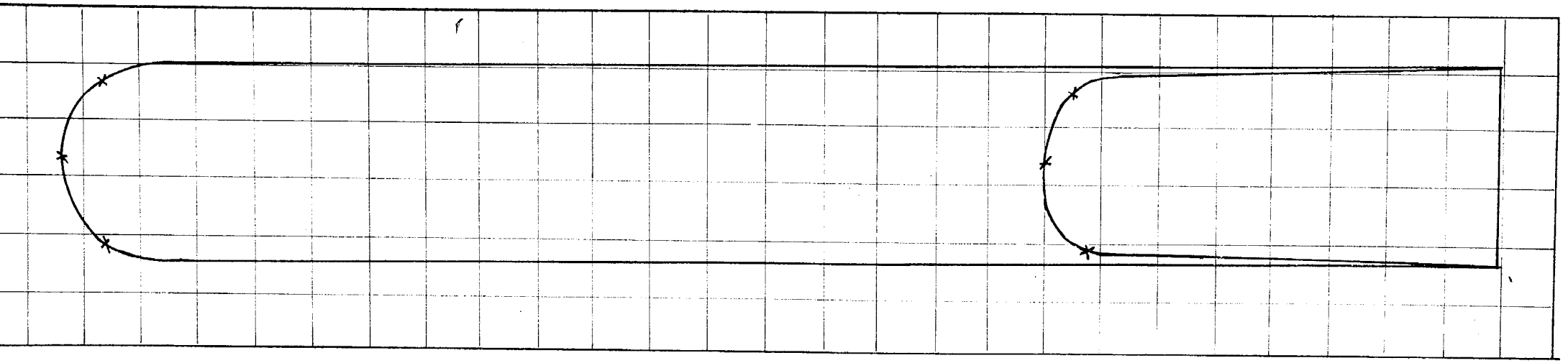

POSITION 5 Scales: Velocity: 1 mm = 1 mm/s

Momentum: 1 mm^2 = $\frac{1}{50}$ kgmm/s

Area under Velocity Curve = 3,070 mm^2

Area under Momentum Curve = 7,850 mm^2

BED MATERIAL: $\frac{1}{2}$ mm Diameter Sand

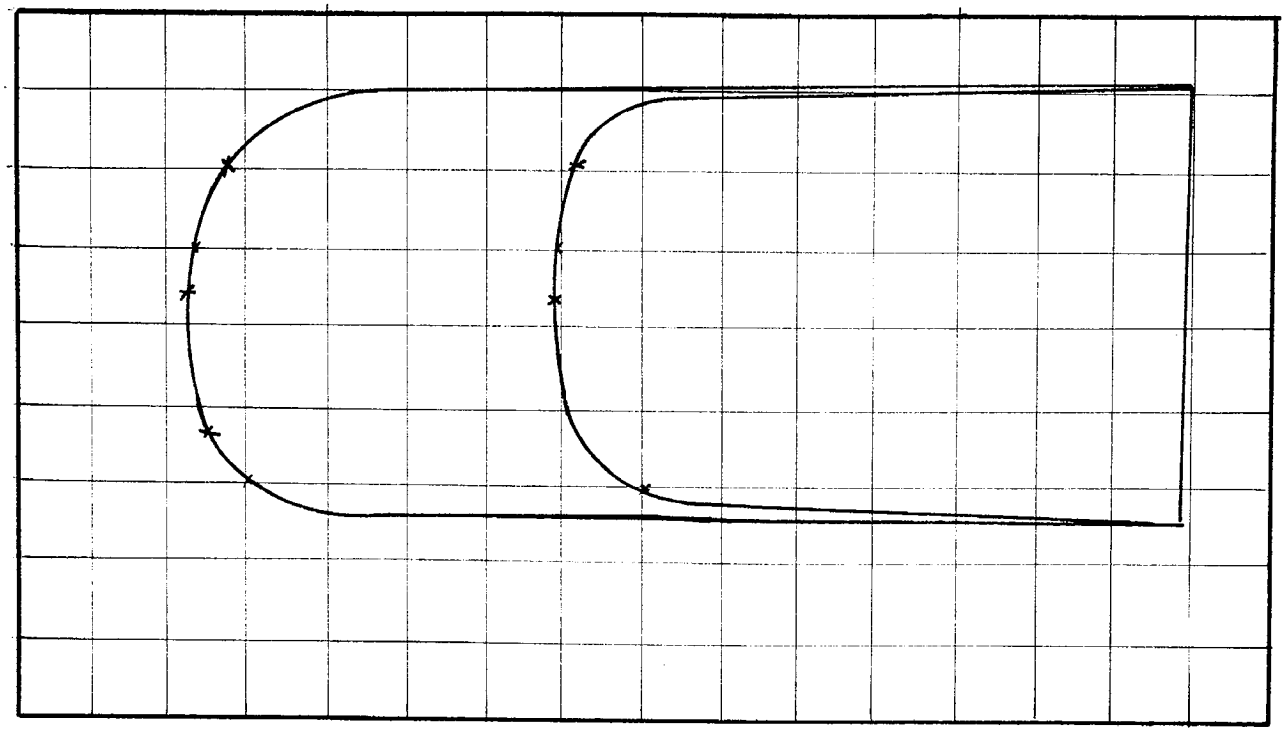

POSITION 1 Scales: Velocity: 1 mm = 1 mm/s

Momentum: 1 mm^2 = $\frac{1}{50}$ kgmm/s

Area under Velocity Curve = 4,020 mm^2

Area under Momentum Curve = 6,400 mm^2

BED MATERIAL $\frac{1}{2}$ mm Diameter Sand

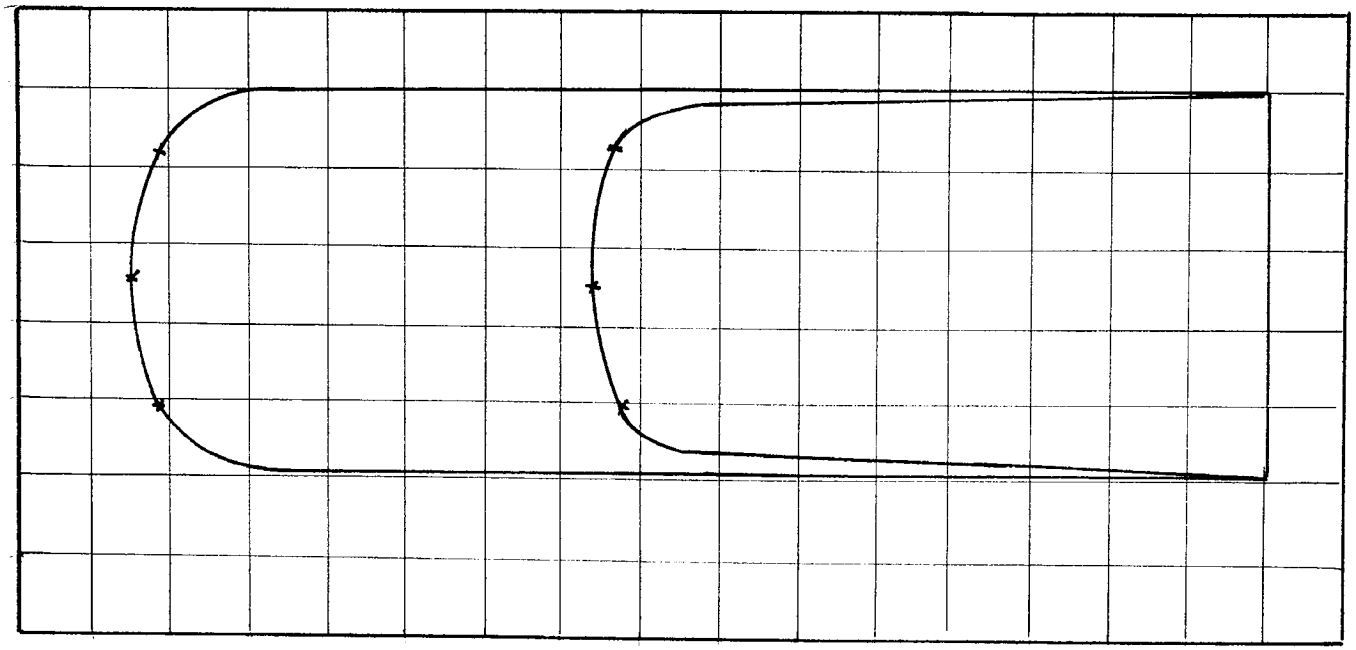

POSITION 2 Scales: Velocity: 1 mm = 1 mm/s

Momentum: 1 mm^2 = $\frac{1}{50}$ kgmm/s

Area under Velocity Curve = 4,050 mm^2

Area under Momentum Curve = 6,420 mm^2

BED MATERIAL: $\frac{1}{2}$ mm Diameter Sand

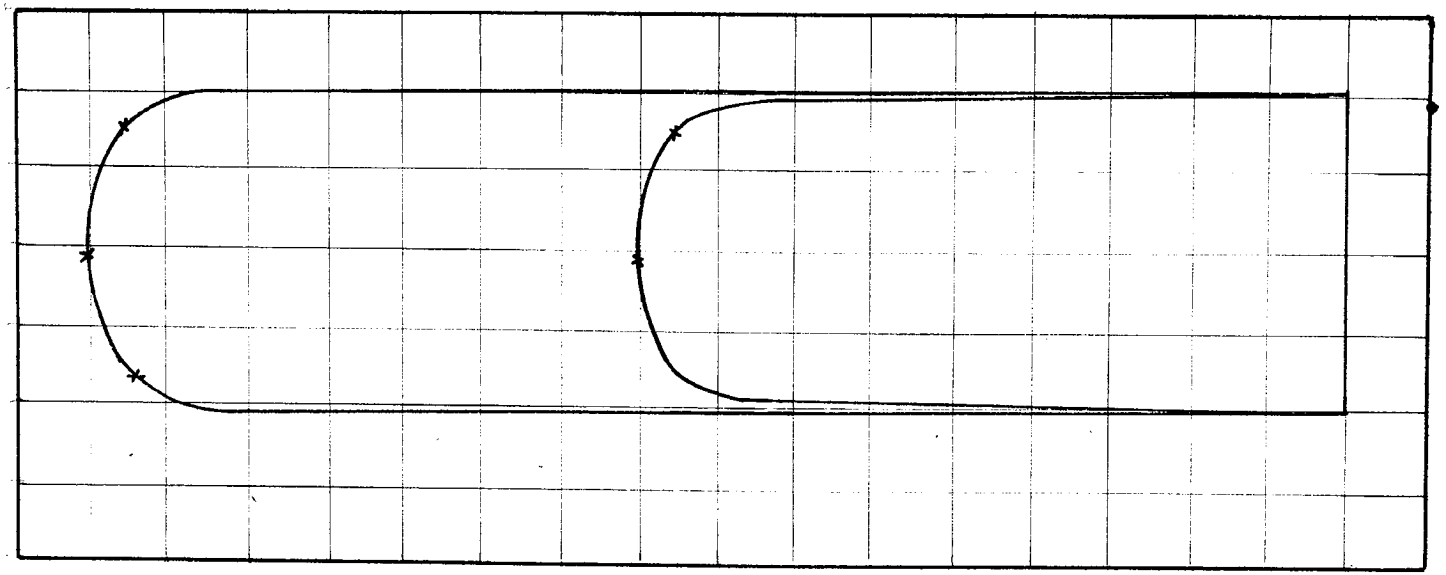

POSITION 3

Scales: Velocity: 1 mm = 1mm/s

Momentum: 1 mm^2 = $\frac{1}{50}$ kgmm/s

Area under Velocity Curve = 4,000 mm^2

Area under Momentum Curve = 6,500 mm^2

BED MATERIAL: $\frac{1}{2}$ mmDiameter Sand

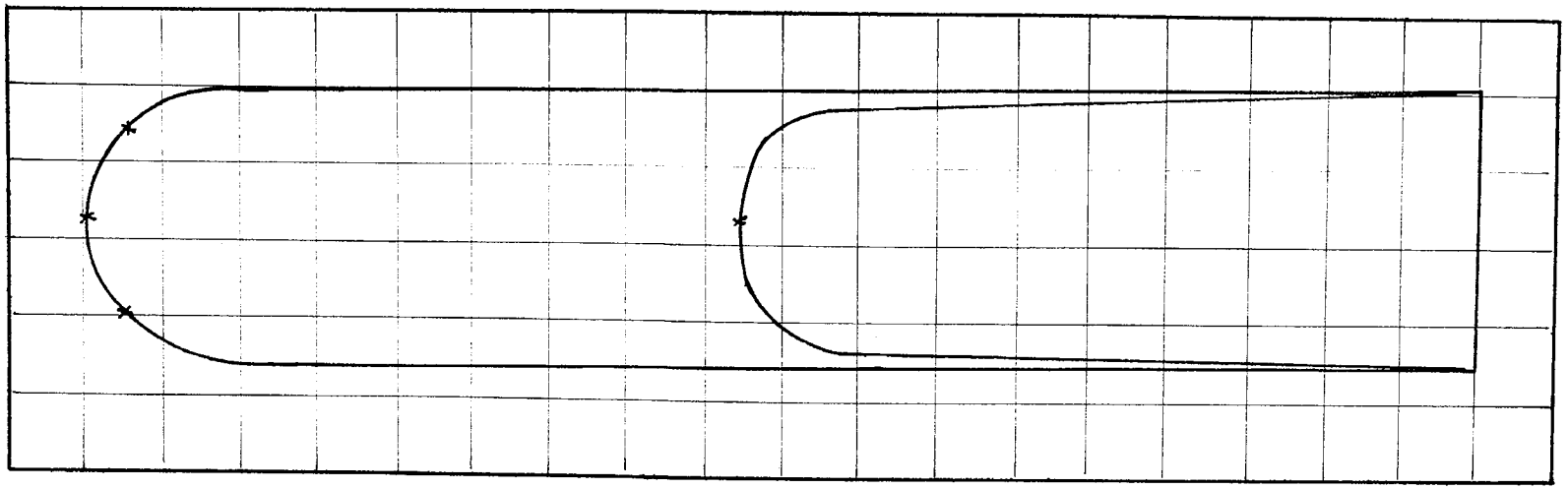

POSITION 4 Scales: Velocity: 1 mm = 1 mm/s

Momentum: 1 mm^2 = $\frac{1}{50}$ kgmm/s

Area under Velocity Curve = 3,800 mm^2

Area under Momentum Curve = 6,430 mm^2

BED MATERIAL: $\frac{1}{2}$ mm Diameter Sand

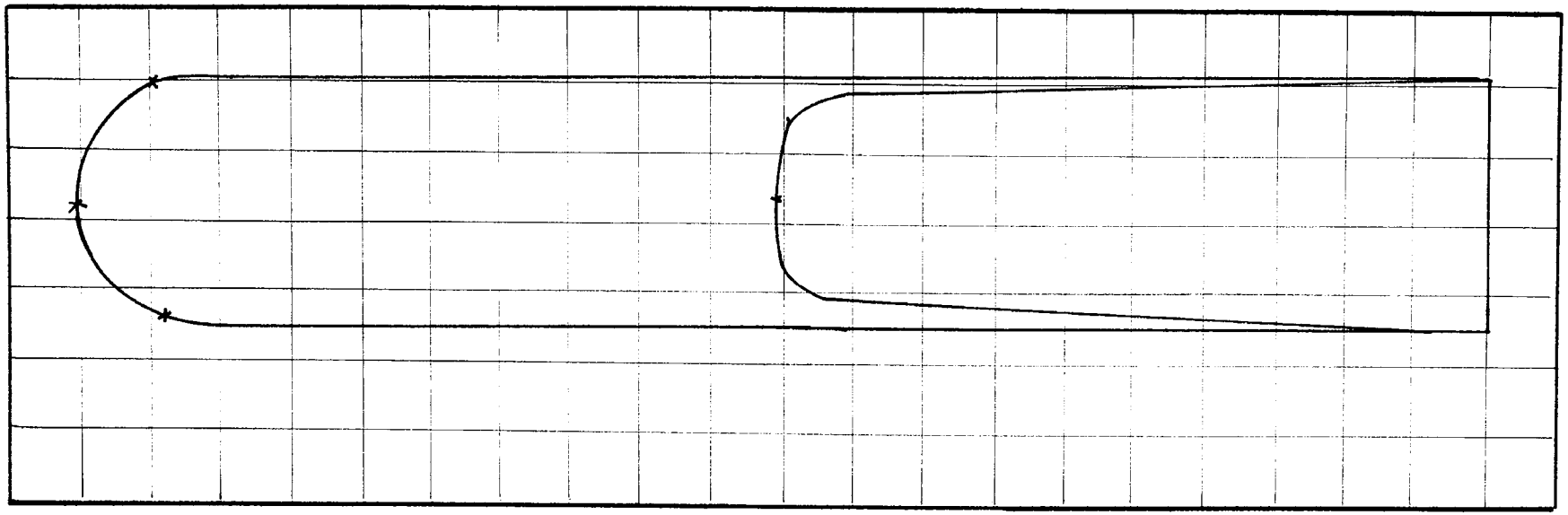

POSITION 5 Scale: Velocity: 1 mm = 1 mm/s

Momentum: 1 mm^2 = $\frac{1}{50}$ kgmm/s

Area under Velocity Curve = 3,850 mm^2

Area under Momentum Curve = 6,550 mm^2

BED MATERIAL: $\frac{1}{2}$ mm Diameter Sand

APPENDIX D

GRAPHS OF BED SHEAR STRESS (J_o)

AGAINST PARTICLE REYNOLDS NUMBER (R_{e_p})

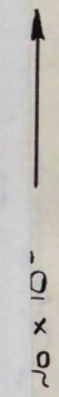

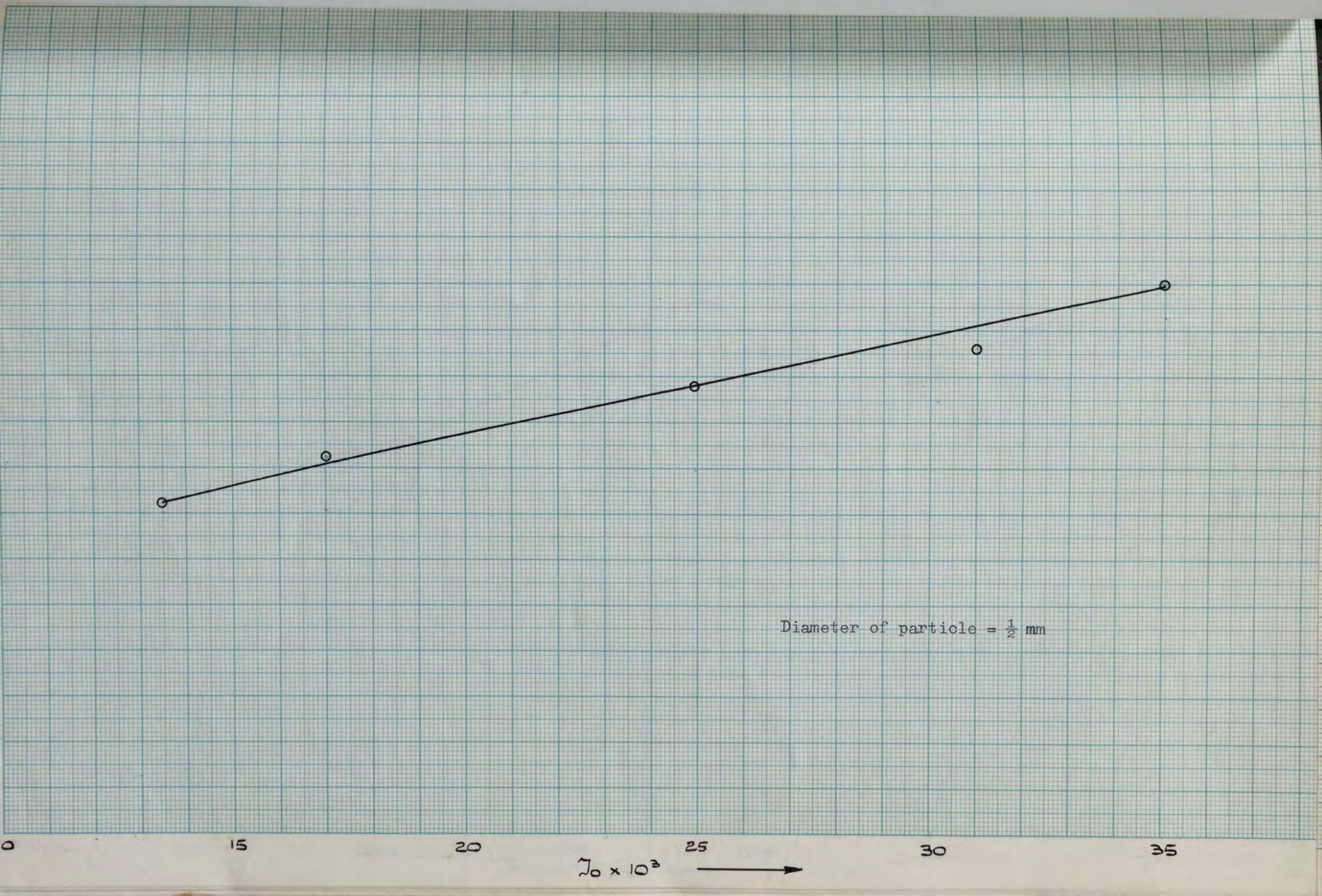
Diameter of particle = $\frac{1}{2}$ mm
0
15
20
25
30
35
$J_0 \times 10^3$

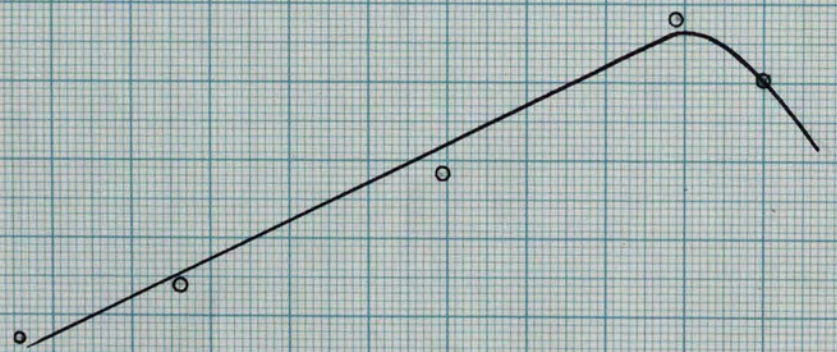

Diameter of particle = $\frac{1}{2}$ mm

0 100 200 300 400

$J_0 \times 10^3$ ⟶

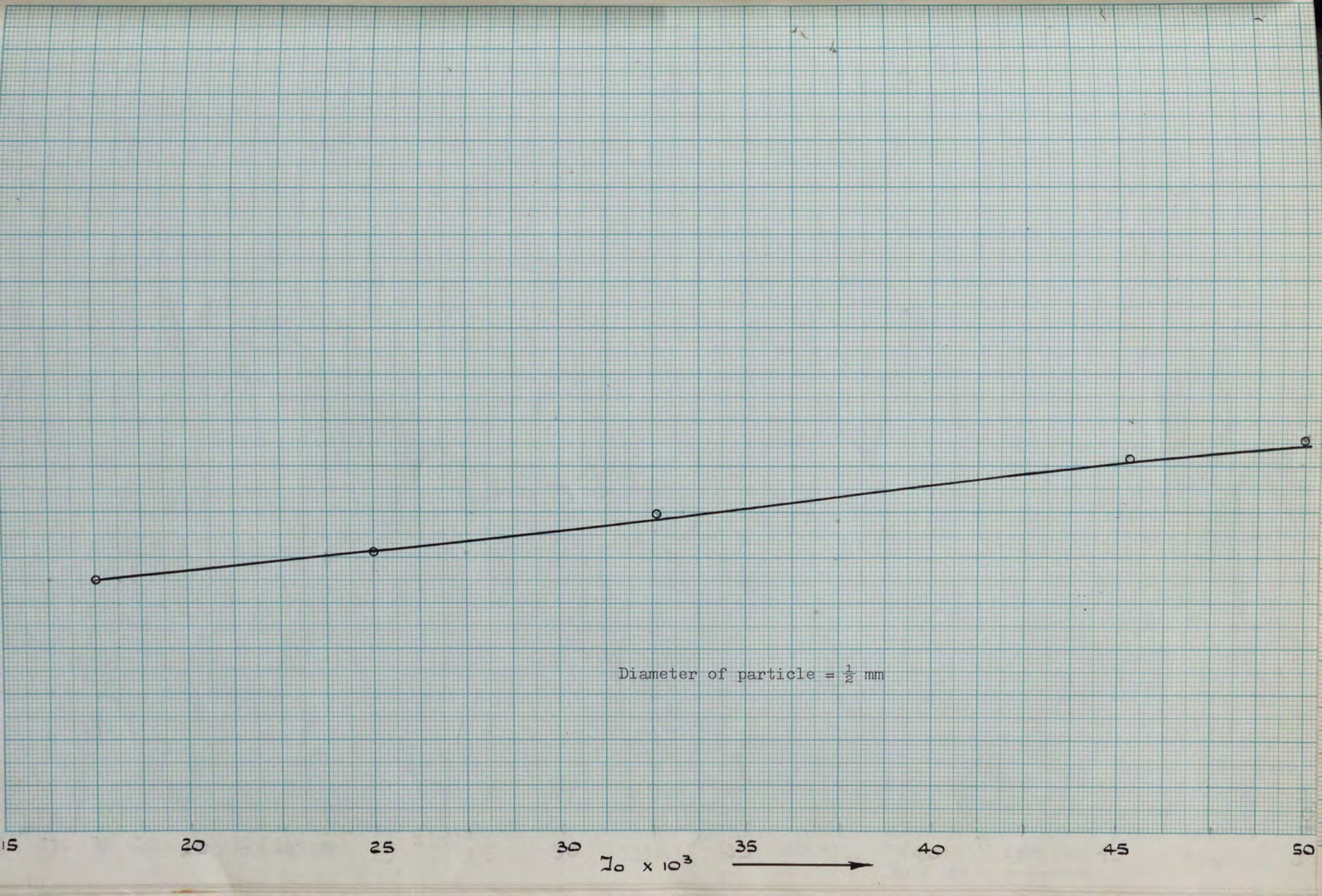
Diameter of particle = $\frac{1}{2}$ mm
15
20
25
30
35
40
45
50
$J_o \times 10^3$

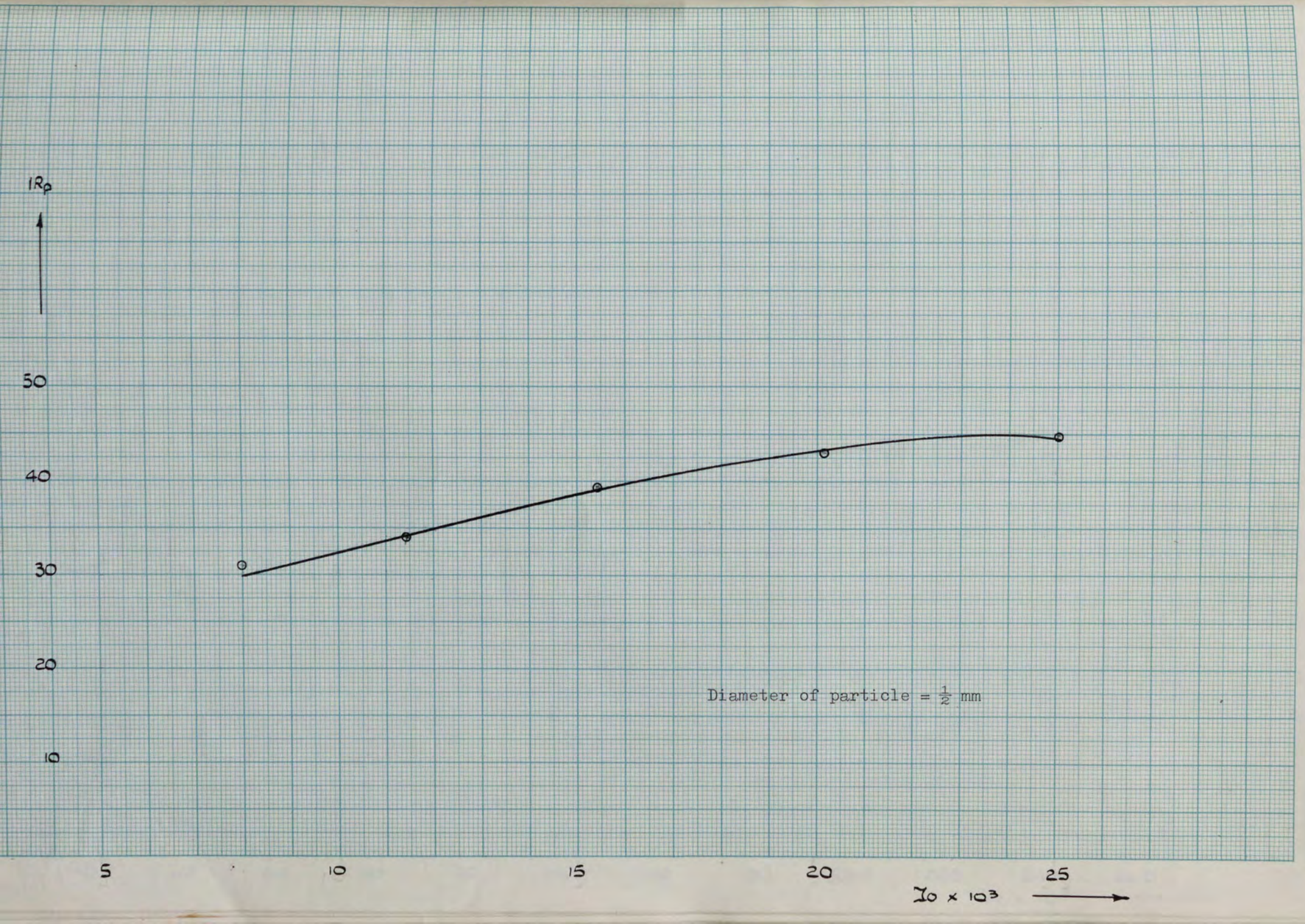
IR_p
50
40
30
20
10
5
10
15
20
25
$I_0 \times 10^3$
Diameter of particle = $\frac{1}{2}$ mm

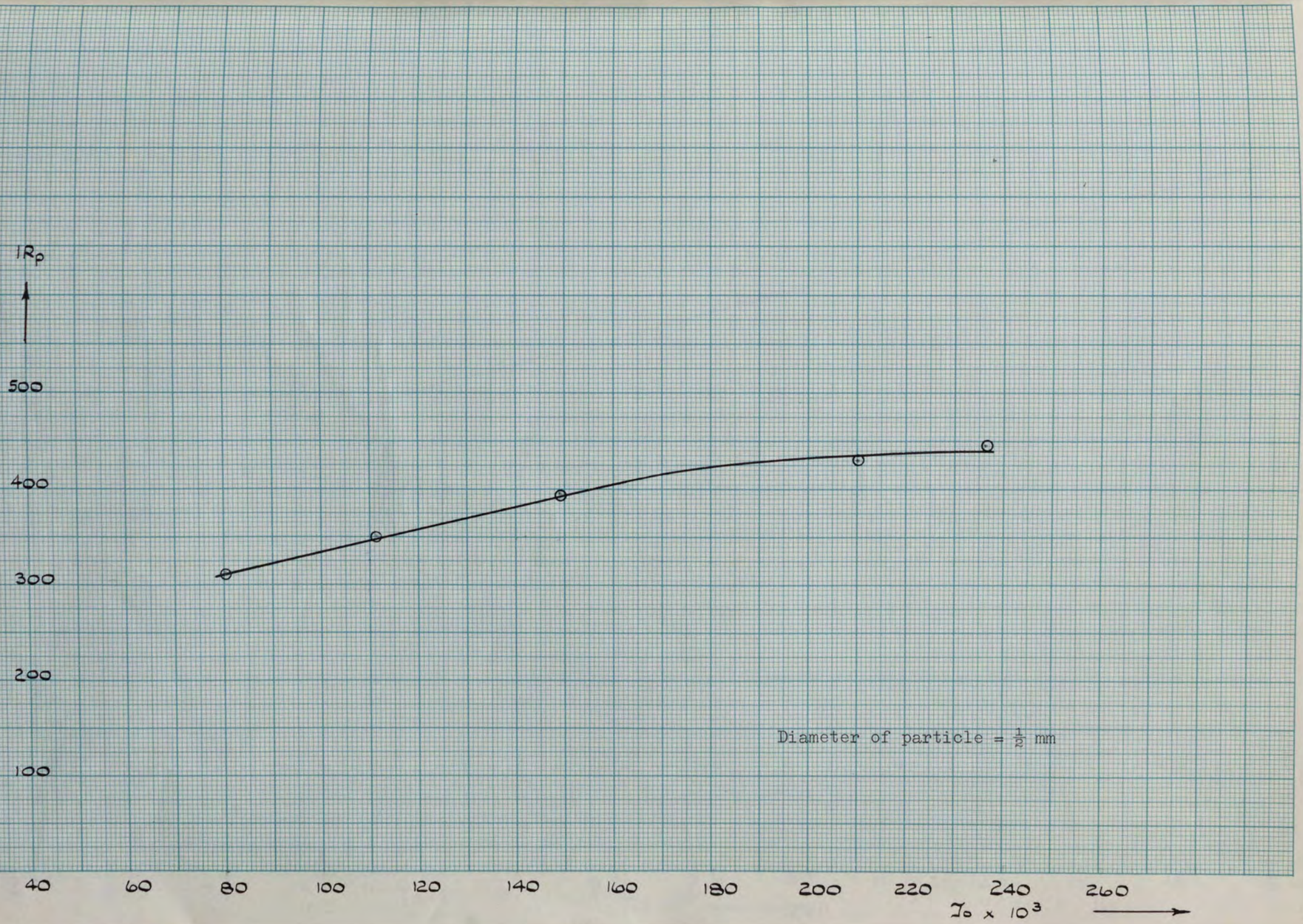
IR_p
500
400
300
200
100
Diameter of particle = $\frac{1}{2}$ mm
40
60
80
100
120
140
160
180
200
220
240
260
$I_o \times 10^3$

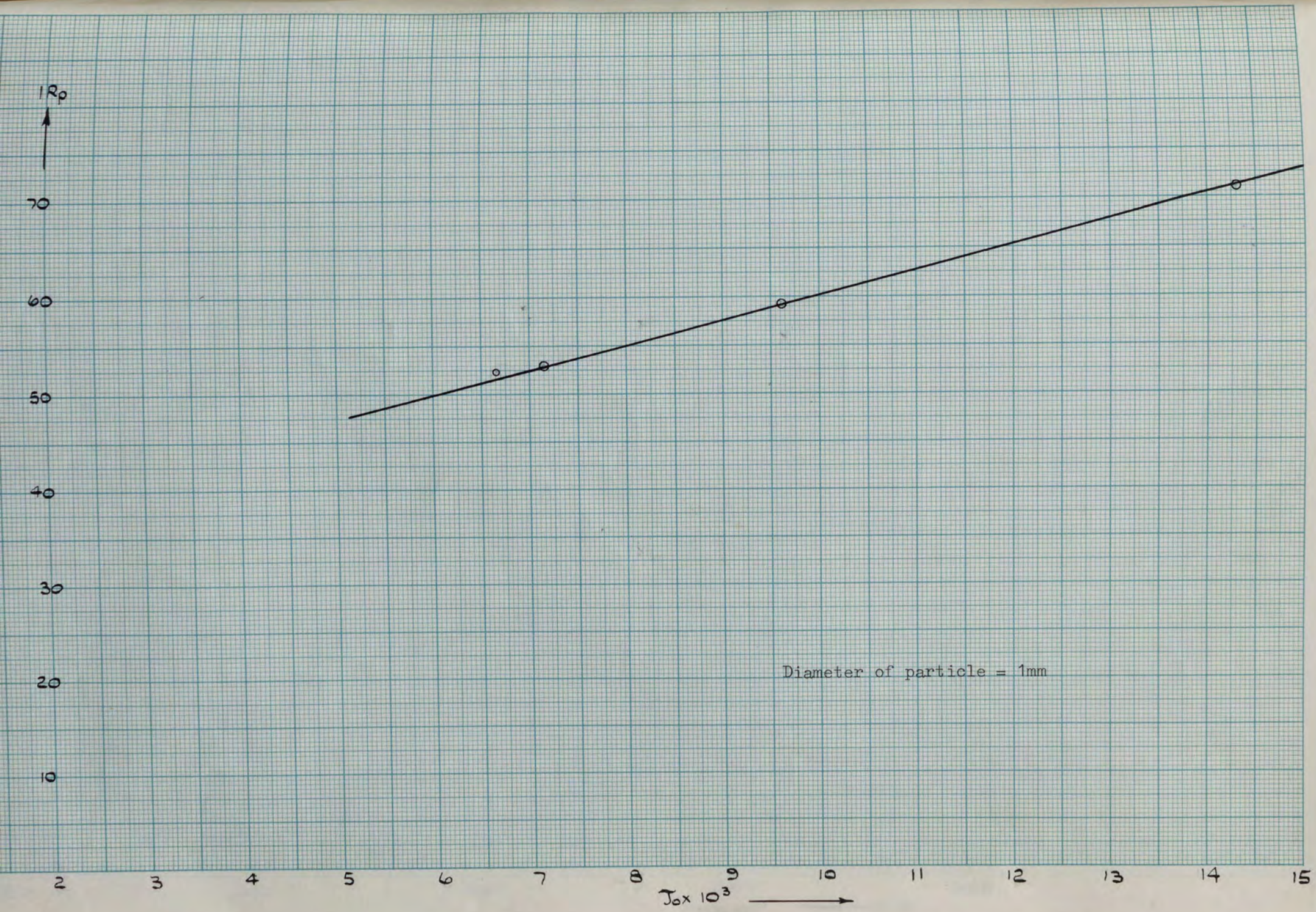
IR_p
70
60
50
40
30
20
10
2
3
4
5
6
7
8
9
10
11
12
13
14
15
$J_o \times 10^3$
Diameter of particle = 1mm

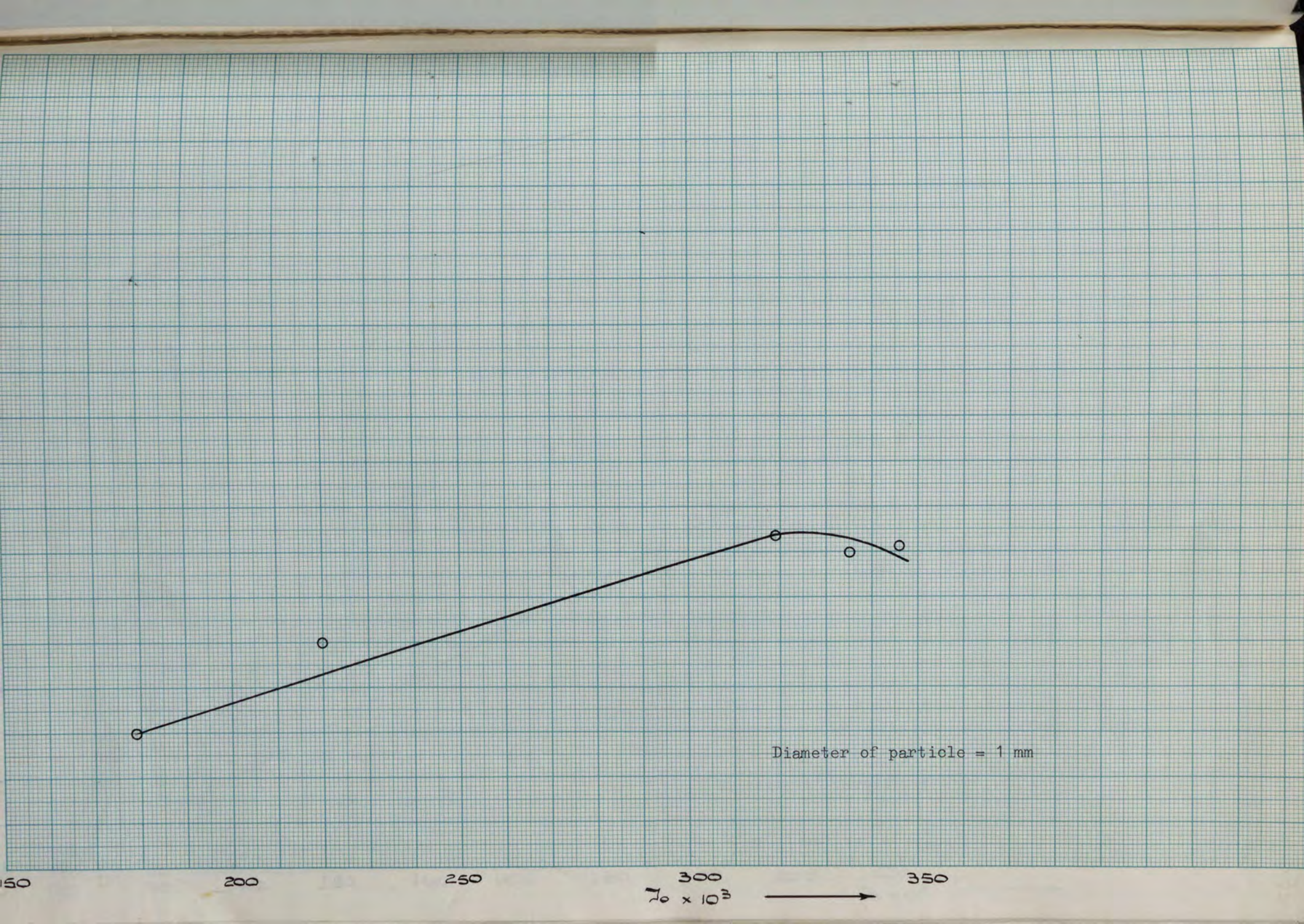
Diameter of particle = 1 mm
150
200
250
300
350
$T_o \times 10^3$

Diameter of particle = 1 mm
$\eta_0 \times 10^3$
120
130
140
150
160
170
180
190
200
220

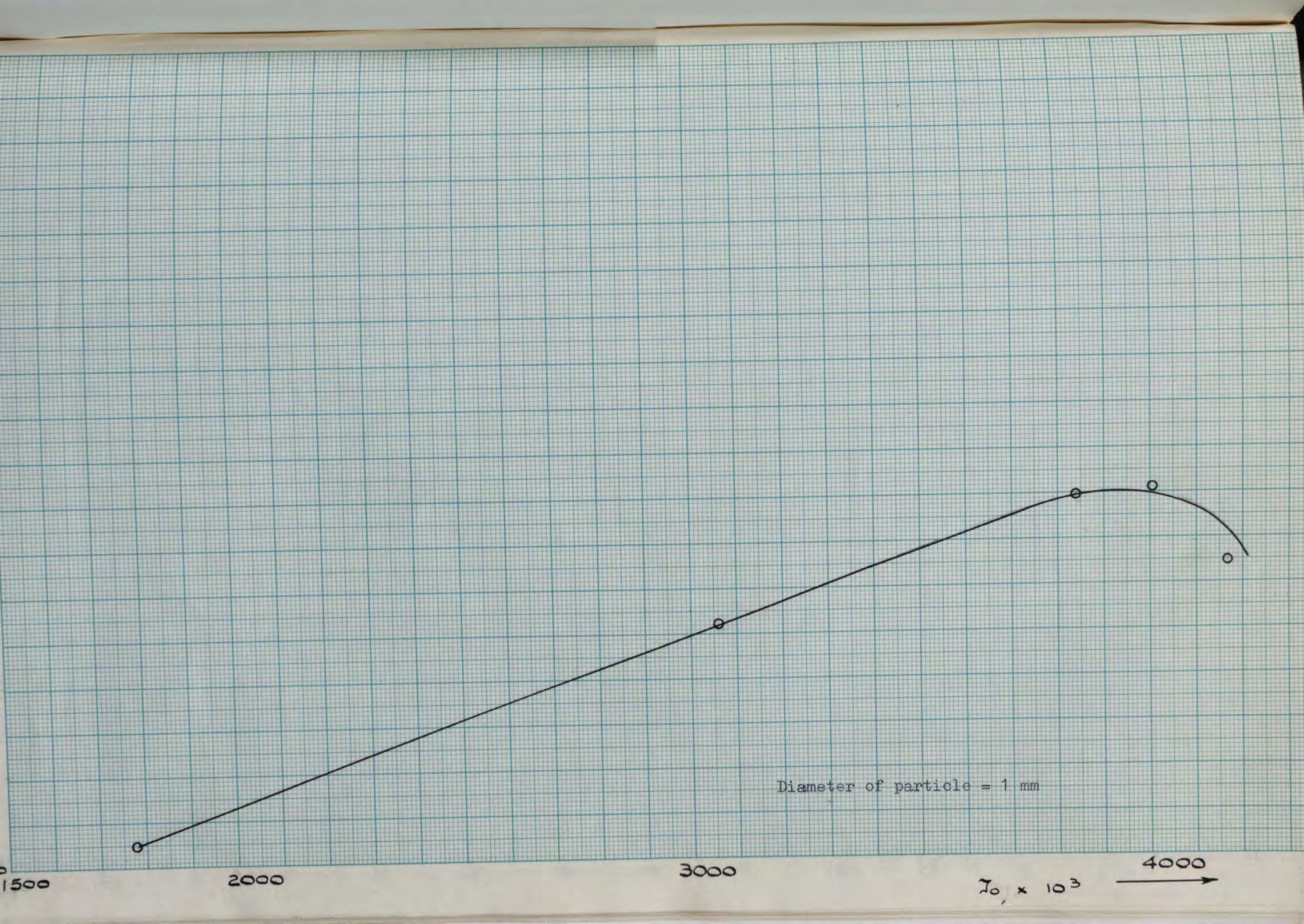
Diameter of particle = 1 mm
1500
2000
3000
4000
$T_0 \times 10^3$

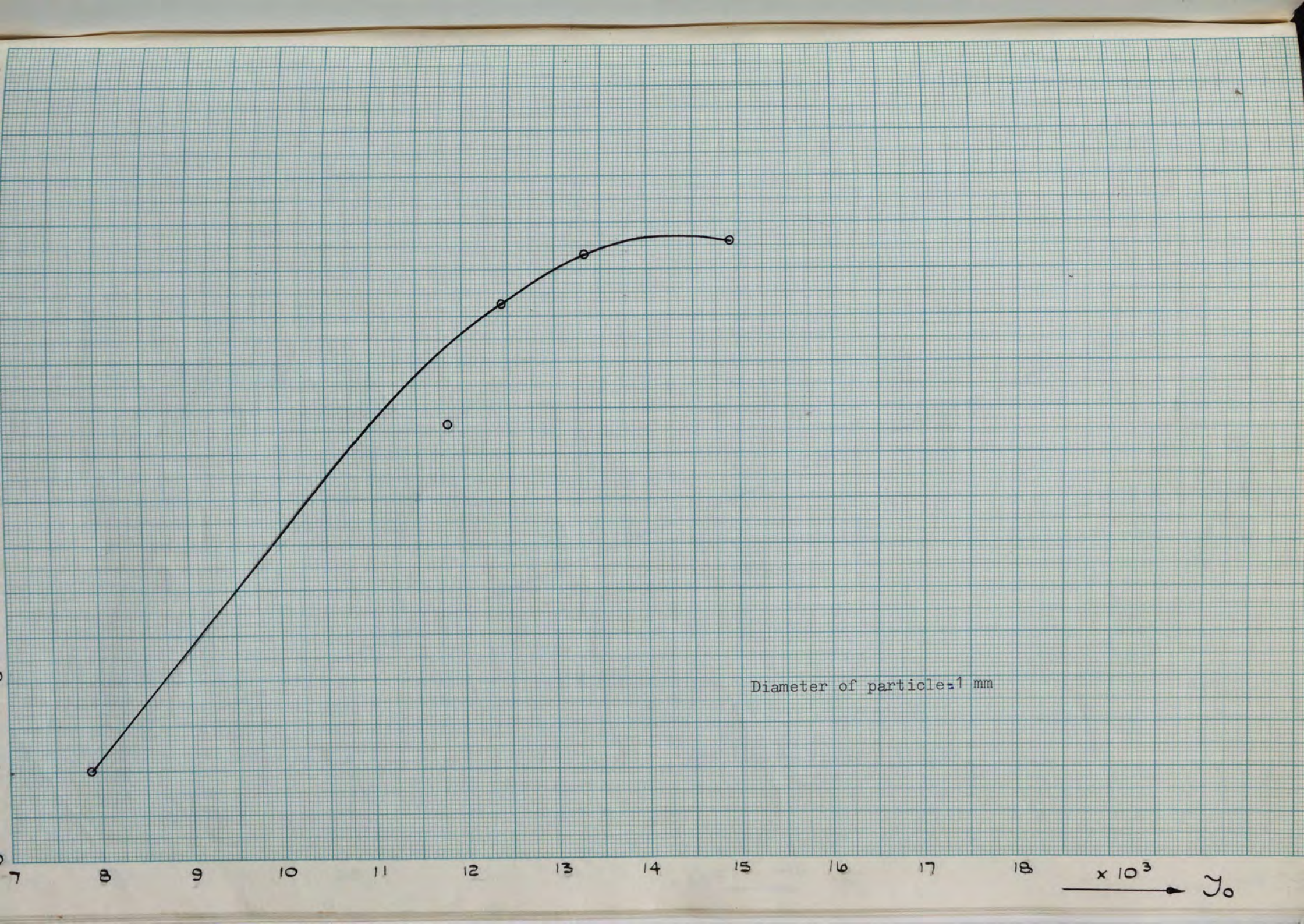
Diameter of particle=1 mm
7
8
9
10
11
12
13
14
15
16
17
18
x 10³
y₀

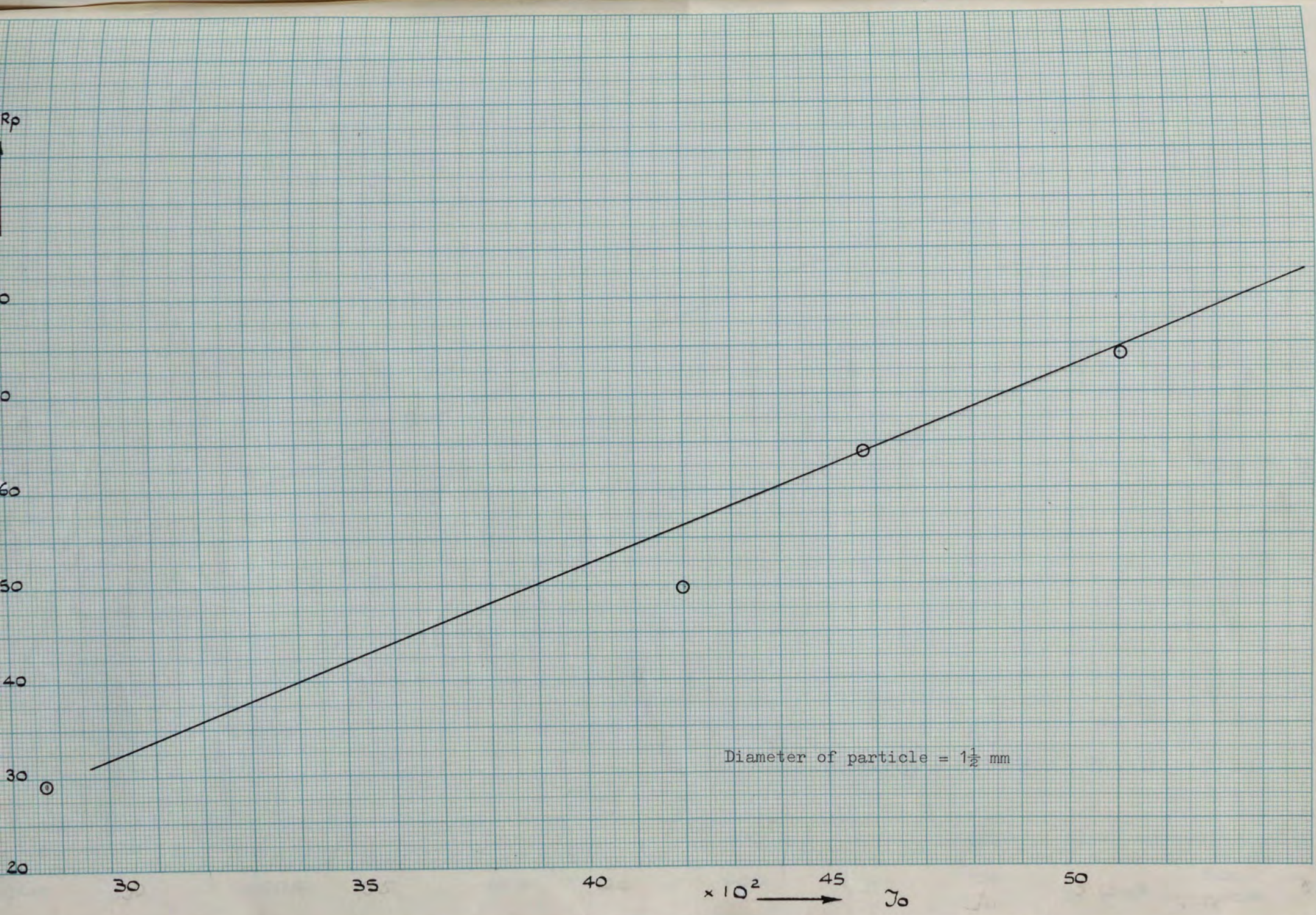
Rp
0
0
60
50
40
30
20
30
35
40
45
50
× 10²
J₀
Diameter of particle = 1½ mm

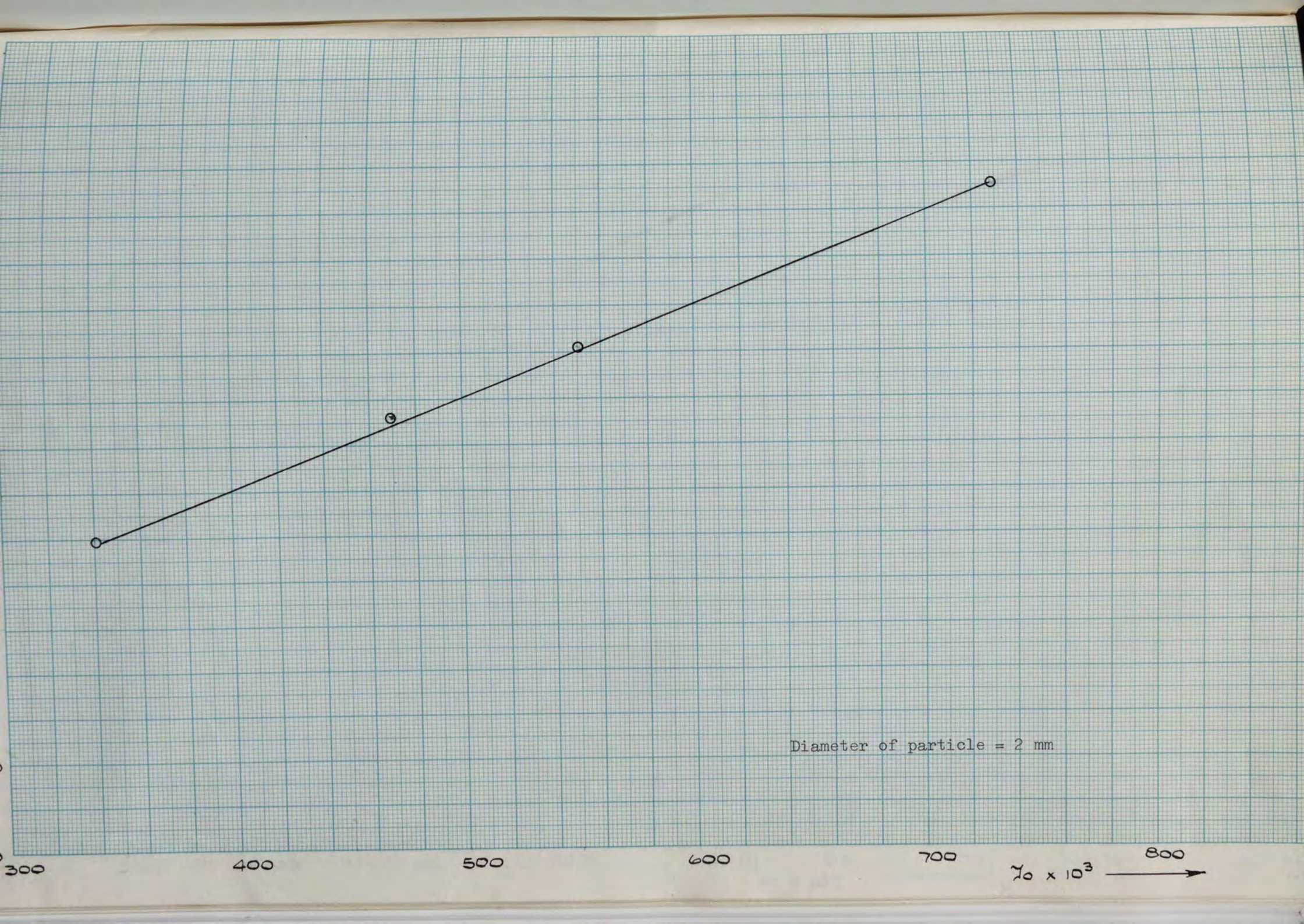
Diameter of particle = 2 mm
300
400
500
600
700
800
$\gamma_o \times 10^3$

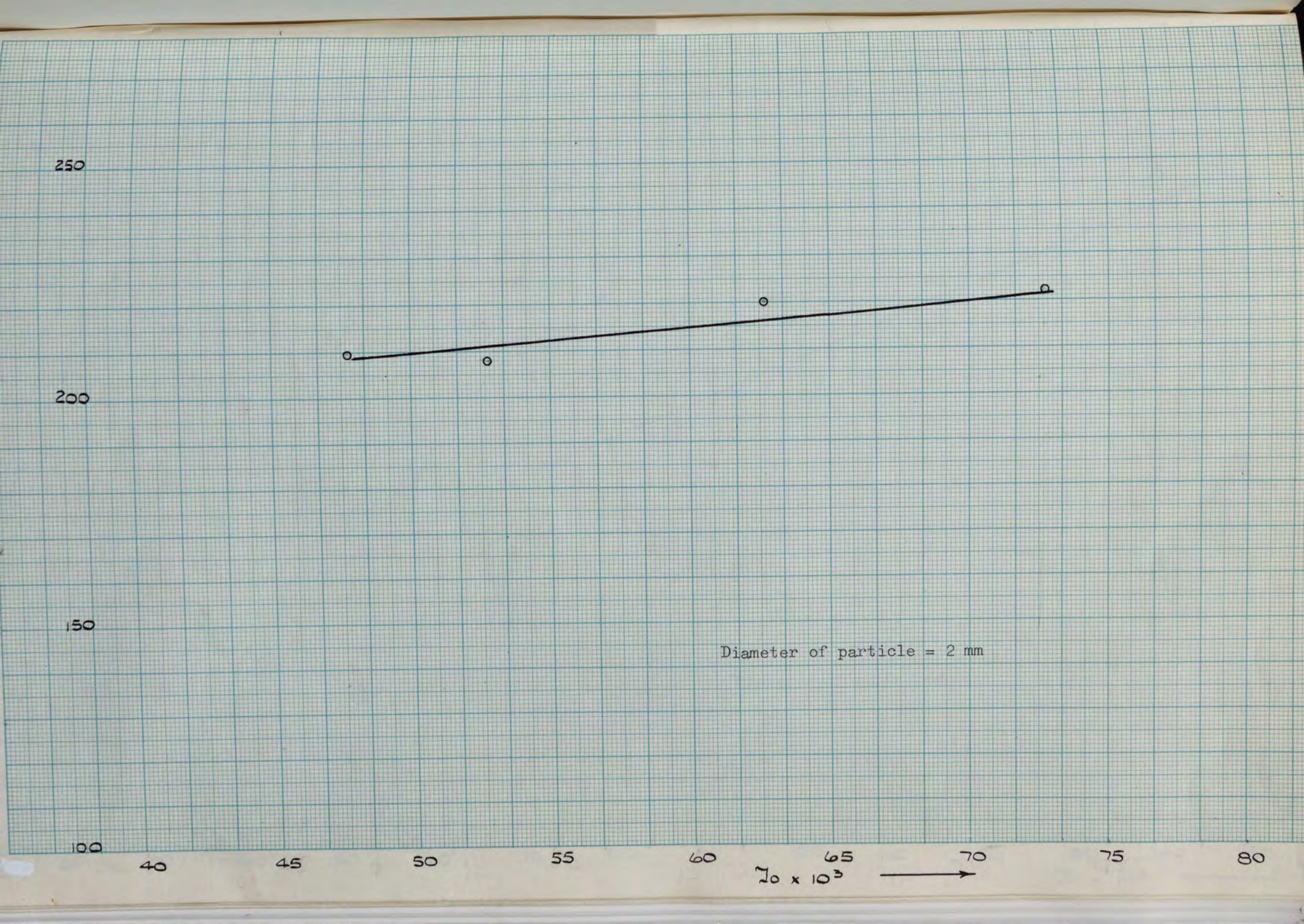
250
200
150
100
40
45
50
55
60
65
70
75
80
Diameter of particle = 2 mm

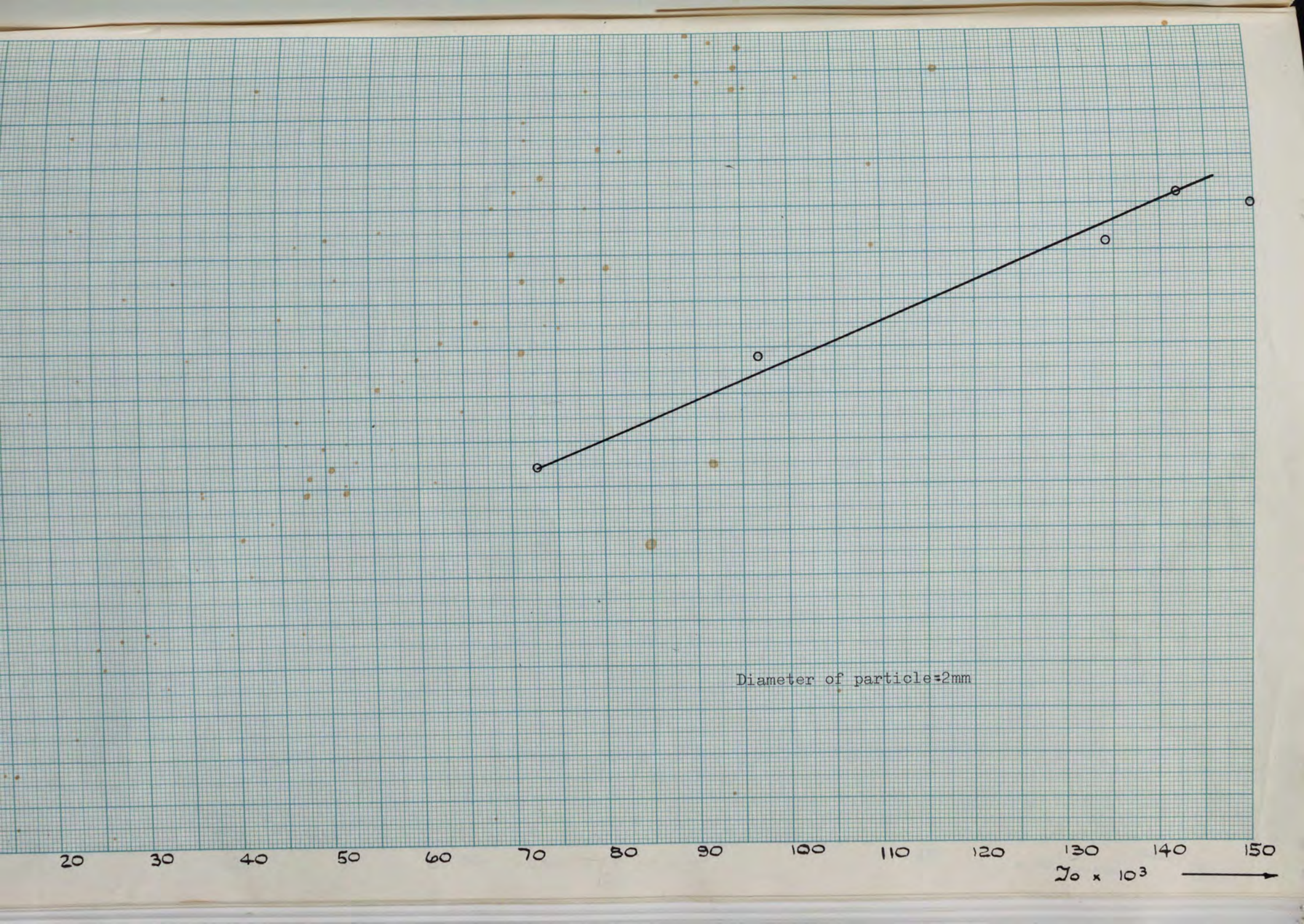
Diameter of particle=2mm
20
30
40
50
60
70
80
90
100
110
120
130
140
150
$J_o \times 10^3$

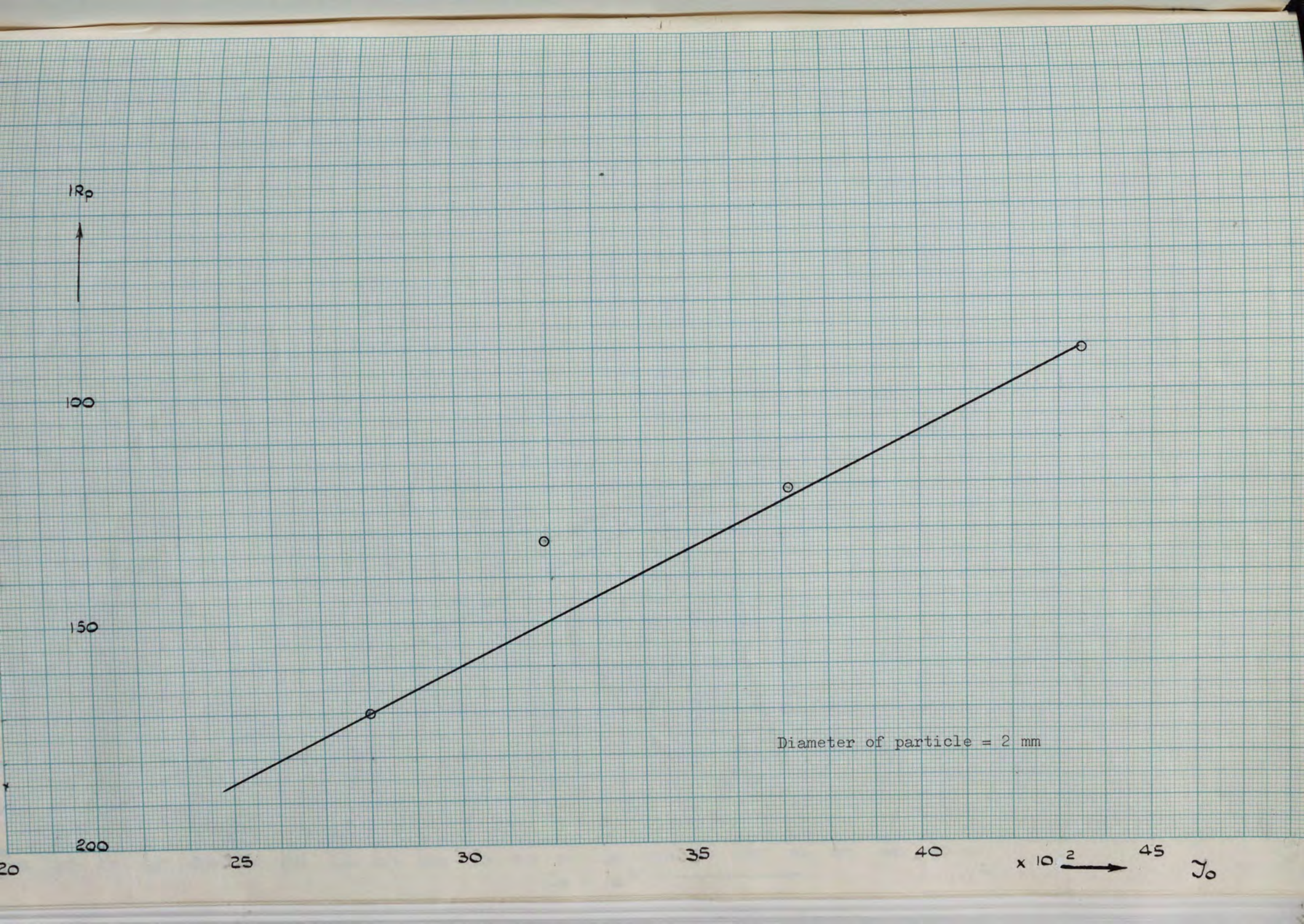
IRp
100
150
200
20
25
30
35
40
45
x 10 2
Jo
Diameter of particle = 2 mm

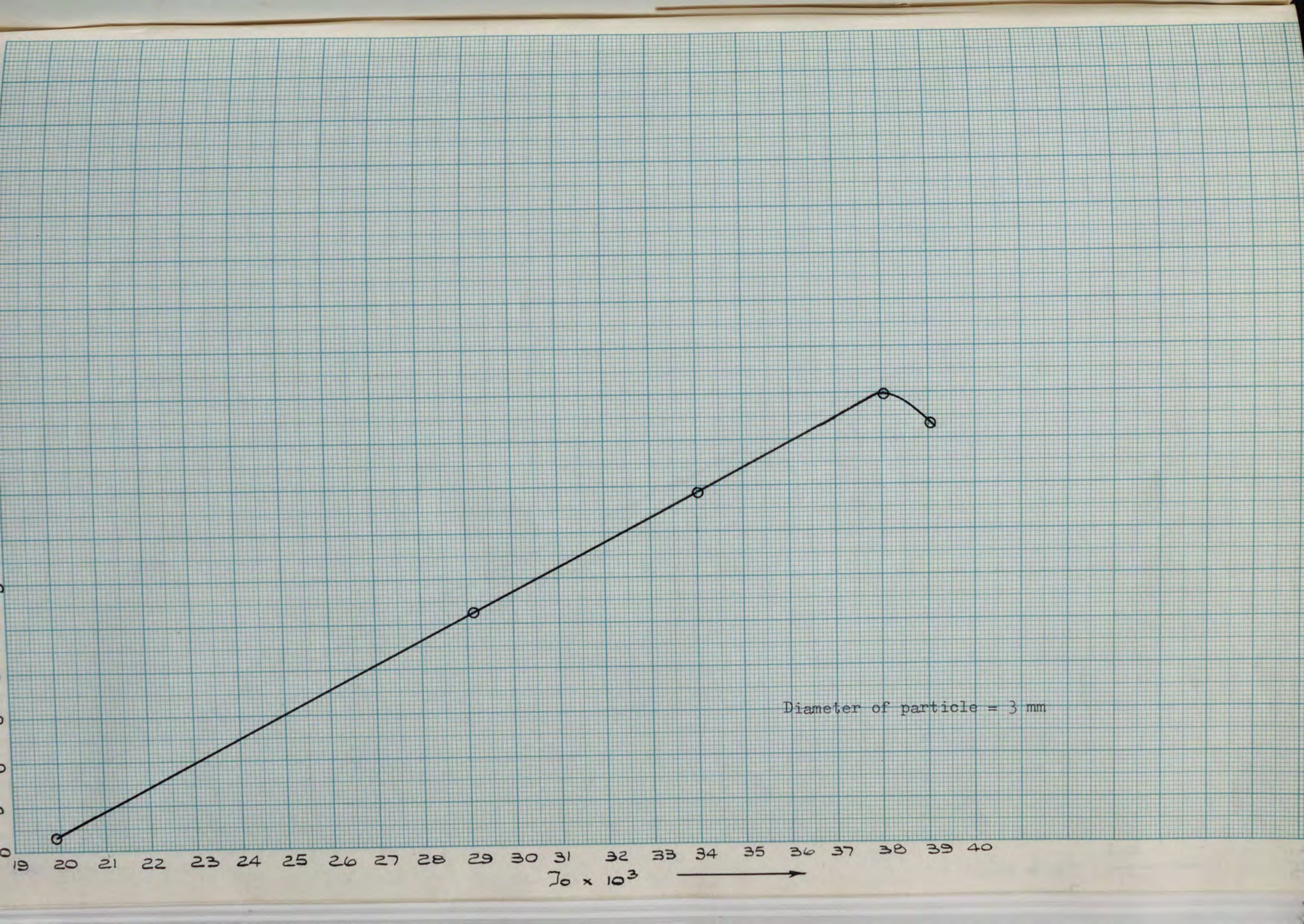
Diameter of particle = 3 mm
19 20 21 22 23 24 25 26 27 28 29 30 31 32 33 34 35 36 37 38 39 40
$J_o \times 10^3$

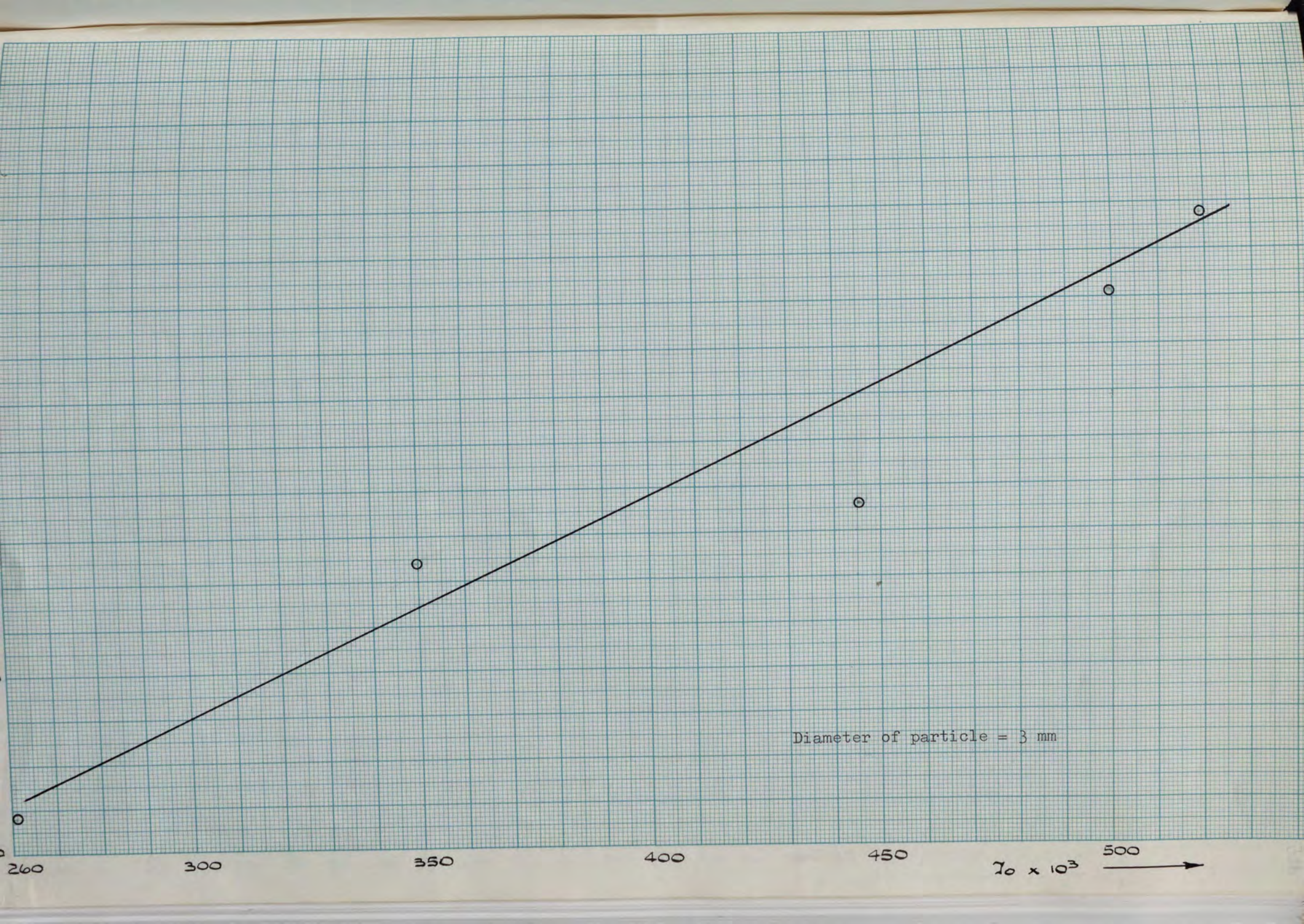
Diameter of particle = 3 mm
260
300
350
400
450
500
$\gamma_o \times 10^3$

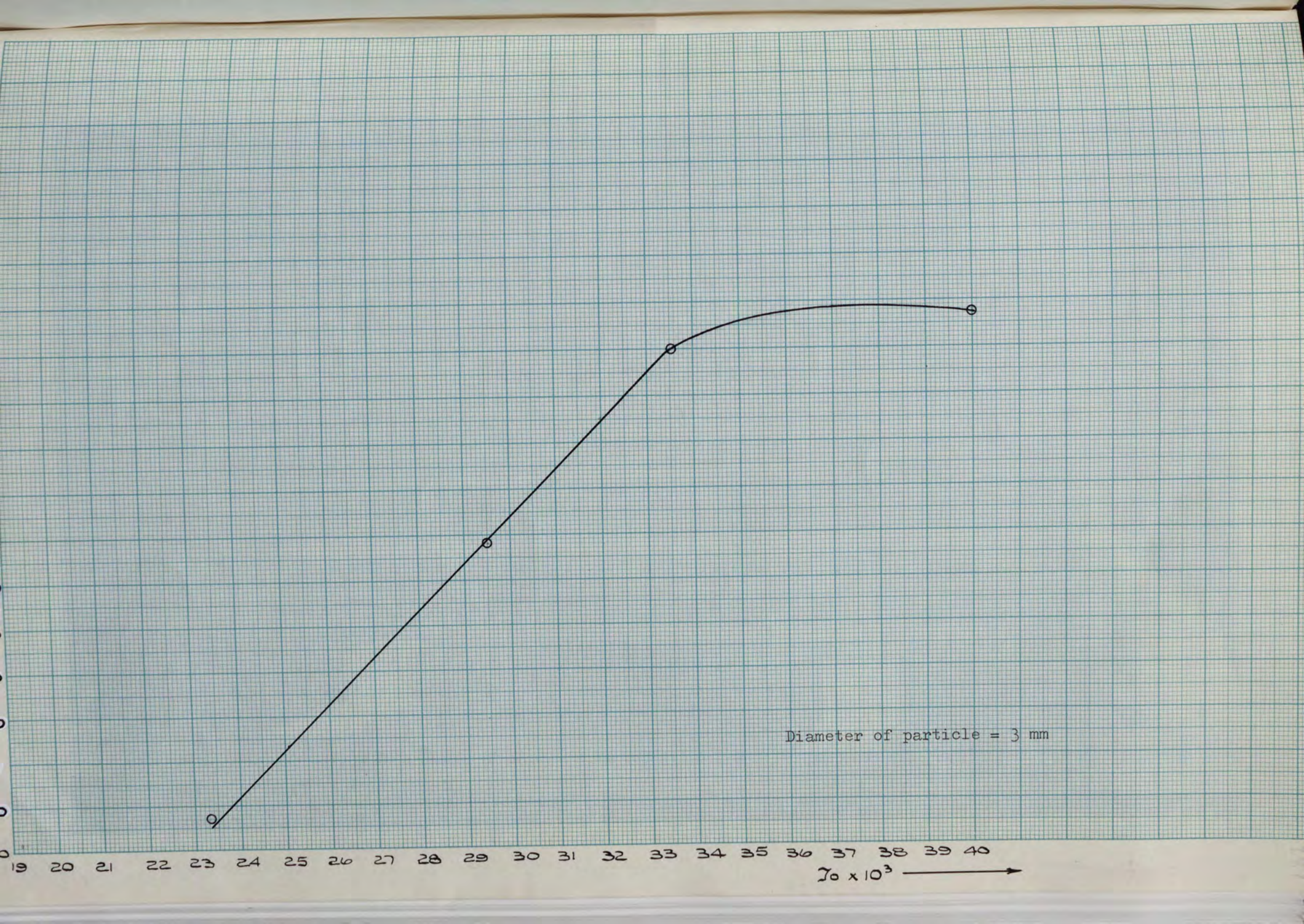
Diameter of particle = 3 mm
19 20 21 22 23 24 25 26 27 28 29 30 31 32 33 34 35 36 37 38 39 40
$\gamma_0 \times 10^3$

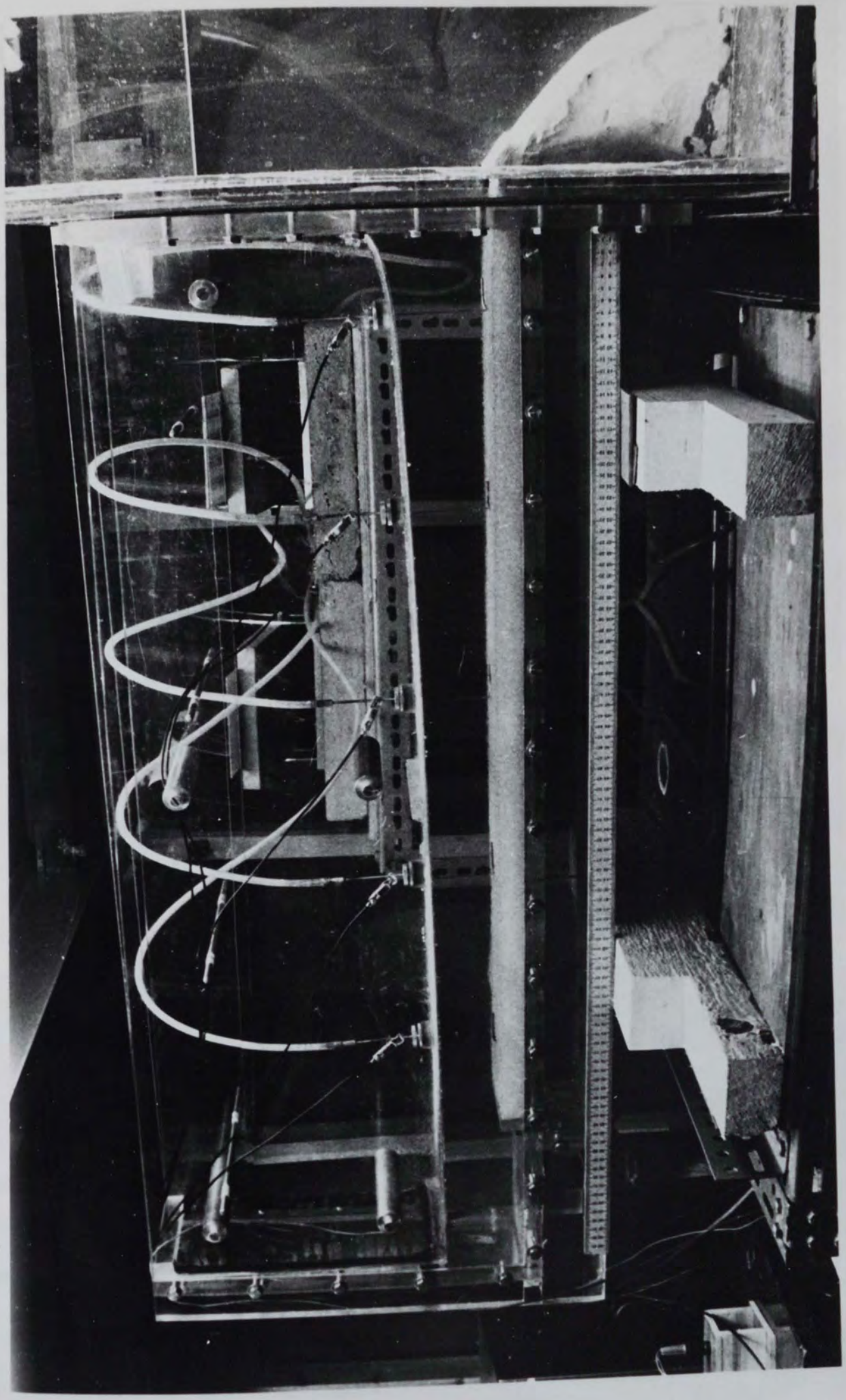

Plate 1

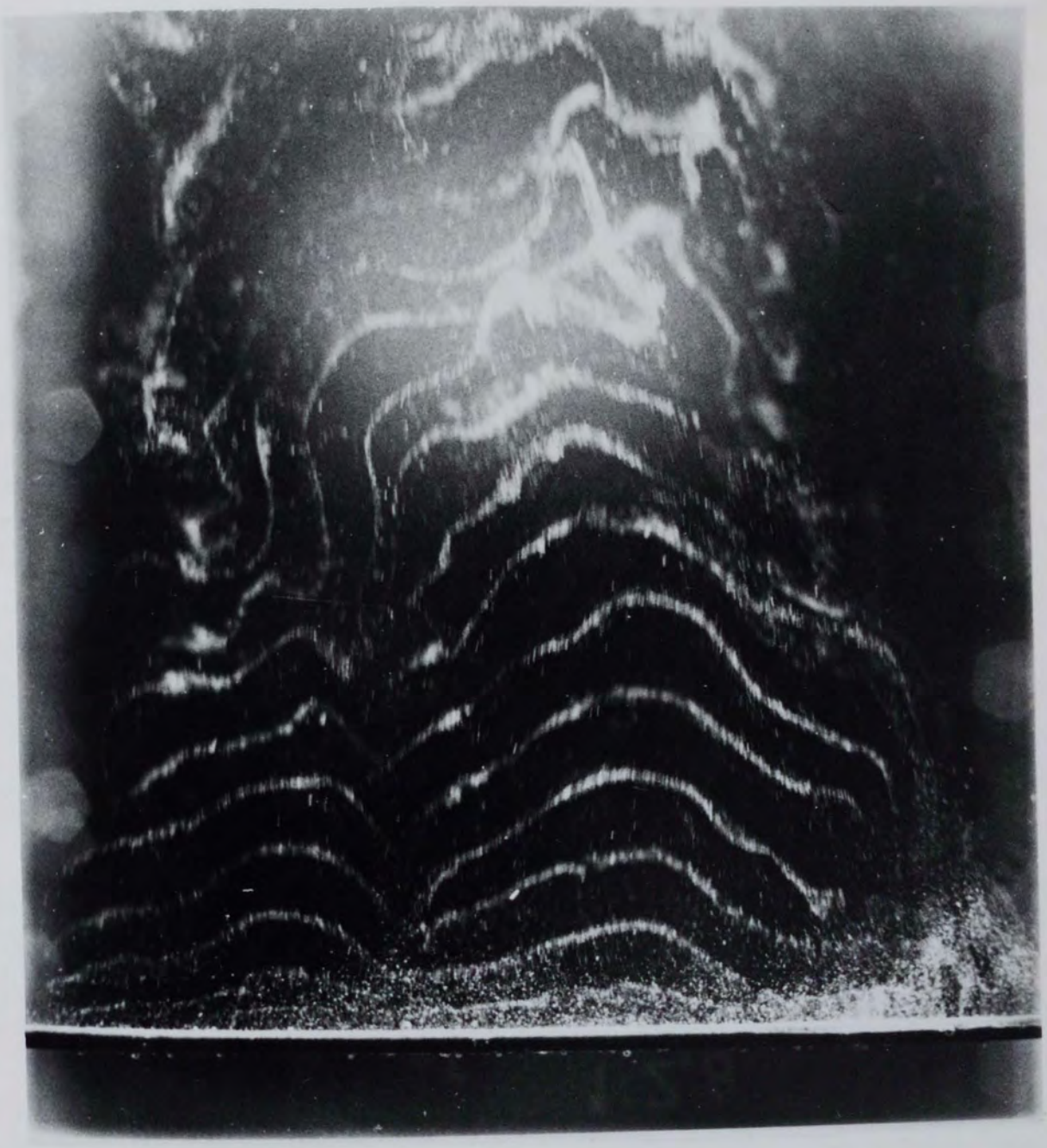

Plate 2

Plate 3

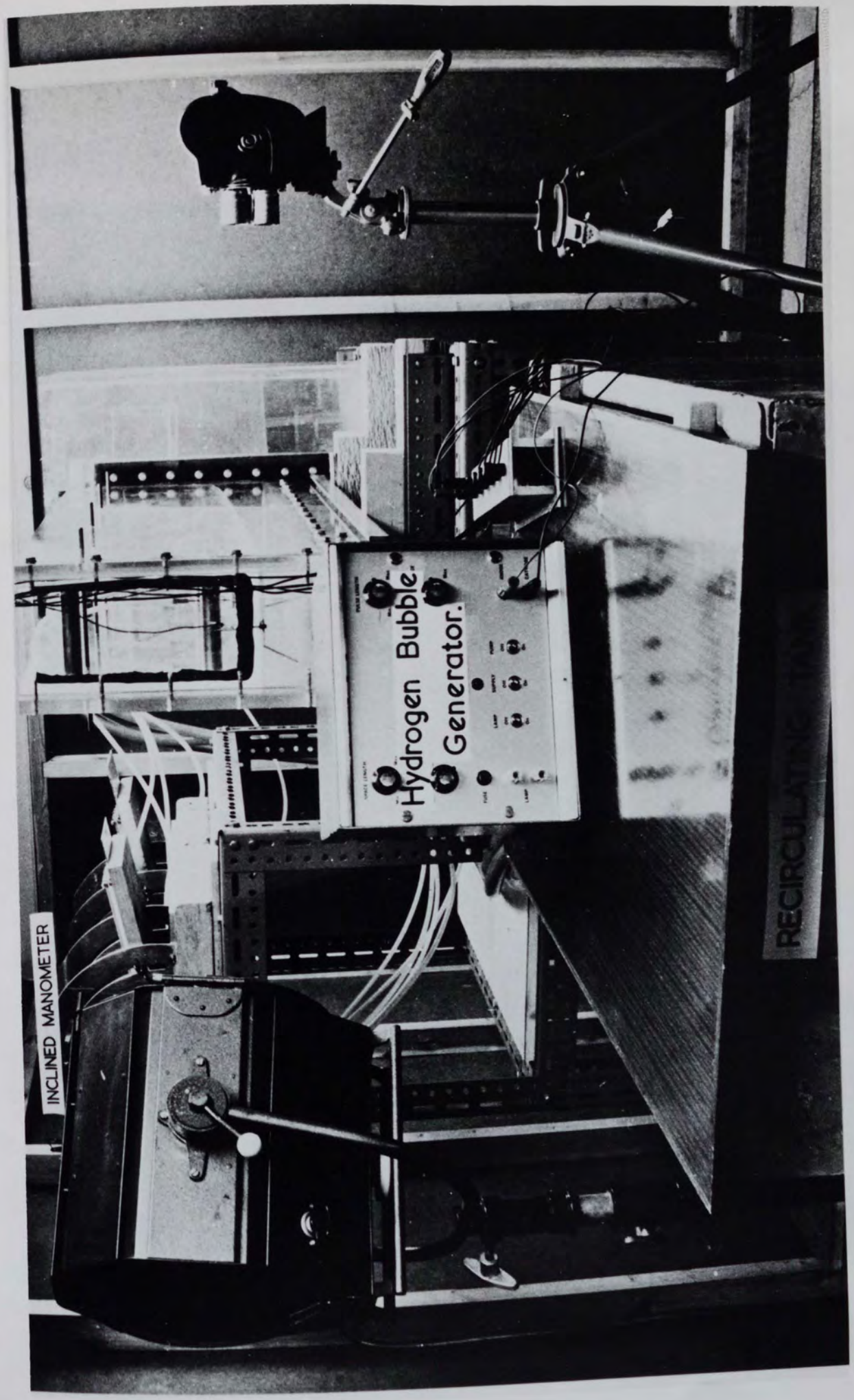
INCLINED MANOMETER
Hydrogen Bubble
Generator.
RECIRCULATING

Plate 4

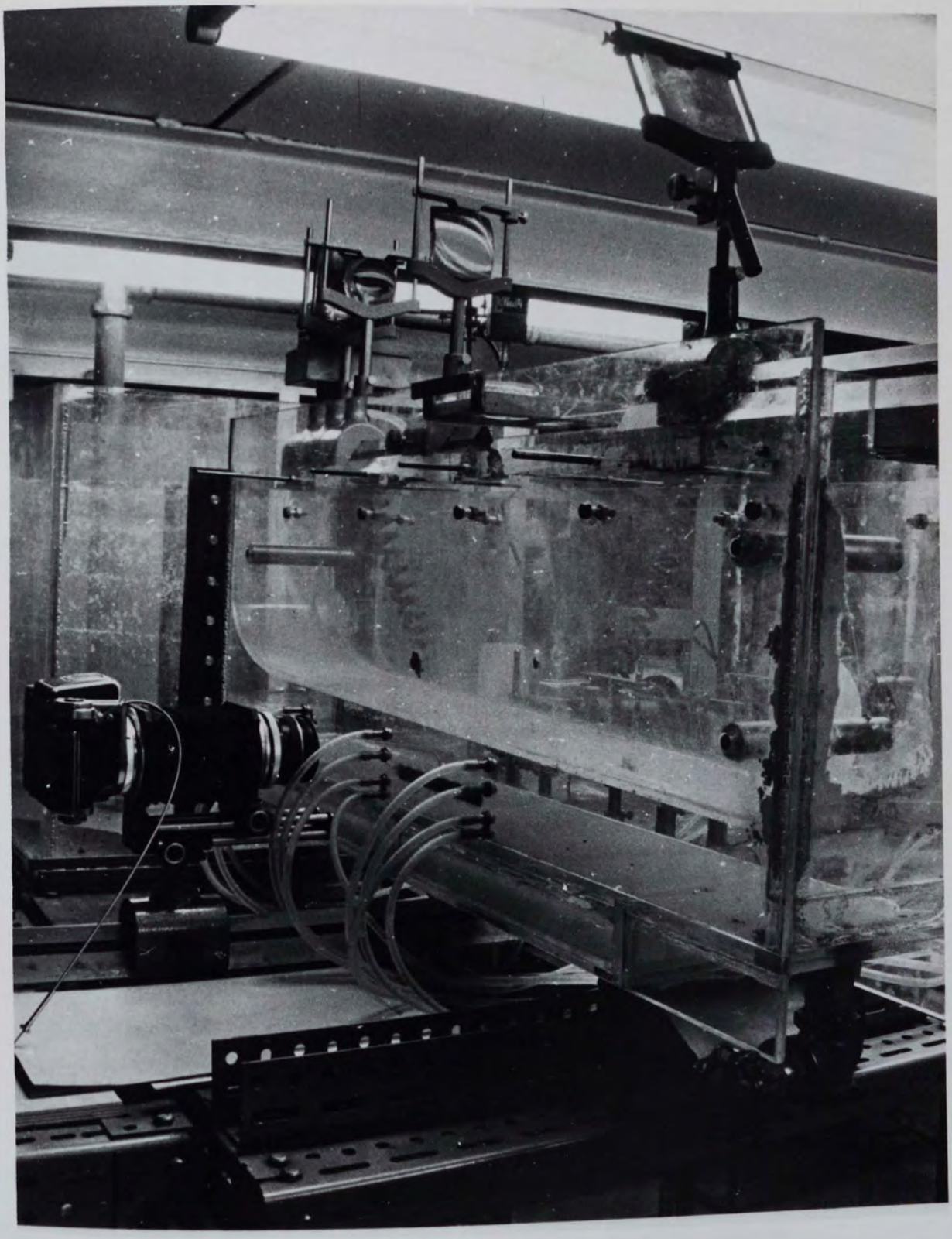

Plate 5

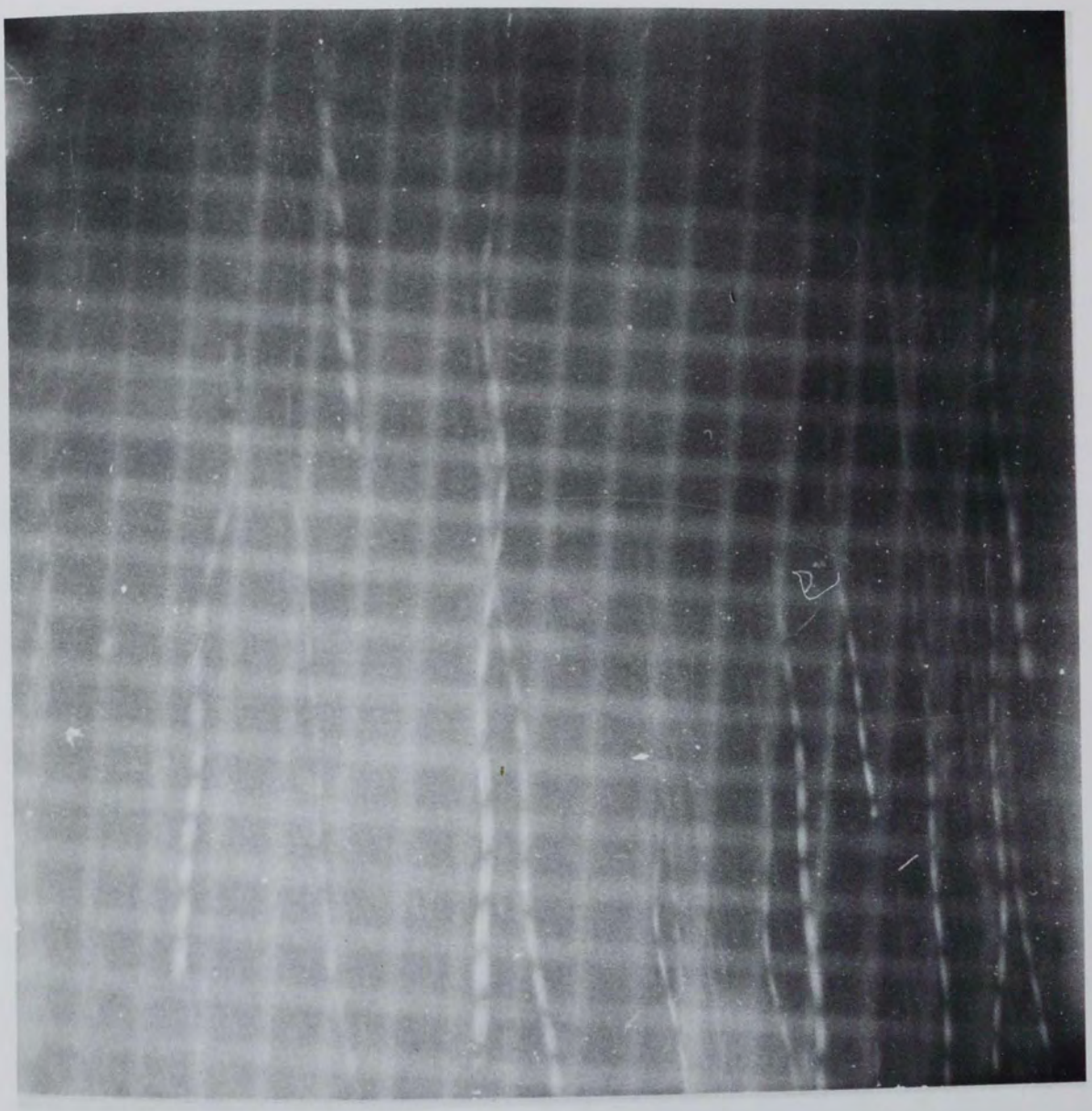

Plate 6

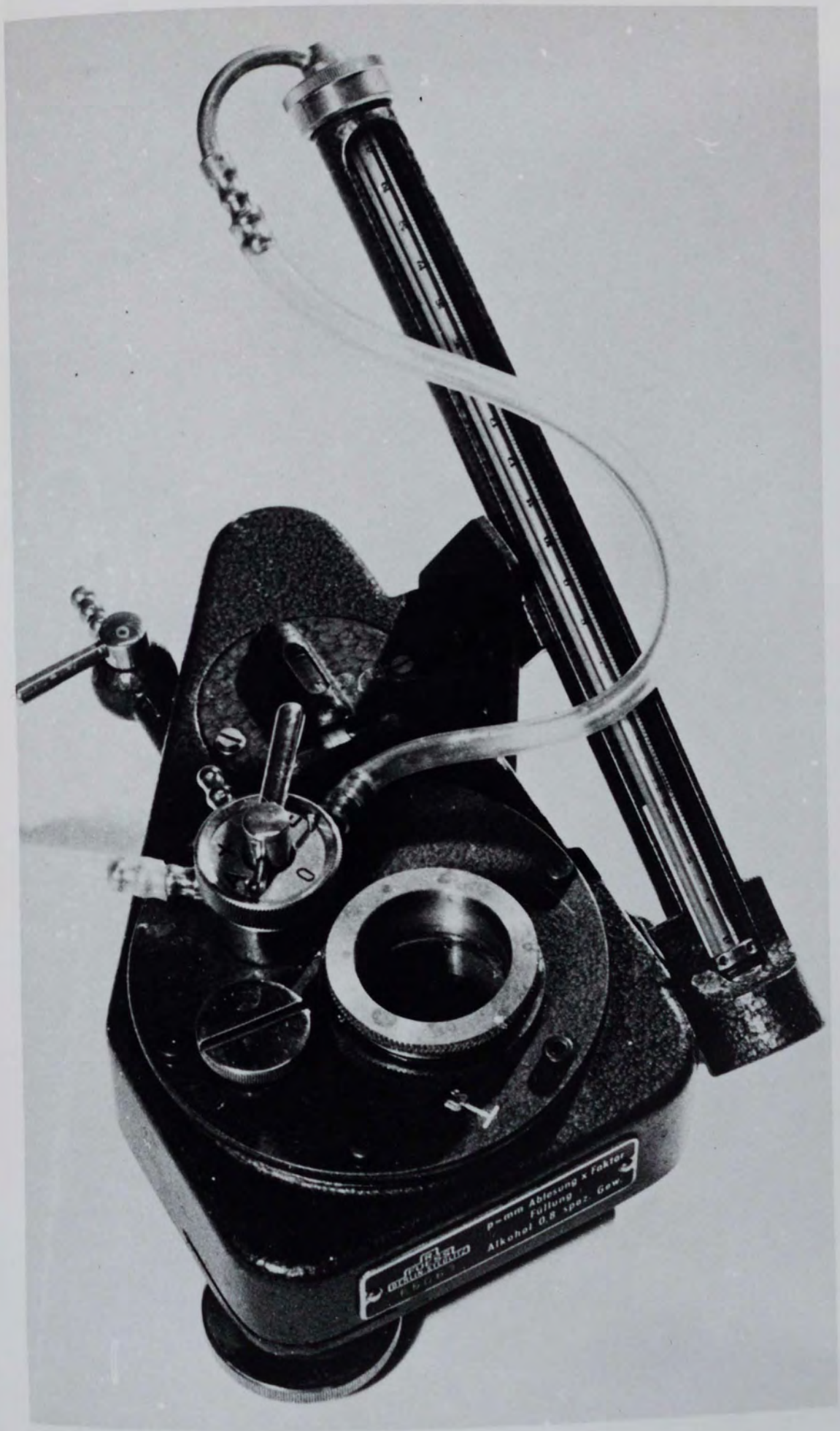

Plate 7

Plate 8

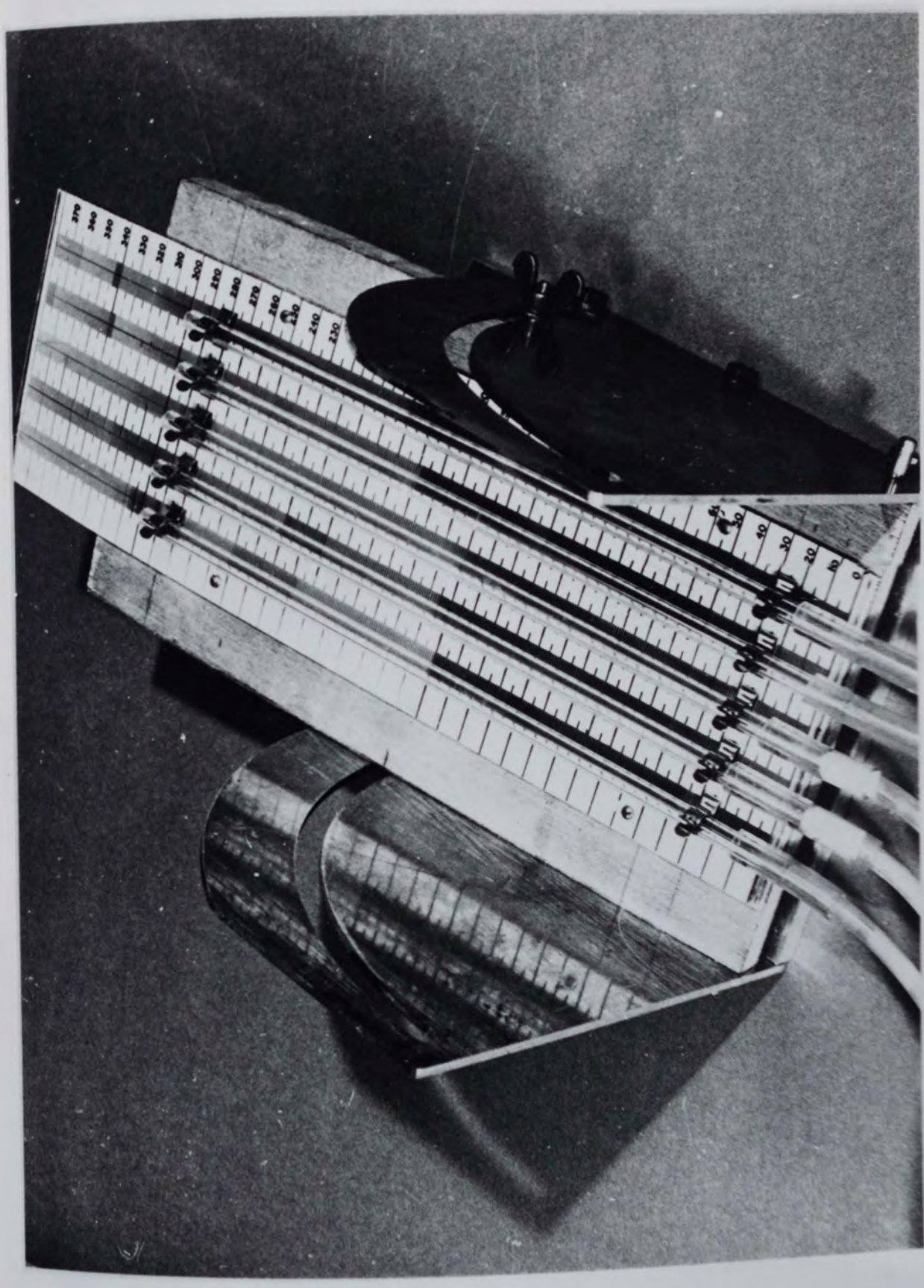

Plate 9

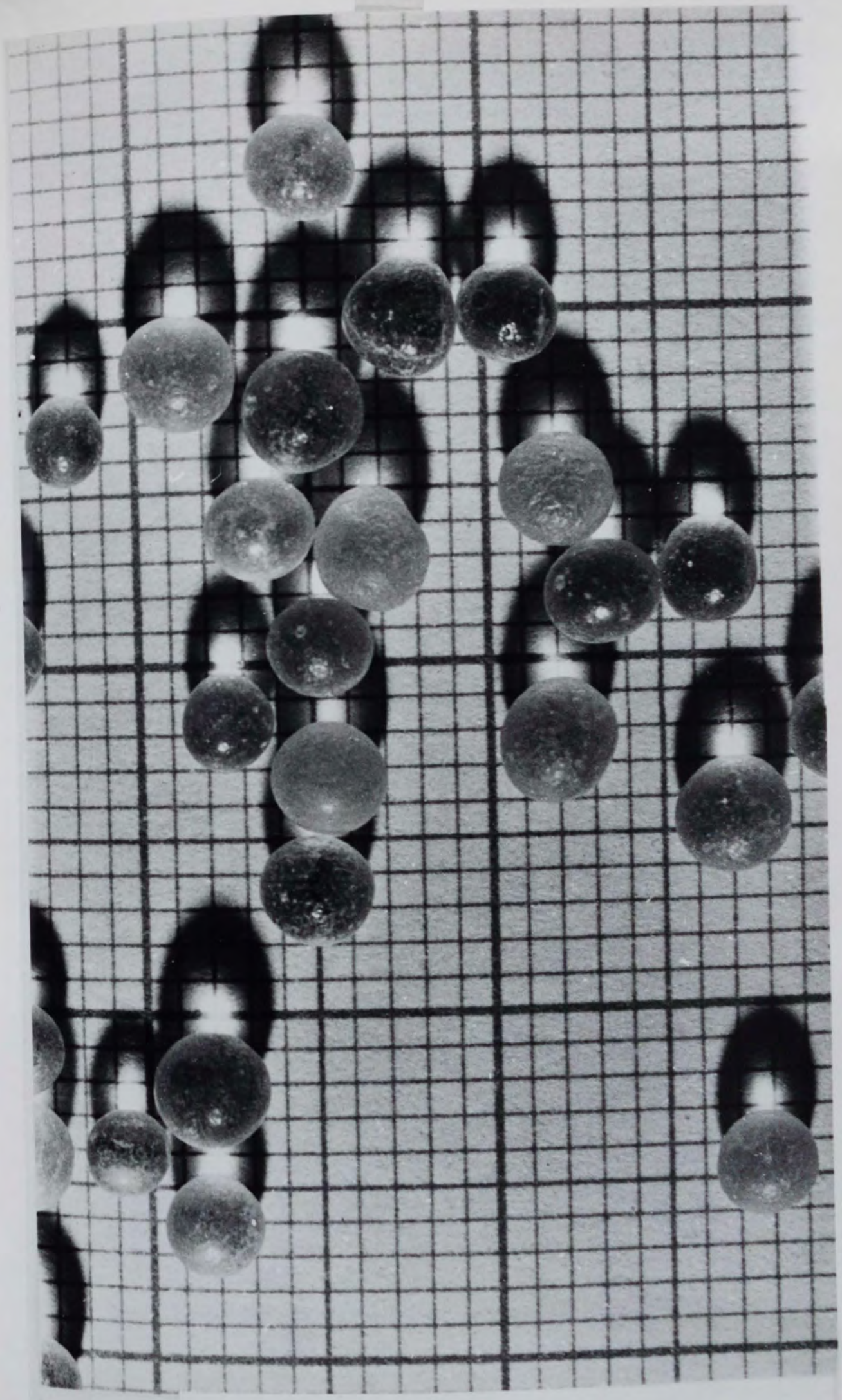

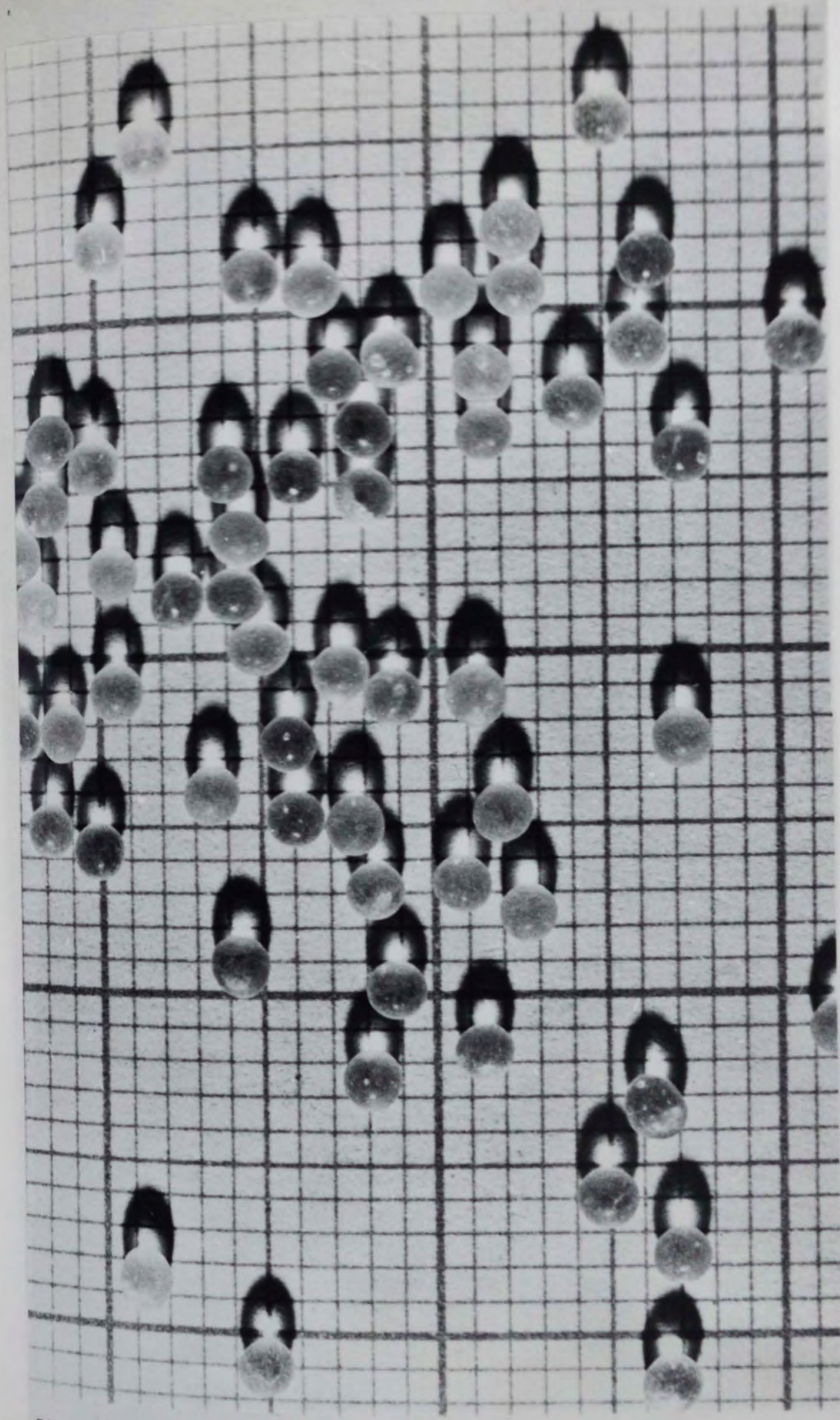

Plate 11

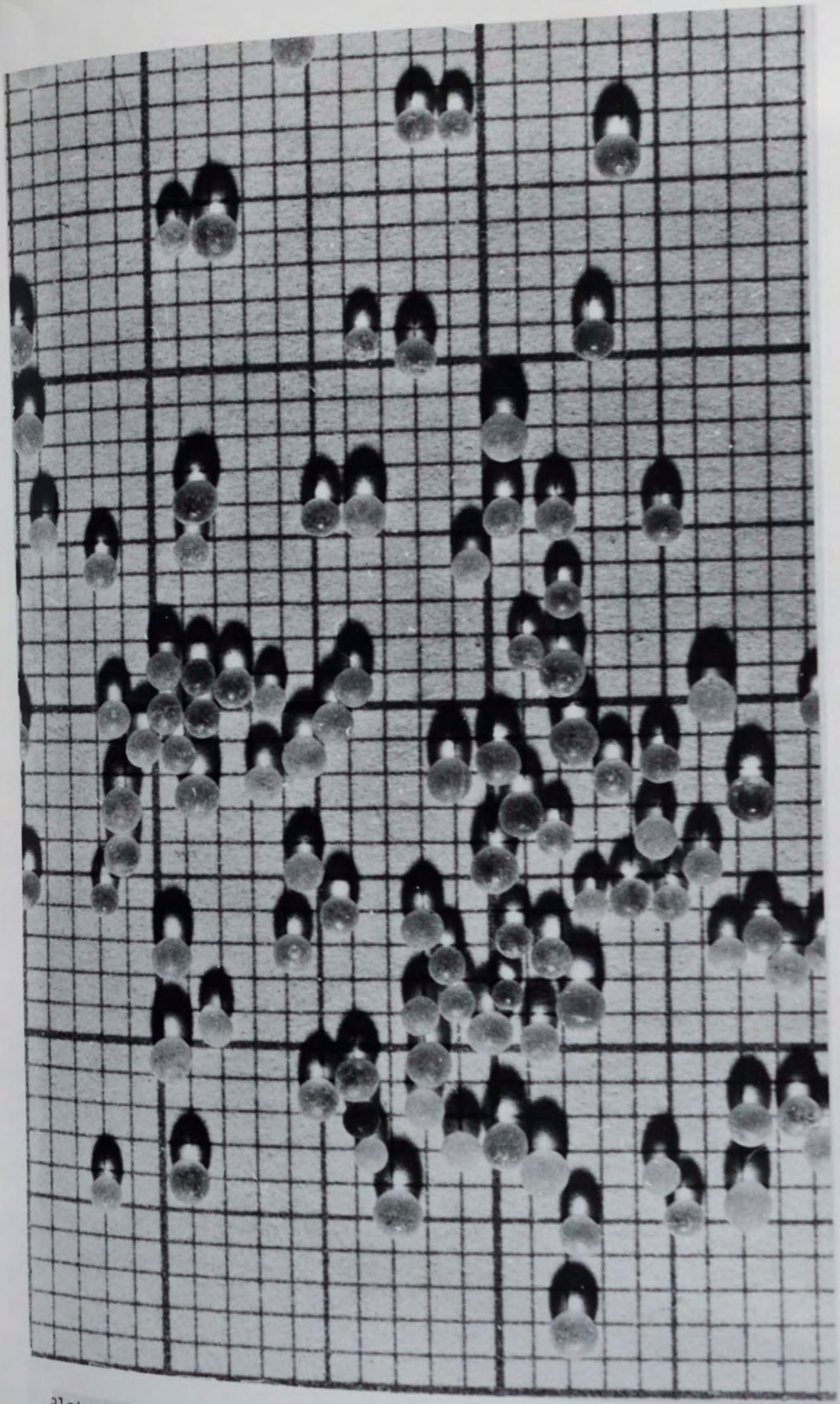

Plate 12

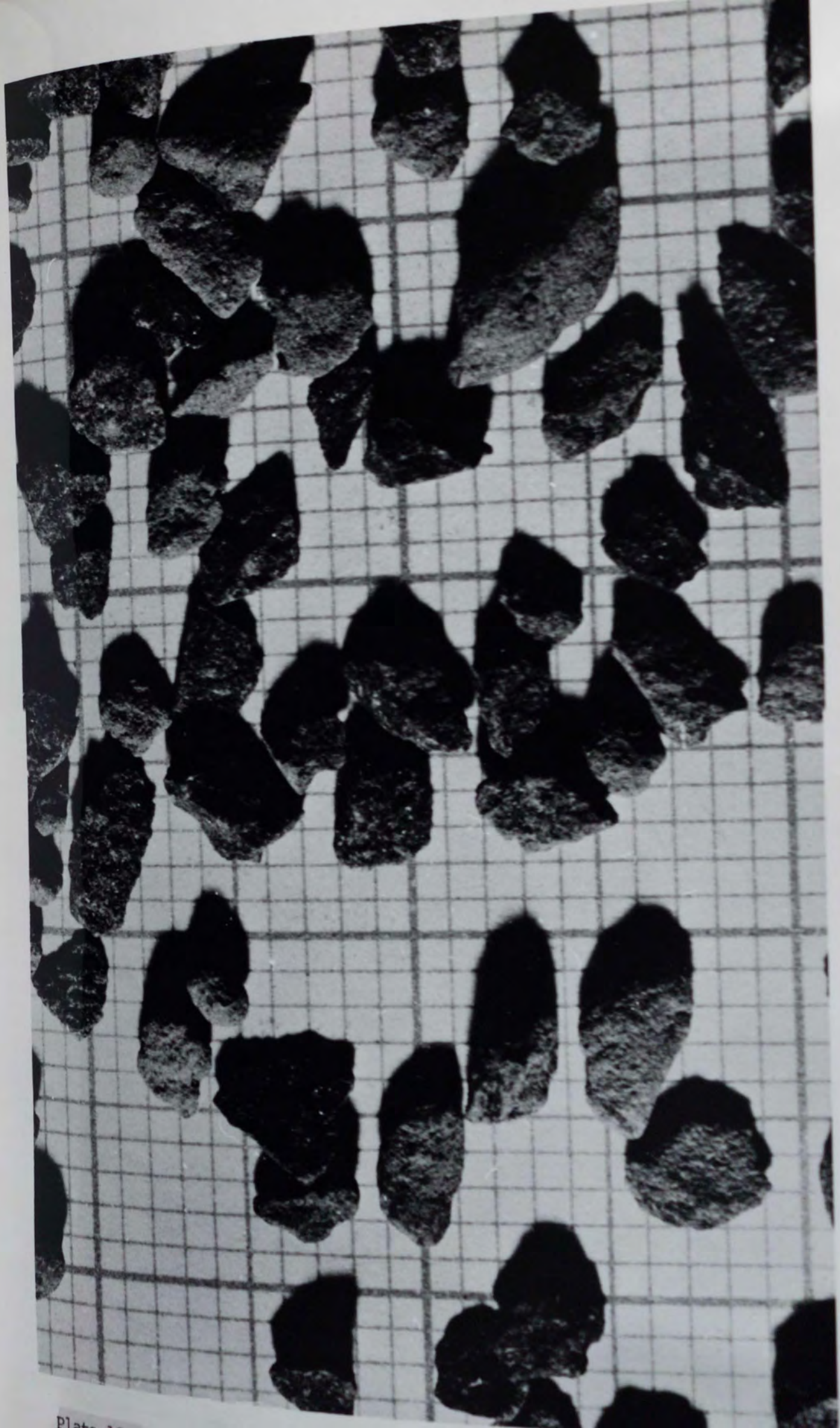

Plate

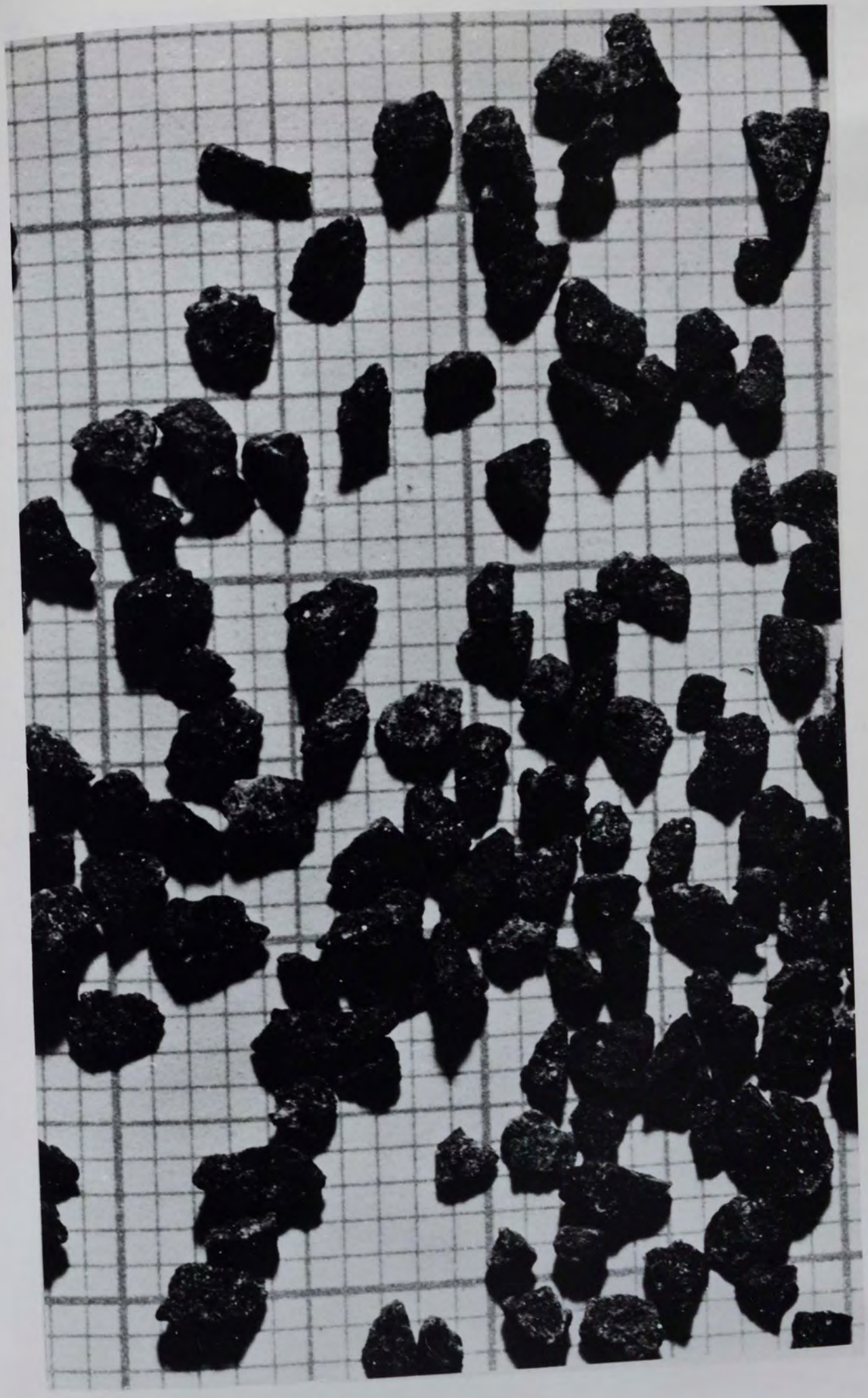

Plate 14

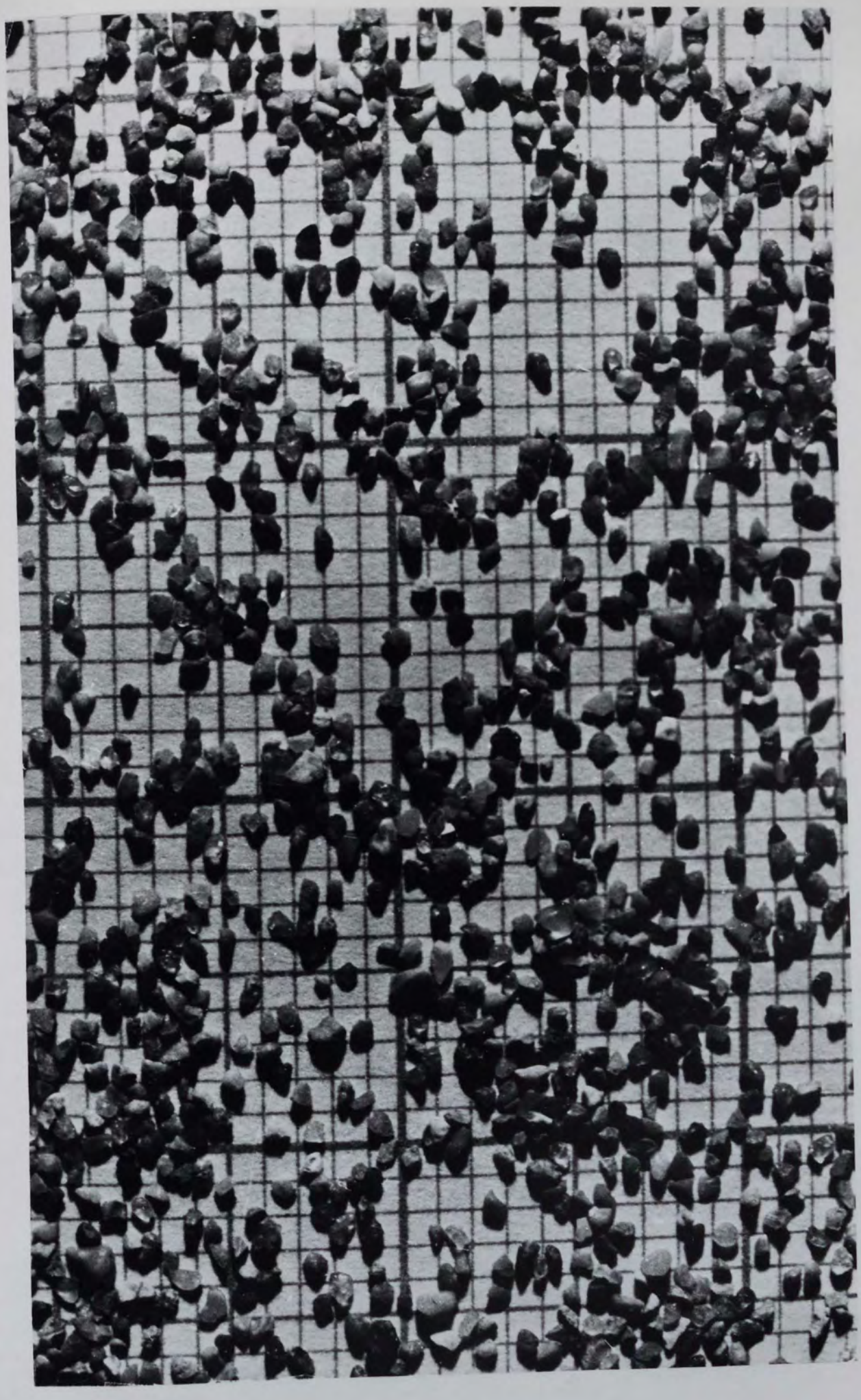

Plate 15

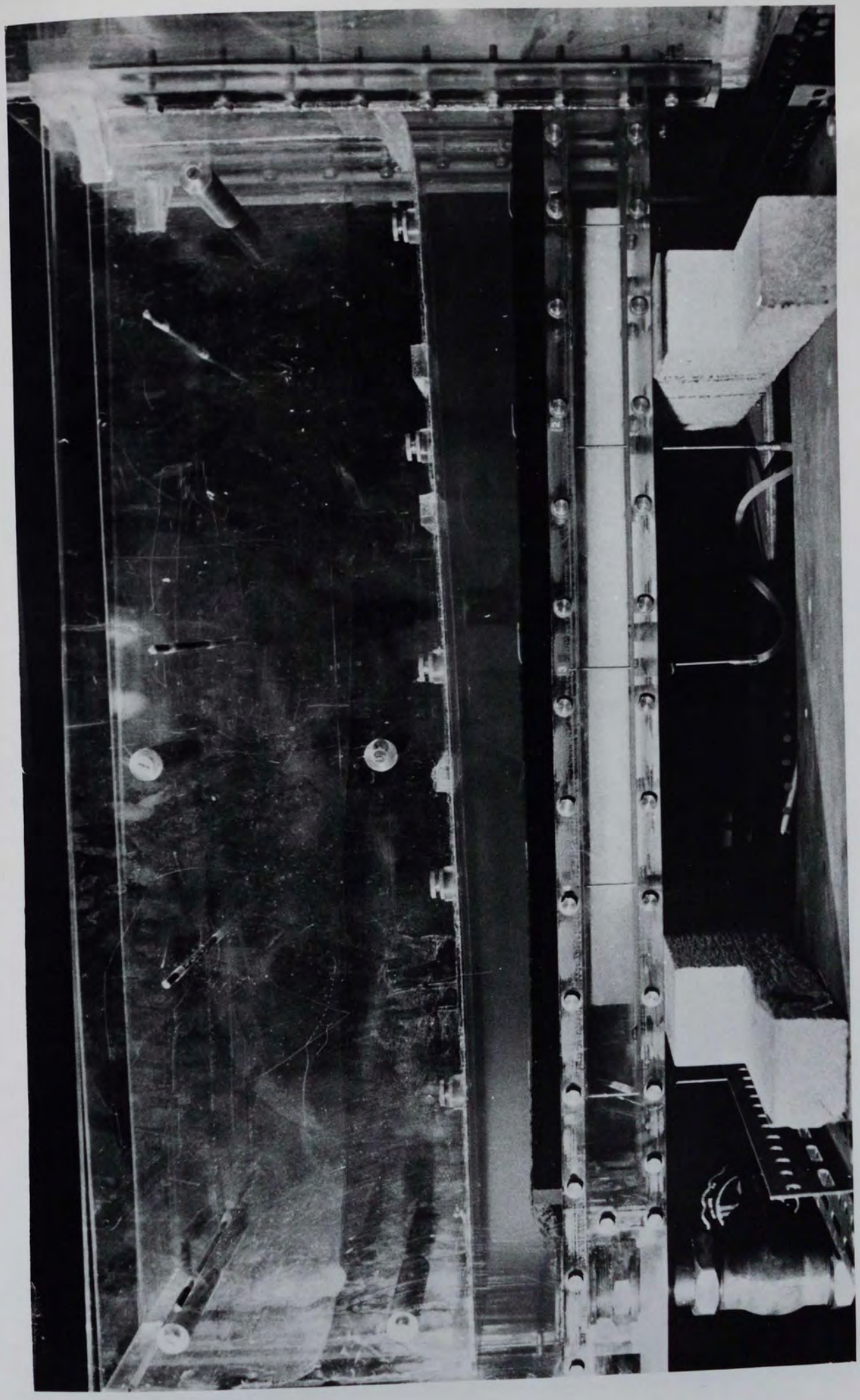

Plate 16

Plate 17

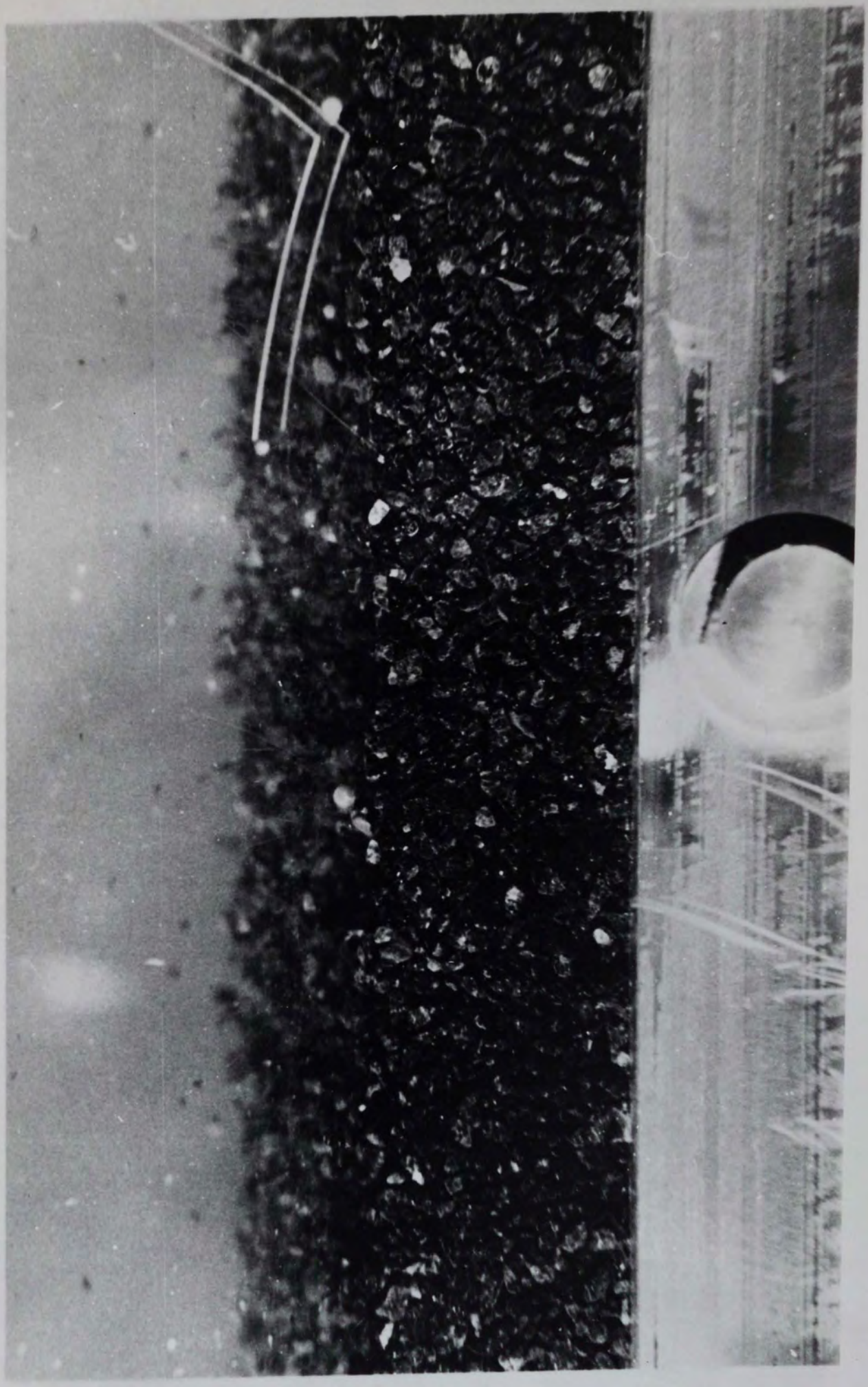

Plate 18